frontiers | Research Topics

Physiological adaptations of insects exposed to different stress conditions, volume II

Edited by
Bin Tang, Bimalendu B. Nath, Lisheng Zhang and Can Li

Published in
Frontiers in Physiology

ISSN 1664-8714
ISBN 978-2-8325-6189-8
DOI 10.3389/978-2-8325-6189-8

About Frontiers

Frontiers is more than just an open access publisher of scholarly articles: it is a pioneering approach to the world of academia, radically improving the way scholarly research is managed. The grand vision of Frontiers is a world where all people have an equal opportunity to seek, share and generate knowledge. Frontiers provides immediate and permanent online open access to all its publications, but this alone is not enough to realize our grand goals.

Frontiers journal series

The Frontiers journal series is a multi-tier and interdisciplinary set of open-access, online journals, promising a paradigm shift from the current review, selection and dissemination processes in academic publishing. All Frontiers journals are driven by researchers for researchers; therefore, they constitute a service to the scholarly community. At the same time, the *Frontiers journal series* operates on a revolutionary invention, the tiered publishing system, initially addressing specific communities of scholars, and gradually climbing up to broader public understanding, thus serving the interests of the lay society, too.

Dedication to quality

Each Frontiers article is a landmark of the highest quality, thanks to genuinely collaborative interactions between authors and review editors, who include some of the world's best academicians. Research must be certified by peers before entering a stream of knowledge that may eventually reach the public - and shape society; therefore, Frontiers only applies the most rigorous and unbiased reviews. Frontiers revolutionizes research publishing by freely delivering the most outstanding research, evaluated with no bias from both the academic and social point of view. By applying the most advanced information technologies, Frontiers is catapulting scholarly publishing into a new generation.

What are Frontiers Research Topics?

Frontiers Research Topics are very popular trademarks of the *Frontiers journals series*: they are collections of at least ten articles, all centered on a particular subject. With their unique mix of varied contributions from Original Research to Review Articles, Frontiers Research Topics unify the most influential researchers, the latest key findings and historical advances in a hot research area.

Find out more on how to host your own Frontiers Research Topic or contribute to one as an author by contacting the Frontiers editorial office: frontiersin.org/about/contact

Physiological adaptations of insects exposed to different stress conditions, volume II

Topic editors

Bin Tang — Hangzhou Normal University, China

Bimalendu B. Nath — Savitribai Phule Pune University, India

Lisheng Zhang — Institute of Plant Protection, Chinese Academy of Agricultural Sciences, China

Can Li — Guiyang University, China

Citation

Tang, B., Nath, B. B., Zhang, L., Li, C., eds. (2025). *Physiological adaptations of insects exposed to different stress conditions, volume II*. Lausanne: Frontiers Media SA. doi: 10.3389/978-2-8325-6189-8

Table of contents

frontiers | Frontiers in Physiology

TYPE Editorial
PUBLISHED 18 March 2025
DOI 10.3389/fphys.2025.1582575

OPEN ACCESS

EDITED AND REVIEWED BY
Silke Sachse,
Max Planck Institute for Chemical Ecology, Germany

*CORRESPONDENCE
Bimalendu B. Nath,
bbnath@gmail.com

RECEIVED 24 February 2025
ACCEPTED 10 March 2025
PUBLISHED 18 March 2025

CITATION
Nath BB (2025) Editorial: Physiological adaptations of insects exposed to different stress conditions, volume II.
Front. Physiol. 16:1582575.
doi: 10.3389/fphys.2025.1582575

Editorial: Physiological adaptations of insects exposed to different stress conditions, volume II

Bimalendu B. Nath[1,2]*

[1]Stress Biology Research Laboratory, Department of Zoology, Savitribai Phule Pune University, Pune, India, [2]Faculty of Science, MIE-SPPU Institute of Higher Education, Doha, Qatar

KEYWORDS

environmental stress, adaptation, insect, stressors, climate change

Editorial on the Research Topic
Physiological adaptations of insects exposed to different stress conditions, volume II

In the contemporary context of swiftly changing environmental conditions, non-human biota must adapt or risk extinction. Insects represent a significant portion of Earth's biodiversity, with estimates of at least 5.5 million species (Stork, 2018). They are incredibly successful at adapting to extreme conditions. Numerous insect groups exhibit remarkable resilience, successfully evolving in response to varying environmental conditions. In recent years, more studies have gained insight into how insects will adapt to these stress pressures via physiological regulation. Recently, insect populations have faced continual stress from suboptimal temperature fluctuations due to global warming, seasonal shifts, moisture imbalances (such as desiccation), nutritional deficiencies stemming from habitat destruction (including deforestation and wildfires), and exposure to a broad range of xenobiotics (like pesticides and insecticides). Many insects have shown exceptional resilience to these multiple stressors, as evidenced by emerging physiological and genomic data reflecting phenotypic plasticity (Chakraborty et al., 2025; McCulloch and Jonathan, 2023). The ability of insects to adapt to various stressors results from complex physiological, genetic, behavioral, and ecological mechanisms. Ongoing research is essential to further understand these adaptations, especially in the context of rapid environmental changes. The adaptive capabilities of insects make them one of the most suitable animal models for examining survival strategies in response to natural and human-induced environmental selection pressures and their evolutionary processes.

The current Research Topic, titled "Physiological Adaptations of Insects Under Varied Stress Conditions," serves as a continuation of the inaugural Research Topic published in Volume I (Tang et al., 2020). Recognizing an increasing interest among biologists focused on environmental stress responses regarding how insects adapt physiologically to different stressors, backed by significant genomic insights—the decision was made to develop this second volume in the series. We opted to broaden our exploration of various stress factors in the backdrop of ecological and evolutionary perspectives through two reviews and nine original research articles.

Furthermore, this current volume represents an ongoing dialogue surrounding recent developments related to insect stress adaptation amidst diverse ecological challenges. The included reviews and research articles explore various adaptive traits through innovative protocols and emerging technologies aimed at filling existing knowledge gaps.

Under persistent selection pressure from chemical insecticides, insects have acquired resistance across various classes of these chemicals. Typically, the development of insecticide resistance within populations comes with a fitness cost that can influence the rate at which this resistance evolves. These fitness costs compromise biological characteristics such as survival rates, reproductive output, hatching success, and lifespan. This trade-off is viewed as indicative of the evolutionary processes driving insect resistance. Gul et al. extensively surveyed the literature on fitness costs induced by insecticide resistance published in the past decade. The review provides an in-depth analysis of these fitness costs, essential for formulating effective strategies to manage insecticide resistance.

The Manchineel, scientifically known as *Hippomane mancinella*—often called the "Death Apple Tree"—is recognized as one of the most poisonous fruits globally. Despite its toxicity, it is the exclusive host plant for the fruit fly species *A. acris*. García-Saldaña et al. described detoxification strategies employed by *Anastrepha acris* larvae. They identified two primary resistance mechanisms present in both species: a structural mechanism that activates cuticle protein biosynthesis—specifically chitin-binding proteins, which likely diminish permeability to harmful substances within the intestine—and a metabolic mechanism that induces serine protease production and enhances xenobiotic metabolism activation.

In recent years, the excessive use of synthetic insecticides has resulted in developing insect populations resistant to these chemicals. Consequently, an increasing focus is on advancing alternative eco-friendly insecticides that can contribute effectively to pest management strategies. Plumbagin has emerged as a significant compound within agricultural chemistry due to its unique mode of action and remarkable efficacy against a wide range of insects. The research conducted by Sun et al. shed light on the specific insecticidal mechanisms associated with plumbagin, offering important insights into its effectiveness as a natural pesticide.

As a promising and sustainable substitute for conventional pesticides, RNAi-based strategies facilitate the development of more eco-friendly and resilient agricultural practices to manage insect pests (Quilez-Molina et al., 2024). A noteworthy investigation by Yang et al. focused on trehalose, which serves as a key precursor in the chitin synthesis pathway within insects. The enzyme trehalose-6-phosphate synthase (TPS) plays an essential role in this biosynthetic process. Through RNA interference (RNAi), inhibiting TPS expression in *Mythimna separata* led to substantial reductions in both trehalose levels and TPS activity. Their findings suggest that RNAi technology may significantly enhance current approaches for controlling infestations of *M. separata*.

In light of the worldwide challenges posed by insect pests and the detrimental impacts of pesticide application, the sterile insect technique (SIT) was devised as early as the 1930s. This method for pest management is gaining increasing interest globally and applies to both minor and extensive operations. The SIT functions as an autocidal control strategy that necessitates large-scale breeding of specific target insects and sterilization through ionizing radiation, followed by systematic release into designated areas to decrease population numbers over successive generations. The spotted cutworm *Xestia c-nigrum* represents a significant pest in agroforestry across temperate and tropical climates in Asia, Europe, North Africa, and North America. Research conducted by Chu et al. focused on detailed dosimetry related to X-ray exposure and its effects on various biological parameters of this irradiated pest. Their results suggest that X-ray irradiation could effectively manage this versatile agricultural threat.

The melon fly, *Z. cucurbitae*, represents a significant insect pest affecting the Cucurbitaceae family globally, damaging over 130 varieties of vegetables and fruits. Previous discussions have highlighted the potential of radiation-mediated approaches as an alternative method for pest management that poses minimal risk to non-target insect species. In a separate investigation, Ahmad et al. focused on uncovering genes influenced by irradiation in *Zeugodacus cucurbitae* that are linked to critical developmental anomalies through comparative transcriptomics and subsequent targeted gene knockdown techniques. Their results provide strong evidence suggesting that irradiation can effectively identify candidate genes essential for developing future RNA interference (RNAi)-based strategies for pest control.

Light traps have been used to monitor and safeguard crops against insect pests for many years. As a crucial component of integrated pest management strategies, these traps have gained popularity in capturing crop-damaging insects while decreasing reliance on chemical pesticides. Recently, there has been significant interest in light trap technology as an environmentally friendly alternative to synthetic pesticide use. The current research conducted by Jiang et al. examined how factors such as duration of light exposure, gender differences, and circadian rhythms affect the phototactic behaviour of female and male *Dastarcus helophoroides* beetles. By employing various wavelengths of light, Jiang et al. analyzed gene expression patterns among females and males subjected to white light exposure. Findings indicated that the beetles exhibited negative phototaxis when exposed to light, suggesting a potential synergistic molecular network governing their response to illumination during nocturnal activity.

Insects are ectothermic organisms, and similar to other ectotherms, their survival, development, and reproduction can be significantly affected by exposure to temperature extremes. Recent research suggests that the threat posed by climate change to insect populations may be greater than earlier assessments have suggested (Johansson et al., 2020). Numerous insect species utilise phenotypic plasticity and genetic diversity to cope with these temperature fluctuations. Nevertheless, relying solely on these plasticity mechanisms is insufficient for many insect populations to withstand extreme temperatures. Consequently, further investigations using key insect models are essential to understanding how insects adapt to extreme thermal variations. In this series, there is one review on cold tolerance strategy and

cryoprotectants, while there are two research articles covering heat stress and extracellular freezing responses. This study provides a theoretical basis for future research on the overwintering and potential distribution and related prediction of *Megabruchidius dorsalis* adults. In their review, Chen et al. examined the cold tolerance mechanisms of the adult seed beetle *M. dorsalis* alongside the effects of low temperatures on its physiological and biochemical processes. This research establishes a theoretical framework for future investigations into overwintering behaviours and potential distribution patterns of *M. dorsalis* adults.

Many species of insects have developed mechanisms to endure extracellular freezing, yet the fundamental principles underlying their natural freeze tolerance are not fully comprehended. Insects often use either freeze tolerance or freeze avoidance strategies; they maintain liquid bodily fluids while permitting ice formation in the extracellular spaces rather than within cellular interiors. Štětina and Koštál conducted a comparative analysis of mitochondrial structural and functional characteristics between larvae phenotypes that are sensitive to freezing and those that exhibit freeze tolerance in the drosophilid fly, *Chymomyza crostata*. Their research revealed that exposure to extracellular freezing triggered a permeability transition in the inner mitochondrial membrane.

Cyrtorhinus lividipennis (Reuter) is a hemipteran predator that targets the brown planthopper (BPH), *Nilaparvata lugens*, which poses a significant threat to rice crops. The effects of global warming are intensifying thermal stress, adversely affecting both the fitness and predatory abilities of *Cyrtorhinus lividipennis*. Consequently, it is crucial to explore how *C. lividipennis* responds to heat stress by identifying key resistance factors that can enhance its survival rates and improve its hunting efficiency under such conditions. Numerous studies have indicated that sphingolipids play a role in regulating responses to thermal stress. Ceramide-degrading enzymes (CDases) are vital metabolic enzymes involved in ceramide metabolism. Research conducted by Chen et al. identified two homologous CDase genes from genomic and transcriptomic databases related to *C. lividipennis*, uncovering potential regulatory mechanisms at play.

Under natural conditions, environmental stress encompasses a multifaceted array of abiotic and biotic factors, often leading organisms to encounter several stressors simultaneously. Investigating the co-variables that affect an organism's reaction to multiple simultaneous stressors, or their combinations is crucial for understanding its threshold limits and homeostatic plasticity. This significant issue was explored by Bomble and Nath using *Drosophila melanogaster* as their model organism. Notably, all types of stressors triggered a shared oxidative stress response regardless of how they were administered. Their research demonstrated the production of reactive nitrogen species (RNS) alongside reactive oxygen species (ROS), establishing a connection between oxidative stress with desiccation, heat exposure, and starvation in *D. melanogaster* larvae. This study represents the first documentation of RONS (reactive oxygen and nitrogen species) generation following combined abiotic stresses in *D. melanogaster*, offering valuable physiologically relevant insights into these processes.

Conclusion

Insects are vital components of ecosystems, and their resilience and adaptability will have significant implications for biodiversity, ecosystem services, and agricultural practices in a changing world. The stress responses and adaptations of insects in a changing environment are complex and multifaceted. As research in this area continues to evolve, it will be essential to integrate findings across disciplines to develop a comprehensive understanding of how insects will cope with ongoing environmental changes. This knowledge is vital for predicting ecological outcomes and informing conservation and agricultural practices.

Author contributions

BN: Writing–original draft, Writing–review and editing.

Funding

The author(s) declare that no financial support was received for the research and/or publication of this article.

Acknowledgments

We sincerely appreciate the reviewers for dedicating their time and providing insightful scientific feedback on submissions. Our gratitude also extends to the editorial team, whose assistance is greatly valued.

Conflict of interest

The author declares that the research was conducted in the absence of any commercial or financial relationships that could be construed as a potential conflict of interest.

Generative AI statement

The author(s) declare that no Generative AI was used in the creation of this manuscript.

Publisher's note

References

Chakraborty, A., Sgro, C. M., and Mirth, C. K. (2025). Untangling plastic responses to combined thermal and dietary stress in insects. *Curr. Opin. Insect Sci.* 66, 101328. doi:10.1016/j.cois.2024.101328

Johansson, F., Orizaola, G., and Nilsson-Örtman, V. (2020). Temperate insects with narrow seasonal activity periods can be as vulnerable to climate change as tropical insect species. *Sci. Rep.* 10, 8822. doi:10.1038/s41598-020-65608-7

McCulloch, G., and Jonathan, M. (2023). Rapid adaptation in a fast-changing world: emerging insights from insect genomics. *world. Glob. Chang. Biol.* 29:943–954. doi:10.1111/gcb.16512

Quilez-Molina, A. I., Niño Sanchez, J., and Merino, D. (2024). The role of polymers in enabling RNAi-based technology for sustainable pest management. *Nat. Commun.* 15, 9158. doi:10.1038/s41467-024-53468-y

Stork, N. E. (2018). How many species of insects and other terrestrial arthropods are there on Earth? *Annu. Rev. Entomol.* 63, 31–45. doi:10.1146/annurev-ento-020117-043348

Tang, B., Wang, S., Desneux, N., and Biondi, A. (2020). (Lausanne: Frontiers Media SA). doi:10.3389/978-2-88966-224-1*Physiological adaptations of insects exposed to different stress conditions*

frontiers | Frontiers in Physiology

TYPE Review
PUBLISHED 11 January 2023
DOI 10.3389/fphys.2022.1118955

OPEN ACCESS

EDITED BY
Bin Tang,
Hangzhou Normal University, China

REVIEWED BY
Hamzeh Izadi,
Vali-E-Asr University of Rafsanjan, Iran
Zong Shixiang,
Beijing Forestry University, China

*CORRESPONDENCE
Cheng-Xu Wu,
✉ cxwu3@gzu.edu.cn

SPECIALTY SECTION
This article was submitted to Invertebrate Physiology,
a section of the journal
Frontiers in Physiology

RECEIVED 08 December 2022
ACCEPTED 30 December 2022
PUBLISHED 11 January 2023

CITATION
Chen S-Y, Zhao R-N, Li Y, Li H-P, Xie M-H, Liu J-F, Yang M-F and Wu C-X (2023), Cold tolerance strategy and cryoprotectants of *Megabruchidius dorsalis* in different temperature and time stresses.
Front. Physiol. 13:1118955.
doi: 10.3389/fphys.2022.1118955

Cold tolerance strategy and cryoprotectants of *Megabruchidius dorsalis* in different temperature and time stresses

Si-Yu Chen[1], Ru-Na Zhao[2], You Li[3], He-Ping Li[1], Ming-Hui Xie[1], Jian-Feng Liu[2], Mao-Fa Yang[2,4] and Cheng-Xu Wu[1]*

[1]College of Forestry, Guizhou University, Guiyang, Guizhou, China, [2]Guizhou Provincial Key Laboratory for Agricultural Pest Management of the Mountainous Region, Scientific Observing and Experiment Station of Crop Pest Guiyang, Ministry of Agriculture, Institute of Entomology, Guizhou University, Guiyang, China, [3]Fujian Province Key Laboratory of Plant Virology, Fujian Agriculture and Forestry University, Vector-Borne Virus Research Center, Fuzhou, China, [4]College of Tobacco Science, Guizhou University, Guiyang, China

The honey locusts (genus *Gleditsia*) are a genus of high-value trees in Asia. Seed beetle, *Megabruchidius dorsalis* (Fåhraeus) (Col.: Chrysomelidae: Bruchinae), is a *Gleditsia* oligophagous pest that causes severe yield reduction. To understand the cold tolerance of *M. dorsalis* adults, this study investigated its cold tolerance strategy and the influence of low temperatures on its physiology and biochemistry. The low-temperature treatments were divided into three groups: long-term temperature acclimation (Group 1; 15°C, or 20°C, or 25°C, or 28°C [control check, CK] for 10 days), short-term low-temperature exposure (Group 2; 0°C or 4°C for 2 h), and long-term low-temperature induction (Group 3; 0°C or 4°C for 1, 3, or 5 d). The supercooling point (SCP; temperature at which spontaneous nucleation and ice lattice growth begin), freezing point (FP; temperature at which insect fluids freeze), low lethal temperature (LLT; temperature at which all individuals are killed), water, lipid, glycerol, and total sugars contents were measured under different temperature stresses. The results showed that *M. dorsalis* adults were a freeze-avoidant species. The SCP and LLT at 28°C were −10.62°C and −19.48°C, respectively. The SCP and FP of long-term temperature acclimation (15°C, or 20°C, or 25°C) were significantly lower than that of the control group (28°C). The water content of the long-term low temperature induction (0°C) group was significantly lower than that of the control group. The lipid and glycerol content in the acclimated group at 20°C and 25°C were significantly higher than in the control group. *M. dorsalis* adults may maintain their biofluids in a supercooled state *via* cryoprotectant accumulation and cryoprotective dehydration to prevent ice nucleation. This study provides a theoretical basis for future research on overwintering and potential distribution and related prediction of *M. dorsalis* adults.

KEYWORDS

***Megabruchidius dorsalis*, temperature acclimation, supercooling point, freezing point, cold-resistant substances**

1 Introduction

Gleditsia is well known for its significant medicinal uses and biological activity, which is a high-value tree species (Ragab et al., 2021). Its seed can be made into edible "snow lotus seeds" (*Gleditsia* kernels) in China. *Megabruchidius dorsalis* (Fåhraeus) (Col.: Chrysomelidae: Bruchinae) is an oligophagous seed pest, mainly infesting *Gleditsia* Lam. plants (Fabaceae),

overwintering as 4th instar larvae and adults in the pod (Ruta et al., 2017; Pintilioaie et al., 2018), which is distributed in Asia and Europe (György and Tuda, 2020). The female adults of *M. dorsalis* deposit eggs on the pods and the larvae hatch and burrow into the seeds until adult emergence (Shimada et al., 2001). The majority of *Gleditsia* seeds will be bored, causing serious economic losses (Lezhenina and Vasilieva, 2020).

Insects are ectothermic animals. The environmental temperature directly affects their adaptability and physiological processes, meaning that temperature affects their survival and distribution (Leather et al., 1993; Régnière et al., 2012; Jaworski and Hilszczański, 2014). Cold hardiness refers to the ability of insects to cope with long- or short-term exposure to low temperatures (Sinclair et al., 2015). The supercooling point (SCP; the temperature at which spontaneous nucleation and ice lattice growth begin) and freezing point (FP; the temperature at which insect fluids freeze) in insects are key markers of their cold tolerance (Lee, 1989; Vétek et al., 2020). The low lethal temperature (LLT; the temperature at which all individuals are killed) and the LT_{50} (median lethal temperature, expected to kill 50% of a population) can be used to estimate the absolute limit of insect survival at low temperatures (Sinclair et al., 2015). Based on SCPs, the cold tolerance strategies of insects can be divided into three main categories: chill susceptibility (mortality occurs without internal ice formation, LT_{50}>SCP), freeze avoidance (survival without internal ice formation and death with internal ice formation, LT_{50} = SCP) and freeze tolerance (tolerate the formation of ice in their body tissues and fluids, LT_{50} < SCP) (Slabber and Chown, 2004; Bemani et al., 2012; Sinclair et al., 2015). Insects can adjust their SCP to cope with cold stress accompanying latitude increases. For example, Xie et al. (2015) discovered that tropical populations of *Ostrinia furnacalis* had higher SCPs than temperate populations, and warm temperate populations were mainly intermediate between temperate and tropical populations.

Insects adapt to cold temperatures through physiological and biochemical adjustments in the body. When exposed to low temperatures or overwintering, insects may limit their activity and metabolism by regulating lipids and carbohydrate contents (Arrese and Soulages, 2010; Sinclair and Marshall, 2018; Hasanvand et al., 2020). Low molecular weight carbohydrates and polyols are important cryoprotectants (Fuller, 2004). The SCP of *Anoplophora glabripennis* was negatively correlated with the contents of low molecular weight sugars (glucose and mannitol) and glycerol, implying that *A. glabripennis* decreased their SCP and enhanced cold resistance by increasing the concentrations of these compounds in winter (Feng et al., 2016). Cryoprotective dehydration is one of the strategies that insects adapt to cold conditions (Clark et al., 2009; Guillén et al., 2022), namely by reducing water content and increasing biofluid concentrations to enhance their supercooling ability, or reducing damage from freezing of biofluids (Zachariassen, 1985; Zhao et al., 2019; Pei et al., 2020).

Rapid cold hardening (after minutes to about 3 h of exposure to low temperatures) can affect a range of cold hardiness parameters, and cold acclimation (days to weeks) also has a significant effect on cold tolerance (Teets and Denlinger, 2013; Jakobs et al., 2015). According to the beneficial acclimation hypothesis, the association of insect adaptive acclimation with SCP can support the cold limit, which is related to acclimation temperature and exposure time (Hemmati et al., 2014; Noor-Ul-ane and Jung, 2021). The SCP of *Phthorimaea operculella* (Aryal and Jung, 2018) and *Helicopter assulta* (Cha and Lee, 2016) decreased significantly after cold acclimation. Insects exposed to cold acclimation before overwintering in natural circumstances improve their capacity to withstand freezing temperatures (Wu et al., 2016).

Understanding insect cold tolerance and variations in their content of cold tolerance-related substances are critical for determining the occurrence trends, distribution range, and overwintering limits (Prasanna et al., 2018). In China, the damage caused by *M. dorsalis* in Guizhou Province (Guiyang: 106°37′48″E 26°38′N) is more severe than that in Henan Province (Zhengzhou: 113°37′ E, 34°44′ N). Based on this phenomenon and temperature differences between these two provinces (Figure 1), the supercooling point, freezing point, water content, lipid content, glycerol content, and total sugar content of *M. dorsalis* adults were measured under conditions of long-term temperature acclimation (15°C, 20°C, 25°C, 28°C), short-term low-temperature exposure (0°C, 4°C; 2 h), and long-term low-temperature induction (0°C, 4°C; 1, 3, or 5 d), and the low lethal temperature of *M. dorsalis* was also determined at 28°C. These results preliminarily determined the cold tolerance of this insect and provided a theoretical basis for studying the potential distribution and correlation predictions for *M. dorsalis*.

2 Materials and methods

2.1 Insects

Adults of *M. dorsalis* were collected in October 2020 from *Gleditsia sinensis* Lam. in the vicinity of Zhijin County, Guizhou Province, China (106°03″–106°04″E, 26°32″–26°33″ N) and reared on seeds of *G. sinensis* in plastic boxes (225 × 155 × 80 mm) in a rearing incubator (RXZ–380A–LED, Ningbo Jiangnan Instrument Factory, Ningbo, China) at Forest Conservation Laboratory in the College of Forestry, Guizhou University. The incubator was maintained at 28°C ± 1°C and 65 ± 5% relative humidity with a 14:10-h dark:light photoperiod. All tested samples were continuously bred for more than three generations in plastic finishing boxes that were covered with gauze. After adults emerged, the beetles were separated by sex for further testing according to the morphological characteristics described by Li et al. (2012) and fed with fresh cucumber slices *ad libitum* daily.

2.2 Determination of SCP and FP and cold tolerance

We assessed the effects of low temperatures with different temperatures and time stresses on the cold tolerance of *M. dorsalis*. Healthy adults from the same batch (within 72 h) with uniform size were selected for experiments, and the treatments were divided into three groups: long-term temperature acclimation (Group 1), short-term low-temperature exposure (Group 2), and long-term low-temperature induction (Group 3). In Group 1, the adults were reared at 15°C, or 20°C, or 25°C, or 28°C (control check, CK) for 10 days. In Group 2, the adults were exposed to temperatures of 0°C or 4°C for 2 h. In Group 3, the adults were induced at 0°C or 4°C for 1, 3, or 5 d. Control adults were kept at 28°C, and the feeding conditions were unchanged in this group. All tested adults were alive before the experiments. In all treatments, male and female adults were separated

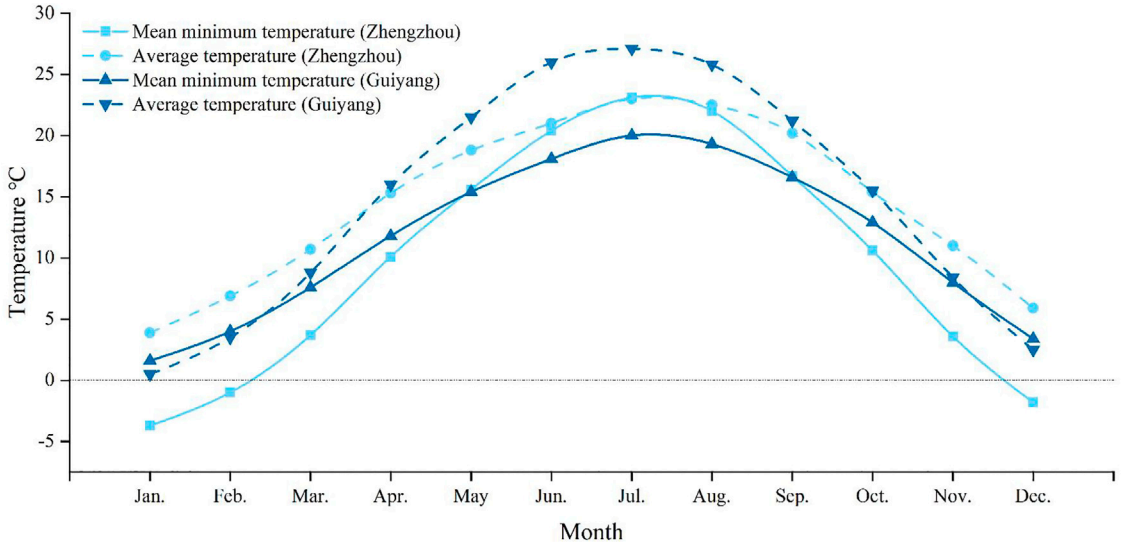

FIGURE 1
The monthly average temperature and monthly mean minimum temperature in Guizhou (Guiyang) and Henan (Zhengzhou) provinces from 1981 to 2010. The data comes from China Meteorological Data Service Centre (http://data.cma.cn/).

and placed on filter paper in Petri dishes (9 cm diameter), and then they were placed in the rearing incubator (Ningbo Jiangnan Instrument Factory, Ningbo, China) or a refrigerator (BCD-576WDPU; Haier, Qingdao, China). The range of temperature fluctuations was ±1°C.

The SCP and FP were measured using the thermocouple method (SUN-V Cold Point For Insect, Peng Cheng Electronic Technology Center of Beijing, China) as described by Sinclair et al. (2015). The abdomens of adults were fixed on a temperature-sensitive probe with transparent tape. The fixed insect bodies and the probe were wrapped with absorbent cotton to prevent rapid cooling of the body and placed together in a low-temperature test box (DW-40L525; Aucama, Qingdao, China) with a constant temperature of -30°C; the temperature was lowered continuously at the rate of 1°C/min. Thirty adults (♀:♂ = 1:1) were measured at each temperature, and data were automatically recorded using the software.

2.3 Low lethal temperature

Healthy adults from the same batch (within 72 h) with uniform size were selected for experiments. Twenty adults (♀:♂ = 1 : 1) were placed on filter paper in Petri dishes (90 mm diameter) and held at lower ranges with seven temperature gradients (−8°C, −10°C, −12°C, −14°C, −16°C, −18°C, or −20°C [resulting in mortality from 0% to 100%]) for 1 hour (DPMS-358, Ningbo Jiangnan Instrument Factory, Ningbo, China). After treatment, *M. dorsalis* adults were placed back in an incubator at normal temperature (25°C) and mortality was evaluated by observing behavioral responses when touched with a small brush (no response considered death). Each treatment was repeated five times. The LLT and LT_{50} were estimated using logistic regression in SAS software (v9.4; SAS Institute, Cary, NC, United States) as described by Sinclair et al. (2015). Logistic regression equation:

$$M(T) = e^{(a+b\times T)} \Big/ \left(1 + e^{(a+b\times T)}\right) \quad (1)$$

T is the temperature of the insect's environment. M(T) is the mortality of insects at temperature T. The a and b are the coefficients of the logistic regression Equation 1. First, the experimental data were inserted into a logistic regression Equation 1 to estimate the parameters a and b, then the known mortality rate was 50% and 100%, and the corresponding temperature was calculated.

2.4 Water and lipid contents

After the same pretreatment as in 2.2, according to the method of Song (2017), 1.5-mL centrifuge tubes were numbered and weighed (W) using an electronic balance (d = 0.0001 g, PR124 ZH/E; Ohouse Instruments [Changzhou] Co., Ltd., Changzhou, China). Four adults (♀:♂ = 1:1) were placed into tubes and their wet weight (fresh weight, FW) was measured. After being placed in an oven (WGL-30B; Taisite, Tianjin, China) at 60°C for 48 h, the dried weight (dry weight, DW) was measured. Five 2-mm grinding beads (bead weight, BW) and 0.2 mL of a 2:1 chloroform–methanol were added into the tube. The insect bodies were crushed using a fully automatic sample freeze-grinding instrument (JXFSTPRP-CL; Jingxin, Shanghai, China), and 0.8 mL of the chloroform–methanol mixture were added. Samples were mixed and centrifuged for 10 min (10000 rpm; Centrifuge 5418 R; Eppendorf, Hamburg, Germany). After removing the supernatant, 1 mL of the chloroform–methonal mixture was added. Centrifuge tubes with residue were placed in an oven (60°C) for 24 h to determine the lean dry weight (LDW). Water content measurements were repeated six times, and lipid content measurements were repeated five times.

$$\text{Water content (\%)} = \left[\frac{[(FW - W) - (DW - W)]}{FW - W}\right] \times 100$$

10.3389/fphys.2022.1118955

$$\text{Lipid content (\%)} = \left[\frac{[(\text{DW} - \text{W}) - (\text{LDW} - \text{W} - \text{BW})]}{\text{DW} - \text{W}}\right] \times 100$$

2.5 Glycerol content

After the same pretreatment as in 2.2, the methods of Song (2017) and Huang (2014) were adopted to make the oxidant, reducing agent (color developer), glycerol standard solution, and standard curve. A 1.5-mL centrifuge tube was weighed (W1) and four treated adults were added and weighed (♀:♂ = 1:1; W2). Five 2-mm grinding beads were added with 200 μL pure water, and the mixture was ground in the tube using a frozen grinding instrument. Then, 1300 μL of pure water were added and mixed thoroughly. Samples were centrifuged (10000 rpm, 10 min) and the supernatant was removed. The oxidation, color development, and optical density (OD) value of the solution were measured, and the corresponding glycerol content was obtained from the standard curve. Measurements were repeated six times per treatment.

$$\text{Glycerol content}\left(\frac{\text{g}}{\text{mg}}\right) = \left[\frac{\left[\text{determination vaules}\left(\frac{\text{g}}{\text{mL}}\right) \times \text{sample dilution (mL)}\right]}{\text{adults weight (W2 - W1) (mg)}}\right]$$

2.6 Total sugar content

After the pretreatment described in 2.1, the total sugar content was measured using a total sugar content assay kit (ZT-2-Y; Suzhou Comin biotechnology Co., Ltd., Suzhou, China) by sampling four adults (♀:♂ = 1 : 1). The adults were weighed with an electronic balance and placed into centrifuge tubes. Then, 0.5 mL of Reagent I and 0.75 mL of distilled water were added, and the mixture was heated in a 95°C water bath for 30 min, before adding 0.5 mL of Reagent II and mixing. The volume was adjusted to 5 mL with distilled water and the tubes were centrifuged (12000 rpm) at 25°C for 10 min. The supernatant was removed, and 40 μL of supernatant was added to 60 μL of reagent III and 40 μL distilled water for determination tubes, and 80 μL of distilled water was added to 60 μL of reagent III as the control tube. Tubes were mixed and heated in a 95°C water bath for 10 min. Then, the final volume was adjusted to 860 μL with distilled water. The absorbance at 540 (A540) nm was then measured using a spectrophotometer (TU-1901; Beijing Persee General Instrument Co., Ltd., China). Measurements were repeated 3–5 times per treatment. The total sugar content was calculated using the following equation:

$$\text{Total sugar content}\left(\frac{\text{mg}}{\text{g}}\right) = \left[\frac{[22.207 \times (\text{determination A} - \text{control A} + 0.0507)]}{\text{fresh weight}}\right]$$

2.7 Statistical analyses

The data were processed using SPSS Statistics 26.0 (IBM Corp., Armonk, NY, United States), and an independent-samples *t*-test or a One-Way ANOVA was used to analyze the data. The Tukey method was used for multiple comparisons, and the Kruskal–Wallis test was used as a non-parametric test for data non-normal distribution or uneven variance. Origin 2018 software (OriginLab Corp., Northampton, MA, United States) was used for mapping. Data are reported as mean ± SE, level of significance in all tests was set at $p < 0.05$. A correlation analysis of trends among mean SCP, temperature,

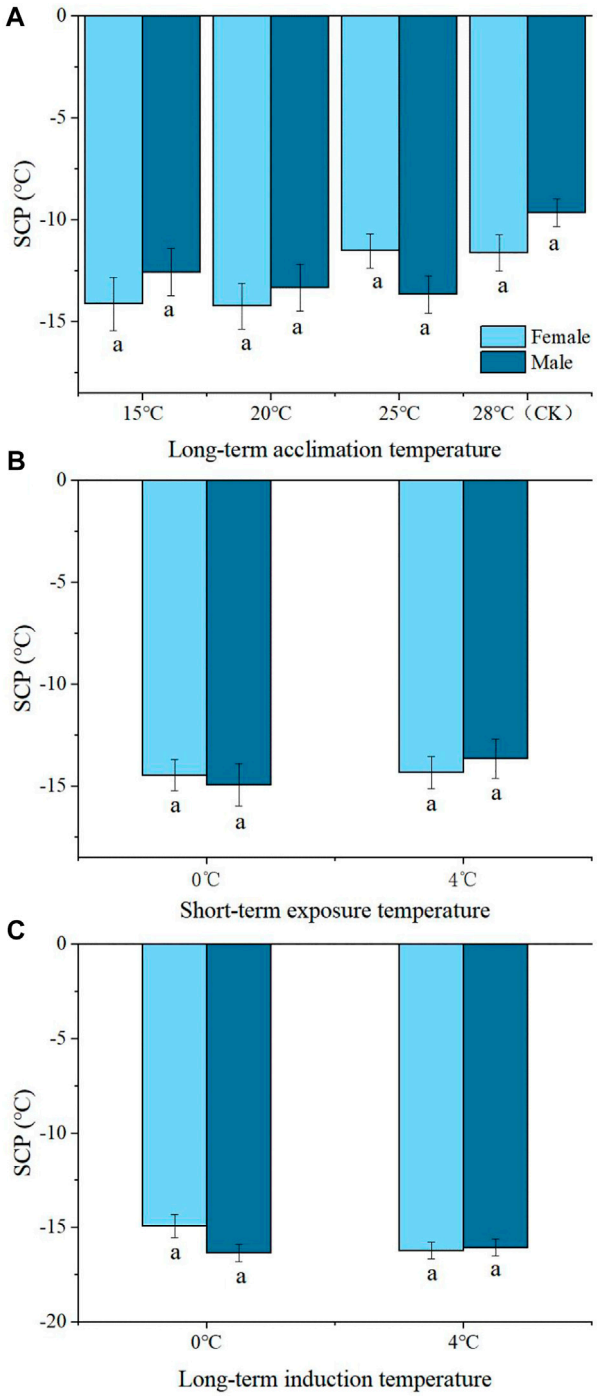

FIGURE 2
The difference of SCP of *Megabruchidius dorsalis* adults under different treatments **(A)**, long-term acclimation temperature; **(B)**, short-term exposure temperature; **(C)**, long-term induction temperature). At the same temperature, the same lowercase letters indicate no significant difference between males and females, the difference between male and female were tested by independent-samples *t*-test ($p < 0.05$).

TABLE 1 Supercooling point and freezing point of female and male adults of *Megabruchidius dorsalis* at different treatments.

Treatments	Times	Temperature (°C)	Gender	SCP (°C)			FP (°C)		
				Mean ± SE	Max	Min	Mean ± SE	Max	Min
CK Control check	<72 h	28	♀+♂	−10.62 ± 0.58	−5.81	−15	−8.66 ± 0.66	−3.15	−12.59
Group 1 long-term temperature acclimation	10 d	15	♀+♂	−13.34 ± 0.86	−5.22	−21.47	−11.39 ± 0.78	−3.95	−18.38
		20	♀+♂	−13.38 ± 0.84	−3.39	−22.14	−11.82 ± 0.77*	−2.17	−18.71
		25	♀+♂	−12.53 ± 0.65	−6.78	−20.82	−10.81 ± 0.64	−4.62	−18.52
Group 2 short-term low temperature exposure	2 h	0	♀+♂	−14.70 ± 0.70*	−6.14	−23.15	−12.74 ± 0.64*	−5.05	−17.86
		4	♀+♂	−14.06 ± 0.56*	−8.7	−18.85	−11.96 ± 0.53*	−6.66	−15.53
Group 3 long-term low temperature induction	1 d	0	♀+♂	−15.51 ± 0.66*	−7.06	−22.04	−13.33 ± 0.58*	−5.26	−18.64
		4	♀+♂	−15.25 ± 0.51*	−8.17	−19.61	−12.96 ± 0.69*	−7.22	−17.31
	3 d	0	♀+♂	−16.32 ± 0.65*	−7.06	−22.04	−14.06 ± 0.49*	−7.19	−19.10
		4	♀+♂	−16.03 ± 0.58*	−9.66	−20.33	−14.18 ± 0.51*	−8.63	−18.74
	5 d	0	♀+♂	−15.09 ± 0.68*	−7.37	−20.47	−12.91 ± 0.58*	−6.95	−17.77
		4	♀+♂	−17.14 ± 0.51*	−9.60	−20.64	−14.41 ± 0.60*	−7.30	−20.56

Note: The asterisk (*) indicated a significant difference between different treatments and control check (Kruskal-wallis test, $p < 0.05$). There are some missing data in Group1, e.g. 20°C: 14 ♀; 25°C: 13 ♀, 12 ♂; 28°C: 10 ♀, 10♂.

water content, lipid content, glycerol content, and total sugar content was performed using the Spearman method (each n = 5).

3 Results

3.1 Supercooling point and freezing point

3.1.1 Sexual differences

There were no significant differences in SCP between male and female adults at 15°C, or 20°C, or 25°C, or 28°C of Group 1 (Figure 2A). Likewise, there was no significant difference in SCP between male and female adults at 0°C or 4°C for 2, or 1, or 3, or 5 d of Group 2 or Group 3. (Figures 2B, C).

3.1.2 Temperature or time difference

The results from the control group (28°C) showed that the SCP was −10.62°C ± 0.63°C and the FP was −8.66°C ± 0.58°C. The SCP of adults acclimated to temperatures from 15°C to 28°C (CK) increased with temperature increases (Table 1). At 20°C, the FP was significantly lower than that at 28°C ($df = 3$, $p = 0.015$) (Table 1). After a short period of exposure to low temperatures, the SCP and FP at 0°C (SCP: $df = 2$, $p = 0.000$; FP: $df = 2$, $p = 0.000$) and 4°C (SCP: $df = 2$, $p = 0.001$, FP: $df = 2$, $p = 0.003$) were significantly lower than those at 28°C (Table 1). The long-term low-temperature induction group SCP and FP at 0°C (SCP: $df = 2$, $p = 0.000$; FP: $df = 2$ $p = 0.000$) and 4°C (SCP: $df = 2$, $p = 0.001$, FP: $df = 2$, $p = 0.003$) were significantly lower than those at 28°C (Table 1).

The results of the long-term low-temperature induction showed that the SCP and FP were significantly lower at 0°C and 4°C than those at 28°C over 1, 3, and 5 d, respectively (0°C: SCP: $df = 3$, $p = 0.000$; FP: $df = 3$, $p = 0.000$; 4°C: SCP: $df = 3$, $p = 0.000$; FP: $df = 3$ $p = 0.000$). However, there were no significant time differences in the SCP and FP of adults induced at 0°C or 4°C for 1, 3, or 5 d, respectively (Table 1).

3.2 Low lethal temperature

The mortality rates of adults in different temperatures could be well-fitted using logistic regression Equation 1. The constant a of Equation 1 was -20.3215 ($\chi^2 = 23.9333$, $p < 0.0001$), and the linear coefficient b was -1.7889 ($\chi^2 = 26.2239$, $p < 0.0001$) (Figure 3). According to the results of the logistic regression, the LLT was estimated to be about -19.48°C and the LT_{50} was about -11.36°C (Figure 3).

3.3 Water and lipid contents

The long-term acclimation showed that the water content of *M. dorsalis* adults at 15°C was significantly higher than that of the 28°C (control group), 20°C, and 25°C ($F = 22.436$, $df = 3$, $p = 0.000$), but other groups showed no significant differences in water content compared with the control group (Figure 4A). The lipid content of adults at 20°C ($F = 16.889$, $df = 3$, $p = 0.004$) and 25°C ($F = 16.889$, $df = 3$, $p = 0.000$) was significantly higher than those of the control group (28°C). There was no significant difference in lipid content between 15°C and 28°C (Figure 4C).

After short-term exposure, the water and lipid content of adults at 0°C were significantly higher than those at 4°C (water content: $df = 2$, $p = 0.011$; lipid content: $F = 4.542$, $df = 2$, $p = 0.028$), but there was no significant difference between 0°C or 4°C and the control group (Figures 4B, D). The water content of adults at 4°C was significantly lower than that of the control group (28°C) ($df = 2$, $p = 0.020$) (Figure 4B). There was no significant difference in lipid content between 0°C and 4°C (Figure 4D).

The body water content of adults induced at 0°C for 1, 3, and 5 d was significantly lower than that of the control group (28°C) ($F = 13.173$, $df = 3$, $p = 0.000$), yet there was no significant difference in body water content between 4 °C and conrol (Figures 5A, B). The lipid content of the adults treated at 0°C for 1 and 3 d was significantly

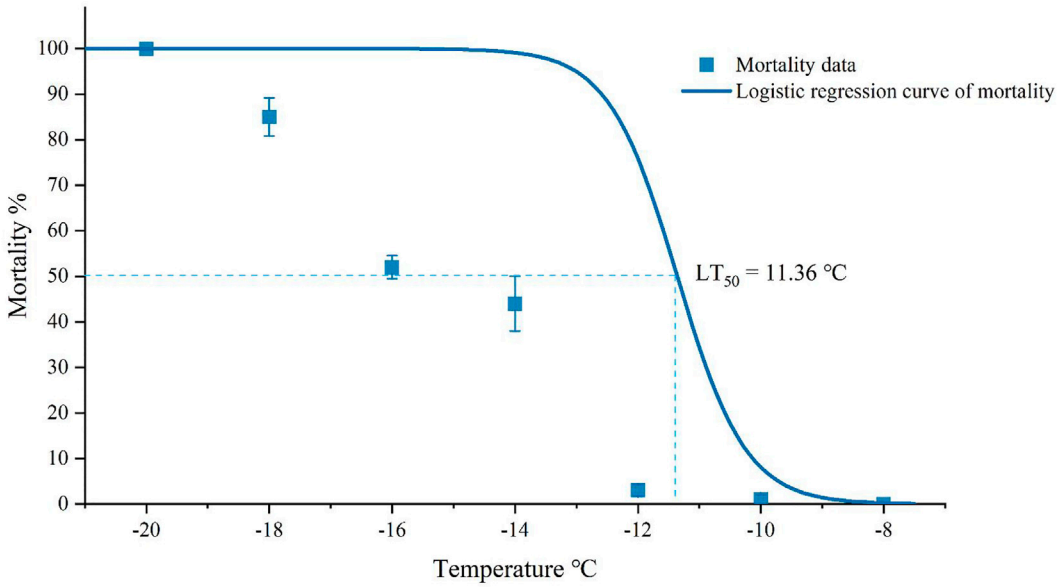

FIGURE 3
Mortality of *Megabruchidius dorsalis* adults after acute (1 hour) low-temperature exposure. The data were Mean ± SE, and lower lethal temperature and LT_{50} were estimated using logistic regression ($p < 0.05$).

higher than that of the control group (1 d: $F = 15.396$, $df = 3$, $p = 0.007$; 3 d: $F = 15.396$, $df = 3$, $p = 0.000$), and that of the adults treated at 0°C for 3 d was significantly higher than that of the adults treated for 5 d ($F = 15.396$, $df = 3$, $p = 0.003$) (Figure 5C). The lipid content in the control group was significantly lower than that in the treatment group at 4°C for 1, 3, and 5 d ($F = 46.432$, $df = 3$, $p = 0.000$), and the lipid content of adults induced at low temperature for 5 d was significantly lower than those induced for 1 d ($F = 46.432$, $df = 3$, $p = 0.000$) and 3 d ($F = 46.432$, $df = 3$, $p = 0.000$) (Figure 5D).

3.4 Glycerol and total sugar contents

After long-term low-temperature acclimation, content of 20°C and 25°C was significantly higher than that of the control group ($F = 26.287$, $df = 3$, $p = 0.000$), but the glycerol content of the adults at 15°C was not significantly different from that of the control group (Figure 4E). At 20°C ($F = 4.027$, $df = 3$, $p = 0.017$), the total sugar content was significantly higher than that of the control group (Figure 4G). At 15°C and at 25°C, there was no significant difference in the values measured in the CK group (Figure 4G).

The contents of glycerol and total sugar at 0°C and 4°C were not significantly different from those of the control group, and there was no significant difference in the contents of glycerol and total sugar between 0°C and 4°C (Figures 4F, H).

The results of the long-term induction showed no significant difference in glycerol content compared to CK after being treated at 0°C or 4°C for 1, 3, or 5 d (Figures 5E, F). The total sugar content in the control group at 4°C was significantly higher than that in the treatment group at 1 d ($F = 11.454$, $df = 3$, $p = 0.002$) and 3 d ($F = 11.454$, $df = 3$, $p = 0.021$) (Figure 5H), yet there was no significant difference in the total sugar content of the adults treated at 0°C for 1, 3, and 5 d (Figure 5G).

3.5 Correlation among the indexes after long-term low temperature acclimation of *M. dorsalis* adults

After long-term low temperature acclimation, there was a significant positive correlation between temperature and SCP, but a significant negative correlation between temperature with water content and total sugar content (Table 2). The SCP exhibited a significant negative correlation with glycerol content and total sugar content, while the glycerol content and total sugar content were both positively correlated with lipid content (Table 2).

4 Discussion

4.1 Supercooling point and low lethal temperature

Supercooling is a significant property related to insect cold tolerance. The lower the SCP or FP, the higher the cold tolerance, and the cold tolerance also partly influences insect distribution (Pei et al., 2020). In general, freeze avoidance is the primary cold tolerance strategy used by insect species in temperate regions of the northern hemisphere (Sinclair and Chown, 2005). The cold tolerance of insects is impacted by both low temperatures and low temperature acclimation time (Salt, 1961). In the present study, there was no significant difference in SCPs between female and male adults of *M. dorsalis* after the three treatments, but the SCP of male *Callosobruchus chinensis* was significantly lower than that of female adults (Song, 2017). Insects can enhance their resistance to cold by either short-term (Chen et al., 1987) or long-term cold exposure (Danks, 1996). Cold acclimation allows insects to withstand cold conditions by lowering

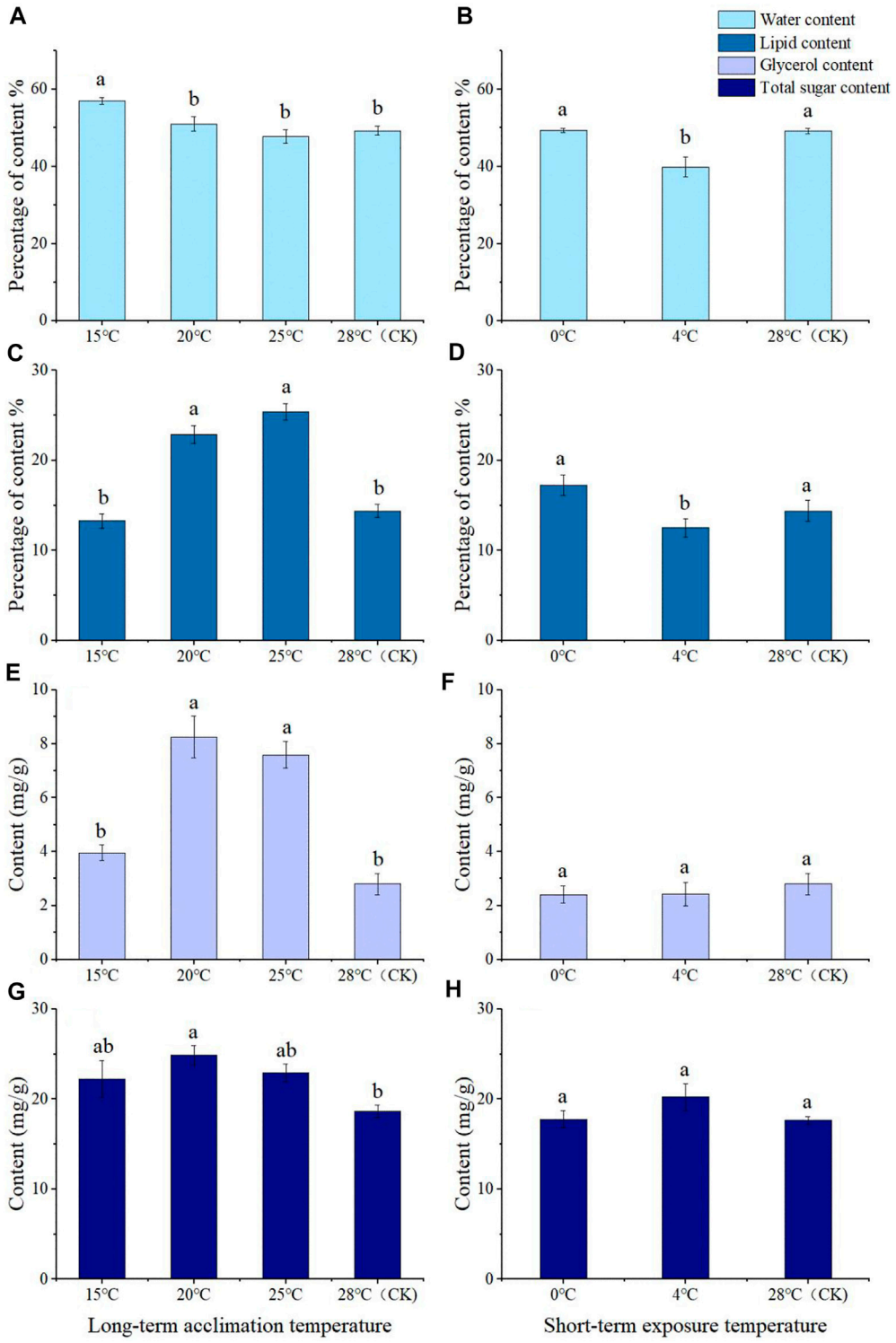

FIGURE 4
Water content **(A,B)**, lipid content **(C,D)**, glycerol content **(E,F)**, and total sugar content **(G,H)** of *Megabruchidius dorsalis* adults after long-term domestication **(A,C,E,G)** or short-term exposure **(B,D,F,H)**. The data were Mean ± SE, and the different lowercase letters indicated a significant difference among temperature treatments under the same physiological indexes (Kruskal–Wallis test, One-Way ANOVA, Tukey, $p < 0.05$).

their SCP (Fuller, 2004; Fujikawa et al., 2018). The SCP and FP of *M. dorsalis* adults acclimated to low temperatures for a long time decreased with decreasing temperature (28°C–15°C), and SCP exhibited a significant positive correlation with temperature. Before overwintering, insects undergo a process of gradual cooling, during which they are physiologically prepared to cope with the cold winter temperatures (Fujikawa et al., 2018). The SCP and FP of *M. dorsalis* adults treated with short-term low-temperature exposure and long-

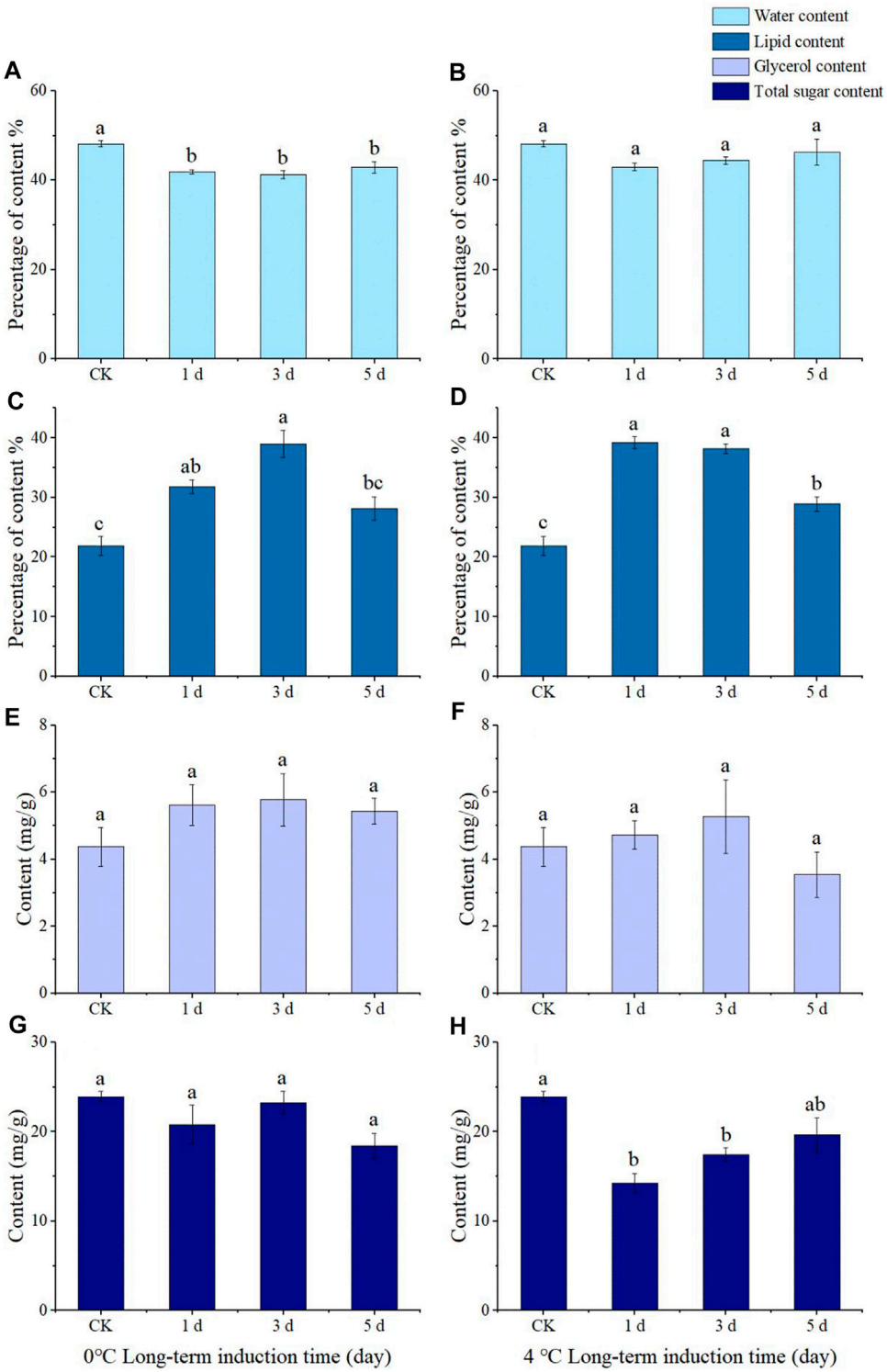

FIGURE 5
Water content **(A,B)**, lipid content **(C,D)**, glycerol content **(E,F)**, and total sugar content **(G,H)** of *Megabruchidius dorsalis* adults induced by long-term low temperature (0°C: A, C, E,G; 4°C: **(B,D,F,H)** for 1, 3, and 5 d.The data were Mean ± SE, and the different lowercase letters indicated a significant difference among time treatments under the same physiological indexes (Kruskal–Wallis test, One-Way ANOVA, Tukey, $p < 0.05$).

term low-temperature induction at 0°C and 4°C were significantly lower than those at 28°C (CK). Both long-term and short-term low-temperature exposure could enhance the cold tolerance of *M. dorsalis* adults, which has similar results in *Sirex noctilio* (Li et al., 2021), *Ips typographus* (Koštál et al., 2011), and *Meligethes aeneus* (Hiiesaar et al., 2011). This suggests that *M. dorsalis* adults, similar to the insects mentioned above, may increase biofluid concentrations to decrease the SCP.

TABLE 2 Spearman correlation coefficient matrix among the indexes after long-term low-temperature acclimation of *Megabruchidius dorsalis* adults.

	Temperature	SCP	Water content	Lipid content	Glycerol content	Total sugar content
Temperature	1					
SCP	0.66**	1				
Water content	−0.733***	−0.388	1			
Lipid content	0.109	−0.385	−0.443	1		
Glycerol content	−0.271	−0.608**	−0.127	0.722***	1	
Total sugar content	−0.473*	−0.552*	0.25	0.564**	0.671**	1

The asterisk (*) indicated a significant correlation among the indexes, * means $p < 0.05$, * * means $p < 0.01$, * * * means $p < 0.001$.

The LT_{50} of *M. dorsalis* in the present study (-11.36°C) was in the range of maximum (-5.8°C) and minimum (-15°C) SCP, and the LLT (-19.48°C) was much lower than the SCP (-10.62°C). The cold tolerance strategy of *M. dorsalis* could be characterized as freeze avoidance from separate measurements of SCP and LLT. Freeze-avoidance species may be susceptible to conditions that promote ice formation (Sinclair et al., 2015). The monthly mean minimum temperature in Zhengzhou in December, January, and February were lower than those in Guiyang, which might be the reason why the damage caused by *M. dorsalis* was more severe in Guizhou than that in Henan province.

4.2 Relationship between cryoprotectants and cold tolerance in *M. dorsalis* adults

Most overwintering insects reduce the damage of biofluids freezing by cryoprotective dehydration, increasing biofluid concentrations, decreasing the SCP, or reducing metabolic activity and energy consumption to increase survival at low temperatures (Koštál et al., 2011; Zhao et al., 2019). The water content of *M. dorsalis* adults at 15°C was significantly higher than that of the control group (at 28°C) under long-term temperature acclimation, which may be caused by differences in *M. dorsalis* behavior (crawling around at 28°C, while crouching at 15°C, personal observation) in this study. The water content was significantly lower than in the control group after short-term cold exposure at 4°C, suggesting that *M. dorsalis* adults might alleviate the damage caused by cold by reducing the water content in their bodies. However, after long-term cold acclimation, the influence of water content on *M. dorsalis* adults' cold tolerance was not significant, similar to results from *Streltzoviella insularis* (Pei et al., 2020).

During overwintering, insects can regulate chemicals related to cold resistance (water, fat, carbohydrates, etc.) in the body through physiological and biochemical reactions and convert chemicals such as sugars into fat (Koštál et al., 2011). This phenomenon may occur before the overwintering onset and during the preparation phase. Fatty compounds can also be hydrolyzed into antifreeze agents such as glycerol to improve cold tolerance, such as in *Dendroctonus armandi* (Wang et al., 2017) and *A. glabripennis* (Feng et al., 2014). After long-term acclimation at 20°C and 25°C, the lipid content of *M. dorsalis* adults was significantly higher than that of the control group, which indicated that *M. dorsalis* adults could tolerate cold conditions by accumulating lipids, similar to the effects of lipid accumulation seen in *A. glabripennis* (Feng et al., 2016). Under the same low-temperature conditions, the lipid content of *M. dorsalis* adults treated for 3 d was significantly higher than those treated for 5 d, indicating that the duration of low-temperature exposure also affected the lipid content.

Glycerol and sugar are important cryoprotectants in insects (Fuller, 2004; Denlinger and Lee, 2010). After acclimation at 20°C, the contents of glycerol and total sugar in *M. dorsalis* adults were significantly higher than those in the control group, and the glycerol content was positively correlated with the lipid and total sugar content, suggesting that the adults resisted cold by accumulating energy and adding antifreeze protectants, which is consistent with the overwintering characteristics of *Pityogenes chalcographus* (Koštál et al., 2014). However, there was no significant difference between the short-term low temperature exposure group and the control group, possibly due to the lack of enough time for glycerol accumulation. After long-term induction at 4°C, the total sugar content of *M. dorsalis* adults treated for 1 d and 3 d was significantly lower than that of the control group. This might reflect the transformation of total sugar in *M. dorsalis* adults into low molecular-weight cryoprotectants, as seen in studies on cold hardiness in *S. insularis* (Qin et al., 2019). In addition, insects regulate cold tolerance by accumulating antifreeze proteins, heat shock proteins, and other proteins related to cold tolerance (Chang et al., 2019).

The cold-resistant strategy of *M. dorsalis* adults is freeze avoidance. The SCP and LLT of *M. dorsalis* adults at 28 °C were -10.62°C and -19.48°C, respectively. The water content of *M. dorsalis* adults after exposure at 4 °C for 2 hours was significantly lower than that of the control group. The contents of glycerol and total sugars in the long-term temperature acclimation group (20 °C) were significantly higher than those in the control group (28 °C). The SCP of *M. dorsalis* adults changed along with environmental temperatures, and the SCP of the long-term acclimation group was positively correlated with environmental temperature, but the SCP was negatively correlated with glycerol content. The glycerol content was significantly positively correlated with the lipid and total sugar content. *M. dorsalis* adults may maintain biofluids in a supercooled state by accumulating cryoprotectants (increasing biofluid concentrations) and cryoprotective dehydration to reduce freezing damage. In this study, the effects of environmental temperature and some metabolic components on the cold resistance of adults of *M. dorsalis* were investigated, but the physiological and molecular mechanisms of the cold hardiness of *M. dorsalis* have not been studied. Future research should focus on the cold tolerance mechanisms of *M. dorsalis*.

Author contributions

All authors listed have made a substantial, direct, and intellectual contribution to the work, and approved it for publication.

Funding

This work was supported by Guizhou Provincial Science and Technology Projects (Qian Ke He Ji Chu-ZK [2022] General 120); Forestry Science and Technology Research Project of Guizhou Province, Grant/Award Numbers [2021] (06); and the Characteristic Forestry Industry Scientific Research Project of Guizhou Province, Grant/Award Numbers: GZMC-ZD20202098. Guizhou province important crop pests natural enemy expansion and application of science and technology innovation personnel team building: Guizhou Kong Science and Technology Cooperation Platform TALENT-CXTD [2021] 004, Construction project of natural enemy expansion breeding room in Guizhou province: Guizhou Development and Reform Investment [2021] 318.

Acknowledgments

We would like to thank Prof. Chen Wenlong of the Institute of Entomology of Guizhou University for his assistance in the use of the supercooling apparatus and Prof. Shi Wangpeng of China Agricultural University for his valuable advice in writing the first draft of this paper.

Conflict of interest

The authors declare that the research was conducted in the absence of any commercial or financial relationships that could be construed as a potential conflict of interest.

Publisher's note

All claims expressed in this article are solely those of the authors and do not necessarily represent those of their affiliated organizations, or those of the publisher, the editors and the reviewers. Any product that may be evaluated in this article, or claim that may be made by its manufacturer, is not guaranteed or endorsed by the publisher.

References

Arrese, E. L., and Soulages, J. L. (2010). Insect fat body: Energy, metabolism, and regulation. *Annu. Rev. Entomol.* 55, 207–225. doi:10.1146/annurev-ento-112408-085356

Aryal, S., and Jung, C. (2018). Cold tolerance characteristics of Korean population of potato tuber moth, *Phthorimaea operculella* (Zeller), (Lepidoptera: Gelechiidae). *Entomol. Res.* 48 (4), 300–307. doi:10.1111/1748-5967.12297

Bemani, M., Izadi, H., Mahdian, K., Khani, A., and Amin, S. M. (2012). Study on the physiology of diapause, cold hardiness and supercooling point of overwintering pupae of the pistachio fruit hull borer, *Arimania comaroffi*. *J. Insect Physiol.* 58 (7), 897–902. doi:10.1016/j.jinsphys.2012.04.003

Cha, W. H., and Lee, D. W. (2016). Identification of rapid cold hardening-related genes in the tobacco budworm, *Helicoverpa assulta*. *J. Asia Pac. Entomol.* 19 (4), 1061–1066. doi:10.1016/j.aspen.2016.09.007

Chang, Y. W., Zhang, X. X., Lu, M. X., Du, Y. Z., and Zhu-Salzman, K. (2019). Molecular cloning and characterization of small heat shock protein genes in the invasive leaf miner fly, liriomyza trifolii. *Genes* 10 (10), 775. doi:10.3390/genes10100775

Chen, C., Denlinger, D. L., and Lee, R. E. (1987). Cold-shock injury and rapid cold hardening in the flesh fly *Sarcophaga crassipalpis*. *Physiol. Zool.* 60, 297–304.

Clark, M. S., Thorne, M. A. S., Purać, J., Burns, G., Hillyard, G., Popović, Ž. D., et al. (2009). Surviving the cold: Molecular analyses of insect cryoprotective dehydration in the Arctic springtail *Megaphorura arctica* (Tullberg). *BMC Genom* 10, 328. doi:10.1186/1471-2164-10-328

Danks, H. V. (1996). The wider integration of studies on insect cold-hardiness. *Eur. J. Entomol.* 93 (3), 383–403.

Denlinger, D. L., and Lee, R. (2010). *Low temperature biology of insects*. Cambridge: Cambridge University Press.

Feng, Y., Xu, L., Li, W., Xu, Z., Cao, M., Wang, J., et al. (2016). Seasonal changes in supercooling capacity and major cryoprotectants of overwintering Asian longhorned beetle (*Anoplophora glabripennis*) larvae. *Agric. For. Entomol.* 18 (3), 302–312. doi:10.1111/afe.12162

Feng, Y., Xu, L., Tian, B., Tao, J., Wang, J., and Zong, S. (2014). Cold hardiness of Asian longhorned beetle (Coleoptera: Cerambycidae) larvae in different populations. *Environ. Entomol.* 43 (5), 1419–1426. doi:10.1603/EN13352

Fujikawa, S., Kuwabara, C., Kasuga, J., and Arakawa, K. (2018). Supercooling-promoting (Anti-ice nucleation) substances. *Adv. Exp. Med. Biol.* 1081, 289–320. doi:10.1007/978-981-13-1244-1_16

Fuller, B. J. (2004). Cryoprotectants: The essential antifreezes to protect life in the frozen state. *Cryo-Letters* 25 (6), 375–388. doi:10.1016/j.cbpb.2004.10.012

Guillén, L., Pascacio-Villafán, C., Osorio-Paz, I., Ortega-Casas, R., Enciso-Ortíz, E., Altúzar-Molina, A., et al. (2022). Coping with global warming: Adult thermal thresholds in four pestiferous *Anastrepha* species determined under experimental laboratory conditions and development/survival times of immatures and adults under natural field conditions. *Front. Physiol.* 13, 991923. doi:10.3389/fphys.2022.991923

György, Z., and Tuda, M. (2020). Host-plant range expansion to *Gymnocladus dioica* by an introduced seed predatory beetle. *Megabruchidius Dorsalis. Entomol. Sci.* 23 (1), 28–32. doi:10.1111/ens.12393

Hasanvand, H., Izadi, H., and Mohammadzadeh, M. (2020). Overwintering physiology and cold tolerance of the sunn pest, *Eurygaster integriceps*, an emphasis on the role of cryoprotectants. *Front. Physiol.* 11 (4), 321. doi:10.3389/fphys.2020.00321

Hemmati, C., Moharramipour, S., and Talebi, A. A. (2014). Effects of cold acclimation, cooling rate and heat stress on cold tolerance of the potato tuber moth *Phthorimaea operculella* (Lepidoptera: Gelechiidae). *Eur. J. Entomology* 111 (4), 487–494. doi:10.14411/eje.2014.063

Hiiesaar, K., Williams, I. H., Mänd, M., Luik, A., Jõgar, K., Metspalu, L., et al. (2011). Supercooling ability and cold hardiness of the pollen beetle *Meligethes aeneus*. *Entomol. Exp. Appl.* 138 (2), 117–127. doi:10.1111/j.1570-7458.2010.01087.x

Huang, N. N. (2014). *Study on tolerance of melon fly,* Bactrocera Cucuribitae *Coquillett to low temperature and its hysiologigal and biochemical mechanisms*. master's thesis (Wu Han: Huazhong Agricultural University).

Jakobs, R., Gariepy, T. D., and Sinclair, B. J. (2015). Adult plasticity of cold tolerance in a continental-temperate population of *Drosophila suzukii*. *J. Insect Physiol.* 79, 1–9. doi:10.1016/j.jinsphys.2015.05.003

Jaworski, T., and Hilszczański, J. (2014). The effect of temperature and humidity changes on insects development their impact on forest ecosystems in the expected climate change. *J. For. Res.* 74 (4), 345–355. doi:10.2478/frp-2013-0033

Koštál, V., Doležal, P., Rozsypal, J., Moravcová, M., Zahradníčková, H., and Šimek, P. (2011). Physiological and biochemical analysis of overwintering and cold tolerance in two Central European populations of the spruce bark beetle, *Ips typographus*. *J. Insect Physiol.* 57 (8), 1136–1146. doi:10.1016/j.jinsphys.2011.03.011

Koštál, V., Miklas, B., Doležal, P., Rozsypal, J., and Zahradníčková, H. (2014). Physiology of cold tolerance in the bark beetle, *Pityogenes chalcographus* and its overwintering in spruce stands. *J. Insect Physiol.* 63 (1), 62–70. doi:10.1016/j.jinsphys.2014.02.007

Leather, S. R., Walters, K. F. A., and Bale, J. S. (1993). *The ecology of insect overwintering*. Cambridge: Cambridge University Press.

Lee, R. E. (1989). Insect cold-hardiness: To freeze or not to freeze. *Bioscience* 39 (5), 308–313. doi:10.2307/1311113

Lezhenina, I. P., and Vasilieva, Y. V. (2020). On the biology of the east Asian seed beetle, *Megabruchidius dorsalis* (Coleoptera, chrysomelidae, bruchinae), an adventive species for Ukraine. *Zoodiversity* 54 (4), 307–316. doi:10.15407/zoo2020.04.307

Li, C., Pei, J., Li, J., Liu, X., Ren, L., and Luo, Y. (2021). Overwintering larval cold tolerance of *sirex noctilio* (Hyme-noptera: Siricidae): Geographic variation in Northeast China. *Insects* 12 (2), 116. doi:10.3390/insects12020116

Noor-Ul-ane, M., and Jung, C. (2021). Characterization of cold tolerance of immature stages of small hive beetle (SHB) *Aethina tumida* murray (coleoptera: Nitidulidae). *Insects* 12 (5), 459. doi:10.3390/insects12050459

Pei, J., Li, C., Ren, L., and Zong, S. (2020). Factors influencing cold hardiness during overwintering of *Streltzoviella insularis* (Lepidoptera: Cossidae). *J. Econ. Entomol.* 113 (3), 1254–1261. doi:10.1093/jee/toaa032

Pintilioaie, A. M., Manci, C. O., Fusu, L., Mitroiu, M. D., and Rădac, A. I. (2018). New invasive bruchine species (Chrysomelidae: Bruchinae) in the fauna of Romania, with a review on their distribution and biology. *Ann. Soc. Entomol. Fr.* 54 (5), 401–409. doi:10.1080/00379271.2018.1506265

Prasanna, B., Huesing, J. E., Eddy, R., and Peschke, V. M. (2018). *A guide for integrated pest management* Fall Armyworm *in Africa*. Available at: https://reliefweb.

int/report/world/fall-armyworm-africa-guide-integrated-pest-management (Accessed February 7, 2018).

Qin, M., Wang, H., Liu, Z., Wang, Y., Zhang, W., and Xu, B. (2019). Changes in cold tolerance during the overwintering period in *Apis mellifera* ligustica. *J. Apic. Res.* 58 (5), 702–709. doi:10.1080/00218839.2019.1634461

Ragab, E. A., Shaheen, U., Bader, A., Elokely, K. M., and Ghoneim, M. M. (2021). Computational study and biological evaluation of isolated saponins from the fruits of *gleditsia aquatica* and *gleditsia caspica*. *Rec. Nat. Prod.* 15 (2), 142–147. doi:10.25135/rnp.202.20.08.1764

Régnière, J., St-Amant, R., and Duval, P. (2012). Predicting insect distributions under climate change from physiological responses: Spruce budworm as an example. *Biol. Invasions* 14 (8), 1571–1586. doi:10.1007/s10530-010-9918-1

Ruta, R., Jaloszynski, P., and Wanat, M. (2017). *Megabruchidius dorsalis* (fåhraeus, 1839) – An invasive seed beetle new to Poland (Coleoptera: Chrysomelidae: Bruchinae). *Entomol. News* 36 (3), 162–166. Available at: https://www.researchgate.net/publication/339900966.

Salt, R. W. (1961). Principles of insect cold-hardiness. *Annu. Rev. Entomol.* 6 (1), 55–74. doi:10.1146/annurev.en.06.010161.000415

Shimada, M., Kurota, H., and Toquenaga, Y. (2001). Regular distribution of larvae and resource monopolization in the seed beetle *Bruchidius dorsalis* infesting seeds of the Japanese honey locust *Gleditsia japonica*. *Popul. Ecol.* 43 (3), 245–252. doi:10.1007/s10144-001-8188-2

Sinclair, B. J., and Chown, S. L. (2005). Climatic variability and hemispheric differences in insect cold tolerance: Support from southern Africa. *Funct. Ecol.* 19 (2), 214–221. doi:10.1111/j.1365-2435.2005.00962.x

Sinclair, B. J., Coello Alvarado, L. E., and Ferguson, L. V. (2015). An invitation to measure insect cold tolerance: Methods, approaches, and workflow. *J. Therm. Biol.* 53, 180–197. doi:10.1016/j.jtherbio.2015.11.003

Sinclair, B. J., and Marshall, K. E. (2018). The many roles of fats in overwintering insects. *J. Exp. Biol.* 221, jeb161836. doi:10.1242/jeb.161836

Slabber, S., and Chown, S. L. (2004). Thermal tolerance and cold hardiness strategy of the sub-Antarctic psocid *Antarctopsocus jeanneli* Badonnel. *Polar Biol.* 28, 56–61. doi:10.1007/s00300-004-0649-6

Song, Y. F. (2017). *Study on tolerance of* Callosobruchus chinensis *(Linnaeus) adults to low temperature and its physiological and biochemical mechanisms*. master's thesis (Chong Qing: Southwest University).

Teets, N., and Denlinger, D. (2013). Physiological mechanisms of seasonal and rapid cold-hardening in insects. *Physiol. Entomol.* 38 (2), 105–116. doi:10.1111/phen.12019

Vétek, G., Fekete, V., Ladányi, M., Cargnus, E., Zandigiacomo, P., Oláh, R., et al. (2020). Cold tolerance strategy and cold hardiness of the invasive zigzag elm sawfly *Aproceros leucopoda* (Hymenoptera: Argidae). *Agric. For. Entomol.* 22 (3), 231–237. doi:10.1111/afe.12376

Wang, J., Gao, G., Zhang, R., Dai, L., and Chen, H. (2017). Metabolism and cold tolerance of Chinese white pine beetle *Dendroctonus armandi* (Coleoptera: Curculionidae: Scolytinae) during the overwintering period. *Agric. For. Entomol.* 19 (1), 10–22. doi:10.1111/afe.12176

Wu, M. J., Xu, Q. Y., Liu, Y., Shi, X. R., Shen, Q. D., Yang, M. M., et al. (2016). The super cooling point change of *Harmonia axyridis* under low temperature stress and its cold-resistance genes' expression analysis. *Zhongguo Nong Ye Ke Xue* 49 (04), 677–685. doi:10.3864/j.issn.0578-1752.2016.04.007

Xie, H. C., Li, D. S., Zhang, H. G., Mason, C. E., Wang, Z. Y., Lu, X., et al. (2015). Seasonal and geographical variation in diapause and cold hardiness of the Asian corn borer, *Ostrinia furnacalis*. *Insect Sci.* 22 (4), 578–586. doi:10.1111/1744-7917.12137

Zachariassen, K. E. (1985). Physiology of cold tolerance in insects. *Physiol. Rev.* 65, 799–832. doi:10.1152/physrev.1985.65.4.799

Zhao, C. C., Yue, L., Wang, Y., Guo, J. Y., and Wan, F. H. (2019). Relationship between copulation and cold hardiness in *Ophraella communa* (Coleoptera: Chrysomelidae). *J. Integr. Agric.* 18 (4), 900–906. doi:10.1016/S2095-3119(19)62591-8

frontiers | Frontiers in Physiology

TYPE Original Research
PUBLISHED 17 January 2023
DOI 10.3389/fphys.2023.1112548

OPEN ACCESS

EDITED BY
Bimalendu B. Nath,
Savitribai Phule Pune University, India

REVIEWED BY
Rita Mukhopadhyaya,
Indian Women Scientist's Association, India
Pawel Marciniak,
Adam Mickiewicz University, Poland

*CORRESPONDENCE
Yanping Luo,
yanpluo2012@hainanu.edu.cn

†These authors have contributed equally to this work

SPECIALTY SECTION
This article was submitted to Invertebrate Physiology, a section of the journal Frontiers in Physiology

RECEIVED 01 December 2022
ACCEPTED 02 January 2023
PUBLISHED 17 January 2023

CITATION
Ahmad S, Jamil M, Jaworski CC and Luo Y (2023), Comparative transcriptomics of the irradiated melon fly (*Zeugodacus cucurbitae*) reveal key developmental genes.
Front. Physiol. 14:1112548.
doi: 10.3389/fphys.2023.1112548

Comparative transcriptomics of the irradiated melon fly (*Zeugodacus cucurbitae*) reveal key developmental genes

Shakil Ahmad[1†], Momana Jamil[1†], Coline C. Jaworski[2,3] and Yanping Luo[1*]

[1]School of Plant Protection, Hainan University, Haikou, Hainan, China, [2]Université Côte d'Azur, INRAE, CNRS, UMR ISA, Nice, France, [3]Beijing Academy of Agriculture and Forestry, Institute of Plant and Environment Protection, Beijing, China

Irradiation can be used as an insect pest management technique to reduce post-harvest yield losses. It causes major physiological changes, impairing insect development and leading to mortality. This technique is used to control the melon fly *Zeugodacus cucurbitae*, a major pest of Cucurbitaceae in Asia. Here, we applied irradiation to melon fly eggs, and the larvae emerged from irradiated eggs were used to conduct comparative transcriptomics and thereby identify key genes involved in the development and survival. We found 561 upregulated and 532 downregulated genes in irradiated flies compared to non-irradiated flies. We also observed abnormal small-body phenotypes in irradiated flies. By screening the 532 downregulated genes, we selected eight candidate genes putatively involved in development based in described functions in public databases and in the literature. We first established the expression profile of each candidate gene. Using RNA interference (RNAi), we individually knocked down each gene in third instar larvae and measured the effects on development. The knockdown of *ImpE2* ecdysone-inducible gene controlling life stage transitions–led to major body size reductions in both pupae and adults. The knockdown of the tyrosine-protein kinase-like tok (Tpk-tok) caused severe body damage to larvae, characterized by swollen and black body parts. Adults subject to knockdown of the eclosion hormone (*Eh_1*) failed to shed their old cuticle which remained attached to their bodies. However, no obvious developmental defects were observed following the knockdown of the heat shock protein 67B1-like (Hsp67), the insulin receptor (*Insr*), the serine/threonine-protein kinase Nek4 (Nek4), the tyrosine-protein kinase transmembrane receptor Ror (*Ror_1*) and the probable insulin-like peptide 1 (*Insp_1*). We argue that irradiation can be successfully used not only as a pest management technique but also for the screening of essential developmental genes in insects *via* comparative transcriptomics. Our results demonstrate that *ImpE2* and *Eh_1* are essential for the development of melon fly and could therefore be promising candidates for the development of RNAi-based pest control strategies.

KEYWORDS

***Zeugodacus cucurbitae*, abiotic stress, insect physiology, gene expression, RNA interference (RNAi), developmental defects**

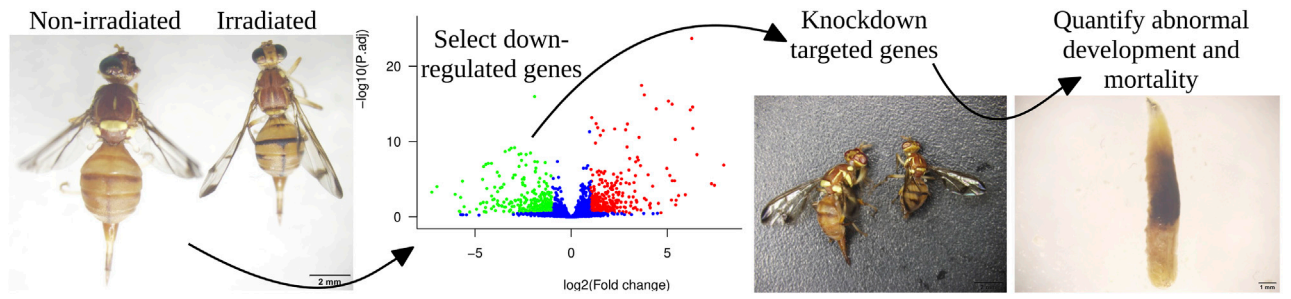

GRAPHICAL ABSTRACT

1 Introduction

Comparative transcriptomics are extremely useful to investigate gene functions even when genomic data are available as a source of bio information. High-throughput sequencing techniques have been widely used to investigate the function of genes linked with insect growth and development. A growing number of developmental transcriptomes have been published, including that of *Bactrocera dorsalis* (Shen et al., 2011; Chen et al., 2018), *Chrysomya megacephala* (Wang et al., 2015), *Trichopria drosophilae* (Zhou et al., 2019), *Cyrtotrachelus buqueti* (Yang et al., 2017), *Dendrolimus punctatus* (Yang et al., 2016), *Bombyx mori* (Ou et al., 2014) and *Phenacoccus solenopsis* (Arya et al., 2018).

The melon fly, *Z. cucurbitae* is a major insect pest of Cucurbitaceae plants worldwide, damaging vegetables and fruits of more than 130 species, including cucumber, pumpkin, watermelon, bitter gourd, tomato and eggplant (Khan et al., 2020). This invasive insect is widely distributed across climatic regions of Central and East Asia (including in China, Pakistan, Bangladesh, India, Nepal, Philippines, and Indonesia) and Oceania (including the Mariana Islands and New Guinea; Dhillon et al., 2005). It has been the target of multiple pest management programmes because of its high reproduction potential, adaptability, and invasion ability (Hoelmer and Daane 2020; Khan et al., 2020; González-Núñez et al., 2021). Insecticides, particularly organophosphates, have been used for decades as the main pest control strategy against the melon fly, despite being moderately effective and harmful to non-target organisms (Desneux et al., 2007).

Irradiation is a potential alternative pest management technique, not harmful to non-target insect species (Ayvaz and Yilmaz, 2015; Cai et al., 2018). Irradiation is used to limit fly growth and reproduction rather than causing severe mortality, because most fresh commodities could not sustain the enormous doses of radiation required to produce 100% acute mortality (Zhang et al., 2015). Nevertheless, insects can develop various physiological and morphological adaptive mechanisms protecting against irradiation (Armisén and Khila 2022). The physiological changes caused by irradiation may be due biochemical and molecular effects of irradiation. For instance, variations in gene and protein expression levels have been observed after irradiation (Marec et al., 2021). The heat shock protein is a possible irradiation marker since it responds to irradiation at high doses (Msaad et al., 2021). Irradiating pupae at a sterilizing dose may affect gene expression in adults (Chang et al., 2015). Such changes in expression levels may disturb pheromone signal processing and central energy generation in *Z. cucurbitae* pupae (Chang et al., 2015).

RNA interference (RNAi) is a reverse-genetic approach used to study insect functional genomics, recently used as a promising tool for gene knockdown in *Z. cucurbitae* (Ahmad et al., 2021b). For instance in *Z. cucurbitae*, the RNAi-mediated suppression of the *ZcVMP26Ab* gene expression resulted in increased desiccation and decreased hatchability of newly laid eggs (Li et al., 2021). Targeting key developmental genes *via* RNAi approaches could cause high levels of developmental defects and mortality in *Z. cucurbitae* (Ahmad et al., 2021b; Jamil et al., 2022). This could lead to potentially less costly and more efficient pest management programs which could be deployed at large scale while being specific and therefore not harmful to non-target insect species. Therefore, it is critical to understand the impacts of irradiation on *Z. cucurbitae* physiology and gene expression levels through a transcriptome analysis for the screening of potential target genes.

Throughout insect development, metamorphoses between life stages, *i.e.*, larva to larva, larva to pupa and pupa to adult, are critical steps. These transitions are initiated and orchestrated by the 20-hydroxyecdysone (20E) (Žitňan et al., 2007), controlling events of apoptosis (type-I programmed-cell death–PCD) and autophagy (type-II PCD), as well as the remodeling of larval tissues and the differentiation of adult tissues from imaginal discs (Yin and Thummel 2005; Ryoo and Baehrecke 2010). The 20E-triggered transcriptional cascade is largely responsible for modulating the metabolic processes through autophagy caspase activity and cell dissociation during the larvae to pupae metamorphosis (Tian et al., 2010; Guo et al., 2012). Another critical step throughout insect development is ecdysis, the periodical shedding of the cuticle. This process is necessary for a marked increase in size, since sclerotized cuticles are virtually inextensible in insects. Cleaning the trachea is one of the most important physiological preparations to ecdysis (Kim et al., 2018).

Signaling pathways of insulin and insulin-like factors (IIS) play a significant role in insect body size regulation (Wu et al., 2016). The insulin receptor (InR) is a transmembrane receptor that activates signal transduction upon insulin binding (Sang et al., 2016). Growth inhibition and malformation were observed in ds*InR*-treated *B. mori* individuals (Zhang et al., 2014).

In the present study, we aim to identify genes impacted by irradiation in *Z. cucurbitae*, and responsible for major developmental defects, using comparative transcriptomics followed by targeted gene knockdown. We knocked down individually eight target genes putatively involved in insect growth, and we investigated the effects of knockdown on *Z. cucurbitae* development. We show that

irradiation can successfully be used to identify candidate genes for the development of future RNAi-based pest management strategies.

2 Materials and methods

2.1 Insect rearing

Z. cucurbitae was reared in 35 cm × 35 cm × 35 cm cages in the insectary of Hainan University [Haikou, Hainan Province, China; temperature: 25°C ± 1°C; humidity: 60% ± 5%; photoperiod (L: D): 14: 10 h] on a 1:3 yeast: sugar diet. Eggs were collected for the experiment by placing cucumber slices in Petri dishes in cages. A Petri dish containing pupae was placed in a new empty cage for adult emergence. Larvae were fed with artificial food following previous studies (Liu et al., 2020; Ahmad et al., 2021b).

2.2 ^{60}Co radiation exposure

25 h old eggs were exposed to ^{60}Co radiation at 50 Gy under free oxygen, at 1.0 Gy/min following previously published studies (Cai et al., 2018; Ahmad et al., 2021a). Experimental replicates were composed of three Petri dishes each containing 100 eggs (diameter of 100 mm; height 15 mm), and three replicates per treatment (irradiated *versus* control) were prepared. To increase hatching and prevent egg desiccation, Petri dishes were covered with a wet filter paper until hatching. Hatched larvae were immediately transferred to the same artificial diet as above. Abnormal phenotypes in irradiated samples were visually observed daily throughout the life cycle from 1st instar to adults. Twenty individuals of 3rd instar from each replicate of both irradiated and non-irradiated groups were frozen with liquid nitrogen and stored at −80°C before RNA extraction for transcriptomic analyses.

2.3 Transcriptome sequencing

1.5 μg of RNA was extracted from each sample. The NEBNext®UltraTM RNA Library Prep Kit for Illumina® (NEB, United States) was used to prepare sequencing libraries. To attribute sequences to samples, unique index codes were added to each sample. Purification of mRNA from total RNA was performed with poly-T oligo-attached magnetic beads. Fragmentation was performed using divalent cations under elevated temperature in NEBNext First Strand Synthesis Reaction Buffer (5X). An M-MuLV reverse transcriptase (RNase H-) primer and random hexamer primer were used to produce first-strand cDNA. DNA polymerase I and RNase H were used to synthesize second-strand cDNA. The remaining overhangs were trimmed into blunt ends using exonuclease/polymerase. To prepare for hybridization, adenylation of the 3′end of DNA fragments was followed by ligation of the hairpin loop structure of NEBNext Adaptor. To select cDNA fragments with a similar length, the library fragments were purified using the AMPure XP system (Beckman Coulter, Beverly, United States) and 3 μl of USER Enzyme (NEB, United States) along with size-selected, adaptor-ligated cDNA at 37°C for 15 min followed by 5 min at 95°C (Utturkar et al., 2015). The PCR was carried out with Phusion High-Fidelity DNA polymerase, Universal DNA polymerase primers, and Index (X) primers. PCR products were purified using the AMPure XP system, and the Agilent Bioanalyzer 2100 was used to verify the quality of the library (Zhang et al., 2015).

We used the HiSeq 4000 PE Cluster Kit (Illumina) to cluster the index-coded samples on the Cluster Generation System following manufacturer instructions. The transcriptome was then sequenced using the Illumina Hiseq 4000 platform to generate 150 bp paired-end reads (Yang et al., 2021). Initial processing of raw fastq data (raw reads) was performed using custom Perl scripts (Ma et al., 2022). Low-quality reads and reads containing adapter and poly-N were first removed from the data. The Q30 and GC content were then calculated in the clean data. We used the clean, high-quality data for all downstream analyses. Reference transcriptomic data for *Z. cucurbitae* (GCF_000806345.2) was downloaded from the NCBI's Sequence Read Archive database. A paired-end alignment of clean reads with the reference was performed using HISAT2 v2.1.0 (Jiang et al., 2022). The number of reads aligned to each reference gene (read depth) was counted using HTSeq v0.11.2. To measure gene expression level, we calculated the FPKM (number of Fragments Per Kilobase of transcript sequence per Millions base pairs sequenced) for each gene using the gene length and its read depth (Nawaz et al., 2018). RNA sequencing raw data has been deposited in the NCBI Sequence Read Archive (SRA; accession number GSE194002).

2.4 Differentially expressed genes (DEGs) and enrichment analysis

We used the DEGseq2 R package version 1.26.0 (Love et al., 2014) to test significant differences in gene expression levels between irradiated replicates and control replicates. The threshold for significantly different expressions was set at $p < .05$, a minimum of 1.5 fold change in expression level ($|\log2 \text{(fold change)}| \geq .58$), and an FPKM >1 in at least one of the six samples (Kumar et al., 2020). Gene expression levels were externally validated by qRT-PCR (Supplemenatry Figure S1). GO (Gene Ontology; http://www.geneontology.org/) significantly enriched pathways were identified using the R package ClusterProfiler with a p-value <.05 (Wu et al., 2021; Chen et al., 2021). KEGG (Kyoto Encyclopedia of Genes and Genomes) significantly enriched pathways were identified using the KEGG Automatic Annotation Server (KAAS, https://www.genome.jp/tools/kaas/) with $p < .05$ (Mao et al., 2005).

2.5 Expression profile and functional characterization of target genes

We observed major developmental defects in irradiated flies, including changes in body size in both pupal and adult flies. Therefore, we focused our mechanistic analysis of irradiation impacts on genes involved in developmental processes. We screened through the significantly downregulated genes in irradiated flies to identify genes previously associated with developmental pathways (GO and KEGG enrichment). Among the most downregulated genes, we selected eight candidates (*Insr*, *Hsp67*, *Tpk-tok*, *Nek4*, *ImpE2*, *Ror_1*, *Eh_1*, and *Insp_1*) for RNAi, based on their previously described role in developmental arrests of many insects species (Vlachou et al., 2006; Ragland et al., 2011; Mizoguchi and Okamoto 2013; Krüger et al., 2015; Lekha et al.,

TABLE 1 Transcriptomic sequencing and assembly quality.

Sample	Raw reads	Clean reads	Q30 (%)	GC content (%)	Total mapped	Mapped ratio (%)
Control1	19084528	18873766	92.16	42.44	16746692	88.73
Control2	20835780	20623263	92.72	42.88	17878306	86.69
Control3	23725619	23434281	92.37	43.23	20338612	86.79
Treatment1	25025265	24790216	92.36	43.46	21359250	86.16
Treatment2	26719132	26403833	92.77	43.58	22778586	86.27
Treatment3	25411483	25117577	92.63	43.23	22010532	87.63

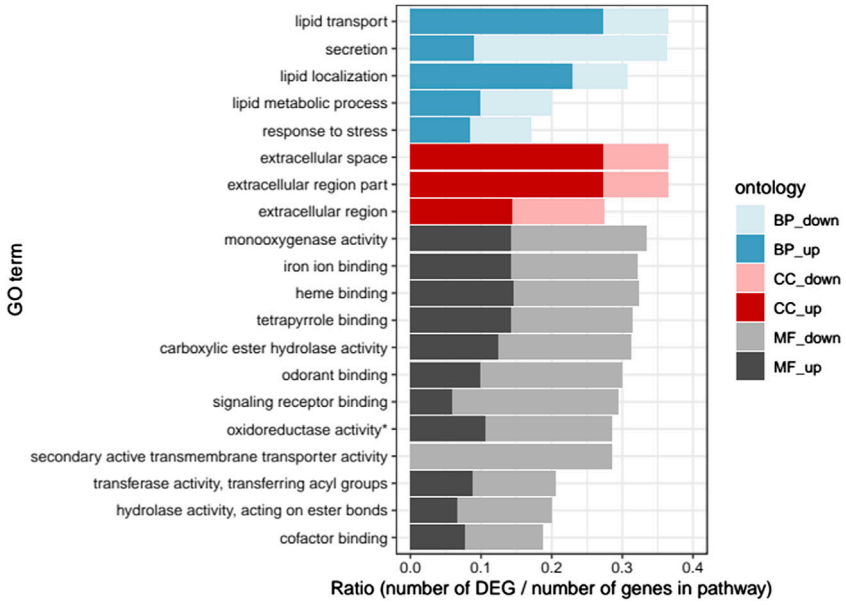

FIGURE 1
Gene ontology enrichment analysis: Ratio of the number of up- and downregulated differentially expressed genes (DEGs) over the total number of genes in each pathway, for the 20 significantly enriched GO pathways ($p < .05$). "BP", biological process; "CC", cellular component; "MF", molecular function; "up", upregulated; "down", downregulated (* oxidoreductase activity acting on paired donors, with incorporation or reduction of molecular oxygen).

2015; Chang et al., 2019; Pérez-Lluch et al., 2020; Saraswathi et al., 2020).

To establish the temporal expression profile of these eight target genes, partial cDNA fragments of each gene were cloned. For this, total RNA was extracted using TRI reagent. The first strand of cDNA was synthesized using the HiScript R III 1st Strand cDNA Synthesis Kit. RNA was extracted from *Z. cucurbitae* flies at each developmental stage (eggs, 1st instar, 2nd instar, 3rd instar, pupae and adults). We analysed amplified products using agarose gel electrophoresis (1.2% agarose gel) and purified them using a Universal DNA Purification kit (Tiangen, China). We then performed RT-qPCR to verify the identity of gene fragments using SYBR R Premix Ex TaqTM II (TliRNaseH Plus) (Takara, Japan) on an ABI 7500 instrument (United States). Three biological replicates of each gene expression were performed using a PCR reaction containing 10 µl SYBER Green mix, 1 µl cDNA, 1 µl forward and reverse primers and 7 µl water (ddH2O). Gene expression levels were normalized using *EFα1* and *Actin* as internal controls (Jamil et al., 2022), and the $2^{-\Delta\Delta CT}$ method was used to calculate the gene relative expression level (Livak and Schmittgen 2001). Similar protocols were used to evaluate gene silencing efficiency.

To assess the function of each target gene in development, we used RNAi to individually knock down each gene and measure the effects on body size, development, and survival of *Z. cucurbitae*. T7 RiboMAXTM Express RNAi System (Promega, United States) was used to synthesize dsRNAs specific to each gene. Each primer used for PCR contained a 5′ T7RNA polymerase binding site (GAATTAATA CGACTCACTATAGGGAGA) followed by the gene-specific sequence. The obtained dsRNA products were purified following the manufacturer's instructions, and the integrity and quantities of all synthesized dsRNAs were determined using 1.2% agarose gel electrophoresis. Purified dsRNAs were diluted in nuclease-free water, and their concentration was measured using the NanoDrop2000 spectrophotometer. The green fluorescent protein (GFP) dsRNA was used as a negative control. Eight groups of 3rd instar larvae of *Z. cucurbitae* were fed with an artificial diet treated

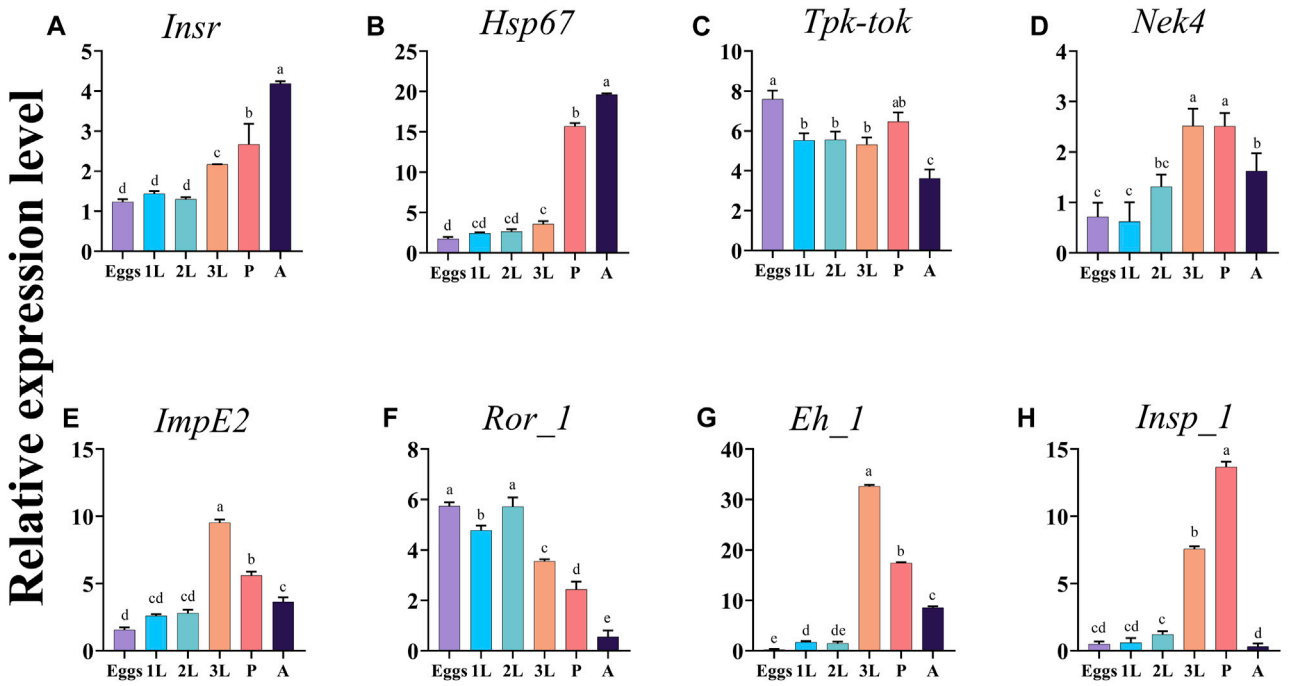

FIGURE 2
Expression profiles of the eight target genes *Insr*, *Hsp67*, *Tpk-tok*, *Nek4*, *ImpE2*, *Ror_1*, *Eh_1*, and *Insp_1* in different developmental stages of *Z. cucurbitae*. Eggs, 1st instar (1L), 2nd instar (2L), 3rd instar (3L), Pupae (P) and Adults (A). Values represent means ± SD. Different letters above the bars indicate significant differences at $p < .05$ (Tukey's tests). *EFα1* and *Actin* were used as internal controls and the $2^{-\Delta\Delta CT}$ method was used to calculate the gene relative expression level.

with each gene-specific dsRNA for 24 h (h) and then shifted to another treated fresh food for another 24 h. The control group was fed with dsGFP-treated food (food treated with RNA silencing the Green Fluorescent Protein, used as a marker). The treated food was obtained by mixing 60 µl of dsRNA (1,000 ng/µl) with 6 g artificial of food. Three biological replicates were performed for each treatment (each of the eight genes) and control group, with 60 larvae in each replicate. Two larvae at 0 h, 12 h, 24 h, and 36 h post-feeding from each replicate were used for RNA extraction to quantify the silencing efficiency. Abnormal Phenotypes and survival ratios of the remaining 52 individuals were observed throughout the developmental stages until adult sexual maturity. All the primers along with gene id of the target genes are presented in Supplemenatry Table S2.

2.5 Statistical analysis

All statistical analyses were performed using R Core Team (2022). Independent linear regressions were performed to measure differences in the expression level of each target gene among life stages. The significance of the life stage fixed effect was tested using a one-way ANOVA, followed by mean comparisons using a Tukey test (function "TukeyHSD", library "stats"; R Core Team, 2022). The effect of gene knockdown on the eight target gene expression levels at different times after feeding compared to control was tested using separate linear regressions for each gene. The treatment (knockdown vs. dsGFP control) in interaction with time after feeding (0, 12, 24 or 36 h) implemented as a factor were used as fixed effects. The significance of the interaction was tested with an ANOVA. This was followed by mean comparisons using the function "emmeans" (library "emmeans"; Lenth, 2022), testing differences in expression levels between control and knockdown treatment for each time.

3 Results

3.1 Quality of the transcriptomic assembly

The transcriptomic sequencing of *Z. cucurbitae* generated 19,084,528, 20,835,780 and 23,725,619 raw reads for the control replicates and 25,025,265, 26,719,132 and 25,411,483 raw reads the for irradiated replicates. After removing low-quality reads, 62,931,310 and 76,311,626 clean reads were generated in total for the control and the irradiated group respectively, and they were mapped to the reference genome. The percentage of total mapped genes ranged from 86% to 89% across replicates, reflecting the high sequencing quality (Table 1). The high-quality score (Q30) was over 92%, the GC content was above 43%, and the mapped ratio exceeded 87%.

3.2 Differentially expressed genes (DEGs)

1,093 genes showed a significant difference in expression levels between irradiated flies and control flies. Among these DEGs, 561 were upregulated and 532 were downregulated in the irradiated group compared to the non-irradiated group (Supplemenatry Figure S2). Gene expression levels were validated using qRT-PCR, and DEG expression levels were not significantly different in the transcriptomic data compared to qRT-PCR data

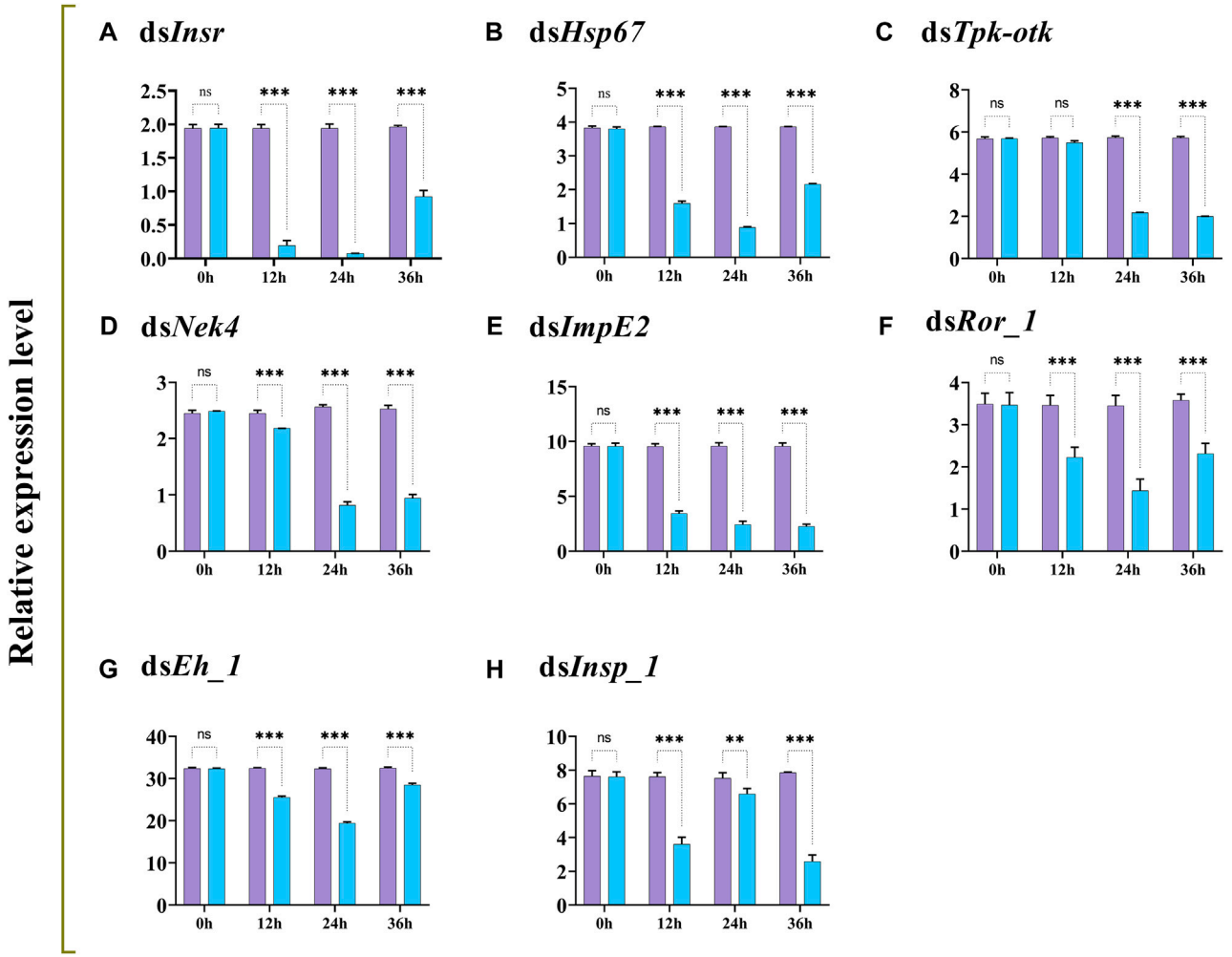

FIGURE 3
Relative expression profiles (mean ± SD; N = 3 replicates per treatment) of *Insr*, *Hsp67*, *Tpk-tok*, *Nek4*, *ImpE2*, *Ror_1*, *Eh_1* and *Insp_1* in *Z. cucurbitae* larvae at different times after feeding on gene-specific dsRNA (treatment; blue) compared to dsGFP (control; purple). *$p < .05$; **$p < .01$; ***$p < .001$; ns, no significant difference. *EFα1* and *Actin* were used as internal controls and the $2^{-\Delta\Delta CT}$ method was used to calculate the gene relative expression level.

(Supplemenatry Figure S1). Among all DEGs, two yolk protein vitellogenin-1 and vitellogenin-1-like were highly upregulated by ~2,900 times and 600 times, respectively. Serine protease persephone-like, ctenidin-3-like, defensin-A-like, glycine-rich RNA-binding protein GRP2A-like and Gram-negative bacteria-binding protein 2-like genes were also amongst the most enriched DEGs in the irradiated group (by > 4,000, >700, >200, >600, and >150 times, respectively). Cell death abnormality protein 1, farnesol dehydrogenase-like, and 20-hydroxyecdysone protein genes were highly downregulated in the irradiated group, with expression levels 150, 65, and 54 times lower, respectively.

Twenty GO terms were found significantly enriched in the DEGs (Figure 1). All pathways except one were enriched with both up- and downregulated DEGs. The most enriched pathways in biological processes were lipid transport and lipid regulation (mostly upregulated DEGs) as well as secretion (mostly downregulated DEGs). In cellular components, the most enriched pathways were extracellular space and extracellular region parts (mostly upregulated DEGs). Finally, in molecular functions, the most enriched pathways were monoxygenase activity and hydrolase activity as well as iron ion, heme, tetrapyrrole, odorant and signalling receptor binding functions, with slightly more down-than upregulated DEGs.

358 KEGG pathways were significantly enriched in irradiated flies, of which 164 were downregulated and 194 were upregulated. Among the 15% most enriched downregulated pathways, we found steroid biosynthesis, protein kinases, metabolism of xenobiotics by Cytochrome P450, exosome, and DNA replication proteins (Supplemenatry Figure S3B), which are pathways associated with developmental defects. Among the 15% most enriched upregulated pathways, we found apoptosis, AMPK signalling pathway, Cytochrome P450, enzymes with EC numbers, peptidases and inhibitors, and protein processing in endoplasmic reticulum (Supplemenatry Figure S3A), which are pathways associated with defence mechanisms.

3.3 Temporal expression of target genes

The expression analysis of the eight target genes *Insr*, *Hsp67*, *Tpk-tok*, *Nek4*, *ImpE2*, *Ror_1*, *Eh_1*, and *Insp_1* showed that their expression pattern varied among almost all developmental stages (Figure 2). *Insr* and *Hsp67* expression levels were the highest in adults, followed by pupae (Figures 2A, B). *Tpk-tok* was highly

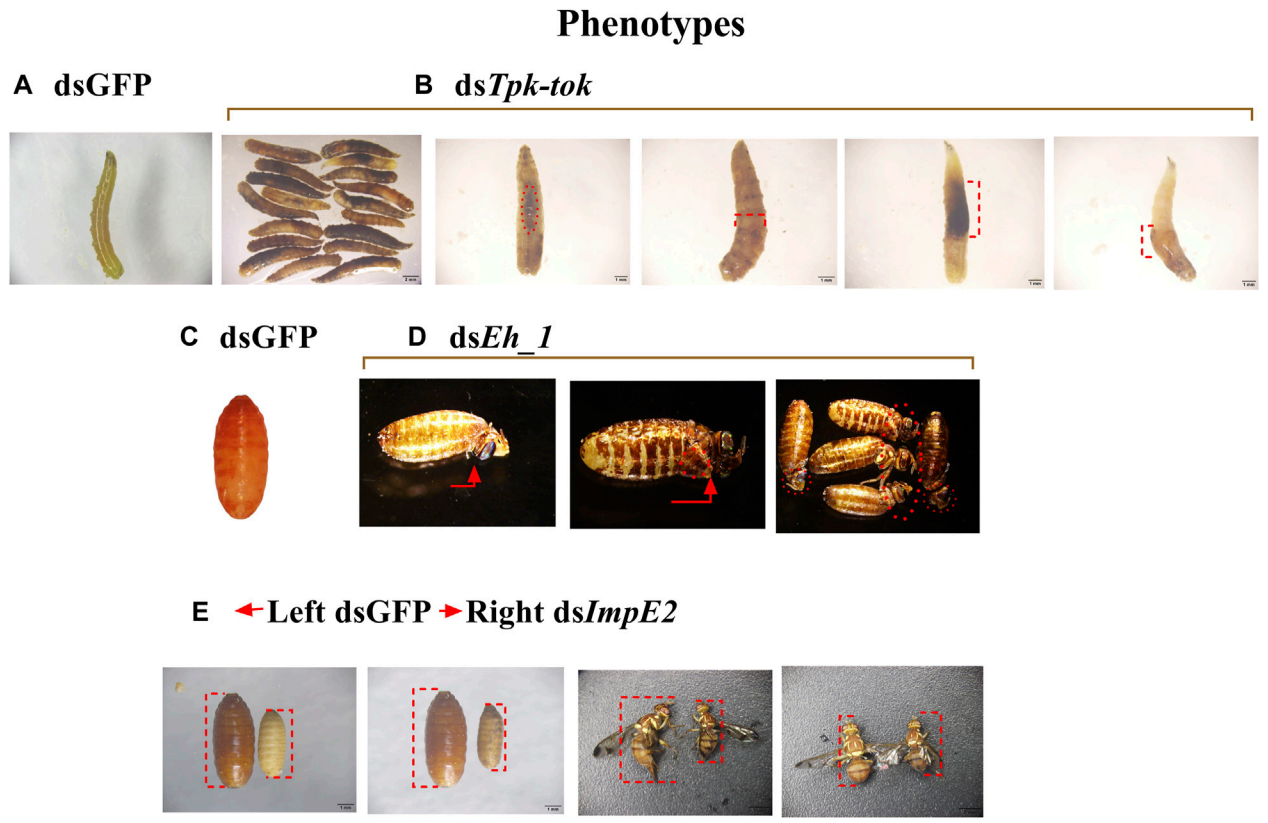

FIGURE 4
Developmental defects observed in *Z. cucurbitae* flies after the knockdown of **(B)** *Tpk-tok*, **(D)** *Eh_1* and **(E)** *ImpE2* genes. **(A)** 3rd instar of *Z. cucurbitae* after feeding on dsGFP-enriched food (control flies). **(C)** Normal pupae from the dsGFP control treatment. Red lines and circles represent the insect body's damage, blockage, and swell portion in **(B)** and reduced body size in **(E)**, while red arrows show the old insect cuticle still attached to their body in **(D)**.

expressed in eggs, then its expression level remained the same in 1st, 2nd, and 3rd instar, then significantly increased in the pupal stage (Figure 2C). The expression levels of *Nek4, Eh_1* and *ImpE2* were highest in the 3rd instar, followed by pupae and adults (Figures 2D, E, G). *Ror_1* was expressed in all the developmental stages, and the highest expression was recorded in eggs and 2nd instar, followed by 1st, 3rd instar and pupae (Figure 2F). The expression level *Insp_1* was highest in 3rd instar followed by pupae and 2nd instar (Figure 2H).

3.4 Effects of dsRNA oral feeding on target genes expression

The transcript levels of *Insr*, *Hsp67*, *Tpk-tok*, *Nek4*, *ImpE2*, *Ror_1*, *Eh_1*, and *Insp_1* were significantly reduced 12–36 h after feeding on dsRNA-enriched food compared to the control group, except *Tpk-tok* which expression level was not significantly reduced before 24 h (Figure 3).

3.5 Genes silencing effects on insect development and survival

Silencing of *Insr*, *Hsp6*, *Nek4*, *Ror_1,* and *Insp_1* did not visibly alter *Z. cucurbitae*'s phenotype at any developmental stage. However, the silencing of *Tpk-tok* caused severe defects in 39.5% of larvae 36 h after feeding compared to the control flies (Figures 4B, 5A). The larval body was distorted in the abdomen section. The middle part of the larvae near the anterior portion became blackish and 60% of the larvae died before pre-pupation stage (Figures 4B, 5A). Few larvae developed into the quiescent stage (about 96 h after ecdysis into final instar) when fed with *Tpk-tok* dsRNA. In contrast, *Eh_1*-silenced flies were able to molt to the pupal stage, and the shedding of the larval cuticle was completed. However, 26% flies fed with ds*Eh_1*-enriched food died at the pupal-adult eclosion stage, when the flies failed to shed their old cuticle and remain attached to their body, showing incomplete ecdysis (Figures 4D, 5A). Also 36.5% of the flies were recorded with the same abnormal phenotypes as when fed with ds*Tpk-tok* (Figures 4D, 5A). Finally, the knockdown of *ImpE2* had no effect on larval growth or survival but significantly reduced the body size in 50.7% of both pupal and adult flies compared to control flies (Figures 4E, 5A). A 12 h delay in adult eclosion was also observed due to *ImpE2* silencing compared to the control.

Knockdown of *Hsp67* decreased the survival of newly emerged adults by 71% compared to control-fed larvae (Figure 5). Similarly, the knockdown of *Ror_1* significantly decreased adult survival by 51% before the treated flies reached the sexual maturity stage. In contrast, the knockdown of *Tpk-tok* caused severe developmental defects in the larval stage compared to dsGFP leading to 57% of larval mortality. Similarly, the knockdown of *Eh_1* caused 26% mortality at the pupal stage (Figure 5).

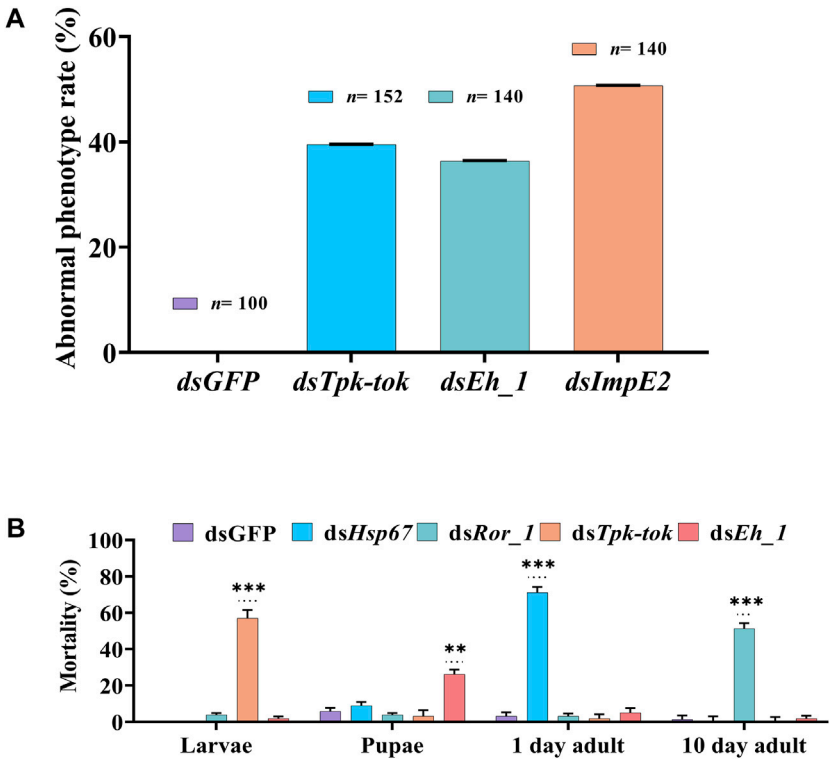

FIGURE 5
Abnormal phenotypes and Mortality observed in different developmental stages of *Z. cucurbitae*. **(A)** Percentage of observed abnormalities after dsRNA delivery of target genes and dsGFP (Control). **(B)** Percentage of insect mortality post feeding dsRNA of target genes compared to the control group. Values represent means % ± SD. Data were analysed using Duncan's test.*$p < .05$; **$p < .01$; ***$p < .001$; ns no statistically significant difference compared to control.

4 Discussion

We identified and characterized the function of key genes involved in the development and survival of *Z. cucurbitae* using ^{60}Co irradiation as a screening tool. We found 1,093 differentially expressed genes (DEGs) in irradiated flies, including 561 upregulated and 532 downregulated genes. Among these, we selected eight DEGs based on their putative function described in the literature (Vlachou et al., 2006; Ragland et al., 2011; Mizoguchi and Okamoto, 2013; Krüger et al., 2015; Lekha et al., 2015; Chang et al., 2019; Pérez-Lluch et al., 2020; Saraswathi et al., 2020), and we knocked down these genes individually to assess their role in the development of *Z. cucurbitae*. Successful knockdown of orally delivered dsRNA for target gene in artificial diet was reported previously in *Z. cucurbitae* (Ahmad et al., 2021b; Jamil et al., 2022). The knockdown of two genes, *ImpE2* and *Tpk-tok*, caused major developmental defects. This study reports key genes involved in the development of melon fly, a highly resistant insect pest and could be used for RNAi based management.

The expression level of the ecdysone receptor (EcR) target gene *ImpE2* was the highest in third instar larvae, followed by pupae and adults. *EcR* is essential for insect molting and metamorphosis (Yin and Thummel 2005; Žitňan et al., 2007; Ryoo and Baehrecke 2010). Due to tissue- and stage-specific mechanisms, *20E* is essential but sufficient for inducing autophagy and apoptosis in larval tissues, primarily through upregulation of several apoptosis and *Atg* genes (Lee et al., 2003; Yin and Thummel 2005; Liu et al., 2013). We observed that the suppression of *20E* through the knockdown of *ImpE2* at the larval stage caused precocious pupation and reduced pupal and adult body size. In insects, the larval stage determines the final body size analogously to the juvenile stage in humans (Edgar 2006; Mirth and Riddiford 2007). In general, insects with reduced body size suffer from either slow larval development or premature pupation, which shortens the larval developmental period (Colombani et al., 2003; Edgar 2006; Mirth and Riddiford 2007). Under *ImpE2* knockdown, we observed that larval body size was not affected but the transition to the pupal stage happened earlier than in control flies, which is a non-feeding stage of the insect. Thus, the smaller body size of flies is likely to be caused by precocious pupation due to the knockdown of *ImpE2*. Precocious or delayed pupation has been observed previously in many insects (Mirth et al., 2005; Layalle et al., 2008).

We found that suppressing *Tpk-tok* transcripts impaired larval development and ultimately caused mortality, highlighting its major role in *Z. cucurbitae* development and survival. Consistent to our findings, a previous study reported the involvement of tyrosine kinase (TK) in the development and survival of *Schistosoma mansoni* (Tavares et al., 2020). This pathway has an essential role in body development: receptor tyrosine kinase (RTK) signalling emerged as a key evolutionary strategy for transmitting extracellular information. Cells use this pathway to transduce extracellular cues, which contributes extensively to developmental processes. Previous studies reported that the ERK signalling pathway contributed to stopping the meiotic metaphase II in insects (Yamamoto et al., 2008), to egg

fertilization (Yamamoto et al., 2013), and to vitellogenesis (Han et al., 2020). However, it is still unclear whether ERK signalling affects insect development or survival, as most of these studies investigated their role at the cellular level only. A knockdown of *Fer*, a TK from FES protein family in *Caenorhabditis elegans* (Nematoda: Rhabditidae), revealed that this protein is important for nematode epidermal differentiation (Putzke et al., 2005).

Similarly to *ImpE2*, the transcript level of *Eh_1* had the highest expression in third instar larvae, followed by pupae and adults and its silencing stopped the pupa to adult transition, when the flies failed to shed their old cuticle which remained attached to their body. We found that *Eh_1* transcripts were detected from egg to adult stage, and the mRNA levels were high in pupae and adults. Comparably, *EH* was found to be expressed in pre-pupae, five-day-old pupae, and early adults in *T. castaneum* (Arakane et al., 2008). The temporal expression indicates that *EH* likely exerts its function in the larvae-pupa-adult transition in *T. castaneum* (Arakane et al., 2008) and *L. decemlineata* (Shen et al., 2021), consistent with our findings in *Z. cucurbitae*. Also consistent with our results, the knockdown of *Eh_1* in the model insects *D. melanogaster* (McNabb et al., 1997; Clark et al., 2004; Krüger et al., 2015; Scott et al., 2020) and *T. castaneum* caused severe impairment in pupation and adult eclosion (Arakane et al., 2008). The ds*EH* delivery in *T. castaneum* through injection disrupted pre-ecdysis and consequently inhibited ecdysis during adult emergence but did not affect the larval-pupal transformation (Arakane et al., 2008). Altogether, these findings provide experimental evidence that the role of *Eh_1* in ecdysis during the pupae-to-adult transition seems conserved across insect species, including *Z. cucurbitae*.

Another gene of the insulin signalling pathway *Ror_1* was expressed in all the developmental stages. The highest expression was recorded in eggs and second instar larvae, followed by first and third instar larvae and pupae. When silencing *Ror_1* in larvae, no effects were observed on larval development, but most of the emerged adults died before reaching the sexual maturity stage. There were no differences in insect survival and development when *Nek4* and *Insp 1* were knockdown compared to non-treated larvae. Their expression was highest in the pupal stage, followed by third instar larvae. These results suggest different roles of each gene of the insulin-signalling pathway in *Z. cucurbitae*. The knockdown of *Insr* had no effects on the development and lifespan of *Z. cucurbitae*. Fontana et al. (2010) found no consensus on the function of *Insr* in insects, but Kenyon (2010) reported that the longevity of honeybee workers increased after silencing the IIS pathway, while it decreased following the suppression of *irs*. Knockdown of *HSP* caused up to 90% mortality in larvae and adults of the emerald ash borer *Agrilus planipennis* (Rodrigues et al., 2018). However, in the current study, the knockdown of *Hsp67* caused significant mortality in one-day-old adults but did not affect their physiology. A variety of proteotoxic tolerances is modulated by heat shock proteins (HSPs), originally identified as stress-responsive proteins (Feder and Hofmann 1999; Sørensen et al., 2003).

We have evidenced target genes involved in the development and survival of the major cucurbitae pest *Z. cucurbitae*. While enhancing the knowledge of the role of these genes in insect development, we suggest that *ImpE2,* involved in body regulation and *Tpk-tok* larval lethal gene could be potential targets for the development of RNAi-based pest control strategies against *Z. cucurbitae*, a major pest of a range of vegetables post-harvest. Such pest management strategies could be more efficient while less harmful to food crops and to non-target insects than chemical methods.

Data availability statement

The datasets presented in this study can be found in online repositories. The names of the repository/repositories and accession number(s) can be found in the article/Supplementary Material.

Author contributions

SA, MJ, and YL initiated the projects and wrote the manuscript. SA and MJ conducted the experiments. CJ and SA performed the analysis and revised the manuscript. All authors contributed to the article and approved the submitted version.

Funding

This research was funded by Hainan Provincial Natural Science Foundation Youth Fund Project (322QN254), Hainan Province Science and Technology Special Fund (ZDKJ2021007 and ZDYF2022XDNY138), NSFC (31860513).

Conflict of interest

The authors declare that the research was conducted in the absence of any commercial or financial relationships that could be construed as a potential conflict of interest.

Publisher's note

Supplementary material

The Supplementary Material for this article can be found online at: https://www.frontiersin.org/articles/10.3389/fphys.2023.1112548/full#supplementary-material

References

Ahmad, S., Hussain, A., Ullah, F., Jamil, M., Ali, A., Ali, S., et al. (2021a). ^{60}Co-γ radiation alters developmental stages of *Zeugodacus cucurbitae* (Diptera: Tephritidae) through apoptosis pathways gene expression. *J. Insect Sci.* 21, 16. doi:10.1093/jisesa/ieab080

Ahmad, S., Jamil, M., Fahim, M., Zhang, S., Ullah, F., Lyu, B., et al. (2021b). RNAi-Mediated Knockdown of Imaginal Disc Growth Factors (IDGFs) genes causes developmental malformation and mortality in melon fly, *Zeugodacus cucurbitae*. *Front. Genet.* 12, 691382. doi:10.3389/fgene.2021.691382

Arakane, Y., Li, B., Muthukrishnan, S., Beeman, R. W., Kramer, K. J., and Park, Y. (2008). Functional analysis of four neuropeptides, EH, ETH, CCAP and bursicon, and their receptors in adult ecdysis behavior of the red flour beetle, *Tribolium castaneum*. *Mech. Dev.* 125, 984–995. doi:10.1016/j.mod.2008.09.002

Armisén, D., and Khila, A. (2022). Genomics of the semi-aquatic bugs (heteroptera; gerromorpha): Recent advances toward establishing a model lineage for the study of phenotypic evolution. *Curr. Opin. Insect Sci.* 50, 100870. doi:10.1016/j.cois.2021.12.010

Arya, S., Dhar, Y., Upadhyay, S., Asif, M., and Verma, P. (2018). De novo characterization of Phenacoccus solenopsis transcriptome and analysis of gene expression profiling during development and hormone biosynthesis. *Sci. Rep.* 8, 7573–7613. doi:10.1038/s41598-018-25845-3

Ayvaz, A., and Yilmaz, S. (2015). "Ionizing radiation disinfestation treatments against pest insects," in *Evolution of ionizing radiation research*. Editor M. Nenoi (Rijeka: IntechOpen). Ch. 10. doi:10.5772/60923

Cai, P., Hong, J., Wang, C., Yang, Y., Yi, C., Chen, J., et al. (2018). Effects of Co-60 radiation on the activities of three main antioxidant enzymes in *Bactrocera dorsalis* (Hendel) (Diptera: Tephritidae). *J. Asia-Pacific Entomology* 21, 345–351. doi:10.1016/j.aspen.2018.01.006

Chang, C., Villalun, M., Geib, S., Goodman, C., Ringbauer, J., and Stanley, D. (2015). Pupal X-ray irradiation influences protein expression in adults of the oriental fruit fly, *Bactrocera dorsalis*. *J. Insect Physiology* 76, 7–16. doi:10.1016/j.jinsphys.2015.03.002

Chang, B. H., Cui, B., Ullah, H., Li, S., Hao, K., Tu, X., et al. (2019). Role of PTP/PTK trans activated insulin-like signalling pathway in regulation of grasshopper (*Oedaleus asiaticus*) development. *Environ. Sci. Pollut. Res.* 26, 8312–8324. doi:10.1007/s11356-019-04212-3

Chen, E., Hou, Q., Dou, W., Wei, D., Yue, Y., Yang, R., et al. (2018). RNA-seq analysis of gene expression changes during pupariation in *Bactrocera dorsalis* (Hendel) (Diptera: Tephritidae). *BMC Genomics* 19, 693–716. doi:10.1186/s12864-018-5077-z

Chen, J., Guo, Y., Huang, S., Zhan, H., Zhang, M., Wang, J., et al. (2021). Integration of transcriptome and proteome reveals molecular mechanisms underlying stress responses of the cutworm, *Spodoptera litura*, exposed to different levels of lead (Pb). *Chemosphere* 283, 131205. doi:10.1016/j.chemosphere.2021.131205

Clark, A., Del Campo, M., and Ewer, J. (2004). Neuroendocrine control of larval ecdysis behavior in *Drosophila*: Complex regulation by partially redundant neuropeptides. *J. Neurosci.* 24, 4283–4292. doi:10.1523/JNEUROSCI.4938-03.2004

Colombani, J., Raisin, S., Pantalacci, S., Radimerski, T., Montagne, J., and Léopold, P. (2003). A nutrient sensor mechanism controls *Drosophila* growth. *Cell.* 114, 739–749. doi:10.1016/s0092-8674(03)00713-x

Desneux, N., Decourtye, A., and Delpuech, J. (2007). The sublethal effects of pesticides on beneficial arthropods. *Annu. Rev. Entomology* 52, 81–106. doi:10.1146/annurev.ento.52.110405.091440

Dhillon, M., Singh, R., Naresh, J., and Sharma, H. (2005). The melon fruit fly, *Bactrocera cucurbitae*: A review of its biology and management. *J. Insect Sci.* 5, 40. doi:10.1093/jis/5.1.40

Edgar, B. (2006). How flies get their size: Genetics meets physiology. *Nat. Rev. Genet.* 7, 907–916. doi:10.1038/nrg1989

Feder, M., and Hofmann, G. (1999). Heat-shock proteins, molecular chaperones, and the stress response: Evolutionary and ecological physiology. *Annu. Rev. physiology* 61, 243–282. doi:10.1146/annurev.physiol.61.1.243

Fontana, L., Partridge, L., and Longo, V. (2010). Extending healthy life span—From yeast to humans. *Science* 328, 321–326. doi:10.1126/science.1172539

González-Núñez, M., Pascual, S., Cobo, A., Seris, E., Cobos, G., Fernández, C., et al. (2021). Copper and kaolin sprays as tools for controlling the olive fruit fly. *Entomol. Gen.* 41, 97–110. doi:10.1127/entomologia/2020/0930

Guo, E., He, Q., Liu, S., Tian, L., Sheng, Z., Peng, Q., et al. (2012). MET is required for the maximal action of 20-hydroxyecdysone during *Bombyx* metamorphosis. *PlosOne* 7, e53256. doi:10.1371/journal.pone.0053256

Han, B., Zhang, T., Feng, Y., Liu, X., Zhang, L., Chen, H., et al. (2020). Two insulin receptors coordinate oogenesis and oviposition via two pathways in the green lacewing, Chrysopa pallens. *J. Insect Physiology* 123, 104049. doi:10.1016/j.jinsphys.2020.104049

Hoelmer, K. A., and Daane, K. M. (2020). Assessment of Asobara japonica as a potential biological control agent for the spotted wing drosophila, *Drosophila suzukii*. *Entomol. Gen.* 41 (1), 1–12. doi:10.1127/entomologia/2020/1100

Jamil, M., Ahmad, S., Ran, Y., Ma, S., Cao, F., Lin, X., et al. (2022). *Argonaute1* and *gawky* are required for the development and reproduction of melon fly, *Zeugodacus cucurbitae*. *Front. Genet.* 13, 880000. doi:10.3389/fgene.2022.880000

Jiang, F., Liang, L., Wang, J., and Zhu, S. (2022). Chromosome-level genome assembly of *Bactrocera dorsalis* reveals its adaptation and invasion mechanisms. *Commun. Biol.* 5, 25–11. doi:10.1038/s42003-021-02966-6

Kenyon, C. (2010). Erratum: The genetics of ageing. *Nature* 467, 622. doi:10.1038/nature09047

Khan, M., Khuhro, N., Awais, M., Memon, R., and Asif, . (2020). Functional response of the pupal parasitoid, Dirhinus giffardii towards two fruit fly species, Bactrocera zonata and B. cucurbitae. *Entomol. Gen.* 27, 87–88. doi:10.2174/092986652702191216112811

Kim, D., Kim, Y., and Adams, M. (2018). Endocrine regulation of airway clearance in *Drosophila*. *Proceeding Natl. Acad. Sci.* 115, 1535–1540. doi:10.1073/pnas.1717257115

Krüger, E., Mena, W., Lahr, E. C., Johnson, E. C., and Ewer, J. (2015). Genetic analysis of Eclosion hormone action during *Drosophila* larval ecdysis. *Development* 142, 4279–4287. doi:10.1242/dev.126995

Kumar, S., Li, G., Yang, J., Huang, X., Ji, Q., Zhou, K., et al. (2020). Investigation of an antioxidative system for salinity tolerance in *Oenanthe javanica*. *Antioxidants* 9, 940. doi:10.3390/antiox9100940

Layalle, S., Arquier, N., and Léopold, P. (2008). The TOR pathway couples nutrition and developmental timing in *Drosophila*. *Dev. Cell.* 15, 568–577. doi:10.1016/j.devcel.2008.08.003

Lee, C., Clough, E., Yellon, P., Teslovich, T., Stephan, D., and Baehrecke, E. (2003). Genome-wide analyses of steroid-and radiation-triggered programmed cell death in *Drosophila*. *Curr. Biol.* 13, 350–357. doi:10.1016/s0960-9822(03)00085-x

Lekha, G., Gupta, T., Awasthi, A. K., Murthy, G. N., Trivedy, K., and Ponnuvel, K. M. (2015). Genome wide microarray based expression profiles associated with *BmNPV* resistance and susceptibility in Indian silkworm races of *Bombyx mori*. *Genomics* 106, 393–403. doi:10.1016/j.ygeno.2015.09.002

Lenth, R. (2022). *emmeans: Estimated marginal means, aka least-squares means*. R package version 1.8.1-1. Available at: https://CRAN.R-project.org/package=emmeans.

Li, W., Song, Y., Xu, H., Wei, D., and Wang, J. (2021). Vitelline membrane protein gene *ZcVMP26Ab* and its role in preventing water loss in *Zeugodacus cucurbitae* (Coquillett) embryos. *Entomol. Gen.* 41, 279–288. doi:10.1127/entomologia/2021/1037

Liu, H., Jia, Q., Tettamanti, G., and Li, S. (2013). Balancing crosstalk between 20-hydroxyecdysone-induced autophagy and caspase activity in the fat body during *Drosophila* larval-prepupal transition. *Insect Biochem. Mol. Biol.* 43, 1068–1078. doi:10.1016/j.ibmb.2013.09.001

Liu, X., Lin, X., Li, J., Li, F., Cao, F., and Yan, R. (2020). A novel solid artificial diet for *Zeugodacus cucurbitae* (Diptera: Tephritidae) larvae with fitness parameters assessed by two-sex life table. *J. insect Sci.* 20, 21. doi:10.1093/jisesa/ieaa058

Livak, K. J., and Schmittgen, T. D. J. M. (2001). Analysis of relative gene expression data using real-time quantitative PCR and the $2^{-\Delta\Delta CT}$ method. *Methods* 25, 402–408. doi:10.1006/meth.2001.1262

Love, M. I., Huber, W., and Anders, S. (2014). Moderated estimation of fold change and dispersion for RNA-Seq data with DESeq2. *Genome Biology* 15. doi:10.1186/s13059-014-0550-8

Ma, Q., Cong, Y., Feng, L., Liu, C., Yang, W., Xin, Y., et al. (2022). Effects of mixed culture fermentation of Bacillus amyloliquefaciens and Trichoderma longibrachiatum on its constituent strains and the biocontrol of tomato Fusarium wilt. *J. Appl. Microbiol.* 132, 532–546. doi:10.1111/jam.15208

Mao, X., Cai, T., Olyarchuk, J., and Wei, L. (2005). Automated genome annotation and pathway identification using the KEGG Orthology (KO) as a controlled vocabulary. *Bioinformatics* 21, 3787–3793. doi:10.1093/bioinformatics/bti430

Marec, F., Bloem, S., and Carpenter, J. (2021). *Inherited sterility in insects, sterile insect technique*. Dordrecht: Springer.

Mcnabb, S., Baker, J., Agapite, J., Steller, H., Riddiford, L., and Truman, J. (1997). Disruption of a behavioral sequence by targeted death of peptidergic neurons in *Drosophila*. *Neuron* 19, 813–823. doi:10.1016/s0896-6273(00)80963-0

Mirth, C., and Riddiford, L. (2007). Size assessment and growth control: How adult size is determined in insects. *BioEssays news Rev. Mol. Cell. Dev. Biol.* 29 (4), 344–355. doi:10.1002/bies.20552

Mirth, C., Truman, J., and Riddiford, L. (2005). The role of the prothoracic gland in determining critical weight for metamorphosis in *Drosophila melanogaster*. *Curr. Biol.* 15, 1796–1807. doi:10.1016/j.cub.2005.09.017

Mizoguchi, A., and Okamoto, N. (2013). Insulin-like and IGF-like peptides in the silkmoth *Bombyx mori*: Discovery, structure, secretion, and function. *Front. Physiol.* 4, 217. doi:10.3389/fphys.2013.00217

Msaad, G., Charaabi, K., Hamden, H., Djobbi, W., Fadhl, S., Mosbah, A., et al. (2021). Probiotic based-diet effect on the immune response and induced stress in irradiated mass reared *Ceratitis capitata* males (Diptera: Tephritidae) destined for the release in the sterile insect technique programs. *PlosOne* 16, e0257097. doi:10.1371/journal.pone.0257097

Nawaz, M., Hafeez, M., Mabubu, J., Dawar, F., Li, X., Khan, M., et al. (2018). Transcriptomic analysis of differentially expressed genes and related pathways in *Harmonia axyridis* after sulfoxaflor exposure. *Int. J. Biol. Macromol.* 119, 157–165. doi:10.1016/j.ijbiomac.2018.07.032

Ou, J., Deng, H., Zheng, S., Huang, L., Feng, Q., and Liu, L. (2014). Transcriptomic analysis of developmental features of *Bombyx mori* wing disc during metamorphosis. *BMC Genomics* 15, 820–915. doi:10.1186/1471-2164-15-820

Pérez-Lluch, S., Klein, C. C., Breschi, A., Ruiz-Romero, M., Abad, A., Palumbo, E., et al. (2020). bsAS, an antisense long non-coding RNA, essential for correct wing development

through regulation of blistered/DSRF isoform usage. *PLoS Genet.* 16, e1009245. doi:10.1371/journal.pgen.1009245

Putzke, A. P., Hikita, S. T., Clegg, D. O., and Rothman, J. H. (2005). Essential kinase-independent role of a Fer-like non-receptor tyrosine kinase in *Caenorhabditis elegans* morphogenesis. *Development* 132, 3185–3195. doi:10.1242/dev.01900

R Core Team (2022). *R: A language and environment for statistical computing*. Vienna, Austria: R Foundation for Statistical Computing. Available at: https://www.R-project.org/.

Ragland, G. J., Egan, S. P., Feder, J. L., Berlocher, S. H., and Hahn, D. A. (2011). Developmental trajectories of gene expression reveal candidates for diapause termination: A key life-history transition in the apple maggot fly *Rhagoletis pomonella*. *J. Exp. Biol.* 214, 3948–3959. doi:10.1242/jeb.061085

Rodrigues, T., Duan, J., Palli, S., and Rieske, L. (2018). Identification of highly effective target genes for RNAi-mediated control of emerald ash borer, *Agrilus planipennis*. *Sci. Rep.* 8, 5020. doi:10.1038/s41598-018-23216-6

Ryoo, H., and Baehrecke, E. (2010). Distinct death mechanisms in *Drosophila* development. *Curr. Opin. Cell. Biol.* 22 (6), 889–895. doi:10.1016/j.ceb.2010.08.022

Sang, M., Li, C., Wu, W., and Li, B. (2016). Identification and evolution of two insulin receptor genes involved in *Tribolium castaneum* development and reproduction. *Gene* 585 (2), 196–204. doi:10.1016/j.gene.2016.02.034

Saraswathi, S., Chaitra, B. S., Tannavi, K., Mamtha, R., Sowrabha, R., Rao, K. V., et al. (2020). Proteome analysis of male accessory gland secretions in *Leucinodes orbonalis* Guenee (Lepidoptera: Crambidae), a *Solanum melongena* L. pest. *Arch. Insect Biochem. Physiol.* 104, e21672. doi:10.1002/arch.21672

Scott, R., Diao, F., Silva, V., Park, S., Luan, H., Ewer, J., et al. (2020). Non-canonical eclosion hormone-expressing cells regulate *Drosophila* ecdysis. *iScience* 23, 101108. doi:10.1016/j.isci.2020.101108

Shen, G., Dou, W., Niu, J., Jiang, H., Yang, W., Jia, F., et al. (2011). Transcriptome analysis of the oriental fruit fly (*Bactrocera dorsalis*). *PlosOne* 6, e29127. doi:10.1371/journal.pone.0029127

Shen, C., Jin, L., Fu, K., Guo, W., and Li, G. (2021). Eclosion hormone functions in larva-pupa-adult ecdysis in *Leptinotarsa decemlineata*. *J. Asia-Pacific Entomology* 24, 141–150. doi:10.1016/j.aspen.2020.12.004

Sørensen, J., Kristensen, T., and Loeschcke, V. (2003). The evolutionary and ecological role of heat shock proteins. *Ecol. Lett.* 6, 1025–1037. doi:10.1046/j.1461-0248.2003.00528.x

Tavares, N. C., Gava, S. G., Torres, G. P., de Paiva, C. Ê. S., Moreira, B. P., Lunkes, F. M. N., et al. (2020). *Schistosoma mansoni* FES tyrosine kinase involvement in the mammalian schistosomiasis outcome and miracidia infection capability in *Biomphalaria glabrata*. *Front. Microbiol.* 11, 963. doi:10.3389/fmicb.2020.00963

Tian, L., Guo, E., Diao, Y., Zhou, S., Peng, Q., Cao, Y., et al. (2010). Genome-wide regulation of innate immunity by juvenile hormone and 20-hydroxyecdysone in the *Bombyx* fat body. *BMC Genomics* 11, 549–612. doi:10.1186/1471-2164-11-549

Utturkar, S., Klingeman, D., Bruno-Barcena, J., Chinn, M., Grunden, A., Köpke, M., et al. (2015). Sequence data for Clostridium autoethanogenum using three generations of sequencing technologies. *Sci. Data* 2, 150014–150019. doi:10.1038/sdata.2015.14

Vlachou, D., Schlegelmilch, T., Runn, E., Mendes, A., and Kafatos, F. C. (2006). The developmental migration of Plasmodium in mosquitoes. *Curr. Opin. Genet. Dev.* 16, 384–391. doi:10.1016/j.gde.2006.06.012

Wang, X., Xiong, M., Lei, C., and Zhu, F. (2015). The developmental transcriptome of the synanthropic fly *Chrysomya megacephala* and insights into olfactory proteins. *BMC Genomics* 16, 1–12. doi:10.1186/s12864-014-1200-y

Wu, Y., Yang, W., Xie, Y., Xu, K., Tian, Y., Yuan, G., et al. (2016). Molecular characterization and functional analysis of Bd*FoxO* gene in the oriental fruit fly, *Bactrocera dorsalis* (Diptera: Tephritidae). *Gene* 578, 219–224. doi:10.1016/j.gene.2015.12.029

Wu, T., Hu, E., Xu, S., Chen, M., Guo, P., Dai, Z., et al. (2021). cluster Profiler 4.0: A Universal Enrichment Tool for Interpreting Omics Data. *The Innovation* 2 (3), 100141. doi:10.1016/j.xinn.2021.100141

Yamamoto, D., Tachibana, K., Sumitani, M., Lee, J., and Hatakeyama, M. (2008). Involvement of Mos-MEK-MAPK pathway in cytostatic factor (CSF) arrest in eggs of the parthenogenetic insect, Athalia rosae. *Mech. Dev.* 125, 996–1008. doi:10.1016/j.mod.2008.08.004

Yamamoto, D., Hatakeyama, M., and Matsuoka, H. (2013). Artificial activation of mature unfertilized eggs in the malaria vector mosquito, *Anopheles stephensi* (Diptera, Culicidae). *J. Exp. Biol.* 216, 2960–2966. doi:10.1242/jeb.084293

Yang, C., Yang, P., Li, J., Yang, F., and Zhang, A. (2016). Transcriptome characterization of *Dendrolimus punctatus* and expression profiles at different developmental stages. *PlosOne* 11, e0161667. doi:10.1371/journal.pone.0161667

Yang, H., Su, T., Yang, W., Yang, C., Lu, L., and Chen, Z. (2017). The developmental transcriptome of the bamboo snout beetle *Cyrtotrachelus buqueti* and insights into candidate pheromone-binding proteins. *PlosOne* 12, e0179807. doi:10.1371/journal.pone.0179807

Yang, C., Meng, J., Yao, M., and Zhang, C. (2021). Transcriptome analysis of *Myzus persicae* to UV-B stress. *J. Insect Sci.* 21, 7. doi:10.1093/jisesa/ieab033

Yin, V. P., and Thummel, C. S. (2005). Mechanisms of steroid-triggered programmed cell death in Drosophila. *Seminars Cell. & Dev. Biol.* 16, 237–243. doi:10.1016/j.semcdb.2004.12.007

Zhang, Z., Teng, X., Chen, M., and Li, F. (2014). Orthologs of human disease associated genes and RNAi analysis of silencing insulin receptor gene in *Bombyx mori*. *Int. J. Mol. Sci.* 15, 18102–18116. doi:10.3390/ijms151018102

Zhang, K., Luo, L., Chen, X., Hu, M., Hu, Q., Gong, L., et al. (2015). Molecular effects of irradiation (Cobalt-60) on the control of *Panonychus citri* (Acari: Tetranychidae). *Int. J. Mol. Sci.* 16, 26964–26977. doi:10.3390/ijms161126004

Zhou, S., Zhou, Y., Wang, Y., Chen, J., Pang, L., Pan, Z., et al. (2019). The developmental transcriptome of *Trichopria drosophilae* (Hymenoptera: Diapriidae) and insights into cuticular protein genes. *Comp. Biochem. Physiol. Part D. Genomics Proteomics* 29, 245–254. doi:10.1016/j.cbd.2018.12.005

Žitňan, D., Kim, Y., Žitňanová, I., Roller, L., and Adams, M. (2007). Complex steroid–peptide–receptor cascade controls insect ecdysis. *General Comp. Endocrinol.* 153, 88–96. doi:10.1016/j.ygcen.2007.04.002

frontiers | Frontiers in Physiology

TYPE Original Research
PUBLISHED 13 February 2023
DOI 10.3389/fphys.2023.1109661

OPEN ACCESS

EDITED BY
Bimalendu B. Nath,
Savitribai Phule Pune University, India

REVIEWED BY
Pin-Jun Wan,
China National Rice Research Institute (CAAS), China
LinQuan Ge,
Yangzhou University, China

*CORRESPONDENCE
Dong Fan,
dnfd@163.com

SPECIALTY SECTION
This article was submitted to Invertebrate Physiology, a section of the journal Frontiers in Physiology

RECEIVED 28 November 2022
ACCEPTED 02 February 2023
PUBLISHED 13 February 2023

CITATION
Yang H-J, Cui M-Y, Zhao X-H, Zhang C-Y, Hu Y-S and Fan D (2023), Trehalose-6-phosphate synthase regulates chitin synthesis in *Mythimna separata*. *Front. Physiol.* 14:1109661. doi: 10.3389/fphys.2023.1109661

Trehalose-6-phosphate synthase regulates chitin synthesis in *Mythimna separata*

Hong-Jia Yang, Meng-Yao Cui, Xiao-Hui Zhao, Chun-Yu Zhang, Yu-Shuo Hu and Dong Fan*

College of Plant Protection, Northeast Agricultural University, Harbin, China

Trehalose is a substrate for the chitin synthesis pathway in insects. Thus, it directly affects chitin synthesis and metabolism. Trehalose-6-phosphate synthase (TPS) is a crucial enzyme in the trehalose synthesis pathway in insects, but its functions in *Mythimna separata* remain unclear. In this study, a *TPS*-encoding sequence in *M. separata* (*MsTPS*) was cloned and characterized. Its expression patterns at different developmental stages and in diverse tissues were investigated. The results indicated that *MsTPS* was expressed at all analyzed developmental stages, with peak expression levels in the pupal stage. Moreover, *MsTPS* was expressed in the foregut, midgut, hindgut, fat body, salivary gland, Malpighian tubules, and integument, with the highest expression levels in the fat body. The inhibition of *MsTPS* expression *via* RNA interference (RNAi) resulted in significant decreases in the trehalose content and TPS activity. It also resulted in significant changes in *Chitin synthase* (*MsCHSA* and *MsCHSB*) expression, and significantly decrease the chitin content in the midgut and integument of *M. separata*. Additionally, the silencing of *MsTPS* was associated with a significant decrease in *M. separata* weight, larval feed intake, and ability to utilize food. It also induced abnormal phenotypic changes and increased the *M. separata* mortality and malformation rates. Hence, *MsTPS* is important for *M. separata* chitin synthesis. The results of this study also suggest RNAi technology may be useful for enhancing the methods used to control *M. separata* infestations.

KEYWORDS

***Mythimna separata*, trehalose-6-phosphate synthase, chitin, trehalose, RNAi**

1 Introduction

Trehalose, which is an important blood sugar in insects, accounts for 80%–90% of the carbohydrate content in the insect hemolymph. It is present in almost all insect tissues and is a crucial source of energy (Hottiger et al., 1987). Trehalose synthesis is an important process affecting insect growth and development, physiological homeostasis, ovum formation, and energy metabolism (Santos et al., 2012). In insects, trehalose is synthesized mainly through the TPS/TPP pathway. Specifically, trehalose-6-phosphate is a product of a reaction between uridine diphosphate glucose and glucose-6-phosphate catalyzed by trehalose-6-phosphate synthase (TPS). Trehalose-6-phosphate phosphatase (TPP) then converts trehalose-6-phosphate to trehalose (Giaever et al., 1988; Strom and Kaasen, 1993; Shukla et al., 2015; Yang et al., 2017). Previous studies revealed that trehalose is synthesized in the fat body of insects (Shukla et al., 2015; Yang et al., 2017). Subsequent research confirmed that *TPS* genes are highly expressed in insect fat body (Chen et al., 2020). TPS is a key enzyme in the trehalose synthesis pathway in insects. Although TPP has been detected in some insects,

most insects contain only TPS (Tang et al., 2014). To date, the *TPS* sequences in more than 50 insect species have been cloned (Tang et al., 2018). Among insects, *Drosophila melanogaster* was the first to have its *TPS* gene cloned (Chen et al., 2002), after which the *TPS* genes of *Locusta migratoria* (Cui and Xia, 2009), *Leptinotarsa decemlineata* (Shi et al., 2016), *Diaphorina citri* (Song et al., 2021) and other insects were cloned. These genes encode proteins comprising approximately 800 amino acids, with two highly conserved TPS and TPP domains.

The synthesis, transformation, and modification of chitin are critical for insect growth and development. Trehalose is considered to be the main substrate for chitin synthesis (Shi et al., 2016; Xiong et al., 2016). The silencing of *TPS* genes in insects can affect the trehalose and chitin contents, while also leading to abnormal molting, growth, and development, and may even lead to death. In an earlier study, after *TcTPS* expression was inhibited in *Tribolium castaneum*, the *CHS1* expression level increased significantly at 72 h, whereas the *CHS2* expression level decreased significantly at 48 and 72 h. Moreover, some of the tested insects were unable to pupate normally and their chitin content decreased (Chen et al., 2018). Another study demonstrated that the inhibition of *SeTPS* expression in *Spodoptera exigua* leads to a decrease in the trehalose content as well as mortality rates of 50.94% and 66.76% at 48 and 204 h, respectively (Tang et al., 2010). The injection of *Bactrocera minax* larvae with dsRNA to silence *BmTPS* expression reportedly significantly decreases the TPS activity, trehalose content, and the expression of three key genes in the chitin biosynthesis pathway, ultimately resulting in an abnormal phenotype and a mortality rate of 52% (Xiong et al., 2016).

Mythimna separata (Lepidoptera: Noctuidae) is a polyphagous insect that mainly infests corn, wheat, rice, sorghum, and other food crops. It is distributed worldwide (Zhang et al., 2018). At sufficiently high densities, *M. separata* can seriously decrease agricultural production. In this study, we identified a *TPS* cDNA sequence in the *M. separata* transcriptome database. The spatiotemporal expression pattern of *MsTPS* was analyzed. Furthermore, *MsTPS* was functionally characterized on the basis of RNA interference (RNAi) experiments. The results of this study may be useful for developing new methods for controlling *M. separata*.

2 Materials and methods

2.1 Insect rearing

Mythimna separata larvae were collected from Xiangyang Station of Northeast Agricultural University (Harbin, China) and transferred to an artificial climate chamber for the rearing of several generations. The incubation conditions were as follows: temperature, 25°C ± 1°C; humidity, 60%–70%; photoperiod, 14-h light:10-h dark cycle. Larvae were fed fresh corn leaves and adults were fed 5% honey water until they laid eggs.

2.2 Cloning of *MsTPS* cDNA

Various larval instars were collected and flash-frozen in liquid nitrogen for the subsequent transcriptome sequencing, which was performed by Annoroad Gene Technology company (Beijing, China). The *M. separata* transcriptome database was screened for the *TPS* sequence, which was then analyzed and compared with the sequences in the NCBI database.

Total RNA was extracted from fourth instar larvae using TRIzol (Invitrogen, Carlsbad, CA, United States) according to the manufacturer's instructions. First-strand cDNA was synthesized from 1.0 μg total RNA using the ReverTra Ace qPCR RT Master Mix with gDNA Remover (Toyobo, Shanghai, China). On the basis of the screened sequence, primers *MsTPS*-F and *MsTPS*-R (Supplementary Table S1) were designed using the Primer Premier 5.0 software for the PCR amplification of the *MsTPS* sequence. The synthesized cDNA served as the template for the PCR. The PCR amplification product was then purified using the Monarch Gel Extraction kit (NEB, Ipswich, MA, United States), inserted into the Trans1-T1 cloning vector (TransGen Biotech, Beijing, China), and sequenced to confirm its accuracy.

2.3 Amino acid sequence analysis and phylogenetic tree construction

The obtained *MsTPS* sequence was registered and deposited in the NCBI database (https://www.ncbi.nlm.nih.gov/). The *MsTPS* open reading frame was predicted and translated using ORF Finder (https://www.ncbi.nlm.nih.gov/orffinder/). The isoelectric point and molecular weight of the encoded amino acid sequence were predicted using the Expasy Compute pI/Mw online tool (https://www.expasy.org/). Its conserved domains were detected using the SMART online program (http://smart.embl-heidelberg.de/). Additionally, 31 known insect TPS amino acid sequences were downloaded from the NCBI database for the construction of a phylogenetic tree according to the maximum likelihood method with best-fitting model of MEGA7.0, with 1,000 bootstrap replicates (Kumar et al., 2016).

2.4 Spatiotemporal *MsTPS* expression pattern

Total RNA was extracted from insects at different developmental stages (i.e., first-day first to sixth instar larvae, prepupae, pupae, and adults) and from various tissues (i.e., foregut, midgut, hindgut, fat body, salivary gland, Malpighian tubules, and integument). The *MsTPS* expression levels in different *M. separata* developmental stages and tissues were analyzed by quantitative real-time PCR (qRT-PCR), with *Msβ-actin* (GenBank accession number: GQ856238) and *MsGAPDH* (glyceraldehyde-3-phosphate dehydrogenase; GenBank accession number: HM055756) used as reference genes. Primer Premier 5.0 was used to design qRT-PCR primer pairs *MsTPS*-q-F and *MsTPS*-q-R, *Msβ-actin*-q-F and *Msβ-actin*-q-R, and *MsGAPDH*-q-F and *MsGAPDH*-q-R (Supplementary Table S1). The qRT-PCR mixture comprised 2 μl cDNA, 6.8 μl ddH_2O, 0.6 μl sense and anti-sense primers, and 10 μl THUNDERBIRD SYBR qPCR Mix kit (Toyobo, Shanghai, China). The qRT-PCR was performed using the SimpliAmp PCR instrument (Thermo Fisher Scientific, MA, United States of America), with the following PCR conditions:

95°C for 3 min; 40 cycles of 94°C for 10 s and 57°C for 30 s. The data were recorded using the Bio-Rad CFX Manager 3.1 software. Melting curves were checked to assess the specificity of the qRT-PCR. Moreover, primer efficiency was validated before analyzing gene expression. The qRT-PCR was completed using three technical replicates and three biological replicates.

2.5 SiRNA synthesis and interference

For the RNAi analysis, siRNA sequences for *MsTPS* (GCGUUA CAGGAACAGGUUUTT and AAACCUGUUCCUGUAACG CTT) as well as for the negative control (UUCUCCGAACGU GUCACGUTT and ACGUGACACGUUCGGAGAATT) were synthesized (GenePharma, Shanghai, China) (Guo et al., 2018). The siRNA sequences were diluted and dissolved in DEPC-treated water for a final concentration of 20 μM. The first-day fourth instar larvae were injected with 2 μl siRNA for *MsTPS* or the negative control using a microsyringe. The larvae were fed normally after the injection.

2.6 Post-RNAi *MsTPS* expression

Larvae were collected at 3, 6, 12, 24, 48, 72, and 96 h after the injection of siRNA. Total RNA was extracted from the larvae and then reverse transcribed to cDNA for an analysis of *MsTPS* expression by qRT-PCR.

2.7 Effect of *MsTPS* silencing on *chitin synthase* gene expression

To explore the effect of *MsTPS* silencing on the expression of *MsCHSA* (GenBank accession number: KT948989) and *MsCHSB* (GenBank accession number: KY348776), Primer Premier 5.0 was used to design qRT-PCR primer pairs *MsCHSA*-q-F and *MsCHSA*-q-R as well as *MsCHSB*-q-F and *MsCHSB*-q-R (Supplementary Table S1). The *MsCHSA* and *MsCHSB* expression levels were analyzed using the cDNA that was used for the post-RNAi examination of *MsTPS* expression.

2.8 Post-RNAi TPS activity

Larvae collected at 3, 6, 12, 24, 48, 72, and 96 h after the injection of siRNA were used to measure the MsTPS activity according to the instructions for the Insect TPS Enzyme-linked Immunoassay (ELISA) kit (Jiangsu Meibiao Biotechnology Co., Ltd., Jiangsu, China). The protein concentrations of the samples were determined on the basis of Coomassie brilliant blue staining as previously described (Bradford, 1976), with a standard curve prepared using bovine serum albumin (Takara, Dalian, China). Briefly, 20 μl each sample and 180 μL Coomassie brilliant blue dye (Takara) were added to a 96-well plate, which was then incubated at room temperature for 5 min before the absorbance at 595 nm was measured.

2.9 Post-RNAi trehalose content

A previously reported method was used to determine the trehalose content (Steele, 1988; Ge et al., 2011) of three replicates of larvae collected at 3, 6, 12, 24, 48, 72, and 96 h after the injection of siRNA. A standard curve was prepared with trehalose concentrations of 0.05, 0.1, 0.2, 0.4, 0.6, 0.8, and 1.6 mmol/L. Each sample was placed in a sterilized homogenizer and then ground after 1 mL PBS (pH 7.4) was added. The samples were centrifuged at 5,000 *g* for 20 min at 4°C. The supernatants were collected and added to a 96-well plate. Following the addition of 5 μl 1% H_2SO_4 solution to each well, the 96-well plate was heated at 90°C for 10 min and then cooled on ice. Next, 5 μl 30% KOH solution was added to each well and then the 96-well plate was heated at 90°C for 10 min. After cooling the 96-well plate on ice, 100 μl chromogenic agent (0.02 g anthranone in 10 ml 80% H_2SO_4 solution) was added to each well, after which the 96-well plate was heated at 90°C for 10 min and then inserted into a microplate reader (Tecan, Hombrechtikon, Switzerland). The absorbance at 630 nm was recorded for each sample. The protein concentrations of the samples were determined as previously described (Bradford, 1976).

2.10 Post-RNAi chitin contents in the midgut and integument

A previously reported method was used to determine the chitin content (Arakane et al., 2005) of larvae collected and weighed at 3, 6, 12, 24, 48, 72, and 96 h after the injection of siRNA. Each analysis was performed using three replicates of 15 larvae. The larvae were dissected in normal saline to obtain the midgut and integument samples, which were placed in a 1.5-mL centrifuge tube and then ground to a powder in liquid nitrogen. After adding 500 μl 6% KOH solution, the ground samples were heated at 80°C for 90 min and then centrifuged at 12,000 *g* for 20 min at 4°C. The supernatant was discarded and each sample was suspended in 1 mL PBS buffer and then centrifuged at 12,000 *g* for 20 min at 4°C. After discarding the supernatant, each sample was resuspended in 200 μl Mcllvaine buffer (pH 6.0) (Tianzd, Beijing, China). To hydrolyze chitin to *N*-acetyl glucosamine (GlcNAc), 50 μl chitinase from *Streptomyces griseus* (Sigma-Aldrich, Shanghai, China) was added to individual samples, which were then incubated for 72 h at 37°C.

The GlcNAc concentrations were determined using a modified Morgan-Elson assay (Reissig et al., 1955). Briefly, various GlcNAc concentrations (0.00025, 0.0005, 0.001, 0.002, 0.004, and 0.008 mol/L) were used as standards. The samples incubated for 72 h were centrifuged at 12,000 *g* for 20 min at 4°C. For each sample, 10 μl supernatant and different GlcNAc standards were added to new centrifuge tubes. Next, 10 μL 0.27 mol/L sodium tetraborate was added to individual samples, which were then heated at 99.9°C for 10 min. The samples were immediately cooled to room temperature and then mixed with 100 μl 10% DMAB solution (10 g p-dimethylaminobenzaldehyde in a solution comprising 12.5 ml concentrated hydrochloric acid and 87.5 ml glacial acetic acid, diluted 1:10 with glacial acetic acid). The samples were heated at 37°C for 20 min and then centrifuged at 12,000 *g* for 5 min at 4°C. An 80-μl aliquot of each sample was transferred

to a 96-well plate, and the absorbance at 585 nm was recorded. Standard curves were prepared using the different GlcNAc concentrations.

2.11 Effects of *MsTPS* silencing on the ability of *M. separata* to utilize food

Fourth instar larvae were injected with 2 μL siRNA targeting *MsTPS* using a microsyringe. The control larvae were injected with 2 μl negative control siRNA. The larvae were subsequently fed normally (i.e., fresh corn leaves). At 3, 6, 12, 24, 48, 72, and 96 h after the injection of siRNA, larvae, remaining corn leaves, and excreta were placed in a 70°C oven and dried until they reached a constant weight. The following indices were recorded: 1) fresh weight of the larvae before the experiment; 2) fresh weight of the corn leaves before feeding; 3) dry weight of the remaining corn leaves for each time-point; 4) dry weight of the excreta (Zhao et al., 2017). The analysis was completed using three replicates of 15 larvae.

To determine the dry weight of the larvae before the experiment, 45 larvae from the same batch were selected at the beginning of the experiment and divided into three replicates. The fresh weight of the larvae was recorded. The larvae were then dried to obtain the dry weight. The larval dry weight:fresh weight ratio was calculated. The dry weight of the larvae before the experiment was calculated according to the dry weight:fresh weight ratio. The dry weight of the fresh corn leaves before feeding was similarly determined.

The ability of insects to digest and use food was evaluated on the basis of nutritional indices, including increase in dry weight W), larval feed intake B), relative growth rate (RGR), relative consumption rate (RCR), efficiency of the conversion of digested food (ECD), efficiency of the conversion of ingested food (ECI), and approximate digestibility (AD). These indices were calculated as follows (Waldbauer, 1968; Mole and Zera, 1993).

- W (g) = dry weight of larvae after the experiment − dry weight of larvae before the experiment
- B (g) = leaf dry weight before feeding − leaf dry weight after feeding
- RGR $[g\cdot(g\cdot h)^{-1}]$ = W/(dry weight of larvae before the experiment × experiment time)
- RCR $[g\cdot(g\cdot h)^{-1}]$ = B/(dry weight of larvae before the experiment × experiment time)
- ECD (%) = [W/(B− dry weight of excreta)] × 100
- ECI (%) = (W/B) × 100
- AD (%) = [(B− dry weight of excreta)/B] × 100

2.12 Effects of *MsTPS* silencing on *M. separata* growth and development

Fourth instar larvae were injected with 2 μl siRNA targeting *MsTPS* using a microsyringe. The control larvae were injected with 2 μl negative control siRNA. The larvae were subsequently fed normally (i.e., fresh corn leaves). Five replicates were prepared, with 30 larvae per group. The larvae were examined every 6 h. The time of death, the time of each molting, and the weight after each molting were recorded to detect abnormal molting. Finally, the mortality rates at 24, 48, and 72 h were calculated. The time required for the fifth instar larvae, sixth instar larvae, and pupae to develop was recorded. The weight of the fifth instar larvae, sixth instar larvae, and pupae was determined. The rates of abnormal molting and pupation were calculated.

The Helicon Focus digital photograph depth-of-field processing tool and the Helicon Remote camera control software were used to photograph and analyze (5–20 focal planes) the insects that exhibited abnormal development.

2.13 Statistical analysis

The qRT-PCR data were analyzed according to a published $2^{-\Delta\Delta CT}$ method (Jo et al., 2002). Statistical analysis was carried out with GraphPad Prism 9.3.0 software. Outliers were removed using Grubbs' test (GraphPad online software). Shapiro-Wilk's test was used to check normality in distribution. Resulting pairs were compared using the Student's t-test. One-way ANOVA was applied to determine the significant differences ($p < 0.05$) for different groups by using the Tukey's test. Then the results were plotted using the software GraphPad Prism 9.3.0.

3 Results

3.1 Analysis of the *MsTPS* cDNA and amino acid sequences

A novel *M. separata TPS* cDNA sequence (*MsTPS*; GenBank accession number: MN832898) was identified on the basis of transcriptome sequencing data. A sequence analysis revealed that the *MsTPS* cDNA is 4,551 bp long, with an open reading frame comprising 2,490 bp. The encoded protein (829 amino acids) has an isoelectric point of 6.68 and a molecular weight of 93.01 kDa. Moreover, it includes two conserved domains, namely, TPS (amino acids 19–499) and TPP (amino acids 537–762).

3.2 Phylogenetic analysis of MsTPS

In the phylogenetic tree constructed for MsTPS and other insect TPS sequences, MsTPS was clustered with the TPS of *S. exigua* (ABM66814), *Spodoptera litura* (XP_022814358), and *Spodoptera frugiperda* (XP_035433508), indicative of a relatively close relationship. It was also clustered with the TPS of *Helicoverpa armigera* (XP_021201246), *Bombyx mori* (XP_004926812), *Manduca sexta* (XP_030020846), *Papilio xuthus* (XP_013178239), *Antheraea pernyi* (ARD05072), and *Heortia vitessoides* (AYO46920). In contrast, MsTPS was distantly related to the TPS of *Aphis glycines* (QII15889) (Supplementary Figure S1). The clustering of TPS from

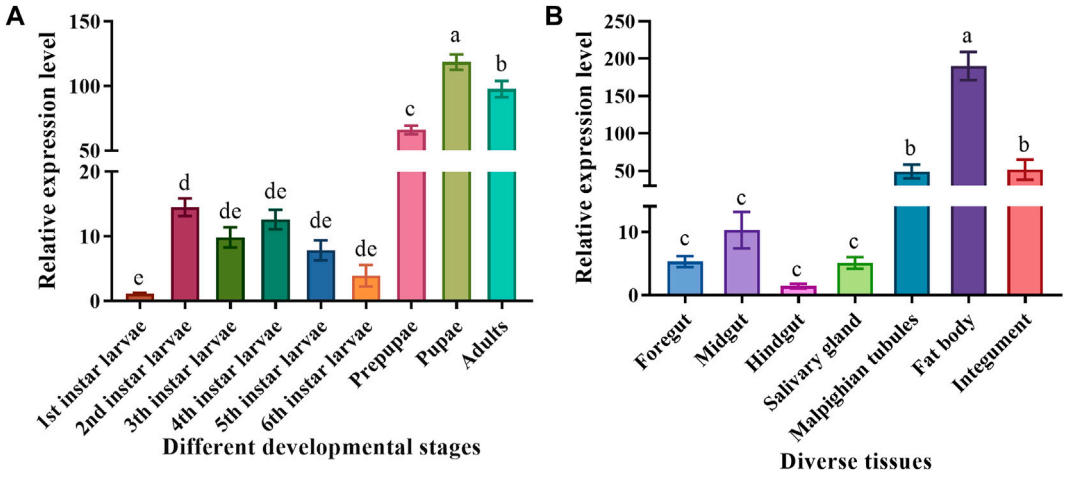

FIGURE 1
Spatiotemporal *MsTPS* expression pattern in different developmental stages **(A)** and in diverse tissues **(B)** of *M. separata*. The qRT-PCR data for *MsTPS* were analyzed using the $2^{-\Delta\Delta CT}$ method to determine relative expression levels, which were calculated as the mean ± SE. The expression data were normalized on the basis of the geometric mean of the expression of two reference genes (encoding *β*-actin and glyceraldehyde-3-phosphate dehydrogenase). The GraphPad Prism software was used for the data analysis. Different letters indicate significant differences ($p < 0.05$) according to the Tukey's test.

various species was basically consistent with the morphological classification of these insects.

3.3 Spatiotemporal *MsTPS* expression pattern

To clarify the *MsTPS* expression pattern during different *M. separata* developmental stages, the larvae, prepupae, pupae, and adults were analyzed by qRT-PCR. The results showed that *MsTPS* was expressed in all examined *M. separata* developmental stages, but the relative *MsTPS* expression level was lowest in the first instar larvae. Additionally, *MsTPS* was expressed at significantly higher levels in the prepupal, pupal, and adult stages than in the larval stages. The peak *MsTPS* expression level, which was detected in the pupal stage, was 107.76-fold and 1.19-fold higher than the corresponding expression levels in the first instar larval stage and the adult stage, respectively (Figure 1A).

To explore the *MsTPS* expression pattern in diverse *M. separata* tissues, the fourth instar larvae were dissected to obtain the following seven tissues: foregut, midgut, hindgut, fat body, salivary gland, Malpighian tubules, and integument. The results of the qRT-PCR analysis indicated *MsTPS* was expressed in all examined tissues. The relative *MsTPS* expression level was lowest in the hindgut. The *MsTPS* expression levels were significantly higher in the Malpighian tubules and integument than in the foregut, midgut, hindgut, and salivary gland. The *MsTPS* expression level in the integument was higher than that in the Malpighian tubules, but this difference was not significant. The highest *MsTPS* expression level, which was detected in the fat body, was 3.51-fold and 134.87-fold higher than the corresponding expression levels in the integument and the hindgut, respectively (Figure 1B).

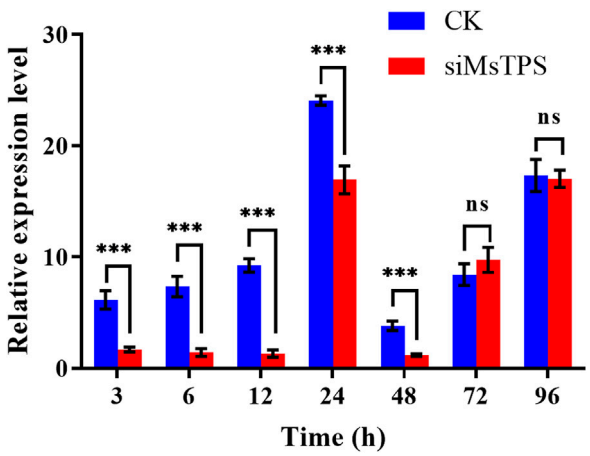

FIGURE 2
Expression of *MsTPS* at different post-RNAi time-points. The relative *MsTPS* expression levels were determined by qRT-PCR and the $2^{-\Delta\Delta CT}$ data analysis method. The expression data are provided as the mean ± SE. Data were normalized against the expression data for two reference genes (encoding *β*-actin and glyceraldehyde-3-phosphate dehydrogenase). Statistical analyses were performed using the GraphPad Prism software. Statistically significant differences by *t*-test at same treatment time shown as asterisks (*$p < 0.05$, **$p < 0.01$, ***$p < 0.001$, ns > 0.05).

3.4 Post-RNAi *MsTPS* silencing efficiency

To assess how efficiently *MsTPS* was silenced by RNAi, the fourth instar larvae were injected with equal amounts of siRNA for *MsTPS* and the negative control. The *MsTPS* expression level was analyzed at 3, 6, 12, 24, 48, 72, and 96 h after the injection. At the 3, 6, 12, 24, and 48 h time-points, the *MsTPS* expression levels were extremely significantly lower in the treated group than in

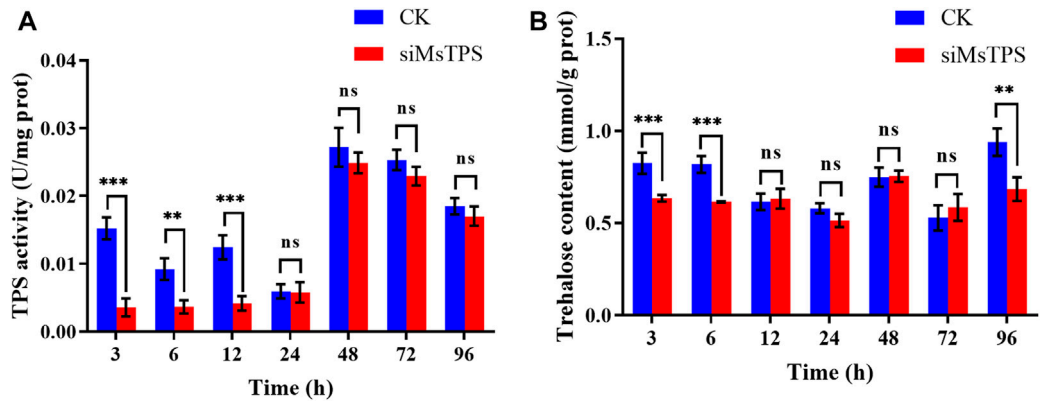

FIGURE 3
M. separata TPS activity **(A)** and trehalose content **(B)** at different time-points after the *MsTPS* RNAi treatment. Data are presented as the mean ± SE. Statistical analyses were performed using the GraphPad Prism software. Statistically significant differences by *t*-test at same treatment time shown as asterisks (*$p < 0.05$, **$p < 0.01$, ***$p < 0.001$, ns > 0.05).

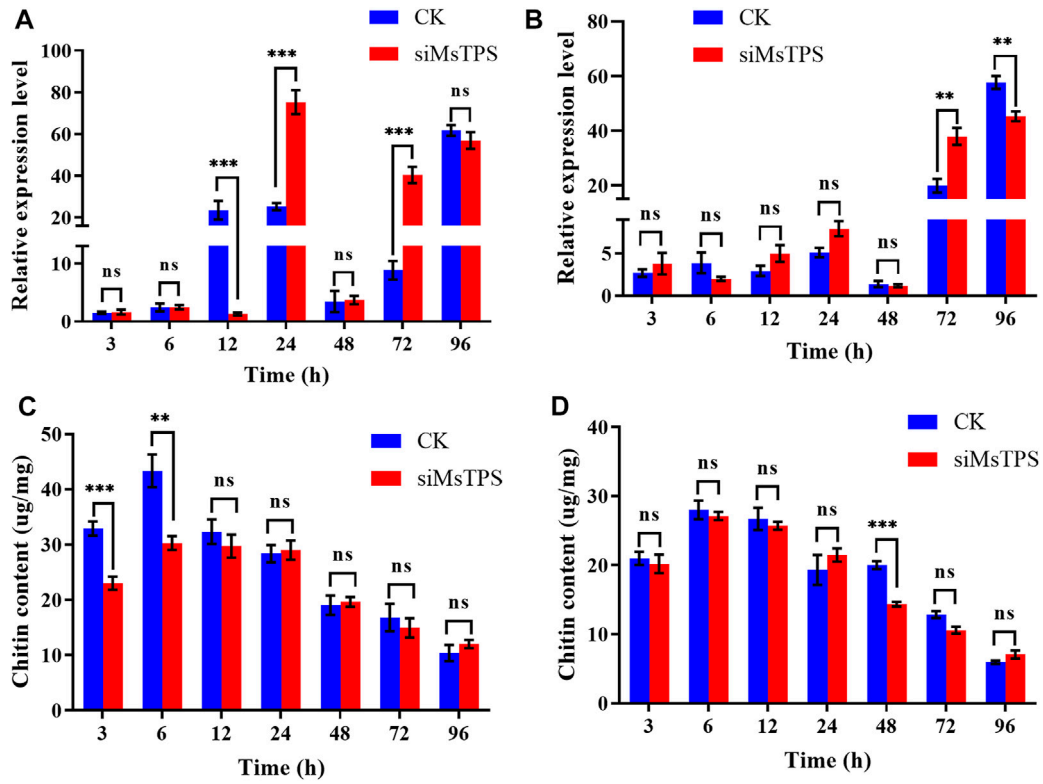

FIGURE 4
Effect of the silencing of *MsTPS* on *chitin synthase* gene expression and the chitin content. **(A)** Expression of *MsCHSA* at different time-points after the *MsTPS* RNAi treatment. **(B)** Expression of *MsCHSB* at different time-points after the *MsTPS* RNAi treatment. **(C)** Chitin content in the *M. separata* integument at different time-points after the *MsTPS* RNAi treatment. **(D)** Chitin content in the *M. separata* midgut at different time-points after the *MsTPS* RNAi treatment. Relative *MsTPS* expression levels were determined by qRT-PCR and the $2^{-\Delta\Delta CT}$ data analysis method. Expression data are provided as the mean ± SE. Data were normalized against the expression data for two reference genes (encoding *β*-actin and glyceraldehyde-3-phosphate dehydrogenase). Statistical analyses were performed using the GraphPad Prism software. Statistically significant differences by *t*-test at same treatment time shown as asterisks (*$p < 0.05$, **$p < 0.01$, ***$p < 0.001$, ns > 0.05).

the control group, with inhibition rates of 72.48%, 86.46%, 85.80%, 29.58%, and 69.35%, respectively. Although the *MsTPS* expression levels increased at 72 and 96 h, there was no significant difference in the expression levels of the treated and control groups (Figure 2). Therefore, *MsTPS* was most efficiently silenced at 6 h post-injection.

3.5 Changes in the TPS activity and trehalose content after the silencing of *MsTPS*

To functionally characterize *MsTPS*, the TPS activity and trehalose content in *M. separata* were analyzed at 3, 6, 12, 24, 48, 72, and 96 h post-RNAi treatment. Compared with the control, the TPS activity at 3, 6, and 12 h post-RNAi treatment decreased by 76.52%, 52.86%, and 54.22%, respectively. In contrast, there were no significant differences in TPS activity between the treated and control groups at the 24, 48, 72, and 96 h time-points (Figure 3A). Compared with the control level, the trehalose content decreased extremely significantly when *MsTPS* was silenced for 3, 6, and 96 h (decreased by 23.17%, 24.88%, and 27.15%, respectively). There were no significant differences in the trehalose content between the treated and control groups at the 12, 24, 48, and 72 h time-points (Figure 3B).

3.6 Analysis of *chitin synthase* gene expression and chitin content after the silencing of *MsTPS*

To investigate whether the silencing of *MsTPS* affected the expression of *MsCHS*, larvae were collected at 3, 6, 12, 24, 48, 72, and 96 h after the RNAi treatment for an examination of *MsCHSA* and *MsCHSB* expression. At the 12 h time-point, *MsCHSA* was expressed at a significantly lower level in the treated group than in the control group, and the silencing of *MsTPS* significantly increased the *MsCHSA* expression at the 24 and 72 h time-points (Figure 4A). In addition, the silencing of *MsTPS* significantly increased the *MsCHSB* expression at 72 h time-point and significantly decreased at 96 h time-point (Figure 4B). The results implying that inhibited *MsTPS* expression adversely affected *MsCHS* expression.

To elucidate the effect of *MsTPS* on the *M. separata* chitin content, the larvae were dissected at 3, 6, 12, 24, 48, 72, and 96 h after the RNAi treatment to obtain the midgut and integument, which were subsequently examined regarding their chitin contents. The results showed that the silencing of *MsTPS* extremely significantly decreased the integument chitin content by 29.99% and 30.12% at the 3 and 6 h time-points, respectively (Figure 4C). Additionly, the silencing of *MsTPS* significantly decreased the midgut chitin content by 28.31% at 48 h time-point (Figure 4D).

3.7 Effects of the silencing of *MsTPS* on the ability of *M. separata* to utilize food

To investigate the effect of the silencing of *MsTPS* on the ability of *M. separata* to utilize food, the larvae at 3, 6, 12, 24, 48, 72, and 96 h after the RNAi treatment were examined regarding specific nutritional indices. The silencing of *MsTPS* resulted in a significant decrease in the *M. separata* dry weight at 96 h post-RNAi treatment. Moreover, the larval feed intake significantly decreased at the 6, 12, 24, 48, and 96 h post-RNAi treatment time-points. The silencing of *MsTPS* significantly decreased the relative growth rate and the relative consumption rate at 6 and 96 h. Furthermore, the RNAi treatment also significantly decreased the efficiency of the conversion of ingested food at 6 h, the approximate digestibility at 24 h, and the efficiency of the conversion of digested food at 6, 48, and 96 h Table 1. Accordingly, the silencing of *MsTPS* adversely affected the ability of *M. separata* to utilize food.

3.8 Effects of the silencing of *MsTPS* on *M. separata* growth and development

To determine the effect of the silencing of *MsTPS* on growth and development, the *M. separata* growth and molting processes following the RNAi treatment were analyzed. The silencing of *MsTPS* resulted in a significant increase in the *M. separata* mortality rate at 24, 48, and 72 h (Figure 5A). The RNAi treatment also significantly prolonged the time required for *M. separata* larvae to develop into 5th-instar larvae, 6th-instar larvae, and pupae (Figure 5B). Furthermore, the RNAi treatment also resulted in a significant decrease in the weight of the sixth instar larvae (Figure 5C). Additionally, compared with the control samples, three distinct phenotypic differences were evident in the *M. separata* in which *MsTPS* was silenced (Figure 6A). First, larvae were unable to molt normally before dying. Second, partially deformed fifth instar larvae retained the cuticle from the fourth instar larvae. Third, some larvae were too small after molting. Moreover, *M. separata* pupation abnormalities were detected (Figure 6B). More specifically, some larvae failed to pupate and some pupae were too small. The rates of abnormal molting and pupation were 7.33% and 12.67%, respectively. The phenotypes of the control samples were relatively consistent.

4 Discussion

As a stress protectant, reserve carbohydrate, transport sugar, stress-related metabolite, and energy source, trehalose affects insect growth and development, molting, flying, overwintering, and other life cycle-related activities (Delorge et al., 2015). making it the most important carbohydrate in insect hemolymphs. In insects, trehalose is primarily synthesized in the TPS/TPP pathway. In this study, the *M. separata TPP* sequence was not detected in the screened transcriptome database. Earlier research revealed that TPS alone can mediate trehalose synthesis (Tang et al., 2018).

The *H. armigera HaTPS* gene is reportedly expressed during all developmental stages, with peak expression in the late sixth larval instar stage (Xu et al., 2009). In the current study, *MsTPS* was expressed in all examined *M. separata* developmental stages, with the lowest and highest expression levels detected in the first instar larvae and pupae, respectively.

The *MsTPS* expression pattern detected in this study was basically consistent with the published expression data for other insects. For example, in *L. migratoria*, *LmTPS* is reportedly mainly expressed in the fat body, but it is also expressed at low levels in the muscle tissue, hemolymph, and intestinal tract (Cui and Xia, 2009). In insects, trehalose is produced in fat body, which is also where *TPS* is mainly expressed (Chung, 2008; Tang et al., 2010). Trehalose, which is considered to be a source of stored energy and carbon, provides energy for insect growth and development, molting, and flying (Chung, 2008). The differential expression of *TPS* can affect the trehalose content in insects (Chen et al., 2010). Because TPS is a key enzyme in the trehalose synthesis pathway, it substantially

TABLE 1 Nutritional indices for *M. separata* at different time-points after the silencing of *MsTPS* by RNA interference.

Different treatments	Increase in dry weight (g)	Larval feed intake (g)	Relative growth rate (RGR) [g·(g·h)$^{-1}$]	Relative consumption rate (RCR) [g·(g·h)$^{-1}$]	Efficiency of conversion of digested food (ECD) (%)	Efficiency of conversion of ingested food (ECI) (%)	Approximate digestibility (AD) (%)
CK 3 h	0.0011 ± 0.0001	0.0041 ± 0.0004	0.0272 ± 0.0028	0.0665 ± 0.0042	47.8742 ± 3.7111	45.2026 ± 3.4430	34.9422 ± 1.5141
si*MsTPS* 3 h	0.0012 ± 0.0001	0.0034 ± 0.0002	0.0310 ± 0.0025	0.0936 ± 0.0112	36.6965 ± 1.0191	37.1864 ± 5.1471	17.2634 ± 2.6476
CK 6 h	0.0032 ± 0.0004	0.0075 ± 0.0002	0.0533 ± 0.0017	0.1313 ± 0.0030	62.0886 ± 1.8594	40.5954 ± 0.6848	44.2561 ± 3.0418
si*MsTPS* 6 h	0.0019 ± 0.0003	0.0047 ± 0.0003**	0.0358 ± 0.0007***	0.0845 ± 0.0012***	35.3609 ± 2.1302***	31.6680 ± 0.7596***	49.7342 ± 3.4406
CK 12 h	0.0039 ± 0.0003	0.0175 ± 0.0001	0.0305 ± 0.0034	0.1295 ± 0.0052	60.6653 ± 4.1909	23.3671 ± 2.9765	34.2510 ± 3.7892
si*MsTPS* 12 h	0.0029 ± 0.0001	0.0126 ± 0.0003***	0.0285 ± 0.0006	0.1238 ± 0.0052	65.4516 ± 3.9655	23.1928 ± 1.3121	34.6162 ± 4.8562
CK 24 h	0.0056 ± 0.0006	0.0232 ± 0.0007	0.0224 ± 0.0027	0.0862 ± 0.0058	51.5945 ± 6.8708	29.3519 ± 2.6503	33.1562 ± 1.4946
si*MsTPS* 24 h	0.0043 ± 0.0008	0.0187 ± 0.0006*	0.0184 ± 0.0038	0.0922 ± 0.0147	37.6385 ± 3.7035	21.7770 ± 3.2105	16.9277 ± 0.0248***
CK 48 h	0.0090 ± 0.0005	0.0469 ± 0.0016	0.0180 ± 0.0015	0.0874 ± 0.0074	68.0102 ± 2.2610	20.7333 ± 1.1907	32.2014 ± 1.7239
si*MsTPS* 48 h	0.0096 ± 0.0008	0.0383 ± 0.0010*	0.0173 ± 0.0001	0.0723 ± 0.0037	52.9722 ± 1.6787**	24.5142 ± 1.4579	31.6346 ± 2.0366
CK 72 h	0.0139 ± 0.0004	0.0661 ± 0.0010	0.0179 ± 0.0010	0.0907 ± 0.0040	63.5514 ± 4.5886	20.1489 ± 0.4596	28.6223 ± 0.6498
si*MsTPS* 72 h	0.0148 ± 0.0009	0.0612 ± 0.0011	0.0187 ± 0.0004	0.0868 ± 0.0016	47.0318 ± 5.9473	22.7698 ± 1.2078	31.8150 ± 2.3600
CK 96 h	0.0387 ± 0.0002	0.1041 ± 0.0021	0.0365 ± 0.0005	0.1021 ± 0.0013	75.1708 ± 1.5756	38.7818 ± 0.9244	14.1180 ± 0.7698
si*MsTPS* 96 h	0.0292 ± 0.0011**	0.0788 ± 0.0036**	0.0272 ± 0.0009**	0.0669 ± 0.0053**	49.2176 ± 1.7186***	42.4051 ± 4.0393	11.4601 ± 1.2654

Data are presented as the mean ± SE. Statistical analyses were performed using the GraphPad Prism software. Statistically significant differences by *t*-test at same treatment time shown as asterisks (*$p < 0.05$, **$p < 0.01$, ***$p < 0.001$).

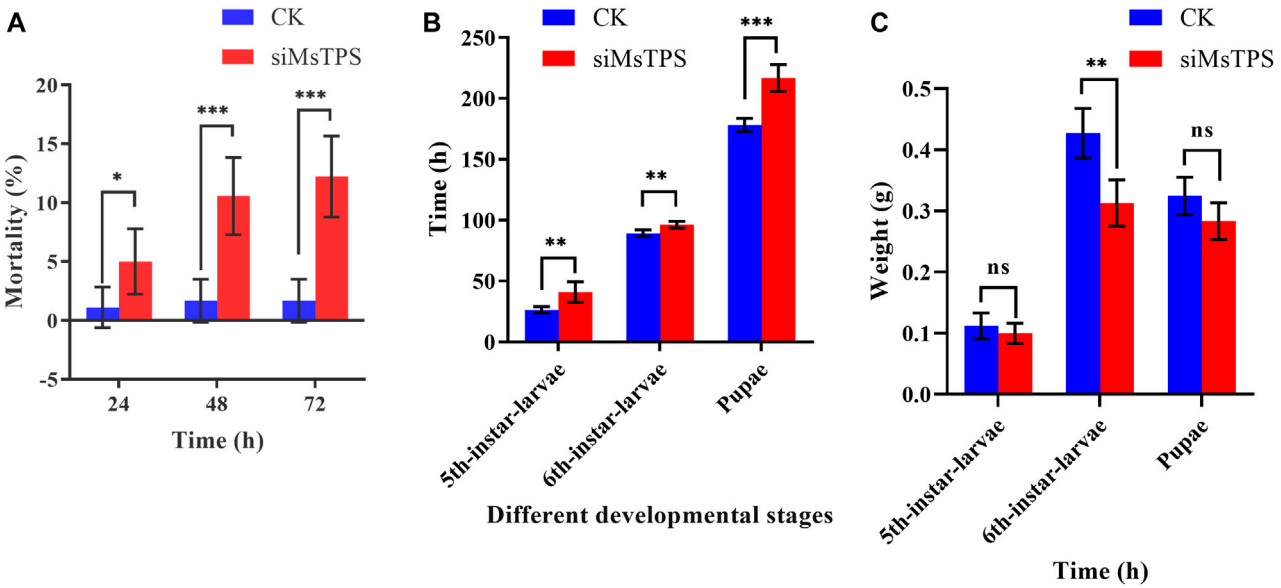

FIGURE 5
Effect of the silencing of *MsTPS* on *M. separata* mortality **(A)**, developmental time **(B)**, and weight **(C)**. Data are presented as the mean ± SE. Statistically significant differences by *t*-test at same treatment time shown as asterisks (*$p < 0.05$, **$p < 0.01$, ***$p < 0.001$, ns > 0.05).

affects trehalose production. In arthropods, *TPS* expression directly affects the trehalose content (Shi and Chung, 2014). In the current study, *MsTPS* expression was inhibited *via* RNAi, which resulted in changes to TPS activity and the trehalose content in *M. separata*.

Insect molting requires chitin synthesis and degradation pathways (Zhu et al., 2016). Trehalose is a substrate for insect chitin synthesis pathways. Studies have demonstrated that an imbalance in the trehalose synthesis and degradation in insects is associated with changes in the expression levels of related genes in the chitin synthesis pathway, with

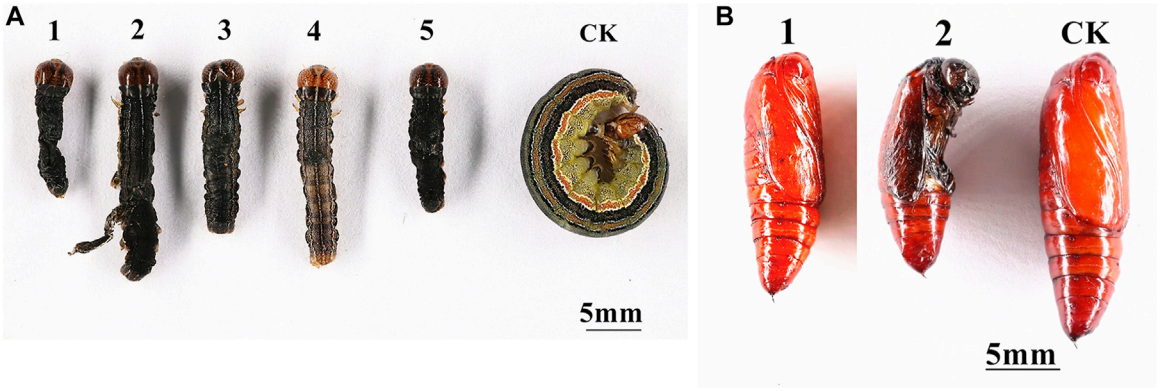

FIGURE 6
Effects of the silencing of *MsTPS* on *M. separata* molting **(A)** and pupation **(B)**. **(A)** 1, 3, and 5: larvae were unable to molt normally before dying; 2: larvae retained the cuticle from the fourth instar larvae; 4: larvae were too small after molting. **(B)** 1: larvae failed to pupate; 2: pupae were too small.

significant decreases in the chitin contents resulting in molting abnormalities and high mortality rates (Tang et al., 2016; Zhao et al., 2016). Moreover, suppressed *TPS* expression in insects leads to abnormal molting and death (Tang et al., 2016; Yang et al., 2017; Chen et al., 2018). In the current study, the silencing of *MsTPS* significantly affected *MsCHSA* and *MsCHSB* expression and significantly decreased the integument and midgut chitin content. Additionally, the RNAi treatment significantly increased the *M. separata* mortality rate and the time required for larvae and pupae to develop, whereas it significantly decreased the weight of the sixth instar larvae, while also leading to abnormal molting and pupation. These findings are in accordance with the results of earlier analyses of other insects. In previous investigations involving *Nilaparvata lugens*, inhibited *NlTPS1* expression resulted in malformation and mortality rates of 20% and 30%, respectively (Chen et al., 2010; Yang et al., 2017). In another study, decreases in the *TPS* expression level in *S. exigua* led to mortality rates of 50.94% and 66.76% at 48 and 204 h, respectively (Tang et al., 2010). Additionally, injecting the third instar larvae of *B. minax* with dsRNA for *BmTPS* reportedly results in abnormal phenotypic changes and a mortality rate of 52% (Xiong et al., 2016). Our results are also in keeping with previous research showing that inhibition of *TPS* gene can lead to malformation and increased mortality rate of insects.

Previous research on *L. decemlineata* revealed that compared with the controls, insects in which *LdTPS* expression is inhibited consume more leaves and are heavier, but they have less chitin (Shi et al., 2016). In the present study, the silencing of *MsTPS* had significant detrimental effects on the ability of *M. separata* to utilize food. These findings were not completely consistent with the reported results for *L. decemlineata*. After the RNAi-based silencing of *MsTPS*, the *M. separata* dry weight and larval feed intake decreased significantly, but the change in the chitin content was consistent with that detected in *L. decemlineata*. An earlier study indicated that the trehalose concentration in insects can modulate insect feeding behaviors (Thompson, 2003). In this study, the silencing of *MsTPS* in *M. separata* resulted in a significant decrease in the trehalose content, thus the decrease of the ability to utilize food which may be related to the decrease in the trehalose content. In this study, it was found the chitin content in the peritrophic membrane significantly decreased in response to the silencing of *MsTPS*. The significant decrease in the ability of *M. separata* to utilize food might be associated with alterations to the peritrophic membrane structure and decreases in the chitin content, but this will need to be experimentally verified.

Data availability statement

The datasets presented in this study can be found in online repositories. The names of the repository/repositories and accession number(s) can be found below: The MsTPS cloned in this study has been recorded into NCBI repository. GenBank accession number: MN832898. https://www.ncbi.nlm.nih.gov/nuccore/MN832898.1/; Transcriptome Sequencing clean reads were submitted to NCBI SRA database: PRJNA919163.

Author contributions

Conceptualization, H-JY and DF; methodology, H-JY and M-YC; software, H-JY; validation, M-YC and X-HZ; formal analysis, H-JY; data curation, H-JY, Y-SH, and C-YZ; writing–original draft preparation, H-JY; writing–review and editing, DF; funding acquisition, DF. All authors have read and agreed to the published version of the manuscript.

Funding

This research was funded by the National Key Research and Development Program (grant no. 2018YFD0201000).

Acknowledgments

We thank Liwen Bianji (Edanz) (www.liwenbianji.cn) for editing the English text of a draft of this manuscript.

Conflict of interest

The authors declare that the research was conducted in the absence of any commercial or financial relationships that could be construed as a potential conflict of interest.

Publisher's note

All claims expressed in this article are solely those of the authors and do not necessarily represent those of their affiliated organizations, or those of the publisher, the editors and the reviewers. Any product that may be evaluated in this article, or claim that may be made by its manufacturer, is not guaranteed or endorsed by the publisher.

Supplementary material

The Supplementary Material for this article can be found online at: https://www.frontiersin.org/articles/10.3389/fphys.2023.1109661/full#supplementary-material

References

Arakane, Y., Muthukrishnan, S., Kramer, K. J., Specht, C. A., Tomoyasu, Y., Lorenzen, M. D., et al. (2005). The *Tribolium chitin synthase* genes *TcCHS1* and *TcCHS2* are specialized for synthesis of epidermal cuticle and midgut peritrophic matrix. *Insect Mol. Biol.* 14 (5), 453–463. doi:10.1111/j.1365-2583.2005.00576.x

Bradford, M. M. (1976). A rapid and sensitive method for the quantitation of microgram quantities of protein utilizing the principle of protein-dye binding. *Anal. Biochem.* 72 (1-2), 248–254. doi:10.1006/abio.1976.9999

Chen, J. X., Lu, Z. H., Wang, C. Y., Chen, J., and Lin, T. (2020). RNA interference of a *trehalose-6-phosphate synthase* gene reveals its roles in the biosynthesis of chitin and lipids in *Heortia vitessoides* (Lepidoptera: Crambidae). *Insect Sci.* 27 (2), 212–223. doi:10.1111/1744-7917.12650

Chen, J., Zhang, D., Yao, Q., Zhang, J., Dong, X., Tian, H., et al. (2010). Feeding-based RNA interference of a *trehalose phosphate synthase* gene in the Brown planthopper. *Nil. Lugens. Insect Mol. Biol.* 19 (6), 777–786. doi:10.1111/j.1365-2583.2010.01038.x

Chen, Q., Ma, E., Behar, K. L., Xu, T., and Handan, G. G. (2002). Role of trehalose phosphate synthase in anoxia tolerance and development in *Drosophila melanogaster*. *J. Biol. Chem.* 277 (5), 3274–3279. doi:10.1074/jbc.M109479200

Chen, Q. W., Jin, S., Zhang, L., Shen, Q. D., Wei, P., Wei, Z. M., et al. (2018). Regulatory functions of trehalose-6-phosphate synthase in the chitin biosynthesis pathway in *Tribolium castaneum* (Coleoptera: Tenebrionidae) revealed by RNA interference. *B. Entomol. Res.* 108 (3), 388–399. doi:10.1017/S000748531700089X

Chung, J. S. (2008). A *trehalose 6-phosphate synthase* gene of the hemocytes of the blue crab, *Callinectes sapidus*: Cloning, the expression, its enzyme activity and relationship to hemolymph trehalose levels. *Saline Syst.* 4 (1), 18. doi:10.1186/1746-1448-4-18

Cui, S. Y., and Xia, Y. X. (2009). Isolation and characterization of the *trehalose-6-phosphate synthase* gene from *Locusta migratoria manilensis*. *Insect Sci.* 16 (4), 287–295. doi:10.1111/j.1744-7917.2009.01268.x

Delorge, I., Figueroa, C. M., Feil, R., Lunn, J. E., and Van, D. P. (2015). Trehalose-6-phosphate synthase 1 is not the only active TPS in *Arabidopsis thaliana*. Arabidopsis thaliana. *Biochem. J.* 466 (2), 283–290. doi:10.1042/BJ20141322

Ge, L. Q., Zhao, K. F., Huang, L. J., and Wu, J. C. (2011). The effects of triazophos on the trehalose content, trehalase activity and their gene expression in the Brown planthopper *Nilaparvata lugens* (Hemiptera: Delphacidae). *Pestic. Biochem. Physiol.* 100 (2), 172–181. doi:10.1016/j.pestbp.2011.03.007

Giaever, H. M., Styrvold, O. B., Kaasen, I., and Strom, A. R. (1988). Biochemical and genetic characterization of osmoregulatory trehalose synthesis in *Escherichia coli*. *J. Bacteriol.* 170 (6), 2841–2849. doi:10.1128/jb.170.6.2841-2849.1988

Guo, X., Wang, Y., Sinakevitch, I., Lei, H., and Smith, B. H. (2018). Comparison of RNAi knockdown effect of tyramine receptor 1 induced by dsRNA and siRNA in brains of the honey bee, *Apis mellifera*. *J. Insect Physiol.* 111, 47–52. doi:10.1016/j.jinsphys.2018.10.005

Hottiger, T., Boller, T., and Wiemken, A. (1987). Rapid changes of heat and desiccation tolerance correlated with changes of trehalose content in *Saccharomyces cerevisiae* cells subjected to temperature shifts. *FEBS Lett.* 220 (1), 113–115. doi:10.1016/0014-5793(87)80886-4

Jo, V., Katleen, D. P., Filip, P., Bruce, P., Nadine, V. R., Anne, D. P., et al. (2002). Accurate normalization of real-time quantitative RT-PCR data by geometric averaging of multiple internal control genes. *Genome Biol.* 3 (7), RESEARCH0034. doi:10.1186/gb-2002-3-7-research0034

Kumar, S., Stecher, G., and Tamura, K. (2016). MEGA7: Molecular evolutionary genetics analysis version 7.0 for bigger datasets. *Mol. Biol. Evol.* 33 (7), 1870–1874. doi:10.1093/molbev/msw054

Mole, S., and Zera, A. J. (1993). Differential allocation of resources underlies the dispersal-reproduction trade-off in the wing-dimorphic cricket, *Gryllus rubens*. *Oecologia* 93 (1), 121–127. doi:10.1007/BF00321201

Reissig, J. L., Strominger, J. L., and Leloir, L. F. (1955). A modified colorimetric method for the estimation of N-acetylamino sugars. *J. Biol. Chem.* 217 (2), 959–966. doi:10.1016/s0021-9258(18)65959-9

Santos, R., Alves-Bezerra, M., Rosas-Oliveira, R., Majerowicz, D., Meyer-Fernandes, J. R., Gondim, K. C., et al. (2012). Gene identification and enzymatic properties of a membrane-bound trehalase from the ovary of *Rhodnius prolixus*. *Arch. Insect Biochem. Physiol.* 81 (4), 199–213. doi:10.1002/arch.21043

Shi, J. F., Xu, Q. Y., Sun, Q. K., Meng, Q. W., Mu, L. L., Guo, W. C., et al. (2016). Physiological roles of trehalose in Leptinotarsa larvae revealed by RNA interference of *trehalose-6-phosphate synthase* and *trehalase* genes. *Insect biochem. Mol. Biol.* 77, 52–68. doi:10.1016/j.ibmb.2016.07.012

Shi, Q., and Chung, J. S. (2014). Trehalose metabolism in the blue crab *Callinectes sapidus*: Isolation of multiple structural cDNA isoforms of *trehalose-6-phosphate synthase* and their expression in muscles. *Gene* 536 (1), 105–113. doi:10.1016/j.gene.2013.11.070

Shukla, E., Thorat, L. J., Nath, B. B., and Gaikwad, S. M. (2015). Insect trehalase: Physiological significance and potential applications. *Glycobiology* 25 (4), 357–367. doi:10.1093/glycob/cwu125

Song, J. C., Lu, Z. J., Yi, L., and Yu, H. Z. (2021). Functional Characterization of a *trehalose-6-phosphate synthase* in *Diaphorina citri* revealed by RNA interference and transcriptome sequencing. *Insects* 12 (12), 1074. doi:10.3390/insects12121074

Steele, J. E. (1988). Occurrence of a hyperglycæmic factor in the corpus cardiacum of an insect. *Nature* 192 (4803), 680–681. doi:10.1038/192680a0

Strom, A. R., and Kaasen, I. (1993). Trehalose metabolism in *Escherichia coli*: Stress protection and stress regulation of gene expression. *Mol. Microbiol.* 8 (2), 205–210. doi:10.1111/j.1365-2958.1993.tb01564.x

Tang, B., Chen, J., Yao, Q., Pan, Z. Q., Xu, W. H., Wang, S. G., et al. (2010). Characterization of a *trehalose-6-phosphate synthase* gene from *Spodoptera exigua* and its function identification through RNA interference. *J. Insect Physiol.* 56 (7), 813–821. doi:10.1016/j.jinsphys.2010.02.009

Tang, B., Qin, Z., Shi, Z. K., Wang, S., Guo, X. J., Wang, S. G., et al. (2014). Trehalase in *Harmonia axyridis* (Coleoptera: Coccinellidae): Effects on beetle locomotory activity and the correlation with trehalose metabolism under starvation conditions. *Appl. Entomol. Zool.* 49 (2), 255–264. doi:10.1007/s13355-014-0244-4

Tang, B., Wang, S., Wang, S. G., Wang, H. J., Zhang, J. Y., and Cui, S. Y. (2018). Invertebrate *trehalose-6-phosphate synthase* gene: Genetic architecture, biochemistry, physiological function, and potential applications. *Front. Physiol.* 9, 30. doi:10.3389/fphys.2018.00030

Tang, B., Wei, P., Zhao, L. N., Shi, Z. K., Shen, Q. D., Yang, M. M., et al. (2016). Knockdown of five *trehalase* genes using RNA interference regulates the gene expression of the chitin biosynthesis pathway in *Tribolium castaneum*. *Bmc Biotechnol.* 16 (1), 67. doi:10.1186/s12896-016-0297-2

Thompson, S. N. (2003). Trehalose-the insect 'blood' sugar. *Adv. Insect Physiol.* 31, 205–285. doi:10.1016/S0065-2806(03)31004-5

Waldbauer, G. P. (1968). The consumption and utilization of food by insects. *Adv. Insect Physiol.* 5, 229–288. doi:10.1016/s0065-2806(08)60230-1

Xiong, K. C., Wang, J., Li, J. H., Deng, Y. Q., Pu, P., Fan, H., et al. (2016). RNA interference of a *trehalose-6-phosphate synthase* gene reveals its roles during larval-pupal metamorphosis in *Bactrocera minax* (Diptera: Tephritidae). *J. Insect Physiol.* 91-92, 84–92. doi:10.1016/j.jinsphys.2016.07.003

Xu, J., Bao, B., Zhang, Z. F., Yi, Y. Z., and Xu, W. H. (2009). Identification of a novel gene encoding the trehalose phosphate synthase in the cotton bollworm, *Helicoverpa armigera*. *Glycobiology* 19 (3), 250–257. doi:10.1093/glycob/cwn127

Yang, M. M., Zhao, L. N., Shen, Q. D., Xie, G. Q., Wang, S. G., and Tang, B. (2017). Knockdown of two *trehalose-6-phosphate synthases* severely affects chitin metabolism gene expression in the Brown planthopper *Nilaparvata lugens*. *Pest Manag. Sci.* 73 (1), 206–216. doi:10.1002/ps.4287

Zhang, Z., Zhang, Y. H., Wang, J., Liu, J., Tang, Q. B., Li, X. R., et al. (2018). Analysis on the migration of first-generation *Mythimna separata* (Walker) in China in 2013. *J. Integr. Agric.* 17 (7), 1527–1537. doi:10.1016/S2095-3119(17)61885-9

Zhao, L. N., Yang, M. M., Shen, Q. D., Liu, X. J., Shi, Z. K., Wang, S. G., et al. (2016). Functional characterization of three *trehalase* genes regulating the chitin metabolism pathway in rice Brown planthopper using RNA interference. *Sci. Rep.* 6, 27841. doi:10.1038/srep27841

Zhao, L. Q., Liao, H. Y., Zeng, Y., Wu, H. J., and Zhu, D. H. (2017). Food digestion capability and digestive enzyme activity in female adults of the wing-dimorphic cricket *Velarifictorus ornatus*. *Entomol. Exp. Appl.* 163 (1), 35–42. doi:10.1111/eea.12563

Zhu, K. Y., Merzendorfer, H., Zhang, W. Q., Zhang, J. Z., and Muthukrishnan, S. (2016). Biosynthesis, turnover, and functions of chitin in insects. *Annu. Rev. Entomol.* 61, 177–196. doi:10.1146/annurev-ento-010715-023933

frontiers | Frontiers in Physiology

TYPE Original Research
PUBLISHED 09 May 2023
DOI 10.3389/fphys.2023.1160846

OPEN ACCESS

EDITED BY
Bimalendu B. Nath,
Savitribai Phule Pune University, India

REVIEWED BY
Ali R. Bandani,
University of Tehran, Iran
Kai Liu,
Zhongkai University of Agriculture and Engineering, China

*CORRESPONDENCE
Zeng-Rong Zhu,
zrzhu@zju.edu.cn
Xiao-Xiao Shi,
shixiao6656@163.com

RECEIVED 07 February 2023
ACCEPTED 24 April 2023
PUBLISHED 09 May 2023

CITATION
Chen M, Shi X-X, Wang N, Zhang C, Shi Z-Y, Zhou W-W and Zhu Z-R (2023), Alkaline ceramidase (*ClAC*) inhibition enhances heat stress response in *Cyrtorhinus lividipennis* (Reuter). *Front. Physiol.* 14:1160846. doi: 10.3389/fphys.2023.1160846

Alkaline ceramidase (*ClAC*) inhibition enhances heat stress response in *Cyrtorhinus lividipennis* (Reuter)

Min Chen[1], Xiao-Xiao Shi[2]*, Ni Wang[1], Chao Zhang[1], Zhe-Yi Shi[1], Wen-Wu Zhou[1] and Zeng-Rong Zhu[1,3]*

[1]State Key Laboratory of Rice Biology and Breeding, Key Laboratory of Molecular Biology of Crop Pathogens and Insects, Ministry of Agriculture, Institute of Insect Sciences, Zhejiang University, Hangzhou, China, [2]Zhejiang Academy of Forestry, Hangzhou, China, [3]Hainan Research Institute, Zhejiang University, Sanya, China

Ceramidases (CDases) are vital sphingolipid enzymes involved in organismal growth and development. They have been reported as key mediators of thermal stress response. However, whether and how CDase responds to heat stress in insects remain unclear. Herein, we identified two CDase genes, *C. lividipennis* alkaline ceramidase (*ClAC*) and neutral ceramidase (*ClNC*), by searching the transcriptome and genome databases of the mirid bug, *Cyrtorhinus lividipennis*, an important natural predator of planthoppers. Quantitative PCR (qPCR) analysis showed that both *ClNC* and *ClAC* were highly expressed in nymphs than in adults. *ClAC* was especially highly expressed in the head, thorax, and legs, while *ClNC* was widely expressed in the tested organs. Only the *ClAC* transcription was significantly affected by heat stress. Knocking down *ClAC* increased the *C. lividipennis* nymph survival rate under heat stress. The transcriptome and lipidomics data showed that the RNA interference-mediated suppression of *ClAC* significantly upregulated the transcription level of *catalase* (*CAT*) and the content of long-chain base ceramides, including C16-, C18-, C24-, and C31- ceramides. In *C. lividipennis* nymphs, *ClAC* played an important role in heat stress response, and the upregulation of nymph survival rate might be caused by variation in the ceramide levels and transcriptional changes in *CDase* downstream genes. This study improves our understanding of the physiological functions of insect CDase under heat stress and provides valuable insights into the nature enemy application.

KEYWORDS

ceramidase, *Cyrtorhinus lividipennis*, heat stress, catalase, ceramide, nature enemy

1 Introduction

Rice (*Oryza sativa*) is the most important food crop in the world with over half of the global population depending on this food resource (Project, 2005; Lou et al., 2014). The brown planthopper (BPH), *Nilaparvata lugens*, not only directly feeds on the rice plant but also transmits plant viruses (Liu et al., 2018). Since the Green Revolution, pesticide abuse increased the insect drug resistance and caused BPH outbreaks, which have seriously threatened rice production and affected human life (Bottrell and Schoenly, 2012). Thus, the biological control of BPH has increasing importance and is considered the sustainable strategy to avoid the shortcomings of chemical control (Lou et al., 2014). *Cyrtorhinus*

lividipennis (Reuter), a hemipteran predator, is a dominant natural enemy of BPH. It feeds on BPH eggs and nymphs, thus effectively controlling the BPH population and playing an important role in BPH biological control (Matsumura et al., 2005; Sigsgaard, 2007; Preetha et al., 2010; Liu et al., 2018). However, with the acceleration of global warming, thermal stress is weakening the fitness and predatory capacity of *C. lividipennis* (Bai et al., 2022). Therefore, it is urgently required to investigate how *C. lividipennis* reacts to heat stress such as identifying the key resistance effectors to increase its survival rate under heat stress and improve its predation performance.

Sphingolipids play structural roles in cellular membranes and act as bioactive signaling molecules involved in multiple cell regulatory functions (Bartke and Hannun, 2009). Ceramides, located in the central part of sphingolipid metabolism, are the precursors of multiple complex sphingolipids (Kitatani et al., 2008; Gault et al., 2010; Young et al., 2013). Many research studies have demonstrated that sphingolipids participate in the regulation of thermal stress response. CDases are the most important metabolic enzymes of ceramides, hydrolyzing ceramides into free fatty acids and sphingosine (Mao and Obeid, 2008). CDases are divided into three subfamilies, including acid CDase (aCDase), neutral CDase (nCDase), and alkaline CDase (alCDase). nCDase have proved to be involved in the heat stress response of BPH (Shi et al., 2018). Serine palmitoyltransferase (*SPT*), localized in the first step of sphingolipid biosynthesis, is required for the accumulation of trehalose, a thermoprotectant in yeast cells under heat stress (Dickson et al., 1997; Jenkins et al., 1997; Dickson et al., 2006). Sphingosine-1-phosphate (S1P), a product of sphingosine (Sph) phosphorylation, enhanced the survival rate of *Arabidopsis* cell under heat stress by reducing programmed cell death (Alden et al., 2011). External addition of S1P could reduce the deleterious effect of heat stress on the development of bovine oocytes (Roth and Hansen, 2004). In mouse cells, ceramide and S1P activated the synthesis of heat shock proteins (HSPs) during heat shock response (Chang et al., 1995; Kozawa et al., 1999). The aforementioned data indicate the intimate relationship between sphingolipid metabolism and thermal responses. However, the involvement of sphingolipids in heat resistance in the predator *C. lividipennis* has not been extensively studied.

In this research, we first identified two *CDase* homologous genes from the *C. lividipennis* genomic and transcriptomic databases. Then, the relative expression and phylogenetic analysis of CDases were conducted to understand the characteristics of these enzymes. Using the technology of RNA interference (RNAi), we clarified the biological roles of *ClAC* in thermal tolerance. Finally, transcriptome and lipid metabolome analyses were performed to reveal the potential regulatory mechanism.

2 Materials and methods

2.1 Insect rearing

C. lividipennis and their prey, BPH, were collected from a paddy field on the Zijingang campus of Zhejiang University, Hangzhou, China. The BPH population was maintained on susceptible rice seedlings of cv. Taichung Native 1 (TN1). *C. lividipennis* was reared in cages with fresh rice seedlings and sufficient prey. The environmental chamber parameters were set as 26 °C ± 1 °C, 70% ± 10% relative humidity, and a 14:10 h light: dark photoperiod, as described by Bai et al. (2022).

2.2 Sequence analysis

The homologous genes of *C. lividipennis CDase* were identified in the transcriptome data and genome data through local blast using *CDases* of *Homo sapiens*, BPH, and *Mus musculus* as queries. The phylogenetic analysis of ClAC and ClNC proteins was performed using MEGA X software (http://www.megasoftware.net/). A phylogenetic tree was constructed using the neighbor-joining and Poisson correction methods based on CDase protein sequences and setting the bootstrap value for 1,000 trials.

2.3 Sample collection

The sample collected for the stage-specific expression pattern analysis were eggs (n = 100), first instar nymphs (n = 50), second instar nymphs (n = 50), third instar nymphs (n = 15), fourth instar nymphs (n = 10), fifth instar nymphs (n = 10), and newly emerged females (n = 5) and males (n = 5). Tissues including the head, thorax, leg, integument, midgut, and fat body were dissected from third nymphs (n = 50). The third instar nymphs were collected after exposure under 26 °C and 38 °C for 6 h or 24 h (n = 5) to analyze the differently expressed genes induced by thermal stress. Three biological replicates were collected for each sample, then snap-frozen in liquid nitrogen and stored at −80 °C.

2.4 RNA isolation and quantitative real time polymerase chain reaction (qRT-PCR)

Total RNA was isolated using the TRIzol reagent (Invitrogen, Carlsbad, CA, United States), and cDNA was prepared following the manufacturer's protocol using *Evo M-MLV* RT Mix Kit with gDNA clean (Accurate Biotechnology). The qRT-PCR reaction was prepared with the SYBR Green premix *Pro Taq* HS qPCR Kit (Accurate Biotechnology) and performed using the CFX96 Real Time System (Bio-Rad Laboratories, Hercules, CA, United States). Each biological replicate had three technical replicates. The primers (Supplementary Table S1) employed for qRT-PCR were designed by Primer3 (v.0.4.0) (https://bioinfo.ut.ee/primer3-0.4.0/) based on the transcriptomic sequences. The standard curve method was employed to calculate the relative transcript levels. The housekeeping gene *GAPDH* was used as the internal reference gene.

2.5 RNA interference

ClAC and *Green Fluorescent Protein* (*GFP*) gene fragments were amplified using primers containing the T7 promoter (Supplementary Table S1). The cloned PCR products were used as templates to synthesize dsRNAs using the Thermo T7 Transcription Kit (TOYOBO). The DNA or RNA concentrations were measured by a NanoDrop 2000 Spectrophotometer (Thermo Fisher Scientific). The dsRNA

products were diluted to 1000 μg/μL and stored at −80 °C for subsequent experiments. The dsRNA of *ClAC* (dsAC) and dsRNA of *GFP* (dsGFP) were separately microinjected into the mesothorax of third instar nymphs after anesthetizing with CO_2. The treated third nymphs recovered in 30 min after microinjection were used for the following experiments. Three biological replicates ($n = 5$) were randomly collected for the measurement of RNAi efficiency.

2.6 Survival rate

The dsRNA-injected third instar nymphs were separately reared in 38 °C or 26 °C incubators for 12 h intervals to assess their survival rate. Six replicates were performed for each treatment. For each biological replicate, 12–16 injected third instar nymphs were transferred onto one BPH-oviposited rice plant, which was replaced in each glass tube every day to provide enough food resources for *C. lividipennis*.

2.7 Transcriptome sequencing

The dsAC-injected or dsGFP-injected third nymphs were reared at 38 °C for 24 h, and then sampled for the RNA extraction. Total RNA was extracted from 10 treated individuals for each sample. Three biological replicates were performed for both dsAC and dsGFP treatments. Illumina sequencing and cDNA library construction were carried out at Novogene (Beijing, China). The differentially expressed genes with padj<0.05 and |log2FoldChange|>0 were selected for the Gene Ontology (GO) and Kyoto Encyclopedia of Genes and Genomes (KEGG) analyses.

2.8 Lipidomic profiling

For each sample, 50 mg of dsAC-injected or dsGFP-injected third instar nymphs in total fresh weight were collected after rearing under 38 °C for 24 h. Six biological replicates were performed for both dsAC and dsGFP treatments. The lipid extraction and lipidomic profiling protocols were conducted at Metware Biotechnology laboratories (Wuhan, China). Significantly regulated metabolites between groups were determined by variable importance in projection (VIP) ≥ 1 and | log2 Fold Change| (|Log2FC|) ≥ 1.0.

2.9 Statistical analysis

The statistical values were shown as means ± standard error of the mean (SEM). One-way ANOVA and LSD test ($p<0.05$) were performed by Data Processing System (DPS) (Tang and Zhang, 2013). Student's t-test was carried out in GraphPad Prism software (Swift, 1997).

3 Results

3.1 Expression patterns and phylogenetic analysis of *C. lividipennis* CDases

To understand the CDases of *C. lividipennis*, we totally found two CDases from *C. lividipennis* (*ClAC* and *ClNC*). We analyzed their evolutionary relationships with CDases from humans, mice, plants, fishes, and other insects. The phylogenetic tree showed that *ClAC* was clustered into the aCDase group and closely related to the aCDases of the hemipteran insects *Cimex lectularius* and *L. striatellus*. Meanwhile, *ClNC* was clustered into the branch of nCDases and closely related to the hemipteran insect *C. lectularius* (Figure 1A). To further understand the biological function of these two CDases, the relative transcription levels of *ClAC* and *ClNC* across different developmental stages or tissues were investigated. The results showed that *ClAC* was expressed the highest in first and second nymphs, followed by eggs, third nymphs, fourth nymphs, females, and was the lowest in fifth nymphs and males. *ClNC* was expressed at a higher level in first to fourth nymphs than in eggs and fifth nymphs, and exhibited the lowest expression in adults (Figure 1B, C). These results indicated that *ClAC* and *ClNC* were more highly expressed in *C. lividipennis* early nymphs than adults. However, *ClAC* was higher expressed in the head, thorax, and legs than that the integument, midgut, and fat body, while *ClNC* showed no significant transcriptional differences between all studied tissues (Figure 1D, E). In conclusion, *C. lividipennis* had two CDases: one aCDase (ClAC) and one nCDase (ClNC), and both were conserved among hemipteran insect species. The transcription data on *ClAC* and *ClNC* suggested that *ClAC* and *ClNC* played different roles throughout the development of *C. lividipennis*.

3.2 The transcription level of *ClAC* was significantly increased under heat stress

In order to reveal the relationship between sphingolipid metabolism and insect stress responses, we monitored the transcript levels of *ClAC* and *ClNC* after thermal treatment. The transcription of *ClAC* was first upregulated by two times after stressful heat treatment (38 °C) for 6 h, while it decreased to the normal level in the next 24 h (Figure 2A). Compared with the control group reared at the regular temperature (26 °C), the transcription of *ClNC* showed no significant differences under heat stress (38 °C) during all 24-hours treatments (Figure 2B). Meanwhile, the transcription levels of other sphingolipid genes, including *serine palmitoyltransferase* (*ClSPT*), *3-keto dihydrosphingosine reductase* (*ClKDSR*), *sphingolipid delta -desaturase* (*ClDES*), *sphingosine kinase* (*ClSK*), *sphingosine-1-phosphate phosphatase* (*ClS1PP*), *sphingomyelin synthase* (*ClSMS*), *sphingomyelinase* (*ClSMase*), and *ceramide glucosyltransferase* (*ClCGT*), were also monitored after heat treatment. The results showed that except for *ClAC*, *ClKDSR*, and *ClS1PP*, the sphingolipid genes had no significant transcriptional variation after the high-temperature treatment (Supplementary Figure S1). *ClKDSR* and *ClS1PP* were upregulated 1.9 times and 1.7 times, respectively, after stressful heat treatment (38 °C) for 6 h. These data indicated that *ClAC*, compared to *ClNC* or other sphingolipid genes, played more critical roles against heat stress in *C. lividipennis*.

3.3 Knocking down *ClAC* increased the survival rate of *C. lividipennis* under heat stress

In order to investigate the roles of *ClAC* in heat stress response, we knocked down the expression of *ClAC* through RNAi. The

10.3389/fphys.2023.1160846

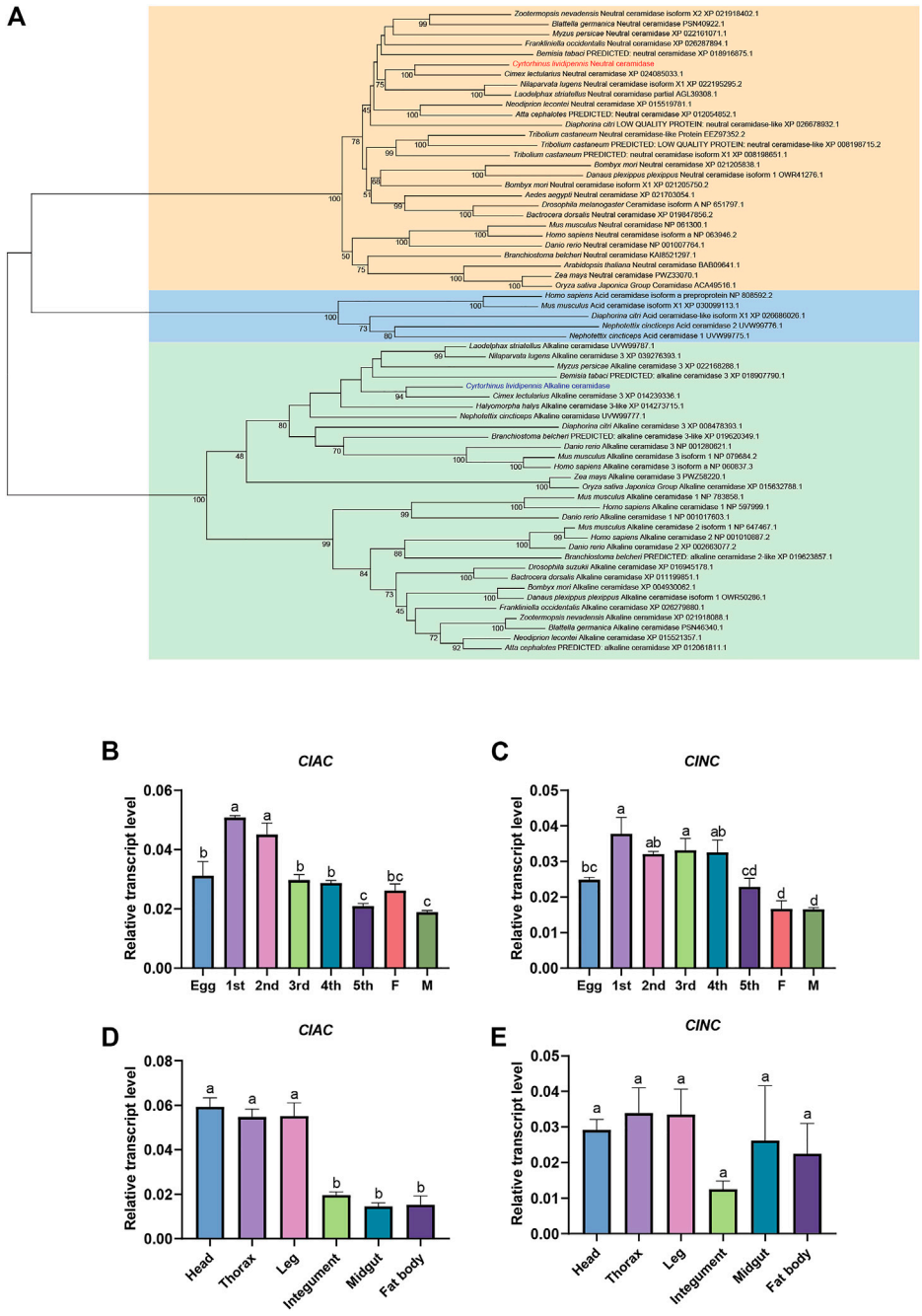

FIGURE 1
Expression patterns and phylogenetic analysis of *C. lividipennis* ceramidase. **(A)** Phylogenetic analysis of ClAC and ClNC with the homologous proteins. The neighbor-joining and Poisson correction methods were used to construct the phylogenetic tree based on ceramidase protein sequences. The bootstrap replication value was set to 1000. Relative transcript levels of *ClAC* **(B)** and *ClNC* **(C)** in eggs, nymphs, and adults. 1st, first instar nymph; 2nd, second instar nymph; 3rd, third instar nymph; 4th, fourth instar nymph; 5th, fifth instar nymph; F, female; M, male. Relative transcript levels *ClAC* **(D)** and *ClNC* **(E)** in different tissues. The error bar indicates the mean ± SEM of three independent biological replicates. Different letters indicate significant differences ($p < 0.05$).

relative transcript levels of *ClAC* were measured at 1 day or 2 days after the injection of dsRNA of *ClAC* (dsAC). Below 26 ˚C or 38 ˚C incubation, the injection of dsAC significantly inhibited the transcription of *ClAC*, and this transcriptional decline could last for two days (Figure 3A, C). Compared with the control group (the dsGFP-injected nymphs), nymphs with lower *ClAC* expression (dsAC-injected nymphs) showed no significant difference in the survival rate at 26 ˚C (Figure 3B). When the rearing temperature was 38 ˚C, the dsAC-injected *C. lividipennis* had higher survival rate than the dsGFP-injected group (Figure 3D). This indicated that lower *ClAC* expression increased the survival rate of *C. lividipennis* nymphs under heat stress. However, the mechanism through

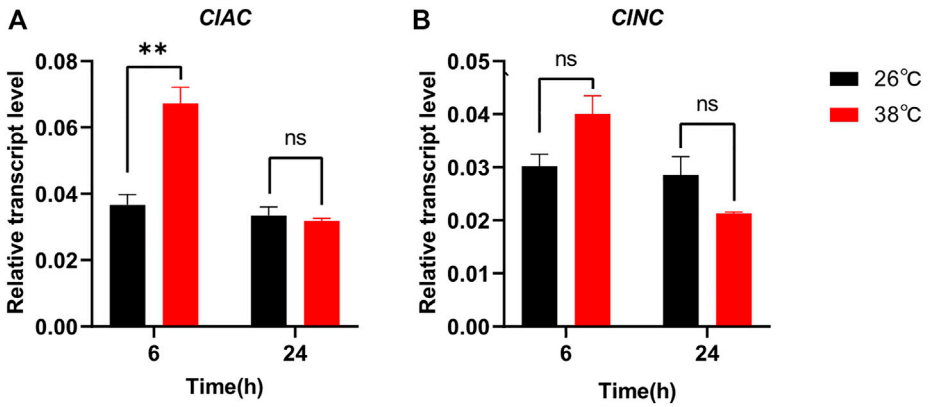

FIGURE 2
Relative transcript levels of *ClAC* **(A)** and *ClNC* **(B)** after thermal treatment. The gene transcription of *C. lividipennis* treated at 38 ˚C was shown by red bars and that at 26 ˚C by black bars. The error bar indicates the mean ± SEM of three independent biological replicates. Significant differences are indicated by "*" at $p<0.05$ and "**" at $p < 0.01$.

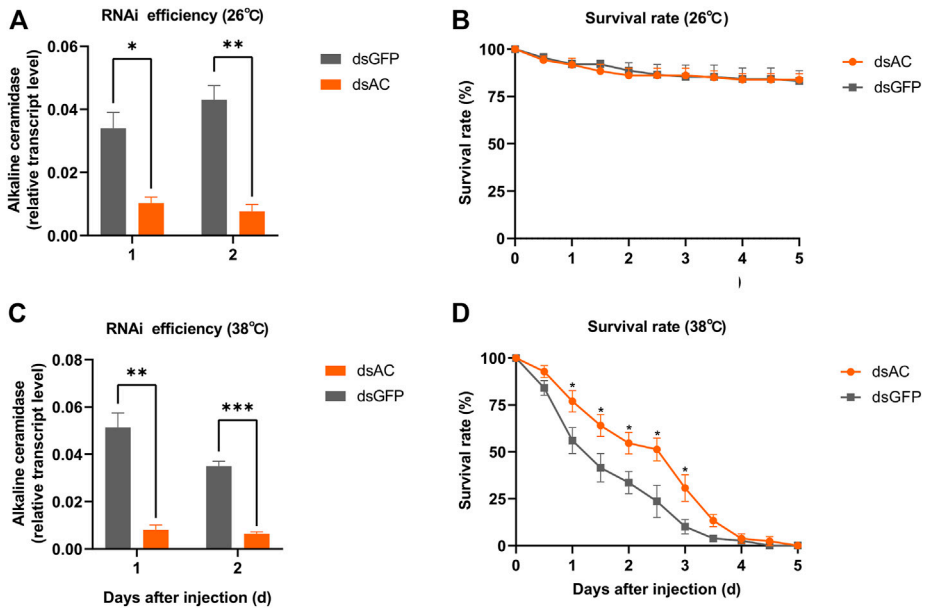

FIGURE 3
Roles of *ClAC* of *C. lividipennis* under heat stress. The relative transcription levels of *ClAC* at 26 ˚C **(A)** and 38 ˚C **(C)** after dsRNA injection. The error bar indicates the mean ± SEM of three independent biological replicates. The survival rate of third nymphs injected with dsAC (orange) and dsGFP (gray) at 12 h intervals below 26 ˚C **(B)** and 38 ˚C **(D)**. dsAC, dsRNA of *ClAC*; dsGFP, dsRNA of *GFP*. The error bar indicates the mean ± SEM of six independent biological replicates (n = 12–16 insects). Significant differences are indicated by "*" at $p < 0.05$, "**" at $p < 0.01$, and "***" at $p < 0.001$.

which *ClAC* mediates the heat stress responses in *C. lividipennis* is still unknown.

3.4 Transcriptome analysis

In order to further understand the mediating role of *ClAC* in heat responses, the transcriptome of third nymphs at the first day after dsRNA injection was analyzed. A total of 1214 differentially expressed genes (DEGs) were detected between the two groups. Compared with dsGFP-injected nymphs, the transcription of 286 genes was upregulated, while that of 928 genes were downregulated in dsAC-injected third nymphs (Figure 4A). KEGG enrichment revealed that the DEGs were mainly involved in peroxisome (nine DEGs), cutin, suberine, and wax biosynthesis (seven DEGs), and longevity regulating pathways (nine DEGs) (Figure 4B). In the longevity regulating pathway, the transcription of *catalase* (*CAT*), *alcohol-*

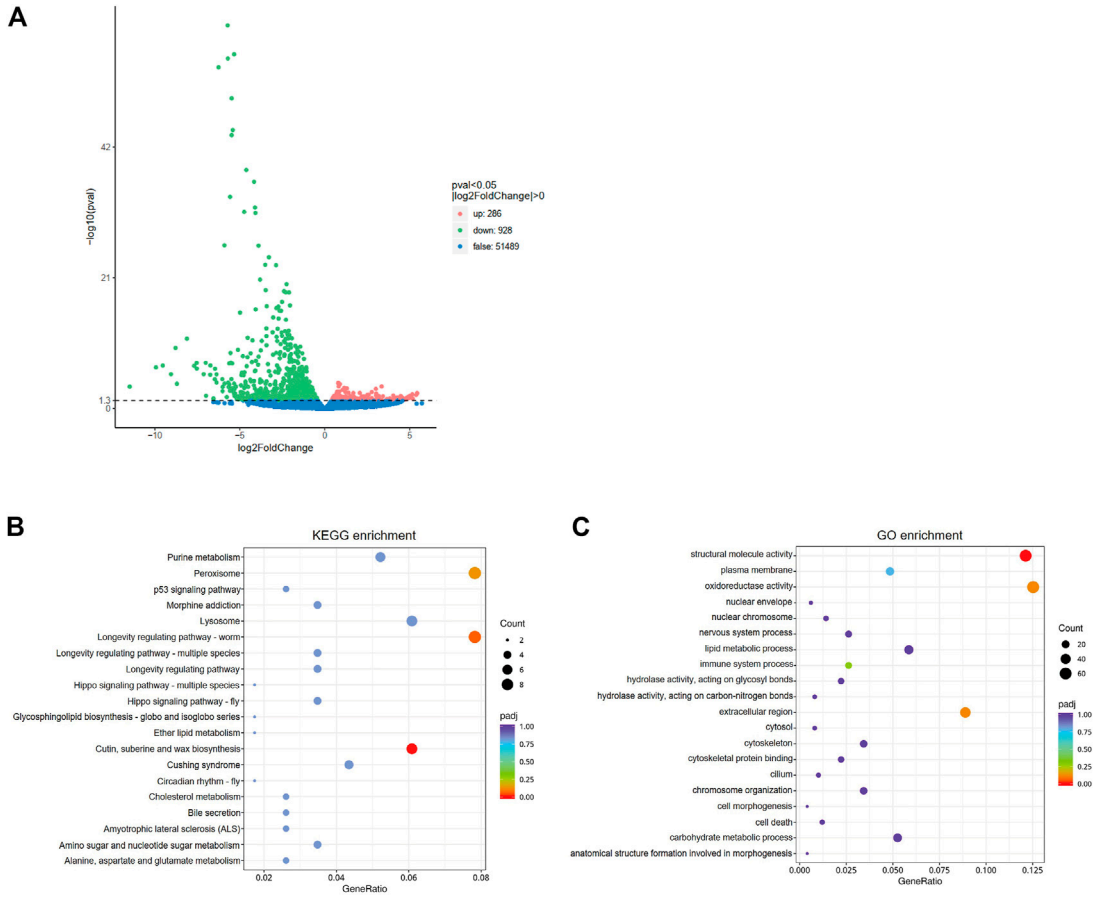

FIGURE 4
Analysis of comparative transcriptome data. **(A)** Volcano plot of differentially expressed genes (DEGs) between dsAC and dsGFP treatments. The red, green, and blue dots represent significantly upregulated genes, significantly downregulated genes, and non-significantly different genes, respectively. DEGs are filtered based on the criteria of padj<0.05 and |log2FoldChange|>0. The most enriched KEGG pathway **(B)** and GO terms **(C)** of DEGs. The sizes of the dots represent the number of DEGs, and the colors represent the enrichment level of DEGs.

forming fatty acyl-CoA reductase (*FARD-1*), and *stearoyl-CoA desaturase* (*FAT-6*) were significantly varied (Supplementary Figure S2). GO enrichment analysis showed that DEGs were mostly clustered in the structural molecule activity, oxidoreductase activity, and extracellular region (Figure 4C). To reveal the relationship between *ClAC* and oxidoreductase, we quantified the transcript levels of oxidoreductase-related genes including two *CAT* (*ClCAT1* and *ClCAT2*), two *glutathione peroxidases* (*ClGPX1* and *ClGPX2*), five *peroxidases* (*ClPOD1 to ClPOD5*), and five *superoxide dismutases* (*ClSOD1 to ClSOD5*). The transcription of *ClCAT1* instead of other genes was significantly increased by 2.2 times in the dsAC-injected third nymphs (Supplementary Figure S3). Moreover, we quantified the relative transcription levels of other sphingolipid genes after knocking down *ClAC*. The qPCR results showed that the transcript level of *ClKDSR* and acid sphingomyelinase *2* (*ClaSMase2*) were upregulated by 1.9 times and 1.3 times, respectively, while other sphingolipid genes had no significant transcription difference between the dsAC-injected nymphs (Supplementary Figure S4).

3.5 Lipid profiling analysis

Lipid profiling was conducted after the transcriptional inhibition of *ClAC* to investigate the metabolic functions of *ClAC* and reveal the network between sphingolipids and other metabolites. A total of 32 differential lipid metabolites (DLMs) were detected, of which 19 DLMs were significantly increased and 13 DLMs were significantly decreased (Supplementary Figure S5A). The KEGG enrichment of DLMs showed that 13 of the 32 DLMs were enriched in the sphingolipid pathway (41%) (Supplementary Figure S5B). These sphingolipids included 10 ceramides (Cer), 1 ceramide-1-phosphate (CerP), and 2 glucosylceramides (GlucoCer). Cer(t18:0/24:0(2OH)) and Cer(t18:0/24:0) were upregulated by 3.9 and 2.1 times, respectively. Ceramides, including Cer(d18:1/18:1), Cer(d18:1/18:0), Cer(d18:1/16:0), Cer(d18:1/24:1), and Cer(d18:1/18:2) were increased by 3.8, 3.8, 5.2, 7.5, and 2.3 times, respectively. The ultra-long chain ceramide Cer(d28:2/31:1(2OH)) was significantly increased by 2.2 times. A trace amount of dihydroceramide Cer(d18:0/16:0(2OH)) (0.23 nmol/g) was detected in dsAC-injected nymphs after high-temperature

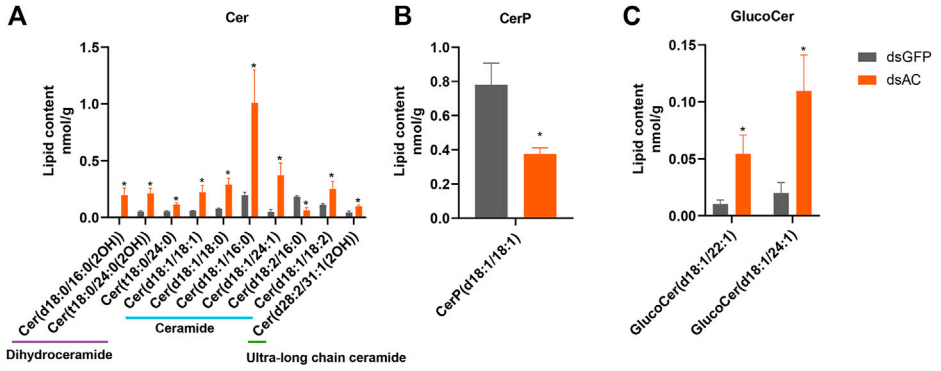

FIGURE 5
Sphingolipid levels after dsAC- and dsGFP-injection. The levels of ceramides **(A)**, ceramide-1-phosphate **(B),** and glucoceramide **(C)** in *C. lividipennis* nymphs after dsAC- and dsGFP-injection. dsAC-injected group, orange column; dsGFP-injected group, gray column. Significant differences are shown by "*" at VIP (VIP ≥ 1) and absolute log2FC (|log2FC| ≥ 1.0).

treatment, while none were observed in the dsGFP-injected nymphs. The levels of Cer(d18:2/16:0) and CerP(d18:1/18:1) were significantly decreased by 41% and 48%, respectively. Meanwhile, GlucoCer(d18:1/22:1) and GlucoCer(d18:1/24:1) were significantly increased by 5.2 and 4.6 times, respectively (Figure 5). In conclusion, most ceramides were increased after *ClAC* inhibition, and *ClAC* mainly mediated the levels of C18 sphingo-based ceramides and their glycosylation derivatives (GlucoCers) in the response to heat stress.

4 Discussion

CDases are classified according to their optimal pH for enzymatic activity (Mao et al., 2001). The types of CDase vary among different organisms. Therefore, it is necessary to investigate the CDase categories for their functional analysis. Five CDase homologs genes have been identified from humans, including one aCDase, one nCDase, and three alCDases (Coant et al., 2017). Two CDases were found in the hemipteran insect *Nephotettix cincticeps* (Zhang et al., 2021). Similar to *C. lividipennis*, the nCDase and alCDase of *Drosophila* (CDase and Dacer) were reported, whereas no aCDase homologs have been identified (Yoshimura et al., 2002; Acharya and Acharya, 2005; Yuan et al., 2011). The nCDase and alCDase were also reported in the hemipteran insect *Laodelphax striatellus* (Zhou et al., 2013; Zhang et al., 2021). The phylogenetic analysis demonstrated that CDases are highly conserved between insects, while the biological function of different type CDases vary among different insect species. The alCDase of *Drosophila* (*Dacer*) was highly expressed in the pupal stage and significantly affected the longevity of *Drosophila* (Yang et al., 2010; Zhang et al., 2019). The nCDase of *Tribolium castaneum* showed high expression in adults, but its biological functions had not been demonstrated (Zhou et al., 2011).The nCDase of BPH was highly expressed in female adults and played essential roles in the reproduction of the insect (Shi et al., 2018; Shi et al., 2021). Different from BPH or *Tribolium castaneum*, both *ClNC* and *ClAC* had high expression in the early nymph stages. The relative transcript levels of genes involved in the *de novo* biosynthetic pathway and sphingomyelinase pathway were tested to observe ceramide metabolism across *C. lividipennis* different developmental stages (Supplementary Figure S6). In the *de novo* biosynthetic pathway, *ClSPT2*, *ClKDSR*, and *ClCS* were highly expressed in eggs, followed by nymphs and females, and exhibited the lowest levels in males. *ClDES* was highly expressed in nymphs, while was lowest in eggs and adults. It suggested high levels of ceramides might synthesize from the *de novo* biosynthetic pathway. In the sphingomyelinase pathway, sphingomyelinases (*ClnSMase*, *ClaSMase1*, and *ClaSMase2*) hydrolyze sphingomyelin to ceramide, while sphingomyelin synthases (*ClSMS*) synthesize ceramide into sphingomyelin (Gault et al., 2010). The relative transcription data showed that *ClnSMase* was highly expressed in eggs and nymphs, and lowest in adults. Coordinated with *ClAC* and *ClNC*, the expression of *ClaSMase1* and *ClaSMase2* were highest in the first nymph, decreased from the first to fifth nymph, and lowest in eggs and adults, indicating ClAC or ClNC might hydrolyze the ceramides produced by ClSMases. Moreover, *ClSMS* was also higher expressed in first nymphs than in other development stages. These results showed that the sphingolipid genes are more highly expressed in early nymph stages than in the adults, indicating the ceramide metabolism was more active in *C. lividipennis* nymphs. In order to maintain a balance of ceramide metabolism, *ClAC* and *ClNC* were supposed to be highly expressed to degrade the excessive ceramides in nymphs. In BPH, the transcript level of nCDase was upregulated under heat stress and knocking down of nCDase increased the female survival rate (Shi et al., 2018). Meanwhile, our results showed that *ClAC* instead of *ClNC* responded to the thermal threat in *C. lividipennis*, suggesting that *ClNC* played different roles together with *ClAC*, and the function of *ClNC* need to be further investigated.

In the present study, we attempted to explain how *ClAC* mediated the high temperature resistance in *C. lividipennis* through transcriptome and lipodomics analysis. For the transcription level, the inhibition of *ClAC* directly mediated the transcription of longevity-related genes and other sphingolipid metabolism-related genes (*ClKDSR* and *ClaSMase2*) to control the hyper thermal responses in *C. lividipennis*. As previously reported, thermal stress induces the generation of reactive oxygen

species (ROS), including superoxide anion ($O2^-$), hydroxyl radicals (^-OH), and hydrogen peroxide (H_2O_2), which can cause oxidative damages and lead to cell death in living organisms (Cui et al., 2011). Antioxidants are necessary to reduce the content of ROS and improve the cellular fitness. Enzymatic antioxidants, such as SOD, CAT, POD, and GPX, have been identified as ROS scavengers (Wang et al., 2001). CAT as one of the primary antioxidant enzymes protects organisms from oxidative damage by catalyzing hydrogen peroxide into water and oxygen (Wang et al., 2001). CAT was also reported to play important roles in the thermal tolerance of insects. Suppressing *CAT* significantly reduced the survival rate of *Myzus persicae* under heat stress (Li et al., 2021). In the whitefly *Bemisia tabaci*, CAT help to adapt to high temperature by scavenging excessive ROS (Liang et al., 2022). The transcript level and activities of *CAT* were enhanced to reduce the production of ROS in mutant *Dacer*, aiding resistance to paraquat-induced oxidative stress (Yang et al., 2010; Zhang et al., 2019). Therefore, we speculated that the high expression of *CAT* after *ClAC* inhibition in *C. lividipennis* might enhance the antioxidant ability of nymphs against the abundant ROS caused by heat stress. However, sphingolipids as the non-enzymatic antioxidants, especially for the ceramides, have been demonstrated to mediate oxidoreductase and maintain cellular redox homeostasis by regulating antioxidant enzymes (García-Caparrós et al., 2021). C2 ceramide inhibited ROS production and cell death in H_2O_2-treated rat primary astrocytes by increasing the expression of phase II antioxidant enzymes, including heme oxygenase-1 (HO-1), NAD(P)H:quinine oxidoreductase 1 (NQO1), and superoxide dismutase (SOD), attesting to the therapeutic potential of C2 ceramide for various oxidative stress-associated diseases (Jung et al., 2016). The treatment of ceramide and ascorbic acid increased the activities of POD and SOD, thus significantly reduced the oxidative damages and maintained the storage quality of strawberries (Zhao et al., 2019). Taken together, the change in ceramide levels after *ClAC* inhibition might mediate the expression of *CAT* and affect the survival rate of *C. lividipennis* under heat stress. Moreover, the *ClKDSR* and *ClaSMase2* closely regulated the ceramide levels through *ClAC* than other sphingolipid gene in *C. lividipennis*.

For the metabolite level, ceramides are not only the essential structural compositions of plasma membranes (Fabri et al., 2020), but also the signaling molecules mediating cellular growth, apoptosis, or death (Okazaki et al., 1998). Ceramides were demonstrated to play important roles in stress tolerance. The loss of the ceramide synthase gene *hyl-2* made *Caenorhabditis elegans* more sensitive to heat shock and anoxia, which indicated that the specific ceramides synthesized by *hyl-2* were required for the stress responses (Menuz et al., 2009). The C16-ceramide synthesized by ceramide synthase 6 had anti-apoptotic roles in tumor cells when encountering endoplasmic reticulum (ER) stress (Senkal et al., 2010). The variation in ceramide species and concentration affected the plasma membrane fluidity. Due to the reduced ceramide levels after ceramide transfer protein (CERT) inhibition, the vesicles were loosely packed, less homogenous, and non-discrete in the plasma membrane of *Dcert* (Rao et al., 2007). The increased fluidity of plasma membrane made *Dcert* mutants more susceptible to oxidative damage (Rao et al., 2007). In addition, ceramides with different acyl-chains had different impact on the membrane biophysical properties. Sandra *et al.* found that saturated ceramides (C16-, C18-, and C24-) were preferred to form gel domains over unsaturated ceramides (C18:1- and C24:1-) in phosphatidylcholine model membranes, and the gel domain formed by C16-ceramide was larger and more stable than that formed by C18-ceramide (Pinto et al., 2011). In the present study, the increased ceramide levels proved the hydrolysis function of *ClAC* as the CDase in *C. lividipennis*. Saturated Cer (d18:1/16:0) was the most abundant species and unsaturated Cer (d18:1/24:1) was the most significantly increased species after *ClAC* inhibition, indicating that Cer (d18:1/16:0) and Cer (d18:1/24:1) were the dominant ceramide species catalyzed by *ClAC*. Cer (d18:1/16:0) reached the highest level compared to other ceramides and might be associated with plasma membrane fluidity. Thus, we proposed that this molecule might play an important role in enhancing the cell membrane stability and in turn upregulate the resistance to oxidative stress.

Most entomology studies have profiled CDases in the model insect *D. melanogaster* and other insect pests such as BPH. However, the CDases profiles have not been studied in natural enemy insects. We found two CDases, *ClAC* and *ClNC*, in *C. lividipennis* and demonstrated that *ClAC* is essential in heat stress response. Metabolically, *ClAC* mediated the ceramide levels and directly regulated the oxidoreductase-related genes at the transcription level. Our results suggested that inhibiting *ClAC* increased the survival rate of *C. lividipennis* nymphs, which was regulated by the alteration of ceramide levels and *ClAC* downstream genes. This study validated the *ClAC* functions and provides valuable information for improving the heat stress tolerance of *C. lividipennis* and other natural enemies of pest insects. Further study should be conducted to construct a sphingolipid gene network to enhance sphingolipid applications in green and sustainable biological pest control.

Data availability statement

The datasets presented in this study can be found in online repositories. The names of the repository/repositories and accession number(s) can be found at: https://www.ncbi.nlm.nih.gov/bioproject/PRJNA932139.

Author contributions

MC, X-XS, and Z-RZ conceived and proposed the idea and designed the study. MC performed the experiments and data analysis. MC and X-XS contributed to writing and reading the manuscript. NW, CZ, Z-YS, and W-WZ provided guidance and assistants for the experiment. All authors contributed to the article and approved the submitted version.

Funding

This work was financially supported by the National Natural Science Foundation of China (Grant Nos. 31901875 and 31871962).

Acknowledgments

The authors thank YL Bai, YD Zhang, and other laboratory mates for their kind cooperation during the research.

Conflict of interest

The authors declare that the research was conducted in the absence of any commercial or financial relationships that could be construed as a potential conflict of interest.

Publisher's note

All claims expressed in this article are solely those of the authors and do not necessarily represent those of their affiliated organizations, or those of the publisher, the editors, and the reviewers. Any product that may be evaluated in this article, or claim that may be made by its manufacturer, is not guaranteed or endorsed by the publisher.

Supplementary material

The Supplementary Material for this article can be found online at: https://www.frontiersin.org/articles/10.3389/fphys.2023.1160846/full#supplementary-material

References

Acharya, U, and Acharya, JK (2005). Enzymes of sphingolipid metabolism in *Drosophila melanogaster*. *Cell Mol Life Sci* 62 (2), 128–42. doi:10.1007/s00018-004-4254-1

Alden, KP, Dhondt-Cordelier, S, McDonald, KL, Reape, TJ, Ng, CK-Y, McCabe, PF, et al. (2011). Sphingolipid long chain base phosphates can regulate apoptotic-like programmed cell death in plants. *Biochemical and Biophysical Research Communications* 410 (3), 574–80. doi:10.1016/j.bbrc.2011.06.028

Bai, YL, Quais, MK, Zhou, WW, and Zhu, ZR (2022). Consequences of elevated temperature on the biology, predation, and competitiveness of two mirid predators in the rice ecosystem. *Journal of Pest Science* 95, 901–16. doi:10.1007/s10340-021-01414-y

Bartke, N, and Hannun, YA (2009). Bioactive sphingolipids: metabolism and function. *Journal of Lipid Research* 50, S91–S96. doi:10.1194/jlr.R800080-JLR200

Bottrell, DG, and Schoenly, KG (2012). Resurrecting the ghost of green revolutions past: The brown planthopper as a recurring threat to high-yielding rice production in tropical Asia. *Journal of Asia-Pacific Entomology* 15 (1), 122–40. doi:10.1016/j.aspen.2011.09.004

Chang, Y, Abe, A, and Shayman, JA (1995). Ceramide formation during heat shock: a potential mediator of alpha B-crystallin transcription. *The Proceedings of the National Academy of Sciences* 92 (26), 12275–9. doi:10.1073/pnas.92.26.12275

Coant, N, Sakamoto, W, Mao, C, and Hannun, YA (2017). Ceramidases, roles in sphingolipid metabolism and in health and disease. *Advances in Biological Regulation* 63, 122–31. doi:10.1016/j.jbior.2016.10.002

Cui, Y, Du, Y, Lu, M, and Qiang, C (2011). Antioxidant responses of *Chilo suppressalis* (Lepidoptera: Pyralidae) larvae exposed to thermal stress. *Journal of Thermal Biology* 36 (5), 292–7. doi:10.1016/j.jtherbio.2011.04.003

Dickson, RC, Nagiec, EE, Skrzypek, M, Tillman, P, Wells, GB, and Lester, RL (1997). Sphingolipids are potential heat stress signals in *Saccharomyces*. *Journal of Biological Chemistry* 272 (48), 30196–200. doi:10.1074/jbc.272.48.30196

Dickson, RC, Sumanasekera, C, and Lester, RL (2006). Functions and metabolism of sphingolipids in *Saccharomyces cerevisiae*. *Progress in Lipid Research* 45 (6), 447–65. doi:10.1016/j.plipres.2006.03.004

Fabri, J, de Sa, NP, Malavazi, I, and Del Poeta, M (2020). The dynamics and role of sphingolipids in eukaryotic organisms upon thermal adaptation. *Progress in Lipid Research* 80, 101063. doi:10.1016/j.plipres.2020.101063

García-Caparrós, P, Filippis, LD, Gul, A, Hasanuzzaman, M, Ozturk, M, Altay, V, et al. (2021). Oxidative Stress and Antioxidant Metabolism under Adverse Environmental Conditions : a Review. *The Botanical Review* 87, 421–66. doi:10.1007/s12229-020-09231-1

Gault, CR, Obeid, LM, and Hannun, YA (2010). "An overview of sphingolipid metabolism: from synthesis to breakdown," in *Sphingolipids as Signaling and Regulatory Molecules* Editors C Chalfant and MD Poeta (New York: Springer New York), 1–23.

Jenkins, GM, Richards, A, Wahl, T, Mao, C, Obeid, L, and Hannun, Y (1997). Involvement of yeast sphingolipids in the heat stress response of *Saccharomyces cerevisiae*. *Journal of Biological Chemistry* 272 (51), 32566–72. doi:10.1074/jbc.272.51.32566

Jung, JS, Choi, MJ, Ko, HM, and Kim, HS (2016). Short-chain C2 ceramide induces heme oxygenase-1 expression by upregulating AMPK and MAPK signaling pathways in rat primary astrocytes. *Neurochemistry International* 94, 39–47. doi:10.1016/j.neuint.2016.02.004

Kitatani, K, Idkowiak-Baldys, J, and Hannun, YA (2008). The sphingolipid salvage pathway in ceramide metabolism and signaling. *Cellular Signalling* 20 (6), 1010–8. doi:10.1016/j.cellsig.2007.12.006

Kozawa, O, Niwa, M, Matsuno, H, Tokuda, H, Miwa, M, Ito, H, et al. (1999). Sphingosine 1-phosphate induces heat shock protein 27 via p38 mitogen-activated protein kinase activation in osteoblasts. *Journal of Bone and Mineral Research* 14 (10), 1761–7. doi:10.1359/jbmr.1999.14.10.1761

Li, MY, Wang, Y, Lei, X, Xu, CT, Wang, DD, Liu, S, et al. (2021). Molecular characterization of a catalase gene from the green peach aphid (*Myzus persicae*). *Archives of Insect Biochemistry and Physiology* 108 (2), e21835. doi:10.1002/arch.21835

Liang, P, Ning, J, Wang, W, Zhu, P, Gui, L, Xie, W, et al. (2022). Catalase promotes whitefly adaptation to high temperature by eliminating reactive oxygen species. *Insect Science* 2022, 1–16. doi:10.1111/1744-7917.13157

Liu, SY, Zhao, J, Hamada, C, Cai, WL, Khan, M, Zou, YL, et al. (2018). Identification of attractants from plant essential oils for *Cyrtorhinus lividipennis*, an important predator of rice planthoppers. *Journal of Pest Science* 92 (2), 769–80. doi:10.1007/s10340-018-1054-1

Lou, Y-G, Zhang, G-R, Zhang, W-Q, Hu, Y, and Zhang, J (2014). Reprint of: Biological control of rice insect pests in China. *Biological Control* 68, 103–16. doi:10.1016/j.biocontrol.2013.09.018

Mao, C, and Obeid, LM (2008). Ceramidases: regulators of cellular responses mediated by ceramide, sphingosine, and sphingosine-1-phosphate. *Biochimica et Biophysica Acta (BBA) - Molecular and Cell Biology of Lipids* 1781 (9), 424–34. doi:10.1016/j.bbalip.2008.06.002

Mao, C, Xu, R, Szulc, ZM, Bielawska, A, Galadari, SH, and Obeid, LM (2001). Cloning and characterization of a novel human alkaline ceramidase. A mammalian enzyme that hydrolyzes phytoceramide. *The Journal of Biological Chemistry* 276 (28), 26577–88. doi:10.1074/jbc.M102818200

Matsumura, M, Urano, S, and Suzuki, Y (2005). "Evaluating augmentative releases of the mirid bug *Cyrtorhinus lividipennis* to suppress brown planthopper *Nilaparvata lugens* in open paddy fields." In. *Rice is Life: Scientific Perspectives for the 21st Century*. (Manila: International Rice Research Institute).

Menuz, V, Howell, KS, Gentina, S, Epstein, S, Riezman, I, Fornallaz-Mulhauser, M, et al. (2009). Protection of *C. elegans* from anoxia by HYL-2 ceramide synthase. *Science* 324 (5925), 381–4. doi:10.1126/science.1168532

Okazaki, T, Kondo, T, Kitano, T, and Tashima, M (1998). Diversity and Complexity of Ceramide Signalling in Apoptosis. *Cellular Signalling* 10 (10), 685–92. doi:10.1016/s0898-6568(98)00035-7

Pinto, SN, Silva, LC, Futerman, AH, and Prieto, M (2011). Effect of ceramide structure on membrane biophysical properties: the role of acyl chain length and unsaturation. *Biochimica et Biophysica Acta* 1808 (11), 2753–60. doi:10.1016/j.bbamem.2011.07.023

Preetha, G, Stanley, J, Suresh, S, and Samiyappan, R (2010). Risk assessment of insecticides used in rice on miridbug, *Cyrtorhinus lividipennis* Reuter, the important predator of brown planthopper, *Nilaparvata lugens* (Stal). *Chemosphere* 80 (5), 498–503. doi:10.1016/j.chemosphere.2010.04.070

Project, IRGS (2005). The map-based sequence of the rice genome. *Nature* 436 (7052), 793–800. doi:10.1038/nature03895

Rao, RP, Yuan, C, Allegood, JC, Rawat, SS, Edwards, MB, Wang, X, et al. (2007). Ceramide transfer protein function is essential for normal oxidative stress response and lifespan. *The Proceedings of the National Academy of Sciences* 104 (27), 11364–9. doi:10.1073/pnas.0705049104

Roth, Z, and Hansen, PJ (2004). Sphingosine 1-phosphate protects bovine oocytes from heat shock during maturation. *Biological of Reproduction* 71 (6), 2072–8. doi:10.1095/biolreprod.104.031989

Senkal, CE, Ponnusamy, S, Bielawski, J, Hannun, YA, and Ogretmen, B (2010). Antiapoptotic roles of ceramide-synthase-6-generated C_{16}-ceramide via selective regulation of the ATF6/CHOP arm of ER-stress-response pathways. *The FASEB Journal* 24 (1), 296–308. doi:10.1096/fj.09-135087

Shi, XX, Huang, YJ, Begum, MA, Zhu, MF, Li, FQ, Zhang, MJ, et al. (2018). A neutral ceramidase, *NlnCDase*, is involved in the stress responses of brown planthopper, *Nilaparvata lugens* (Stal). *Scientific Reports* 8 (1), 1130. doi:10.1038/s41598-018-19219-y

Shi, XX, Zhu, MF, Wang, N, Huang, YJ, Zhang, MJ, Zhang, C, et al. (2021). Neutral Ceramidase Is Required for the Reproduction of Brown Planthopper, *Nilaparvata lugens* (Stal). *Frontiers in Physiology* 12, 629532. doi:10.3389/fphys.2021.629532

Sigsgaard, L (2007). Early season natural control of the brown planthopper, *Nilaparvata lugens*: the contribution and interaction of two spider species and a predatory bug. *Bulletin of Entomological Research* 97 (5), 533–44. doi:10.1017/S0007485307005196

Swift, ML (1997). GraphPad prism, data analysis, and scientific graphing. *Journal of chemical information and computer sciences* 37 (2), 411–2. doi:10.1021/ci960402j

Tang, QY, and Zhang, CX (2013). Data Processing System (DPS) software with experimental design, statistical analysis and data mining developed for use in entomological research. *Insect Science* 20 (2), 254–60. doi:10.1111/j.1744-7917.2012.01519.x

Wang, Y, Oberley, LW, and Murhammer, DW (2001). Antioxidant defense systems of two lipidopteran insect cell lines. *Free Radic Biol Med* 30 (11), 1254–62. doi:10.1016/s0891-5849(01)00520-2

Yang, Q, Gong, ZJ, Zhou, Y, Yuan, JQ, Cheng, JA, Tian, L, et al. (2010). Role of *Drosophila* alkaline ceramidase (*Dacer*) in *Drosophila* development and longevity. *Cell Mol Life Sci* 67 (9), 1477–90. doi:10.1007/s00018-010-0260-7

Yoshimura, Y, Okino, N, Tani, M, and Ito, M (2002). Molecular cloning and characterization of a secretory neutral ceramidase of *Drosophila melanogaster*. *Journal of Biochemical* 132 (2), 229–36. doi:10.1093/oxfordjournals.jbchem.a003215

Young, MM, Kester, M, and Wang, HG (2013). Sphingolipids: regulators of crosstalk between apoptosis and autophagy. *Journal of Lipid Research* 54 (1), 5–19. doi:10.1194/jlr.R031278

Yuan, C, Rao, RP, Jesmin, N, Bamba, T, Nagashima, K, Pascual, A, et al. (2011). CDase is a pan-ceramidase in *Drosophila*. *Molecular Biology of the Cell* 22 (1), 33–43. doi:10.1091/mbc.E10-05-0453

Zhang, CH, Zhang, MJ, Shi, XX, Mao, C, and Zhu, ZR (2019). Alkaline Ceramidase Mediates the Oxidative Stress Response in *Drosophila melanogaster* Through Sphingosine. *Journal of Insect Science* 19 (3), 13. doi:10.1093/jisesa/iez042

Zhang, MJ, Shi, XX, Bai, YL, Zhou, WW, and Zhu, ZR (2021). Sphingolipid composition and metabolism differ in three auchenorrhynchous pests of rice. *Journal of Asia-Pacific Entomology* 24 (3), 772–9. doi:10.1016/j.aspen.2021.06.013

Zhao, HN, Liu, SW, Chen, MG, Li, J, Huang, DD, and Zhu, SH (2019). Synergistic effects of ascorbic acid and plant-derived ceramide to enhance storability and boost antioxidant systems of postharvest strawberries. *Journal of the Science of Food and Agriculture* 99 (14), 6562–71. doi:10.1002/jsfa.9937

Zhou, Y, Lin, XW, Yang, Q, Zhang, YR, Yuan, JQ, Lin, XD, et al. (2011). Molecular cloning and characterization of neutral ceramidase homologue from the red flour beetle, *Tribolium castaneum*. *Biochimie* 93 (7), 1124–31. doi:10.1016/j.biochi.2011.03.009

Zhou, Y, Lin, XW, Zhang, YR, Huang, YJ, Zhang, CH, Yang, Q, et al. (2013). Identification and biochemical characterization of *Laodelphax striatellus* neutral ceramidase. *Insect Molecular Biology* 22 (4), 366–75. doi:10.1111/imb.12028

frontiers | Frontiers in Physiology

TYPE Review
PUBLISHED 19 October 2023
DOI 10.3389/fphys.2023.1238111

OPEN ACCESS

EDITED BY
Bin Tang,
Hangzhou Normal University, China

REVIEWED BY
Muhammad Umair Sial,
University of Agriculture, Faisalabad, Pakistan
Govindaraju Ramkumar,
Indian Institute of Horticultural Research (ICAR), India
Asad Ali,
Abdul Wali Khan University, Pakistan

*CORRESPONDENCE
Nicolas Desneux,
nicolas.desneux@inrae.fr
Xiaoxia Liu,
liuxiaoxia611@cau.edu.cn

RECEIVED 10 June 2023
ACCEPTED 22 September 2023
PUBLISHED 19 October 2023

CITATION
Gul H, Gadratagi BG, Güncan A, Tyagi S, Ullah F, Desneux N and Liu X (2023), Fitness costs of resistance to insecticides in insects.
Front. Physiol. 14:1238111.
doi: 10.3389/fphys.2023.1238111

Fitness costs of resistance to insecticides in insects

Hina Gul [1], Basana Gowda Gadratagi[2], Ali Güncan [3], Saniya Tyagi[4], Farman Ullah [5], Nicolas Desneux[6]* and Xiaoxia Liu[1]*

[1]MARA Key Laboratory of Pest Monitoring and Green Management, Department of Entomology, College of Plant Protection, China Agricultural University, Beijing, China, [2]Division of Crop Protection, ICAR-National Rice Research Institute, Cuttack, Odisha, India, [3]Department of Plant Protection, Faculty of Agriculture, Ordu University, Ordu, Türkiye, [4]Department of Entomology, BRD PG College, Deoria, Uttar Pradesh, India, [5]State Key Laboratory for Managing Biotic and Chemical Threats to the Quality and Safety of Agro-products, Institute of Plant Protection and Microbiology, Zhejiang Academy of Agricultural Sciences, Hangzhou, China, [6]Université Côte d'Azur, INRAE, CNRS, UMR, ISA, Nice, France

The chemical application is considered one of the most crucial methods for controlling insect pests, especially in intensive farming practices. Owing to the chemical application, insect pests are exposed to toxic chemical insecticides along with other stress factors in the environment. Insects require energy and resources for survival and adaptation to cope with these conditions. Also, insects use behavioral, physiological, and genetic mechanisms to combat stressors, like new environments, which may include chemicals insecticides. Sometimes, the continuous selection pressure of insecticides is metabolically costly, which leads to resistance development through constitutive upregulation of detoxification genes and/or target-site mutations. These actions are costly and can potentially affect the biological traits, including development and reproduction parameters and other key variables that ultimately affect the overall fitness of insects. This review synthesizes published in-depth information on fitness costs induced by insecticide resistance in insect pests in the past decade. It thereby highlights the insecticides resistant to insect populations that might help design integrated pest management (IPM) programs for controlling the spread of resistant populations.

KEYWORDS

integrated pest management, selection pressure, ecotoxicology, toxins, fitness costs, life table, biological traits

1 Introduction

Insect pests cause severe agricultural damage, leading to high financial and environmental costs worldwide. Despite multiple possible alternative pest management methods (Lu et al., 2012; Gurr et al., 2017; Jactel et al., 2019; Verheggen et al., 2022), chemical pesticides are usually the most commonly used method to control insect pests (Deguine et al., 2021). However, under continuous selection pressure of chemical insecticides, insects have developed resistance against different groups of insecticides (Koo et al., 2014; Ma et al., 2019; Ullah et al., 2020a; Pires et al., 2021; Li et al., 2022a). Fitness is the quantitative representation of an organism reproductive success. Fitness costs are a trade-off between biological traits in which alleles confer higher fitness in one condition, such as selection pressure to insecticides, while reduced fitness in another condition, such as without insecticide selection (Ullah et al., 2020b; Singarayan et al., 2021).

Fitness costs related to insecticide resistance occur in insects when the development of insecticide resistance is accompanied by energy costs or significant physiological disadvantages that affect the fitness of the target insects compared to their susceptible counterparts in the population (Kliot and Ghanim, 2012). Fitness costs are linked not only with insecticide resistance development but also with several other phenomena. Fitness costs are associated when insects adapt to new habitats, combat different stressors, and adapt to toxic secondary metabolites of new host plants (Kliot and Ghanim, 2012). The most common mechanisms of insecticide resistance included 1) metabolic detoxification due to the expression of metabolic genes, 2) target site mutations, 3) decreased penetration/increased excretion, and 4) behavioral resistance. The upregulation of detoxification genes is linked with insecticide resistance, resulting in fitness costs following the resource and energy reallocation due to the expense of metabolic and developmental processes (Grigoraki et al., 2017).

The genes responsible for resistance may be of homozygous (RR) or heterozygous (Rr) genotype. It is essential to know the genetic background of the resistance genes to study the fitness costs attached to it. Since heterozygotes may be relatively prevalent in the early phases of pesticide selection, the fitness costs in heterozygote-resistant strains are more important than in the homozygote-resistant population. It is necessary to conduct further research on the dominance of any putative pleiotropic effects of resistance in these heterozygous individuals [for details, check these key documents 15,16]. Under certain conditions, fitness costs in an insecticide-resistant insect pest population showed reduced survival and reproduction and slowed the evolution of resistance (Ullah et al., 2020c). The fitness of insecticide-resistant populations is impacted by the development of insecticide resistance, which is often associated with a high energetic cost (Grigoraki et al., 2017). Several studies reported fitness costs associated with different classes of insecticide resistance on insect pest species such as *Thrips hawaiiensis*, *Aphis gossypii*, *Nilaparvata lugens*, *Plutella xylostella*, *Spodoptera* spp., *Aedes* spp., *Bradysia odoriphaga*, and *Musca domestica* (Abbas et al., 2016a; Steinbach et al., 2017; Zhang et al., 2018a; Fu et al., 2018; Ullah et al., 2020c; Shan et al., 2021; Ullah et al., 2021) (Figure 1). To better understand the manifestation of these fitness costs and the scope of this phenomena, Freeman et al. (2021) did a detailed review of literature on studies that examined the fitness costs of pesticide resistance and examined each class of insecticide individually and collectively. In 60% of the trials, pesticide resistance has a cost, especially for reversion of resistance and reproduction measurements, according to more than 170 papers on the fitness costs of insecticide resistance. There were variances among insecticide classes, with fitness costs being more seldom observed for organochlorines.

Our current review presents the body of literature on fitness costs due to insecticide resistance in a few important insect orders along with fitness advantage over a decade. Though a few reviews have been published on fitness cost associated with insecticide resistance, they are mostly based on the class of insecticides (Bass, 2017; Freeman et al., 2021). In-depth knowledge about the fitness costs induced by any insecticide might help design an integrated pest management (IPM) program to control the spread of a resistant population of insect pests. In this review, we have structured our discussion through insect orders to explore the fitness costs induced by various class of insecticides based on studies conducted over the past decade.

2 Blattodea

Blattodea contains about 3,500 to 4,000 species of cockroaches identified, which can be divided into five families: Cryptocercidae, Blattidae, Blattellidae, Blaberidae, and Polyphagidae. The most important pest specie was the German cockroach, *Blattella germanica*. Its extraordinary ability to acquire resistance to harmful insecticides was a prime example of adaptive evolution. The most frequent approach to control *B. germanica* in homes, flats, and commercial kitchens was to apply insecticides (Dingha et al., 2013; Wang et al., 2019a). *Blattella germanica* transmits several microorganisms (Lee et al., 2021), causes allergic reactions (Eggleston, 2017; Wang et al., 2020a; Lee et al., 2021), and poses a health risk because it serves as a mechanical vector for a variety of harmful bacteria (Brenner and Kramer, 2019). Many factors, including physiological resistance to the insecticide, cross-resistance (Abbas and Shad, 2015), and contamination of the insecticide deposit, can affect the effectiveness of insecticides used to control *B. germanica* (Lee et al., 2022). During resistance onset, the fitness cost may be high, but as resistance advances with constant selection pressure, these costs may be reduced or eliminated due to the replacement of high energetic resistance alleles with lesser ones or due to the selection of modifier alleles that reduce the fitness costs (Basit, 2019).

Insects with resistant genotypes pay an energetic cost that reduces their fitness compared to susceptible conspecifics. Hemiptera, Diptera, Coleoptera, and Lepidoptera have all been observed with this trait (Kliot and Ghanim, 2012; Mengoni and Alzogaray, 2018; Castellanos et al., 2019). Compared to other resistant strains of German cockroach, certain pyrethrin- and allethrin-resistant cockroaches have an irregular pattern of development among the nymphs and a lower total fecundity (Zhang and Yang, 2019). Insecticide-resistance is typically connected with life history costs that prevent it from being fixed. Fitness-related costs had delayed developmental stages and shorter adult lifespan (Hardstone et al., 2014). Experimental conditions, including feeding, relative humidity and temperature, strain origin, aggregation effects, and pesticide category, may influence cost variations (Zhang et al., 2017; Wang et al., 2020b; Chong et al., 2022). Jensen et al. (2016) showed that indoxacarb-selected cockroaches had poorer survival to maturity, decreased adult body size, and prolonged development time with reinforcing interactions, showing that poor nutritional condition might increase the cost of pesticide adaptation and fitness costs via interactions with insecticide resistance.

3 Thysanoptera

Like other insect orders, insecticide resistance among thrips species poses a significant challenge to effective pest management strategies. Understanding the interplay between insecticide resistance and associated fitness costs is critical. The studies show case diverse insights into the dynamics of insecticide resistance. The study by Nakao et al. (2014) investigated the developmental and ovipositional behaviors of pyrethroid-resistant and pyrethroid-susceptible strains of

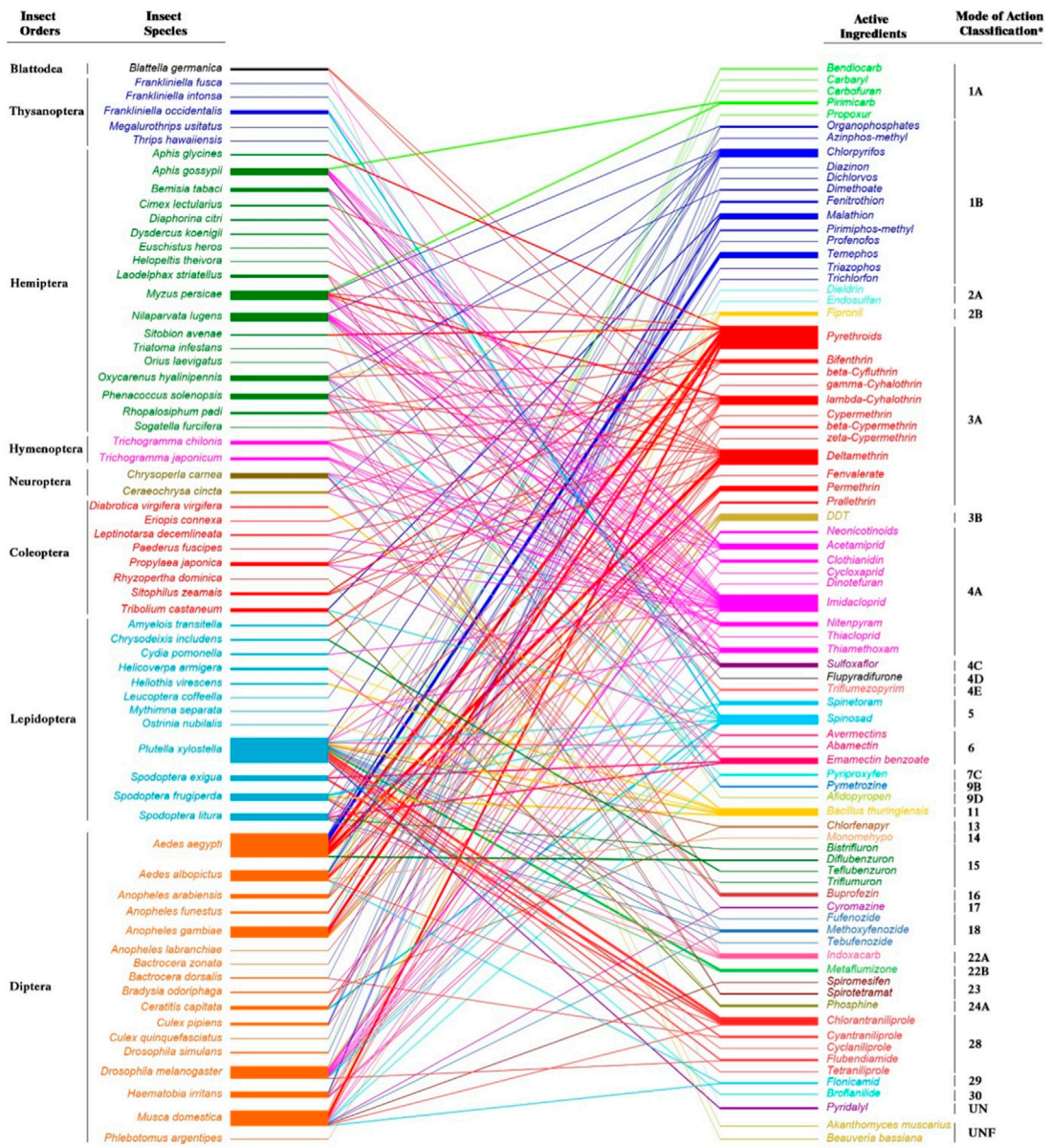

FIGURE 1
Studies about fitness costs of insect pest species associated with different insecticides with Mode of Action Classification. The width of the bars denote the number of studies in the literature of the last decade reviewed from Science Citation Index Expanded within the Clarivate Web of Science database (https://www.webofscience.com) using "insecticide", "fitness", and "resistance" as keywords. *According to the Insecticide Resistance Action Committee (IRAC, https://irac-online.org/, Edition: 10.5, March 2023) Mode of Action Classification Groups: 1: Acetylcholinesterase (AChE) inhibitors; 1A Carbamates, 1B Organophosphates. 2: GABA-gated chloride channel blockers; 2A Cyclodieneorganochlorines, 2B Phenylpyrazoles. 3: Sodium channel modulators; 3A Pyrethroids, 3B DDT, Methoxychlor. 4: Nicotinic acetylcholine receptor (nAChR) competitive modulators; 4A Neonicotinoids, 4C Sulfoximines, 4D Butenolides, 4E Mesoionics. 5: Nicotinic acetylcholinereceptor(nAChR) allostericmodulators–Site I; Spinosyns. 6: Glutamate-gatedchloride channel (GluCl) allostericmodulators; Avermectins, Milbemycins. 7: Juvenile hormone mimics; 7C Pyriproxyfen. 9: Chordotonal organ TRPV channel modulators; 9B Pyridine azomethine derivatives, 9D Pyropenes. 11: Microbial disruptors of insect midgut membranes; *11 Bacillus thuringiensis*. 13: Uncouplers of oxidative phosphorylation via disruption of the proton gradient; Pyrroles, Dinitrophenols, Sulfluramid. 14: Nicotinic acetylcholine receptor (nAChR) channel blockers; Nereistoxin analogues. 15: Inhibitors of chitin biosynthesis affecting CHS1; Benzoylureas. 16: Inhibitors of chitin biosynthesis, type 1; Buprofezin. 17: Moulting disruptors, Dipteran; Cyromazine. 18: Ecdysone receptor agonists; Diacylhydrazines. 22: Voltage-dependent sodium channel blockers; 22A Oxadiazines, 22B Semicarbazones. 23: Inhibitors of acetyl CoA carboxylase; Tetronic and Tetramicacid derivatives. 24: Mitochondrial complex IV electron transport inhibitors; 24A Phosphides. 28: Ryanodine receptor modulators; Diamides. 29: Chordotonal organ nicotinamidase inhibitors; Flonicamid. 30: GABA-gated chloride channel allosteric modulators; Meta-diamides, Isoxazolines. UN: Compounds of unknown or uncertain MoA; Pyridalyl. UNF: Fungal agents.

Thrips tabaci (Thysanoptera: Thripidae), on different persimmon and green bean varieties. Despite differences in pyrethroid susceptibility, the pyrethroid-resistant strains had lower fecundity than susceptible strains on green bean leaves, suggesting that resistance did not substantially affect other aspects of pest behavior in commercial persimmon orchards. Gao et al. (2014) enrich the discourse by unraveling

cross-resistance patterns and the biochemical mechanisms driving resistance to thiamethoxam in *F. occidentalis* (Thysanoptera: Thripidae), displaying low survival in first instar larvae, pupation percentage and fecundity in resistant ones. Li et al. (2017) reveal that spinosad resistance can lead to decreased fecundity and reduced body size and affect the feeding behaviors of *F. occidentalis*. Wan et al. (2021), delve into the intricate relationship between spinosad resistance and transmission efficiency of Tomato spotted wilt orthotospovirus (TSWV) by *F. occidentalis*, further underlining the potential impacts of resistance on vector competence and concluded that spinosad resistance in *F. occidentalis* reduced pupation rate, sex ratio and male longevity and increased vector competence. On the other hand, the influence of host plants emerges as a crucial factor in thrips resistance dynamics. Li et al. (2022b) highlight how spinetoram resistance may alter the host preference of *F. occidentalis*, potentially driven by shifts in detoxification enzyme activities. In addition, cost of spinetoram resistance leads shorter preadult and adult longevity in tested hosts, i.e., broader bean and eggplant. Fu et al. (2018), highlights the rapid increase in resistance to spinetoram in *Thrips hawaiiensis* (Thysanoptera: Thripidae), accompanied by a decline in resistance ratios over generations. Similarly, Hua et al. (2023), demonstrate how spinosad resistance in *F. occidentalis* (Thysanoptera: Thripidae), incurs fitness costs, affecting fecundity and ovary development. Furthermore, the complexity of resistance in pest management strategies is evident in the study by Chappell et al. (2019), which demonstrates that fitness costs of imidacloprid resistance in *Frankliniella fusca* (Thysanoptera: Thripidae), may not necessarily impede resistance evolution alone, as consistent insecticide use can offset these costs. The study by Wang et al. (2020c) determined that the *F. occidentalis*, exhibited high susceptibility to the insecticide pyridalyl in field populations from 2016 to 2017 in China. However, a laboratory-selected pyridalyl-resistant strain showed no cross-resistance to other insecticides, and its resistance was inhibited by piperonyl butoxide and diethyl maleate. The pyridaly resistant *F. occidentalis* strain had lower pupation and emergence rates and reduced female fecundity, indicating resistance-related fitness costs. The study by Fu et al. (2022) found that the extensive use of spinetoram in controlling two closely related thrips, *Megalurothrips usitatus* and *F. intonsa* (Thysanoptera: Thripidae), led to the displacement of *F. intonsa* by *M. usitatus* on cowpea crops due to interspecific competition. Exposure to spinetoram favored *M. usitatus* dominance, and the development of higher resistance to spinetoram in *M. usitatus* compared to *F. intonsa* suggests a connection between resistance evolution and competitive interactions. After laboratory selection, both species showed increased resistance, with *M. usitatus* having higher resistance and no associated fitness costs, potentially explaining the recent dominance shift. In contrast, spinetoram resistant *F. intonsa* showed a lower net reproduction rate, intrinsic rate of increase and finite rate of increase.

By synthesizing insights from these diverse studies, the complicated relationships between resistance, fitness costs, and host interactions are paramount in devising effective pest management strategies against thrips pest species.

4 Hemiptera

Hemipterans suck the sap from plants' vascular system, which can lead to the yellowing, drying and wilting of plants. Additionally, in the case of planthoppers and leafhoppers, a more severe symptom known as "hopper burn" can be observed if the extent of damage is high. These insects also serve as vectors for several plant diseases, enabling their control as a critical component in disease management (Shi et al., 2014). Hemipterans, such as aphids, whiteflies, and plantoppers, are generally of small size with a short life cycle and high fecundity, which enable the use of insecticide as the most feasible option for their control. However, more frequent use of insecticides develops resistance in hemipterans against them with varying effects on their fitness traits. Resistance build-up and associated fitness trade-offs in insects have been extensively studied individually for various insecticidal groups, such as organophosphates, carbamates, pyrethroids, and neonicotinoids (Saeed et al., 2021; Ullah et al., 2022; Valmorbida et al., 2022; Walsh et al., 2022). The common finding in all of the above studies is that after cessation of selection pressure of insecticides, which leads to the reversion of resistance, the earlier resistant insect strains could compensate for the reduced biological fitness in more or less time. Likewise, recently, such studies have also been documented for combination insecticides. In a study on cabbage aphid, *Brevicoryne brassicae* in Iran, exposure to multiple sublethal doses of thiamethoxam-lambda cyhalothrin, a combination of a neonicotinoid and a pyrethroid, had shown an adverse effect on their offsprings' reproductive rate, survival rate, and fecundity. This could be due to increased toxicity, leading to high selection pressure on insects, which was apparent only from the first generation (Mahmoodi et al., 2020). One of the most devastating hemipterans, i.e., whitefly, *Bemisia tabaci*, showed slow development, low survival, and reduced egg laying due to its resistance to acetamiprid (Roy et al., 2019). The extended nymphal period was also reported due to resistance to pyriproxyfen, an insect growth regulator (Singh and Chandi, 2019). In Korea, there is a prevalence of genetic displacement of cluster 2 over 1 in *B. tabaci* populations primarily based on its high resistance levels to thiamethoxam compared to cluster 1. Higher LC_{50} values of the cluster 2 population for thiamethoxam are due to the metabolic factor rendered by elevated cytochrome P450 activity (Park et al., 2021).

The brown planthopper, *N. lugens*, is the most significant insect pest in the world's main rice-growing areas. It has gained resistance to many insecticide classes over time (Malathi et al., 2017). A recent example is its resistance to triflumezopyrim, which inhibits the nicotinic acetylcholine receptor and belongs to a new family of mesoionic insecticides (Liao et al., 2021; Qin et al., 2021). All the important biological parameters, such as lifespan, female adult period, fecundity, and hatchability, were decreased in the resistant strain compared to the susceptible strain, resulting in a relative fitness of 0.62 (Qin et al., 2021). The pre-adult time and total pre-oviposition duration were increased. Additionally, there was a general decline in the resistant population (Qin et al., 2021). Similar patterns of decline in the biological fitness of *N. lugens* strains resistant to imidacloprid (Sanada-Morimura et al., 2019), nitenpyram (Zhang et al., 2018a), sulfoxaflor (Liao et al., 2019), and clothianidin (Jin et al., 2021) were also observed. The reduced fitness of insects in the presence of insecticides will slow down resistance build-up. However, in the case of hemipterans, their high fecundity and shorter life cycle will aid in developing resistance

quickly and presumably regain their full health potential rapidly in the insecticide-free environment (Qin et al., 2021).

5 Hymenoptera

As pesticides are an integral part of the crop ecosystem to manage agricultural pests and diseases, they can have a variety of direct (lethal) and indirect (sublethal) effects on target and non-target organisms (Ndakidemi et al., 2016). The adverse consequences of insecticides on natural enemies are frequently cited as a major barrier to implementing Integrated Pest Management (IPM) programs (Ndakidemi et al., 2016). Although pesticide resistance in beneficial insects was less understood, it has been established in several species (Biondi et al., 2015; Sparks and Nauen, 2015; Lommen et al., 2017; Overton et al., 2021; Schmidt-Jeffris et al., 2021; Tanda et al., 2022). Natural enemies are more vulnerable to pesticides than herbivorous insect pests (Bielza et al., 2020). Parasitic Hymenoptera is less likely to develop resistance compared to other insects (Bielza et al., 2016). *Trichogramma* spp. egg parasitoids are among the most important biological control agents of Lepidoptera pests globally and enable controlling insect pests before they damage plants (Sithanantham et al., 2013; El-Arnaouty et al., 2014; Huang et al., 2020; Zang et al., 2021; Zhang et al., 2021). The use of *Trichogramma* wasps has been developed through extensive applied research (Wang et al., 2014; Du et al., 2018; Hou et al., 2018; Wang et al., 2019b; Gontijo et al., 2019; Guo et al., 2019; Wang et al., 2021; Zhang et al., 2021), their use being mostly through artificial inundative releases (El-Arnaouty et al., 2014; Huang et al., 2020; Zang et al., 2021), although natural parasitism has been reported for possible conservation biological control (Biondi et al., 2013; Bagheri et al., 2019; Salas Gervassio et al., 2019). They are used for biological control of many insect pests on various crops, e.g., vegetables and tree crops, and stored products (Chailleux et al., 2013; Marchioro et al., 2015; Khan and Ruberson, 2017; Gontijo et al., 2019; Qu et al., 2020; Zang et al., 2021).

Based on numerous laboratory and field investigations, most studies have focused on sublethal effects rather than examining the fitness costs of insecticides in Hymenopteran insects. In the study by Xie et al. (2022) the researchers aimed to develop insecticide-tolerant strains of *Trichogramma* parasitoids, which are used as biocontrol agents against lepidopteran rice pests in rice fields. They exposed *Trichogramma japonicum* and *Trichogramma chilonis* to sublethal doses of imidacloprid, thiamethoxam, buprofezin, and nitenpyram targeting rice planthoppers in a laboratory setting. *Trichogramma japonicum* showed the highest increase in tolerance to imidacloprid after successive treatments, and *T. chilonis* also displayed increased tolerance to these insecticides. Over time, the emergence and deformity rates of the treated *Trichogramma* species gradually recovered, and the fecundity of *T. japonicum* treated with thiamethoxam was significantly higher compared to the control, while *T. chilonis* treated with certain insecticides exhibited differences in fecundity. The study suggests that developing insecticide-tolerant *Trichogramma* strains, especially pairing *T. japonicum* with imidacloprid, could enhance the integration of biological control methods with traditional chemical strategies in integrated pest management for rice agroecosystems.

Trichogramma spp. wasps are particularly vulnerable to most broad-spectrum insecticides (Cheng et al., 2018). As a result, pesticides and *Trichogramma* spp. have traditionally been thought to be incompatible as pesticides negatively impact the parasitoids' fitness in agroecosystems. An example of this scenario was documented by Tabebordbar et al. (2020) that Metasystox, dichlorodiphenyltrichloroethane (DDT), and Metasystox negatively affected *Trichogramma evanescens* by decreasing longevity and fecundity, as well as increasing adult mortality after their emergence.

Several novel insecticides, e.g., methoxyfenozide, tebufenozide and spinosad, have been developed and tested against lepidopteran pests in cotton to overcome insecticide resistance, support natural enemies, and reduce health concerns (Sifakis et al., 2017). The effect of certain pesticides on emergence appears to be associated with the preimaginal development stage at the time of exposure (Amandeep et al., 2012; Khan and Ruberson, 2017).

The impact of resistant pest populations on natural enemies in the action of pesticides has yet to be determined. The interference identified in the performance of *T. pretiosum* emphasizes the necessity of understanding how improper insecticide use can harm the fitness of the natural enemy. On the other hand, *T. pretiosum* can still be utilized in IPM management programs since it maintains its effectiveness even in the presence of resistant populations in the field whenever host eggs of *S. frugiperda* populations had some resistance when over six generations of exposure to metaflumizone, the biological activity of *T. pretiosum* was decreased (Barbosa et al., 2021). It was discovered that eggs originating from the resistant population had lower parasitism percentages, emergence, and parasitoids/eggs, but females from the susceptible population survived longer than those from the resistant population. However, neither the sex ratio nor the male longevity was altered.

Pesticide resistance results from mutations that replace alleles, and the selection pressure (Van Leeuwen et al., 2020) enhances the genotypic diversity of the original population. Due to its intricacy, the co-evolutionary process that combines parasitoids and hosts in the field (Martinez et al., 2014) cannot be examined in laboratory settings. Consequently, the interference in the examined biological parameters was at its greatest. When the host may acquire physiological resistance, the parasitoids evolve tactics to combat this resistance (George et al., 2021).

Cotesia plutellae was a prominent natural enemy of the diamondback moth. *P. xylostella* had developed extensive resistance to various insecticides, including microbiological Bt formulations, and had been a devastating pest of brassica crops (Sparks et al., 2012; Li et al., 2016; Lin et al., 2020; Banazeer et al., 2021). In laboratory investigations, the effects of Bt plants on a larval endoparasitoid of both Bt-susceptible and Bt-resistant *P. xylostella* strains were compared to the deadly effects of Cry1Ac-expressing transgenic oilseed rape (*Brassica napus*) on the endoparasitoid, *Cotesia plutellae*. Resistant *P. xylostella* larvae feeding on highly resistant Bt plants were ideal hosts for *C. plutellae* growth.

The resistance mechanisms in aphids have been linked to fitness costs that are both inhibitory and pleiotropic. But sometimes, parasitoids can take advantage of trade-offs in the insecticide-resistant clone to counteract insecticide resistance. For example, the parasitization (mummification) rate of *Aphidius ervi* towards the insecticide-resistant (knockdown resistance (kdr) Sitobion avenae) clones was noticeably higher than their insecticide-susceptible

counterparts (Sitobion avenae). This might be due to the smaller heterozygous (kdr-SR) clones' ineffective warding behavior (Jackson et al., 2020). This is consistent with Onstad and Flexner (2023), who discovered that insecticide-resistant peach potato aphids (*Myzus persicae*) were mummified at a higher rate than their insecticide susceptible counterparts. When selected for by a higher trophic level, pesticide resistance genes sometimes cause maladaptive behaviors that have a detrimental pleiotropic effect on fitness. For example, eight parthenogenetic *M. persicae* clones (representing various pesticide resistance genotypes) were subjected to alarm pheromones to confirm the degree of response. The clones were then exposed to adult female parasitoids, *Diaeretiella rapae,* both in the presence and absence of measured amounts of alarm pheromone. Results exhibited that clones with a consistently high alarm response (insecticide-susceptible forms) when compared to aphids with a low alarm response (insecticide-resistant forms), displayed a variety of behaviors during and after parasitoid attack that were significantly associated with greater survival (avoidance of parasitism) (Onstad and Flexner, 2023).

6 Neuroptera

The detrimental consequences of insecticide use on natural enemies have been a significant focal point within pest management science. Lacewings stand out as crucial natural predators because of their capability to control a wide range of pests and are naturally distributed extensively across various agricultural production areas. Using insecticide-resistant natural enemies can potentially suppress pests in numerous cropping systems where chemical pest management is a prevalent approach. The primary focus of insecticide resistance research has been directed towards common green lacewing, *Chrysoperla carnea* (Neuroptera: Chrysopidae).

For example, a study by Mansoor et al. (2013) involved selecting a field-collected population of the common green lacewing *C. carnea* for resistance to the insecticide emamectin benzoate in a laboratory setting. The emamectin benzoate resistant *C. carnea* population demonstrated higher emergence rates in adults, increased fecundity, egg hatchability, and shorter developmental times than the susceptible population. Population growth rates, including intrinsic rate of increase and biotic potential, were also higher in the emamectin benzoate-selected population than in the susceptible population. Another study by Abbas et al. (2014) involved selecting a field-collected population of the common green lacewing *C. carnea* with the insecticide spinosad, and the spinosad-resistant population exhibited a relative fitness advantage, with higher adult emergence rates, fecundity, hatchability, and shorter developmental times as a fitness cost of resistance. The study also found that the spinosad-selected population displayed higher growth rates and biotic potential compared to a susceptible laboratory population. Rodrigo et al. (2019) investigated the susceptibility of different lacewing species, including *Ceraeochrysa cincta*, *Ceraeochrysa cubana*, *Ceraeochrysa paraguaria*, and *Chrysoperla externa* (Neuroptera: Chrysopidae), to bifenthrin, chlorpyrifos, and imidacloprid insecticides in citrus orchards managed under both organic and conventional pest management systems. They found that *C. cincta* populations from conventional management systems had lower egg-hatching rates but faster life cycles, i.e., shorter egg and larval developmental times and higher population growth. Mansoor and Shad (2022a) investigated the resistance development potential of the field-collected *C. carnea*, when subjected to selection with cyromazine and methoxyfenozide, and the results of the study indicate no significant difference between sex ratios and adult mortality in cyromazine and methoxyfenozide selected strains. The studies about cross-resistance patterns and realized heritability also hold significant importance. This exploration spans diverse insecticide classes—like acetamiprid, buprofezin, methoxyfenozide, and nitenpyram—evaluated for their effects on *C. carnea* to understand resistance mechanisms (Mansoor et al., 2017; Mansoor and Shad, 2019; Mansoor and Shad, 2020; Mansoor and Shad, 2022b).

These studies have set the stage for using insecticide-resistant lacewings as a valuable biocontrol agent in controlling important crop pests, especially in cases where chemicals are currently necessary.

7 Coleoptera

Despite having over 250,000 species, the Coleoptera order does not include as many agricultural pests as Hemiptera and Lepidoptera. Regardless, pests in this family do enormous damage to agriculture and forestry throughout their life cycles, both as larvae and adults (Patole, 2017). Many of these were pests of storage, wreaking havoc on grain and other seed silos, and also dried plant material. In tropical regions, the maize weevil, *Sitophilus zeamais* Motschulsky (Coleoptera: Curculionidae), is an important pest of stored grains, primarily maize (Ojo and Omoloye, 2016; Nwosu, 2018). Insecticide resistance and fitness studies of this insect have been a major concern all-round year due to the overreliance on pesticides for control (Haddi et al., 2018).

The fitness costs induced by insecticide resistance are a typical assumption in insecticide resistance evolution models. (Vézilier et al., 2013; Cordeiro et al., 2017; Guedes et al., 2017). These costs are most likely the result of an energy imbalance, which diverts energy away from the core physiological processes and towards pesticide resistance (Von Santos et al., 2013; Cordeiro et al., 2017). Despite this, fitness losses associated with pesticide resistance in the absence of insecticides are not ubiquitous, although they often occur (Vézilier et al., 2013). Demographic and competition research using insecticide-susceptible and insecticide-resistant maize weevil strains revealed that certain strains have fitness costs associated with pesticide resistance while others do not (Guedes et al., 2017).

According to Guedes et al. (2009), in both areas, the behavioral patterns of insect movement varied with the population. The different locomotor patterns observed among *S. zeamais* populations may be attributed to the difference in insect metabolism, which can affect insect behavior. However, these differences were not related to the activity of carbohydrate and lipid-metabolizing enzymes in the maize weevil populations studied. Greater body mass and energy storage in *S. zeamais,* resulting in higher respiration rates, were linked to lower fitness costs associated with pesticide resistance (Araújo et al., 2008; Cordeiro et al., 2017; Guedes et al., 2017). Similarly, Araújo et al. (2008) observed that in

the absence of insecticides, resistance is typically linked with fitness losses, but prior selection with these chemicals may encourage the evolution of fitness modifier genes that attenuate such costs. In pesticide-resistant strains' enzymes exhibited higher serine- and cysteine-proteolytic and cellulolytic activity, and kinetic characteristics revealed that cysteine-proteinase and cellulase activities were more essential in reducing the cost of insecticide resistance in maize weevil strains (Araújo et al., 2008).

Colorado potato beetle, *Leptinotarsa decemlineata*, has been the subject of many resistance and fitness studies. *L. decemlineata* strains resistant to OPs and pyrethroids have been discovered in various regions of the world (Freeman et al., 2021). Experiments on lab strains of the beetle with Bt resistance revealed that the resistant lines had a higher fitness cost than their susceptible equivalents. However, the resistance levels decreased dramatically after only five generations without selection pressure (Jisha et al., 2013).

Genetic research and early findings suggest that fitness disadvantages associated with phosphine resistance have been predicted (Mau et al., 2012; Bajracharya, 2013; Collins et al., 2017; Aulicky et al., 2019). In the three species of the red flour beetle (*Tribolium castaneum*), the lesser grain borer (*Rhyzopertha dominica*), and the saw-toothed grain beetle (*Oryzaephilus surinamensis*), resistance to phosphine is associated with a fitness cost, which can potentially compromise the fixation and dispersal of resistant genotypes. In some cases, years of rigorous selection for phosphine resistance may have favored suppressing the negative consequences, reducing the fitness costs normally associated with it. In pyrethroid-resistant populations of *S. zeamais*, such mitigation has already been described (Cordeiro et al., 2017; Guedes et al., 2017). Resistance prevalence data also benchmark against which management performance can be measured (Daglish et al., 2015; Bughio and Wilkins, 2021). The prevailing mechanism of phosphine resistance in these insects involves a reduced uptake of the fumigant, a process designated as active exclusion (Nguyen et al., 2015). This process may be closely related to the insect respiration rate, which is not usually determined in studies of resistance to phosphine. Respiration is also a good index of the physiological responses of insects to the environment to which it is exposed (Wang et al., 2020d). The assumption of an insecticide resistance fitness cost is based on the acquisition of adaptability to a new environment, one contaminated with insecticides. Current findings support previous findings that resistant *S. oryzae* and *S. zeamais* populations had lower fecundity and growth rates than susceptible populations (Daglish et al., 2014). Differences in the biological parameters affecting the growth rate of insect populations are fundamental to insecticide resistance management because, in this case, the frequency of resistant individuals can decrease with time (Gould et al., 2018). However, resistant strains may have a fitness advantage under particular conditions, and resistant individuals may not decrease over time (Guedes et al., 2009). The population of each species produced carbon dioxide, and the instantaneous rate of population expansion (r_i) was associated with their resistance ratios at LC_{50}. There was a strong correlation between respiration rate and phosphine resistance in all species of stored-product pests. Populations with lower carbon dioxide generation had a greater resistance ratio (Wang et al., 2020d), indicating that the decreased respiration rate represents the physiological foundation of resistance to phosphine via lowering the insect's fumigant intake (Nguyen et al., 2015; Alnajim, 2020). In contrast, groups with a greater r_i exhibited lower resistance ratios, which may imply a reduced reproduction rate in resistant populations compared to susceptible ones. This lends weight to the idea that allocating energy for forming defense mechanisms against pesticides would lower the reproductive potential of resistant populations (Cordeiro et al., 2017). Unlike susceptible populations, resistant populations of *S. oryzae*, *S. zeamais*, and *Cryptolestes ferrugineus* exhibited decreased fertility and growth rates (Daglish et al., 2014; Chakraborty and Madhumathi, 2020). In the absence of insecticides, pesticide resistance is typically linked with an increase in the cost of adaptation. Due to the reallocation of resources from a fundamental physiological function to the defense against insecticides, favoring their survival at the price of their reproduction, these expenditures diminish the reproductive success of resistant individuals (Bass et al., 2014; Cordeiro et al., 2017). Adaptive costs associated with pesticide resistance have been documented in some populations of *S. zeamais* (Cordeiro et al., 2017; Guedes et al., 2017). Consumption of oxygen and generation of carbon dioxide is related to metabolism and might indicate energy expenditures (Chown et al., 2016; Abbas et al., 2020). Modifications in fat body shape reflect the availability and mobilization of energy reserves for the individual's maintenance, resulting in its survival when exposed to harmful chemicals (Cordeiro et al., 2017). These patterns and study techniques were created in investigations with populations of pyrethroid-resistant maize weevils (Cordeiro et al., 2017), where the resistant population demonstrated greater respiration rate and body mass than the susceptible and another resistant population, demonstrating a reduction of fitness costs. Araújo et al. (2008) report that populations of *S. zeamais* with varying degrees of pesticide sensitivity accumulate and mobilize energy stores differently. These changes enable *S. zeamais* to survive hazardous chemicals better without sacrificing reproductive fitness. Enzymatic tests using carbohydrate- and lipid-metabolizing enzymes measured the activity levels of trehalase, glycogen phosphorylase, lipase, glycosidase, amylase, and respirometry bioassays in two insecticide-resistant populations with (resistance cost) or without (no-cost resistance) associated fitness cost and an insecticide-susceptible population. The group with no cost resistance had much greater body mass and respiration rate than the other two populations, which were comparable. The levels of permethrin resistance, body mass, and respiration rates reported in the above research support those of Guedes et al. (2017), who postulated that an insecticide-resistant population's greater respiration rate, body mass, and energy reserves reduce the fitness penalty generally associated with pesticide resistance. This mitigation maintains pesticide resistance mechanisms without interfering with other physiological functions, like reproduction.

Amylase cleaves starch and similar polysaccharides, enabling their ultimate storage and utilization as an energy source. It then becomes the substrate of another set of carbohydrases (such as glycosidase and trehalase) that hydrolyze oligosaccharides and disaccharides (Harrison et al., 2012). Trehalase, found in many insects, breaks down trehalose into glucose (Dolezal and Toth, 2014; Kaur et al., 2014; Rodríguez et al., 2015). Lipases are involved in lipid digestion and mobilization, but our *in vitro* bioassays could not tell the difference (Dolezal and Toth, 2014; Jiang et al., 2016). Lipid hydrolysis was more efficient in the resistant population with a cost,

whereas starch digestion was more efficient in the resistant group with no cost. The increased activity of amylases in the resistant no-cost population indicates their superior efficiency in extracting energy from food and storing it, resulting in a bigger body mass (Cordeiro et al., 2017). The increased trehalose activity in the resistant cost group likely indicates better energy mobilization, reducing the likelihood of its buildup and resulting rise in body mass. It is difficult to determine the significance of increased lipase activity in the resistant cost population since the enzyme source was the whole insect body, and the lipase classes (involved in fat digestion or lipid mobilization) were not differentiated. Nevertheless, given the increased trehalase activity and the obvious existence of resistance costs in the resistant cost group (Cordeiro et al., 2017; Guedes et al., 2017), the higher lipase activity reported in this population indicates more lipid mobilization. The no-cost-resistant population has a bigger body mass than the cost-resistant population. It is more resistant and likely needs more energy mobilization to maintain its higher pesticide resistance (Cordeiro et al., 2017; Guedes et al., 2017).

8 Lepidoptera

The caterpillars and rarely moths of the order Lepidoptera are known for their herbivory on vast crops. These insects feed using chewing and biting mouthparts and devour vegetation through nibbling, boring, mining, etc. Hence, large-scale systemic, as well as contact insecticides, have been used to manage lepidopterans, eventually developing resistance against them (Hafeez et al., 2022; Kenis et al., 2023). Recently, genetically modified crops have also developed resistance in insects despite the rate of resistance development being slower than that of insecticides (Fernandez-Cornejo et al., 2014). For example, Bt cotton, which produces toxins against cotton bollworms upon ingestion, has developed resistance to these insects, which is somewhat counteracted or delayed by their reduced fitness (Carrière et al., 2019). *Pectinophora gossypiella* is resistant to the Cry1Ac toxin generated by Bt cotton due to a gene mutation that inhibits cadherin protein binding to Cry1Ac (Fabrick et al., 2014; Wang et al., 2019c). Furthermore, its resistance to Cry2Ab is due to a mutation of the ATP-binding cassette transporter gene (Heckel, 2015; Mathew et al., 2018). Higher levels of gossypol in traditional cottonseed enhanced the fitness cost of *P. gossypiella* to Bt cotton by affecting survival (Carrière et al., 2019). Also, using biological control agents, multiple toxins, non-Bt refuge and defensive plant compounds, such as gossypol, will reduce/delay the resistance development (Carrière et al., 2019). The insect populations with the non-recessive mode of inheritance of resistance face an early decline in susceptibility, yet high fitness costs associated with them also help delay it (Ullah et al., 2020b).

Research conducted on the widespread fall armyworm, *S. frugiperda*, has documented numerous instances of its resistance and consequent detrimental impact on its biological fitness to a variety of Bt toxins and multiple insecticidal classes, namely, benzoylureas and pyrethroids. Additionally, relatively new insecticides like spinetoram and metaflumizone have shown the same effects on this insect (Barbosa et al., 2020). One example of organophosphate is chlorpyriphos, a widely used insecticide against *S. frugiperda*. Its resistant strains exhibited lower survival, developmental period, pupal weights, fecundity, and fertility life table parameters (Garlet et al., 2021). In another wide-scale used diamide insecticide, chlorantraniliprole, the field-collected resistant strain showed reduced fitness based on population history parameters compared to the near-isogenic resistant strain. This highlighted the importance of using the suitable genetic background of the crop for fitness costs-related studies (Elias et al., 2022). Shan et al. (2021) reported the trade-offs between chlorantraniliprole resistance and chemical communication as well as the fitness cost of insecticide resistance in *P. xylostella*.

Due to its resistance to 97 pesticides, the diamondback moth, *Plutellaxylostella*, is regarded as the most difficult pest of the Brassicaceae family to eradicate (IRAC, 2020). In several nations, it is resistant to almost all key insecticidal groups, including Bt. Since 2010, Japanese farmers have used the rotation of pesticides with varied modes of action for resistance management. Nonetheless, this technique produces variations in their mortalities (Uesugi, 2021) (IRAC 2019). Fitness costs related to using insecticides could be a possible reason for this disparity, resulting in varying susceptibility against the different modes of action affecting resistance stability (Jouzani et al., 2017). Bt, spinosyns, pyridalyl, and aver-mectins/milbemycins may become key components of the rotation approach because their high fitness costs lead to steady and high susceptibility (Jouzani et al., 2017; Yin et al., 2019; Uesugi, 2021; Kumar et al., 2022).

9 Diptera

The dipterans represent agricultural, domestic and medically important pests, which have suffered immense insecticidal exposure. *Musca domestica* is a classic example of insecticidal resistance reported in insects (Roca-Acevedo et al., 2023). It is broadly resistant to all the major insecticidal groups, such as organochlorides, organophosphates, carbamates, and pyrethroids, and has been linked to its reduced fitness for one or more traits. Some such examples are spiromesifen (Alam et al., 2020), chlorantraniliprole (Shah and Shad, 2020), spinosad (Khan, 2018), pyriproxyfen (Shah et al., 2015), methoxyfenozide (Shah et al., 2017), fipronil (Abbas et al., 2016a), lambda-cyhalothrin (Abbas et al., 2016b) and imidacloprid (Abbas et al., 2015a). Houseflies develop resistance to insecticides to varying degrees depending on the chemical and its mode of action, which is partly a function of how often and for how long they are exposed to the chemicals. In the absence of insecticides, there will be a reversion of resistance in the process of regaining reduced fitness (Abbas et al., 2015b).

The susceptibility also varies according to season, frequency of application, and the insecticidal group due to changing biological parameters or termination of insecticide exposure in off season (Abbas et al., 2015b). Additionally, pesticide cross-resistance and multiple-resistance contribute to a decrease in sensitivity. Cross-resistance between organophosphates and pyrethroids owing to the presence of detoxifying enzymes such as esterases is one example (Muthusamy et al., 2014). The long use of pyrethroids and DDT to control houseflies has resulted in resistance build-up, mainly attributed to the *kdr* gene family involving multiple alleles (Bass et al., 2014). Interestingly, the lowest resistance imparting *kdr-his*

allele is present in two-third of flies' population in the United States. In contrast, *kdr* and *super-kdr* alleles were less prevalent despite imparting higher resistance (Rinkevich et al., 2013). This may be due to decreased fitness costs associated with *kdr-his* alleles, showing that the biology of flies plays a role in disseminating some resistance-conferring alleles (Sun et al., 2016; Hanai et al., 2018).

There have been reports of resistance to many organophosphate and carbamate chemicals (Low et al., 2013) in *Liriomyza sativae* (Askari-Saryazdi et al., 2015), *Drosophila melanogaster* (Hubhachen et al., 2022), *B. tabaci* (Renault et al., 2023) with a reduction or increase in acetylcholinesterase sensitivity as the major resistance mechanism. Metabolic enzymes as the driving force for altered susceptibility is also prevalent, for example, in *M. domestica* against chlorantraniliprole,- utilizing cytochrome P450 monooxygenase and esterase detoxifying enzymes (Shah and Shad, 2020). Interestingly, there was a varied response of detoxifying enzymes on resistance due to differential insecticidal exposure in different life stages of insects. For example, resistance to chlorpyriphos was more observed in the larval than in the adult stage in *Anopheles gambiae* and *L. sativae* (Askari-Saryazdi et al., 2015). Differential entry routes and chemical properties can force insects to cope with these stress conditions differently in diverse life stages at the cost of their biological fitness (Mastrantonio et al., 2019).

Fruit flies, which are polyphagous, multivoltine, and agriculturally important insect pests, are resistant to various chemicals. One such example is the resistance of a peach fruit fly strain to trichlorfon, an organophosphate, which showed a reduction in relative fitness up to 0.52 (Abubakar et al., 2021). A similar trend was also found for *Bactrocera dorsalis* concerning this specific chemical (Chen et al., 2015). The reduced fitness traits included fecundity, pupal weight, reduced larval duration, number of future larvae, and net reproductive rate, with no difference in biotic potential and intrinsic rate relative to unselected strains (Chen et al., 2015).

It is known that pesticide resistance severely influences mosquito fitness overall and has a number of detrimental impacts on its growth and reproduction features (Diniz et al., 2015; Osoro et al., 2021; Gonzalez-Santillan et al., 2022; Parker-Crockett et al., 2022). The insecticides temephos and deltamethrin are not effective against the laboratory-created strain of *Aedes aegypti* known as *Aedes* Rio, which was developed from field mosquito populations of Rio de Janeiro. Compared to Rockefeller's laboratory reference strain, pleiotropic effects that led to a fitness cost that metabolic and target site resistance mechanisms may have induced evolved in the original populations. However, due to this diminished fitness, the *A. aegypti* Rio strain did not become infected with or spread the Zika virus (Dos Santos et al., 2020).

The understanding of molecular biology has assisted us in predicting the costs associated with various resistance mechanisms. Bass (2017) critically reviewed the literature on fitness costs in the absence of pesticides. The resistance alleles can develop from pre-existing polymorphisms, and sexual differences can also sustain resistance-associated variation. For resistance induced by *kdr* and *RDL* genes, heterozygous (RS) male *A. gambiae* demonstrated greater mating success than their homozygous resistant (RR) equivalents. This shows that in this instance, homozygous target site resistance has a cost in terms of decreased mating success (Platt et al., 2015).

Most arthropod species have complex connections with symbiotic bacteria and depend on microorganisms for reproduction, development, metabolism, and immunity (Douglas, 2015). The disruption of these commensal bacteria may have detrimental consequences on the physiology of insects, leading to mortality or diminished fitness. For instance, adult tsetse flies given a blood meal containing the antibiotic tetracycline and lice fed on four different medicines exhibited immediate mortality (Weiss et al., 2012). In growing nymphs of the omnivorous American cockroach, removing symbiotic bacteria from the stomach with metronidazole impeded weight gain (Bauer et al., 2015). The elimination of bacterial symbionts may alter not just the longevity and fertility of insects but also their susceptibility to insecticides (Pietri and Liang, 2018). Insecticide resistance in the bean bug, *Riptortus pedestris*, and oriental fruit fly, *B. dorsalis*, has been linked to the synthesis of detoxifying enzymes by Proteobacteria in the midgut, and antibiotic treatments may restore sensitivity to resistant individuals (Kikuchi et al., 2012; Cheng et al., 2017). According to (Pietri et al., 2018), microbiota contributes to both physiological and evolutionary elements of pesticide resistance, suggesting that targeting this community might be a useful tactic. Meanwhile, the gut microbiota also acquired insecticide resistance, contributing to host resistance (Engel and Moran, 2013). Pesticide resistance altered the makeup of the gut microbiota of cockroaches, altering the growth and development of insect hosts. Prior research has examined insecticide resistance mechanisms in German cockroaches regarding target site insensitivity, epidermal permeability, behavioral resistance, and metabolic detoxification (Boopathy et al., 2022), indicating that the gut microbiota may potentially play a part in the resistance process.

Cai et al. (2020) reported that cypermethrin resistance in *B. germanica* affected the development of ovaries and the expression of proteins with different functions in the ovaries, resulting in fecundity defects in the cypermethrin-resistant (R) strain of *B. germanica*, which reflected as fitness disadvantages. The R strain of *B. germanica* showed an even greater ootheca shedding rate, a much lower number of hatched and surviving nymphs, a significantly higher percentage of females in the population, and aberrant ovarian development than the sensitive (S) strains. Consequently, the metabolic variations required to overcome the negative effects of pesticides might result in an energy exchange that changes energy allocation and, eventually, the insect's fundamental requirements. The fitness cost caused by pesticide resistance is crucial for preventing the development of resistance.

This unique integrated pest management (IPM) technique might be used to develop pesticide synergists that inhibit insecticide metabolism in pest microbiota and biocontrol agents (Zhang et al., 2018b; Zhang and Yang, 2019). Given the substantial fitness costs associated with resistance, insecticide rotation may be a viable resistance control strategy. Identifying fitness costs associated with insecticidal resistance may restrict the spread of resistant populations and enable IPM programs to target resistant populations efficiently.

10 Fitness advantage

The phenomena of fitness cost or advantage in relation to the resistance of insecticides are familiar in the insect species. Identifying fitness advantages can be useful in deciding integrated pest management by curbing the spread of resistant populations. Fitness costs and resistant individuals spread in the population are directly proportional, thereby becoming an important parameter in decision-making (Kliot and Ghanim, 2012). The major purpose behind investigating the fitness advantage due to insecticide resistance is to monitor the resistance levels over time in environments distinctly exposed to insecticides (Hawkins et al., 2019). Furthermore, if the principal mechanism selected for resistance is known, the genotyping of resistance genes in place and time scales render important assumptions about their fitness advantage (Belinato and Martins, 2016).

The resistant (R) and susceptible (S) *Eriopis connexa* (Germar) populations are crossed, and the performance of the F1 offspring and resistance maintenance over F1, F2, and F3 progenies was assessed (Lira et al., 2016). Compared to the R population, the heterozygous F1 progeny exhibited much higher fecundity and longevity. These findings showed that when beetles from the R population are released and mated with the S population, the field progeny retain the resistance phenotype with an advantage over the parental R population in terms of increased egg production and longer survival. A life table analysis of fenvalerate on the brown planthopper, *N. lugens* indicated that the resistant strain (G4 and G8) demonstrated an improved female ratio, copulation rate, and fecundity. However, the resistant strain had a reduced hatchability. The number of offspring in the G8 generation was higher than that in the G4 generation, and resistant strains in generations G4 and G8 demonstrated a fitness advantage (1.04 and 1.11) (Ling et al., 2011). When an organism faces a niche change and adapts to a new environment, a fitness advantage is a phenomenon that manifests. If the evolutionary pressure lasts for a number of generations, it is possible that other genetic alterations will take place to reduce the negative impacts of the first adaptation and improve it such that there are no longer any fitness costs. The existence of fitness advantages during the laboratory conditions is also important in the evaluation of specific traits.

11 Conclusion

Chemical application remains a prevalent strategy for global insect pest control. However, the widespread use of chemical insecticides subjects both intended targets and unintended species to toxic compounds and concurrent stressors. In these challenges, insects must allocate energy and resources for survival and adaptation. Insects counteract the effects of toxic chemicals by employing behavioral, physiological, and genetic defenses. The persistent selective pressure from insecticide usage can lead to resistance development through mechanisms such as upregulation of detoxification genes and target-site mutations.

Numerous studies have underscored the resource-intensive nature of these defense mechanisms, impacting vital biological traits like development and reproduction and other pivotal factors influencing insect fitness. However, future studies should focus on determining the underlying molecular mechanisms of fitness costs associated with insecticide resistance. Such insights can potentially guide the development of effective resistance management strategies for sustainable insect control programs. Furthermore, validating laboratory findings by quantitatively assessing resistance across various fitness matrices within field contexts is imperative. This comprehensive approach is necessary to comprehensively elucidate the intricate interplay between resistance development and fitness costs in agroecosystems at the community level.

Author contributions

All authors listed have made a substantial, direct, and intellectual contribution to the work and approved it for publication.

Funding

This work was supported by the National Key R&D Program of China (2022YFD1400300).

Conflict of interest

The authors declare that the research was conducted in the absence of any commercial or financial relationships that could be construed as a potential conflict of interest.

Publisher's note

References

Abbas, N., and Shad, S. A. (2015). Assessment of resistance risk to lambda-cyhalothrin and cross-resistance to four other insecticides in the house fly, *Musca domestica* L.(Diptera: muscidae). *Parasitol. Res.* 114, 2629–2637. doi:10.1007/s00436-015-4467-2

Abbas, N., Mansoor, M. M., Shad, S. A., Pathan, A. K., Waheed, A., Ejaz, M., et al. (2014). Fitness cost and realized heritability of resistance to spinosad in *Chrysoperla carnea* (neuroptera: chrysopidae). *Bull. Entomol. Res.* 104 (6), 707–715. doi:10.1017/S0007485314000522

Abbas, N., Khan, H., and Shad, S. A. (2015a). Cross-resistance, stability, and fitness cost of resistance to imidacloprid in *Musca domestica* L.,(Diptera: muscidae). *Parasitol. Res.* 114, 247–255. doi:10.1007/s00436-014-4186-0

Abbas, N., Ijaz, M., Shad, S. A., and Khan, H. (2015b). Stability of field-selected resistance to conventional and newer chemistry insecticides in the house fly, *Musca domestica* L.(Diptera: muscidae). *Neotropical Entomol.* 44, 402–409. doi:10.1007/s13744-015-0290-9

Abbas, N., Shah, R. M., Shad, S. A., and Azher, F. (2016a). Dominant fitness costs of resistance to fipronil in *Musca domestica* linnaeus (Diptera: muscidae). *Vet. Parasitol.* 226, 78–82. doi:10.1016/j.vetpar.2016.06.035

Abbas, N., Shah, R. M., Shad, S. A., Iqbal, N., and Razaq, M. (2016b). Biological trait analysis and stability of lambda-cyhalothrin resistance in the house fly, *Musca domestica* L.(Diptera: muscidae). *Parasitol. Res.* 115, 2073–2080. doi:10.1007/s00436-016-4952-2

Abbas, W., Withers, P. C., and Evans, T. A. (2020). Water costs of gas exchange by a speckled cockroach and a darkling beetle. *Insects* 11 (9), 632. doi:10.3390/insects11090632

Abubakar, M., Ali, H., Shad, S. A., Anees, M., and Binyameen, M. (2021). Trichlorfon resistance: its stability and impacts on biological parameters of *Bactrocera zonata* (Diptera: tephritidae). *Appl. Entomol. Zool.* 56 (4), 473–482. doi:10.1007/s13355-021-00754-6

Alam, M., Shah, R. M., Shad, S. A., and Binyameen, M. (2020). Fitness cost, realized heritability and stability of resistance to spiromesifen in house fly, *Musca domestica* L.(Diptera: muscidae). *Pestic. Biochem. Phys.* 168, 104648. doi:10.1016/j.pestbp.2020.104648

Alnajim, I. A. (2020). "Comparison of physiological and metabolic changes between phosphine resistant and susceptible strains of Rhyzopertha dominica (Fabricius) and *Tribolium castaneum* (Herbst)," (Perth, Australia: Murdoch University). Doctoral dissertation.

Amandeep, K., Singh, N. N., and Mukesh, K. (2012). Persistent toxicity of insecticides on biotic potential of *Trichogramma brasiliensis* ashmead (Hymenoptera: trichogrammatidae), an egg parasitoid of tomato fruit borer. *Indian J. Entomol.* 74 (4), 359–365.

Araújo, R. A., Guedes, R. N., Oliveira, M. G., and Ferreira, G. H. (2008). Enhanced proteolytic and cellulolytic activity in insecticide-resistant strains of the maize weevil, *Sitophilus zeamais*. *J. Stored Prod. Res.* 44 (4), 354–359. doi:10.1016/j.jspr.2008.03.006

Askari-Saryazdi, G., Hejazi, M. J., Ferguson, J. S., and Rashidi, M. R. (2015). Selection for chlorpyrifos resistance in *Liriomyza sativae* blanchard: cross-resistance patterns, stability and biochemical mechanisms. *Pestic. Biochem. Phys.* 124, 86–92. doi:10.1016/j.pestbp.2015.05.002

Aulicky, R., Stejskal, V., and Frydova, B. (2019). Field validation of phosphine efficacy on the first recorded resistant strains of *Sitophilus granarius* and *Tribolium castaneum* from the Czech Republic. *J. Stored Prod. Res.* 81, 107–113. doi:10.1016/j.jspr.2019.02.003

Bagheri, A., Askari Seyahooei, M., Fathipour, Y., Famil, M., Koohpayma, F., Mohammadi-Rad, A., et al. (2019). Ecofriendly managing of *Helicoverpa armigera* in tomato field by releasing *Trichogramma evanescence* and *Habrobracon hebetor*. *J. Crop Prot.* 8, 11–19.

Bajracharya, N. S. (2013). *Phosphine resistance in stored-product insect pests: Management and fitness cost*. Oklahoma State University.

Banazeer, A., Afzal, M. B., Hassan, S., Ijaz, M., Shad, S. A., and Serrão, J. E. (2021). Status of insecticide resistance in *Plutella xylostella* (linnaeus)(Lepidoptera: plutellidae) from 1997 to 2019: cross-resistance, genetics, biological costs, underlying mechanisms, and implications for management. *Phytoparasitica* 50, 465–485. doi:10.1007/s12600-021-00959-z

Barbosa, M. G., Andre, T. P., Pontes, A. D., Souza, S. A., Oliveira, N. R., and Pastori, P. L. (2020). Insecticide rotation and adaptive fitness cost underlying insecticide resistance management for *Spodoptera frugiperda* (Lepidoptera: noctuidae). *Neotrop Entomol.* 49, 882–892. doi:10.1007/s13744-020-00800-y

Barbosa, M. G., Souza, S. A., André, T. P., Pontes, A. D., Teixeira, C. S., Pereira, F. F., et al. (2021). Do fall armyworm's Metaflumizone resistante populations affect the activity of *Trichogramma pretiosum*? *Braz. J. Biol.* 83, e245273. doi:10.1590/1519-6984.245273

Basit, M. (2019). Status of insecticide resistance in *Bemisia tabaci*: resistance, cross-resistance, stability of resistance, genetics and fitness costs. *Phytoparasitica* 47 (2), 207–225. doi:10.1007/s12600-019-00722-5

Bass, C., Puinean, A. M., Zimmer, C. T., Denholm, I., Field, L. M., Foster, S. P., et al. (2014). The evolution of insecticide resistance in the peach potato aphid, *Myzus persicae*. *Insect Biochem. Mol. Biol.* 51, 41–51. doi:10.1016/j.ibmb.2014.05.003

Bass, C. (2017). Does resistance really carry a fitness cost? *Curr. Opin. Insect Sci.* 21, 39–46. doi:10.1016/j.cois.2017.04.011

Bauer, E., Lampert, N., Mikaelyan, A., Köhler, T., Maekawa, K., and Brune, A. (2015). Physicochemical conditions, metabolites and community structure of the bacterial microbiota in the gut of wood-feeding cockroaches (Blaberidae: panesthiinae). *FEMS Microbiol. Ecol.* 91 (2), 1–14. doi:10.1093/femsec/fiu028

Belinato, T. A., and Martins, A. J. (2016). Insecticide resistance and fitness cost. *InTech*. doi:10.1093/femsec/fiu028

Bielza, P. (2016). "Insecticide resistance in natural enemies," in *Advances in insect control and resistance management*. Editors A. Horowitz and I. Ishaaya (Cham: Springer), 313–329. doi:10.1007/978-3-319-31800-4-16

Bielza, P., Balanza, V., Cifuentes, D., and Mendoza, J. E. (2020). Challenges facing arthropod biological control: identifying traits for genetic improvement of predators in protected crops. *Pest Manag. Sci.* 76 (11), 3517–3526. doi:10.1002/ps.5857

Biondi, A., Chailleux, A., Lambion, J., Han, P., Zappalà, L., and Desneux, N. (2013). Indigenous natural enemies attacking *Tuta absoluta* (Lepidoptera: gelechiidae) in southern France. *Egypt J. Biol. Pest Control* 23 (1), 117–121.

Biondi, A., Campolo, O., Desneux, N., Siscaro, G., Palmeri, V., and Zappalà, L. (2015). Life stage-dependent susceptibility of *Aphytis melinus* DeBach (Hymenoptera: aphelinidae) to two pesticides commonly used in citrus orchards. *Chemosphere* 128, 142–147. doi:10.1016/j.chemosphere.2015.01.034

Boopathy, B., Rajan, A., and Radhakrishnan, M. (2022). Ozone: an alternative fumigant in controlling the stored product insects and pests: a status report. *Ozone Sci. Eng.* 44 (1), 79–95. doi:10.1080/01919512.2021.1933899

Brenner, R. J., and Kramer, R. D. (2019). "Cockroaches (blattaria)," in *Medical and veterinary entomology* (United States: Academic Press), 61–77.

Bughio, F. M., and Wilkins, R. M. (2021). Fitness in a malathion resistant *Tribolium castaneum* strain; feeding, growth and digestion. *J. Stored Prod. Res.* 92, 101814. doi:10.1016/j.jspr.2021.101814

Cai, T., Huang, Y. H., and Zhang, F. (2020). Ovarian morphological features and proteome reveal fecundity fitness disadvantages in β-cypermethrin-resistant strains of *Blattella germanica* (L.)(Blattodea: blattellidae). *Pestic. Biochem. Phys.* 170, 104682. doi:10.1016/j.pestbp.2020.104682

Carrière, Y., Yelich, A. J., Degain, B. A., Harpold, V. S., Unnithan, G. C., Kim, J. H., et al. (2019). Gossypol in cottonseed increases the fitness cost of resistance to Bt cotton in pink bollworm. *Crop Prot.* 126, 104914. doi:10.1016/j.cropro.2019.104914

Castellanos, N. L., Haddi, K., Carvalho, G. A., de Paulo, P. D., Hirose, E., Guedes, R. N., et al. (2019). Imidacloprid resistance in the neotropical brown stink bug *Euschistus heros*: selection and fitness costs. *J. Pest Sci.* 92, 847–860. doi:10.1007/s10340-018-1048-z

Chailleux, A., Biondi, A., Han, P., Tabone, E., and Desneux, N. (2013). Suitability of the pest–plant system *Tuta absoluta* (Lepidoptera: gelechiidae)–tomato for *Trichogramma* (Hymenoptera: trichogrammatidae) parasitoids and insights for biological control. *J. Econ. Entomol.* 106 (6), 2310–2321. doi:10.1603/ec13092

Chakraborty, D., and Madhumathi, T. (2020). Present scenario of insecticide resistance in Rusty grain beetle, *Cryptolestes ferrugenius* (stephens) to malathion and deltamethrin in Andhra Pradesh, India. *Int. J. Curr. Microbiol. App Sci.* 9 (6), 4180–4188. doi:10.20546/ijcmas.2020.906.489

Chappell, T. M., Huseth, A. S., and Kennedy, G. G. (2019). Stability of neonicotinoid sensitivity in *Frankliniella fusca* populations found in agroecosystems of the southeastern USA. *Pest Manag. Sci.* 75 (6), 1539–1545. doi:10.1002/ps.5319

Chen, L., Liu, X., Wu, S., Zhu, Y., Zeng, L., and Lu, Y. (2015). A comparative study of the population biology of trichlorfon-resistant strains of the oriental fruit fly, *Bactrocera dorsalis* (Diptera: Tephritdae). *Acta Entomol. Sin.* 58 (8), 864–871.

Cheng, J., Lee, X., Gao, W., Chen, Y., Pan, W., and Tang, Y. (2017). Effect of biochar on the bioavailability of difenoconazole and microbial community composition in a pesticide-contaminated soil. *Appl. Soil Ecol.* 121, 185–192. doi:10.1016/j.apsoil.2017.10.009

Cheng, S., Lin, R., Wang, L., Qiu, Q., Qu, M., Ren, X., et al. (2018). Comparative susceptibility of thirteen selected pesticides to three different insect egg parasitoid *Trichogramma* species. *Ecotoxicol. Environ. Saf.* 166, 86–91. doi:10.1016/j.ecoenv.2018.09.050

Chong, H. K., Peng, M. H., Liu, K. L., Singham, G. V., and Neoh, K. B. (2022). Role of social aggregation in the fitness cost of pyrethroid-resistant German cockroaches. *J. Appl. Entomol.* 146 (10), 1320–1332. doi:10.1111/jen.13070

Chown, S. L., Haupt, T. M., and Sinclair, B. J. (2016). Similar metabolic rate-temperature relationships after acclimation at constant and fluctuating temperatures in caterpillars of a sub-Antarctic moth. *J. Insect Phys.* 85, 10–16. doi:10.1016/j.jinsphys.2015.11.010

Collins, P. J., Falk, M. G., Nayak, M. K., Emery, R. N., and Holloway, J. C. (2017). Monitoring resistance to phosphine in the lesser grain borer, *Rhyzopertha dominica*, in Australia: a national analysis of trends, storage types and geography in relation to resistance detections. *J. Stored Prod. Res.* 70, 25–36. doi:10.1016/j.jspr.2016.10.006

Cordeiro, E. M., Corrêa, A. S., Rosi-Denadai, C. A., Tomé, H. V., and Guedes, R. N. (2017). Insecticide resistance and size assortative mating in females of the maize weevil (*Sitophilus zeamais*). *Pest Manag. Sci.* 73 (5), 823–829. doi:10.1002/ps.4437

Daglish, G. J., Nayak, M. K., and Pavic, H. (2014). Phosphine resistance in *Sitophilus oryzae* (L.) from eastern Australia: inheritance, fitness and prevalence. *J. Stored Prod. Res.* 59, 237–244. doi:10.1016/j.jspr.2014.03.007

Daglish, G. J., Nayak, M. K., Pavic, H., and Smith, L. W. (2015). Prevalence and potential fitness cost of weak phosphine resistance in *Tribolium castaneum* (Herbst) in eastern Australia. *J. Stored Prod. Res.* 61, 54–58. doi:10.1016/j.jspr.2014.11.005

Deguine, J. P., Aubertot, J. N., Flor, R. J., Lescourret, F., Wyckhuys, K. A., and Ratnadass, A. (2021). Integrated pest management: good intentions, hard realities. A review. *Agron. Sustain Dev.* 41 (3), 38. doi:10.1007/s13593-021-00689-w

Dingha, B., Jackai, L., Monteverdi, R. H., and Ibrahim, J. (2013). Pest control practices for the German cockroach (blattodea: blattellidae): a survey of rural residents in North Carolina. *Fla. Entomol.* 96 (3), 1009–1015. doi:10.1653/024.096.0339

Diniz, D. F., Melo-Santos, M. A., Santos, E. M., Beserra, E. B., Helvecio, E., de Carvalho-Leandro, D., et al. (2015). Fitness cost in field and laboratory *Aedes aegypti* populations associated with resistance to the insecticide temephos. *Parasites vectors* 8 (1), 662–665. doi:10.1186/s13071-015-1276-5

Dolezal, A. G., and Toth, A. L. (2014). Honey bee sociogenomics: a genome-scale perspective on bee social behavior and health. *Apidologie* 45, 375–395. doi:10.1007/s13592-013-0251-4

Dos Santos, C. R., de Melo Rodovalho, C., Jablonka, W., Martins, A. J., Lima, J. B., dos Santos Dias, L., et al. (2020). Insecticide resistance, fitness and susceptibility to Zika infection of an interbred *Aedes aegypti* population from Rio de Janeiro, Brazil. *Parasites Vectors* 13 (1), 293–294. doi:10.1186/s13071-020-04166-3

Douglas, A. E. (2015). Multiorganismal insects: diversity and function of resident microorganisms. *Annu. Rev. Entomol.* 60, 17–34. doi:10.1146/annurev-ento-010814-020822

Du, W. M., Xu, J., Hou, Y. Y., Lin, Y., Zang, L. S., Yang, X., et al. (2018). *Trichogramma* parasitoids can distinguish between fertilized and unfertilized host eggs. *J. Pest Sci.* 91, 771–780. doi:10.1007/s10340-017-0919-z

Eggleston, P. A. (2017). Cockroach allergy and urban asthma. *J. Allergy Clin. Immunol. Pract.* 140 (2), 389–390. doi:10.1016/j.jaci.2017.04.033

El-Arnaouty, S. A., Galal, H. H., Afifi, A. I., Beyssat, V., Pizzol, J., Desneux, N., et al. (2014). Assessment of two *Trichogramma* species for the control of *Tuta absoluta* in North African tomato greenhouses. *Afr. Entomol.* 22 (4), 801–809. doi:10.4001/003.022.0410

Elias, O. P. F., Hideo, K. R., Omoto, C., and Sartori, G. A. (2022). Fitness costs associated with chlorantraniliprole resistance in *Spodoptera frugiperda* (Lepidoptera: noctuidae) strains with different genetic backgrounds. *Pest Manag. Sci.* 78 (3), 1279–1286. doi:10.1002/ps.6746

Engel, P., and Moran, N. A. (2013). The gut microbiota of insects–diversity in structure and function. *FEMS Microbiol. Rev.* 37 (5), 699–735. doi:10.1111/1574-6976.12025

Fabrick, J. A., Ponnuraj, J., Singh, A., Tanwar, R. K., Unnithan, G. C., Yelich, A. J., et al. (2014). Alternative splicing and highly variable cadherin transcripts associated with field-evolved resistance of pink bollworm to Bt cotton in India. *PloS One* 9 (5), e97900. doi:10.1371/journal.pone.0097900

Fernandez-Cornejo, J., Wechsler, S., Livingston, M., and Mitchell, L. (2014). *Genetically engineered crops in the United States*. United States: USDA-ERS Economic Research Report.

Freeman, J. C., Smith, L. B., Silva, J. J., Fan, Y., Sun, H., and Scott, J. G. (2021). Fitness studies of insecticide resistant strains: lessons learned and future directions. *Pest Manag. Sci.* 77 (9), 3847–3856. doi:10.1002/ps.6306

Fu, B., Li, Q., Qiu, H., Tang, L., Zeng, D., Liu, K., et al. (2018). Resistance development, stability, cross-resistance potential, biological fitness and biochemical mechanisms of spinetoram resistance in *Thrips hawaiiensis* (thysanoptera: thripidae). *Pest Manage Sci.* 74 (7), 1564–1574. doi:10.1002/ps.4887

Fu, B., Tao, M., Xue, H., Jin, H., Liu, K., Qiu, H., et al. (2022). Spinetoram resistance drives interspecific competition between *Megalurothrips usitatus* and *Frankliniella intonsa*. *Pest Manag. Sci.* 78 (6), 2129–2140. doi:10.1002/ps.6839

Gao, C. F., Ma, S. Z., Shan, C. H., and Wu, S. F. (2014). Thiamethoxam resistance selected in the western flower thrips *Frankliniella occidentalis* (thysanoptera: thripidae): cross-resistance patterns, possible biochemical mechanisms and fitness costs analysis. *Pestic. Biochem. Phys.* 114, 90–96. doi:10.1016/j.pestbp.2014.06.009

Garlet, C. G., Moreira, R. P., Gubiani, P. D., Palharini, R. B., Farias, J. R., and Bernardi, O. (2021). Fitness cost of chlorpyrifos resistance in *Spodoptera frugiperda* (Lepidoptera: noctuidae) on different host plants. *Environ. Entomol.* 50 (4), 898–908. doi:10.1093/ee/nvab046

George, J., Glover, J. P., Gore, J., Crow, W. D., and Reddy, G. V. (2021). Biology, ecology, and pest management of the tarnished plant bug, *Lygus lineolaris* (Palisot de Beauvois) in southern row crops. *Insects* 12 (9), 807. doi:10.3390/insects12090807

Gontijo, L., Cascone, P., Giorgini, M., Michelozzi, M., Rodrigues, H. S., Spiezia, G., et al. (2019). Relative importance of host and plant semiochemicals in the foraging behavior of *Trichogramma achaeae*, an egg parasitoid of *Tuta absoluta*. *J. Pest Sci.* 92 (4), 1479–1488. doi:10.1007/s10340-019-01091-y

Gonzalez-Santillan, F. J., Contreras-Perera, Y., Davila-Barboza, J. A., Juache-Villagrana, A. E., Gutierrez-Rodriguez, S. M., Ponce-Garcia, G., et al. (2022). Fitness cost of sequential selection with deltamethrin in *Aedes aegypti* (Diptera: culicidae). *J. Med. Entomol.* 59 (3), 930–939. doi:10.1093/jme/tjac032

Gould, F., Brown, Z. S., and Kuzma, J. (2018). Wicked evolution: can we address the sociobiological dilemma of pesticide resistance? *Science* 360 (6390), 728–732. doi:10.1126/science.aar3780

Grigoraki, L., Pipini, D., Labbe, P., Chaskopoulou, A., Weill, M., and Vontas, J. (2017). Carboxylesterase gene amplifications associated with insecticide resistance in *Aedes albopictus*: geographical distribution and evolutionary origin. *PLoS Negl. Trop. Dis.* 11 (4), e0005533. doi:10.1371/journal.pntd.0005533

Guedes, N. M., Guedes, R. N., Ferreira, G. H., and Silva, L. B. (2009). Flight take-off and walking behavior of insecticide-susceptible and–resistant strains of *Sitophilus zeamais* exposed to deltamethrin. *Bull. Entomol. Res.* 99 (4), 393–400. doi:10.1017/S0007485309006610

Guedes, N. M., Guedes, R. N., Campbell, J. F., and Throne, J. E. (2017). Mating behaviour and reproductive output in insecticide-resistant and-susceptible strains of the maize weevil (*Sitophilus zeamais*). *Ann. App Biol.* 170 (3), 415–424. doi:10.1111/aab.12346

Guo, X., Di, N., Chen, X., Zhu, Z., Zhang, F., Tang, B., et al. (2019). Performance of *Trichogramma pintoi* when parasitizing eggs of the oriental fruit moth *Grapholita molesta*. *Entomol. Gen.* 39, 239–249. doi:10.1127/entomologia/2019/0853

Gurr, G. M., Wratten, S. D., Landis, D. A., and You, M. (2017). Habitat management to suppress pest populations: progress and prospects. *Annu. Rev. Entomol.* 62, 91–109. doi:10.1146/annurev-ento-031616-035050

Haddi, K., Valbon, W. R., Viteri Jumbo, L. O., de Oliveira, L. O., Guedes, R. N., and Oliveira, E. E. (2018). Diversity and convergence of mechanisms involved in pyrethroid resistance in the stored grain weevils, *Sitophilus* spp. *Sci. Rep.* 8 (1), 16361. doi:10.1038/s41598-018-34513-5

Hafeez, M., Li, X., Ullah, F., Zhang, Z., Zhang, J., Huang, J., et al. (2022). Characterization of indoxacarb resistance in the fall armyworm: selection, inheritance, cross-resistance, possible biochemical mechanisms, and fitness costs. *Biology* 11 (12), 1718. doi:10.3390/biology11121718

Hanai, D., Hardstone Yoshimizu, M., and Scott, J. G. (2018). The insecticide resistance allele kdr-his has a fitness cost in the absence of insecticide exposure. *J. Econ. Entomol.* 111 (6), 2992–2995. doi:10.1093/jee/toy300

Hardstone, M. C., Huang, X., Harrington, L. C., and Scott, J. G. (2014). Differences in development, glycogen, and lipid content associated with cytochrome P450-mediated permethrin resistance in *Culex pipiens quinquefasciatus* (Diptera: culicidae). *J. Med. Entomol.* 47 (2), 188–198. doi:10.1603/me09131

Harrison, J. F., Woods, H. A., and Roberts, S. P. (2012). *Ecological and environmental physiology of insects*. Oxford: OUP Oxford.

Hawkins, N. J., Bass, C., Dixon, A., and Neve, P. (2019). The evolutionary origins of pesticide resistance. *Biol. Rev.* 94 (1), 135–155. doi:10.1111/brv.12440

Heckel, D. G. (2015). *Roles of ABC proteins in the mechanism and management of Bt resistance. InBt resistance: Characterization and strategies for GM crops producing* Bacillus thuringiensis *toxins*. Wallingford UK: CABI, 98–106.

Hou, Y. Y., Yang, X., Zang, L. S., Zhang, C., Monticelli, L. S., and Desneux, N. (2018). Effect of oriental armyworm Mythimna separata egg age on the parasitism and host suitability for five *Trichogramma* species. *J. Pest Sci.* 91, 1181–1189. doi:10.1007/s10340-018-0980-2

Hua, D., Li, X., Yuan, J., Tao, M., Zhang, K., Zheng, X., et al. (2023). Fitness cost of spinosad resistance related to vitellogenin in *Frankliniella occidentalis* (Pergande). *Pest Manag. Sci.* 79 (2), 771–780. doi:10.1002/ps.7253

Huang, N. X., Jaworski, C. C., Desneux, N., Zhang, F., Yang, P. Y., and Wang, S. (2020). Long-term and large-scale releases of *Trichogramma* promote pesticide decrease in maize in northeastern China. *Entomol. Gen.* 40 (4), 331–335. doi:10.1127/entomologia/2020/0994

Hubhachen, Z., Pointon, H., Perkins, J. A., Van Timmeren, S., Pittendrigh, B., and Isaacs, R. (2022). Resistance to multiple insecticide classes in the vinegar fly *Drosophila melanogaster* (Diptera: drosophilidae) in Michigan vineyards. *J. Econ. Entomol.* 115 (6), 2020–2028. doi:10.1093/jee/toac155

Jackson, G. E., Malloch, G., McNamara, L., and Little, D. (2020). Grain aphids (*Sitobion avenae*) with knockdown resistance (kdr) to insecticide exhibit fitness trade-offs, including increased vulnerability to the natural enemy *Aphidius ervi*. *Plos One* 15 (11), e0230541. doi:10.1371/journal.pone.0230541

Jactel, H., Verheggen, F., Thiéry, D., Escobar-Gutiérrez, A. J., Gachet, E., Desneux, N., and Neonicotinoids Working Group (2019). Alternatives to neonicotinoids. *Environ. Int.* 129, 423–429. doi:10.1016/j.envint.2019.04.045

Jensen, K., Ko, A. E., Schal, C., and Silverman, J. (2016). Insecticide resistance and nutrition interactively shape life-history parameters in German cockroaches. *Sci. Rep.* 6 (1), 28731. doi:10.1038/srep28731

Jiang, Y. P., Li, L., Liu, Z. Y., You, L. L., Wu, Y., Xu, B., et al. (2016). Adipose triglyceride lipase (Atgl) mediates the antibiotic jinggangmycin-stimulated reproduction in the brown planthopper, *Nilaparvata lugens* Stål. *Sci. Rep.* 6 (1), 18984. doi:10.1038/srep18984

Jin, R., Mao, K., Xu, P., Wang, Y., Liao, X., Wan, H., et al. (2021). Inheritance mode and fitness costs of clothianidin resistance in brown planthopper, *Nilaparvata lugens* (Stål). *Crop Prot.* 140, 105414. doi:10.1016/j.cropro.2020.105414

Jisha, V. N., Smitha, R. B., and Benjamin, S. (2013). An overview on the crystal toxins from *Bacillus thuringiensis*. *Adv. Microbiol.* 3 (05), 462–472. doi:10.4236/aim.2013.35062

Jouzani, G. S., Valijanian, E., and Sharafi, R. (2017). Bacillus thuringiensis: a successful insecticide with new environmental features and tidings. *Appl. Microbiol. Biotechnol.* 101, 2691–2711. doi:10.1007/s00253-017-8175-y

Kaur, R., Kaur, N., and Gupta, A. K. (2014). Structural features, substrate specificity, kinetic properties of insect α-amylase and specificity of plant α-amylase inhibitors. *Pestic. Biochem. Phys.* 116, 83–93. doi:10.1016/j.pestbp.2014.09.005

Kenis, M., Benelli, G., Biondi, A., Calatayud, P. A., Day, R., Desneux, N., et al. (2023). Invasiveness, biology, ecology, and management of the fall armyworm, *Spodoptera frugiperda*. *Entomol. Gen.* 43, 187–241. doi:10.1127/entomologia/2022/1659

Khan, M. A., and Ruberson, J. R. (2017). Lethal effects of selected novel pesticides on immature stages of *Trichogramma pretiosum* (Hymenoptera: trichogrammatidae). *Pest Manag. Sci.* 73 (12), 2465–2472. doi:10.1002/ps.4639

Khan, H. A. (2018). Spinosad resistance affects biological parameters of *Musca domestica* Linnaeus. *Sci. Rep.* 8 (1), 14031. doi:10.1038/s41598-018-32445-8

Kikuchi, Y., Hayatsu, M., Hosokawa, T., Nagayama, A., Tago, K., and Fukatsu, T. (2012). Symbiont-mediated insecticide resistance. *Proc. Natl. Acad. Sci.* 109 (22), 8618–8622. doi:10.1073/pnas.1200231109

Kliot, A., and Ghanim, M. (2012). Fitness costs associated with insecticide resistance. *Pest Manag. Sci.* 68 (11), 1431–1437. doi:10.1002/ps.3395

Koo, H. N., An, J. J., Park, S. E., Kim, J. I., and Kim, G. H. (2014). Regional susceptibilities to 12 insecticides of melon and cotton aphid, *Aphis gossypii* (Hemiptera: aphididae) and a point mutation associated with imidacloprid resistance. *Crop Prot.* 55, 91–97. doi:10.1016/j.cropro.2013.09.010

Kumar, R. M., Gadratagi, B. G., Paramesh, V., Kumar, P., Madivalar, Y., Narayanappa, N., et al. (2022). Sustainable management of invasive fall armyworm, *Spodoptera frugiperda*. *Agronomy* 12 (9), 2150. doi:10.3390/agronomy12092150

Lee, C. Y., Wang, C., and Rust, M. K. (2021). *German cockroach infestations in the world and their social and economic impacts. Biology and management of the German cockroach*. Clayton South, Victoria, Australia: CSIRO Publishing, 1–16.

Lee, S. H., Choe, D. H., Rust, M. K., and Lee, C. Y. (2022). Reduced susceptibility towards commercial bait insecticides in field German cockroach (blattodea: ectobiidae) populations from California. *J. Econ. Entomol.* 115 (1), 259–265. doi:10.1093/jee/toab244

Li, Z., Feng, X., Liu, S. S., You, M., and Furlong, M. J. (2016). Biology, ecology, and management of the diamondback moth in China. *Annu. Rev. Entomol.* 61, 277–296. doi:10.1146/annurev-ento-010715-023622

Li, X., Wan, Y., Yuan, G., Hussain, S., Xu, B., Xie, W., et al. (2017). Fitness trade-off associated with spinosad resistance in *Frankliniella occidentalis* (thysanoptera: thripidae). *J. Econ. Entomol.* 110 (4), 1755–1763. doi:10.1093/jee/tox122

Li, R., Zhu, B., Liang, P., and Gao, X. (2022a). Identification of carboxylesterase genes contributing to multi-insecticide resistance in *Plutella xylostella* (L.). *Entomol. Gen.* 42 (6), 967–976. doi:10.1127/entomologia/2022/1572

Li, D., Zhi, J., Yue, W., Zhang, T., and Liu, L. (2022b). Resistance to spinetoram affects host adaptability of *Frankliniella occidentalis* (thysanoptera: thripidae) based on detoxifying enzyme activities and an age-stage-two-sex life table. *Environ. Entomol.* 51 (4), 780–789. doi:10.1093/ee/nvac053

Liao, X., Mao, K., Ali, E., Jin, R., Li, Z., Li, W., et al. (2019). Inheritance and fitness costs of sulfoxaflor resistance in *Nilaparvata lugens* (Stål). *Pest Manag. Sci.* 75 (11), 2981–2988. doi:10.1002/ps.5412

Liao, X., Xu, P. F., Gong, P. P., Wan, H., and Li, J. H. (2021). Current susceptibilities of brown planthopper *Nilaparvata lugens* to triflumezopyrim and other frequently used insecticides in China. *Insect Sci.* 28 (1), 115–126. doi:10.1111/1744-7917.12764

Lin, J., Yu, X. Q., Wang, Q., Tao, X., Li, J., Zhang, S., et al. (2020). Immune responses to *Bacillus thuringiensis* in the midgut of the diamondback moth, *Plutella xylostella*. *Dev. Comp. Immunol.* 107, 103661. doi:10.1016/j.dci.2020.103661

Ling, S., Zhang, H., and Zhang, R. (2011). Effect of fenvalerate on the reproduction and fitness costs of the brown planthopper, Nilaparvata lugens and its resistance mechanism. *Pestic. Biochem. Phys.* 101 (3), 148–153. doi:10.1016/j.pestbp.2011.08.009

Lira, R. A., Rodrigues, A. R., and Torres, J. B. (2016). Fitness advantage in heterozygous ladybird beetle *Eriopis connexa* (Germar) resistant to lambda-cyhalothrin. *Neotrop Entomol.* 45, 573–579. doi:10.1007/s13744-016-0407-9

Lommen, S. T., de Jong, P. W., and Pannebakker, B. A. (2017). It is time to bridge the gap between exploring and exploiting: prospects for utilizing intraspecific genetic variation to optimize arthropods for augmentative pest control–a review. *Entomol. Exp. Appl.* 162 (2), 108–123. doi:10.1111/eea.12510

Low, V. L., Chen, C. D., Lee, H. L., Tan, T. K., Chen, C. F., Leong, C. S., et al. (2013). Enzymatic characterization of insecticide resistance mechanisms in field populations of Malaysian *Culex quinquefasciatus* say (Diptera: culicidae). *PloS One* 8 (11), e79928. doi:10.1371/journal.pone.0079928

Lu, Y., Wu, K., Jiang, Y., Guo, Y., and Desneux, N. (2012). Widespread adoption of Bt cotton and insecticide decrease promotes biocontrol services. *Nature* 487 (7407), 362–365. doi:10.1038/nature11153

Ma, K., Tang, Q., Zhang, B., Liang, P., Wang, B., and Gao, X. (2019). Overexpression of multiple cytochrome P450 genes associated with sulfoxaflor resistance in *Aphis gossypii* Glover. *Pestic. Biochem. Phys.* 157, 204–210. doi:10.1016/j.pestbp.2019.03.021

Mahmoodi, L., Mehrkhou, F., Guz, N., Forouzan, M., and Atlihan, R. (2020). Sublethal effects of three insecticides on fitness parameters and population projection of *Brevicoryne brassicae* (Hemiptera: aphididae). *J. Econ. Entomol.* 113 (6), 2713–2722. doi:10.1093/jee/toaa193

Malathi, V. M., Jalali, S. K., Gowda, D. K., Mohan, M., and Venkatesan, T. (2017). Establishing the role of detoxifying enzymes in field-evolved resistance to various insecticides in the brown planthopper (*Nilaparvata lugens*) in South India. *Insect Sci.* 24 (1), 35–46. doi:10.1111/1744-7917.12254

Mansoor, M. M., and Shad, S. A. (2019). Resistance of green lacewing, *Chrysoperla carnea* (stephens), to buprofezin: cross resistance patterns, preliminary mechanism and realized heritability. *Biol. Control* 129, 123–127. doi:10.1016/j.biocontrol.2018.10.008

Mansoor, M. M., and Shad, S. A. (2020). Genetics, cross-resistance and realized heritability of resistance to acetamiprid in generalist predator, *Chrysoperla carnea* (Steph.)(Neuroptera: chrysopidae). *Egypt. J. Biol. Pest Control* 30 (1), 23. doi:10.1186/s41938-020-0213-x

Mansoor, M. M., and Shad, S. A. (2022a). Risk assessment of cyromazine and methoxyfenozide resistance suggests higher additive genetic but lower environmental variation supporting quick resistance development in non-target *Chrysoperla carnea* (Stephens). *Environ. Monit. Assess.* 194, 66–68. doi:10.1007/s10661-021-09735-2

Mansoor, M. M., and Shad, S. A. (2022b). Methoxyfenozide tolerance in *Chrysoperla carnea*: inheritance, dominance and preliminary detoxification mechanisms. *Plos One* 17 (3), e0265304. doi:10.1371/journal.pone.0265304

Mansoor, M. M., Abbas, N., Shad, S. A., Pathan, A. K., and Razaq, M. (2013). Increased fitness and realized heritability in emamectin benzoate-resistant *Chrysoperla carnea* (neuroptera: chrysopidae). *Ecotoxicol* 22, 1232–1240. doi:10.1007/s10646-013-1111-8

Mansoor, M. M., Raza, A. B., Abbas, N., Aqueel, M. A., and Afzal, M. (2017). Resistance of green lacewing, *Chrysoperla carnea* stephens to nitenpyram: cross-resistance patterns, mechanism, stability, and realized heritability. *Pestic. Biochem. Phys.* 135, 59–63. doi:10.1016/j.pestbp.2016.06.004

Marchioro, C. A., Krechemer, F. S., and Foerster, L. A. (2015). Assessing the total mortality caused by two species of *Trichogramma* on its natural host *Plutella xylostella* (L.) at different temperatures. *Neotrop Entomol.* 44, 270–277. doi:10.1007/s13744-014-0263-4

Martinez, A. J., Ritter, S. G., Doremus, M. R., Russell, J. A., and Oliver, K. M. (2014). Aphid-encoded variability in susceptibility to a parasitoid. *BMC Evol. Biol.* 14 (1), 127–210. doi:10.1186/1471-2148-14-127

Mastrantonio, V., Ferrari, M., Negri, A., Sturmo, T., Favia, G., Porretta, D., et al. (2019). Insecticide exposure triggers a modulated expression of ABC transporter genes in larvae of *Anopheles gambiae* ss. *Insects* 10 (3), 66. doi:10.3390/insects10030066

Mathew, L. G., Ponnuraj, J., Mallappa, B., Chowdary, L. R., Zhang, J., Tay, W. T., et al. (2018). ABC transporter mis-splicing associated with resistance to Bt toxin Cry2Ab in laboratory-and field-selected pink bollworm. *Sci. Rep.* 8 (1), 13531. doi:10.1038/s41598-018-31840-5

Mau, Y. S., Collins, P. J., Daglish, G. J., Nayak, M. K., and Ebert, P. R. (2012). The rph2 gene is responsible for high level resistance to phosphine in independent field strains of *Rhyzopertha dominica*. *Plos One* 7 (3), e34027. doi:10.1371/journal.pone.0034027

Mengoni, S. L., and Alzogaray, R. A. (2018). Deltamethrin-resistant German cockroaches are less sensitive to the insect repellents DEET and IR3535 than non-resistant individuals. *J. Econ. Entomol.* 111 (2), 836–843. doi:10.1093/jee/toy009

Muthusamy, R., Ramkumar, G., Karthi, S., and Shivakumar, M. S. (2014). Biochemical mechanisms of insecticide resistance in field population of dengue vector *Aedes aegypti* (Diptera: culicidae). *Int. J. Mosq. Res.* 1 (2), 1–4.

Nakao, S., Chikamori, C., Asuka, H. O., and Satoshi, T. O. (2014). Relationship between pyrethroid Resistance and attacking persimmon in the onion thrips, *Thrips tabaci* (thysanoptera: thripidae). *Jpn. J. Appl. Entomol. Zool.* 58 (3), 255–262. doi:10.1303/jjaez.2014.255

Ndakidemi, B., Mtei, K., and Ndakidemi, P. A. (2016). Impacts of synthetic and botanical pesticides on beneficial insects. *Agric. Sci.* 7 (06), 364–372. doi:10.4236/as.2016.76038

Nguyen, T. T., Collins, P. J., and Ebert, P. R. (2015). Inheritance and characterization of strong resistance to phosphine in *Sitophilus oryzae* (L.). *PloS One* 10 (4), e0124335. doi:10.1371/journal.pone.0124335

Nwosu, L. C. (2018). Impact of age on the biological activities of *Sitophilus zeamais* (Coleoptera: curculionidae) adults on stored maize: implications for food security and pest management. *J. Econ. Entomol.* 111 (5), 2454–2460. doi:10.1093/jee/toy187

Ojo, J. A., and Omoloye, A. A. (2016). Development and life history of *Sitophilus zeamais* (Coleoptera: curculionidae) on cereal crops. *Adv. Agric.* 2016, 1–8. doi:10.1155/2016/7836379

Onstad, D. W., and Flexner, J. L. (2023). "Insect resistance, natural enemies, and density-dependent processes," in *Insect resistance management* (United States: Academic Press), 381–399.

Osoro, J. K., Machani, M. G., Ochomo, E., Wanjala, C., Omukunda, E., Munga, S., et al. (2021). Insecticide resistance exerts significant fitness costs in immature stages of *Anopheles gambiae* in western Kenya. *Malar. J.* 20 (1), 259. doi:10.1186/s12936-021-03798-9

Overton, K., Hoffmann, A. A., Reynolds, O. L., and Umina, P. A. (2021). Toxicity of insecticides and miticides to natural enemies in Australian grains: A review. *Insects* 12 (2), 187. doi:10.3390/insects12020187

Park, Y., Kim, S., Lee, S. H., and Lee, J. H. (2021). Insecticide resistance trait may contribute to genetic cluster change in *Bemisia tabaci* MED (Hemiptera: aleyrodidae) as a potential driving force. *Pest Manag. Sci.* 77 (7), 3581–3587. doi:10.1002/ps.6412

Parker-Crockett, C., Lloyd, A., Ramirez, D., and Connelly, C. R. (2022). Impacts of differential mosquito control treatment regimens on insecticide susceptibility status of *Aedes aegypti* (Diptera: culicidae). *SN Appl. Sci.* 4 (9), 249. doi:10.1007/s42452-022-05130-9

Patole, S. S. (2017). Review on beetles (Coleopteran): an agricultural major crop pests of the world. *Int. J. Life Sci. Sci. Res.* 3 (6), 1424–1432. doi:10.21276/ijlssr.2017.3.6.1

Pietri, J. E., and Liang, D. (2018). The links between insect symbionts and insecticide resistance: causal relationships and physiological tradeoffs. *Ann. Entomol. Soc. Am.* 111 (3), 92–97. doi:10.1093/aesa/say009

Pietri, J. E., Tiffany, C., and Liang, D. (2018). Disruption of the microbiota affects physiological and evolutionary aspects of insecticide resistance in the German cockroach, an important urban pest. *PloS One* 13 (12), e0207985. doi:10.1371/journal.pone.0207985

Pires, D., Lozano, R. E., Menger, J. P., Andow, D. A., and Koch, R. L. (2021). Identification of point mutations related to pyrethroid resistance in voltage-gated sodium channel genes in *Aphis glycines*. *Entomol. Gen.* 41 (3), 243–255. doi:10.1127/entomologia/2021/1226

Platt, N., Kwiatkowska, R. M., Irving, H., Diabaté, A., Dabire, R., and Wondji, C. S. (2015). Target-site resistance mutations (kdr and RDL), but not metabolic resistance, negatively impact male mating competiveness in the malaria vector *Anopheles gambiae*. *Heredity* 115 (3), 243–252. doi:10.1038/hdy.2015.33

Qin, Y., Xu, P., Jin, R., Li, Z., Ma, K., Wan, H., et al. (2021). Resistance of *Nilaparvata lugens* (Hemiptera: delphacidae) to triflumezopyrim: inheritance and fitness costs. *Pest Manag. Sci.* 77 (12), 5566–5575. doi:10.1002/ps.6598

Qu, Y., Chen, X., Monticelli, L. S., Zhang, F., Desneux, N., Huijie, D., et al. (2020). Parasitism performance of the parasitoid *Trichogramma dendrolimi* on the plum fruit moth *Grapholitha funebrana*. *Entomol. Gen.* 40 (4), 385–395. doi:10.1007/s00294-019-01030-5

Renault, D., Elfiky, A., and Mohamed, A. (2023). Predicting the insecticide-driven mutations in a crop pest insect: evidence for multiple polymorphisms of acetylcholinesterase gene with potential relevance for resistance to chemicals. *Environ. Sci. Pollut. Res.* 30 (7), 18937–18955. doi:10.1007/s11356-022-23309-w

Rinkevich, F. D., Leichter, C. A., Lazo, T. A., Hardstone, M. C., and Scott, J. G. (2013). Variable fitness costs for pyrethroid resistance alleles in the house fly, *Musca domestica*, in the absence of insecticide pressure. *Pestic. Biochem. Phys.* 105 (3), 161–168. doi:10.1016/j.pestbp.2013.01.006

Roca-Acevedo, G., Boscaro, I., and Toloza, A. C. (2023). Global pattern of kdr-type alleles in *Musca domestica* (L.). *Curr. Trop. Med. Rep.* 10 (1), 1–10. doi:10.1007/s40475-022-00281-6

Rodrigo, R. G., Cuervo, R. J. B., Anzolut, S. P., and Takao, Y. P. (2019). Pest management systems and insecticide tolerance of lacewings (neuroptera: chrysopidae). *J. Econ. Entomol.* 112 (3), 1183–1189. doi:10.1093/jee/toz024

Rodríguez, E., Weber, J. M., Pagé, B., Roubik, D. W., Suarez, R. K., and Darveau, C. A. (2015). Setting the pace of life: membrane composition of flight muscle varies with metabolic rate of hovering orchid bees. *Proc. R. Soc. B Biol. Sci.* 282 (1802), 20142232. doi:10.1098/rspb.2014.2232

Roy, D., Bhattacharjee, T., Biswas, A., Ghosh, A., Sarkar, S., Mondal, D., et al. (2019). Resistance monitoring for conventional and new chemistry insecticides on *Bemisia tabaci* genetic group Asia-I in major vegetable crops from India. *Phytoparasitica* 47, 55–66. doi:10.1007/s12600-018-00707-w

Saeed, R., Abbas, N., and Hafez, A. M. (2021). Biological fitness costs in emamectin benzoate-resistant strains of *Dysdercus koenigii*. *Entomol. Gen.* 41 (3), 267–278. doi:10.1127/entomologia/2021/1184

Salas Gervassio, N. G., Aquino, D., Vallina, C., Biondi, A., and Luna, M. G. (2019). A re-examination of *Tuta absoluta* parasitoids in South America for optimized biological control. *J. Pest Sci.* 92 (4), 1343–1357. doi:10.1007/s10340-018-01078-1

Sanada-Morimura, S., Fujii, T., Chien, H. V., Cuong, L. Q., Estoy, G. F., Jr, and Matsumura, M. (2019). Selection for imidacloprid resistance and mode of inheritance in the brown planthopper, *Nilaparvata lugens*. *Pest Manag. Sci.* 75 (8), 2271–2277. doi:10.1002/ps.5364

Schmidt-Jeffris, R. A., Beers, E. H., and Sater, C. (2021). Meta-analysis and review of pesticide non-target effects on phytoseiids, key biological control agents. *Pest Manag. Sci.* 77 (11), 4848–4862. doi:10.1002/ps.6531

Shah, R. M., and Shad, S. A. (2020). House fly resistance to chlorantraniliprole: cross resistance patterns, stability and associated fitness costs. *Pest Manag. Sci.* 76 (5), 1866–1873. doi:10.1002/ps.5716

Shah, R. M., Shad, S. A., and Abbas, N. (2015). Mechanism, stability and fitness cost of resistance to pyriproxyfen in the house fly, *Musca domestica* L.(Diptera: muscidae). *Pestic. Biochem. Phys.* 119, 67–73. doi:10.1016/j.pestbp.2015.02.003

Shah, R. M., Shad, S. A., and Abbas, N. (2017). Methoxyfenozide resistance of the housefly, *Musca domestica* L.(Diptera: muscidae): cross-resistance patterns, stability and associated fitness costs. *Pest Manag. Sci.* 73 (1), 254–261. doi:10.1002/ps.4296

Shan, J., Zhu, B., Gu, S., Liang, P., and Gao, X. (2021). Development of resistance to chlorantraniliprole represses sex pheromone responses in male *Plutella xylostella* (L.). *Entomol. Gen.* 41 (6), 615–625. doi:10.1127/entomologia/2021/1359

Shi, R., Zhao, H., and Tang, S. (2014). Global dynamic analysis of a vector-borne plant disease model. *Adv. Differ. Equ.* 1, 59–16. doi:10.1186/1687-1847-2014-59

Sifakis, S., Androutsopoulos, V. P., Tsatsakis, A. M., and Spandidos, D. A. (2017). Human exposure to endocrine disrupting chemicals: effects on the male and female reproductive systems. *Environ. Toxicol. Pharmacol.* 51, 56–70. doi:10.1016/j.etap.2017.02.024

Singarayan, V. T., Jagadeesan, R., Nayak, M. K., Ebert, P. R., and Daglish, G. J. (2021). Gene introgression in assessing fitness costs associated with phosphine resistance in the rusty grain beetle. *J. Pest Sci.* 94, 1415–1426. doi:10.1007/s10340-020-01315-6

Singh, S., and Chandi, A. K. (2019). Physiological influences of pyriproxyfen, a juvenile hormone analogue, on *Bemisia tabaci* (Gennadius). *Agric. Res. J.* 56 (3), 444–452. doi:10.5958/2395-146x.2019.00071.1

S. Sithanantham, C. R. Ballal, S. K. Jalali, and N. Bakthavatsalam (Editors) (2013). *Biological control of insect pests using egg parasitoids* (India: Springer), 15.

Sparks, T. C., and Nauen, R. (2015). IRAC: mode of action classification and insecticide resistance management. *Pestic. Biochem. Phys.* 121, 122–128. doi:10.1016/j.pestbp.2014.11.014

Sparks, T. C., Dripps, J. E., Watson, G. B., and Paroonagian, D. (2012). Resistance and cross-resistance to the spinosyns–a review and analysis. *Pestic. Biochem. Phys.* 102 (1), 1–10. doi:10.1016/j.pestbp.2011.11.004

Steinbach, D., Moritz, G., and Nauen, R. (2017). Fitness costs and life table parameters of highly insecticide-resistant strains of *Plutella xylostella* (L.)(Lepidoptera: plutellidae) at different temperatures. *Pest Manage Sci.* 73 (9), 1789–1797. doi:10.1002/ps.4597

Sun, H., Tong, K. P., Kasai, S., and Scott, J. G. (2016). Overcoming super-knock down resistance (super-kdr) mediated resistance: multi-halogenated benzyl pyrethroids are more toxic to super-kdr than kdr house flies. *Insect Mol. Biol.* 25 (2), 126–137. doi:10.1111/imb.12206

Tabebordbar, F., Shishehbor, P., Ziaee, M., and Sohrabi, F. (2020). Lethal and sublethal effects of two new insecticides spirotetramat and flupyradifurone in comparison to conventional insecticide deltamethrin on *Trichogramma evanescens* (Hymenoptera: trichogrammatidae). *J. Asia Pac Entomol.* 23 (4), 1114–1119. doi:10.1016/j.aspen.2020.09.008

Tanda, A. S., Kumar, M., Tamta, A. K., and Deeksha, M. G. (2022). "Advances in integrated management technology of insect pests of stored grain," in *Advances in integrated pest management technology* (Cham: Springer), 157–196.

Uesugi, R. (2021). Historical changes in the lethal effects of insecticides against the diamondback moth, *Plutella xylostella* (L.). *Pest Manag. Sci.* 77 (7), 3116–3125. doi:10.1002/ps.6344

Ullah, F., Gul, H., Tariq, K., Desneux, N., Gao, X., and Song, D. (2020a). Functional analysis of cytochrome P450 genes linked with acetamiprid resistance in melon aphid, *Aphis gossypii*. *Pestic. Biochem. Phys.* 170, 104687. doi:10.1016/j.pestbp.2020.104687

Ullah, F., Gul, H., Tariq, K., Desneux, N., Gao, X., and Song, D. (2020b). Fitness costs in clothianidin-resistant population of the melon aphid, *Aphis gossypii*. *Plos One* 15 (9), e0238707. doi:10.1371/journal.pone.0238707

Ullah, F., Gul, H., Desneux, N., Said, F., Gao, X., and Song, D. (2020c). Fitness costs in chlorfenapyr-resistant populations of the chive maggot, *Bradysia odoriphaga*. *Ecotoxicology* 29, 407–416. doi:10.1007/s10646-020-02183-7

Ullah, F., Gul, H., Tariq, K., Desneux, N., Gao, X., and Song, D. (2021). Acetamiprid resistance and fitness costs of melon aphid, *Aphis gossypii*: an age-stage, two-sex life table study. *Pestic. Biochem. Phys.* 171, 104729. doi:10.1016/j.pestbp.2020.104729

Ullah, F., Xu, X., Gul, H., Güncan, A., Hafeez, M., Gao, X., et al. (2022). Impact of imidacloprid resistance on the demographic traits and expressions of associated genes in *Aphis gossypii* Glover. *Toxics* 10(11), 658. doi:10.3390/toxics10110658

Valmorbida, I., Coates, B. S., Hodgson, E. W., Ryan, M., and O'Neal, M. E. (2022). Evidence of enhanced reproductive performance and lack-of-fitness costs among soybean aphids, *Aphis glycines*, with varying levels of pyrethroid resistance. *Pest Manag. Sci.* 78 (5), 2000–2010. doi:10.1002/ps.6820

Van Leeuwen, T., Dermauw, W., Mavridis, K., and Vontas, J. (2020). Significance and interpretation of molecular diagnostics for insecticide resistance management of agricultural pests. *Curr. Opin. Insect Sci.* 39, 69–76. doi:10.1016/j.cois.2020.03.006

Verheggen, F., Barrès, B., Bonafos, R., Desneux, N., Escobar-Gutiérrez, A. J., Gachet, E., et al. (2022). Producing sugar beets without neonicotinoids: an evaluation of alternatives for the management of viruses-transmitting aphids. *Entomol. Gen.* 42 (4), 491–498. doi:10.1127/entomologia/2022/1511

Vézilier, J., Nicot, A., De Lorgeril, J., Gandon, S., and Rivero, A. (2013). The impact of insecticide resistance on *Culex pipiens* immunity. *Evol. Appl.* 6 (3), 497–509. doi:10.1111/eva.12037

Von Santos, V. R., Pereira, E. J., Guedes, R. N., and Oliveira, M. G. (2013). Does cypermethrin affect enzyme activity, respiration rate and walking behavior of the maize weevil (*Sitophilus zeamais*)? *Insect Sci.* 20 (3), 358–366. doi:10.1111/j.1744-7917.2012.01529.x

Walsh, L. E., Schmidt, O., Foster, S. P., Varis, C., Grant, J., Malloch, G. L., et al. (2022). Evaluating the impact of pyrethroid insecticide resistance on reproductive fitness in *Sitobion avenae*. *Ann. Appl. Biol.* 180 (3), 361–370. doi:10.1111/aab.12738

Wan, Y., Zheng, X., Xu, B., Xie, W., Wang, S., Zhang, Y., et al. (2021). Insecticide resistance increases the vector competence: A case study in *Frankliniella occidentalis*. *J. Pest Sci.* 94, 83–91. doi:10.1007/s10340-020-01207-9

Wang, Z. Y., He, K. L., Zhang, F., Lu, X., and Babendreier, D. (2014). Mass rearing and release of *Trichogramma* for biological control of insect pests of corn in China. *Biol. Control* 68, 136–144. doi:10.1016/j.biocontrol.2013.06.015

Wang, C., Eiden, A., Cooper, R., Zha, C., and Wang, D. (2019a). Effectiveness of building-wide integrated pest management programs for German cockroach and bed bug in a high-rise apartment building. *J. Integr. Pest Manag.* 10 (1), 33. doi:10.1093/jipm/pmz031

Wang, Y., Xiang, M., Hou, Y. Y., Yang, X., Dai, H., Li, J., et al. (2019b). Impact of egg deposition period on the timing of adult emergence in *Trichogramma* parasitoids. *Entomol. Gen.* 39, 339–346. doi:10.1127/entomologia/2019/0896

Wang, L., Ma, Y., Guo, X., Wan, P., Liu, K., Cong, S., et al. (2019c). Pink bollworm resistance to *Bt* toxin Cry1Ac associated with an insertion in cadherin exon 20. *Toxins* 11 (4), 186. doi:10.3390/toxins11040186

Wang, C., Eiden, A. L., Cooper, R., Zha, C., Wang, D., and Hamilton, R. G. (2020a). Abatement of cockroach allergens by effective cockroach management in apartments. *J. Allergy Clin. Immunol. Pract.* 8 (10), 3608–3609. doi:10.1016/j.jaip.2020.06.040

Wang, L., Walter, G. H., and Furlong, M. J. (2020b). Temperature, deltamethrin-resistance status and performance measures of *Plutella xylostella*: complex responses of insects to environmental variables. *Ecol. Entomol.* 45 (2), 345–354. doi:10.1111/een.12805

Wang, R., Wang, Z., Luo, C., and Yang, G. (2020c). Characterization of pyridalyl resistance in a laboratory-selected strain of *Frankliniella occidentalis*. *Pestic. Biochem. Phys.* 166, 104564. doi:10.1016/j.pestbp.2020.104564

Wang, K., Liu, M., Wang, Y., Song, W., and Tang, P. (2020d). Identification and functional analysis of cytochrome P450 CYP346 family genes associated with phosphine resistance in *Tribolium castaneum*. *Pestic. Biochem. Phys.* 168, 104622. doi:10.1016/j.pestbp.2020.104622

Wang, P., Li, M. J., Bai, Q. R., Ali, A., Desneux, N., Dai, H. J., et al. (2021). Performance of *Trichogramma japonicum* as a vector of *Beauveria bassiana* for parasitizing eggs of rice striped stem borer, *Chilo suppressalis*. *Entomol. Gen.* 41 (2), 147–154. doi:10.1016/j.canrad.2020.06.030

Weiss, B. L., Maltz, M., and Aksoy, S. (2012). Obligate symbionts activate immune system development in the tsetse fly. *J. Immunol. Res.* 188 (7), 3395–3403. doi:10.4049/jimmunol.1103691

Xie, L. C., Jin, L. H., Lu, Y. H., Xu, H. X., Zang, L. S., Tian, J. C., et al. (2022). Resistance of lepidopteran egg parasitoids, *Trichogramma japonicum* and *Trichogramma chilonis*, to insecticides used for control of rice planthoppers. *J. Econ. Entomol.* 115 (2), 446–454. doi:10.1093/jee/toab254

Yin, C., Wang, R., Luo, C., Zhao, K., Wu, Q., Wang, Z., et al. (2019). Monitoring, cross-resistance, inheritance, and synergism of *Plutella xylostella* (Lepidoptera: plutellidae) resistance to pyridalyl in China. *J. Econ. Entomol.* 112 (1), 329–334. doi:10.1093/jee/toy334

Zang, L. S., Wang, S., Zhang, F., and Desneux, N. (2021). Biological control with *Trichogramma* in China: history, present status, and perspectives. *Annu. Rev. Entomol.* 66, 463–484. doi:10.1146/annurev-ento-060120-091620

Zhang, F., and Yang, R. (2019). Life history and functional capacity of the microbiome are altered in beta-cypermethrin-resistant cockroaches. *Int. J. Parasitol.* 49 (9), 715–723. doi:10.1016/j.ijpara.2019.04.006

Zhang, X., Liao, X., Mao, K., Yang, P., Li, D., Alia, E., et al. (2017). The role of detoxifying enzymes in field-evolved resistance to nitenpyram in the brown planthopper *Nilaparvata lugens* in China. *Crop Prot.* 94, 106–114. doi:10.1016/j.cropro.2016.12.022

Zhang, X., Mao, K., Liao, X., He, B., Jin, R., Tang, T., et al. (2018a). Fitness cost of nitenpyram resistance in the brown planthopper *Nilaparvata lugens*. *J. Pest Sci.* 91, 1145–1151. doi:10.1007/s10340-018-0972-2

Zhang, J. H., Zhang, S., Yang, Y. X., Zhang, Y. X., and Liu, Z. W. (2018b). New insight into foregut functions of xenobiotic detoxification in the cockroach *Periplaneta americana*. *Insect Sci.* 25 (6), 978–990. doi:10.1111/1744-7917.12486

Zhang, X., Wang, H. C., Du, W. M., Zang, L. S., Ruan, C. C., Zhang, J. J., et al. (2021). Multi-parasitism: a promising approach to simultaneously produce *Trichogramma chilonis* and *T. dendrolimi* on eggs of *Antheraea pernyi*. *Entomol. Gen.* 41 (6), 627–636. doi:10.1038/s41419-021-03917-z

frontiers | Frontiers in Physiology

TYPE Original Research
PUBLISHED 01 December 2023
DOI 10.3389/fphys.2023.1250836

OPEN ACCESS

EDITED BY
Bin Tang,
Hangzhou Normal University, China

REVIEWED BY
Xiaoling Tan,
Chinese Academy of Agricultural Sciences (CAAS), China
Wei Zhang,
Guizhou University, China

*CORRESPONDENCE
Fei Lyu,
haimolv@foxmail.com
Zhigang Wang,
wzhg432@163.com

†These authors have contributed equally to this work

RECEIVED 30 June 2023
ACCEPTED 22 November 2023
PUBLISHED 01 December 2023

CITATION
Jiang X, Li T, Hai X, Zheng X, Wang Z and Lyu F (2023), Integrated behavior and transcriptomic analysis provide valuable insights into the response mechanisms of *Dastarcus helophoroides* Fairmaire to light exposure.
Front. Physiol. 14:1250836.
doi: 10.3389/fphys.2023.1250836

Integrated behavior and transcriptomic analysis provide valuable insights into the response mechanisms of *Dastarcus helophoroides* Fairmaire to light exposure

Xianglan Jiang[1†], Tengfei Li[1†], Xiaoxia Hai[1], Xiang Zheng[2], Zhigang Wang[1*] and Fei Lyu[1*]

[1]College of Forestry, Hebei Agricultural University, Baoding, Hebei, China, [2]Laboratory of Enzyme Preparation, Hebei Research Institute of Microbiology Co., Ltd., Baoding, Hebei, China

Light traps have been widely used to monitor and manage pest populations, but natural enemies are also influenced. The *Dastarcus helophoroides* Fairmaire is an important species of natural enemy for longhorn beetles. However, the molecular mechanism of *D. helophoroides* in response to light exposure is still scarce. Here, integrated behavioral, comparative transcriptome and weighted gene co-expression network analyses were applied to investigate gene expression profiles in the head of *D. helophoroides* at different light exposure time. The results showed that the phototactic response rates of adults were 1.67%–22.5% and females and males displayed a negative phototaxis under different light exposure [6.31×10^{18} (photos/m^2/s)]; the trapping rates of female and male were influenced significantly by light exposure time, diel rhythm, and light wavelength in the behavioral data. Furthermore, transcriptome data showed that a total of 1,052 significantly differentially expressed genes (DEGs) were identified under different light exposure times relative to dark adaptation. Bioinformatics analyses revealed that the "ECM-receptor interaction," "focal adhesion," "PI3K-Akt signaling," and "lysosome" pathways were significantly downregulated with increasing light exposure time. Furthermore, nine DEGs were identified as hub genes using WGCNA analysis. The results revealed molecular mechanism in negative phototactic behavior response of *D. helophoroides* under the light exposure with relative high intensity, and provided valuable insights into the underlying molecular response mechanism of nocturnal beetles to light stress.

KEYWORDS

***Dastartcus helophoroides*, natural enemy, phototactic behavior, nocturnal beetles, transcriptome, ECM-receptor interaction**

1 Introduction

With global landscape and climate change, insect pests have widespread and frequent outbreaks, seriously damaging agricultural and forest services for human wellbeing, particularly the expansion of invasive pests in nonnative ranges (Scherm et al., 2000; Mina et al., 2022). In many countries, chemical pesticides are still the primary control

strategy for pests, but excessive utilization of pesticides has led to problems, such as reducing biodiversity of insects in freshwater and terrestrial systems (Beketov et al., 2013), polluting the environment, increasing pest resistance to pesticides, and contributing to global insect pollinator declines (Basset and Lamarre, 2019). Insect pest management has become one of the biggest challenges, such as on organic farms (Kim et al., 2019). Natural enemies are alternative and environmentally friendly means to control insect pests and have received wide attention worldwide (Landis et al., 2000).

The ectoparasitoid beetle, *Dastartcus helophoroides* Fairmaire (Coleptera: Bothrideridae) is distributed widely in Kyushu and Osaka in Japan, Korea and China (Lyu et al., 2014). This beetle is an important parasitoid of several longhorned beetles in its native range, including *Anoplophora glabripennis* Motschulsky (Haack et al., 2010), *Monochamus alternatus* Hope (Lyu et al., 2014), and *Batocera horsfieldi* Hope (Yang et al., 2014). These longhorn beetles are phytophagous: the larvae usually bore in the large branches and trunks of woody plants, ranging from alive to moribund to dead and decomposing (Hanks, 1999). Many longhorn beetle species cause tremendous economic and ecological losses in forests worldwide, including insect vectors of nematodes (Zhou et al., 2023), such as *A. glabripennis* and the genus *Monochamus*. The *A. glabripennis* is a polyphagous xylophage native to Asia and ranked as one of the top 100 worst invasive species worldwide in North America and Europe (Branco et al., 2022). Potential losses of widespread *A. glabripennis* outbreaks in compensatory value were equal to approximately 12% of the total economic losses caused by forest pests and diseases in China, exceeding more than US$1.5 billion (Golec et al., 2018). Outside its native range, estimations of potential economic losses exceed US$1 trillion if adjusted to 2021 values, and approximately 35% of urban trees have been destroyed in the USA (Branco et al., 2022). Pine wood nematodes is transported between host trees by cerambycid beetles of the genus *Monochamus*, and approximately 1.7 million hectares were infected in 19 provinces in 2021, destroying 14 million trees in China's pine forests (Yu et al., 2023).

Insects use visual and chemical cues from intra- and interspecific communication and the environment to mediate their activities and behaviors, such as reproduction, and foraging, and even to organize and maintain social structures in social insects (Nieri et al., 2022). Many different stimuli signals have often been applied to pest management, such as chemicals, lights, colors, sounds and vibrations (Fleming et al., 2005; Kim et al., 2019; Cavaletto et al., 2021; Van der Kooi et al., 2021; Zapponi et al., 2022). In cerambycid beetles, pheromone-baited traps are a common tool for detecting and sampling insects for surveillance, eradication, or management, and pheromones of more than 100 cerambycid species have been identified to date, including sex attractant pheromones, aggregation-sex pheromones, and nonvolatile contact pheromones (Hanks and Millar, 2016). However, semiochemical-based traps baited with a mixture of host kairomones (plant volatile organic compounds) and/or sex pheromones have still not reached operational efficacy for some Cerambycid beetles in field bioassays; for example, the trapping number of approximately 80% (34/43) of longhorn beetle species was fewer than 10 beetles per 10–14 days (Nehme et al., 2010; Ray et al., 2012; Wickham et al., 2012; Hanks and Millar, 2013; Wickham et al., 2014; Silva et al., 2016; Wickham et al., 2016; Zhu et al., 2017; Xu et al., 2020) (Supplementary Figure S1). Therefore, an effective trapping tool needs to be developed for some longhorn beetles with limited semiochemical-based trapping effects in the future.

Light traps are widely used to monitor and manage the population density of insect pests, and play an important role in physical pest control (Kim et al., 2019). Due to natural light is present in the daytime, the target pest is usually a crepuscular or nocturnal insect, and at least some of the activity occurs at night (Kim et al., 2019; Nieri et al., 2022). Both foraging and mating behavior in *A. glabripennis* adults occur throughout the day, and the peaking of foraging behavior occurs at night (21:30) (Lyu et al., 2015a). In addition, the mating behavior of *M. alternatus* also took place throughout the day, particularly during the peak time of activity at night (18:00–24:00) (Luo et al., 2012). Longhorn beetles *Phymatodes aereus*, *Anelaphus pumilus*, and *Massicus raddei* are also nocturnal insects (Mitchell et al., 2015). These results suggested that a light-trapping strategy may be used to monitor and manage the population density of Cerambycid beetles. Although light traps can be used to attract and kill insect pest populations, they can also kill the natural enemies of pests (Luo and Chen, 2016). Therefore, the phototactic behavioral responses of natural enemies should be considered when light traps are used to monitor and manage target insect pests.

The phototactic behavior of insects not only depends on the characteristics of the light source, including light wavelength and intensity, but the other conditions also influence phototactic behavior response rates, such as rhythmicity with photoperiod, light exposure time, sex and gene expression (Kim et al., 2019; Kooi et al., 2021). Although the results of previous study showed that near-infrared light (NIR, 700 nm) is most suitable in attracting *D. helophoroides* adults, the phototactic response of *D. helophoroides* have broad spectrum of light (from UV to NIR) and the response rates were not significant difference between UV, blue, green and NIR lights (Wang et al., 2021). In addition, near infrared light (NIR,700 nm) were used to trap Cerambycid beetles has been rarely reported. In the field, UV (or violet), blue, and green lights are usually used to attract and kill target insect pests, including Cerambycid beetles (Luo and Chen, 2016). For example, the beetles (Coleoptera) show a preference for UV, violet (350–440) and green (500–560) wavelength spectra (Kim et al., 2019; Van der Kooi et al., 2021). UV-black-light-blue light traps captured more Cerambycid beetles (*Arhopaus ferus*) than yellow light traps (Pawson et al., 2009). UV (365 nm) and violet light (420 and 435 nm) are the most suitable wavelengths for attracting adult *A. glabripennis* at night (Jiang et al., 2023a). Therefore, in order to decrease the trapping rate of natural enemy (*D. helophoroides*) in the light traps, it is of great significance to reveal the response mechanism of *D. helophoroides* adults for the UV and visible lights.

The behavioral and physiological changes of insects under light exposure are well established (Kim et al., 2019; Kooi et al., 2021) and are tightly related to gene expression and regulation (Futahashi et al., 2015). RNA-Seq is a powerful tool for the analysis of DEGs, the discovery of novel transcripts, and the identification of key genes (Trapnell et al., 2010). It has been widely utilized in various fields ranging from agriculture to medicine, investigating gene expression changes in response to light exposure and other biotic and abiotic stresses (Hong et al., 2020; Chen et al., 2022). In *Diaphorina citri* adults, 841 upregulated differential expressed genes (DEGs) and 932 downregulated DEGs, and DEGs play key roles in physiological

and biochemical responses such as oxidative stress, protein denaturation, inflammation and tumor development after blue light (400 nm) exposure (Wang F. F. et al., 2023). While 40 DEGs were upregulated and 413 DEGs were downregulated in the *Bemisia tabaci* after ultraviolet-A radiation, and DEGs were mainly involved in physiological and biochemical responses, including anti-oxidation and detoxification, protein turnover, metabolism (Khan et al., 2023). Many studies have shown that downregulated DEGs are significantly greater than upregulated DEGs after different light exposures and the antioxidant activity is decreased (Cui et al., 2021; Khan et al., 2023). However, these data are insufficient to fully understand the molecular mechanisms underlying the response to light exposure, especially in nocturnal Coleoptera beetles.

In the present study, we investigated the influence of light exposure time, sex, and diel rhythm on the phototactic behavioral response of female and male *D. helophoroides* under light with different wavelengths, and the gene expression profiles of females and males under white light exposure. Due to UV, violet (350–440 nm) and green (500–560 nm) wavelength spectra were often used to trap Cerambycid beetles, therefore, 6 LED light wavelengths, which were UV (365 nm), violet (420 nm and 435 nm), green (515 nm), and red (600 nm and 660 nm), were selected to investigate the effect of exposure time on the phototactic behavioral responses of females and males, thus providing an appropriate test condition for the next experiment. Then, we displayed the phototactic behavioral responses of females and males under different light wavelengths at five time slots to show diel rhythm on the phototactic behavioral response. Finally, at the transcriptome level, we investigated the gene expression profiles of females and males under different light exposure times (15 and 120 min) of white light relative to dark conditions (control treatment) to explore the response mechanism for light exposure. Thus, these results not only can provide valuable information for the monitoring and management of population density and prediction, but also may expand the understanding of the molecular response mechanism in the nocturnal beetle *D. helophoroides* to light exposure.

2 Materials and methods

2.1 Insects

Adults of the beetle *D. helophoroides* were provided by the Institute of Entomology, College of Agriculture Vocational of Beijing. The first generation of the wild population was collected from parasitized larvae and pupae of *A. glabripennis*. A substitute hosts (*Thyestilla gebleri* Fald.) were used to rear larvae. Adults were reared at 25°C and 60% ± 10% relative humidity under an LD cycle of 16:8 h (light: 500 lx and dark 0 lx) in an artificial climate chamber (RXZ-500D, Jiangnan Instrument Factory, Ningbo, China). The insects were provided water in moist cotton balls placed on the centrifuge tube and were fed *Tenebrio molitor* L. larvae that were dried by the stove at 60 °C. Female and male adults were distinguished by the end angle of the anal plate under a dissecting microscope (Olympus SZ51, Tokyo, Japan) according to Tang et al. (2007). Approximately 30–60 days after emergence adults were used in our experiment, and all females and males were able to mate and oviposit normally (female) in our experiment.

2.2 Experimental apparatus and light sources

To observe the phototactic behavior of *D. helophoroides* in the different conditions, a light-dark alternative apparatus with an opaque black acrylic board was self-designed based on a previous study (Figures 1A, B) (Jiang et al., 2023a). The apparatus comprised two test chambers (L = 50 cm × H = 30 cm × W = 30 cm) at right angles to each other, which provided an activity space for beetles to respond to different wavelength LED lights, and an activity chamber (L = 30 cm × H = 30 cm × W = 30 cm), which provided adequate space for insect movement. The side of the test chamber near the light source area was called the light area (Figure 1B, a), and the other side without the light source area was called the dark area (Figure 1B, b). To conveniently observe the behavior of beetles, transparent acrylic boards were used on the top side of the light and dark areas. Half of the top of the chamber (Figure 1B, f) was used with a moveable transparent acrylic board to facilitate the removal and observation of insects after the test. At the tops of the activity chamber, we drilled a hole with 10 cm diameter (Figure 1, d) to introduce test insects, and then placed a transparent acrylic board on the hole to prevent insect escape when *D. helophoroides* was added to the activity chamber. A transparent and opaque acrylic board was fitted on the end of the light and dark areas to prevent insect escape and facilitate light transmission, respectively. We set up two baffle boards with opaque black acrylic (Figure 1, e) between the test and activity chambers. Only the LED light resource was turned on in the light area when the baffle was pushed down (Figure 1, a). The LED light resource was spread in the light area (Figure 1, a) and activity chamber (Figure 1, c), and there was no light in the dark area (Figure 1, b) when the baffle was removed. The number of test insects in the phototaxis areas within 30 cm was regarded as the positive trapping number of females and males, while the number of insects was used as the negative trapping number of adults in the dark area. To avoid the effect of light reflection, opaque black acrylic boards were used in the outer and inner of chambers, except for the top side of the light and dark areas, to facilitate the observation of test insects. All experiments were tested under a completely dark environment in an air-conditioned room to maintain a constant temperature of 25°C ± 1°C and 65% ± 10% RH.

Fourteen monochromatic LED lamps distributing ultraviolet (UV) and visible light were used as light stimuli at the end of the light area, including 365, 385, 400, 420, 435, 475, 500, 515, 560, 595, 600, 630, and 660 nm (Jiang et al., 2023a). All LED lamps were made by Shenzhen Xinhongxian Electronics Technology Co., Ltd. (Shenzhen, China), and the power of each lamp was 20 W. A rheostat was connected LED lights to adjust the light intensity. Due to females and males were attracted by light passing through a transparent acrylic board rather than under direct light, the light irradiance at the center of the activity chamber was measured by a high-speed spectrometer (HSU–100S, Asahi Spectra Co. Ltd., Tokyo) with sensor fiber. The intensity of the light in photons

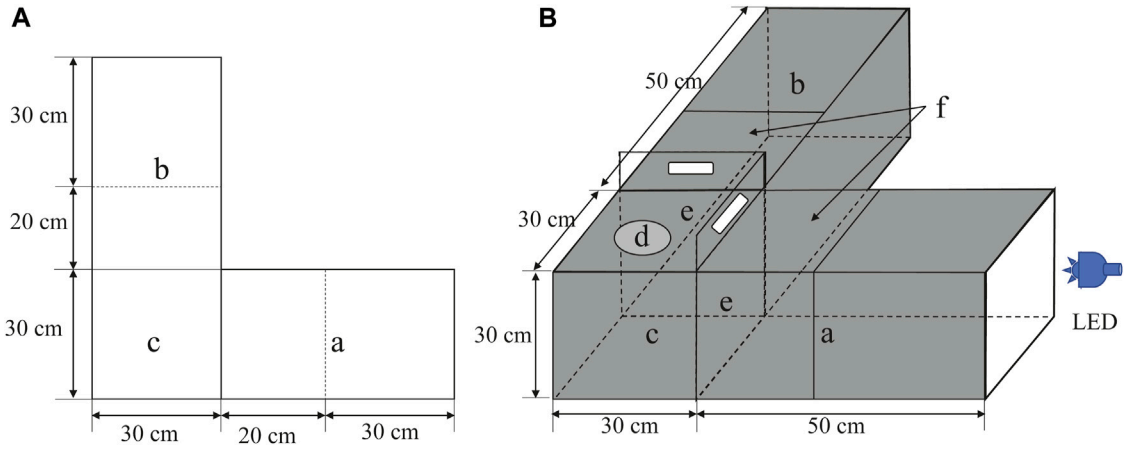

FIGURE 1
Schematic diagram of the behavioral bioassay chamber. **(A)** planar diagram, **(B)** stereoscopic diagram. Storage chambers (a and b); activity chamber (c); test insect release point (d); black opaque acrylic boards (e) and moveable transparent acrylic board (f). LED: light emitting diode.

per second per area was adjusted and maintained at 6.31×10^{18} (photos/m^2/s) (Miyatake et al., 2016).

2.3 Behavioral experiments

A series of dual-choice experiments were displayed to determine the effect of exposure time, diel rhythm, and light wavelength on the phototactic behavioral response of female and male *D. helophoroides* in a completely dark indoor environment. Different light sources were installed at the end of the light area, while no light sources were installed at the end of the dark area. Twenty adult females or males were used as one replicate to test the phototactic behavioral response of adults. In each test, adults were placed in the activity chamber to adapt to the dark environment for 2 h, and then the LED lamps were turned on. When the baffles were removed from the junction between the activity and the test chambers, the timer was started. The number of females and males was recorded in the light, dark and release areas, respectively. To avoid residual adult volatile cues, the activity and test chamber was wiped with hexane and air-dried between trials.

2.3.1 Effect of exposure time on phototactic behavioral responses

UV, violet (350–440) and green (500–560) wavelength spectra were often used to trap Cerambycid beetles in field (Kim et al., 2019; Van der Kooi et al., 2021). Red light was also the preferred source of light for adult *D. helophoroides* (Wang et al., 2021). Therefore, six wavelength spectra (365, 420, 435, 515, 600, and 660 nm) were selected to analyze the effect of exposure time on the behavioral responses of adults in the time slot 19:00–21:00 to provide a suitable light exposure time for the next test. We installed 6 different wavelength LED lights at the end of the light area, while no lights were installed at the end of the dark area. The number of beetles in the light area, dark area and release area were recorded at 15, 30, 45, 60, 75, 90, 105, and 120 min during the observation period, respectively. Twelve replicates were measured at each light wavelength.

2.3.2 Monochromatic LED light preference in different time slots

To determine the effect of different wavelengths on the phototactic behavioral responses of female and male *D. helophoroides*, a series of experiments were conducted in 5 different time slots (9:00–11:00, 14:00–16:00, 19:00–21:00, 0:00–2:00, and 5:00–7:00). The female or male beetles either crawled or flew into the light or dark area from the activity chamber. The number of beetles in the light area, dark area and release area was recorded after an illumination time of 15 min based on the results of "Effect of exposure time on the phototactic behavioral responses" test. The samples of females and males were 6 replicates per time slot, and thirty replicates at five time slots were measured for 14 wavelengths of light (365–660 nm).

2.4 Transcription analysis

2.4.1 Transcriptome sequencing, assembly, and functional annotation

Approximately 500 (female and male) heads of adult *D. helophoroides* were used for RNA extraction in the 6 different treatments, including dark adaptation of 120 min, light exposure time of 15 and 120 min after 120 min dark adaptation (white light intensity: 6.31×10^{18} (photos/m^2/s)). Total head RNA was extracted using TRIzol Reagent (Invitrogen, Waltham, MA, United States) based on the manufacturer's standard protocol. Then, the extracted RNA was determined using a 5,300 Bioanalyser (Agilent) and quantified using an ND-2000 (NanoDrop Technologies), respectively. Only high-quality RNA samples (OD260/280 = 1.8–2.2, OD260/230 ≥ 2.0, RIN≥6.5, 28S:18S ≥ 1.0, >1 μg) were used to construct the sequencing library. The total head RNA samples were sent to Shanghai Majorbio Bio-pharm Biotechnology Co., Ltd. (Shanghai, China) for RNA quality testing, library construction, and sequencing at a depth of 6.84 G according to

the manufacturer's instructions (Illumina, San Diego, CA). All data have been uploaded in the NCBI Sequence Read Archive (SRA) database (http://www.ncbi.nlm.nih.gov/bioproject/987166). Afterward, the clean data were mapped to the reference genome of *D. helophoroides* using HISAT2 software (Zhang et al., 2023). All mapped genes were aligned into public databases using Diamond (v0.8.22, E-value 1e-5), including the NCBI non-redundant nucleotide sequences (NR), Swiss-Prot, gene ontology (GO), Kyoto Encyclopedia of Genes and Genomes (KEGG), clusters of orthologous groups of proteins (KOG/COG/eggNOG), and protein family (Pfam) databases as described previously (Liu et al., 2023).

2.4.2 Screening of DEGs, GO and KEGG enrichment analysis

The expression level of genes was calculated according to the fragments per kilobase of exon model per million mapping read values (FPKM) method to identify differentially expressed genes (DEGs) between two different samples. Differential expression analysis of different treatments was displayed using DESeq2 (http://bioconductor.org/packages/stats/bioc/DESeq2/) according to an absolute value of Log_2 FC (fold change) ≥ 1.0 and a false discovery rate (FDR) < 0.05. Furthermore, GO and KEGG functional enrichment analyses were performed to identify which DEGs were significantly enriched in GO terms and KEGG pathways at Benjamini–Hochberg (BH) - corrected FDR <0.05 compared with the whole-transcriptome background. Goatools and KOBAS were used to determine GO functional enrichment and KEGG pathways, respectively (Xie et al., 2011).

2.4.3 Short time-series expression miner (STEM) analysis

STEM analysis was used to investigate the dynamic expression of DEGs in beetles in response to light exposure (Ernst and Bar-Joseph, 2006). In the STEM analysis, the light exposure time and the calculated Log2 value of the ratio of their mRNA levels (in FPKM) at light exposure of 15 or 120 min to the control (dark adaptation = 0 min) were used as the horizontal and vertical coordinates. Subsequently, total DEGs were clustered into distinct and significant temporal expression clusters using default settings according to previous studies described (Zheng et al., 2020; Wang Z. et al., 2023).

2.4.4 WGCNA and gene-gene interaction analyses

An unsigned topological overlap matrix (TOM) was used to construct the WGCNA network according to the following parameters: the network type was signed, soft power was 14, min module size was 30, minKMEtoStay was 0.3, and merge cut height was 0.25 (Wang Z. et al., 2023; Liu et al., 2023). A correlation heatmap was constructed between the modules and traits after the cluster analysis of the modules. The module eigengene value was calculated to determine the association of modules with each light exposure time for 18 samples. The STRING database (v11.5, https://cn.string-db.org/) was used to analyze GGI predictions of hub genes, and Cytoscape software (v3.9.1) was used to visualize the interaction network from STRING (Shannon et al., 2003; Szklarczyk et al., 2020).

2.4.5 Quantitative real-time PCR (qRT-PCR) analysis

The DEGs from the transcriptome data were randomly selected to confirm the RNA-seq data and identify their transcript levels using qRT-PCR method. We used Primer Premier 5.0 software to design the primers based on the selected transcript sequence, and then these selected genes were amplified (Supplementary Table S1). We used a CFX96 Touch Deep Well Real-Time PCR Detection System (Bio-Rad, Hercules, CA, United States) to perform qRT-PCR test. The relative expression levels of mRNA were calculated with the GAPDH gene, which is an internal control gene, using the $2^{-\Delta\Delta CT}$ method (Livak and Schmittgen, 2001). Three biological replicates were measured for each treatment.

2.5 Statistical analysis

To evaluate the trapping ability of different light sources for female and male *D. helophoroides* at different treatments, the trapping rate was used as an important parameter to evaluate the trapping ability of LED lights.

The trapping rate was calculated using the following formula:

$$Trapping\ rate\ (\%) = \frac{Number\ of\ beetles\ in\ light\ area}{Total\ number\ of\ test\ beetles} \times 100 \quad (1)$$

Furthermore, in "Monochromatic LED light preference" experiment, the preference index (PI) was also used as an important parameter to evaluate the preference of beetles for light wavelengths. The formula is as follows:

$$\mathrm{PI}\ (\%) = \frac{Number\ of\ beetles\ in\ light\ area - Number\ of\ beetles\ in\ dark\ area}{Number\ of\ beetles\ in\ light\ area + Number\ of\ beetles\ in\ dark\ area} \quad (2)$$

The effects of light exposure time, diel rhythm, and light wavelength on the phototactic response of female and male beetles on trapping rate were analyzed using Generalize linear model (GLM) with a Poisson distribution and a log link function and followed by the Bonferroni test. Non-responders were recorded but excluded from the analysis. All experimental data were statistically analyzed using SPSS Statistics v. 21.0 (IBM Corp., Armonk, NY, USA) for Windows.

3 Results

3.1 Phototactic behavioral response of male and female *D. helophoroides*

3.1.1 Effect of exposure time on the phototactic behavioral response

The trapping rates of females and males showed different changes under the 6 LED light wavelengths (Figure 2). The trapping rate of females at 420 and 600 nm, and that of males at 515 nm decreased gradually when the exposure time was prolonged (female, 420 nm: $X^2 = 48.000$, $df = 7$, $p < 0.001$, 600 nm: $X^2 = 88.085$, $df = 7$, $p < 0.001$; male, 515 nm: $X^2 = 67.051$, $df = 7$, $p < 0.001$); and the trapping rate of adults at light exposure 15 min was higher than at 120 min. The trapping rates of females and males show no

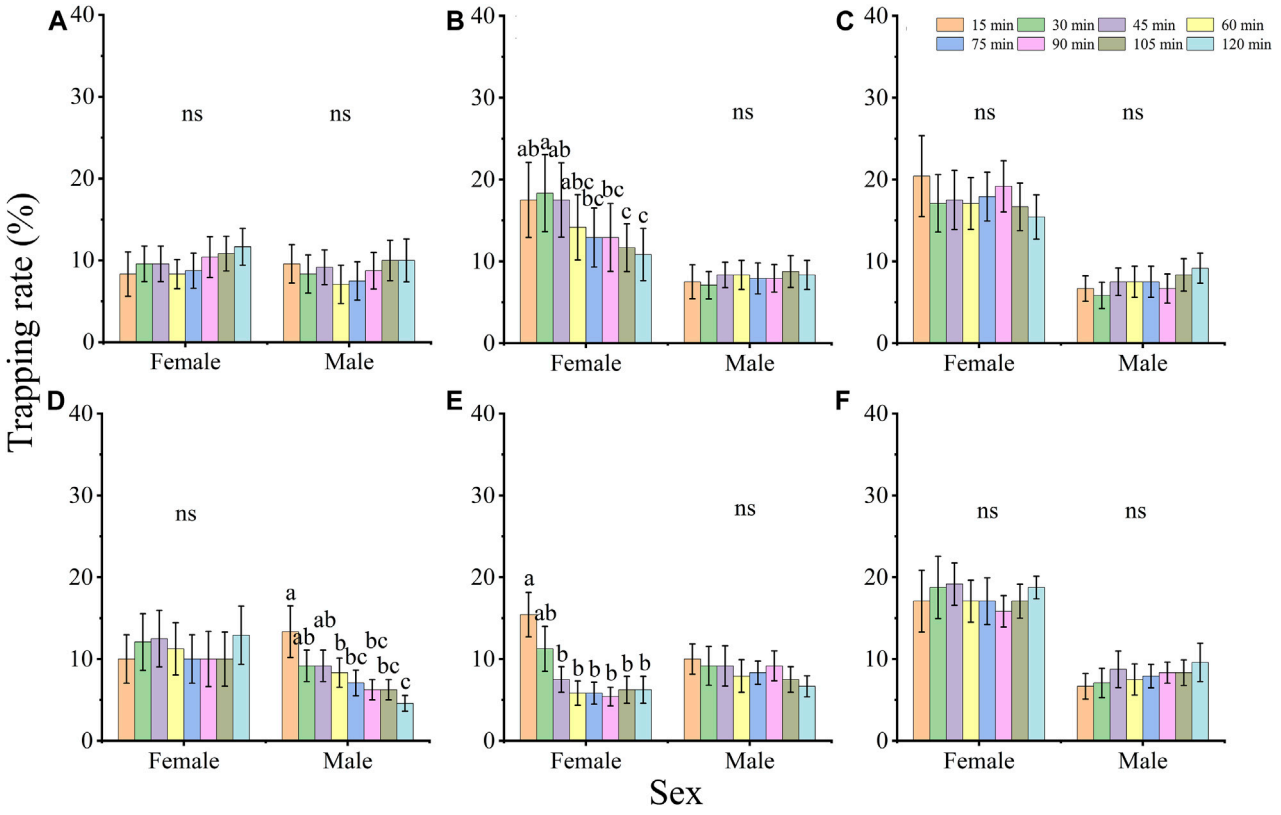

FIGURE 2
The effect of exposure time on the phototactic behavioral response rate of adults *D. helophorides* at wavelengths of 365 nm **(A)**, 420 nm **(B)**, 435 nm **(C)**, 515 nm **(D)**, 600 nm **(E)** and 660 nm **(F)**. The significant differences in phototactic behavioral responses to LED lights among different exposure times were analyzed using GLM with Poisson distribution and a log link function followed by Bonferroni test; α = 0.05. The samples of females and males were 12 replicates. The data are presented as the mean ± SE.

significant difference among the different exposure times under the other wavelengths (females, 365 nm: $X^2 = 12.441$, $p = 0.087$, 435 nm: $X^2 = 10.968$, $p = 0.140$, 515 nm: $X^2 = 11.599$, $p = 0.115$, 660 nm: $X^2 = 6.324$, $p = 0.502$; males, 365 nm: $X^2 = 12.240$, $p = 0.093$, 420 nm: $X^2 = 3.094$, $p = 0.876$, 435 nm: $X^2 = 12.148$, $p = 0.096$, 600 nm: $X^2 = 12.427$, $p = 0.087$, 660 nm: $X^2 = 9.197$, $p = 0.239$; all $df = 7$).

3.1.2 Monochromatic LED light preference in different time slots

To compare the effect of diel rhythm on phototactic behavioral responses, the trapping rates of females and males were compared at five different time slots (Figure 3). The behavioral responses of females and males showed a significantly difference among 5 time slots, except for those of males under 500 nm ($X^2 = 2.432$, $df = 4$, $p = 0.657$) and females under 660 nm ($X^2 = 8.541$, $df = 4$, $p = 0.074$). Under 515 and 630 nm illumination, both males and females exhibited higher preference at night (19:00–2:00) than at other time slots, but the highest trapping rates of males and females were 13.33% and 10.00% (515 nm) and 13.33% and 17.50% (630 nm), respectively (Figures 3A, B; 515 nm, male: $X^2 = 38.412$, $df = 4$, $p < 0.001$, female: $X^2 = 11.768$, $df = 4$, $p = 0.019$; 630 nm, male: $X^2 = 81.094$, $df = 4$, $p < 0.001$, female: $X^2 = 16.005$, $df = 4$, $p = 0.003$). Moreover, the trapping rates of males at 385 and 455 nm and females at 420, 435, 475, and 560 nm showed higher preference at night (19:00–2:00) than during the day (Figure 3), while those of males at 400 nm, and females at 455 nm and 595 nm showed higher phototactic responses during the day (14:00–16:00) (Figure 3).

Furthermore, both females and males showed a significant difference among the phototactic behavioral responses of adults under 14 different wavelength LED cues (Figure 4 A and C; male: $X^2 = 164.338$, $df = 13$, $p < 0.001$; female: $X^2 = 333.859$, $df = 13$, $p < 0.001$). Males and females exhibited different preferences under 14 different LED lamps. Males showed the highest preference for 400, 455, and 600 nm, followed by 385 and 660 nm (Figure 4A), while females exhibited the highest preference at 660 nm, followed by 600, 630, 435 and 455 nm (Figure 4C). The trapping rates of males were 10.83%, 10.67% and 10.67% under 400, 455, and 600 nm LED lights, respectively (Figure 4A), while the trapping rate of females was 15.83% under 660 nm (Figure 4C). The lowest trapping rate of males and females was in the blue-green region (male: 475 nm, 5.17%, female: 500 nm, 5.50%). The preference index of females and males showed that the beetles had distinct negative phototaxis under illumination with different wavelengths (Figures 4B, D).

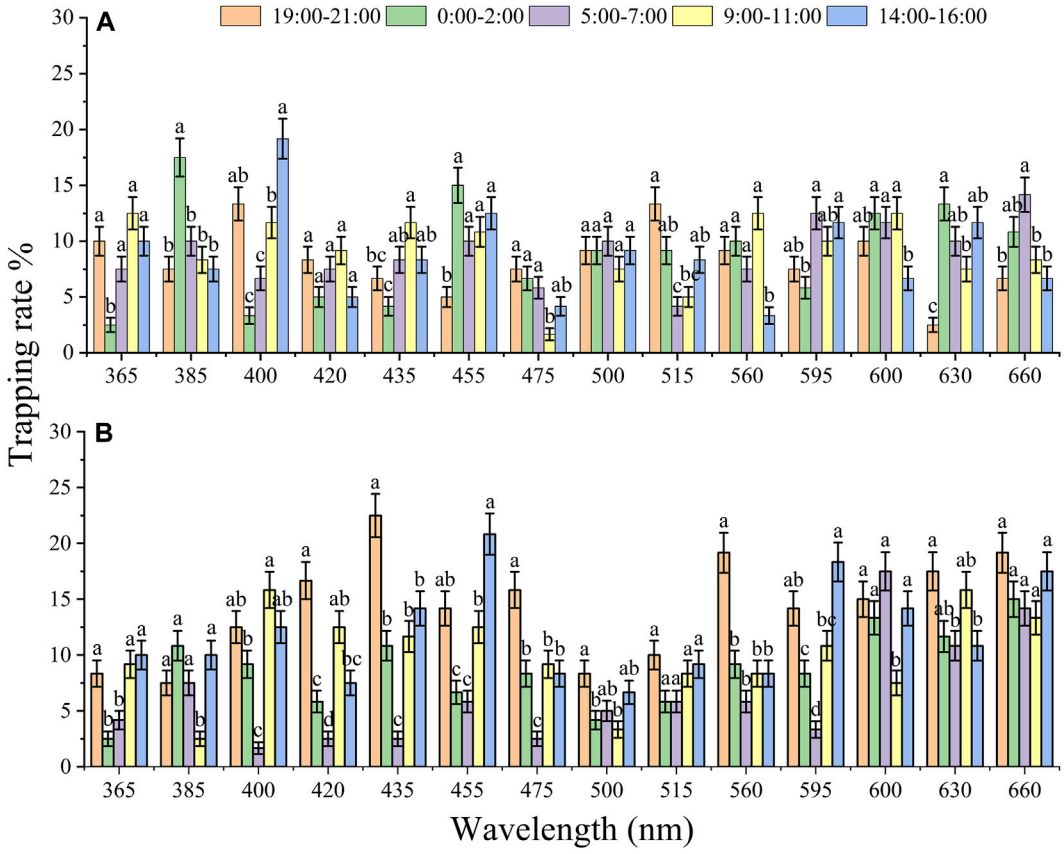

FIGURE 3
The effect of diel rhythm on the phototactic response rate of males **(A)** and females **(B)**. The significant difference was analyzed by GLM with Poisson distribution and a log link function followed by Bonferroni test; α = 0.05, and the same lowercase letters on top of the bar indicate no significant difference under the same wavelength. The samples of females and males were 6 replicates per time slots. The data are presented as the mean ± SE.

3.2 Head transcriptome sequencing of *D. helophoroides*

3.2.1 RNA sequence analysis

To further investigate the underlying molecular mechanisms of light signal recognition of *D. helophoroides*, we performed a time-course transcriptome analysis using head samples of female and male beetles exposed to white light for different lengths of time (0, 15, or 120 min). Eighteen samples were subjected to RNA-Seq, which produced approximately 140.96 G (6.84 Gb of data for each sample). Quality scores were more than 98.04% and 94.08% at the levels of Q20 and Q30, respectively (Supplementary Table S2). Subsequently, the clean reads of each sample were mapped to the reference genome, and the mapping rate ranged from 88.08% to 90.41% (Supplementary Table S3). A total of 14,890 genes were mapped, and 2,164 new genes were found and generated 29,851 transcripts in these transcriptome sequences. There were 13,647 transcripts (45.7%) with lengths ≥1,800 bp, 7,525 transcripts (25.2%) in the range 1,000–1,800 bp, and 8,679 (29.1%) with lengths ≤1,000 bp in our transcriptome datasets (Figure 5A). Among 14,890 genes, 92.01% (13,700 genes) were annotated via the NR database, 86.00% (12,805 genes) were annotated via the COG database, 77.71% (11,571 genes) were annotated via the GO database, 75.57% (11,252 genes) were annotated via the Pfam database, 70.79% (10,541 genes) were annotated via the Swiss-Prot database, and 62.00% (12,805 genes) were annotated via the KEGG database (Figure 5B).

3.2.2 Identification of differentially expressed genes (DEGs)

Differentially expressed genes were identified using DESeq 2. A total of 1,052 DEGs were identified in *D. helophoroides* via pairwise comparisons, among which 403, 566, 493, and 428 DEGs were obtained in the four comparisons of dark adaptation and light adaptation after light exposure for 15 and 120 min (L15F vs. L0F, L120F vs. L0F, L15M vs. L0M, L120M vs. L0M), respectively (Figure 5C). Furthermore, the results showed that there were very few genes in the common upregulated and downregulated comparison of males with females under the same light exposure times (Figures 5F, G), while the genes were relatively lot up- or downregulated uniquely in the comparisons between L15F vs. L0F, L120F vs. L0F, L15M vs. L0M, and L120M vs. L0M (Figures 5D, E, H, I).

3.2.3 Functional classification of DEG responses to light and dark adaptation

To reveal the effect of light treatment on the transcriptomes of females and males relative to dark treatment, GO enrichment

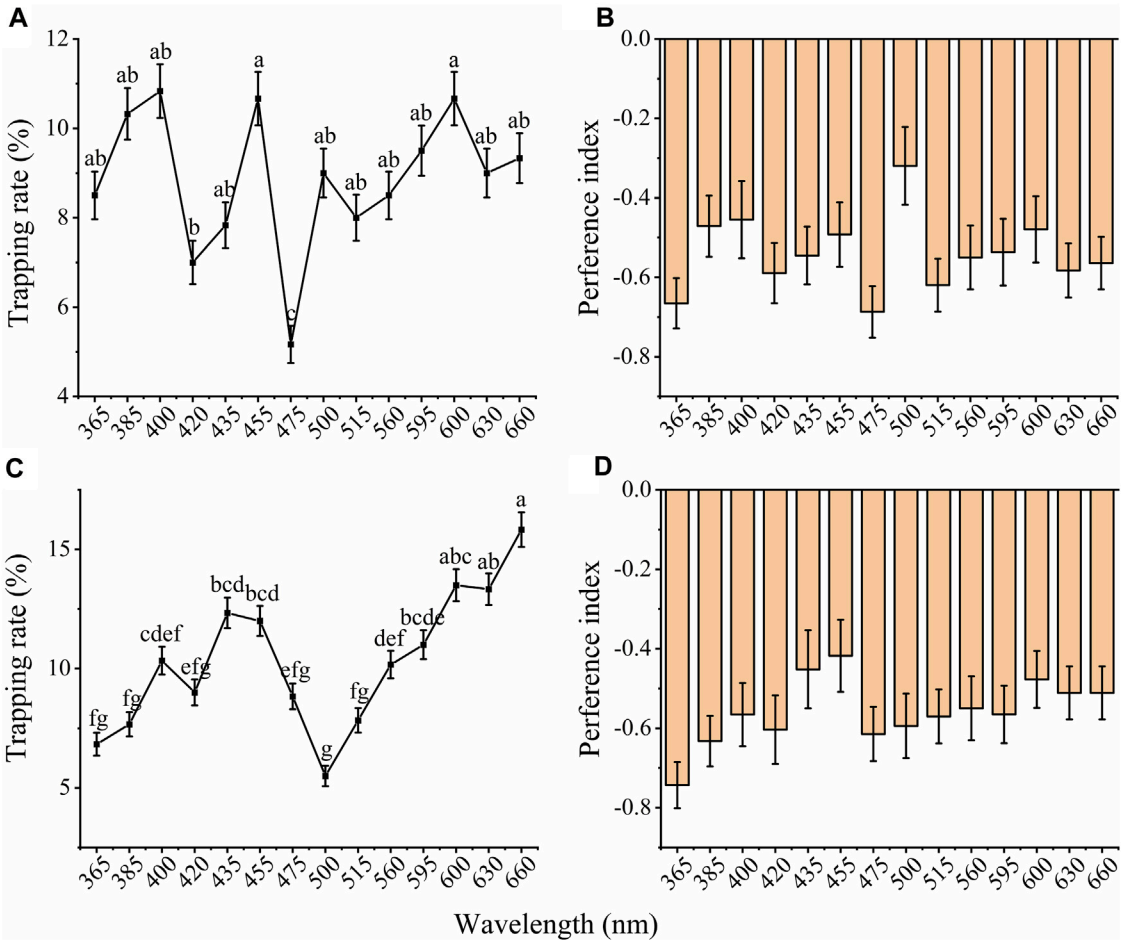

FIGURE 4
Total trapping rates and preference index of males and females to different wavelengths of light. The total trapping rate of males **(A)** and females **(C)**. The preference index of males **(B)** and females **(D)** to different wavelengths of light. The significant difference was analyzed by GLM with Poisson distribution and a log link function followed by Bonferroni test; and the same lowercase letters on top of the line indicate no significant difference. The samples of females and males were 30 replicates per wavelengths. The data are presented as the mean ± SE.

analysis was used to classify the DEGs (Figure 6A). The GO terms of both females and males were markedly enriched in "cell morphogenesis," "cell morphogenesis involved in differentiation" (biological process), "basement membrane", "extracellular region," "collagen-containing extracellular matrix," "extracellular matrix," "external encapsulating structure" (cellular component), and "chitin binding" (molecular function) (Figure 6A).

To further display the biological function of DEGs, the DEGs were analyzed using KEGG pathway analysis based on the KEGG database. The top pathways were displayed for the prominent enriched DEGs between light exposure and dark conditions (Figure 6B). In the L120F vs. L0F and L15F vs. L0F comparisons in female, 242 and 155 DEGs were annotated to 190 and 186 KEGG pathways, respectively (Supplementary Tables S4, S5), while in the L120M vs. L0M, L15M vs. L0M comparisons in males, 190 and 238 DEGs were annotated to 215 and 242 KEGG pathways, respectively (Supplementary Tables S6, S7). These DEGs were significantly enriched in "ECM-receptor interaction," "Focal adhesion," "PI3K-Akt signaling pathway," and "Lysosome" (Figure 6B).

3.2.4 STEM analysis of the DEGs in the response to light exposure

To further explore the expression patterns of these DEGs, hierarchical clustering was performed on their expression profiles at different treatment times. The results showed that the DEGs were divided into two groups, including dark treatment (L0F and L0M) and light treatment (L15F, L120F, L15M, and L120M) (Figure 7A). Sub-clustering analysis showed that the relative expression of DEGs changed pattern with prolonged light exposure time (Figures 7B, C).

Furthermore, STEM analysis was performed to further explore the expression patterns of these DEGs at different treatment times in females and males (Figures 7D–K). The DEGs were clustered into eight distinct temporal expression patterns in females and males, and three clusters in the male comparison and four clusters in the female comparison showed significant change patterns following light exposure time (Figures 7D–K, $p < 0.03$). The other cluster showed no significant change patterns (Supplementary Figures S2A–H). The predominant profiles revealed that the expression patterns of most DEGs were rapidly induced within the first 15 min of light exposure (Figures 7D–K). However, there was no significant

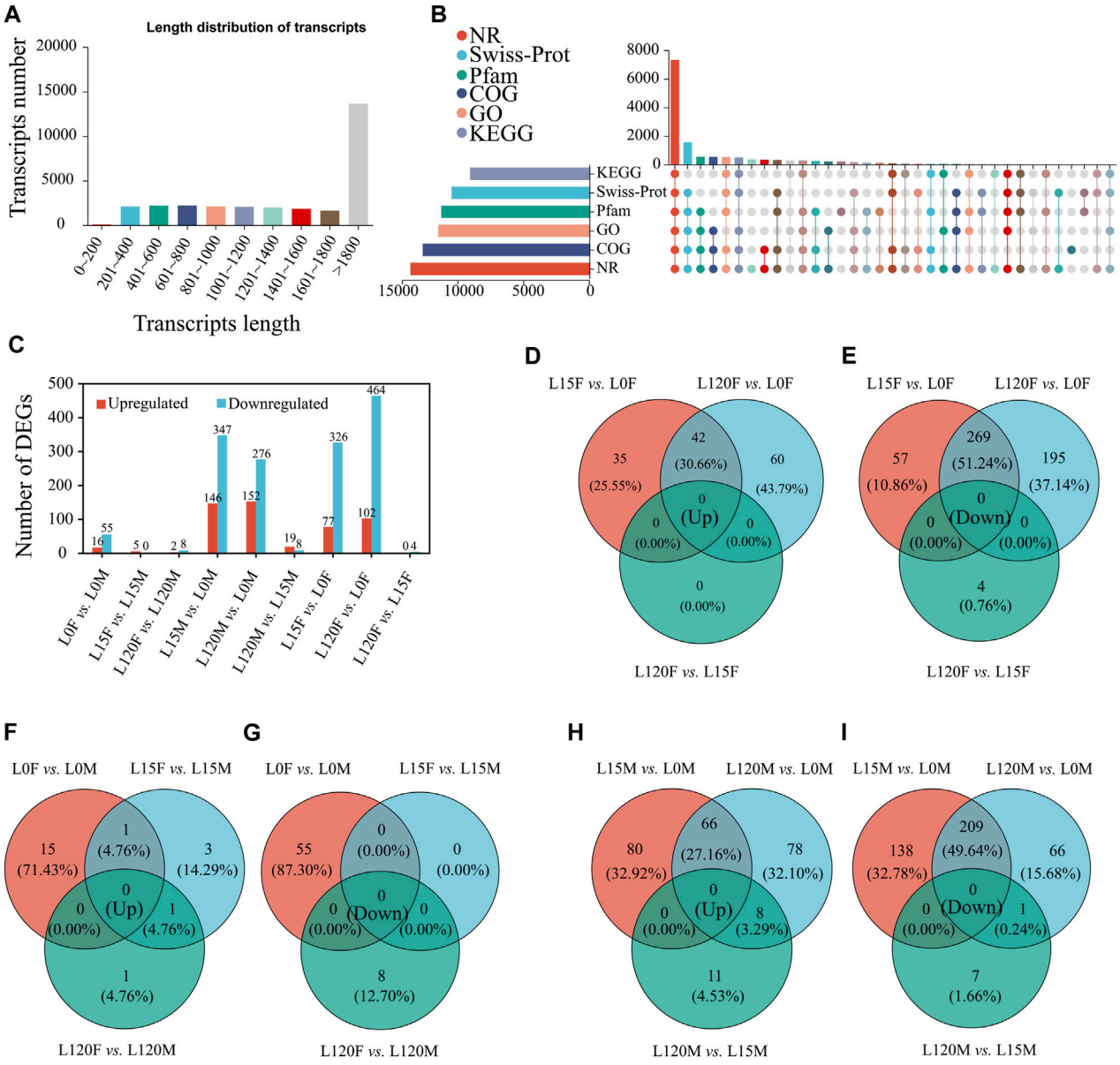

FIGURE 5
Illumina sequencing of the heads of adults *D. helophorides* under the different light exposure times. **(A)** The length distribution of all assembled transcripts. **(B)** The number of genes annotated via different databases, including NCBI non-redundant protein database (NR), NCBI non-redundant nucleotide database (NT), Swiss-Prot, gene ontology (GO), Kyoto Encyclopedia of Genes and Genomes (KEGG), clusters of orthologous groups of proteins (KOG), and protein family (Pfam). **(C)** Classification information of annotated GO terms. **(C)** the number of DEGs in the different treatments. The Venn diagram of upregulated and downregulated genes in the comparisons of females **(D,E)**, females and males **(F,G)**, and males **(H,I)**.

difference in the expression patterns of DEGs between light exposure for 15 and 120 min.

3.2.5 WGCNA analysis of the DEGs in the response to light exposure

A total of 1,052 was performed to further explore key gene co-expression modules in the head of *D. helophoroides* in response to light exposure at different times (0, 15, 120 min) (Supplementary Table S8). Three different co-expression modules were identified to mark different colors based on the similarity in the expression of DEGs (Figure 8A). DEGs in the same co-expression module showed distinct expression profiles in the head of *D. helophoroides* at different light exposure times, especially the blue and turquoise modules (Figure 8B). The blue module of 232 genes had the strongest negative correlation with dark adaptation in males (R = −0.646, p = 0.00378) and a weak correlation with light exposure for 120 min in females (R = 0.474, p = 0.0469), while the turquoise module of 404 genes had the strongest positive correlation with dark adaptation in female (R = 0.646, p = 0.00378). The grey module of 44 genes had the strongest correlation with dark adaptation in males (R = 0.532, p = 0.0231) (Figure 8B).

To identify the hub genes in the module, the key genes with a high connectively degree were screened in the co-expression network modules. In the blue modules, the genes (evm.TU.HIC_ASM_8.152) were involved in phosphatidylinositol binding, (evm.TU.HIC_ASM_7.1150) belonged

10.3389/fphys.2023.1250836

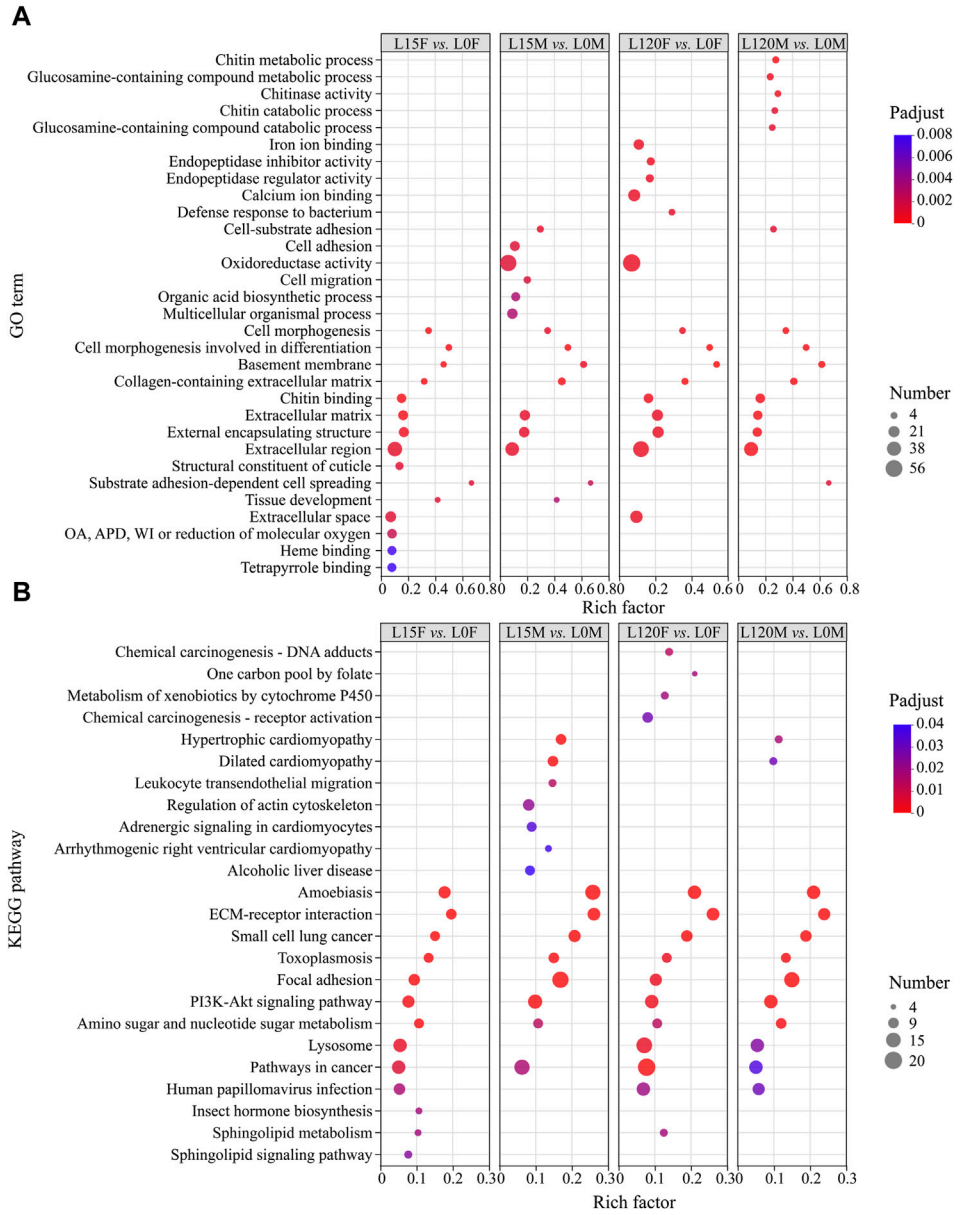

FIGURE 6
The gene Ontology (GO) term **(A)** and Kyoto Encyclopedia of Genes and Genomes (KEGG) pathway **(B)** enrichment analysis of all DEGs in the different comparisons. OA, APD, oxidoreductase activity, acting on paired donors, with incorporation or reduction of molecular oxygen.

to the integral component of membrane, and (evm.TU.HIC_ASM_10.101) were responsible for sensory perception of light stimulus (Supplementary Table S9). In the turquoise, (evm.TU.HIC_ASM_2.289) was involved in the integral component of the membrane, (evm.TU.HIC_ASM_9.491) was related to flavin adenine dinucleotide binding, and (evm.TU.HIC_ASM_4.1260) and (evm.TU.HIC_AS-M_8.362) encoded calcium ion binding protein (Supplementary Table S10). In the grey modules, (evm.TU.HIC_ASM_8.361) participated in calcium channel activity, and (evm.TU.H-IC_ASM_4.921) was related to transmembrane transporter activity (Supplementary Table S11).

All genes from three modules were subjected to KEGG enrichment analysis, showed that the turquoise module genes were significantly enriched in "ECM-receptor interaction," "Focal adhesion" and "PI3K-Akt signaling pathway" (p <0.001) (Figure 8C). Additionally, the pathways "Amino sugar and nucleotide sugar metabolism," "Metabolism of xenobiotics by cytochrome P450," and "Sphingolipid metabolism" also displayed an adjusted p-value <0.05. These results suggest that these KEGG pathways may have an important role in the response of *D. helophoroides* to light exposure, especially those pathways with $p < 0.001$ (Figure 8C). Furthermore, to our surprise, human disease pathways were enriched significantly, such as "Small cell lung cancer," "Arrhythmogenic right ventricular cardiomyopathy" ($p <$ 0.01). Furthermore, blue module gene were enriched significantly in "Caffeine metabolism" (Supplementary Table S13, $p < 0.01$), the other KEGG pathway were no significantly enriched (Supplementary Tables S13, S14, $p > 0.05$).

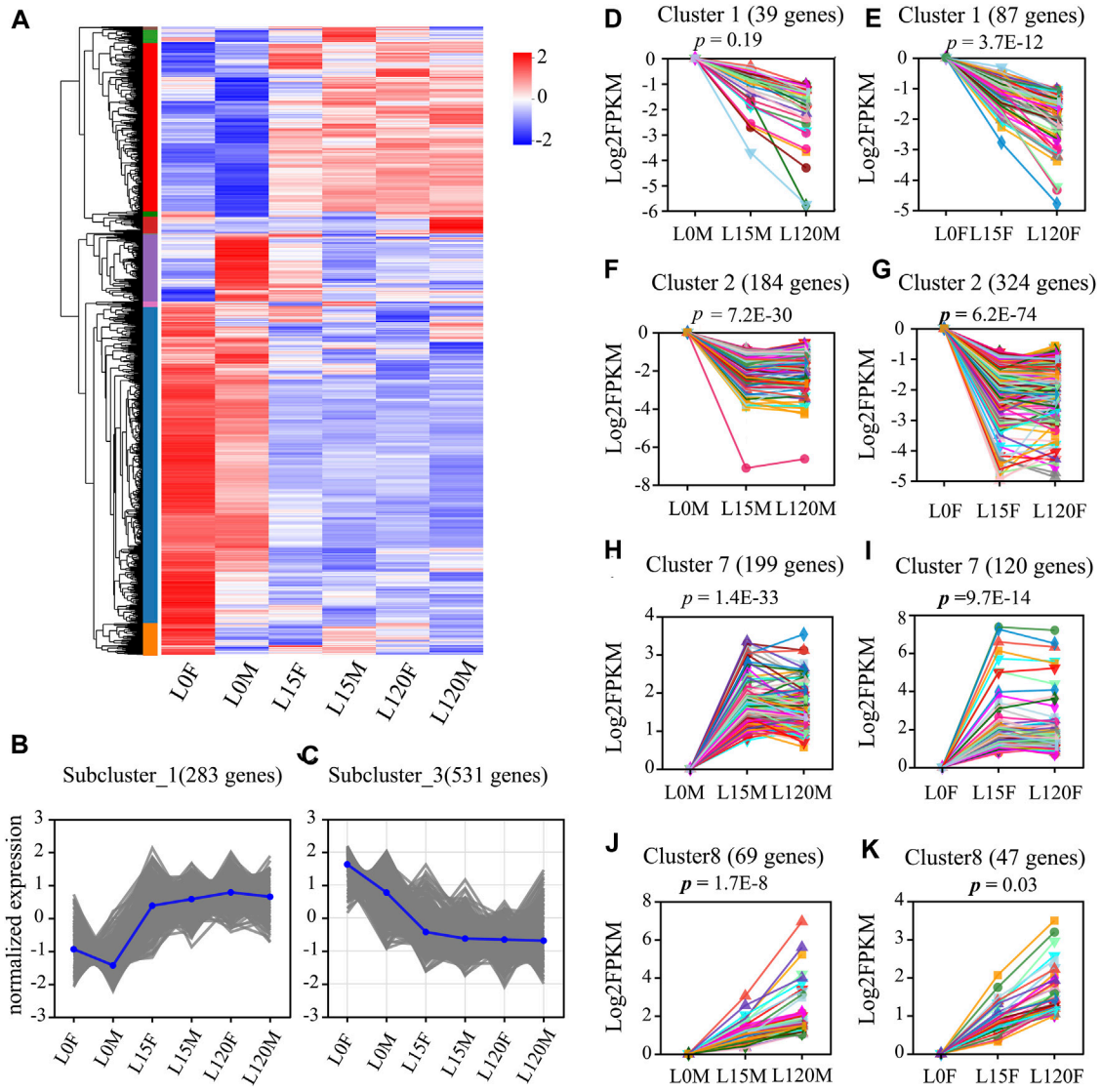

FIGURE 7
Summary of differentially expressed genes (DEGs) in the head of *D. helophorides* under the different light exposure times. **(A)** Expression profiles of the DEGs at light exposure time points of female and male (0, 15, 120 min) using a heatmap. **(B,C)** Two of the subclusters were showed. **(D–K)** Temporal expression analysis of the DEGs in the head of *D. helophorides* following light exposure at 0, 15 and 120 min using STEM software (male: D, F, H, and J; female: **(E,G,I,K)**. There data from 15 to 120 min were normalized using log2 compared to dark adaption (light exposure 0 min).

As mentioned above, the "ECM-receptor interaction," "Focal adhesion" and "PI3K-Akt signaling pathway" pathways, which had adjusted *p* values of 2.59 E−11, 8.67E-06, and 3.17E-05, respectively, were ranked number one, four, and five in all downregulated KEGG pathways following light exposure (Figure 8C; Supplementary Table S12). Furthermore, "Lysosome" was also enriched in the comparison L15F vs. L0F, L120F vs. L0F, and L120M vs. L0M (Figure 6B, $p < 0.05$). Therefore, total 30 DEGs from four pathway-related were further analyzed using GGI networks (Figure 8D). As shown in Figure 8D, we detected 30 DEGs in four pathways interacting with each other, such as cell migration, cell morphogenesis involved in differentiation (evm.TU.HIC_ASM_8.978), (evm.TU.HIC_ASM_0.1096, 1,097, 1,098), (MSTRG.130), and (evm.TU.ORIGINAL_488.1); basement membrane (evm.TU.HIC_ASM_10.534), (evm.TU.HIC_ASM_10.526); integrin-mediated signaling pathway (evm.TU.HIC_ASM_11.701), (evm.TU.HIC_ASM_12.1091) (Supplementary Table S15). Notably, cell migration and cell morphogenesis involved in differentiation (evm.TU.HIC_ASM_8.978) were downregulated by 2.03–2.78 times following light exposure (Supplementary Table S16); the basement membrane (evm.TU.HIC_ASM_10.534), and (evm.TU.HIC_ASM_10.526) were downregulated by 2.33–2.96 times following light exposure (Supplementary Table S16).

3.2.6 Validation of differentially expressed genes by qPCR

To validate the expression patterns of DEGs in the RNA-seq results, qRT-PCR was selected to quantify 9 genes, including

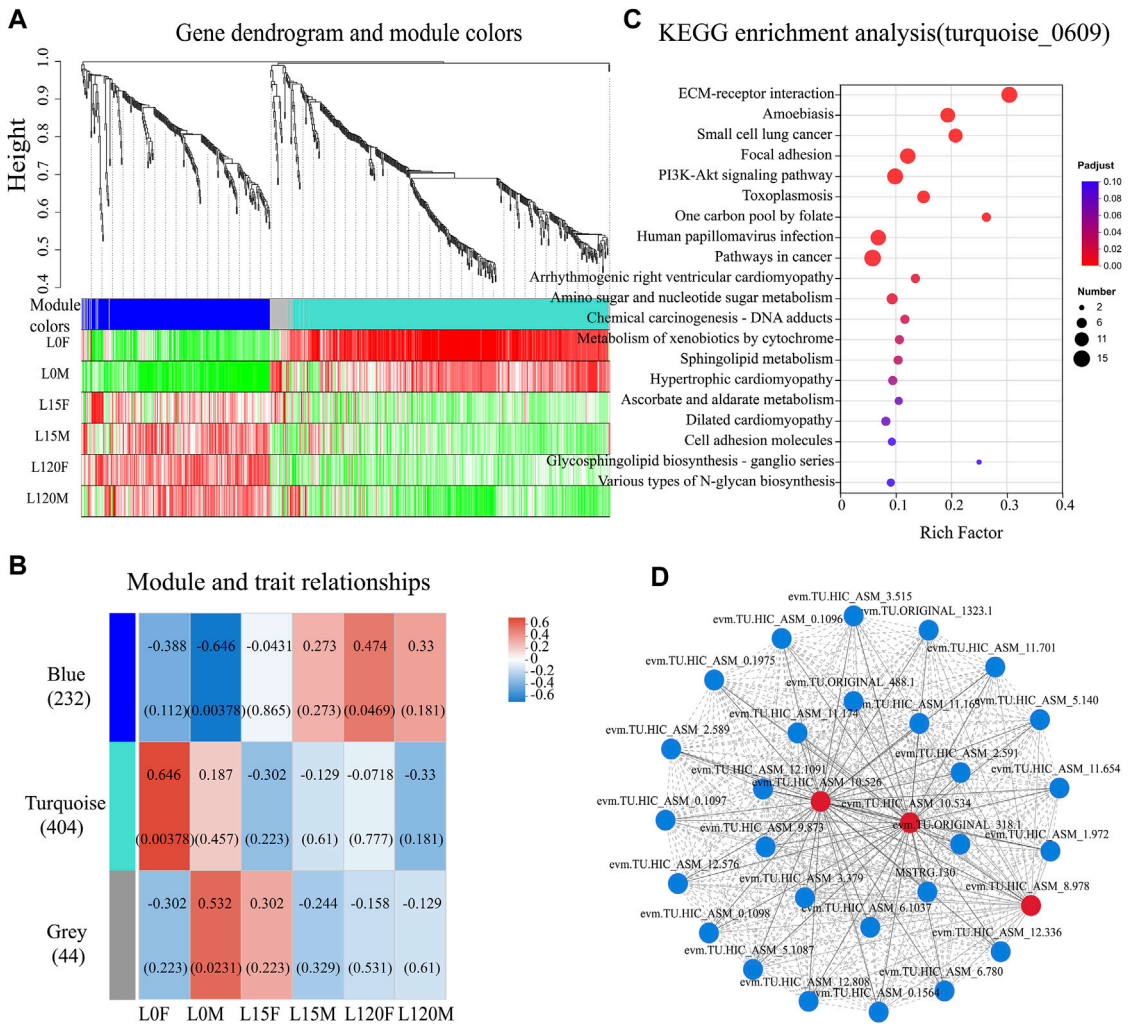

FIGURE 8
Weighted gene co-expression network analysis (WGCNA), KEGG and gene-gene interaction (GGI) analysis for differentially expressed genes (DEGs) in the head transcriptome data. **(A)** the 1,052 DEGs were clustered three co-expression modules using WGCNA analysis. **(B)** Correlation between module and trait. A correlation analysis between the module and different light exposure times (0, 15, and 120 min) of female and male. **(C)** The genes in the turquoise module were subjected to KEGG enrichment analysis. The top 20 enriched KEGG terms were displayed. **(D)** GGI networks of the DEGs belonging to "ECM-receptor interaction," "Focal adhesion," "PI3K-Akt signaling pathway," and "Lysosome" (Downregulated genes).

basement membrane (evm.TU.HIC_ASM_10.526), The experimental results showed that the expression levels of genes were similar to the results from RNA-seq (Figure 7A; Figure 9, and Supplementary Table S8). Such as, the expression levels of (evm.TU.HIC_ASM_10.526, evm.TU.HIC_ASM_2.1264) were downregulated under light exposure with 15 min, while there was no significant difference between light exposure for 15 and 120 min.

4 Discussion

To decrease negative effect of chemical pesticides on the environment, the taxis of insects to artificial lights are widely used to detect, monitor and manage insect pests (Kim et al., 2019; Van der Kooi et al., 2021), such as Tenebrionidae, Curculionidae, Pselaphidae, Silvanidae, Cerambycidae and Scolytinae (Park and Lee, 2017; Marchioro et al., 2020). However, traps with artificial lights can also attract many natural enemies when they are used to detect and manage insect pests (Luo and Chen, 2016; Kim et al., 2019). Therefore, the trapping ability of lights for natural enemies of pests should also be considered in the monitoring and detection of insect pests (Bian et al., 2018). The ectoparasitoid beetle *D. helophoroides* is an important natural enemy of wood-boring insects and is widely used in controlling cerambycid beetles, including *A. glabripennis* and *M. alternatus* (Wang L. et al., 2023; Lyu et al., 2023; Zhang et al., 2023). Therefore, it is vital to explore the response mechanisms of ectoparasitoid beetles to light cue cognition at behavioral and molecular level. Our results showed that female and male *D. helophoroides* have negative or weak phototaxis at a certain light intensity, and it was influenced by light exposure time, diel rhythm, sex, and light wavelength.

Previous studies have shown that *D. helophoroides* adults are attracted by NIR light with a peak wavelength of 700 nm and an

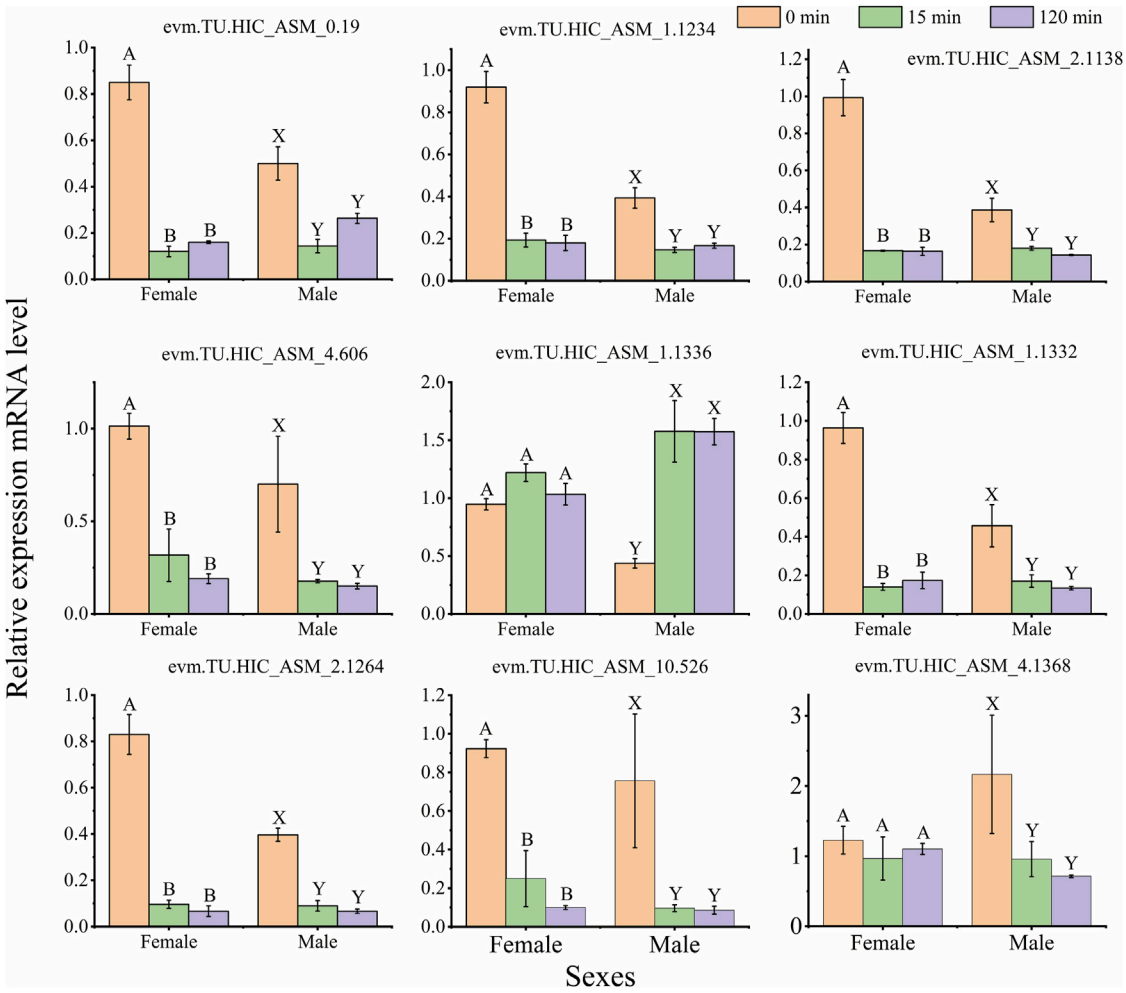

FIGURE 9
Quantitative PCR (qPCR) data for the mRNA expression profiles of differentially expressed genes (DEGs) in the female and male. The same capital letters on top of the bar indicate no significant difference (Tukey's test, α = 0.05; Female: A, B, C; Male: X, Y, Z). The data indicates mean ± standard deviation (SD) (n = 3 biological replicates).

intensity at 7 lux, and the highest phototactic response rate is approximately more than 60% in the near-infrared light region (Wang et al., 2021). In the present study, males showed the highest preference for 400, 455, and 600 nm (Figure 4A), while females exhibited the highest preference at 660 nm (Figure 4C). The trapping rates were approximately 10.67%–15.83%. We speculate that the light intensity may cause a significant difference between the two studies. In previous study showed that phototactic behavioral rate of adults decreased with increasing light intensity (Wang et al., 2021). In this study, a 6.31×10^{18} (photos/m^2/s) light intensity (approximately 180 lx) was used, which may also contribute to the low trapping rates of adults.

The trapping rate of females and males was also affected by light exposure time. For example, the trapping rate of females at 420 and 600 nm and males at 515 nm under the light exposure with 15 min was higher than under 120 min (Figures 2B, D, E), so the samples were selected in the light exposure time with 0, 15 and 120 min after dark adaptation in transcriptomic analysis. Moreover, the trapping rate was not significantly different between 15 and 120 min (Figures 2A, C, F). In transcriptomic and qRT-PCR data, there was not significant difference in the majority of gene expression (Figure 7A; Figure 9). Therefore, the treatment sample time interval should be extended to response monochromatic light radiation in the further study.

Previous studies have shown that Coleoptera beetles display a preference for UV, violet and green wavelength spectra (350–440 and 500–560 nm) (Kim et al., 2019; Van der Kooi et al., 2021). Using the same behavioral response chamber, both females and males *A. glabripennis* displayed higher phototactic responses under illumination with 420 and 435 nm wavelengths (violet and blue) at night, with an approximately 74%–82% trapping rate (Jiang et al., 2023a). UV light traps were more attractive to *Arhopalus ferus* and *Prionoplus reticularis* (longhorn beetles) than their adjacent two yellow lights (Pawson and Watt, 2009). UV-blue light traps captured 2–4 times more bark beetles *Hylurgus ligniperda* and *Hylastes ater* beetles than traps baited with other wavelengths in New Zealand (Pawson et al., 2009). These results suggested that UV and blue light traps can be used to detect and control wood boring pests, including longhorn and bark beetles. In this study, females

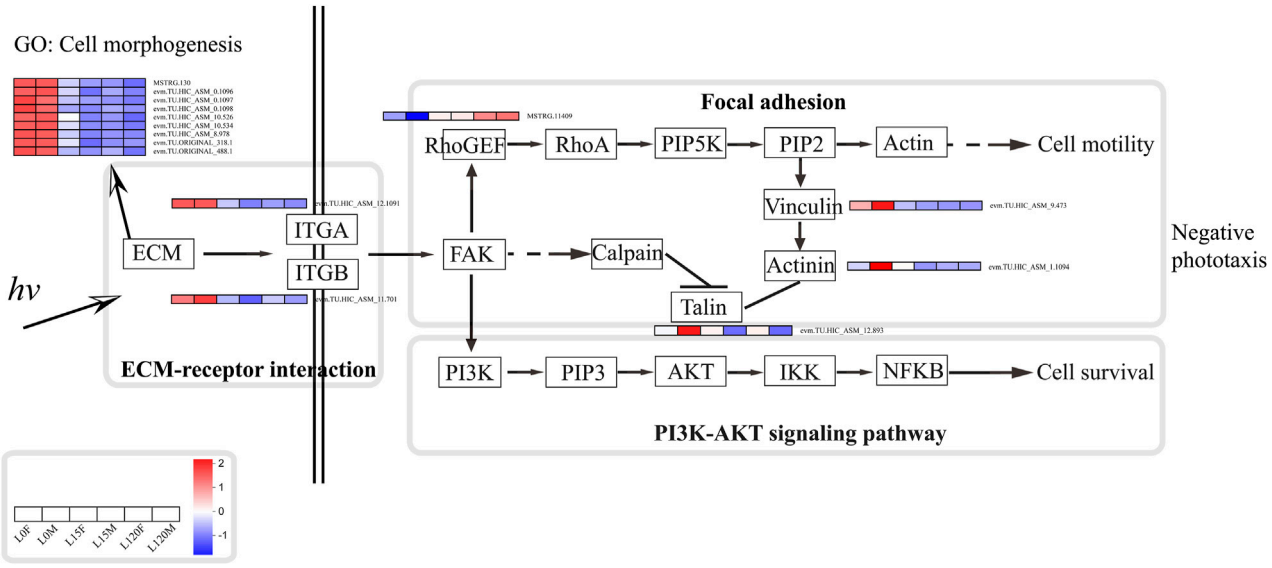

FIGURE 10
Schematic diagram of the potential response mechanisms of *D. helophorides* involved in light exposure.

showed a higher preference for 420, 435, 475, 560, and 630 nm at night from 19:00–21:00 (Figure 3B), but the trapping rate decreased with increasing light intensity (Wang et al., 2021). Therefore, light intensity should be enhanced to reduce the trapping of *D. helophoroides* when UV and blue light traps are used to detect and manage wood boring pests.

Previous studies have shown that the 24-h rhythm of locomotor activity in female and male *D. helophoroides* was elevated in the dark phase and reduced in the light phase, and the peak of locomotor activity occurred at 20:30–22:30 during the dark period, while that of adults hardly occurred during light period, indicating that they are nocturnal insects (Lyu et al., 2015b; Lyu et al., 2015c). Further researches showed that increasing the light duration during the dark phase significantly decreased the activity percentage of locomotor, disturbing the normal rhythm of locomotor activity. Moreover, the oviposition ability of females was decreased under light (1, 10, and 100 lx) exposure at night relative to no light (0 lx) at night (Jiang et al., 2023b). In this study, female and male adults exhibited negative phototaxis for LED lights (Figures 5B, D), which is an adaptation strategy to avoid the adverse influence of light exposure.

In the organism response to abiotic stress, a comparative transcriptome analysis was performed using RNA-Seq to examine the cellular responses of plants and animals in response to heavy metals, heat, drought, pathogenesis and insect stress, and up- and downregulated DEGs were identified and analyzed, and potential regulatory mechanisms were speculated or verified under adverse situations (Sun et al., 2022; Wang Z. et al., 2023; Liu et al., 2023). For example, RNA-Seq was used in crayfish experiments under Cu stress, and 4,662 DEGs, including 3,534 upregulated and 1,128 downregulated DEGs, were identified (Wang Z. et al., 2023). In the present study, a total of 1,052 DEGs were identified in the head of *D. helophoroides* following light exposure for 15 and 120 min, and different comparison groups had different up- and downregulation (Figures 5C–I). These results indicated that transcriptional alterations occurred in the head of this beetle during light exposure for 15 and 120 min relative to dark adoption. STEM analysis revealed that 3 clusters (DEGs) significantly changed in male and 4 clusters significantly changed in females (Figures 7D–K), suggesting that differential response strategies may be employed by female and male beetle at different light exposure times. This corroborates the results of behavioral experiments (Figure 2) that showed that trapping rate changes were observed under different light exposures.

Our previous study showed that the locomotor activity percentage of beetles under the light phase was significantly lower than that under the dark phase, suggesting that long-term light exposure can derange temporal adaptation and decrease organism fitness (Jiang et al., 2023b). In the present study, KEGG pathway analysis showed that the lysosome pathway was enriched (Figure 6B), and all of the relative genes in this pathway were downregulated under light exposure for 15 and 120 min relative to dark adaptation, suggesting that the function of this pathway decreased under light exposure. The autophagy lysosome pathway is a major mechanism for degrading intracellular macromolecules, which is also known to protect adult cells against irreversible states (Fujimaki et al., 2019; Lawrence and Zoncu, 2019). In addition, a previous study also showed that reducing lysosomal function drove cells progressively deeper into quiescence depth, and even into a senescence-like irreversibly arrested state (Fujimaki et al., 2019). Reducing lysosomal function may suggest that light illumination may have a negative effect on this nocturnal beetle. Thus, in transcriptome level, the results also showed that female and male adults have a lower or negative phototactic behavioral response rates to light illumination (Figure 4).

In addition, the focal adhesion pathway was also significantly enriched statistically in the 15 and 120 min light exposure groups (female and male) relative to dark adaptation (Figure 6B and 8 C,

Supplementary Table S12, $p_{adjust} < 0.001$). Focal adhesions are key modulators of cellular responses to biotic and abiotic stimuli in cell proliferation, differentiation, and motility (Wehrle-Haller, 2012). In crustaceans, focal adhesions have been reported to be involved in Cd, Pb and Cu tolerance through transcriptomic and proteomic approaches (Lu et al., 2019; Jiao et al., 2021; Wang Z. et al., 2023). In crayfish, focal adhesion pathway plays a critical role in the crayfish response to Cu stress and that upregulation of hub genes may increase the survival capacity of crayfish (Wang Z. et al., 2023). However, in our study, genes linked to focal adhesion were significantly downregulated under light exposure for 15 and 120 min relative to dark adaptation (Figure 6B; Supplementary Table S16). In the real environment, there is a significant difference between light stresses and heavy metal stresses. The heavy metal pollutants in aquatic environments are generally widespread. For example, Cu ions are significantly enriched in water, sediment, and cultured fish species around aquaculture farms in the Yangtze River and Taihu Lake, East China (Rajeshkumar et al., 2018; Xiong et al., 2020). Crustacean animals hardly choose the optimal living environment through migration, while nocturnal insects can select a suitable habitat to avoid light exposure through migration. Therefore, crustacean animals may decrease the influence of heavy metals through an upregulated focal adhesion pathway, while the focal adhesion pathway was downregulated in nocturnal insects under light exposure relative to the normal environment (dark adaptation) to impact normal physiological activity.

Furthermore, focal adhesions are specialized sites within the cell, where mechanical force generated within the cell is transmitted to the surrounding ECM, thus influencing its organization and also contributing to cell migration (Burridge, 2017). The compound eye of insects usually regulates the length and shape of the cone, the cross-sectional areas and shapes of the rhabdoms, and the movement of pigment cells to adapt to changes in light and dark environments (Insausti et al., 2013; Chen et al., 2019). For example, cones of *M. alternatus* were 14.67 ± 0.51 μm in length and formed a conical shape with a narrow and pointed proximal end in the light-adapted state, while cones were much shorter (5.57 ± 0.16 μm) and had a disc-shaped structure with a round and blunt proximal end in the dark-adapted state. The cross-sectional area of the rhabdom decreases by approximately 35% in the light-adapted state relative to that of the dark-adapted state (Wen et al., 2020). Furthermore, photoreceptors have a light/dark adaptation mechanism for adjusting light sensitivity through changes in rhodopsin levels and cellular location in the crepuscular mosquito *Anopheles gambiae* (Moon et al., 2014). In the present study, GO annotation analysis showed that the DEGs were significantly enriched in cell morphogenesis, cell morphogenesis involved in differentiation, basement membrane, and substrate adhesion-dependent cell spreading under light exposure for 15 and 120 min relative to dark conditions (Figure 6A), suggesting some of cell redistribution during change in the light and dark environment. Moreover, DEGs that were enriched in the focal adhesion pathway were mainly distributed in the cell motility and eventually into regulation of actin cytoskeleton (Figure 10; Supplementary Figure S3). For arthropods, rhodopsin was present within the cytoplasmic compartment during daylight timepoints, while it moved to the rhabdomeres only under dark conditions to enhance visual capability in a low light environment (Sacunas et al., 2002; Hu et al., 2012; Moon et al., 2014). Therefore, these DEGs may regulate changes in cone, rhabdom and pigment cell length and shape to enhance light signal recognition ability. Whether these DEGs can regulate changes in cone cells, movement of pigment cells and cross-sectional areas and shapes of the rhabdoms requires further experiments.

Based on the results from this study and other previous studies (Macias-Muñoz et al., 2019), a potential synergistic molecular network can be proposed for the nocturnal beetle *D. helophoroides* in response to light exposure (Figure 10). When light photons were received by photoreceptor cells, genes related to the ECM-receptor interaction pathway are downregulated, such as MSTRG. 130, evm.TU.HIC_ASM_0.1906, 1,097, 1,098, evm.TU.HIC_ASM_10.534, and evm.TU.HIC_ASM_8.978 were downregulated under light exposure (15 and 120 min) relative to dark adaptation (Figure 10). Furthermore, these genes also regulated cell morphogenesis and differentiation to decrease the amount of received light quantum, reducing cellular damage. Subsequently, ITGA (evm.TU.HIC_ASM_12.1091) and ITGB (evm.TU.HIC_ASM_11.701) were downregulated; and then on the one hand, RhoGEF was upregulated to further influence the focal adhesion pathway; on the other hand, PI3K-AKT signaling pathway was regulated, impacting cell motility and survival. Finally, beetles showed negative phototaxis under light exposure.

Data availability statement

RNA sequencing raw data has been deposited in the NCBI Sequence Read Archive (SRA, https://www.ncbi.nlm.nih.gov/sra/, accession numbers SRR25020620 to SRR25020637).

Ethics statement

The manuscript presents research on animals that do not require ethical approval for their study.

Author contributions

Conceptualization, ZW and FL; methodology, FL, XH, and XZ; formal analysis, XJ, FL, TL, and XZ; investigation, XJ, TL, and XH; writing–original draft preparation, XJ, TL, and FL; writing–review and editing, FL; supervision, FL; project administration, ZW and FL; funding acquisition, FL. All authors contributed to the article and approved the submitted version.

Funding

This research was funded by the National Natural Science Foundation of China (No. 32171800), the Natural Science Foundation of Hebei Province of China (No. C2019204276), and

the Basic Scientific Research of Universities in Hebei Province of China (No. KY202008).

Acknowledgments

We thank the personnel at Hebei Agricultural University (Yao Yijian, Wang Hanxu, Zhang Yimeng, and Zhou Mingyuan) for their assistance with data collection. We thank Prof. Tang Guanghui and Dr. Zhang Zhengqing at Northwest Agriculture and Forestry University for share Genomic data. We also thank the National Natural Science Foundation of China (No. 32171800), the Natural Science Foundation of Hebei Province of China (No. C2019204276), and the Basic Scientific Research of Universities in Hebei Province of China (No. KY202008) for their generous support.

Conflict of interest

Author XZ was employed by Hebei Research Institute of Microbiology Co., Ltd.

The remaining authors declare that the research was conducted in the absence of any commercial or financial relationships that could be construed as a potential conflict of interest.

Publisher's note

Supplementary material

The Supplementary Material for this article can be found online at: https://www.frontiersin.org/articles/10.3389/fphys.2023.1250836/full#supplementary-material

References

Basset, Y., and Lamarre, G. (2019). Toward a world that values insects. *Science* 364 (6447), 1230–1231. doi:10.1126/science.aaw7071

Beketov, M. A., Kefford, B. J., Schafer, R. B., and Liess, M. (2013). Pesticides reduce regional biodiversity of stream invertebrates. *Proc. Natl. Acad. Sci. U. S. A.* 110 (27), 11039–11043. doi:10.1073/pnas.1305618110

Bian, L., Cai, X. M., Luo, Z. X., Li, Z. Q., and Chen, Z. M. (2018). Decreased capture of natural enemies of pests in light traps with light-emitting diode technology. *Ann. Appl. Biol.* 173 (3), 251–260. doi:10.1111/aab.12458

Branco, S., Faccoli, M., Brockerhoff, E. G., Roux, G., Jactel, H., Desneux, N., et al. (2022). Preventing invasions of Asian longhorn beetle and citrus longhorn beetle: are we on the right track? *J. Pest Sci.* 95, 41–66. doi:10.1007/s10340-021-01431-x

Burridge, K. (2017). Focal adhesions: a personal perspective on a half century of progress. *FEBS J.* 284 (20), 3355–3361. doi:10.1111/febs.14195

Cavaletto, G., Faccoli, M., Marini, L., Spaethe, J., Giannone, F., Moino, S., et al. (2021). Exploiting trap color to improve surveys of longhorn beetles. *J. Pest Sci.* 94 (3), 871–883. doi:10.1007/s10340-020-01303-w

Chen, Q. X., Chen, Y. W., and Li, W. L. (2019). Ultrastructural comparison of the compound eyes of the Asian corn borer *Ostrinia furnacalis* (Lepidoptera: crambidae) under light/dark adaptation. *Arthropod Struct. Dev.* 53, 100901. doi:10.1016/j.asd.2019.100901

Chen, X., Wang, J., Wang, R., Zhang, D., Chu, S., Yang, X., et al. (2022). Insights into growth-promoting effect of nanomaterials: using transcriptomics and metabolomics to reveal the molecular mechanisms of MWCNTs in enhancing hyperaccumulator under heavy metal(loid)s stress. *J. Hazard. Mater.* 439, 129640. doi:10.1016/j.jhazmat.2022.129640

Cui, H., Zeng, Y., Reddy, G. V. P., Gao, F., Li, Z., and Zhao, Z. (2021). UV radiation increases mortality and decreases the antioxidant activity in a tephritid fly. *Food Energy Secur.* 10 (3), e297. doi:10.1002/fes3.297

Ernst, J., and Bar-Joseph, Z. (2006). STEM: a tool for the analysis of short time series gene expression data. *BMC Bioinforma.* 7 (1), 191. doi:10.1186/1471-2105-7-191

Fleming, M. R., Bhardwaj, M. C., Janowiak, J., Shield, J. E., Roy, R., Agrawal, D. K., et al. (2005). Noncontact ultrasound detection of exotic insects in wood packing materials. *For. Prod. J.* 55 (6), 33–37.

Fujimaki, K., Li, R., Chen, H., Della Croce, K., Zhang, H. H., Xing, J., et al. (2019). Graded regulation of cellular quiescence depth between proliferation and senescence by a lysosomal dimmer switch. *Proc. Natl. Acad. Sci. U. S. A.* 116 (45), 22624–22634. doi:10.1073/pnas.1915905116

Futahashi, R., Kawahara-Miki, R., Kinoshita, M., Yoshitake, K., Yajima, S., Arikawa, K., et al. (2015). Extraordinary diversity of visual opsin genes in dragonflies. *Proc. Natl. Acad. Sci. U. S. A.* 112 (11), 1247–1256. doi:10.1073/pnas.1424670112

Golec, J. R., Li, F., Cao, L., Wang, X., and Duan, J. J. (2018). Mortality factors of *Anoplophora glabripennis* (Coleoptera: Cerambycidae) infesting *Salix* and *Populus* in central, northwest, and northeast China. *Biol. Control* 126, 198–208. doi:10.1016/j.biocontrol.2018.05.015

Haack, R. A., Herard, F., Sun, J., and Turgeon, J. J. (2010). Managing invasive populations of Asian longhorned beetle and citrus longhorned beetle: a worldwide perspective. *Annu. Rev. Entomology* 55, 521–546. doi:10.1146/annurev-ento-112408-085427

Hanks, L. M. (1999). Influence of the larval host plant on reproductive strategies of Cerambycid beetles. *Annu. Rev. Entomology* 44 (1), 483–505. doi:10.1146/annurev.ento.44.1.483

Hanks, L. M., and Millar, J. G. (2013). Field bioassays of cerambycid pheromones reveal widespread parsimony of pheromone structures, enhancement by host plant volatiles, and antagonism by components from heterospecifics. *Chemoecology* 23 (1), 21–44. doi:10.1007/s00049-012-0116-8

Hanks, L. M., and Millar, J. G. (2016). Sex and aggregation-sex pheromones of Cerambycid beetles: basic science and practical applications. *J. Chem. Ecol.* 42 (7), 631–654. doi:10.1007/s10886-016-0733-8

Hong, M., Tao, S., Zhang, L., Diao, L. T., Huang, X., Huang, S., et al. (2020). RNA sequencing: new technologies and applications in cancer research. *J. Hematol. Oncol.* 13 (1), 166. doi:10.1186/s13045-020-01005-x

Hu, X., Leming, M. T., Metoxen, A. J., Whaley, M. A., and O'Tousa, J. E. (2012). Light-mediated control of rhodopsin movement in mosquito photoreceptors. *J. Neurosci.* 32 (40), 13661–13667. doi:10.1523/jneurosci.1816-12.2012

Insausti, T. C., Le Gall, M., and Lazzari, C. R. (2013). Oxidative stress, photodamage and the role of screening pigments in insect eyes. *J. Exp. Biol.* 216 (17), 3200–3207. doi:10.1242/jeb.082818

Jiang, X., Hai, X., Bi, Y., Zhao, F., Wang, Z., and Lyu, F. (2023a). Research on photoinduction-based technology for trapping Asian longhorned beetle (*Anoplophora glabripennis* (Motschulsky, 1853) (Coleoptera: Cerambycidae). *Insects* 14 (5), 465. doi:10.3390/insects14050465

Jiang, X., Ren, Z., Hai, X., Zhang, L., Wang, Z., and Lyu, F. (2023b). Exposure to artificial light at night mediates the locomotion activity and oviposition capacity of *Dastarcus helophoroides* (Fairmaire). *Front. Physiology* 14, 1063601. doi:10.3389/fphys.2023.1063601

Jiao, L., Dai, T., Jin, M., Sun, P., and Zhou, Q. (2021). Transcriptome analysis of the Hepatopancreas in the *Litopenaeus vannamei* responding to the lead stress. *Biol. Trace Elem. Res.* 199 (3), 1100–1109. doi:10.1007/s12011-020-02235-3

Khan, M. M., Rothenberg, D. O., Shahfahad Qiu, B. L., and Zhu, Z. R. (2023). Identification and transcriptional profiling of UV-A-responsive genes in *Bemisia tabaci*. *Ecotoxicol. Environ. Saf.* 263, 115300. doi:10.1016/j.ecoenv.2023.115300

Kim, K., Huang, Q., and Lei, C. (2019). Advances in insect phototaxis and application to pest management: a review. *Pest Manag. Sci.* 75 (12), 3135–3143. doi:10.1002/ps.5536

Kooi, C., Stavenga, D. G., Arikawa, K., Belui, G., and Kelber, A. (2021). Evolution of insect color vision: from spectral sensitivity to visual ecology. *Annu. Rev. Entomology* 66 (1), 435–461. doi:10.1146/annurev-ento-061720-071644

Landis, D. A., Wratten, S. D., and Gurr, G. M. (2000). Habitat management to conserve natural enemies of arthropod pests in agriculture. *Annu. Rev. Entomology* 45 (1), 175–201. doi:10.1146/annurev.ento.45.1.175

Lawrence, R. E., and Zoncu, R. (2019). The lysosome as a cellular centre for signalling, metabolism and quality control. *Nat. Cell Biol.* 21 (2), 133–142. doi:10.1038/s41556-018-0244-7

Liu, H., Jiao, Q., Fan, L., Jiang, Y., Alyemeni, M. N., Ahmad, P., et al. (2023). Integrated physio-biochemical and transcriptomic analysis revealed mechanism underlying of Si-mediated alleviation to cadmium toxicity in wheat. *J. Hazard. Mater.* 452, 131366. doi:10.1016/j.jhazmat.2023.131366

Livak, K. J., and Schmittgen, T. D. (2001). Analysis of relative gene expression data using real-time quantitative PCR and the 2(-Delta Delta C(T)) Method. *Methods* 25 (4), 402–408. doi:10.1006/meth.2001.1262

Lu, Z., Wang, S., Shan, X., Ji, C., and Wu, H. (2019). Differential biological effects in two pedigrees of clam *Ruditapes philippinarum* exposed to cadmium using iTRAQ-based proteomics. *Environ. Toxicol. Pharmacol.* 65, 66–72. doi:10.1016/j.etap.2018.12.002

Luo, C., and Chen, Y. (2016). Phototactic behavior of *Scleroderma guani* (hymenoptera: bethylidae) - parasitoid of *Pissodes punctatus* (Coleoptera: Curculionidae). *J. Insect Behav.* 29 (6), 605–614. doi:10.1007/s10905-016-9584-y

Luo, Y., Xu, H., Meng, J., and Fan, J. (2012). Mating behavior and characteristics of *Monochamus alternatus*. *J. Zhejiang Agric. For. Univ.* 29 (5), 795–798. doi:10.11833/j.issn.2095-0756.2012.05.025

Lyu, F., Hai, X., and Wang, Z. (2023). A review of the host plant location and recognition mechanisms of Asian longhorn beetle. *Insects* 14 (3), 292. doi:10.3390/insects14030292

Lyu, F., Hai, X., Wang, Z., Yan, A., Bi, Y., and Liu, B. (2015a). Diurnal rhythm of four types of adult behaviors of *Anoplophora glabripennis*. *J. Northeast For. Univ.* 43 (9), 90–95. doi:10.13759/j.cnki.dlxb.20150721.013

Lyu, F., Hai, X. X., Wang, Z. G., Liu, B. X., Yan, A. H., and Bi, Y. G. (2014). Research progress in *Dastarcus helophoroides* Fairmaire (Bothrideridae), an important natural enemy of the longhorn beetle pests. *Sci. Seric.* 40 (6), 1107–1113. doi:10.13441/j.cnki.cykx.2014.06.026

Lyu, F., Hai, X. X., Wang, Z. G., Liu, B. X., Yan, A. H., and Bi, Y. G. (2015b). Circadian behaviors of the parasitic beetles, *Dastarcus helophoroides* (Fairmaire) (Coleptera: Bothrideridae) under artificial light/dark conditions. *Acta Entomol. Sin.* 58 (6), 658–664. doi:10.16380/j.kcxb.2015.06.010

Lyu, F., Hai, X. X., Wang, Z. G., Yan, A. H., Bi, Y. G., and Liu, B. X. (2015c). Diurnal rhythm of adult behavior of *Dastarcus helophoroides* Fairmaire, the parasitic natural enemy of *Apriona germari*. *Sci. Seric.* 41 (2), 239–246. doi:10.13441/j.cnki.cykx.2015.02.007

Macias-Muñoz, A., Rangel Olguin, A. G., and Briscoe, A. D. (2019). Evolution of phototransduction genes in Lepidoptera. *Genome Biol. Evol.* 11 (8), 2107–2124. doi:10.1093/gbe/evz150

Marchioro, M., Battisti, A., and Faccoli, M. (2020). Light traps in shipping containers: a new tool for the early detection of insect alien species. *J. Econ. Entomology* 113 (4), 1718–1724. doi:10.1093/jee/toaa098

Mina, M., Messier, C., Duveneck, M. J., Fortin, M. J., and Aquilue, N. (2022). Managing for the unexpected: building resilient forest landscapes to cope with global change. *Glob. Change Biol.* 28 (14), 4323–4341. doi:10.1111/gcb.16197

Mitchell, R. F., Reagel, P. F., Wong, J. C. H., Meier, L. R., Silva, W. D., Mongold-Diers, J., et al. (2015). Cerambycid beetle species with similar pheromones are segregated by phenology and minor pheromone components. *J. Chem. Ecol.* 41 (5), 431–440. doi:10.1007/s10886-015-0571-0

Miyatake, T., Yokoi, T., Fuchikawa, T., Korehisa, N., Kamura, T., Nanba, K., et al. (2016). Monitoring and detecting the cigarette Beetle (Coleoptera: anobiidae) using ultraviolet (LED) direct and reflected lights and/or pheromone traps in a laboratory and a storehouse. *J. Econ. Entomology* 109, 2551–2560. doi:10.1093/jee/tow225

Moon, Y. M., Metoxen, A. J., Leming, M. T., Whaley, M. A., and O'Tousa, J. E. (2014). Rhodopsin management during the light–dark cycle of *Anopheles gambiae* mosquitoes. *J. Insect Physiology* 70, 88–93. doi:10.1016/j.jinsphys.2014.09.006

Nehme, M. E., Keena, M. A., Zhang, A., Baker, T. C., Xu, Z., and Hoover, K. (2010). Evaluating the use of male-produced pheromone components and plant volatiles in two trap designs to monitor *Anoplophora glabripennis*. *Environ. Entomol.* 39 (1), 169–176. doi:10.1603/EN09177

Nieri, R., Anfora, G., Mazzoni, V., and Stacconi, M. (2022). Semiochemicals, semiophysicals and their integration for the development of innovative multi-modal systems for agricultural pests' monitoring and control. *Entomol. Gen.* 42 (2), 167–183. doi:10.1127/entomologia/2021/1236

Park, J.-H., and Lee, H.-S. (2017). Phototactic behavioral response of agricultural insects and stored-product insects to light-emitting diodes (LEDs). *Appl. Biol. Chem.* 60 (2), 137–144. doi:10.1007/s13765-017-0263-2

Pawson, S., and Watt, M. (2009). An experimental test of a visual-based push-pull strategy for control of wood boring phytosanitary pests. *Agric. For. Entomology* 11 (3), 239–245. doi:10.1111/j.1461-9563.2009.00436.x

Pawson, S. M., Watt, M. S., and Brockerhoff, E. G. (2009). Using differential responses to light spectra as a monitoring and control tool for *Arhopalus ferus* (Coleoptera: Cerambycidae) and other exotic wood-boring pests. *J. Econ. Entomology* 102 (1), 79–85. doi:10.1603/029.102.0112

Rajeshkumar, S., Liu, Y., Zhang, X., Ravikumar, B., Bai, G., and Li, X. (2018). Studies on seasonal pollution of heavy metals in water, sediment, fish and oyster from the Meiliang Bay of Taihu Lake in China. *Chemosphere* 191, 626–638. doi:10.1016/j.chemosphere.2017.10.078

Ray, A. M., Barbour, J. D., McElfresh, J. S., Moreira, J. A., Swift, I., Wright, I. M., et al. (2012). 2,3-Hexanediols as sex attractants and a female-produced sex pheromone for cerambycid beetles in the prionine genus *Tragosoma*. *J. Chem. Ecol.* 38 (9), 1151–1158. doi:10.1007/s10886-012-0181-z

Sacunas, R. B., Papuga, M. O., Malone, M. A., Pearson, A. C., Jr., Marjanovic, M., Stroope, D. G., et al. (2002). Multiple mechanisms of rhabdom shedding in the lateral eye of *Limulus polyphemus*. *J. Comp. Neurology* 449 (1), 26–42. doi:10.1002/cne.10263

Scherm, H., Sutherst, R. W., Harrington, R., and Ingram, J. S. I. (2000). Global networking for assessment of impacts of global change on plant pests. *Environ. Pollut.* 108, 333–341. doi:10.1016/S0269-7491(99)00212-2

Shannon, P., Markiel, A., Ozier, O., Baliga, N. S., Wang, J. T., Ramage, D., et al. (2003). Cytoscape: a software environment for integrated models of biomolecular interaction networks. *Genome Res.* 13 (11), 2498–2504. doi:10.1101/gr.1239303

Silva, W. D., Millar, J. G., Hanks, L. M., and Bento, J. M. (2016). (6E,8Z)-6,8-pentadecadienal, a novel attractant pheromone produced by males of the Cerambycid beetles *Chlorida festiva* and *Chlorida costata*. *J. Chem. Ecol.* 42 (10), 1082–1085. doi:10.1007/s10886-016-0742-7

Sun, X., Feng, D., Liu, M., Qin, R., Li, Y., Lu, Y., et al. (2022). Single-cell transcriptome reveals dominant subgenome expression and transcriptional response to heat stress in Chinese cabbage. *Genome Biol.* 23 (1), 262. doi:10.1186/s13059-022-02834-4

Szklarczyk, D., Gable, A. L., Nastou, K. C., Lyon, D., Kirsch, R., Pyysalo, S., et al. (2020). The STRING database in 2021: customizable protein–protein networks, and functional characterization of user-uploaded gene/measurement sets. *Nucleic Acids Res.* 49 (D1), D605–D612. doi:10.1093/nar/gkaa1074

Tang, H., Yang, Z. Q., and Zhang, Y. N. (2007). Technical researches on distinguishing female and male alive adults of the main parasite of longhorn beetles, *Dastarcus helophoroides* (Coleoptera: Bothrideridae) without injuring. *Acta Zootaxonomica Sin.* 32, 649–654. doi:10.3969/j.issn.1000-0739.2007.03.032

Trapnell, C., Williams, B. A., Pertea, G., Mortazavi, A., Kwan, G., van Baren, M. J., et al. (2010). Transcript assembly and quantification by RNA-Seq reveals unannotated transcripts and isoform switching during cell differentiation. *Nat. Biotechnol.* 28 (5), 511–515. doi:10.1038/nbt.1621

Van der Kooi, C. J., Stavenga, D. G., Arikawa, K., Belusic, G., and Kelber, A. (2021). Evolution of insect color vision: from spectral sensitivity to visual ecology. *Annu. Rev. Entomology* 66, 435–461. doi:10.1146/annurev-ento-061720-071644

Wang, F. F., Wang, M. H., Zhang, M. K., Qin, P., Cuthbertson, A. G. S., Lei, C. L., et al. (2023a). Blue light stimulates light stress and phototactic behavior when received in the brain of *Diaphorina citri*. *Ecotoxicolgy Environ. Saf.* 251, 114519. doi:10.1016/j.ecoenv.2023.114519

Wang, L., Li, C., Luo, Y., Wang, G., Dou, Z., Haq, I. U., et al. (2023b). Current and future control of the wood-boring pest *Anoplophora glabripennis*. *Insect Sci.* doi:10.1111/1744-7917.13187

Wang, Q., Guo, Z., Zhang, J., Chen, Y., Zhou, J., Pan, Y., et al. (2021). Phototactic behavioral response of the ectoparasitoid beetle *Dastarcus helophoroides* (Coleoptera: Bothrideridae): evidence for attraction by near-infrared light. *J. Econ. Entomology* 114 (4), 1549–1556. doi:10.1093/jee/toab120

Wang, Z., Yang, L., Zhou, F., Li, J., Wu, X., Zhong, X., et al. (2023c). Integrated comparative transcriptome and weighted gene co-expression network analysis provide valuable insights into the response mechanisms of crayfish (*Procambarus clarkii*) to copper stress. *J. Hazard. Mater.* 448, 130820. doi:10.1016/j.jhazmat.2023.130820

Wehrle-Haller, B. (2012). Structure and function of focal adhesions. *Curr. Opin. Cell Biol.* 24 (1), 116–124. doi:10.1016/j.ceb.2011.11.001

Wen, C., Ma, T., Deng, Y., Liu, C., Liang, S., Wen, J., et al. (2020). Morphological and optical features of the apposition compound eye of *Monochamus alternatus* Hope (Coleoptera: Cerambycidae). *Micron* 128, 102769. doi:10.1016/j.micron.2019.102769

Wickham, J. D., Harrison, R. D., Lu, W., Guo, Z., Millar, J. G., Hanks, L. M., et al. (2014). Generic lures attract cerambycid beetles in a tropical montane rain forest in southern China. *J. Econ. Entomology* 107 (1), 259–267. doi:10.1603/ec13333

Wickham, J. D., Millar, J. G., Hanks, L. M., Zou, Y., Wong, J. C., Harrison, R. D., et al. (2016). (2R,3S)-2,3-Octanediol, a female-produced sex pheromone of *Megopis costipennis* (Coleoptera: Cerambycidae: Prioninae). *Environ. Entomol.* 45 (1), 223–228. doi:10.1093/ee/nvv176

Wickham, J. D., Xu, Z., and Teale, S. A. (2012). Evidence for a female-produced, long range pheromone of *Anoplophora glabripennis* (Coleoptera: Cerambycidae). *Insect Sci.* 19 (3), 355–371. doi:10.1111/j.1744-7917.2012.01504.x

Xie, C., Mao, X., Huang, J., Ding, Y., Wu, J., Dong, S., et al. (2011). KOBAS 2.0: a web server for annotation and identification of enriched pathways and diseases. *Nucleic Acids Res.* 39, W316–W322. doi:10.1093/nar/gkr483

Xiong, B., Xu, T., Li, R., Johnson, D., Ren, D., Liu, H., et al. (2020). Heavy metal accumulation and health risk assessment of crayfish collected from cultivated and uncultivated ponds in the Middle Reach of Yangtze River. *Sci. Total Environ.* 739, 139963. doi:10.1016/j.scitotenv.2020.139963

Xu, T., Hansen, L., Cha, D. H., Hao, D., Zhang, L., and Teale, S. A. (2020). Identification of a female-produced pheromone in a destructive invasive species: asian longhorn beetle, *Anoplophora glabripennis*. *J. Pest Sci.* 93 (4), 1321–1332. doi:10.1007/s10340-020-01229-3

Yang, Z. Q., Wang, X. Y., and Zhang, Y. N. (2014). Recent advances in biological control of important native and invasive forest pests in China. *Biol. Control* 68, 117–128. doi:10.1016/j.biocontrol.2013.06.010

Yu, L., Zhan, Z., Ren, L., Li, H., Huang, H., and Luo, Y. (2023). Impact of stand- and landscape-level variables on pine wilt disease-caused tree mortality in pine forests. *Pest Manag. Sci.* 79, 1791–1799. doi:10.1002/ps.7357

Zapponi, L., Nieri, R., Zaffaroni-Caorsi, V., Pugno, N. M., and Mazzoni, V. (2022). Vibrational calling signals improve the efficacy of pheromone traps to capture the brown marmorated stink bug. *J. Pest Sci.* 96, 587–597. doi:10.1007/s10340-022-01533-0

Zhang, Z., Pei, P., Zhang, M., Li, F., and Tang, G. (2023). Chromosome-level genome assembly of *Dastarcus helophoroides* provides insights into CYP450 genes expression upon insecticide exposure. *Pest Manag. Sci.* 79 (4), 1467–1482. doi:10.1002/ps.7319

Zheng, Y., Yuan, J., Gu, Z., Yang, G., Li, T., and Chen, J. (2020). Transcriptome alterations in female *Daphnia* (*Daphnia magna*) exposed to 17β-estradiol. *Environ. Pollut.* 261, 114208. doi:10.1016/j.envpol.2020.114208

Zhou, L., Liu, W., Bai, L., Liu, H., Wang, J., Ma, X., et al. (2023). Female's war: a story of the invasion and competitive displacement between two xylophilus group nematode species. *J. Pest Sci.* 96, 1301–1311. doi:10.1007/s10340-023-01603-x

Zhu, N., Zhang, D., Wu, L., Hu, Q., and Fan, J. (2017). Attractiveness of aggregation pheromone and host plant volatiles to *Anoplophora glabripennis* and *A. chinensis* (Coleoptera: Cerambycidae). *Acta Entomol. Sin.* 60 (4), 421–430. doi:10.16380/j.kcxb.2017.04.007

frontiers | Frontiers in Physiology

TYPE Original Research
PUBLISHED 18 January 2024
DOI 10.3389/fphys.2024.1263475

OPEN ACCESS

EDITED BY
Bimalendu B. Nath,
Savitribai Phule Pune University, India

REVIEWED BY
Pawel Marciniak,
Adam Mickiewicz University, Poland
Rita Mukhopadhyaya,
Indian Women Scientists Association, India

*CORRESPONDENCE
Martín Aluja,
martin.aluja@inecol.mx
Daniel Cerqueda-García,
daniel.cerqueda@inecol.mx

RECEIVED 19 July 2023
ACCEPTED 08 January 2024
PUBLISHED 18 January 2024

CITATION
García-Saldaña EA, Cerqueda-García D, Ibarra-Laclette E and Aluja M (2024), Insights into the differences related to the resistance mechanisms to the highly toxic fruit *Hippomane mancinella* (Malpighiales: Euphorbiaceae) between the larvae of the sister species *Anastrepha acris* and *Anastrepha ludens* (Diptera: Tephritidae) through comparative transcriptomics.
Front. Physiol. 15:1263475.
doi: 10.3389/fphys.2024.1263475

Insights into the differences related to the resistance mechanisms to the highly toxic fruit *Hippomane mancinella* (Malpighiales: Euphorbiaceae) between the larvae of the sister species *Anastrepha acris* and *Anastrepha ludens* (Diptera: Tephritidae) through comparative transcriptomics

Essicka A. García-Saldaña[1], Daniel Cerqueda-García[1]*, Enrique Ibarra-Laclette[2] and Martín Aluja[1]*

[1]Clúster Científico y Tecnológico BioMimic®, Red de Manejo Biorracional de Plagas y Vectores, Instituto de Ecología, A C–INECOL, Xalapa, Veracruz, Mexico, [2]Clúster Científico y Tecnológico BioMimic®, Red de Estudios Moleculares Avanzados, Instituto de Ecología, A C–INECOL, Xalapa, Veracruz, Mexico

The Manchineel, *Hippomane mancinella* ("Death Apple Tree") is one of the most toxic fruits worldwide and nevertheless is the host plant of the monophagous fruit fly species *Anastrepha acris* (Diptera: Tephritidae). Here we aimed at elucidating the detoxification mechanisms in larvae of *A. acris* reared on a diet enriched with the toxic fruit (6% lyophilizate) through comparative transcriptomics. We compared the performance of *A. acris* larvae with that of the sister *species A. ludens,* a highly polyphagous pest species that is unable to infest *H. mancinella* in nature. The transcriptional alterations in *A. ludens* were significantly greater than in *A. acris*. We mainly found two resistance mechanisms in both species: structural, activating cuticle protein biosynthesis (chitin-binding proteins likely reducing permeability to toxic compounds in the intestine), and metabolic, triggering biosynthesis of serine proteases and xenobiotic metabolism activation by glutathione-S-transferases and cytochrome P450 oxidoreductase. Some cuticle proteins and serine proteases were not orthologous between both species, suggesting that in *A. acris*, a structural resistance mechanism has been selected allowing specialization to the highly toxic host plant. Our results represent a nice example of how two phylogenetically close species diverged over recent evolutionary time related to resistance mechanisms to plant secondary metabolites.

KEYWORDS

Herbivory, detoxification mechanisms, transcriptomics, *Anastrepha acris*, *Anastrepha ludens*, Diptera: Tephritidae, *Hippomane mancinella*

1 Introduction

Insects are the most diverse group of animals on earth with over a million documented species, many being essential for ecosystem functionality (Grimaldi and Engel, 2005). Their ecological significance spans from nutrient cycling and plant pollination to serving as food sources for many taxa (Scudder, 2017). Moreover, certain insect species have profound economic impacts given their pest status and the interactions that ensue when completing their life cycles in commercially valuable plants/fruits (Lemelin et al., 2016). One such interaction is the resistance/tolerance to the toxic compounds found in certain fruits, which partially protect plants from herbivores (Weng et al., 2012). Understanding the resistance mechanisms to these toxic compounds can provide insights into insects' evolutionary adaptations and survival strategies, especially when considering closely related species (Aluja and Mangan, 2008; Ali and Agrawal, 2012; Giron et al., 2018).

A particularly important group of insects is represented by the true fruit flies (Diptera: Tephritidae) which includes more than 5,000 species (Norrbom, 2010; Liquido et al., 2019). As part of their life history, fruit fly females lay their eggs inside their host's pulp or seeds, where they find favorable conditions for the growth and development of their larvae (Aluja and Mangan, 2008). This behavior causes certain fruit fly species to affect a wide range of commercially valuable fruit crops, limiting international trade of agricultural products (Aluja and Mangan, 2008). In fact, some of these fruit flies are listed among the fruit-tree pest insect species with the greatest economic impact worldwide (White and Elson-Harris, 1992). Among these species, those belonging to the *Anastrepha* genus are one of the most relevant in Mexico and the Neotropics (Hernández-Ortiz et al., 2010). Such is the case of *Anastrepha ludens* (Loew) (Diptera: Tephritidae), commonly known as the Mexican Fruit Fly.

Anastrepha ludens is classified as a highly polyphagous pest, due to its feeding habits which confer it the ability to attack many plant species of several families, including many economically important fruit species such as mango (*Mangifera indica* L.; Anacardiaceae), citrus (*Citrus aurantium* L. or *Citrus x sinensis* L.; Rutaceae), peach (*Prunus persica* L.; Rosaceae), and pepper (*Capsicum pubescens* Ruiz y Pav.; Solanaceae) (Birke et al., 2015; Birke and Aluja, 2018); or wild fruit species, including *Casimiroa edulis* La Llave and Lex (also known as white sapote or matasano) and *C. greggii* (S. Watson) F. Chiang (commonly known as yellow chapote), both within the Rutaceae family. These last two species are the purported ancestral hosts of *A. ludens* (Birke et al., 2015).

In contrast to highly polyphagous tephritid species (*i.e.*, *A. ludens*, the Oriental fruit fly - *Bactrocera dorsalis* Hendel, or the Mediterranean fruit fly - *Ceratitis capitata* Wiedemann), there are other fruit fly species with strict monophagous feeding habits. A good example of a monophagous fruit fly is represented by *B. oleae* Gmelin, commonly known as the Olive Fly. This fly specializes in infesting the fruit of *Olea europaeae* L (olive tree), which contains high levels of phenolic compounds (up to 14% dry weight-based), many of them being active against insects (Ben-Yosef et al., 2015). Among these compounds, Oleuropein, a glucid that is lethal to *Bactrocera oleae* larvae, stands out. Despite this, the larvae of *B. oleae* can develop optimally in the fruit of the olive tree, because it hosts the bacterium *Candidatus Erwinia dacicola* (Enterobacteriaceae), a symbiont found in its digestive tract that assists the larvae to catabolize oleuropein (Ben-Yosef et al., 2015). A similar association between a key bacterium degrading toxic polyphenols (*i.e.*, *Komagataeibacter*) and a fruit fly (the stenophagous *A. striata*) was recently reported (Ochoa-Sánchez et al., 2022). Here we chose as study model another fruit fly species adapted to monophagy: *Anastrepha acris* Stone (Diptera: Tephritidae), which is phylogenetically very close to *A. ludens* (Mengual et al., 2017), but exclusively infests fruits of *Hippomane mancinella* L (Malpighiales: Euphorbiaceae) (Aluja and Norrbom, 2000; Aluja et al., 2020). *Hippomane mancinella* is a tree that produces a fruit commonly known as "Apple of Death", which is highly toxic to many animals, including humans and insects (Rao, 1974; Adolf and Hecker, 1984).

Recently, Aluja et al. (2020) analyzed the interaction between *H. mancinella, A. acris,* and *A. ludens*, and found that diets enriched with different concentrations of dried fruit pulp of *H. mancinella* have a differential effect on the development of the larvae of both species. Not surprisingly, in *A. ludens* they found that *H. mancinella* produces a more pronounced, negative impact on larvae development as there is no natural association between the fly and this toxic fruit in nature. For example, only 0.08% of *A. ludens* larvae developed into pupae in a diet supplemented with 12.5% *H. mancinella* compared with *A. acris* larvae, which fully metamorphosed into pupae and viable adults. However, the number and weight of the exposed pupae decreased as concentration increased. This study nicely complemented the classical literature on the topic of specialized insects dealing with toxic plants (*e.g.*, Berenbaum et al., 1989; Adler et al., 1995; Zalucki et al., 2001; Agrawal and Kurashige, 2003; Harvey et al., 2007). It becomes clear that monophagous species (*i.e.*, highly specialized ones) are not totally immune to plant defense, but they have developed physiological adaptations which allow individuals to cope with deleterious allelochemicals contained in their hosts, exhibiting greater tolerance to these chemicals than polyphagous species. The active compounds reported in *H. mancinella* include the ellagitannins Hippomanin A and B, phenylpropanoids, coumarins, and flavonoids (*e.g.*, naringenin, kaempferol, hesperidin, and quercetin) (Rao, 1974; Aluja et al., 2020). Hippomanin A (a hydrolyzable tannin) is the main active, toxic compound of *H. mancinella* fruit. When it undergoes acid hydrolysis, it yields glucose, ellagic acid, and gallic acid (Rao, 1974; Rao, 1977). However, Hippomanin A was not detected in any of the developmental stages of *A. acris* and neither in its parasitoid; *Doryctobracon areolatus* (Szépligeti) (Hymenoptera: *Braconidae*), which suggests that *A. acris* developed detoxification mechanisms to metabolize it (Aluja et al., 2020).

Despite their economic importance, there is still scant work aimed at understanding the mechanisms used by fruit flies to defend themselves from the toxic specialized metabolites of their plant hosts. In this sense, gene expression studies can be helpful in our quest to elucidate the metabolic impact of plant compounds on herbivorous insects and their effects on their feeding behavior and development (Thitz et al., 2020). For example, Wang et al. (2020) and Zhao et al. (2022) tested the reaction of *Spodoptera litura* (Fabricius) (Lepidoptera: Noctuidae) fed on a diet enriched with tannins. They found that the genes encoding for proteins involved in xenobiotic metabolism (*e.g.*, cytochrome, and glutathione-related

proteins) and digestive enzymes (*e.g.,* lipases and carbohydrases), were highly regulated in the midgut upon diet intake. In *Helicoverpa armigera* (Hübner) (Lepidoptera: Noctuidae) moth, Zheng et al. (2022) evaluated the transcriptomic changes in response to gossypol and tannic acid and identified several transcript-encoding-enzymes involved in immunity, digestion, and detoxification metabolism, including glutathione S-transferases (GSTs), UDP-glucosyl-transferases (UGTs), hydrolases, serine-proteases, lipases, Hsp20, or aldehyde dehydrogenases, explaining how tannins are degraded within the digestive tract of the insect (Zheng et al., 2022). Celorio-Mancera et al. (2011) evaluated the defensive mechanisms of the generalist insect *H. armigera* against the toxic compounds produced by plants within the genus *Gossypium* L (Malvales: Malvaceae). These authors determined that some phytoregulators (*i.e.*, jasmonic acid, salicylic acid, and ethylene) and phenolic compounds modified the transcriptional responses of the larvae at the primary metabolism level and activated its stress response (Celorio-Mancera et al., 2011).

Based on all the above, but particularly following the emphatic call by Ali and Agrawal (2012) recommending the study of related insects with contrasting feeding habits to foster a deeper understanding of the many mechanisms behind herbivory, here we applied a comparative transcriptomic approach to identify the response of *A. acris* and *A. ludens* larvae when fed a lyophilized extract of *H. mancinella*. The latter, to gain insight into the resistance and detoxification mechanisms used by these sister species to overcome the effects of toxic phytochemicals. Based on the "phytochemical coevolution theory/hypothesis" (Cornell and Hawkins, 2003), we predicted that albeit their close phylogenetic relationship, *A. acris*, the strict specialist, would have evolved resistance/degrading mechanisms that the congener, the broad generalist, either lost or never developed during evolution.

2 Materials and methods

2.1 Biological material

To obtain wild specimens of *A. acris* and *A. ludens*, we made collections of infested host fruit in nature. For this, we collected a total of 65 kg of *H. mancinella* (host of *A. acris*) and 60 kg of *Citrus x aurantium* (bitter orange; host of *A. ludens*). The first were collected at Punta Mita (20° 46′19.58"N, 105° 30′38.79"W) and Lo de Marcos (20° 57′13.28"N, 105° 21′59.09"W) in the state of Nayarit, Mexico during July 2020. Infested *C. x aurantium* fruits were collected in September 2020, in Alborada, Veracruz, Mexico (19° 26′49.8"N, 96° 52′24.5"W). The criteria used to determine infestation status in fruit was the identification of small holes in the fruit skin or brown spots (indicating fruit decomposition), both of which are signs of oviposition and larval feeding activity inside the fruit. In addition, 15 kg of uninfested *H. mancinella* fruit were also collected and frozen in liquid nitrogen in the field. These samples were used to lyophilize the pulp used for the experimental diets, following the protocol described by Aluja et al. (2020).

The field-collected material was processed in the laboratories of the Biorational Pest and Vector Management Network (RMBPV), embedded in the BioMimic® Scientific and Technological Cluster, Instituto de Ecología, A.C. (INECOL) in Coatepec, Veracruz, Mexico. Methods described in Aluja et al. (2020) were followed to process infested fruit and collect the larvae/pupae yielded by the fruit.

2.2 Egg collection

Adult and sexually mature flies of each species were distributed in 15 30 × 30 × 30 cm transparent acrylic cages, at a density of 30 ♀ and 15 ♂'s (a total of 450 ♀ and 225 ♂). Inside each cage, we placed containers maintained with water, food (*i.e.*, hydrolyzed protein and sugar in a 1: 3 w/w ratio), with a photoperiod of 12:12 h L:D, at 27°C ± 1°C and 70% ± 5% of relative humidity (RH). For the egg collection, a green cloth, balloon-shaped oviposition device was introduced into each cage, filled with a 0.2% sodium benzoate solution as conservative (Pascacio-Villafán et al., 2018). The devices placed in the *A. acris* cages were impregnated with a mixture of sterile water and 50% of the volume with lyophilized pulp of *H. mancinella* because preliminary observations showed that females do not oviposit in *H. mancinella*-free mixtures. Devices used for *A. ludens* oviposition were free of the *H. mancinella* lyophilizate. Oviposition devices (*i.e.,* egg-collection devices) were retrieved every day after exposing them to flies for 24 h, until the flies stopped producing offspring/eggs (*i.e.*, approximately two and a half months for both species). The eggs were placed on the top of a black cloth placed over moistened cotton, with 5 mL of 0.2% sodium benzoate in plastic Petri dishes (6 cm in diameter) and were incubated in the dark at 29°C ± 1°C and 70% ± 5% RH. The eggs hatched after ca. Three days and the larvae were transferred to Petri dishes (6 cm in diameter) containing the experimental diets described below.

2.3 Transcriptomic experiment

To compare the gene expression of *A. acris* and *A. ludens* larvae in response to lyophilized pulp of *H. mancinella*, we mixed 6% of the lyophilizate with an artificial diet. The artificial diet consisted of a mixture of guar gum (0.096%), nipagin (methylparaben, 0.096%), sodium benzoate (0.38%), citric acid (0.42%), corn flour (5.1%), yeast (5.78%), sugar (7.9%), cob powder (18.3%) and distilled water (61.88%) (as described in Aluja et al., 2020). We determined the concentration used in this study based on a previous one (Aluja et al., 2020), where we reported that *A. acris* larvae can survive until the pupal stage with negligible negative effect up to a concentration of ~30% of *H. mancinella* pulp mixed with an artificial diet, but *A. ludens* larvae reached their survival limit when exposed to a proportion of 12.5% of pulp in the artificial diet (>99% of the larvae died). Therefore, here we used the sub-lethal dose of 6% of lyophilized pulp as the experimental treatment to be able to compare both species.

In the case of the control treatment, larvae were fed with the same artificial diet but without the addition of the toxic *H. mancinella* lyophilizate. This control setup was crucial in establishing baseline gene expression levels in both species under standard dietary conditions. Fifty newly eclosed larvae of each fly species were placed in a 60 mm diameter Petri dish, with 16 g of diet (artificial diet with 6% or without *H. mancinella* lyophilizate). These larvae were kept at 29°C ± 1°C, 70% ± 5% of RH, and were fed for

10 days, until the third instar. Three larvae were taken from each Petri dish and preserved in five volumes of RNAlater® (Qiagen), then they were frozen in liquid nitrogen and kept at −80°C (Oppert et al., 2012).

Formal transcriptomic analyses considered three larvae × three replicates × two conditions = 18 larvae per species (36 larvae in total). Each replicate consisted of a pool of three larvae. Replicates were collected during identical but independent and randomized experimental runs, with independent observations, but with strictly controlled environmental conditions. RNA extractions were made with the RNeasy® Plant mini-Kit (Qiagen©; Hilden, Germany). Total RNA concentration was quantified in a NanoDrop® spectrophotometer (ND-1000, NanoDrop Technologies; Wilmington, DE, United States), while its integrity was verified on 1% agarose gel.

Prior to sequencing, the RIN (RNA integrity number) of each sample was estimated using the Agilent 2,100 Bioanalyzer® capillary electrophoresis system (Agilent Technologies©; Palo Alto, CA, United States). Only samples with a RIN >8 were considered for sequencing. The construction of the libraries was achieved with the TruSeq® RNA Sample Preparation v2 kit (Illumina®; San Diego, CA). Each library was normalized to a final concentration of 20 mM and was sequenced on NextSeq500® equipment (Illumina©; San Diego, CA), using a paired 2 × 150 bp format, at the sequencing unit of the Instituto de Ecología, A.C. (INECOL).

2.4 Bioinformatic analysis

The analysis workflow to process the Illumina paired-end (2 × 150) raw reads was performed in the High-Performance Cluster at the Instituto de Ecología A.C. (INECOL; Xalapa Veracruz, Mexico). A *de novo* transcriptome assembly was performed for each species. For each library, the Illumina adapters were removed, the first 10 bp of the raw reads were trimmed, and the low-quality sequences were cleaned, considering a minimum QScore quality value of 20, using the Trim galore v0.4.5 (Krueger, 2012) and Cutadapt v1.9.1 (Martin, 2011) software. The sequencing quality of each dataset was checked using the FastQC program (http://www.bioinformatics.babraham.ac.uk/projects/fastqc). A single *de novo* transcriptome assembly was generated for each species using the Trinity software with default parameters (Grabherr et al., 2011). After the assembly, we obtained the unigenes or transcripts which were processed with the SeqClean program to remove the poly A tails (https://sourceforge.net/projects/seqclean). To reduce redundant sequences and errors generated by insertions or deletions in the transcriptomes of each species, the coding regions of the unigenes were identified and the reading frames were corrected with the AlignWise software, taking as reference an insect's genomes database (Evans and Loose, 2015). To reduce redundancy, unigenes were clustered at 95% similarity with the CD-HIT program (Li and Godzik, 2006). To estimate the transcripts' abundance, the raw libraries were mapped with the Salmon software against the transcriptome assembly of their respective species (Patro et al., 2017). The differentially expressed unigenes (DEGs) were calculated with DEseq2 software (Love et al., 2014) in the R Studio 4.1.0 under R (R Development Core Team, 2021). We focused on contrasting the gene expression between control and treatment groups to identify Differentially Expressed Genes (DEGs). Initially, we filtered out transcripts exhibiting less than 10 transcripts per million (tpm). Subsequently, for the identification of DEGs, we applied a threshold criterion were unigenes exhibiting a fold change (FC) of ≥1 or ≤ −1, coupled with an adjusted *p*-value (*p*-adj, corrected for False Discovery Rate, FDR) of less than 0.05, were considered significant. This approach allowed us to robustly determine genes that were significantly upregulated or downregulated in the treatment group compared to the control. To explore the results, the up and downregulated set of DEGs per experiment were visualized as volcano plots, Pearson´s correlations, PCAs, heatmaps, and pie charts, with the R Studio 4.1.0 software (R Development Core Team, 2021), using the ggrepel (Slowikowski, 2021), EnhancedVolcano (Blighe et al., 2021), magrittr (Milton-Bache and Wickham, 2020), corrplot (Wei and Simko, 2021), pcaExplorer (Marini and Binder, 2019), cluster (Maechler et al., 2021), pheatmap (Kolde, 2019), dplyr (Wickham et al., 2021), ggplot2 (Wickham, 2016) and ggpubr (Kassambara, 2020) packages. Then, the protein IDs and the amino acid sequences were obtained from the sets of DEGs, to obtain the functional annotation. The functional annotation assignments were performed using the eggNOG-mapper website (Cantalapiedra et al., 2021), specifying a minimum hit e-value = 0, minimum hit bit-score = 60, Percentage identity = 40, minimum % of query coverage = 40, minimum % of subject coverage = 40, only transferring annotations from one-to-one orthology, with experimental evidence only and realigning queries to the whole PFAM DB. The Pathway-tool 13.0 software (Karp et al., 2010) was used to perform the metabolic reconstruction. For this, we used the gff3 annotation file obtained from eggNOG. The reconstruction was done with the PathoLogic algorithm, using the taxonomic pruning option to avoid false positives or pathways not present in tephritids, with a pathway prediction score cutoff of 0.15. Those reconstructed pathways associated with differential genes were identified and their $\log_2$ (FC) was plotted as a heatmap.

We used the heuristic tool Proteinortho (Lechner et al., 2011) to detect orthology between coding proteins of *A. ludens* and *A. acris*. Input data were the aminoacid sequences codified by the corrected ORFs by AlignWise (Evans and Loose, 2015). We used "Proteinortho parameters" as default (Lechner et al., 2011).

3 Results

3.1 *De novo* transcriptome assembly

The minimum and maximum number of raw reads obtained in the libraries of *A. acris* was 21,886,356 and 27,284,901 (with a mean of 24,776,710.3 and a standard deviation 1,983,057.6), and for *A. ludens* was 22,962,425 and 26,517,707 (with a mean of 24,936,771.2 and standard deviation 1,455,172.4). After trimming the mean number of reads was 24,727,965.8 (standard deviation 1,984,655.3) for *A. acris* and 24,896,660.5 (standard deviation 1,451,546.2) for *A. ludens*. The statistics of the transcriptomes of both species are shown in Table 1.

TABLE 1 General statistics of the *de-novo* transcriptome assembly of *A. acris* and *A. ludens*.

Parameters	*A. acris*	*A. ludens*
Total of unigenes ("genes")	112,572	141,660
Total of transcripts ("contigs or transcripts")	187,958	232,187
Percent GC	39.21%	39.12%
Transcripts/contigs with N50 (bp)	1834	1,491
Median contig length (bp)	403	379
Median unigene length (bp)	344	322
Mean contig length (bp)	886.53	787.92
Mean unigene length (bp)	653.02	591.52
Total assembled bases of contigs	166,629,799	182,945,902
Total assembled bases of unigenes	73,511,905	83,794,024
Unigenes >10 tpm	29,592	32,216
DEGs downregulated	31	64
DEGs upregulated	22	184
Percentage of DEGs downregulated with annotation	87.1%	93.7%
Percentage of DEGs upregulated with annotation	97.4%	80.4%
DEGs downregulated with COG	25	60
DEGs upregulated with COG	21	147
DEGs downregulated with Pfam	23	58
DEGs upregulated with Pfam	10	146

3.2 Transcriptome overview of DGEs found in *A. acris* and *A. ludens*

In the PCA analysis, libraries generated from both *A. acris* and *A. ludens* were clustered according to the treatments (highlighted in circles). Respectively, 33% and 60% of the observed variance were explained by the first of two components. While the separation between the variables was evident (Figures 1A, B), no replicates were detected as outliers (Figures 1C, D).

Comparing the transcripts expressed by the larvae developed in the diet enriched with *H. mancinella* lyophilizates, we found a greater number of deregulated unigenes in *A. ludens*, compared to *A. acris*: 64 unigenes were repressed (downregulated) and 184 were overexpressed (upregulated) (with a $\log_2$ Fold change ≥ and ≤1) (Figures 2A, B). Much fewer transcripts were altered in *A. acris*: 31 were repressed and 22 overexpressed (Figures 2A, B). We observed a clear separation between up and downregulated unigenes in the heatmaps in both species that developed in a *H. mancinella* enriched diet. Importantly, the three replicates of each species indicate reproducibility (Figure 3).

In both species, DEGs were related mainly to cuticle biosynthesis, hypoxia, and xenobiotic metabolism. However, *A. ludens* exhibited a higher number of DEGs compared to *A. acris* (Table 2). In both species, several transcripts encoding for chitin-binding and cuticle structural constituent proteins (Chitin_bind_4, Cuticle_4) were identified (in *A. acris* a total of 4 and 40 in *A. ludens*), as well as transcripts encoding hemocyanin proteins (Hemocyanin_C, Hemocyanin_M, Hemocyanin_N) (in *A. acris* a total of 2 and 10 in *A. ludens*). We detected several upregulated transcripts involved in the metabolism of xenobiotics (mainly in Phase one of detoxification) and with redox activity such as P450, COX3, Cytochrom_B, GST_C, GST_N, 3HCDH, adh_short_C2, Aldo_ket_red and Malic_M (in *A. acris* a total of 3 and 19 in *A. ludens*). Also, we detected the upregulation of transcripts encoding for Trypsin and serine proteases involved in digestive processes as well as in the proteolytic activation of zymogens, such as Prophenoloxidase (in *A. acris* a total of 3 and 21 in *A. ludens*) (Table 2). However, only in *A. ludens* did we detect the upregulation of transcripts encoding proteins related to fermentative pathways, such as G6PD, 6PGD-NAD_binding. In *A. ludens*, the downregulated transcripts are related to signal transduction processes, transport, ubiquitination, and proteins with kinase activity, such as PI3K, FAT, DUF, and HECT. In *A. acris*, repressed transcripts include those encoding for SNARE proteins, involved in the fusion of vesicles with the membrane (Table 2). Please note that we are providing a Supplementary Data Sheet that includes the differentially expressed genes for both species with their log fold changes, annotations, and nucleotide sequences.

We found a larger number of differential pathways mapped in *A. ludens* compared to *A. acris* (Figure 4). In *A. ludens*, we observed the activation of detoxification (*i.e.*, Glutathione-peroxide redox reactions, 4-hydroxy-2-nonenal detoxification), pigment (*i.e.*, Pheomelanin biosynthesis, and L-dopa and L-dopachrome biosynthesis), and fermentative metabolic pathways (*i.e.*, glycolysis III, gluconeogenesis III,

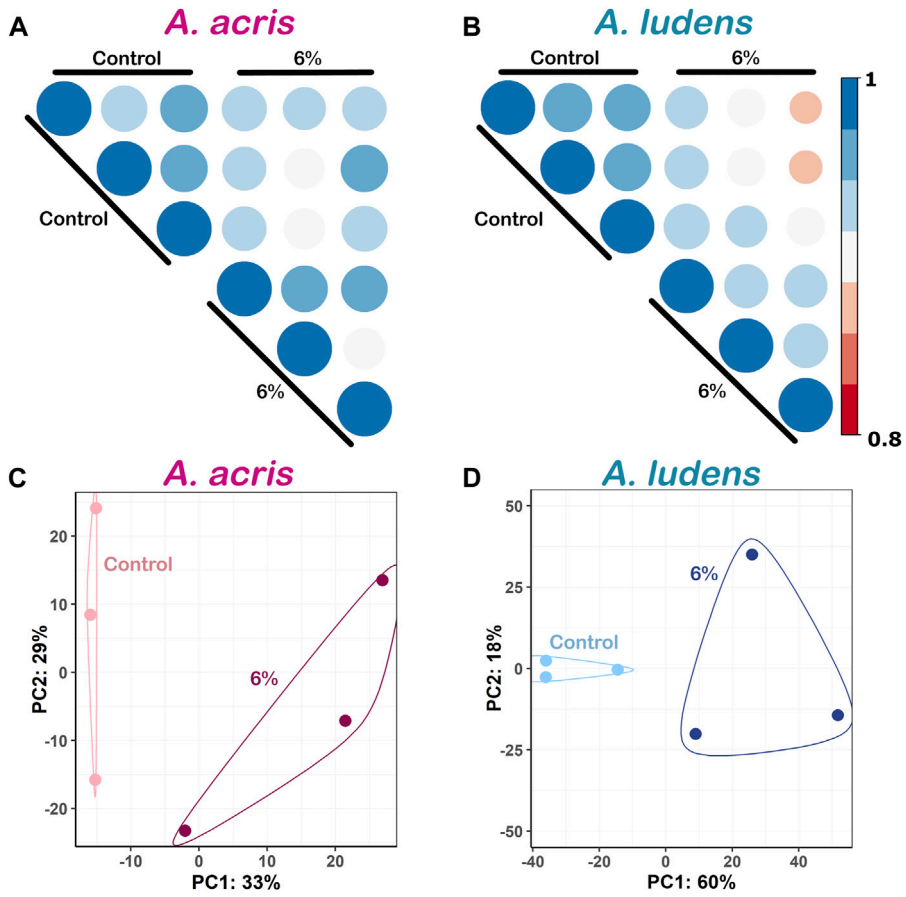

FIGURE 1
Exploratory plots of the transcriptomic differences between the species *A. acris* and *A. ludens* and between treatments. **(A)** and **(B)** Pearson's correlation analysis of the DEGs between the replicas. All replicas had correlation values >0.8. **(C)** and **(D)** Principal component analysis (PCA) of the DEGs from both species. Each point represents a biological replica. The values in the *y* and *x*-axes represent the variation percentages explained by their respective main components.

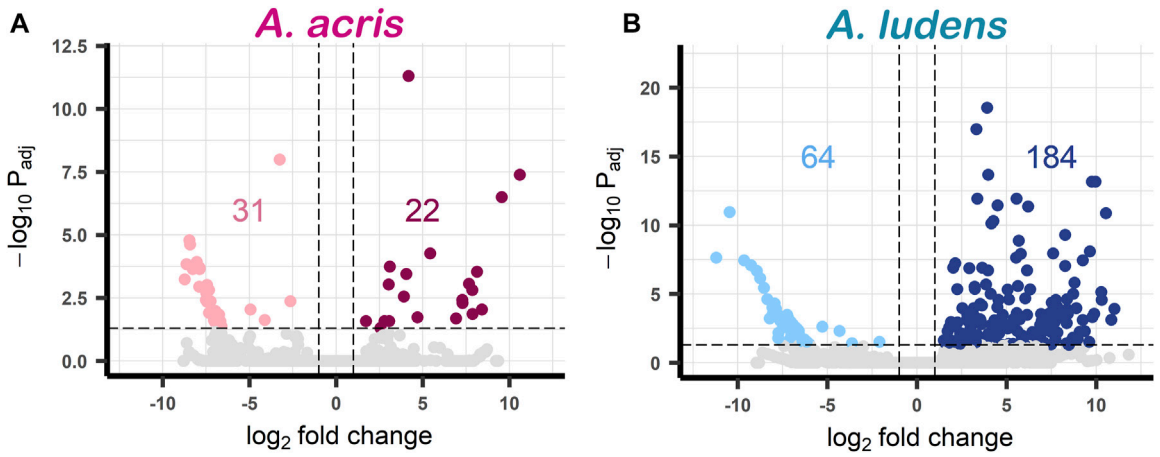

FIGURE 2
Volcano plots of DEGs found in **(A)** *A. acris* and **(B)** *A. ludens* in response to 6% *H. mancinella* lyophilizates mixed in an artificial rearing medium. The dotted horizontal line indicates the−log Padj = 0.05 and the dotted vertical lines indicate the $\log_2$ Fold change ≥1 and ≤ −1. The statistically significant DEGs are colored points (reds and blues). On the left side those that were repressed "downregulated" (pink and light blue) and on the right the overexpressed unigenes "upregulated" (cherry and navy blue) are highlighted. Non-DEGs are shown in gray.

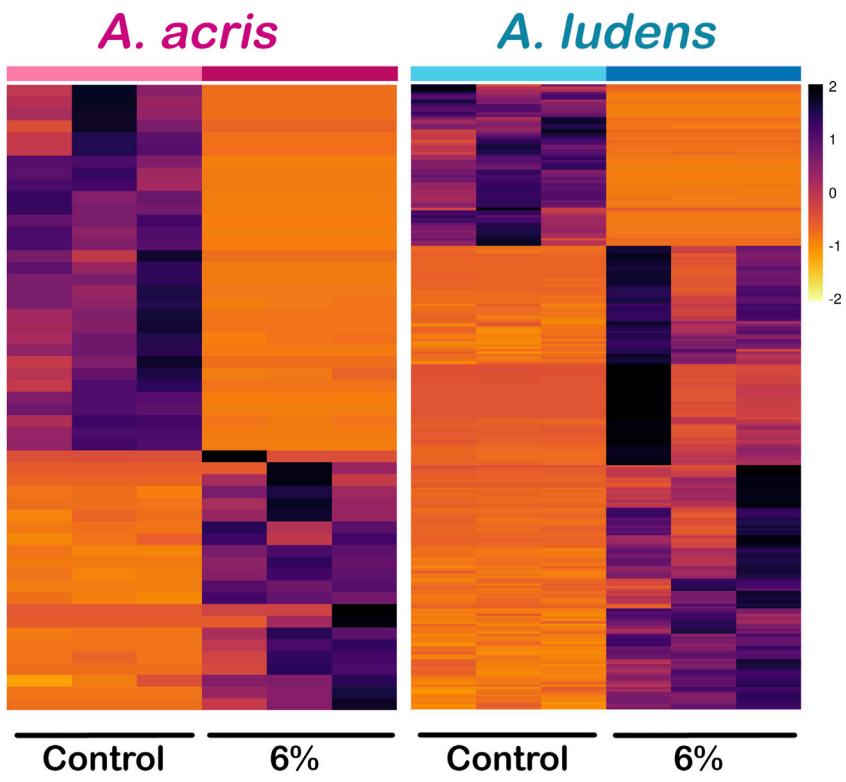

FIGURE 3
Heatmap of differentially expressed unigenes (DEG) of *A. acris* and *A. ludens* exposed to 6% *H. mancinella* lyophilizates mixed in an artificial rearing medium. The scale indicates the $\log_2$. Fold change of each of the DEGs and each column corresponds to a replica.

homolactic fermentation, D-galactose degradation I, and the pentose-phosphate pathway). Also, in *A. ludens* we observed the repression of the protein ubiquitination process, transcripts encoding for proteins involved in the biosynthesis and degradation of amino acids (including Methionine, Isoleucine, Cysteine, Threonine, and Glutamine) and the 3-phosphoinositide biosynthesis (PI3-K); this last (PI3K) was also repressed in *A. acris* (Figure 4). The only route repressed exclusively in *A. acris* was the anandamine degradation pathways (Figure 4).

4 Discussion

The study of the molecular responses of herbivorous insects to plant chemical defenses can be useful in our quest to better understand the mechanisms/metabolic routes that are activated to cope with toxic allelochemicals. Using a transcriptomic approach, here we sought to identify the regulated genes in the larvae of two closely phylogenetically related fruit flies with contrasting feeding habits (*i.e.*, monophagous vs. polyphagous), *A. acris* and *A. ludens*, when they are exposed to the pulp of *H. mancinella*, a plant that produces fruit that is highly toxic. In both species, an alteration was observed in the levels of transcript expression coding for enzymes related to cuticle biosynthesis, hypoxia, protease activity (trypsin and serine proteases) and metabolism of xenobiotics (*i.e.*, responses to abiotic stress) (Table 2). However, a higher number of these transcripts were only recorded in *A. ludens* compared to *A. acris*, the species that thrives in *H. mancinella* (Table 2). In addition to these transcripts found, we were able to map the phosphoinositol biosynthesis pathway (PI3K) in both species (Figure 4). On the other hand, activation in routes related to fermentative metabolism (energy production) and repression of pathways involved in the process of ubiquitination and biosynthesis and degradation of amino acids was only identified in *A. ludens* (Figure 4). The only pathway exclusively affected in *A. acris* was the degradation of anandamides (Figure 4). As will be discussed in what follows, it is likely that the lower regulation observed in *A. acris*, the strict specialist, is likely due to the fact that: 1) larvae of this species have the resistance mechanisms to effectively counteract the negative effects of the toxic allelochemicals present in *H. mancinella* fruit; 2) the low concentration of *H. mancinella* lyophilizate mixed in the diet in which the larvae were reared did not stress the larvae of *A. acris* enough as in nature they are exposed to higher concentrations (an aspect we are currently investigating); 3) these larvae might possibly have a symbiotic intestinal microbiota that facilitates the metabolization of the toxic compounds present in the pulp of *H. mancinella* (something we will research in a future study). Contrary to our prediction, it appears that *A. ludens*, the sister species that evolved into a broad generalist, has maintained most of the broad resistance mechanisms that it shares with *A. acris* which were expressed when exposed to the toxic diet it does not encounter in nature. But *A. ludens* appears to not have developed the specialized biochemical pathways or structural defensive mechanisms *A. acris* possesses that enable it to thrive in the highly toxic *H. mancinella*. A comparative genomics study would be necessary to shed definitive light on this.

The fruit of *H. mancinella* is rich in bioactive polyphenols, such as the ellagitannin Hippomannin A, considered the most toxic compound present in this fruit (Schaeffer et al., 1954; Lauter and Foote, 1955; Rao, 1974; Rao, 1977; Barbehenn et al., 2006;

10.3389/fphys.2024.1263475

TABLE 2 Annotation of the relevant up and downregulated DEGs identified in *A. acris* and *A. ludens* larvae in response to 6% *H. mancinella* lyophilizates mixed in an artificial rearing medium. ID, gene identifier; log_2FC, mean of unigenes with the same PFAM; Total, number of unigenes from the same PFAM; PFAM, name of the protein family to which the enzyme it encodes belongs (obtained from the description of the eggNOG-mapper website).

	Regul	PFAM	log_2FC	p-value	Total	Description
A. acris	Up	Chitin_bind_4	6.69	0.0056	4	Structural constituent of cuticle
		Protease serine-type, Rhomboid	3.07	0.0091	4	Serine-type endopeptidase activity. It is involved in the biological process described with proteolysis
		ADAM_spacer1,Pep_M12B_propep, Reprolysin,TSP_1	7.85	0.0015	1	Involved in the biological process related to proteolysis
		Hemocyanin_C, Hemocyanin_M, Hemocyanin_N	3.98	0.0016	2	Hemocyanin, all-alpha domain
		Cytochrom_B_C, Cytochrome_B	1.73	0.0262	1	Component of the ubiquinol-cytochrome c reductase complex that is part of the mitochondrial respiratory chain. The b-c1 complex mediates electron transfer from ubiquinol to cytochrome c
		P450	8.42	0.0091	1	Heme binding. It is involved in the biological process described with oxidation-reduction process
		COX3	2.57	0.0494	1	Subunits I, II and III form the functional core of the enzyme complex. Component of the cytochrome c oxidase, the last enzyme in the mitochondrial electron transport chain, drives oxidative phosphorylation
	Down	SNARE	−6.61	0.0421	1	SNARE domain: Facilitate the fusion of vesicles, responsible for the transport of molecules
A. ludens	Up	Chitin_bind_4	7.83	0.0097	37	Structural constituent of cuticle
		Trypsin, CLIP, Peptidase_S28, Peptidase_S10	4.75	0.0039	21	Serine-type endopeptidase or carboxypeptidase activity. It is involved in the biological process described with proteolysis
		Hemocyanin_C, Hemocyanin_M, Hemocyanin_N	3.45	0.0258	10	Oxidoreductase activity. It is involved in the biological process described with metabolic process. Hemocyanin, all-alpha domain
		3HCDH, 3HCDH_N	3.37	0.0018	5	3-hydroxyacyl-CoA dehydrogenase activity. It is involved in the biological process described with oxidation-reduction process
		6PGD, NAD_binding_2	3.21	0.0004	1	Catalyzes the oxidative decarboxylation of 6-phosphogluconate to ribulose 5-phosphate and CO(2), with concomitant reduction of NADP to NADPH
		adh_short_C2	4.66	0.0003	4	Oxidoreductase activity. It is involved in the biological process described with metabolic process
		Aldo_ket_red	2.43	0.0388	4	It is involved in the biological process described with oxidation-reduction processes
		p450	3.74	0.0001	3	Heme binding. It is involved in the biological process described with oxidation-reduction process
		Cuticle protein	4.81	0.0027	3	Cuticle protein
		GST_C, GST_C_3, GST_N, GST_N_3	1.92	0.0130	2	Conjugation of reduced glutathione to a wide number of exogenous and endogenous hydrophobic electrophiles
		Malic_M, malic	1.71	0.0051	1	It is involved in the biological process described with oxidation-reduction processes
		G6PD_C, G6PD_N	2.12	0.0496	1	Catalyzes the rate-limiting step of the oxidative pentose-phosphate pathway, which represents a route for the dissimilation of carbohydrates besides glycolysis
	Down	PI3K_C2,PI3K_p85B,PI3K_rbd,PI3Ka,PI3_PI4_kinase	−6.93	0.0056	2	Phosphotransferase activity, alcohol group as acceptor. It is involved in the biological process described with phosphatidylinositol phosphorylation
		FAT,FATC, PI3_PI4_kinase	−7.27	0.0027	1	Belongs to the PI3 PI4-kinase family
		C2, HECT,WW	−6.5	0.034	1	Ubiquitin-protein transferase activity

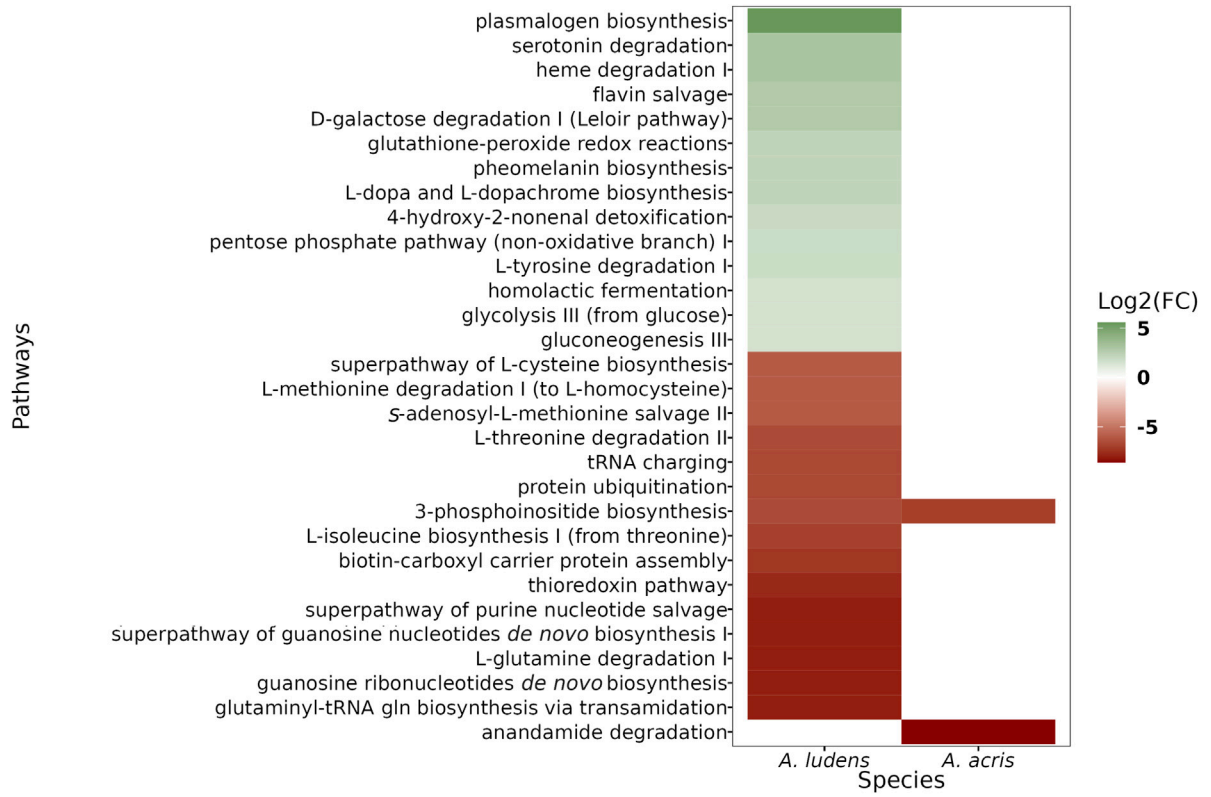

FIGURE 4
Heatmap of differential metabolic pathways found in *A. acris* and *A. ludens* larvae that were reared in an artificial diet containing 6% *H. mancinella* pulp lyophylizates. The activated pathways are shown in green (or shades thereof) and the repressed ones, in ochre red.

Aluja et al., 2020). The first defense line of insects to face these secondary metabolites is the cuticle. The larval cuticle is a physical barrier that can limit the passage of toxic compounds from the environment to the hemolymph (Pryor et al., 1947; Barrett, 1983; Ashida and Brey, 1995; 1997). We found upregulation of transcripts that encode for cuticle proteins (chitin-binding proteins) in both species (Table 2) and could be related to a response leading to the reinforcement of the cuticle of the larvae. In insects, an increase in the thickness of the cuticle has been related to resistance against secondary metabolites present in plants and insecticides (Balabanidou et al., 2018). For example, when larvae of *Spodoptera frugiperda* were exposed to camptothecin (a pentacyclic quinoline alkaloid isolated from *Camptotheca acuminata* Decne.), histopathological changes were observed in the midgut structure, followed by upregulation of several genes encoding for cuticular proteins (Shu et al., 2021). Consistent with this, we found that of the upregulated cuticle-proteins, 28 were not orthologous in *A. ludens*, and four were not orthologous in *A. acris*. We note, however, that many of these Unigenes were partial, and this could have biased the resolution of the orthology detection procedure followed. If the above is true, then the damage generated by the pulp of lyophilized *H. mancinella* could first occur through cuticular disruption. Considering this, *A. acris* can likely reinforce the resistance against *H. mancinella* by adapting its cuticle through structural proteins in the cuticle that are more efficient than those found in *A. ludens*, a species whose larvae are not naturally exposed to the toxicants in the fruit of this plant.

We also identified many transcripts encoding proteases, including trypsin (Table 2). Trypsin is a non-specific serine endopeptidase responsible for the maturation of various zymogens such as prophenoloxidase (important for immune responses) (Ashida and Brey, 1997; Perdomo-Morales et al., 2007; Soares et al., 2011; Lu et al., 2014; Wu et al., 2015). Prophenoloxidase is synthesized in insect hemocytes, actively transported into the cuticle through the epidermis, and randomly distributed in the endocuticle of the body wall (Ashida and Brey, 1997). Since phenoloxidase (mature version of phenoloxidase) is central to the immune response, as it can oxidize phenolic compounds to induce melanization of the cuticle, it is likely that the phenoloxidase system actively participates as a defense mechanism in response to *H. mancinella* compounds (Lu et al., 2014; Wu et al., 2015).

In insects there is an antagonistic interaction between the ingestion of phenols and the assimilation of nutrients, which can cause an inhibition of the digestion of carbohydrates or proteins, affecting their nutrition, growth, and development (Schopf, 1986; Felton et al., 1992; Haukioja et al., 2002; Pascacio-Villafán et al., 2016; Punia et al., 2020; Thitz et al., 2020). This antagonistic interaction is produced due to the inhibition of digestive enzymes by polyphenols. In the case of ellagitannins, it has been documented that they can inhibit alfa-amylase and trypsin activity (McDougall and Stewart, 2005). Many phytophagous insects counteract the polyphenols' effect by a high protease synthesis rate (Brioschi et al., 2007; Spit et al., 2014; Zhu-Salzman and Zeng, 2015), a mechanism we identified in both fly species in this study. We identified the upregulation of trypsin and serine proteases, 21 in *A. ludens* and four in *A. acris*. However, our results suggest differences in these enzymes in both flies, with two peptidases in *A. acris* not being orthologous with *A. ludens*. On the

other hand, 13 peptidases present in *A. ludens* were not orthologous in *A. acris*.

Interestingly, one non-orthologous serine-type endopeptidase in *A. acris* is a rhomboid-like1 protein. Rhomboid serine proteases, together with ADAM (a disintegrin and metalloproteinase) proteins, are involved in the Epidermal Growth Factor Receptor (EGFR) pathway, catalyzing the cleavage of membrane-tethered epidermal growth factor (EGF)-like ligands, being a regulator and activator of EGFR (Lee et al., 2001; Urban, 2002; Blobel, 2005). In *A. acris*, a homologous of the ADAM metalloprotease was upregulated (Unigen: acris005570). In *Drosophila*, EGFR regulates the penetration resistance to the insecticide avermectin, regulating the chitin synthesis and promoting the increment of peritrophic membrane thickness in larvae resistant to avermectin (Chen et al., 2016). Interestingly in human cells, EGFR activation can be inhibited by epigallocatechin-gallate, triggering the internalization of the EGFR (Adachi et al., 2007; Adachi et al., 2008). Even though the EGFR pathway seems conserved in all eukaryotes, differences could exist between *A. ludens* and *A. acris*, based on the difference in the rhomboid protein, that hypothetically could be related to the maturation of the EGFR-ligand.

When *A. ludens* larvae are reared in diets or fruit containing high concentrations of phenolic compounds (*e.g.*, *Malus domestica* Borkh), a reduction in egg production, larval weight, and an increase in larval development and pupation times has been recorded (Aluja et al., 2014; Pascacio-Villafán et al., 2014). The induction of deformities was also observed in pupae, as well as an increase in mortality and the duration of the biological cycle, which lasts up to three times more compared to larvae reared on natural hosts such as grapefruit, with a lower content of phenolic compounds (Aluja et al., 2014; Pascacio-Villafán et al., 2014). At a molecular level, phenolic compounds bind to the amino acid-building proteins in the diet and/or to digestive tract enzymes (Schopf, 1986; Felton and Duffey, 1991). This happens because the aromatic rings of amino acids and polyphenols interact through π-type interactions, destabilizing the tridimensional structure of proteins, which induces protein denaturation and coalescence with other proteins (Adamczyk et al., 2012; Chen et al., 2019). These effects inactivate the function of the proteins affected, and the biological processes in which they participate (Haslam, 2007; Spalinger et al., 2010; Adamczyk et al., 2012). Tannins, a particular class of polyphenols, can produce high levels of semiquinones and quinones, which affect the redox status of the cell contributing to poor absorption of nutrients and generation of cytotoxic effects in the affected tissues (Appel, 1993; Salminen et al., 2004; Barbehenn et al., 2005; Barbehenn and Constabel, 2011).

In addition, and in contrast to what was observed in *A. acris*, in *A. ludens* a high number of transcripts that encode for proteins involved in energy processes and in the biosynthesis and degradation of amino acids were found (Figure 4). So, not surprisingly, the larvae of *A. ludens* suffered more metabolic changes than *A. acris*. For example, we observed the activation of fermentative pathways, inferring that energy metabolism was one of the most affected aspects in *A. ludens*. This effect was not observed in *A. acris*, suggesting that the basal defense mechanisms of *A. acris* were sufficient to prevent the metabolic effects observed in *A. ludens*.

The transcriptional responses of both phylogenetically related species involve the activation of transcripts that encode for similar enzymes, such as enzymes with heme-binding sites, proteases, or chitin-binding enzymes (Table 2). It is likely that the high concentration of tannins present in the pulp of *H. mancinella*, together with the metal chelating activity of the o-dihydroxyphenyl groups of tannins, causes a decrease in the bioavailability of iron, copper, and other metallic macro or micronutrients (McDonald et al., 1996; Afsana et al., 2004; Fiesel et al., 2015; Delimont et al., 2017). So, if tannins were chelating metals, proteins that have an active site coordinated with metal ions, such as those with heme groups, would become dysfunctional. For example, the activation of genes that encode for hemocyanin (a heme-containing protein) could cause a decrease in the oxygen transport activity through the hemolymph (Engel and Brouwer, 1991; Martin and Hose, 1995). Therefore, if the tannins are interfering with the oxygen transport activity, and favoring hypoxic conditions, a plausible countermeasure to compensate hypoxia could be the transcriptional activation of hemocyanins (Engel and Brouwer, 1991; Martin and Hose, 1995; Salminen and Karonen, 2011). Also, the decrease in the concentration of oxygen available in the hemolymph would explain the activation of the fermentative pathways observed in *A. ludens*. Usually, the activation of fermentative pathways leads to the rapid production of energy, but this process is insufficient when these conditions are maintained for a long time, affecting the metabolic performance of the organism (Hoback and Stanley, 2001).

In both species, the activation of genes coding for proteins related to the metabolism of xenobiotics and in oxidation-reduction processes was also found (Table 2). As was the case with other defensive responses, in *A. ludens* the number of these transcripts was much higher compared to *A. acris*. In this sense, the activation of transcripts related to the first stage of xenobiotic metabolism is relevant, since these enzymes represent one of the first lines of defense against toxic compounds (Li et al., 2007). So, the activation of transcripts encoding for P450 monooxygenase enzymes, glutathione-S-transferases, and transporters could be related to the coordinated response of detoxification pathways and toxin excretion (Chahine and O'Donnell, 2012; Zheng et al., 2022). In future studies, it would be of interest to identify the anatomical site where these transcripts are altered.

Repression of signaling via phosphoinositides was also identified in both species. For example, in *A. ludens* the transcript of phosphatidylinositol 4, 5-bisphosphate kinase (PI3K) was specifically repressed (Figure 4). PI3K is an important regulator of cell growth in insects, as it inhibits the signaling that leads to a reduction in body size, tissue growth, and starvation (Britton et al., 2002; Lin and Smagghe, 2019). This happens because PI3K activity is regulated by the availability of protein in the diet and coordinates cellular metabolism based on the nutritional conditions of the individual (Britton et al., 2002).

Notably, in *A. acris*, the anandamide degradation pathway was repressed (Figure 4). Anandamide is a bioactive fatty acid amide widely studied in mammals that functions as a messenger molecule regulating feeding behavior (*e.g.*, hunger, and satiety perception), among other functions (Sharkey et al., 2014). However, in insects, there are few studies on the metabolism of anandamide and its functions (Ban et al., 2003; Farrell and Merkler, 2008; Tortoriello et al., 2013; Jeffries et al., 2014).

In other study models such as the plant *Arabidopsis thaliana*, it has been reported that fungi toxin elimination occurs via a vesicle-mediated transport which is translocated from the plasma membrane to vacuoles (Wang et al., 2020). This mechanism, which is not exclusive to plants, could occur also in insects in which the detoxification strategy includes catabolism and the sequestration of plant-defense secondary metabolites. The above can explain, at least in part, why proteins like SNARE are

differentially expressed. SNARE proteins represent a superfamily of small, mostly membrane-anchored proteins that catalyze the fusion of membranes in all eukaryotic cells (Margiotta, 2022).

5 Conclusion

The larvae of *A. acris* and *A. ludens* responded at a transcriptional level to counteract the negative effects caused by the ingestion of *H. mancinella* pulp, expressing overall similar mechanisms. However, in *A. ludens* the number of transcripts altered was much greater than in *A. acris*. These transcriptional responses of both species were mainly related to hypoxia, cuticle biosynthesis, and xenobiotic metabolism. Our results indicate that *A. acris* can easily handle a low level of toxicity in *H. mancinella* lyophilizates added to an artificial diet (6%), but additional experiments with higher concentrations of the toxicants in the fruit are needed to fully understand the biochemical/molecular mechanisms larvae of this species use to degrade or block these deleterious allelochemicals. From our results it becomes clear that during the divergence of these phylogenetically close species, *A. acris* developed adaptations to deal with the toxicants of its only known host, whereas *A. ludens*, following another evolutionary path, maintained certain common biochemical routes, expressed here when exposed to the toxicants of a fruit that is not a host in nature, and apparently lost others that inhibit its development in *H. mancinella*. But further research is needed to clarify if *A. acris* indeed evolved novel toxicant degradation/blocking routes, or if its gut contains symbiotic bacteria that are the ones that metabolize the toxicants. This is needed as in this study we studied the transcriptome of entire larvae, including the gut. In future studies we will concentrate on the gut and the bacteria contained in it. Further research is also needed on possible morphological adaptations in the midgut of the larvae (e.g., thickness of gut walls) through which the entrance of toxicants via the gut into the hemolymph could be blocked.

Data availability statement

The raw datasets for this study can be found in the Sequence Read Archive (SRA) of the National Center for Biotechnology Information (NCBI) under the accession number PRJNA957832.

Ethics statement

The manuscript presents research on animals that do not require ethical approval for their study.

Author contributions

EG-S: Data curation, Investigation, Software, Visualization, Writing–original draft. DC-G: Data curation, Formal Analysis, Software, Supervision, Visualization, Writing–review and editing. EI-L: Conceptualization, Methodology, Supervision, Writing–review and editing. MA: Conceptualization, Funding acquisition, Methodology, Supervision, Writing–original draft, Writing–review and editing.

Funding

The author(s) declare financial support was received for the research, authorship, and/or publication of this article. This work was funded by grants to MA from the Campaña Nacional Contra Moscas de la Fruta via an Agreement between the Consejo Nacional Consultivo Fitosanitario (CONACOFI) and INECOL (Project Numbers 41013–2019, 80124–2020 and 80147–2021). Additional funds in the form of salaries as well as research facilities and equipment were provided by INECOL to MA and EIL.

Acknowledgments

We gratefully acknowledge the valuable contributions to the research being reported here made during tutorial exams by Dr. Jing-Ke Weng, Massachusetts Institute of Technology. We gratefully acknowledge the expert technical help provided by Emilio Acosta Velasco, Erick J. Enciso Ortíz, Alma R. Altúzar Molina and Juan Carlos Conde Alarcón. We also gratefully acknowledge the technical assistance of Alexandro G. Alonso S., who prepared and sequenced the libraries. Alma R. Altúzar Molina also provided editorial help and helped us format the final version of the manuscript. We also acknowledge the critical support provided by Emanuel Villafán de la Torre, manager of INECOL's supercomputing center where all bioinformatic analyses were run. We finally acknowledge the comments made during tutorial exams and the considerable time investment during a first failed attempt at bioinformatically analyzing the data by Dr. Jesús Alejandro Zamora Briseño (Instituto de Ecología, A.C—INECOL). This publication reports the results of a master's degree thesis by EAG-S directed by MA. EG-S gratefully acknowledges a fellowship from the Consejo Nacional de Ciencia y Tecnología–CONACyT.

Conflict of interest

The authors declare that the research was conducted in the absence of any commercial or financial relationships that could be construed as a potential conflict of interest.

Publisher's note

Supplementary material

The Supplementary Material for this article can be found online at: https://www.frontiersin.org/articles/10.3389/fphys.2024.1263475/full#supplementary-material

References

Adachi, S., Nagao, T., Ingolfsson, H. I., Maxfield, F. R., Andersen, O. S., Kopelovich, L., et al. (2007). The inhibitory effect of (−)-Epigallocatechin Gallate on activation of the epidermal growth factor receptor is associated with altered lipid order in HT29 colon cancer cells. *Cancer Res.* 67, 6493–6501. doi:10.1158/0008-5472.CAN-07-0411

Adachi, S., Nagao, T., To, S., Joe, A. K., Shimizu, M., Matsushima-Nishiwaki, R., et al. (2008). (-)-Epigallocatechin gallate causes internalization of the epidermal growth factor receptor in human colon cancer cells. *Carcinogenesis* 29, 1986–1993. doi:10.1093/carcin/bgn128

Adamczyk, B., Salminen, J.-P., Smolander, and A., and Kitunen, V. (2012). Precipitation of proteins by tannins: effects of concentration, protein/tannin ratio and pH. *Int. J. Food Sci. Technol.* 47, 875–878. doi:10.1111/j.1365-2621.2011.02911.x

Adler, L. S., Schmitt, J., and Bowers, M. D. (1995). Genetic variation in defensive chemistry in *Plantago lanceolata* (Plantaginaceae) and its effect on the specialist herbivore *Junonia coenia* (Nymphalidae). *Oecologia* 101, 75–85. doi:10.1007/BF00328903

Adolf, W., and Hecker, E. (1984). On the active principles of the spurge family, X. Skin irritants, cocarcinogens, and cryptic cocarcinogens from the latex of the manchineel tree. *J. Nat. Prod.* 47, 482–496. doi:10.1021/np50033a015

Afsana, K., Shiga, K., Ishizuka, S., and Hara, H. (2004). Reducing effect of ingesting tannic acid on the absorption of iron, but not of zinc, copper, and manganese by rats. *Biosci. Biotechnol. Biochem.* 68, 584–592. doi:10.1271/bbb.68.584

Agrawal, A. A., and Kurashige, N. S. (2003). A role for isothiocyanates in plant resistance against the specialist herbivore *Pieris rapae*. *J. Chem. Ecol.* 29, 1403–1415. doi:10.1023/A:1024265420375

Ali, J. G., and Agrawal, A. A. (2012). Specialist *versus* generalist insect herbivores and plant defense. *Trends Plant Sci.* 17, 293–302. doi:10.1016/j.tplants.2012.02.006

Aluja, M., Birke, A., Ceymann, M., Guillén, L., Arrigoni, E., Baumgartner, D., et al. (2014). Agroecosystem resilience to an invasive insect species that could expand its geographical range in response to global climate change. *Agric. Ecosyst. Environ.* 186, 54–63. doi:10.1016/j.agee.2014.01.017

Aluja, M., and Mangan, R. L. (2008). Fruit fly (Diptera: Tephritidae) host status determination: critical conceptual, methodological, and regulatory considerations. *Annu. Rev. Entomol.* 53, 473–502. doi:10.1146/annurev.ento.53.103106.093350

Aluja, M., and Norrbom, A. L. (2000). *Fruit flies (Tephritidae): phylogeny and evolution of behavior*. Boca Raton, FL: CRC Press.

Aluja, M., Pascacio-Villafán, C., Altúzar-Molina, A., Monribot-Villanueva, J., Guerrero-Analco, J. A., Enciso, E., et al. (2020). Insights into the interaction between the monophagous tephritid fly *Anastrepha acris* and its highly toxic host *Hippomane mancinella* (Euphorbiaceae). *J. Chem. Ecol.* 46, 430–441. doi:10.1007/s10886-020-01164-8

Appel, H. M. (1993). Phenolics in ecological interactions: the importance of oxidation. *J. Chem. Ecol.* 19, 1521–1552. doi:10.1007/BF00984895

Ashida, M., and Brey, P. T. (1995). Role of the integument in insect defense: pro-phenol oxidase cascade in the cuticular matrix. *Proc. Natl. Acad. Sci. U.S.A.* 92, 10698–10702. doi:10.1073/pnas.92.23.10698

Ashida, M., and Brey, P. T. (1997). "Recent advances in research on the insect phenoloxidase cascade," in *Molecular mechanisms of immune responses in insects*. Editors P. T. Brey and D. Hultmark (London: Chapman and Hall), 135–172.

Balabanidou, V., Grigoraki, L., and Vontas, J. (2018). Insect cuticle: a critical determinant of insecticide resistance. *Curr. Opin. Insect Sci.* 27, 68–74. doi:10.1016/j.cois.2018.03.001

Ban, L., Scaloni, A., Brandazza, A., Angeli, S., Zhang, L., Yan, Y., et al. (2003). Chemosensory proteins of *Locusta migratoria*. *Insect Mol. Biol.* 12, 125–134. doi:10.1046/j.1365-2583.2003.00394.x

Barbehenn, R., Cheek, S., Gasperut, A., Lister, E., and Maben, R. (2005). Phenolic compounds in Red Oak and Sugar Maple leaves have prooxidant activities in the midgut fluids of *Malacosoma disstria* and *Orgyia leucostigma* caterpillars. *J. Chem. Ecol.* 31, 969–988. doi:10.1007/s10886-005-4242-4

Barbehenn, R. V., and Constabel, P. C. (2011). Tannins in plant-herbivore interactions. *Phytochem* 72, 1551–1565. doi:10.1016/j.phytochem.2011.01.040

Barbehenn, R. V., Jones, C. P., Hagerman, A. E., Karonen, M., and Salminen, J. P. (2006). Ellagitannins have greater oxidative activities than condensed tannins and galloyl glucoses at high pH: potential impact on caterpillars. *J. Chem. Ecol.* 32, 2253–2267. doi:10.1007/s10886-006-9143-7

Barrett, F. M. (1983). Purification of phenolic compounds and a phenoloxidase from larval cuticle of the red-humped oakworm, *Symmerista cannicosta* Francl. *Arch. Insect Biochem. Physiol.* 1, 213–223. doi:10.1002/arch.940010304

Ben-Yosef, M., Pasternak, Z., Jurkevitch, E., and Yuval, B. (2015). Symbiotic bacteria enable olive fly larvae to overcome host defences. *R. Soc. Open Sci.* 2, 150170. doi:10.1098/rsos.150170

Berenbaum, M., Zangerl, A. R., and Lee, K. (1989). Chemical barriers to adaptation by a specialist herbivore. *Oecologia* 80, 501–506. doi:10.1007/BF00380073

Birke, A., Acosta, E., and Aluja, M. (2015). Limits to the host range of the highly polyphagous tephritid fruit fly *Anastrepha ludens* in its natural habitat. *Bull. Entomol. Res.* 105, 743–753. doi:10.1017/S0007485315000711

Birke, A., and Aluja, M. (2018). Do mothers really know best? Complexities in testing the preference-performance hypothesis in polyphagous frugivorous fruit flies. *Bull. Entomol. Res.* 108, 674–684. doi:10.1017/S0007485317001213

Blighe, K., Rana, S., and Lewis, M. (2021). Enhanced Volcano: publication-ready volcano plots with enhanced colouring and labeling. R Package Version 1.10.0. Available at: https://github.com/kevinblighe/EnhancedVolcano.

Blobel, C. P. (2005). ADAMs: key components in EGFR signalling and development. *Nat. Rev. Mol. Cell Biol.* 6, 32–43. doi:10.1038/nrm1548

Brioschi, D., Nadalini, L. D., Bengtson, M. H., Sogayar, M. C., Moura, D. S., and Silva-Filho, M. C. (2007). General up regulation of *Spodoptera frugiperda* trypsins and chymotrypsins allows its adaptation to soybean proteinase inhibitor. *Insect biochem. Mol. Biol.* 37, 1283–1290. doi:10.1016/j.ibmb.2007.07.016

Britton, J. S., Lockwood, W. K., Li, L., Cohen, S. M., and Edgar, B. A. (2002). Drosophila's insulin/PI3-kinase pathway coordinates cellular metabolism with nutritional conditions. *Dev. Cell.* 2, 239–249. doi:10.1016/S1534-5807(02)00117-X

Cantalapiedra, C. P., Hernández-Plaza, A., Letunic, I., Bork, P., and Huerta-Cepas, J. (2021). EggNOG-mapper v2: functional annotation, orthology assignments, and domain prediction at the metagenomic scale. *Mol. Biol. Evol.* 38, 5825–5829. doi:10.1093/molbev/msab293

Celorio-Mancera, M. D., Ahn, S. J., Vogel, H., and Heckel, D. G. (2011). Transcriptional responses underlying the hormetic and detrimental effects of the plant secondary metabolite gossypol on the generalist herbivore *Helicoverpa armigera*. *BMC Genom* 12, 575. doi:10.1186/1471-2164-12-575

Chahine, S. C. A., O'Donnell, M. J., and O'Donnell, M. J. (2012). Genetic knockdown of a single organic anion transporter alters the expression of functionally related genes in Malpighian tubules of *Drosophila melanogaster*. *J. Exp. Biol.* 215, 2601–2610. doi:10.1242/jeb.071100

Chen, G., Wang, S., Feng, B., Jiang, B., and Miao, M. (2019). Interaction between soybean protein and tea polyphenols under high pressure. *Food Chem.* 277, 632–638. doi:10.1016/j.foodchem.2018.11.024

Chen, L.-P., Wang, P., Sun, Y. J., and Wu, Y. J. (2016). Direct interaction of avermectin with epidermal growth factor receptor mediates the penetration resistance in *Drosophila* larvae. *Open Biol.* 6, 150231. doi:10.1098/rsob.150231

Cornell, H. V., and Hawkins, B. A. (2003). Herbivore responses to plant secondary compounds: a test of phytochemical coevolution theory. *Am. Nat.* 161, 507–522. doi:10.1086/368346

Delimont, N. M., Haub, M. D., and Lindshield, B. L. (2017). The impact of tannin consumption on iron bioavailability and status: a narrative review. *Curr. Dev. Nutr.* 1, 1–12. doi:10.3945/cdn.116.000042

Engel, D. W., and Brouwer, M. (1991). Short-term metallothionein and copper changes in blue crabs at ecdysis. *Biol. Bull.* 180, 447–452. doi:10.2307/1542345

Evans, T., and Loose, M. (2015). AlignWise: a tool for identifying protein-coding sequence and correcting frame-shifts. *BMC Bioinform* 16, 376. doi:10.1186/s12859-015-0813-8

Farrell, E. K., and Merkler, D. J. (2008). Biosynthesis, degradation, and pharmacological importance of the fatty acid amides. *Drug Discov. Today.* 13, 558–568. doi:10.1016/j.drudis.2008.02.006

Felton, G. W., Donato, K. K., Broadway, R. M., and Duffey, S. S. (1992). Impact of oxidized plant phenolics on the nutritional quality of dietar protein to a noctuid herbivore, *Spodoptera exigua*. *J. Insect Physiol.* 38, 277–285. doi:10.1016/0022-1910(92)90128-Z

Felton, G. W., and Duffey, S. S. (1991). Reassessment of the role of gut alkalinity and detergency in insect herbivory. *J. Chem. Ecol.* 17, 1821–1836. doi:10.1007/BF00993731

Fiesel, A., Ehrmann, M., Gessner, D. K., Most, E., and Eder, K. (2015). Effects of polyphenol-rich plant products from grape or hop as feed supplements on iron, zinc, and copper status in piglets. *Arch. Anim. Nutr.* 69, 276–284. doi:10.1080/1745039X.2015.1057065

Giron, D., Dubreuil, G., Bennett, A., Dedeine, F., Dicke, M., Erb, M., et al. (2018). Promises and challenges in insect-plant interactions. *Entomol. Exp. Appl.* 166, 319–343. doi:10.1111/eea.12679

Grabherr, M. G., Haas, B. J., Yassour, M., Levin, J. Z., Thompson, D. A., Amit, I., et al. (2011). Full-length transcriptome assembly from RNA-Seq data without a reference genome. *Nat. Biotechnol.* 29, 644–652. doi:10.1038/nbt.1883

Grimaldi, D., and Engel, M. S. (2005). *Evolution of the insects*. New York, Melbourne: Cambridge University Press.

Harvey, J. A., Van Dam, N. M., Witjes, L. M., Soler, R., and Gols, R. (2007). Effects of dietary nicotine on the development of an insect herbivore, its parasitoid and secondary

hyperparasitoid over four trophic levels. *Ecol. Entomol.* 32, 15–23. doi:10.1111/j.1365-2311.2006.00838.x

Haslam, E. (2007). Vegetable tannins – lessons of a phytochemical lifetime. *Phytochemy* 68, 2713–2721. doi:10.1016/j.phytochem.2007.09.009

Haukioja, E., Ossipov, V., and Lempa, K. (2002). Interactive effects of leaf maturation and phenolics on consumption and growth of a geometrid moth. *Entomol. Exp. Appl.* 104, 125–136. doi:10.1046/j.1570-7458.2002.00999.x

Hernández-Ortiz, V., Guillén-Aguilar, J., and López, L. (2010). "Taxonomía e identificación de moscas de la fruta de importancia económica en América," in *Moscas de la Fruta: fundamentos y Procedimientos para su Manejo*. Editors P. Montoya, J. Toledo, and E. Hernández (México: S and G), 49–79. D. F.

Hoback, W. W., and Stanley, D. W. (2001). Insects in hypoxia. *J. Insect Physiol.* 47, 533–542. doi:10.1016/S0022-1910(00)00153-0

Jeffries, K. A., Dempsey, D. R., Behari, A. L., Anderson, R. L., and Merkler, D. J. (2014). *Drosophila melanogaster* as a model system to study long-chain fatty acid amide metabolism. *FEBS Lett.* 588, 1596–1602. doi:10.1016/j.febslet.2014.02.051

Karp, P. D., Paley, S. M., Krummenacker, M., Latendresse, M., Dale, J. M., Lee, T. J., et al. (2010). Pathway Tools version 13.0: integrated software for pathway/genome informatics and systems biology. *Brief. Bioinform.* 11, 40–79. doi:10.1093/bib/bbp043

Kassambara, A. (2020). Ggpubr: 'ggplot2' based publication ready plots. R Package Version 0.4.0. Available at: https://CRAN.R-project.org/package=ggpubr.

Kolde, R. (2019). Pheatmap: pretty heatmaps. R Package Version 1.0.12. Available at: https://CRAN.R-project.org/package=pheatmap.

Krueger, F. (2012). Trim Galore: a wrapper tool around Cutadapt and FastQC to consistently apply quality and adapter trimming to FastQ files, with some extra functionality for MspI-digested RRBS-type (Reduced Representation Bisufite-Seq) libraries. Available at: http://www.bioinformatics.babraham.ac.uk/projects/trim_galore/.

Lauter, W. M., and Foote, P. A. (1955). Investigation of the toxic principles of *Hippomane mancinella* L. II. Preliminary isolation of a toxic principle of the fruit. *J. Am. Pharm. Assoc.* 44, 361–363. doi:10.1002/jps.3030440616

Lechner, M., Findeiß, S., Steiner, L., Marz, M., Stadler, P. F., and Prohaska, S. J. (2011). Proteinortho: detection of (co-) orthologs in large-scale analysis. *BMC bioinform* 12, 124–129. doi:10.1186/1471-2105-12-124

Lee, J. R., Urban, S., Garvey, C. F., and Freeman, M. (2001). Regulated intracellular ligand transport and proteolysis control EGF signal activation in *Drosophila*. *Cell* 107, 161–171. doi:10.1016/S0092-8674(01)00526-8

Lemelin, R. H., Harper, R. W., Dampier, J., Bowles, R., and Balika, D. (2016). Humans, insects, and their interaction: a multi-faceted analysis. *Anim. Sci. J.* 5, 65–79. Available at: https://ro.uow.edu.au/asj/vol5/iss1/5.

Li, W., and Godzik, A. (2006). Cd-hit: a fast program for clustering and comparing large sets of protein or nucleotide sequences. *Bioinform* 22, 1658–1659. doi:10.1093/bioinformatics/btl158

Li, X., Schuler, M. A., and Berenbaum, M. R. (2007). Molecular mechanisms of metabolic resistance to synthetic and natural xenobiotics. *Annu. Rev. Entomol.* 52, 231–253. doi:10.1146/annurev.ento.51.110104.151104

Lin, X., and Smagghe, G. (2019). Roles of the insulin signaling pathway in insect development and organ growth. *Peptides* 122, 169923. doi:10.1016/j.peptides.2018.02.001

Liquido, N. J., McQuate, G. T., Suiter, K. A., Norrbom, A. L., Yee, W. L., and Chang, C. L. (2019). "Compendium of fruit fly host plant information. The USDA primary reference in establishing fruit fly regulated host plants," in *Areawide management of fruit fly pests*. Editors D. Pérez-Staples, F. Díaz-Fleischer, P. Montoya, and M. T. Vera (Boca Raton, FL: CRC Press), 363–368.

Love, M. I., Huber, W., and Anders, S. (2014). Moderated estimation of fold change and dispersion for RNA-seq data with DESeq2. *Genome Biol.* 15, 550. doi:10.1186/s13059-014-0550-8

Lu, A., Zhang, Q., Zhang, J., Yang, B., Wu, K., Xie, W., et al. (2014). Insect prophenoloxidase: the view beyond immunity. *Front. Physiol.* 5, 252. doi:10.3389/fphys.2014.00252

Maechler, M., Rousseeuw, P., Struyf, A., Hubert, M., and Hornik, K. (2021). *Cluster analysis basics and extensions*. R Package Version 2.1.2. Available at: https://CRAN.R-project.org/package=cluster.

Margiotta, A. (2022). Membrane fusion and SNAREs: interaction with ras proteins. *Int. J. Mol. Sci.* 23, 8067. doi:10.3390/ijms23158067

Marini, F., and Binder, H. (2019). pcaExplorer: an R/Bioconductor package for interacting with RNA-seq principal components. *BMC Bioinforma.* 20, 331. doi:10.1186/s12859-019-2879-1

Martin, G. G., and Hose, J. E. (1995). "Circulation, the blood and disease," in *Biology of the lobster*, Homarus americanus. Editor J. R. Factor (San Diego: Academic Press), 465–495.

Martin, M. (2011). Cutadapt removes adapter sequences from high-throughput sequencing reads. *EMBnet J.* 17, 10–12. doi:10.14806/ej.17.1.200

McDonald, M., Mila, I., and Scalbert, A. (1996). Precipitation of metal ions by plant polyphenols: optimal conditions and origin of precipitation. *J. Agric. Food Chem.* 44, 599–606. doi:10.1021/jf950459q

McDougall, G. J., and Stewart, D. (2005). The inhibitory effects of berry polyphenols on digestive enzymes. *BioFactors* 23, 189–195. doi:10.1002/biof.5520230403

Mengual, X., Kerr, P., Norrbom, A. L., Barr, N. B., Lewis, M. L., Stapelfeldt, A. M., et al. (2017). Phylogenetic relationships of the tribe Toxotrypanini (Diptera: Tephritidae) based on molecular characters. *Molec. Phyl. Evol.* 113, 84–112. doi:10.1016/j.ympev.2017.05.011

Milton-Bache, S., and Wickham, H. (2020). Magrittr: a forward-pipe operator for R. R package version 2.0.1. Available at: https://CRAN.R-project.org/package=magrittr.

Norrbom, A. L. (2010). "Tephritidae (fruit flies, moscas de Frutas)," in *Manual of central American Diptera*. Editors B. V. Brown, A. Borkent, J. M. Cumming, D. M. Wood, N. E Woodley, and M. A. Zumbado (Ottawa: NRC Research Press), 909–954.

Ochoa-Sánchez, M., Cerqueda-García, D., Moya, A., Ibarra-Laclette, E., Altúzar-Molina, A., Desgarennes, D., et al. (2022). Bitter friends are not always toxic: the loss of acetic acid bacteria and the absence of *Komagataeibacter* in the gut microbiota of the polyphagous fly *Anastrepha ludens* could inhibit its development in *Psidium guajava* in contrast to *A. striata* and *A. fraterculus* that flourish in this host. *Front. Microbiol.* 13, 979817. doi:10.3389/fmicb.2022.979817

Oppert, B., Martynov, A. G., and Elpidina, E. N. (2012). *Bacillus thuringiensis* Cry3Aa protoxin intoxication of *Tenebrio molitor* induces widespread changes in the expression of serine peptidase transcripts. *Comp. Biochem. Physiol. Part D. Genomics Proteomics.* 7, 233–242. doi:10.1016/j.cbd.2012.03.005

Pascacio-Villafán, C., Guillén, L., Williams, T., and Aluja, M. (2018). Effects of larval density and support substrate in liquid diet on productivity and quality of artificially reared *Anastrepha ludens* (Diptera: Tephritidae). *J. Econ. Entomol.* 111, 2281–2287. doi:10.1093/jee/toy221

Pascacio-Villafán, C., Lapointe, S., Williams, T., Sivinski, J., Niedz, R., and Aluja, M. (2014). Mixture-amount design and response surface modeling to assess the effects of flavonoids and phenolic acids on developmental performance of *Anastrepha ludens*. *J. Chem. Ecol.* 40, 297–306. doi:10.1007/s10886-014-0404-6

Pascacio-Villafán, C., Williams, T., Birke, A., and Aluja, M. (2016). Nutritional and non-nutritional food components modulate phenotypic variation but not physiological trade-offs in an insect. *Sci. Rep.* 6, 29413. doi:10.1038/srep29413

Patro, R., Duggal, G., Love, M. I., Irizarry, R. A., and Kingsford, C. (2017). Salmon provides fast and bias-aware quantification of transcript expression. *Nat. Methods.* 14, 417–419. doi:10.1038/nmeth.4197

Perdomo-Morales, R., Montero-Alejo, V., Perera, E., Pardo-Ruiz, Z., and Alonso-Jiménez, E. (2007). Phenoloxidase activity in the hemolymph of the spiny lobster *Panulirus argus*. *Fish. Shellfish Immunol.* 23, 1187–1195. doi:10.1016/j.fsi.2007.04.001

Pryor, M. G. M., Russell, P. B., and Todd, A. R. (1947). Phenolic substances concerned in hardening the insect cuticle. *Nature* 159, 399–400. doi:10.1038/159399a0

Punia, A., Singh Chauhan, N., Kaur, S., and Kaur Sohal, S. (2020). Effect of ellagic acid on the larvae of *Spodoptera litura* (Lepidoptera: Noctuidae) and its parasitoid *Bracon hebetor* (Hymenoptera: braconidae). *J. Asia-Pac. Entomol.* 23, 660–665. doi:10.1016/j.aspen.2020.05.008

Rao, K. V. (1974). Toxic principles of *Hippomane mancinella* I. *Planta Med.* 25, 166–171. doi:10.1055/s-0028-1097927

Rao, K. V. (1977). Toxic principles of *Hippomane mancinella*. II structure of Hippomanin A. *Lloydia*. *Lloydia* 40, 169–172. Available at: https://pubmed.ncbi.nlm.nih.gov/875644/.

R Development Core Team (2021). *R: a language and environment for statistical computing*. Vienna, Austria: R Foundation for Statistical Computing.

Salminen, J. P., and Karonen, M. (2011). Chemical ecology of tannins and other phenolics: we need a change in approach. *Funct. Ecol.* 25, 325–338. doi:10.1111/j.1365-2435.2010.01826.x

Salminen, J. P., Roslin, T., Karonen, M., Sinkkonen, J., Pihlaja, K., and Pulkkinen, P. (2004). Seasonal variation in the content of hydrolyzable tannins, flavonoid glycosides, and proanthocyanidins in oak leaves. *J. Chem. Ecol.* 30, 1693–1711. doi:10.1023/b:joec.0000042396.40756.b7

Schaeffer, H. J., Lauter, W. M., and Foote, P. A. (1954). A preliminary phytochemical study of *Hippomane mancinella* L. *J. Am. Pharm. Assoc.* 43, 43–45. doi:10.1002/jps.3030430115

Schopf, R. (1986). The effect of secondary needle compounds on the development of phytophagous insects. *For. Ecol. Manag.* 15, 55–64. doi:10.1016/0378-1127(86)90089-7

Scudder, G. G. E. (2017). "The importance of insects,". *Insect biodiversity: science and society*. Editors R. G. Foottit and P. H. Adler (Chichester, UK: Wiley-Blackwell), 9–43.

Sharkey, K. A., Darmani, N. A., and Parker, L. A. (2014). Regulation of nausea and vomiting by cannabinoids and the endocannabinoid system. *Eur. J. Pharmacol.* 722, 134–146. doi:10.1016/j.ejphar.2013.09.068

Shu, B., Zou, Y., Yu, H., Zhang, W., Li, X., Cao, L., et al. (2021). Growth inhibition of *Spodoptera frugiperda* larvae by camptothecin correlates with alteration of the structures

and gene expression profiles of the midgut. *BMC Genom* 22, 391–154. doi:10.1186/s12864-021-07726-8

Slowikowski, K. (2021). *ggrepel: automatically position non-overlapping text labels with 'ggplot2*. R package version 0.9.1. Available at: https://CRAN.R-project.org/package=ggrepel.

Soares, T. S., Watanabe, R. M. O., Lemos, F. J. A., and Tanaka, A. S. (2011). Molecular characterization of genes encoding trypsin-like enzymes from *Aedes aegypti* larvae and identification of digestive enzymes. *Gene* 489, 70–75. doi:10.1016/j.gene.2011.08.018

Spalinger, D. E., Collins, W. B., Hanley, T. A., Cassara, N. E., and Carnahan, A. M. (2010). The impact of tannins on protein, dry matter, and energy digestion in moose (*Alces alces*). *Can. J. Zool.* 88, 977–987. doi:10.1139/z10-064

Spit, J., Zels, S., Dillen, S., Holtof, M., Wynant, N., and Vanden Broeck, J. (2014). Effects of different dietary conditions on the expression of trypsin- and chymotrypsin-like protease genes in the digestive system of the Migratory Locust, *Locusta migratoria*. *Insect biochem. Mol. Biol.* 48, 100–109. doi:10.1016/j.ibmb.2014.03.002

Thitz, P., Mehtätalo, L., Välimäki, P., Randriamanana, T., Lännenpää, M., Hagerman, A. E., et al. (2020). Phytochemical shift from condensed tannins to flavonoids in transgenic *Betula pendula* decreases consumption and growth but improves growth efficiency of *Epirrita autumnata* larvae. *J. Chem. Ecol.* 46, 217–231. doi:10.1007/s10886-019-01134-9

Tortoriello, G., Rhodes, B. P., Takacs, S. M., Stuart, J. M., Basnet, A., Raboune, S., et al. (2013). Targeted lipidomics in *Drosophila melanogaster* identifies novel 2-monoacylglycerols and N-acyl amides. *PLoS ONE* 8, e67865. doi:10.1371/journal.pone.0067865

Urban, S. A., Lee, J. R., and Freeman, M. (2002). Family of rhomboid intramembrane proteases activates all *Drosophila* membrane-tethered EGF ligands. *EMBO J.* 21, 4277–4286. doi:10.1093/emboj/cdf434

Wang, L., Zhao, P., Luo, J., Wang, C., Zhu, X., Zhang, L., et al. (2020). Identification and functional analysis of diet-responsive genes in *Spodoptera litura* (Fabricius). *Res. Sq.* doi:10.21203/rs.2.24664/v2

Wei, T., and Simko, V. (2021). *R package 'corrplot': visualization of a correlation matrix (version 0.91)*. Available at: https://github.com/taiyun/corrplot.

Weng, J. K., Philippe, R. N., and Noel, J. P. (2012). The rise of chemodiversity in plants. *Sci* 336, 1667–1670. doi:10.1126/science.1217411

White, I. M., and Elson-Harris, M. M. (1992). *Fruit flies of economic significance: their identification and bionomics*. Wallingford: CAB International.

Wickham, H. (2016). *ggplot2: elegant graphics for data analysis*. New York: Springer-Verlag. Available at: https://github.com/hadley/ggplot2.

Wickham, H., François, R., Henry, L., and Müller, K. (2021). dplyr: a grammar of data manipulation. R Package Version 1.0.7. Available at: https://CRAN.R-project.org/package=dplyr.

Wu, K., Zhang, J., Zhang, Q., Zhu, S., Shao, Q., Clark, K. D., et al. (2015). Plant phenolics are detoxified by prophenoloxidase in the insect gut. *Sci. Rep.* 5, 16823. doi:10.1038/srep16823

Zalucki, M. P., Brower, L. P., and Alonso-M, A. (2001). Detrimental effects of latex and cardiac glycosides on survival and growth of first-instar monarch butterfly larvae *Danaus plexippus* feeding on the sandhill milkweed *Asclepias humistrata*. *Ecol. Entomol.* 26, 212–224. doi:10.1046/j.1365-2311.2001.00313.x

Zhao, P., Xue, H., Zhu, X., Wang, L., Zhang, K., Li, D., et al. (2022). Silencing of cytorome P450 gene CYP321A1 effects tannin detoxification and metabolism in *Spodoptera litura*. *Int. J. Biol. Macromol.* 194, 895–902. doi:10.1016/j.ijbiomac.2021.11.144

Zheng, S., Luo, J., Zhu, X., Gao, X., Hua, H., and Cui, J. (2022). Transcriptomic analysis of salivary gland and proteomic analysis of oral secretion in *Helicoverpa armigera* under cotton plant leaves, gossypol, and tannin stresses. *Genom* 114, 110267. doi:10.1016/j.ygeno.2022.01.004

Zhu-Salzman, K., and Zeng, R. (2015). Insect response to plant defensive protease inhibitors. *Annu. Rev. Entomol.* 60, 233–252. doi:10.1146/annurev-ento-010814-020816

frontiers | Frontiers in Physiology

TYPE Original Research
PUBLISHED 07 February 2024
DOI 10.3389/fphys.2024.1358190

OPEN ACCESS

EDITED BY
Bin Tang,
Hangzhou Normal University, China

REVIEWED BY
Hamzeh Izadi,
Vali-E-Asr University of Rafsanjan, Iran
Annelise Francisco,
Lund University, Sweden

*CORRESPONDENCE
Vladimír Koštál,
kostal@entu.cas.cz

RECEIVED 19 December 2023
ACCEPTED 29 January 2024
PUBLISHED 07 February 2024

CITATION
Štětina T and Koštál V (2024), Extracellular freezing induces a permeability transition in the inner membrane of muscle mitochondria of freeze-sensitive but not freeze-tolerant *Chymomyza costata* larvae.
Front. Physiol. 15:1358190.
doi: 10.3389/fphys.2024.1358190

Extracellular freezing induces a permeability transition in the inner membrane of muscle mitochondria of freeze-sensitive but not freeze-tolerant *Chymomyza costata* larvae

Tomáš Štětina and Vladimír Koštál*

Institute of Entomology, Biology Centre of the Czech Academy of Sciences, České Budějovice, Czechia

Background: Many insect species have evolved the ability to survive extracellular freezing. The search for the underlying principles of their natural freeze tolerance remains hampered by our poor understanding of the mechanistic nature of freezing damage itself.

Objectives: Here, in search of potential primary cellular targets of freezing damage, we compared mitochondrial responses (changes in morphology and physical integrity, respiratory chain protein functionality, and mitochondrial inner membrane (IMM) permeability) in freeze-sensitive vs. freeze-tolerant phenotypes of the larvae of the drosophilid fly, *Chymomyza costata*.

Methods: Larvae were exposed to freezing stress at −30°C for 1 h, which is invariably lethal for the freeze-sensitive phenotype but readily survived by the freeze-tolerant phenotype. Immediately after melting, the metabolic activity of muscle cells was assessed by the Alamar Blue assay, the morphology of muscle mitochondria was examined by transmission electron microscopy, and the functionality of the oxidative phosphorylation system was measured by Oxygraph-2K microrespirometry.

Results: The muscle mitochondria of freeze-tolerant phenotype larvae remained morphologically and functionally intact after freezing stress. In contrast, most mitochondria of the freeze-sensitive phenotype were swollen, their matrix was diluted and enlarged in volume, and the structure of the IMM cristae was lost. Despite this morphological damage, the electron transfer chain proteins remained partially functional in lethally frozen larvae, still exhibiting strong responses to specific respiratory substrates and transferring electrons to oxygen. However, the coupling of electron transfer to ATP synthesis was severely impaired. Based on these results, we formulated a hypothesis linking the observed mitochondrial swelling to a sudden loss of barrier function of the IMM.

KEYWORDS

insects, freeze tolerance, mitochondrial swelling, permeability transition, respiration, oxidative phosphorylation

Introduction

Freezing of body water is lethal for most organisms, but some plants and ectotherms have evolved the ability to survive internal ice formation (i.e., freeze tolerance) (Storey and Storey, 1988; Pearce, 2001). Freeze tolerance is particularly widespread in insects (Asahina, 1970; Sinclair, 1999; Lee, 2010). Ice forms extracellularly in freeze-tolerant organisms, whereas ice formation within their cells is considered lethal (for exceptions, see (Sinclair and Renault, 2010)). Extracellular freezing is an extraordinarily challenging environmental stressor because it combines the deleterious effects of cold, loss of liquid water, elevated osmolality, increased concentrations of protons, calcium, metal ions, and other toxic compounds, anoxia and ischemia, cell shrinkage, mechanical stress, and increased packing of cellular components (Mazur, 1984; Muldrew et al., 2004). The high complexity of freezing stress is an obstacle to experimentation because the hierarchy and importance of individual effects of different stressors on different targets (macromolecules, cellular structures, and processes) are difficult to distinguish. Although considerable knowledge has accumulated over decades, we are still far from an integrative understanding of how cells of naturally freeze-tolerant animals cope with the enormous complexity of freezing stress (Storey and Storey, 2013; Storey and Storey, 2017; Toxopeus and Sinclair, 2018; Teets et al., 2023). Here, we contribute by analyzing the effects of extracellular freezing stress on muscle mitochondrial morphology and function in freeze-sensitive vs. freeze-tolerant phenotypes of naturally freeze-tolerant insects.

Our understanding of how mitochondria in temperate and polar insects adapt to the winter season is still limited (Lubawy et al., 2022; Lebenzon et al., 2023). Overwintering insects are exposed to low ambient temperatures and often spend the winter in diapause—a state of developmental arrest, behavioral inactivity, and deep metabolic suppression (Koštál, 2006; Teets et al., 2023). The relatively low demand for energy turnover, on the one hand, and the high cost of maintaining active mitochondria, on the other hand, led to the evolution of seasonal mitochondrial degradation as an ultimate strategy in some insects. However, such a strategy appears to be exceptional in insects that predictably spend many months of each winter in deep dormancy, such as caterpillars of the moth *Gynaephora groenlandica* that overwinter near the permafrost in Greenland (Kukal et al., 1989; Levin et al., 2003). Some insects, such as the Colorado potato beetle, *Leptinotarsa decemlineata*, at least degrade populations of mitochondria in their seasonally histolyzed flight muscles because the wings are useless in winter (Lebenzon et al., 2022). However, most overwintering insects maintain fully coupled mitochondria capable of oxidizing various substrates throughout the winter. In such insects: 1) the activities of some mitochondrial enzymes may be slightly reduced, as in diapausing larvae of the gall fly *Eurosta solidaginis* and the gall moth *Epiblema scudderiana*, (Ballantyne and Storey, 1985; Joanisse and Storey, 1994; McMullen and Storey, 2008); 2) the relative utilization of different substrates by mitochondrial respiratory complexes may shift, as in cold-acclimated drosophilid flies (Jørgensen et al., 2023); and/or 3) the expression of transcripts encoding the subunits of respiratory complexes may be reduced, as in the cricket *Gryllus veletis* (Toxopeus et al., 2019). Working with the drosophilid fly, *Chymomyza costata*, we showed that winter phenotype larvae (diapausing, cold acclimated) also maintain a high number of fully functional mitochondria in their fat body cells and can effectively protect them from all the deleterious effects associated with extracellular freezing and cryopreservation in liquid nitrogen (Rozsypal et al., 2018; Štětina et al., 2020).

Mitochondria are organelles that remarkably integrate life-sustaining functions and death-promoting activities in eukaryotic cells. Mitochondria are central to cellular energy supply and metabolic transformations, but they also sense changes in the cellular environment and can respond to various physiological imbalances or environmental stressors by inducing cell death pathways (Newmeyer and Ferguson-Miller, 2003; Nunnari and Suomalainen, 2012; Abate et al., 2020; Modesti et al., 2021). It has been hypothesized that the maintenance of mitochondrial integrity and function, while avoiding the induction of death pathways, may be critical for cellular homeostasis and consequently for the survival of the whole organism in ectothermic animals exposed to thermal extremes (Camus et al., 2017; Sokolova, 2018; Chung and Schulte, 2020; Lubawy et al., 2022). Indeed, the experimental evidence available for insects shows that mitochondrial function and integrity are critically affected by cold and freezing stress. For example, data from the vinegar fly *Drosophila melanogaster* show that mitochondrial failure to produce ATP coincides with increased mortality in warm-acclimated flies exposed to chronic cold stress at 4°C for 3 days. Cold-acclimated flies were able to avert both mitochondrial failure and mortality (Colinet et al., 2017). When adult tropical cockroaches *Gromphadorina cocquereliana* were exposed to acute cold shock at 4°C for 3 h, significant changes in respiratory activity, ROS production, and activation of defense systems were detected in their muscle and fat body mitochondria (Chowański et al., 2017). When cockroaches were repeatedly exposed to the same stress for 3 days, an acclimation response was observed as the perturbed mitochondrial parameters returned to homeostasis (Lubawy et al., 2023). We have shown that lethal (but not sublethal) freezing stress applied to summer phenotype (active, warm acclimated) larvae of *C. costata* causes significant swelling of fat body and hindgut mitochondria, resulting in partial loss of tissue respiratory capacity (Štětina et al., 2020). Similar mitochondrial swelling was also observed in mitochondria of Malpighian tubules in lethally frozen larvae of the gall fly, *E. solidaginis* (Collins et al., 1997).

Here, we followed up on our previous observations and compared muscle mitochondrial responses to freezing stress in two contrasting seasonal phenotypes of *C. costata* larvae. The relatively freeze-sensitive (LD, active, warm acclimated, summer phenotype) and freeze-tolerant (SDA, diapause, cold acclimated, winter phenotype) larvae were exposed to freezing stress at −30°C for 1 h, which is lethal for LD larvae but readily survived by SDA larvae (see Materials and Methods for further explanation of LD and SDA abbreviations). We sought answers to the following specific questions: Do muscle mitochondria change their morphology and integrity during freezing stress? Does freezing stress affect the functionality of respiratory complexes in the inner mitochondrial membrane (IMM)? Does freezing stress affect the oxygen consumption capacity and the coupling of the oxidative phosphorylation system (OXPHOS)? Are there differences in

mitochondrial responses to freezing stress between LD and SDA larvae? Answers to these questions may improve our understanding of the mechanisms of freezing injury in *C. costata* larvae. From a broader perspective, our results can contribute to the search for integrative models [sensu (MacMillan, 2019)] of freezing injury and its prevention/repair in naturally freeze-tolerant insects and ectotherms.

Materials and methods

Insects, acclimations, phenotypes, and tissue dissection

A colony of *C. costata*, Sapporo strain (Riihimaa and Kimura, 1988), was reared on artificial diet in MIR 154 incubators (Sanyo Electric, Osaka, Japan) as described previously (Koštál et al., 1998). This study is based on comparative analysis of muscle mitochondrial responses to freezing stress in two phenotype/acclimation variants of *C. costata* larvae. Two phenotype/acclimation variants with contrasting freeze tolerance were generated according to our earlier acclimation protocols (Rozsypal et al., 2018; Grgac et al., 2022; Kučera et al., 2022): 1) active, warm-acclimated (summer phenotype) → freeze-sensitive larvae (abbreviated as LD in earlier papers); 2) diapause, cold-acclimated (winter phenotype) → freeze-tolerant larvae (abbreviated as SDA in earlier papers). Briefly, the LD larvae were reared from eggs to 3rd larval instars (age of 3 weeks) at 18°C under long-day photoperiod (LD, 16 h light:8 h dark), which promotes direct non-diapause development to pupa and adult. The SDA larvae were reared until age of 6 weeks at 18°C under short-day photoperiod (SD, 12 h light:12 h dark)—which induces larval diapause—and were then transferred to constant darkness and progressively cold acclimated over 5 weeks (SDA, 1 week at 11°C, followed by 4 weeks at 4°C). The LD larvae of *C. costata* have limited survival after freezing stress (35% survive slow inoculative extracellular freezing to −5°C, 10% survive to −10°C, and none survive freezing to −20°C or below). In contrast, practically all SDA larvae survive freezing to −30°C or even −75°C, and 42.5% survive and metamorphose into fit adults after 18 months of cryopreservation in liquid nitrogen (Rozsypal et al., 2018).

The larval muscles form a dense three-dimensional system of longitudinal and dorsoventral muscles below the body wall (Wiplfler et al., 2013). We dissected the larvae under binocular microscope and ensured that approximately 90% of the total larval body wall muscle volume was taken from each dissected larva. The larvae were dissected in different buffers for different purposes: 1) for transmission electron microscopy (TEM): in ice-cold phosphate-buffered saline (PBS: 137 mM NaCl, 3 mM KCl, 10.1 mM Na_2HPO_4, and 1.8 mM KH_2PO_4, pH 7.2); 2) for citrate synthase activity assay: in Tris-sucrose buffer (50 mM Tris-HCl, 200 mM sucrose, 1 mM EDTA, 0.1% Triton-X 100, pH 8.0); 3) for Alamar Blue assays and for Oxygraph-2K respirometry: in Schneider's insect medium (Biosera, Nuaillé, France). The dissection of single larva took less than 1 min.

Freezing stress

Whole larvae were exposed to slow inoculative freezing to −30°C using the protocol described earlier (Rozsypal et al., 2018). The protocol consisted of five steps set in a Ministat 240 programmable cryostat (Huber, Offenburg, Germany): 1) 20 min of larval manipulation at 0°C (washing larvae out of the diet, dividing into groups of 20 specimens, and placing them into 3 mL plastic tubes between two layers of moist cellulose); 2) slow freezing to −30°C (with a small ice crystal added on top of the moist cellulose) for 300 min (cooling rate, 0.1°C min^{-1}); 3) keeping larvae at −30°C for 60 min; 4) heating from −30°C to +5°C over 60 min (heating rate, 0.6°C min^{-1}); and 5) keeping at constant +5°C for 10 min to allow complete melting of ice. Adding a small ice crystal at the beginning of step (2) induces inoculative internal freezing in larvae, which starts between −1°C and −3°C and results in freezing of 76% or 68% of total body in LD or SDA larvae, respectively (Rozsypal et al., 2018). This freezing stress is invariably lethal for LD larvae while it is survived by SDA larvae in rates similar to unfrozen controls.

Transmission electron microscopy

The TEM was conducted as described earlier (Des Marteaux et al., 2018; Štětina et al., 2020). Briefly, the larval muscles were dissected in PBS right upon melting—at the end of step (5) of the freezing protocol (control larvae were not frozen). The muscles were fixed overnight in PBS containing 2.5% glutaraldehyde. After washing in PBS, we continued in fixation using 2% OsO_4 (EMS, Hatfield, Pennsylvania) for 2 h, washing in PBS, dehydration in grading acetone solutions (from 30% to 100%), and embedding into resin Embed-812 (EMS). The resin was polymerized at 60°C/24 h and the blocks were sectioned using an ultra-microtome Leica UC6 (Leica microsystems GmbH, Wetzlar, Germany) equipped with DiATOME diamond knife (EMS). The ultra-thin sections (70 nm) were placed on 300-mesh-Cu grids and counter-stained with saturated ethanolic uranyl acetate for 30 min, followed by lead citrate for 20 min. The grids with sections were then coated by carbon film using JEOL JE 4C coater (JEOL, Tokio, Japan), and micrographs were taken by a transmission electron microscope JEOL JEM—1010 1 (JEOL, Tokio, Japan).

Morphology of muscle mitochondria

Based on our earlier study, we focused on mitochondrial swelling as this was the most characteristic response to freezing stress in fat body and hindgut mitochondria of *C. costata* larvae (Štětina et al., 2020). We distinguished three morphological categories 1) normal size, shape, and presence of cristae; 2) transitional (slightly enlarged, rounded, cristae invisible, matrix still containing the electron-dense material); and 3) swollen (large, rounded, OMM sometimes discontinuous—bursting, internal structure lost, matrix showing little or no electron dense material). The examples of mitochondrial morphology scoring are shown in Supplementary Figure S1.

Muscles dissected from five larvae (each larva considered as a biological replicate) of each combination of phenotype/acclimation variant and freezing treatment were collected for TEM analysis. We selected approximately 20 representative TEM micrographs (magnification of ×25,000), taken at different locations of the ultra-thin section, in order to collect morphology scores for several hundred

mitochondria in every single larva (the exact numbers are shown in Supplementary Tables). In total, we scored the morphology of 6,291 muscle mitochondria. A gallery containing all micrographs and scores is available in figshare: https://figshare.com/articles/figure/Gallery_of_mitochondria_pdf/24961422.

Citrate synthase activity

Muscle tissues dissected from 3 × 10 larvae (3 biological replicates, 10 larvae pooled for each replicate) of each combination of phenotype/acclimation variant and freezing treatment were collected for citrate synthase activity assay. The tissue samples were homogenized in 600 µL of the Tris-sucrose buffer using metal-blade homogenizer X 120 (Ingenieurbüro CAT M. Zipperer, Germany) followed by sonication using 4710 Series Ultrasonic Homogenizer (Cole Parmer, Chicago, IL, United States). After the incubation of homogenate for 10 min at 0°C, the samples were centrifuged at 22,000 *g*/10 min/4°C, and the supernatants were used as the source of enzyme. All activity assays were run at constant 25°C. The composition of standard reaction mixture for CS assay was similar as described earlier (Štětina et al., 2020; Grgac et al., 2022): 20 mM imidazole-HCl buffer, pH 7.2; 0.05 mM DTNB reagent (5,5′-dithiobis-2-nitrobenzoic acid); 0.15 mM acetyl CoA; 0.25 mM oxaloacetate. The reaction was initiated by the addition of 25 µL of oxaloacetate solution into 475 µL of reaction mixture and the mercaptid ion formation from CoA-SH (that was released upon synthesis of citrate) was followed by measuring the increase of 412 nm absorbance (DTNB → TNB). The total proteins were measured by bicinchoninic acid assay according to Smith et al. (1985).

Alamar Blue assay of metabolic activity of muscle cells

The alamarBlue™ HS (Invitrogen, Thermo Fisher Scientific, Waltham, Massachusetts, United States) is a cell-viability assay based on a principle that the innate metabolic activity of living cells maintain reducing conditions that result in a chemical reduction of resazurin to resorufin (Alamar Blue reagent), which is accompanied with the change of color that can be measured spectrometrically (Supplementary Figure S2B). The oxidation-reduction potential of the Alamar Blue reagent is intermediate between the final reduction of O_2 and cytochrome *c* oxidase, and Alamar Blue can thus be used as a proxy metabolic indicator of the mitochondrial electron transfer chain activity (Braut-Boucher and Aubery, 2017). However, in addition to mitochondrial reductases, the Alamar Blue reagent is reduced by several other enzymes (Rampersad, 2012), so we conservatively interpret the Alamar Blue reagent reduction as an indicator of cellular metabolic activity.

Muscle tissues dissected from 3 × 5 larvae (3 biological replicates, 5 larvae pooled for each replicate) of each combination of phenotype/acclimation variant and freezing treatment were collected for metabolic activity assay. The tissues were transferred into 200 µL of Schneider's medium in the wells of 96-well EIA/RIA polystyrene plate (Corning, NY, United States). The 10 µL of Alamar Blue reagent was added into each well, mixed, and the plates were incubated at constant 18°C for 6 hours. The metabolic activity was inferred based on gradual color change of the assay from blue to pink. The change of color was recorded by photographing using cell phone and standardized lighting conditions in dark chamber. At the end of assay, at a time of 360 min, the absorbances at 600 nm and 570 nm (resazurin and resorufin, respectively) were taken. In addition, we ran Alamar Blue assays in: 1) blanks (assays without tissue samples); and 2) muscles of LD larvae exposed to heat shocks of 45°C or 65°C for 1 h (both heat shocks are invariably lethal for LD larvae).

Oxygraph-2K respirometry of the OXPHOS complexes I and II

Muscle tissues dissected from 3 × 20 larvae (3 biological replicates, 20 larvae pooled for each replicate, which corresponds to approximately 1–2 mg of tissue in each replicate) of each combination of phenotype/acclimation variant and freezing treatment were collected for microrespirometry using the Oxygraph-2K respirometer (Oroboros Instruments, Innsbruck, Austria). We measured oxygen consumption in permeabilized muscle tissue, which preserves intact mitochondria well integrated into the cellular system and, therefore, provides physiologically relevant insight into mitochondrial function (Kuznetsov et al., 2008). Our experimental approaches were designed basically according to principles described earlier (Pichaud et al., 2013; McDonald et al., 2018; Simard et al., 2018). The dissected muscles were washed 3 times in 1 mL of respiration buffer (115 mM KCl, 10 mM KH_2PO_4, 2 mM $MgCl_2$, 3 mM HEPES, 1 mM EGTA, 0.2% BSA, pH 7.2) and then transferred to 2 mL of respiration buffer in the Oxygraph-2K chamber. All microrespirometry assays were run at constant 25°C. The tissue was permeabilized by 55 µM or 30 µM digitonin for LD and SDA acclimation variants, respectively (see Supplementary Figure S2C for explanation) and the oxygen consumption rates representing the basal respiration prior to adding substrates was taken (this respiration was likely supported by substrates present endogenously in dissected muscle cells). Then, the specific substrates for complexes I and II were added, which stimulated the mitochondrial oxygen flux. In the absence of ADP, this flux mainly represents the compensation of the proton leak (i.e., LEAK state respiration rate). However, since we cannot exclude the possibility that some tissue-endogenous ADP contributed to the oxygen consumption rate, we will refer to this oxygen flux as the substrate-stimulated (SS) oxygen flux. Finally, exogenous ADP was added to further stimulate oxygen consumption and the OXPHOS state respiration rate was estimated (the mitochondrial oxygen flux corresponding to electron transfer chain coupled to phosphorylation and ATP production by complex V, ATP synthase).

The oxygen consumption rates after each addition were estimated when the signal stabilized and were expressed as pmol O_2/(s.10 muscles)$^{-1}$. It was technically difficult to either weight the fresh mass of larval muscle tissue prior to analysis, or quantitatively recover the muscle tissue from respiration vials after the analysis (to measure total protein). Therefore, we normalized the data to 10 muscle tissues which corresponds directly to the reading of Oxygraph-2K [O_2/(s.mL)$^{-1}$], where the total volume is 2 mL and

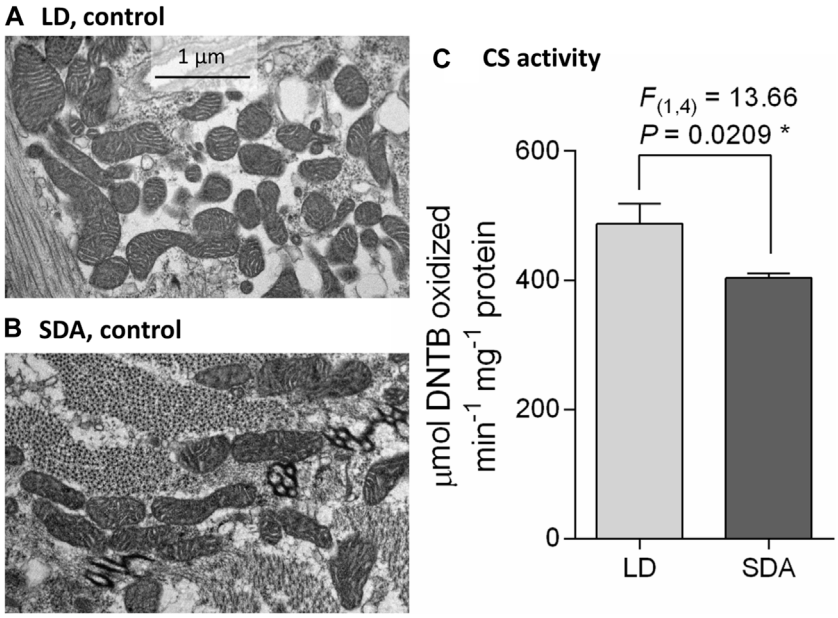

FIGURE 1
Larval muscle mitochondria are morphologically similar in two acclimation variants of *Chymomyza costata*. The transmission electron micrographs taken at a magnification of ×25,000 show examples of typical muscle mitochondria in control (unfrozen) larvae of two phenotypes: **(A)** LD, freeze sensitive; and **(B)** SDA, freeze tolerant. More examples are presented in Supplementary Figure S3, and a gallery containing all micrographs is available in figshare. **(C)** Mean citrate synthase (CS) activity in SDA muscles was 83% of that in LD muscles. Each column shows mean ± SD (n = 3, each replicate is a pool of 10 dissected larval muscle tissues). The difference between LD and SDA larvae was analyzed using ANOVA model (*p < 0.05, significantly different).

20 tissues were pooled. We believe that this normalization is sufficient for comparative purposes. The order of additions was as follows (the concentrations in brackets are the final concentrations in respiration buffer): complex I, 1) the substrates pyruvate (10 mM) and malate (2 mM); 2) the ADP (2.5 mM) to couple the OXPHOS; and rotenone (1 µg.m^{-1}) to inhibit the activity of complex I. Complex II, 1) rotenone (1 µg.m^{-1}) to block the recurrent electron flow to complex I; 2) the substrate succinate (10 mM); 3) ADP (2.5 mM); and 4) KCN (5 mM) to inhibit the whole electron transfer chain by blocking the Complex IV (cytochrome *c* oxidase). The basal, SS, and OXPHOS oxygen consumption rates were used to calculate two parameters separately for complexes I and II: 1) the substrate contribution ratio, SCR = (SS—basal)/basal; and 2) the OXPHOS coupling efficiency = 1—(SS/OXPHOS) (Menail et al., 2022). See Supplementary Figure S2A for schematic depiction of our experimental approaches to the analysis of activity of different complexes of the OXPHOS residing in the inner mitochondrial membrane.

Statistics

Statistical analyses were performed with generalized linear models (GLM) and with linear ANOVA models followed by Tukey's *post hoc* multiple comparison tests when the ANOVA was significant. To respect the assumptions of parametric ANOVA model, the normality of model residuals was checked with Shapiro-Wilk test and the homoscedasticity with the Bartlett test. When the assumptions of parametric model were not met, data were log-transformed. If neither log-transformation have satisfied the assumptions of parametric model, we used the test with rank-transformed response variables. All analyses were performed with the R software version 4.3.2 (R Core Team, 2023), multiple comparisons with the multcomp package (Hothorn et al., 2008). We provide the raw data used for statistical analyses in the Supplementary Tables.

Results

Muscle mitochondria are morphologically similar in LD and SDA control larvae

Mitochondria in the larval muscles of control (unfrozen) larvae were of broadly similar morphology (Figures 1A, B), although the shape of individual mitochondria was highly variable, ranging from spherical to rod-shaped and elongated (see Supplementary Figure S3 for diversity of mitochondrial morphology; a gallery containing all micrographs and scores is available in figshare). On transverse section, the diameter of individual mitochondria did not exceed 1 µm and their length did not exceed 3 µm. The cristae of the inner membrane were well developed. Such mitochondria were classified as "normal" (category 1) (Supplementary Figure S1). There was no apparent difference in mitochondrial number between acclimation variants LD and SDA. However, the citrate synthase activity

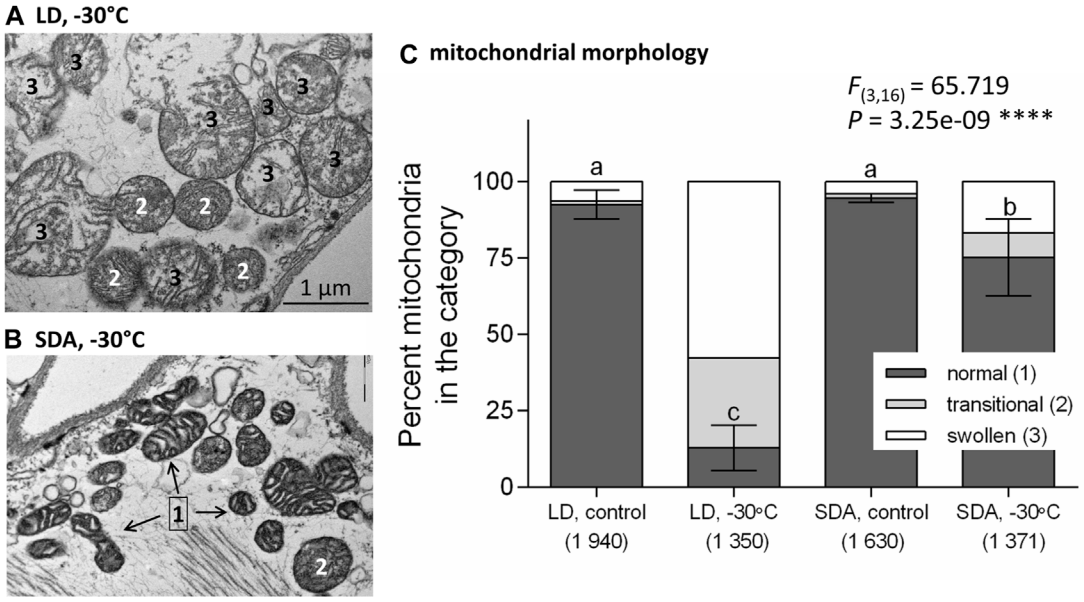

FIGURE 2
Morphological responses of larval muscle mitochondria to freezing stress differed in two acclimation variants of *Chymomyza costata*. The larvae were exposed to slow inoculative freezing to −30°C, which is lethal to freeze-sensitive LD larvae but survived by freeze-tolerant SDA larvae. The muscle tissues were dissected from five larvae of each experimental variant: a combination of acclimation, LD vs. SDA, and treatment. The transmission electron micrographs taken at a magnification of ×25,000 show examples of **(A)** swollen mitochondria in LD larvae in contrast to **(B)** morphologically normal mitochondria of SDA larvae. More examples are presented in Supplementary Figure S4, and a gallery containing all micrographs is available in figshare. **(C)** The relative proportions of mitochondria with morphology classified as normal (1), transitional (2), and swollen (3) (see Supplementary Figure S1 for a classification scale). Each stacked column shows mean proportions of three morphological classes. The variation (±SD) is shown for "normal" class only (n = 5, single larva was taken as an independent replicate, and total numbers of mitochondria classified in each experimental variant are shown in parentheses). Statistical analysis using ANOVA model followed by Tukey's multiple comparisons test was performed for proportions of "normal" mitochondria only, as the proportion of "damaged" mitochondria (transitional + swollen) is only a complement to 100%. Stars represent statistical differences (****p < 0.0001). Columns flanked by different letters are statistically different.

normalized to total protein (a proxy for mitochondrial number) in SDA larval muscles was only 83% of that in LD larval muscles (Figure 1C).

LD mitochondria swell while SDA mitochondria remain intact after freezing stress

Upon freezing stress, most LD mitochondria responded with a characteristic swelling (Figure 2A, see also Supplementary Figure S4A for more examples of swollen mitochondria). The shape became predominantly rounded, the diameter increased to more than 1 µm. The "empty" spaces (loss of electron-dense material) occurred in the mitochondrial matrix, and the structure of the cristae was partially or completely lost. Some mitochondria had discontinuous outer membrane and looked like burst. Such mitochondria were classified as transitional (2) or swollen (3) (Supplementary Figure S1).

In contrast, many SDA mitochondria retained their normal morphology after freezing stress and were classified as category (1) (Figure 2B; Supplementary Figure S4B). Statistical analysis revealed highly significant effect of freezing stress on morphology of mitochondria. While the relative proportion of damaged morphologies (transitional + swollen) increased with freezing stress, the relative proportion of normal morphologies decreased from 92.4% before stress to 12.6% after stress in LD mitochondria, while it decreased much less, from 94.8% to 72.7%, in SDA mitochondria (Figure 2C).

Muscle mitochondria are functionally similar in LD and SDA larvae but respond differently to freezing stress

The results of the Alamar Blue assays, summarized in Figure 3, suggest that the innate metabolic activity of LD muscle cells persists, at least in part, after the organism is killed by freezing or even heat stress. No or little metabolic activity (i.e., no or little change in the color of the assay over 6 h) was observed only in the blanks (no tissue in the assay) and in the muscles of larvae killed by heating to 65°C. Muscles from LD larvae killed by either heating to 45°C or freezing to −30°C still showed clear metabolic activity, as indicated by a change in the color of the assay from blue to pink. Calculation of the ratio of light absorbance at 600/670 nm at 360 min allowed relative quantification of the color change and suggested that the metabolic activity was significantly reduced (but not arrested) by freezing stress in LD muscles compared to either control LD muscles or control and frozen SDA muscles (SDA larvae readily survive freezing stress).

The basal respiration rates of digitonin-permeabilized muscle tissue prior to addition of substrates for complexes I or II were practically equal in the LD and SDA control muscles [10.8 pmol O_2/

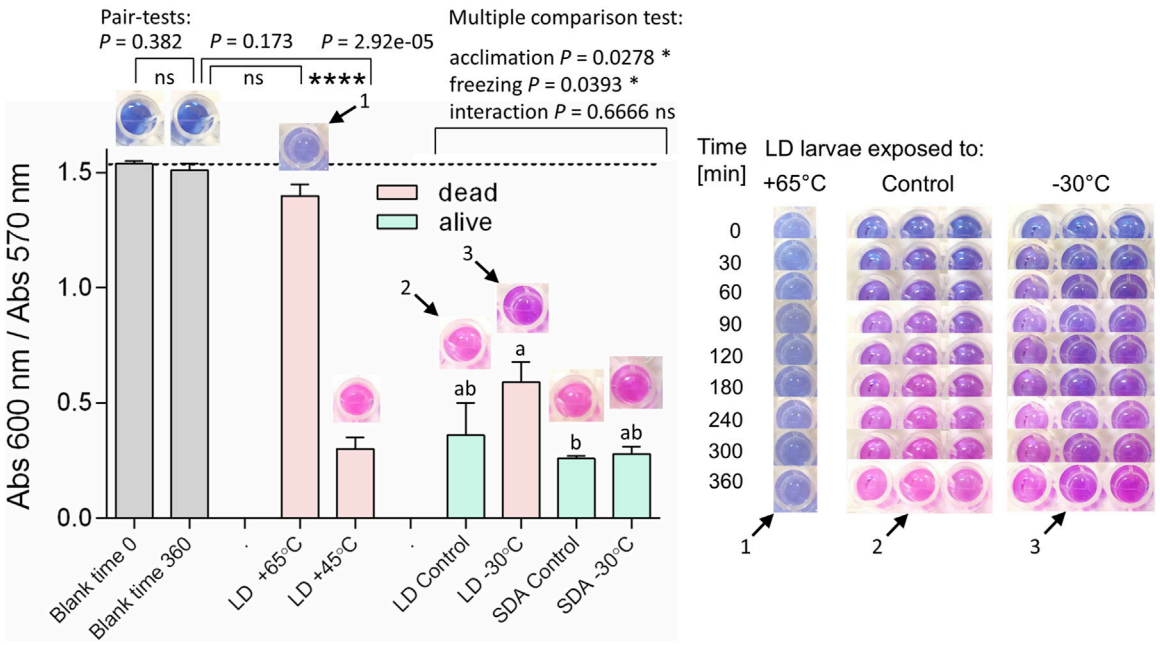

FIGURE 3
The metabolic activity persisted in larval muscle cells of *Chymomyza costata* after the lethal freezing stress. Each column shows mean ± SD (n = 3, each replicate is a pool of five dissected larval muscle tissues) ratio of Alamar Blue assay absorbance at 600/570 nm taken at the incubation time of 360 min (see text and Supplementary Figure S2B for explanations). Abbreviations: LD, freeze-sensitive larvae, SDA, freeze-tolerant larvae. The photographs above each column show examples of the color of Alamar Blue assay after 360 min. The set of photographs on the right show examples of gradual change in color of the Alamar Blue assay from blue (600 nm) to pink (570 nm) over the incubation time in select treatments (single replicate of the LD larvae exposed to heat shock at 65°C; all three replicates of LD control; all three replicates of LD frozen at −30°C). No color change with time of incubation (meaning no metabolic activity) was observed in blank assays (no tissue); minimum change in color was also seen in the assays containing muscle tissue dissected from larvae killed by heating to 65°C; the larvae killed by heating to 45°C, however, still showed a change in color. Similarly, the freeze-sensitive LD larvae killed by freezing stress still showed a significant change in color (meaning some metabolic activity), though this change was slightly slower than the change in color in the assays of control (unfrozen) LD or SDA larvae or frozen SDA larvae (which readily survive the freezing stress). The differences between blanks and heat-stressed LD larvae were statistically analyzed using ANOVA models (see clamps for compared pairs). In order to apply two-way ANOVA model followed by Tukey's multiple comparisons to analyze differences among control and frozen larvae, the rank-transformed response variables were used. Stars represent statistical differences (*$p < 0.05$; ****$p < 0.001$; ns, not significant). Columns flanked by different letters are statistically different.

(s.10 muscles)$^{-1}$] (Figure 4A). In response to freezing stress, the basal respiration rate decreased to 6.1 pmol O_2/(s.10 muscles)$^{-1}$ in the LD muscles, while it marginally increased to 12.8 pmol O_2/(s.10 muscles)$^{-1}$ in the SDA muscles (none of these changes, however, was statistically significant). The substrate contribution ratios were much lower for pyruvate and malate (ranging from 1.1 to 2.1, Figure 4B) than for succinate (ranging from 11.1 to 15.1, Figure 4C). Statistical analysis revealed no significant effects of larval acclimation (LD vs. SDA) or freezing (control vs. −30°C) on the response of complexes I and II to their substrates.

Oxygen consumption rates supported by complex I activity (Figure 5, see Supplementary Figure S5 for examples of original Oxygraph-2K traces of oxygen concentration and flux) decreased significantly after freezing stress in LD larvae (Figure 5A). This decrease in oxygen consumption rate was expressed in all steps of the respirometric analysis, from basal rates, to SS respiration energized by the substrates pyruvate and malate, to OXPHOS respiration of ADP-stimulated mitochondria. In contrast, the rates of oxygen consumption associated with complex I activity were virtually unaffected by freezing stress in SDA larvae (Figure 5B). The response of complex II to freezing stress was generally similar to that of complex I, i.e., the rates of oxygen consumption decreased significantly after freezing stress in LD larvae, whereas the rates remained unchanged after freezing stress in SDA larvae (Supplementary Figures S6, S7). The coupling efficiencies calculated for complexes I and II considerably decreased in response to freezing stress in LD muscles, whereas they remained practically unchanged in SDA muscles (Figure 6).

Discussion

Here we show that switching *C. costata* phenotypes from an active, warm acclimated larva (LD, summer phenotype, freezing sensitive) to a diapausing, cold acclimated larva (SDA, winter phenotype, freezing tolerant) has relatively little effect on muscle mitochondrial numbers, morphology, functionality of OXPHOS complexes, and oxygen consumption (measured at constant 25°C). In contrast, the responses of LD and SDA muscle mitochondria to freezing stress at −30°C were drastically different: while SDA mitochondria remained morphologically and functionally intact, LD mitochondria swelled and became partially dysfunctional. These results confirm and extend our

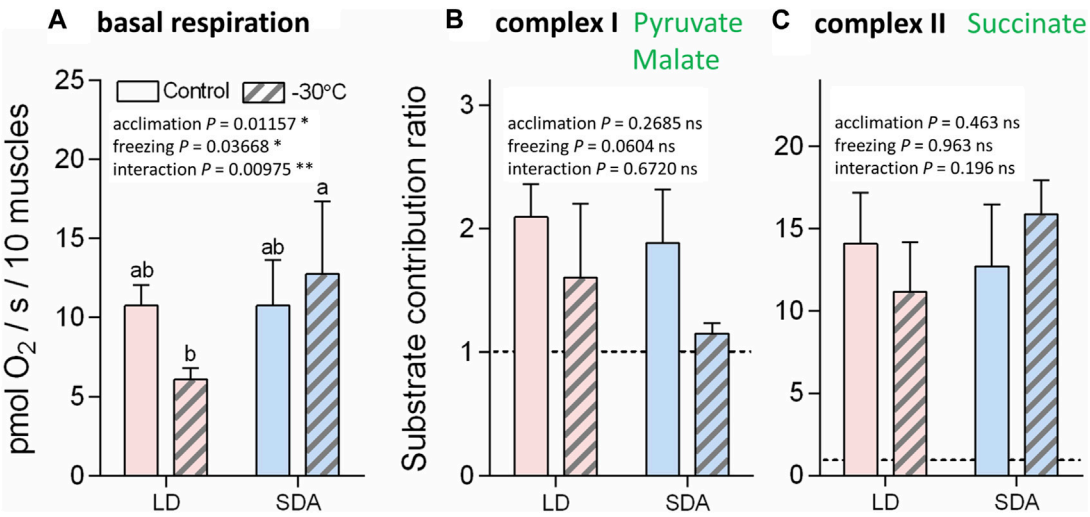

FIGURE 4
The basal respiration rates and substrate contribution ratios of larval muscle mitochondria prior to and after freezing stress in two acclimation variants of *Chymomyza costata*. The freeze-sensitive (LD) and freeze-tolerant (SDA) larvae were exposed to slow inoculative freezing to −30°C. The muscle tissues were dissected right after the freezing stress (or taken from control-unfrozen larvae), permeabilized using digitonin, and the oxygen consumption rates were measured using Oxygraph-2K respirometer prior to addition of any substrates to measure **(A)** the basal respiration. Next, substrates for complex I **(B)** and complex II **(C)** were added and the corresponding increase of oxygen consumption rate was expressed as substrate contribution ratio (SCR, see text for explanation). Each column shows mean ± SD [n = 6 in **(A)** or n = 3 in **(B,C)**, each replicate is a pool of 20 dissected larval muscle tissues]. The differences were statistically analyzed using two-way ANOVA model followed by Tukeys's multiple comparisons test. Stars represent statistical differences (*p < 0.05; **p < 0.01; ns, not significant). Columns flanked by different letters are statistically different. In case of basal respiration **(A)**, the rank-transformed response variables were used.

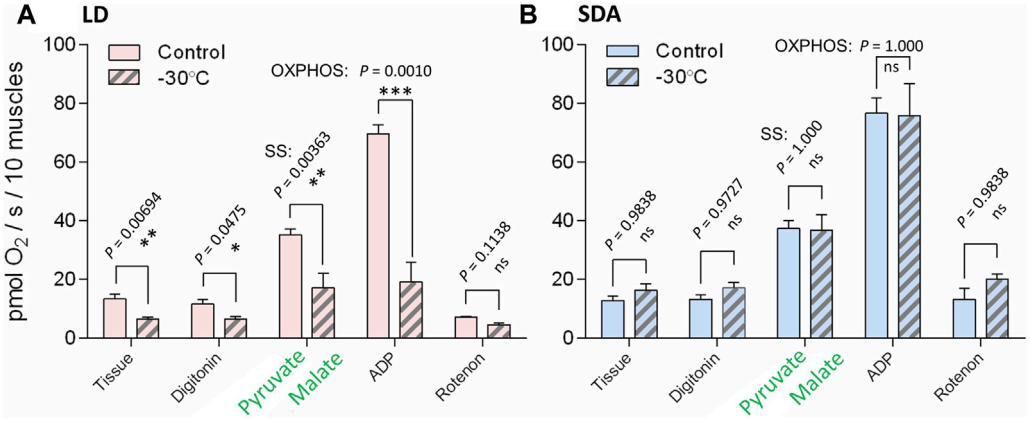

FIGURE 5
The respiration rates linked to activity of complex I were significantly reduced after the freezing stress in the muscles of freeze-sensitive larvae of *Chymomyza costata*. The freeze-sensitive (**A**, LD) and freeze-tolerant (**B**, SDA) larvae were exposed to slow inoculative freezing to −30°C. The muscle tissues were dissected right after the freezing stress (or taken from control-unfrozen larvae), permeabilized using digitonin, and the oxygen consumption rates were measured using Oxygraph-2K respirometer after adding pyruvate and malate—specific substrates for complex I (substrate-stimulated oxygen flux, SS), followed by ADP (OXPHOS state, activity of electron transfer chain coupled to ATP synthase), followed by rotenone—specific inhibitor of complex I (see Supplementary Figure S2A). Each column shows mean ± SD (n = 3, each replicate is a pool of 20 dissected larval muscle tissues). The differences between frozen and control variants (see clamps) were statistically tested using multiple ANOVA models (checked for nested effects). Stars represent statistical differences (*p < 0.05; **p < 0.01; ***p < 0.001; ns, not significant). In case of LD larvae **(A)**, the log-transformed oxygen consumption data were used. See Supplementary Figure S5 for examples of original oxygen flux traces taken by Oxygraph-2K.

previous observations of similar mitochondrial responses to freezing stress in fat body and hindgut tissues of *C. costata* larvae (Štětina et al., 2020). We will discuss mechanisms that may cause the observed freeze-induced mitochondrial dysfunction and physical disintegration, distinguishing between damage to protein respiratory chain complexes and to the inner mitochondrial membrane (IMM) in which the complexes are located.

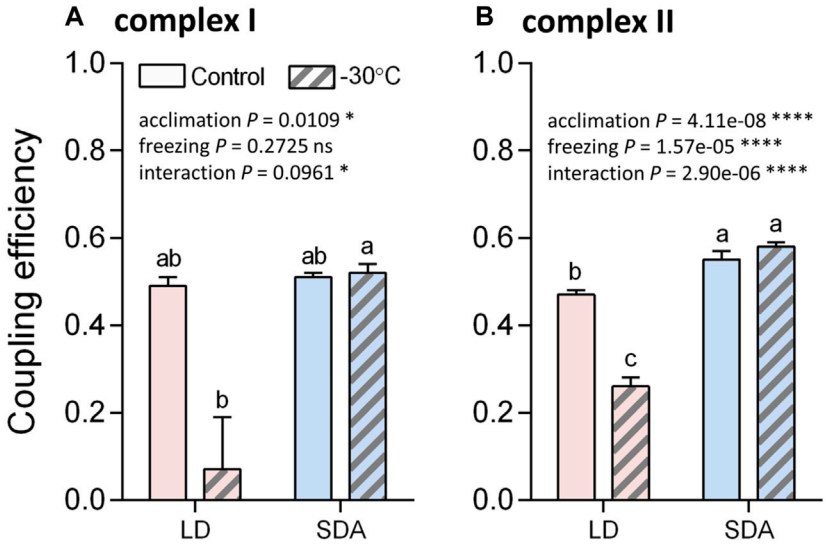

FIGURE 6
The efficiency of coupling between electron transfer chain and ATP synthase significantly decreased after the freezing stress in the muscles of freeze-sensitive larvae of *Chymomyza costata*. The coupling efficiencies were calculated from oxygen flux data (Figures 5 and Supplementary Figure S6), separately for complexes I **(A)** and II **(B)**, using a formula: efficiency = 1−(SS/OXPHOS). Each column shows mean ± SD (n = 3, each replicate is a pool of 20 dissected larval muscle tissues). The differences were statistically analyzed using two-way ANOVA model followed by Tukeys's multiple comparisons test. Stars represent statistical differences (*p < 0.05; ****p < 0.0001; ns, not significant). Columns flanked by different letters are statistically different. In case of complex I **(A)**, the rank-transformed response variables were used.

The protein respiratory chain complexes remain partially functional in lethally frozen insects

Our results suggest that the respiratory complexes in *C. costata* muscle mitochondria survive freeze-induced death of the whole organism with only partial loss of activity. The Alamar Blue assay showed that the metabolic activity of muscle cells slows down, but does not stop, in LD larvae after lethal freezing stress. Oxygraph-2K respirometry confirmed this result, showing that the mitochondrial respiration still proceeds in the muscles of lethally frozen LD larvae. The rate of basal oxygen consumption (without added substrates) decreased to 56.6% in lethally stressed LD larvae compared to unfrozen controls. Nevertheless, complexes I and II still clearly responded to their respective substrates in lethally frozen LD larvae. For example, the succinate-stimulated oxygen consumption (i.e., the succinate contribution ratio) was 11.1-fold higher than the basal consumption rate in lethally frozen LD larvae. These results indicate that the entire electron transfer chain from complex I or II via complexes III and IV to oxygen must have functioned at least partially in lethally stressed LD larvae. Thus, the "proteinaceous component" of the mitochondrial respiratory system in *C. costata* larval muscles appeared to be relatively resistant to freezing stress. In addition, the electron transfer chain complexes were found to be relatively stable even under lethal heat stress. The Alamar Blue assay indicated that metabolically active mitochondria survived in muscle cells of *C. costata* larvae killed by heat stress at 45°C. A higher temperature of 65°C was required to completely "kill" the metabolic activity in *C. costata* muscles, probably via irreversible denaturation of enzymes, including the electron transfer chain proteins. Similar results, showing that *in vitro* mitochondrial respiration still proceeds at temperatures above the upper thermal limit for organismal survival, were obtained for adults of the vinegar fly *D. melanogaster* (Heinrich et al., 2017). Taken together, these results suggest that proteins forming the mitochondrial electron transfer chain in *C. costata* muscle do not represent the first line of sensitivity to thermal stress and retain at least partial activity after organismally lethal freezing stress.

Furthermore, we observed that muscle mitochondria from lethally frozen larvae of *C. costata* are decoupled, i.e., they respond to exogenous ADP with a significantly lower increase in oxygen consumption than mitochondria from control or freeze-tolerant larvae exposed to the same stress. Considering that complexes I-IV of lethally frozen larvae remain partially functional, we speculate that the dissociation between proton gradient generation and its use for ATP synthesis by complex V is caused by increased leakage of the IMM for protons or, more generally, by permeabilization of the IMM and loss of its barrier function.

Lethal freezing stress is associated with permeability transition in IMM

Despite the maintenance of partially functional respiratory complexes I-IV, mitochondria from lethally frozen LD larvae of *C. costata* exhibited morphological changes characteristic of a permeability transition in the IMM: the mitochondrial matrix appeared diluted, the cristae were displaced to the periphery or lost, and the mitochondria were significantly swollen, sometimes showing discontinuous outer membranes (burst). In healthy mitochondria, matrix volume is regulated by constant effluxes of cations (mainly K^+ and Ca^{2+}) across the IMM, which are energized by a steep proton gradient ($\Delta\Psi m$ of about −180 mV) formed by

proton pumping activities of complexes I, III and IV of the electron transfer chain (Kaasik et al., 2007; Javadov et al., 2018). When the IMM loses its barrier function, the proton gradient dissipates, which has two major consequences: first, the mitochondria are decoupled, and second, the regulated efflux of cations is impaired. The resulting colloidosmotic gradient caused by accumulated cations and tightly packed proteins in the matrix will then drive water in and cause mitochondrial swelling (Halestrap, 2009; Bernardi et al., 2023). Both mitochondrial decoupling and swelling have been observed in lethally frozen *C. costata* larvae. The existence of a colloidosmotic gradient in mitochondria of *D. melanogaster* S2 cells was demonstrated by permeabilizing the IMM with either the K^+-specific ionophore valinomycin or the multicoductive pore-forming peptide alamethicin, both of which induced rapid mitochondrial swelling (Von Stockum et al., 2011) strikingly similar to what we observed in tissues from lethally frozen *C. costata*. IMM permeabilization followed by matrix swelling is a typical malformation induced by various pathologies, toxins or environmental stressors (Ghadially, 1988) and also accompanies apoptotic cell death in *D. melanogaster* S2 cells (Abdelwahid et al., 2007) and adult muscle cells (Klein et al., 2014). Taken together, there is little doubt that the mitochondrial swelling observed in lethally frozen *C. costata* larvae is caused by a loss of barrier function of the IMM. However, the cause of this freezing-induced permeability transition remains unclear.

Hypothetical causes of permeability transition in IMM

There are at least two hypothetical explanations, which are not mutually exclusive: the occurrence of phase transitions in the lipid bilayer of the IMM; and the opening of a non-specific large pore in the IMM. The IMM may become porous due to the direct effects of low temperature and freeze dehydration on its lipid bilayer. As the ambient temperature gradually decreases, a specific temperature (T_m) is reached at which the membrane phospholipids begin to transition from the liquid crystalline to the gel phase (Chapman, 1975). According to the theory developed by Quinn (1985), the non-bilayer-forming species, such as phosphatidylethanolamines (PEs), begin to transit earlier (at higher temperatures) than the bilayer-forming phosphatidylcholines. The membrane domains enriched in non-bilayer species are thus formed that are separated from the bilayer species domains. The loss of barrier function then occurs upon rewarming, when the domains of non-bilayer species tend to transition to the hexagonal phase, resulting in disruption of the bilayer structure and subsequent leakage of all solutes across the membrane in both directions. In addition, a decrease in membrane hydration associated with freezing stress can further worsen the situation, as the transition to the hexagonal phase becomes more likely with decreasing hydration of the phospholipid head groups (Quinn, 1985). Insect membranes generally contain a high proportion of non-bilayer forming lipid species (Koštál, 2010). For example, 51% of the phospholipid molecules in *C. costata* larval muscles are PEs and 63% of them carry at least one unsaturated fatty acyl chain (Koštál et al., 2003), making the PE molecules conical in shape and poorly bilayer packing. The composition of the *C. costata* IMM is currently unknown, but the IMM of other animals, including *D. melanogaster*, is known to have a very high content of non-bilayer forming species. In addition to approximately 30 mol% of PEs (Schenkel and Bakovic, 2014), the IMM contains approximately 15–20 mol% of cardiolipins (CLs) (Schlame et al., 2012; Gasanoff et al., 2021). The CL molecules, due to their highly conical molecular shape, are extremely prone to form non-bilayer structures such as inverted micelles and hexagonal phase under certain temperature and hydration conditions (Raison et al., 1971; Quinn, 1985; Hazel, 1995). Thus, the specific lipid composition appears to make the IMM relatively susceptible to loss of integrity due to direct effects of low temperature and low hydration on bilayer phase transitions.

Whether bilayer phase transitions actually occur in *mitochondrial* membranes of LD larvae exposed to freezing stress remains to be investigated. Nevertheless, we have already shown that *plasma* membrane integrity is compromised upon freezing stress in LD larvae but not in SDA larvae, where integrity is likely protected by at least two mechanisms: seasonal restructuring of lipid composition (Koštál et al., 2003); and stabilization by seasonally accumulated proline, trehalose and serum proteins (Grgac et al., 2022). Our unpublished observations confirmed that freezing-induced loss of plasma membrane integrity also occurs in other tissues of LD larvae, including muscle. The loss of plasma membrane integrity is likely to be followed by a massive influx of calcium from the extracellular space into the cytosol, which may have further deleterious consequences for mitochondria. The high cytosolic calcium can activate phospholipase C, which releases inositol phosphates (IPs) from plasma membrane phosphatidylinositols (Kadamur and Ross, 2013). The IPs are important signaling molecules that (among other things) open the calcium channels in the endoplasmic reticulum (ER) (Putney and Tomita, 2012; Kadamur and Ross, 2013), potentially closing the lethal feedback loop by releasing a secondary surge of calcium from the ER into the cytosol. More importantly, high cytosolic calcium is known to be a central player in the mammalian model of mitochondrial permeability transition, which is accompanied by characteristic mitochondrial swelling (Haworth and Hunter, 1979; Hunter and Haworth, 1979; Bernardi et al., 2023).

Putative role of calcium in freezing stress-induced mitochondrial permeability transition

In both mammalian and insect models, high cytosolic calcium is inevitably and rapidly overloaded into the mitochondrial matrix (Bernardi et al., 2023), where it affects at least two targets related to the IMM permeability transition: cardiolipins and the permeability transition pore. First, the high innate tendency of CLs to form non-bilayer structures (see above) is known to be further stimulated by calcium (Verkleij, 1984). The formation of hexagonal non-bilayer structures induced by exogenous calcium was directly observed by freeze-fracture electron microscopy in isolated rat liver mitochondria (van Venetië and Verkleij, 1982). Second, in mammalian mitochondria, exogenous calcium concentrations higher than about 100 μM were shown to induce a permeability transition by opening a large non-selective channel in the IMM - the permeability transition pore

(mPTP). The exact molecular identity of mPTP remains elusive despite decades of intensive efforts (Halestrap, 2009; Chinopoulos, 2018; Bernardi et al., 2023). The short opening of mPTP is thought to serve several regulatory purposes (e.g., reduction of calcium overload, reduction of ROS production). However, the prolonged mPTP openings cause mitochondrial swelling and rupture of the OMM, disrupting mitochondrial energy metabolism and ultimately leading to the induction of cell death pathways (Giorgio et al., 2018). The functional fly (*D. melanogaster*) homolog of mPTP has been characterized (Von Stockum et al., 2011). Although many functional similarities were found, it may differ from mammalian mPTP in that it does not form a large non-selective pore upon stimulation by calcium. No mitochondrial swelling was observed upon stimulation of *D. melanogaster* S2 cells permeabilized with digitonin and exposed to 40–100 μM calcium (Von Stockum et al., 2011). These observations led the authors to name the fly mPTP homologue mCRC—mitochondrial calcium release channel. The proposed function of mCRC under physiological conditions is to respond to relatively small and rapid pulses of calcium overload (e.g., in working muscle) by opening and releasing the excess calcium from the matrix (Von Stockum et al., 2011; Bernardi and von Stockum, 2012). A relative insensitivity of invertebrate mitochondria to doses of exogenous calcium between 100 and 1,000 μM has also been observed in the crustacean *Artemia franciscana* (Menze et al., 2005). However, it should be noted that extracellular calcium concentrations in the hemolymph of *D. melanogaster* larvae are as high as 3,600 μM (Krans et al., 2010). This leaves some room for speculation that much higher concentrations than those tested in *D. melanogaster* (100 μM) could be generated by calcium influx into the cytosol of cells in lethally frozen *C. costata* larvae, and that these concentrations would exert the effects described above either on the CL phase transition or on mCRC opening.

Follow-up studies are needed to assess the validity of the hypothesis of calcium mediation of the mitochondrial permeability transition in freeze-stressed insect cells. For example, in *C. costata* larvae, the experiments are ongoing to monitor the changes in cytosolic calcium levels (using calcium-sensitive probes) before and after freezing stress, while extracellular calcium levels and plasma membrane permeability are manipulated (by culturing tissues in media with differing calcium concentrations, and by permeabilization vs. stabilization of the plasma membrane by digitonin vs. cryoprotectants, respectively). It should also be noted that the influx of exogenous calcium into the cytosol plays a central role in the integrative model currently being constructed to explain chilling injury in chill-sensitive insects (such as the fly *D. melanogaster* or the migratory locust, *Locusta migratoria*) (MacMillan, 2019). Chilling injury is caused by relatively short exposures to mild temperatures, typically above zero. In the *chilling* injury model, the deleterious cascade begins with a change in plasma membrane *function*: the ion motive activity of Na^+/K^+ ATPase decreases with decreasing ambient temperature and cannot keep up with the backward flow of ions. This leads to a loss of ionic and osmotic balance across the body epithelia, resulting in systemic cell membrane depolarization (Koštál et al., 2004; MacMillan et al., 2015; Overgaard and MacMillan, 2017), which in turn causes the opening of the calcium voltage-dependent channels (Bayley et al., 2018; Bayley et al., 2019; Bayley et al., 2020). In the hypothetical *freezing* injury model outlined here, the deleterious cascade would begin with the loss of plasma membrane *structure*. Freezing stress is hypothesized to be associated with the formation of non-bilayer structures in the plasma membrane that are leaky not only to calcium but also to any large and charged molecule (such as Trypan blue).

Conclusion

In conclusion, we have shown that lethal freezing stress in *C. costata* larvae is closely associated with mitochondrial swelling. Since muscle OXPHOS proteins remained at least partially functional after lethal freezing stress, we hypothesized that the permeability transition in the muscle IMM lipid bilayer is primarily responsible for the loss of matrix volume control and subsequent mitochondrial swelling. In the search for plausible mechanistic explanations for the cause of the IMM permeability transition, we outlined two mutually non-exclusive hypotheses, which postulate that: 1) the direct effects of cold and freeze dehydration on IMM lipid bilayer phase transitions may result in the formation of non-bilayer structural defects that render the IMM leaky, and 2) IMM permeabilization is induced by calcium overload of the mitochondrial matrix following the surge of extracellular calcium into the cytosol resulting from loss of plasma membrane integrity. We suggest that further investigation in these two directions may help to understand the mechanistic nature of freeze-induced injury in freeze-sensitive cells and animals.

Data availability statement

The original contributions presented in the study are included in the article/Supplementary Material, further inquiries can be directed to the corresponding author.

Ethics statement

The manuscript presents research on animals that do not require ethical approval for their study.

Author contributions

TS: Conceptualization, Formal Analysis, Investigation, Methodology, Writing—review and editing. VK: Conceptualization, Formal Analysis, Funding acquisition, Methodology, Project administration, Supervision, Validation, Visualization, Writing—original draft, Writing—review and editing.

Funding

The authors declare financial support was received for the research, authorship, and/or publication of this article. The work

on this study was funded by two Czech Science Foundation grants to VK: GAČR 19-13381S and GAČR 23-06518S.

Acknowledgments

We thank Petr Šmilauer (Faculty of Science, University of South Bohemia in České Budějovice, Czech Republic) for his advice on statistical analysis.

Conflict of interest

The authors declare that the research was conducted in the absence of any commercial or financial relationships that could be construed as a potential conflict of interest.

Publisher's note

Supplementary material

The Supplementary Material for this article can be found online at: https://www.frontiersin.org/articles/10.3389/fphys.2024.1358190/full#supplementary-material

References

Abate, M., Festa, A., Falco, M., Lombardi, A., Luce, A., Grimaldi, A., et al. (2020). Mitochondria as playmakers of apoptosis, autophagy and senescence. *Semin. Cell Dev. Biol.* 98, 139–153. doi:10.1016/j.semcdb.2019.05.022

Abdelwahid, E., Yokokura, T., Krieser, R. J., Balasundaram, S., Fowle, W. H., and White, K. (2007). Mitochondrial disruption in *Drosophila* apoptosis. *Dev. Cell* 12, 793–806. doi:10.1016/j.devcel.2007.04.004

Asahina, E. (1970). Frost resistance in insects. *Adv. Insect Physiol.* 6, 1–49. doi:10.1016/S0065-2806(08)60109-5

Ballantyne, J. S., and Storey, K. B. (1985). Characterization of mitochondria isolated from the freezing-tolerant larvae of the goldenrod gall fly (*Eurosta solidaginis*): substrate preferences, salt effects, and pH effects on warm-and cold-acclimated animals. *Can. J. Zool.* 63, 373–379. doi:10.1139/z85-057

Bayley, J. S., Klepke, M. J., Pedersen, T. H., and Overgaard, J. (2019). Cold acclimation modulates voltage gated Ca2+ channel currents and fiber excitability in skeletal muscles of *Locusta migratoria*. *J. Insect Physiol.* 114, 116–124. doi:10.1016/j.jinsphys.2019.03.003

Bayley, J. S., Sørensen, J. G., Moos, M., Koštál, V., and Overgaard, J. (2020). Cold acclimation increases depolarization resistance and tolerance in muscle fibers from a chill-susceptible insect, *Locusta migratoria*. *Am. J. Physiol.-Regul., Integr. Comp. Physiol.* 319, R439–R447. doi:10.1152/ajpregu.00068.2020

Bayley, J. S., Winther, C. B., Andersen, M. K., Grønkjær, C., Nielsen, O. B., Pedersen, T. H., et al. (2018). Cold exposure causes cell death by depolarization-mediated Ca2+ overload in a chill-susceptible insect. *Proc. Natl. Acad. Sci. U. S. A.* 115, E9737–E9744. doi:10.1073/pnas.1813532115

Bernardi, P., Gerle, C., Halestrap, A. P., Jonas, E. A., Karch, J., Mnatsakanyan, N., et al. (2023). Identity, structure, and function of the mitochondrial permeability transition pore: controversies, consensus, recent advances, and future directions. *Cell Death Differ.* 30, 1869–1885. doi:10.1038/s41418-023-01187-0

Bernardi, P., and von Stockum, S. (2012). The permeability transition pore as a Ca2+ release channel: new answers to an old question. *Cell Calcium* 52, 22–27. doi:10.1016/j.ceca.2012.03.004

Braut-Boucher, F., and Aubery, M. (2017). "Fluorescent molecular probes," in *Encyclopedia of specroscopy and spectrometry*. Editors J. C. Lindon, G. E. Tranter, and D. W. Koppenaal (Elsevier), 661–669. ISBN: 978-0-12-803224-4.

Camus, M. F., Wolff, J. N., Sgrò, C. M., and Dowling, D. K. (2017). Experimental support that natural selection has shaped the latitudinal distribution of mitochondrial haplotypes in Australian *Drosophila melanogaster*. *Mol. Biol. Evol.* 34, 2600–2612. doi:10.1093/molbev/msx184

Chapman, D. (1975). Phase transitions and fluidity characteristics of lipids and cell membranes. *Q. Rev. Biophys.* 8, 185–235. doi:10.1017/S0033583500001797

Chinopoulos, C. (2018). Mitochondrial permeability transition pore: back to the drawing board. *Neurochem. Int.* 117, 49–54. doi:10.1016/j.neuint.2017.06.010

Chowański, S., Lubawy, J., Paluch-Lubawa, E., Spochacz, M., Rosiński, G., and Słocińska, M. (2017). The physiological role of fat body and muscle tissues in response to cold stress in the tropical cockroach *Gromphadorhina coquereliana*. *PLoS One* 12, e0173100. doi:10.1371/journal.pone.0173100

Chung, D. J., and Schulte, P. M. (2020). Mitochondria and the thermal limits of ectotherms. *J. Exp. Biol.* 223, jeb227801. doi:10.1242/jeb.227801

Colinet, H., Renault, D., and Roussel, D. (2017). Cold acclimation allows *Drosophila* flies to maintain mitochondrial functioning under cold stress. *Insect biochem. Mol. Biol.* 80, 52–60. doi:10.1016/j.ibmb.2016.11.007

Collins, S. D., Allenspach, A. L., and Lee, R. E., Jr (1997). Ultrastructural effects of lethal freezing on brain, muscle and Malpighian tubules from freeze-tolerant larvae of the gall fly, *Eurosta solidaginis*. *J. Insect Physiol.* 43, 39–45. doi:10.1016/s0022-1910(96)00073-x

Des Marteaux, L. E., Štětina, T., and Koštál, V. (2018). Insect fat body cell morphology and response to cold stress is modulated by acclimation. *J. Exp. Biol.* 221, jeb189647. doi:10.1242/jeb.189647

Gasanoff, E. S., Yaguzhinsky, L. S., and Garab, G. (2021). Cardiolipin, non-bilayer structures and mitochondrial bioenergetics: relevance to cardiovascular disease. *Cells* 10, 1721. doi:10.3390/cells10071721

Ghadially, F. N. (1988). "Mitochondria," in *Ultrastructural pathology of the cell and matrix* (Elsevier), 191–328. ISBN: 9781483192086.

Giorgio, V., Guo, L., Bassot, C., Petronilli, V., and Bernardi, P. (2018). Calcium and regulation of the mitochondrial permeability transition. *Cell Calcium* 70, 56–63. doi:10.1016/j.ceca.2017.05.004

Grgac, R., Rozsypal, J., Des Marteaux, L., Štětina, T., and Koštál, V. (2022). Stabilization of insect cell membranes and soluble enzymes by accumulated cryoprotectants during freezing stress. *Proc. Natl. Acad. Sci. U. S. A.* 119, e2211744119. doi:10.1073/pnas.2211744119

Halestrap, A. P. (2009). What is the mitochondrial permeability transition pore? *J. Mol. Cell. Cardiol.* 46, 821–831. doi:10.1016/j.yjmcc.2009.02.021

Haworth, R. A., and Hunter, D. R. (1979). The Ca2+-induced membrane transition in mitochondria: II. Nature of the Ca2+ trigger site. *Arch. Biochem. Biophys.* 195, 460–467. doi:10.1016/0003-9861(79)90372-2

Hazel, J. R. (1995). Thermal adaptation in biological membranes: is homeoviscous adaptation the explanation? *Annu. Rev. Physiol.* 57, 19–42. doi:10.1146/annurev.ph.57.030195.000315

Heinrich, E. C., Gray, E. M., Ossher, A., Meigher, S., Grun, F., and Bradley, T. J. (2017). Aerobic function in mitochondria persists beyond death by heat stress in insects. *J. Therm. Biol.* 69, 267–274. doi:10.1016/j.jtherbio.2017.08.009

Hothorn, T., Bretz, F., and Westfall, P. (2008). Simultaneous inference in general parametric models. *Biom. J.* 50, 346–363. doi:10.1002/bimj.200810425

Hunter, D. R., and Haworth, R. A. (1979). The Ca2+-induced membrane transition in mitochondria: I. The protective mechanisms. *Arch. Biochem. Biophys.* 195, 453–459. doi:10.1016/0003-9861(79)90371-0

Javadov, S., Chapa-Dubocq, X., and Makarov, V. (2018). Different approaches to modeling analysis of mitochondrial swelling. *Mitochondrion* 38, 58–70. doi:10.1016/j.mito.2017.08.004

Joanisse, D. R., and Storey, K. B. (1994). Mitochondrial enzymes during overwintering in two species of cold-hardy gall insects. *Insect biochem. Mol. Biol.* 24, 145–150. doi:10.1016/0965-1748(94)90080-9

Jørgensen, L. B., Hansen, A. M., Willot, Q., and Overgaard, J. (2023). Balanced mitochondrial function at low temperature is linked to cold adaptation in *Drosophila* species. *J. Exp. Biol.* 226, jeb245439. doi:10.1242/jeb.245439

Kaasik, A., Safiulina, D., Zharkovsky, A., and Veksler, V. (2007). Regulation of mitochondrial matrix volume. *Am. J. Physiol. Cell Physiol.* 292, C157–C163. doi:10.1152/ajpcell.00272.2006

Kadamur, G., and Ross, E. M. (2013). Mammalian phospholipase C. *Annu. Rev. Physiol.* 75, 127–154. doi:10.1146/annurev-physiol-030212-183750

Klein, P., Müller-Rischart, A. K., Motori, E., Schönbauer, C., Schnorrer, F., Winklhofer, K. F., et al. (2014). Ret rescues mitochondrial morphology and muscle degeneration of *Drosophila* Pink1 mutants. *EMBO J.* 33, 341–355. doi:10.1002/embj.201284290

Koštál, V. (2006). Eco-physiological phases of insect diapause. *J. Insect Physiol.* 52, 113–127. doi:10.1016/j.jinsphys.2005.09.008

Koštál, V. (2010). "Cell structural modifications in insects at low temperature," in *Low temperature biology of insects*. Editors D. L. Denlinger and R. Lee (Cambridge: Cambridge University Press), 116–140. ISBN: 978-0-521-88635-2.

Koštál, V., Berková, P., and Šimek, P. (2003). Remodelling of membrane phospholipids during transition to diapause and cold-acclimation in the larvae of *Chymomyza costata* (Drosophilidae). *Comp. Biochem. Physiol. B* 135, 407–419. doi:10.1016/S1096-4959(03)00117-9

Koštál, V., Noguchi, H., Shimada, K., and Hayakawa, Y. (1998). Developmental changes in dopamine levels in larvae of the fly *Chymomyza costata*: comparison between wild-type and mutant-nondiapause strains. *J. Insect Physiol.* 44, 605–614. doi:10.1016/S0022-1910(98)00043-2

Koštál, V., Vambera, J., and Bastl, J. (2004). On the nature of pre-freeze mortality in insects: water balance, ion homeostasis and energy charge in the adults of *Pyrrhocoris apterus*. *J. Exp. Biol.* 207, 1509–1521. doi:10.1242/jeb.00923

Krans, J. L., Parfitt, K. D., Gawera, K. D., Rivlin, P. K., and Hoy, R. R. (2010). The resting membrane potential of *Drosophila melanogaster* larval muscle depends strongly on external calcium concentration. *J. Insect Physiol.* 56, 304–313. doi:10.1016/j.jinsphys.2009.11.002

Kučera, L., Moos, M., Štětina, T., Korbelová, J., Vodrážka, P., Des Marteaux, L., et al. (2022). A mixture of innate cryoprotectants is key for freeze tolerance and cryopreservation of a drosophilid fly larva. *J. Exp. Biol.* 225, jeb243934. doi:10.1242/jeb.243934

Kukal, O., Duman, J. G., and Serianni, A. S. (1989). Cold-induced mitochondrial degradation and cryoprotectant synthesis in freeze-tolerant arctic caterpillars. *J. Comp. Physiol. B* 158, 661–671. doi:10.1007/BF00693004

Kuznetsov, A. V., Veksler, V., Gellerich, F. N., Saks, V., Margreiter, R., and Kunz, W. S. (2008). Analysis of mitochondrial function *in situ* in permeabilized muscle fibers, tissues and cells. *Nat. Protoc.* 3, 965–976. doi:10.1038/nprot.2008.61

Lebenzon, J. E., Denezis, P. W., Mohammad, L., Mathers, K. E., Turnbull, K. F., Staples, J. F., et al. (2022). Reversible mitophagy drives metabolic suppression in diapausing beetles. *Proc. Natl. Acad. Sci. U. S. A.* 119, e2201089119. doi:10.1073/pnas.2201089119

Lebenzon, J. E., Overgaard, J., and Jørgensen, L. B. (2023). Chilled, starved or frozen: insect mitochondrial adaptations to overcome the cold. *Curr. Opin. Insect Sci.* 58, 101076. doi:10.1016/j.cois.2023.101076

Lee, R. E., Jr. (2010). "A primer on insect cold-tolerance," in *Low temperature biology of insects*. Editors D. L. Denlinger and R. E. J. Lee (Cambridge: Cambridge University Press), 3–34. ISBN: 978-0-521-88635-2.

Levin, D., Danks, H., and Barber, S. (2003). Variations in mitochondrial DNA and gene transcription in freezing-tolerant larvae of *Eurosta solidaginis* (Diptera: tephritidae) and *Gynaephora groenlandica* (Lepidoptera: lymantriidae). *Insect Mol. Biol.* 12, 281–289. doi:10.1046/j.1365-2583.2003.00413.x

Lubawy, J., Chowański, S., Adamski, Z., and Słocińska, M. (2022). Mitochondria as a target and central hub of energy division during cold stress in insects. *Front. Zool.* 19, 1. doi:10.1186/s12983-021-00448-3

Lubawy, J., Chowański, S., Colinet, H., and Słocińska, M. (2023). Mitochondrial metabolism and oxidative stress in the tropical cockroach under fluctuating thermal regimes. *J. Exp. Biol.* 226, jeb246287. doi:10.1242/jeb.246287

MacMillan, H. A. (2019). Dissecting cause from consequence: a systematic approach to thermal limits. *J. Exp. Biol.* 222, jeb191593. doi:10.1242/jeb.191593

MacMillan, H. A., Baatrup, E., and Overgaard, J. (2015). Concurrent effects of cold and hyperkalaemia cause insect chilling injury. *Proc. R. Soc. B* 282, 20151483. doi:10.1098/rspb.2015.1483

Mazur, P. (1984). Freezing of living cells: mechanisms and implications. *Am. J. Physiol.* 247, C125–C142. doi:10.1152/ajpcell.1984.247.3.C125

McDonald, A. E., Pichaud, N., and Darveau, C. A. (2018). "Alternative" fuels contributing to mitochondrial electron transport: importance of non-classical pathways in the diversity of animal metabolism. *Comp. Biochem. Physiol. B Biochem. Mol. Biol.* 224, 185–194. doi:10.1016/j.cbpb.2017.11.006

McMullen, D. C., and Storey, K. B. (2008). Mitochondria of cold hardy insects: responses to cold and hypoxia assessed at enzymatic, mRNA and DNA levels. *Insect biochem. Mol. Biol.* 38, 367–373. doi:10.1016/j.ibmb.2007.12.003

Menail, H. A., Cormier, S. B., Ben Youssef, M., Jørgensen, L. B., Vickruck, J. L., Morin, P., Jr, et al. (2022). Flexible thermal sensitivity of mitochondrial oxygen consumption and substrate oxidation in flying insect species. *Front. Physiol.* 13, 897174. doi:10.3389/fphys.2022.897174

Menze, M. A., Hutchinson, K., Laborde, S. M., and Hand, S. C. (2005). Mitochondrial permeability transition in the crustacean *Artemia franciscana*: absence of a calcium-regulated pore in the face of profound calcium storage. *Am. J. Physiol. –Regul. Integr. Comp. Physiol.* 289, R68–R76. doi:10.1152/ajpregu.00844.2004

Modesti, L., Danese, A., Angela Maria Vitto, V., Ramaccini, D., Aguiari, G., Gafà, R., et al. (2021). Mitochondrial Ca2+ signaling in health, disease and therapy. *Cells* 10, 1317. doi:10.3390/cells10061317

Muldrew, K., Acker, J. P., Elliott, J. A., and McGann, L. E. (2004). "The water to ice transition: implications for living cells," in *Life in the frozen state*. Editors B. J. Fuller, N. Lane, and E. E. Benson (Boca Raton, FL: CRC Press), 67–108. ISBN: 0-415-24700-4.

Newmeyer, D. D., and Ferguson-Miller, S. (2003). Mitochondria: releasing power for life and unleashing the machineries of death. *Cell* 112, 481–490. doi:10.1016/S0092-8674(03)00116-8

Nunnari, J., and Suomalainen, A. (2012). Mitochondria: in sickness and in health. *Cell* 148, 1145–1159. doi:10.1016/j.cell.2012.02.035

Overgaard, J., and MacMillan, H. A. (2017). The integrative physiology of insect chill tolerance. *Annu. Rev. Physiol.* 79, 187–208. doi:10.1146/annurev-physiol-022516-034142

Pearce, R. S. (2001). Plant freezing and damage. *Ann. Bot.* 87, 417–424. doi:10.1006/anbo.2000.1352

Pichaud, N., Messmer, M., Correa, C. C., and Ballard, J. W. O. (2013). Diet influences the intake target and mitochondrial functions of *Drosophila melanogaster* males. *Mitochondrion* 13, 817–822. doi:10.1016/j.mito.2013.05.008

Putney, J. W., and Tomita, T. (2012). Phospholipase C signaling and calcium influx. *Adv. Biol. Regul.* 52, 152–164. doi:10.1016/j.advenzreg.2011.09.005

Quinn, P. (1985). A lipid-phase separation model of low-temperature damage to biological membranes. *Cryobiol* 22, 128–146. doi:10.1016/0011-2240(85)90167-1

Raison, J., Lyons, J., Mehlhorn, R., and Keith, A. (1971). Temperature-induced phase changes in mitochondrial membranes detected by spin labeling. *J. Biol. Chem.* 246, 4036–4040. doi:10.1016/S0021-9258(18)62136-2

Rampersad, S. N. (2012). Multiple applications of Alamar Blue as an indicator of metabolic function and cellular health in cell viability bioassays. *Sensors* 12, 12347–12360. doi:10.3390/s120912347

R Core Team (2023). *R: a language and environment for statistical computing*. Vienna, Austria: R Foundation for Statistical Computing. Available at: https://www.R-project.org/.

Riihimaa, A. J., and Kimura, M. T. (1988). A mutant strain of *Chymomyza costata* (Diptera: drosophilidae) insensitive to diapause-inducing action of photoperiod. *Physiol. Entomol.* 13, 441–445. doi:10.1111/j.1365-3032.1988.tb01128.x

Rozsypal, J., Moos, M., Šimek, P., and Koštál, V. (2018). Thermal analysis of ice and glass transitions in insects that do and do not survive freezing. *J. Exp. Biol.* 221, 170464. doi:10.1242/jeb.170464

Schenkel, L. C., and Bakovic, M. (2014). Formation and regulation of mitochondrial membranes. *Int. J. Cell Biol.* 2014, 709828. doi:10.1155/2014/709828

Schlame, M., Blais, S., Edelman-Novemsky, I., Xu, Y., Montecillo, F., Phoon, C. K., et al. (2012). Comparison of cardiolipins from *Drosophila* strains with mutations in putative remodeling enzymes. *Chem. Phys. Lipids* 165, 512–519. doi:10.1016/j.chemphyslip.2012.03.001

Simard, C. J., Pelletier, G., Boudreau, L. H., Hebert-Chatelain, E., and Pichaud, N. (2018). Measurement of mitochondrial oxygen consumption in permeabilized fibers of Drosophila using minimal amounts of tissue. *JoVE J. Vis. Expts.*, e57376. doi:10.3791/57376

Sinclair, B. J. (1999). Insect cold tolerance: how many kinds of frozen? *Eur. J. Entomol.* 96, 157–164.

Sinclair, B. J., and Renault, D. (2010). Intracellular ice formation in insects: unresolved after 50 years? *Comp. Biochem. Physiol. A* 155, 14–18. doi:10.1016/j.cbpa.2009.10.026

Smith, P. E., Krohn, R. I., Hermanson, G., Mallia, A., Gartner, F., Provenzano, M., et al. (1985). Measurement of protein using bicinchoninic acid. *Anal. Biochem.* 150, 76–85. doi:10.1016/0003-2697(85)90442-7

Sokolova, I. (2018). Mitochondrial adaptations to variable environments and their role in animals' stress tolerance. *Integr. Comp. Biol.* 58, 519–531. doi:10.1093/icb/icy017

Štětina, T., Des Marteaux, L., and Koštál, V. (2020). Insect mitochondria as targets of freezing-induced injury. *Proc. R. Soc. B* 287, 20201273. doi:10.1098/rspb.2020.1273

Storey, K. B., and Storey, J. M. (1988). Freeze tolerance in animals. *Physiol. Rev.* 68, 27–84. doi:10.1152/physrev.1988.68.1.27

Storey, K. B., and Storey, J. M. (2013). Molecular biology of freezing tolerance. *Compr. Physiol.* 3, 1283–1308. doi:10.1002/cphy.c130007

Storey, K. B., and Storey, J. M. (2017). Molecular physiology of freeze tolerance in vertebrates. *Physiol. Rev.* 97, 623–665. doi:10.1152/physrev.00016.2016

Teets, N. M., Marshall, K. E., and Reynolds, J. A. (2023). Molecular mechanisms of winter survival. *Annu. Rev. Entomol.* 68, 319–339. doi:10.1146/annurev-ento-120120-095233

Toxopeus, J., Des Marteaux, L. E., and Sinclair, B. J. (2019). How crickets become freeze tolerant: the transcriptomic underpinnings of acclimation in *Gryllus veletis*. *Comp. Biochem. Physiol. D. Genom. Proteom.* 29, 55–66. doi:10.1016/j.cbd.2018.10.007

Toxopeus, J., and Sinclair, B. J. (2018). Mechanisms underlying insect freeze tolerance. *Biol. Rev.* 93, 1891–1914. doi:10.1111/brv.12425

van Venetië, R., and Verkleij, A. J. (1982). Possible role of non-bilayer lipids in the structure of mitochondria. A freeze-fracture electron microscopy study. *Biochim. Biophys. Acta –Biomembr.* 692, 397–405. doi:10.1016/0005-2736(82)90390-X

Verkleij, A. J. (1984). Lipidic intramembranous particles. *Biochim. Biophys. Acta – Rev. Biomembr.* 779, 43–63. doi:10.1016/0304-4157(84)90003-0

Von Stockum, S., Basso, E., Petronilli, V., Sabatelli, P., Forte, M. A., and Bernardi, P. (2011). Properties of Ca2+ transport in mitochondria of *Drosophila melanogaster*. *J. Biol. Chem.* 286, 41163–41170. doi:10.1074/jbc.M111.268375

Wiplfler, B., Schneeberg, K., Löffler, A., Hünefeld, F., Meier, R., and Beutel, R. G. (2013). The skeletomuscular system of the larva of *Drosophila melanogaster* (Drosophilidae, Diptera) – a contribution to the morphology of a model organism. *Arthr. Struct. Devel.* 42, 47–68. doi:10.1016/j.asd.2012.09.005

frontiers | Frontiers in Physiology

TYPE Original Research
PUBLISHED 21 February 2024
DOI 10.3389/fphys.2024.1362991

OPEN ACCESS

EDITED BY
Can Li,
Guiyang University, China

REVIEWED BY
Polychronis Rempoulakis,
NSW Government, Australia
Jalal Jalali Sendi,
University of Guilan, Iran

*CORRESPONDENCE
Yanhui Lu,
luyanhui@caas.cn

RECEIVED 29 December 2023
ACCEPTED 13 February 2024
PUBLISHED 21 February 2024

CITATION
Chu S, Liu B, Li H, Lu K and Lu Y (2024), Effect of X-ray irradiation on the biological parameters of *Xestia c-nigrum*.
Front. Physiol. 15:1362991.
doi: 10.3389/fphys.2024.1362991

Effect of X-ray irradiation on the biological parameters of *Xestia c-nigrum*

Shijiao Chu[1,2], Bing Liu[2,3], Huan Li[2], Keke Lu[2] and Yanhui Lu[2,3]*

[1]College of Agriculture, Shihezi University, Shihezi, China, [2]State Key Laboratory for Biology of Plant Diseases and Insect Pests, Institute of Plant Protection, Chinese Academy of Agricultural Sciences, Beijing, China, [3]Western Agricultural Research Center, Chinese Academy of Agricultural Sciences, Changji, China

The sterile insect technique (SIT) is widely used to control Lepidopteran pests by inducing inherited sterility. The noctuid moth *Xestia c-nigrum* is a polyphagous pest whose subterranean larvae severely injure cereals and some vegetables. The goals of this study were to assess the impact of X-ray irradiation on the development and survival of *X. c-nigrum* and use the data to select suitable sterilizing doses for potential future use in pest management. Batches of male pupae were exposed to 0 (control), 10, 30, 50, 100, 200, 300, or 400 Gy of X-rays, approximately 24 h before adult emergence. Exposure of late-stage pupae to 10–200 Gy of radiation had no significant effect on adult emergence, but all doses (10–400 Gy) reduced adult longevity, the number of spermatophores in mated females, and the number of eggs laid per female in the irradiated parental generation compared with the controls. Exposure to 10 and 30 Gy had no significant effects in the F1 generation on 1) the rate of egg hatch, 2) the duration of larval or pupal development, or 3) adult longevity. However, exposure to 50 Gy reduced the rate of egg hatch in the F1 generation, and when male pupae were exposed to 100 Gy only 1% of the F1 eggs hatched. Also at 100 Gy, the developmental durations of larvae and pupae were significantly prolonged, and longevity of adult moths was reduced. There were no significant differences between the control group and any treatments in 1) the sex ratio of the F1 adults, 2) the duration of F1 pre-oviposition or oviposition periods, or 3) the number of eggs laid per F1 female. Our findings indicate that a dose of 100 Gy can effectively slow pest development and reduce larval survival in the F1 generation. In addition, F1 adults from lines treated with 100 Gy were able to mate and lay eggs, but all F2 eggs failed to hatch. Our results suggest that use of X-ray irradiation has potential to control this polyphagous pest at the regional level.

KEYWORDS

***Xestia c-nigrum*, sterile insect technique, x-ray irradiation, inherited infertility, longevity, survival**

Introduction

The spotted cutworm *Xestia c-nigrum* is an important agroforestry pest found in temperate and tropical regions of Asia, Europe, North Africa, and North America (Subchev et al., 1996). With a wide host range and high reproductive potential, it is an economically important pest (Broad and Boyes, 2022). Typical damage is to plant seedlings in the early spring season, when larvae feed on roots and sever stems at ground level, causing them to

wilt and die (Wright et al., 2010). Due to the larvae's nocturnal activity and underground feeding sites, their presence is often only revealed when the plants are already severely damaged, making them extremely difficult to control (Weng et al., 2019). Despite the use of light traps to monitor the flight period of the adults, it is still difficult to predict their damage (Hrudová et al., 2022). Chemical insecticides are still one of the most effective ways to suppress this pest; however, their widespread application can leave pesticide residues in crops, induce the emergence of highly resistant moths, and harm non-target organisms (Goudarzi et al., 2015).

The advantage of the sterile insect technique (SIT) is that it is specific to the target pest and its action is based on releasing males that confer sterility to females that the males seek out and mate with. This mode of action makes SIT particularly effective at controlling hidden pests, especially those whose larvae burrow or live in the soil (Shelly and Manoukis, 2022; Chen et al., 2023). For example, the release of sterile *Cydia pomonella* male moths in the Similkameen Valley of British Columbia in Canada from 1976 to 1978 resulted in 100% reduction of economic damage in orchards (Proverbs et al., 1982). In 1999, the release of sterile males of the tephritid fly *Ceratitis capitata* in the Hex River Valley in South Africa reduced wild fly populations 6 to 7-fold, greatly reducing crop losses due to this fruit fly (Barnes et al., 2004). SIT has been widely used in many countries against a variety of pests, including fruit flies [*C. capitata* (Plá et al., 2021), *Anastrepha ludens* (Ramírez-Santos et al., 2021), *Zeugodacus cucurbita* (Koyama et al., 2004)]; moths [*Agrotis ipsilon* (Salem et al., 2014), *Agrotis segetum* (Andreev and Martens, 1974), *C. pomonella* (Neven and Wakie, 2020)]; and beetles [*Anoplophora glabripennis* (IDIDS, 2003), *Callosobruchus analis* (Chiluwal et al., 2019)].

Historically, isotopes such as Cobalt 60 (^{60}Co) and Caesium 137 (^{137}Cs) that emit gamma radiation have been employed for sterilization (Klassen and Vreysen, 2021). In the late 1980s, preliminary studies investigated the effect of SIT on *X. c-nigrum* control through the application of gamma radiation, showing that a certain dosage of gamma rays could reduce the percentage of egg hatch in *X. c-nigrum* (Khattak et al., 1989). This study suggested that SIT might be a potential control method for this pest. More recently, studies on the effects of gamma radiation on insects have declined because gamma radiation sources are in need of regular replenishment, are very expensive, and are becoming more difficult to obtain due to stricter regulations (Mastrangelo et al., 2010; Gómez-Simuta et al., 2021). X-ray sources, in contrast, are increasingly employed in research applications due to their affordability, ease of transportation, and superior penetration capabilities compared to gamma rays. In addition, the irradiation process is simple to perform and lower risk (Kumano et al., 2018; Wang et al., 2023). However, the effect of X-ray irradiation on *X. c-nigrum* needs further assessment.

SIT is based on the sterilization of insects through radiation-induced mutations. When applying SIT, it is important to comprehensively consider the selection of the irradiation dose, appropriate release ratio, and dynamics of the target insect population in the release area to achieve the best effects (Judd et al., 2011; Orozco et al., 2013; Woods et al., 2016; Saour et al., 2022; Osouli et al., 2023). In particular, the efficiency of SIT is especially influenced by the correct choice of a suitable radiation dose (Ramírez-Santos et al., 2021). While high doses are obligatory for total sterility in Lepidoptera, such high doses can diminish adult longevity and mating competitiveness (Marec and Vreysen, 2019). In comparison, genetic sterility that manifests in the F1 offspring, which is induced through the use of lower doses of radiation, allows treated insects to retain relatively high mating competitiveness (Li, 2006). For example, Jiang et al. (2022a) found that X-rays applied at 25–150 Gy reduced the fertility of the F1 generation of *Spodoptera litura* without affecting mating ability. However, to determine the most effective sterilization dose for insects, it is important to evaluate several biological characteristics that may be affected by irradiation, including adult emergence rates, adult longevity, egg numbers from irradiated females, hatchability of eggs from such females, and the survival of the larval from these eggs (Zhao et al., 2022).

The aim of this research is to determine the dose of X-ray radiation that most effectively sterilizes pupae and the resulting adults of *X. c-nigrum*. This determination was made by measuring life history parameters, including for adults of the irradiated parental generation (1) adult emergence, longevity, the numbers of spermatophores produced, and numbers of eggs laid per female, as well as (2) in the F1 generation, the egg hatch rate, larval developmental duration, stage survival rates, pupal mass, adult longevity, sex ratio, and per female oviposition, and finally (3) for the F2 generation the hatch rate after X-ray radiation of pupae of the parental generation. These results will aid in the application of sterile insect techniques using X-ray radiation to manage *X. c-nigrum* by determining appropriate sterility parameters.

Materials and methods

Insects sources

In mid-July 2022, during the peak of the *X. c-nigrum* population in field, adults were collected by light-trapping at the Korla Experimental Stations of the Chinese Academy of Agricultural Sciences, Korla city, in southern Xinjiang Province, China. After being trapped, moths were kept in cages covered with gauze for egg laying and provided with a 20% honey solution daily as food. The colony was reared at 24°C ± 1 °C, 50% ± 10% RH, and a 12:12 (L:D) photoperiod. Eggs laid on the gauze were collected daily and held for hatching. Neonate larvae were inserted into glass tubes (2.5 cm dia, 7.5 cm h) and supplied with artificial diet (the main components being wheat germ, casein, agar, sucrose, Wesson's salt mixture, and vitamin mixture, Zhang et al., 2012), with 5–10 larvae per tube. Fresh diet was provided every 2 days. After the larvae reached the fourth instar, they were placed individually in new tubes for pupation, and pupae were examined 10 days later to separate them by sex (Zhang et al., 2020). After egg hatch, larvae and pupae were reared under continuous dark 0:24 h (L:D).

Once this colony was well established, male pupae were collected for use in the irradiation test, isolating pupae approximately 24 h before adult emergence. Pupae used in our study originated from the second or third rearing generations.

X-ray irradiation procedures

An X-ray irradiator (MultiRad 160, Faxitron Bioptics LLC, Tucson, AZ, United States of America) was used as the source of X-rays in our test. X-ray irradiation was done at ambient temperature, with the X-ray machine being operated at 160 kV

and 25 mA, emitting 7.012 Gy/min at the point of irradiation. The machine and procedure were calibrated annually to ensure the accuracy of the dose administered and compliance with nationally recognized safety standards. The sample to be irradiated was placed in the center of the wire stage of the irradiator system, and X-rays are emitted from an X-ray tube positioned at a standard distance above the target. The irradiation voltage, current, and time were determined automatically based on the irradiation dose selected using the control panel. The irradiation doses used as treatments were 0 (no irradiation, i.e., the control), 10, 30, 50, 100, 200, 300, and 400 Gy. When the treatment's dosage had been administered, X-ray emission automatically ended, and the irradiated insects were then removed and used for the lifetable experiment.

Effect of irradiation on insect emergence, longevity, the per female oviposition rate, and the number of spermatophores in mated female in the parental generation

Groups of male pupae were placed in Petri dishes (90 mm dia) 48 h before adult emergence and irradiated with 10, 30, 50, 100, 200, 300, or 400 Gy, together with an untreated control. At least 50 pupae were treated in each group. Irradiation was done in four batches, each including all treatment doses and a control. The irradiated pupae were then transferred to rearing boxes and held until adults emerged. Pupae from which no adults emerged were counted to evaluate emergence rates. Emerged adult males were paired with non-irradiated, virgin females in disposable transparent plastic cups (8 cm dia at the mouth, 5 cm dia at the bottom, and 13 cm h) for mating. Paired moths were supplied with a 20% honey solution.

To determine the effect of treatment on moth oviposition, we evaluated four replicates of 30 pairs of adults for each treatment, including the controls. The mouth of each cup was covered with gauze for oviposition and replaced daily to record egg production. If male moths died, one male moth from the same treatment was added to continue mating with the paired female moths until the female moth died. The boxes with moths were kept under the same conditions as the rearing colony until all adults died. Longevity of the male adults was determined by recording daily mortality in each box.

To determine the effect of treatment on male sperm production and transfer, adults from irradiated male pupae were paired with newly emerged, non-irradiated virgin females. At various time points after pairing (1, 2, 3, 4, 5, and 10 days), females were sacrificed and dissected in a 0.8% NaCl solution, and the number of spermatophores in each female's bursa copulatrix was determined using a stereomicroscope. There were four replicates, each of five pairs, for each treatment, including the controls, and each date of female dissection, for a total of 960 pairs (8 treatments or control x 4 replicates x 5 pairs x 6 time points for dissection).

Effect of irradiation on development and fecundity of the F1 generation

To determine the effect of mating with irradiated males on the fertility of F1 eggs from non-irradiated females, batches of eggs laid 3–5 days after pairing in each treatment were collected to record their hatching rate. There were 300 eggs in each replicate of each treatment, and there were four replicates. Eggs were observed daily to detect hatch, until all the eggs had either hatched or died and dried up. The number of eggs that did not hatch was counted and used as the measure of the level of sterility induced by the irradiation treatments.

After viable eggs from each of the above treatments had hatched, the neonate larvae (within 12 h of hatching) were transferred into glass tubes containing artificial diet and reared until pupation. Larvae that did not pupate normally were scored to measure the survival rate of larvae. Pupal weights were measured 7 days after pupation, for both pupae from which adults emerged and that had died as pupae. The pupal duration and emergence rates for each treatment were determined. There were four replicates, each with 100 individuals, for each treatment, including the controls. The sex of each emerged adult was determined, and the males were then paired with non-irradiated females. Females were not used for further tests. Longevity of adults of both sexes was recorded until all adults had died.

Effect of irradiation on egg hatch rate of F2 generation

To determine the intergenerational effect of irradiated grandparents, F1 males sired by irradiated parental males were paired with unirradiated females. Eggs laid 3–5 days after this pairing were observed for hatching and the number of eggs that did not hatch was taken as the rate of induced sterility in the F2 generation.

Statistical analysis

The eclosion rate of pupae of the irradiated parental generation, and the survival rate of larvae of the F1 generation were all analyzed using generalized linear models (GLM) with binomial distributions. The number of spermatophores in mated females of the parental generation were analyzed using a GLM with a Poisson distribution. Data on adult longevity of the parental generation, the F1 larval and pupal developmental times, adult longevities of F1 males and females (and pooled), F1 pupal weight, sex-ratio (calculated as the proportion of female moths: F/(F + M)), pre-oviposition and oviposition periods, F1 oviposition number, and both F1 and F2 egg hatching rate were analyzed using one-way ANOVAs. Oviposition levels of females of the parental generation were analyzed using a GLM with negative binomial distributions, which was done using the "glm.nb" function within "MASS" package (Venables and Ripley, 2002). Within each GLM or ANOVA analysis, each parameter in the life tables of the F1 generation were compared between the various radiation doses and the control using Dunnett test. For other analyses, multiple comparisons were made using Tukey's Honestly Significant Difference (HSD) correction (for $p < 0.05$). Analysis of the survival from first instars to the adult stage for the F1 generation was done using Cox Regression by the "survifit" function within the "survival" package (Therneau, 2023). All analyses were performed by using R 4.3.1 software (R Development Core Team, 2023).

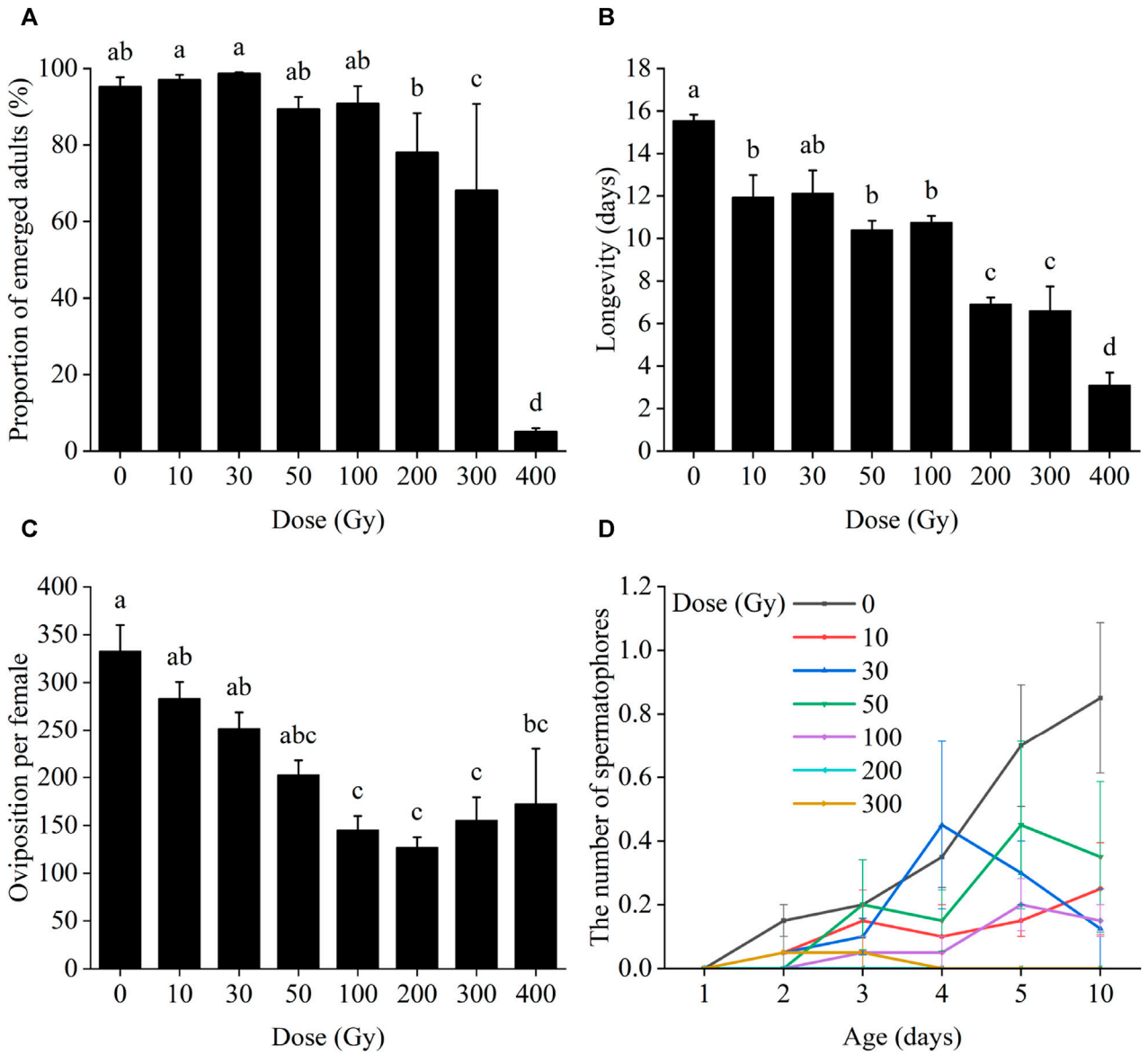

FIGURE 1
Effects of pupal irradiation on **(A)** the proportion of successfully emerged parental adults, **(B)** longevity of adults of the parental generation, **(C)** oviposition per parental female and **(D)** the number of spermatophores of mated females of the parental generation, with different doses. Data are average ±SE; means followed by the same lowercase letters are not statistically different ($p > 0.05$, Tukey HSD).

Results

Effect of irradiation on insect emergence, longevity, the per female oviposition, and the number of spermatophores in mated female in the parental generation

Irradiation of male pupae at doses ≥300 Gy significantly reduced adult emergence compared to the control group (0 Gy) (Figure 1A). Only 68.2% and 5.1% of irradiated male pupae reached the adult stage at 300 and 400 Gy, which was a significant difference between those doses ($\chi^2 = 436.92$, $df = 7$, $p < 0.001$). Male pupal emergence at doses from 10 to 200 Gy, however, did not differ significantly.

Longevity of the male adults of the parental generation decreased progressively with increased radiation doses, changing from 12.13 to 3.11 days from 10 to 400 Gy (Figure 1B). Adult longevity at all doses differed from that of the controls except for 30 Gy ($F_{7,24} = 28.16$, $p < 0.001$), at which dose adult longevity was not significantly different from the control group (12.13 days vs. 15.55).

When male pupae were exposed to radiation and mated with unexposed females, the radiation dosage did not affect the number of eggs laid per female of the same generation until male moths were exposed to 100 Gy or more of radiation ($\chi^2 = 59.58$, $df = 7$, $p < 0.001$; Figure 1C).

The number of successful matings between irradiated males and unirradiated females ranged from 0 to 4, all of which occurred after

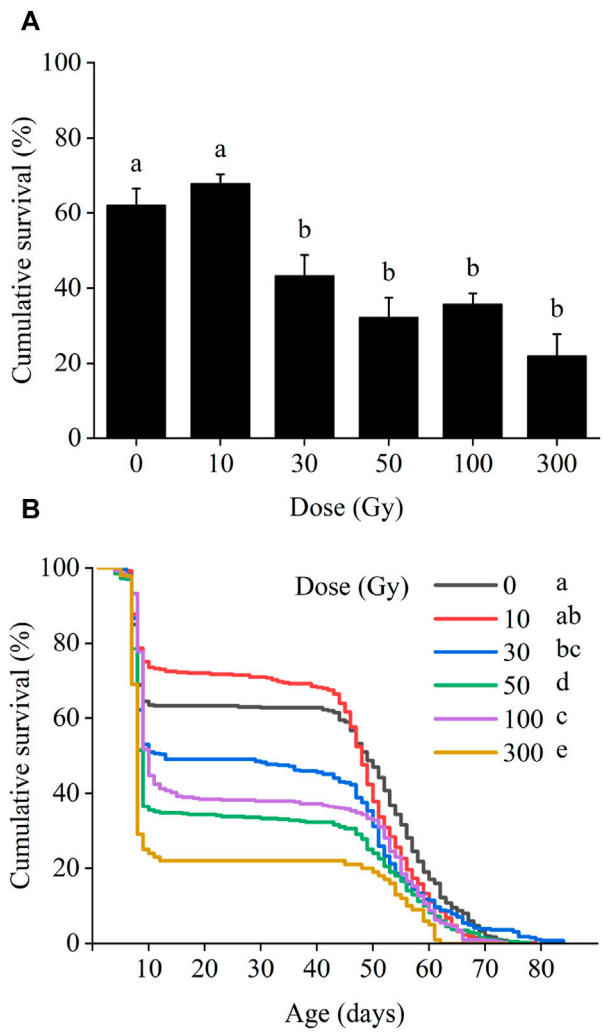

FIGURE 2
Effects of pupal irradiation on the survival rate of **(A)** larvae and **(B)** from first instar larvae to adult death of the F1 generation, with different doses. Data are average ±SE; means followed by the same lowercase letters are not statistically different ($p > 0.05$, Tukey HSD).

day 2 (after pairing). But there were no significant differences between those doses on day 2 ($\chi^2 = 1.69$, $df = 6$, $p = 0.946$), day 3 ($\chi^2 = 1.74$, $df = 6$, $p = 0.942$), day 4 ($\chi^2 = 5.15$, $df = 6$, $p = 0.524$), day 5 ($\chi^2 = 6.94$, $df = 6$, $p = 0.326$) or day 10 ($\chi^2 = 8.16$, $df = 6$, $p = 0.227$) (Figure 1D).

Effect of irradiation on development and fecundity of the F1 generation

In the F1 generation, larval survival was significantly affected by the irradiation dose, with larval survival gradually decreasing as the dose of radiation increased ($\chi^2 = 68.85$, $df = 5$, $p < 0.001$; Figure 2A). Larval survival rates at 10 and 30 Gy were 67.9% and 43.3%, respectively. With increasing irradiation, larval survival declined to 32.3%, 35.8%, and 22.0% following exposure to 50, 100, and 300 Gy, respectively, all of which were statistically different from the control level (62.3%).

Survival from egg hatch was reduced at all radiation doses above 30 Gy ($\chi^2 = 79.15$, $df = 5$, $p < 0.001$). Initially, population survival of the first larval instar was high in all treatments for the first 7 days. However, between 7 and 10 days period from first to second instar larvae, cumulative survival decreased sharply in all treatments including the control and continued to decrease steadily between 10 and 50 days. After 50 days, cumulative survival again declined more sharply until adult death (Figure 2B).

The developmental parameters (see Table 1) of F1 larvae, pupae, and adults following X-ray irradiation of the parental male pupae showed that egg hatch was reduced by increased doses of radiation. At 10 and 30 Gy, egg hatch was 58.9% and 41.3%, respectively, and these values were not significantly different from the control (51.9%); but all doses ≥50 Gy yielded egg hatch rates significantly lower than the control, reaching 0% at 200 and 400 Gy ($F_{5,18} = 10.17$, $p < 0.001$). Different doses of irradiation had significant effects on the duration of all larval instars, including first: $F_{5,18} = 9.79$, $p < 0.001$, second: $F_{5,18} = 15.14$, $p < 0.001$, third: $F_{5,18} = 5.91$, $p = 0.002$, fourth: $F_{5,18} = 4.06$, $p = 0.012$, fifth: $F_{5,18} = 10.67$, $p < 0.001$, sixth: $F_{5,18} = 7.62$, $p < 0.001$, and the whole larval stage ($F_{5,18} = 9.36$, $p < 0.001$), as well as the pupal stage ($F_{5,18} = 5.46$, $p = 0.003$), the first instar larval-pupal stage ($F_{5,18} = 9.79$, $p < 0.001$), and pupal weight ($F_{5,18} = 11.18$, $p < 0.001$) in the F1 generation.

In contrast, longevity and sex ratio were not affected by irradiation: (1) male longevity ($F_{5,18} = 0.69$, $p = 0.635$), (2) female longevity ($F_{5,18} = 1.57$, $p = 0.219$), (3) the longevity of all adults combined ($F_{5,18} = 2.17$, $p = 0.103$), (4) sex ratio ($F_{5,18} = 0.73$, $p = 0.608$). The pre-oviposition period ($F_{5,18} = 2.25$, $p = 0.009$), and oviposition period ($F_{5,18} = 0.93$, $p = 0.482$), and oviposition per female ($F_{5,18} = 0.99$, $p = 0.451$) at all irradiation doses were not significantly different from those of the controls. The results indicate that, in the F1 generation, irradiation of the previous generation's males mainly affected the larvae of the F1 generation.

As for the control moths, the sex ratio (F/(F + M) of irradiated moths was male biased = 0.44–0.36) in the 30–100 Gy irradiation groups. F1 adult longevity did not show significant differences between treatment groups in one-way ANOVA ($p = 0.103$). However, Dunnett's method (which was used to compare with the difference between each treatment group and the control group) revealed that the adult longevity at 100 Gy (9.74 days) was significantly lower than that of the control group, which was 14.20 days ($p = 0.019$; Table 1).

Effect of irradiation on egg hatch of F2 generation

In the F2 generation, egg hatch was significantly reduced as the dose of radiation applied increased ($F_{4,15} = 21.75$, $p < 0.001$; Figure 3). In the control group, the egg hatch rate was 79.6%, but this decreased to 64.5% and 47.0% at 10 and 30 Gy, respectively. These values, however, were not significantly different from the control. However, at 50 Gy and 100 Gy, the rate was reduced to 0%, showing that at these doses no eggs of the F2 generation survived.

TABLE 1 Effect of irradiation (Gy units) on developmental duration and fecundity of F1 generation.

Stage	Parameters	0 (Control)	10	30	50	100	300	*Df*	*F*	*p*
Egg	hatch rate (%)	51.92 ± 8.36	58.85 ± 8.71	41.33 ± 9.06	20.89 ± 4.48 *	1.08 ± 0.77 ***	11.21 ± 8.44 **	5	10.168	<0.001
Larvae	1st instar duration (d)	6.26 ± 0.10	5.74 ± 0.09	6.02 ± 0.18	6.59 ± 0.11	6.92 ± 0.06 *	6.53 ± 0.21	5	9.791	<0.001
	2nd instar duration (d)	3.71 ± 0.10	3.41 ± 0.03	3.65 ± 0.06	4.02 ± 0.06	4.36 ± 0.07 ***	3.90 ± 0.14	5	15.135	<0.001
	3rd instar duration (d)	3.31 ± 0.05	3.27 ± 0.07	3.39 ± 0.18	3.46 ± 0.17	3.95 ± 0.06 *	3.99 ± 0.18 **	5	5.909	0.002
	4th instar duration (d)	3.52 ± 0.07	3.61 ± 0.13	4.11 ± 0.35	3.77 ± 0.08	4.00 ± 0.12	4.53 ± 0.21 **	5	4.057	0.012
	5th instar duration (d)	5.31 ± 0.25	5.78 ± 0.26	5.89 ± 0.35	5.07 ± 0.09	5.28 ± 0.15	7.42 ± 0.36 ***	5	10.606	<0.001
	6th instar duration (d)	7.17 ± 0.24	7.22 ± 0.14	7.88 ± 0.48	8.15 ± 0.16	8.99 ± 0.37 **	9.00 ± 0.20 **	5	7.621	<0.001
	larvae stage duration (d)	26.82 ± 0.64	26.74 ± 0.28	28.63 ± 1.21	29.25 ± 0.35	32.44 ± 0.68 ***	29.63 ± 0.55 *	5	9.356	<0.001
Pupa	Duration (d)	14.22 ± 0.28	14.40 ± 0.12	14.02 ± 0.14	14.53 ± 0.30	15.33 ± 0.09 **	14.53 ± 0.09	5	5.463	0.003
	Mass (mg)	286.96 ± 6.93	253.40 ± 5.82 **	248.22 ± 5.05 ***	294.10 ± 5.20	271.06 ± 5.53	271.55 ± 2.95	5	11.176	<0.001
1st instar larval-pupal duration (d)		41.04 ± 0.85	41.14 ± 0.33	42.00 ± 0.64	43.65 ± 0.64 *	46.39 ± 0.51 ***	43.93 ± 0.82 *	5	9.786	<0.001
Adult	Female longevity (d)	18.48 ± 1.32	14.20 ± 1.07	16.17 ± 0.40	15.12 ± 1.46	12.60 ± 1.37	13.71 ± 3.07	5	1.571	0.219
	Male longevity (d)	10.20 ± 0.54	8.80 ± 0.27	9.09 ± 0.47	9.24 ± 1.20	8.06 ± 0.26	9.04 ± 1.43	5	0.694	0.635
	All adult longevity (d)	14.20 ± 0.86	11.55 ± 0.60	12.19 ± 0.38	11.98 ± 0.90	9.74 ± 0.96 *	11.52 ± 1.66	5	2.171	0.103
	sex ratio (F/(F + M))	0.48 ± 0.05	0.50 ± 0.05	0.44 ± 0.05	0.44 ± 0.03	0.36 ± 0.07	0.48 ± 0.07	5	0.733	0.608
	Pre-oviposition period (d)	5.08 ± 0.79	2.90 ± 0.43	2.53 ± 0.39 *	2.56 ± 0.53	2.91 ± 0.17	2.71 ± 1.13	5	2.247	0.009
	Oviposition period (d)	11.12 ± 0.56	9.75 ± 1.07	11.85 ± 0.49	10.34 ± 1.81	6.93 ± 1.66	10.25 ± 3.27	5	0.934	0.482
	Egg deposited per female	332.34 ± 19.64	261.88 ± 29.89	318.38 ± 52.81	257.42 ± 33.49	164.23 ± 11.67	285.71 ± 127.82	5	0.991	0.451

Data are shown as average ±SE; *df*, *F*, and *p* values are the results after one-way ANOVA, and asterisks in the table indicate significant differences between the treatment groups and the control; $^{*}p < 0.05$, $^{**}p < 0.01$, $^{***}p < 0.001$ (Dunnett's multiple comparisons).

Discussion

The objective of SIT is to prevent the reproduction of females in invasive or established pest populations through the distribution of mass-produced, sterile insects, with particular emphasis on sterile males (Light et al., 2015; Klassen and Vreysen, 2021). The success of SIT is based on the use of a dosage of radiation that sterilizes male insects, but still leaves them as competitive as their fertile counterparts within the target population (M'Saad Guerfali et al., 2011; Pérez-Staples et al., 2012; Kapranas et al., 2022). Sterility can manifest at various life stages of the targeted insect during its reproductive development, such as failure of egg production or hatch, larval mortality, failure to pupate, non-emergence of adults, and sterility of any F1 adults that do emerge (Pérez-Staples et al., 2012; Light et al., 2015; Kapranas et al., 2022).

Following pupal irradiation, rates of adult emergence from irradiated pupae and adult longevity are important measures of the quality of the sterile males being produced (Mastrangelo et al., 2010). Reduction in the emergence rate of male adults after irradiation is a dose responsive outcome, with emergence decreasing as dosage increases. This relationship implies that higher radiation doses can induce morphological damage in male adults, contrary to the goal of SIT (Aksoy et al., 2017). We found that the emergence rate of male pupae of *X. c-nigrum* was not affected by dosage within the range of 10–200 Gy. However, the emergence rate was significantly depressed if the radiation dose was 300 Gy or higher. Also, our results showed that an increase in radiation exposure in male pupae lead to a significant reduction in adult longevity, suggesting that exposure to high levels of radiation may also affect the somatic cells of insects (Brower, 1976).

The number of spermatophores present in a female moth's bursa copulatrix is an indicator of her number of successful matings, with each spermatophore originating uniquely from one male moth (Wu, 2020). In this study, we found that the number of spermatophores transferred to females by irradiated males declined gradually with increasing irradiation dose for each day of pairing. Moreover,

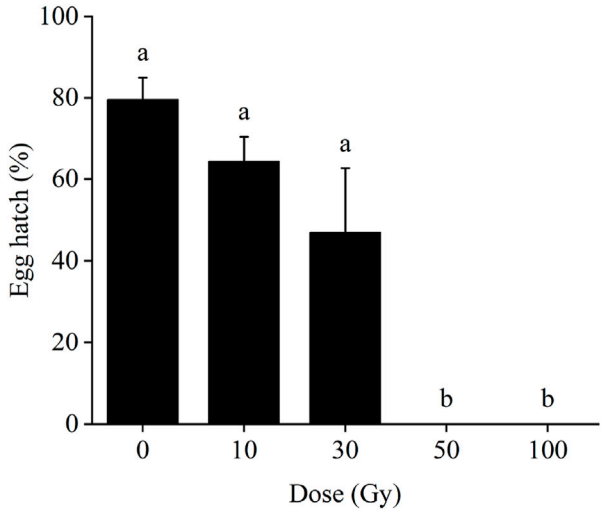

FIGURE 3
Effect of pupal irradiation on egg hatch rate of the F2 generation. Data are average ±SE; means followed by the same lowercase letters are not statistically different ($p > 0.05$, Tukey HSD).

mating virtually ceased at radiation doses exceeding 200 Gy. Meanwhile, the number of spermatophores in the bursa copulatrix of females increased with days of pairing, as seen in a study of *Anopheles arabiensis* (Helinski and Knols, 2009).

Ideally in SIT, an optimum amount of irradiation is used so that the sterility level of treated insects increases and the number of eggs and their hatch rate decreases (Mansour and Mohamad, 2004). In our study, the number of eggs laid by the parental generation was significantly reduced by the radiation treatments, and the rate of egg hatch in the F1 generation was significantly reduced compared to the control at ≥ 100 Gy. These results suggest that X-ray irradiation may damage the reproductive cells and ultimately cause sterility of this pest. Similar findings have been reported for *Drosophila melanogaster* and *Sesamia nonagrioides* (Vaiserman et al., 2004; Aksoy et al., 2017). In contrast, irradiation of *C. pomonella* at 366 Gy with X-rays did not have any impact on egg numbers but significantly reduced egg viability (Zhang et al., 2023). These variations suggest that the effects of irradiation depend on the target species.

Some studies have reported that use of X-rays for irradiation of pupae caused a dose-dependent reduction in larval survival, adult emergence, and, in the next-generation, of fecundity and F1 adult longevity (Kim et al., 2015; Jiang et al., 2022a; Jiang et al., 2022b). In our study, as the irradiation dose increased, the development rates decreased for both larvae and pupae of the F1 generation after irradiation, while the longevity of the adults, the duration of pre-oviposition period and the whole oviposition periods were shortened. Also, there was a reduction in the survival rate of both larvae and the whole period from first instar larvae to adult. In addition, the sex ratio of adults of the F1 generation of moths following the irradiation of their male parent became more male biased as the dose increased. This finding is consistent with research on *Phyllocnistis citrella* using gamma rays at 100–250 Gy and on *Ostrinia nubilalis* using 90–180 Gy (Osouli et al., 2023). Moreover, oviposition per female in the F1 generation declined progressively with increasing irradiation dose, and at the 50 and 100 Gy levels, there was a complete loss of egg hatch in the F2 generation.

This study examined the physiological responses of *X. c-nigrum* to X-ray irradiation, including development and reproduction. However, before these findings can be applied at a field scale, the post-treatment effects of irradiation on moth behaviors such as on flight ability and mating competitiveness, as well as the impact of different ratios of irradiated males to wild moths, need to be examined. Preliminary findings from this study suggest that employing 100 Gy of X-rays irradiation may be effect for SIT programs against *X. c-nigrum*.

Data availability statement

The raw data supporting the conclusion of this article will be made available by the authors, without undue reservation.

Ethics statement

The manuscript presents research on animals that do not require ethical approval for their study.

Author contributions

SC: Writing–original draft, Writing–review and editing, Formal Analysis, Investigation. BL: Formal Analysis, Writing–original draft, Writing–review and editing. HL: Writing–review and editing, Investigation. KL: Investigation, Writing–review and editing. YL: Writing–review and editing, Conceptualization, Data curation, Funding acquisition, Methodology, Project administration, Software, Supervision, Validation, Visualization, Writing–original draft.

Funding

The author(s) declare financial support was received for the research, authorship, and/or publication of this article. This work was supported by the National Key R&D Program of China (2022YFD1400300), China Agriculture Research System of MOF and MARA (CARS-15-19).

Acknowledgments

We thank Xie Wang, Yike Zhou, Yu Zhang, and Wannan Cheng for their contributions to this research.

Conflict of interest

The authors declare that the research was conducted in the absence of any commercial or financial relationships that could be construed as a potential conflict of interest.

Publisher's note

References

Aksoy, H. A., Yazıcı, N., and Erel, Y. (2017). Effects of X-ray irradiation on different stages of *Sesamia nonagrioides* Lefebvre (Lepidoptera: noctuidae) and DNA damage. *Radiat. Phys. Chem.* 130, 148–153. doi:10.1016/j.radphyschem.2016.08.012

Andreev, S. V., and Martens, B. K. (1974). "Research on the technique of radiation sterilisation of insect pests in the USSR," in *IAEA and the FAO of the united nations international atomic energy agency; food and agriculture organization: sterility principle for insect control* (Innsbruck: FAO), 103–114.

Barnes, B. N., Eyles, D. K., and Franz, G. (2004). "South Africa's fruit fly programme – the Hex River Valley pilot project and beyond," in *Proceedings of the 6th international symposium on fruit flies of economic importance*. Editor B. N. Barnes (South Africa: Isteg Scientific Publications), 131–141.

Broad, G. R., and Boyes, D. (2022). The genome sequence of the setaceous Hebrew character, *Xestia c-nigrum*, (Linnaeus, 1758). *Wellcome Open Res.* 7, 295. doi:10.12688/wellcomeopenres.18608.1

Brower, J. H. (1976). Recovery of fertility by irradiated males of the Indian meal moth. *J. Econ. Entomol.* 69 (2), 273–276. doi:10.1093/jee/69.2.273

Chen, C., Aldridge, R. L., Gibson, S., Kline, J., Aryaprema, V., Qualls, W., et al. (2023). Developing the radiation-based sterile insect technique (SIT) for controlling *Aedes aegypti*: identification of a sterilizing dose. *Pest Manag. Sci.* 79 (3), 1175–1183. doi:10.1002/ps.7303

Chiluwal, K., Kim, J., Bae, S. D., Roh, G. H., Park, H. J., and Park, C. G. (2019). Effect of gamma irradiation on fecundity, sterility, and female sex pheromone production of *Callosobruchus chinensis* (Coleoptera: bruchidae). *J. Econ. Entomol.* 112 (1), 156–163. doi:10.1093/jee/toy317

Gómez-Simuta, Y., Parker, A., Cáceres, C., Vreysen, M. J. B., and Yamada, H. (2021). Characterization and dose-mapping of an X-ray blood irradiator to assess application potential for the sterile insect technique (SIT). *Appl. Radiat. Isot.* 176, 109859. doi:10.1016/j.apradiso.2021.109859

Goudarzi, M., Moosavi, M. R., and Asadi, R. (2015). Effects of entomopathogenic nematodes, *Heterorhabditis bacteriophora* (poinar) and *Steinernema carpocapsae* (weiser), in biological control of *Agrotis segetum* (denis and schiffermüller) (Lepidoptera: noctuidae). *Turk. Entomol. Derg.-Tu.* 39 (3), 239–250. doi:10.16970/ted.43220

Helinski, M. E., and Knols, B. G. (2009). Sperm quantity and size variation in un-irradiated and irradiated males of the malaria mosquito *Anopheles arabiensis* Patton. *Acta. Trop.* 109 (1), 64–69. doi:10.1016/j.actatropica.2008.10.002

Hrudová, E., Juroch, J., Svobodová, E., and Balek, J. (2022). Current possibilities and limits of using Noctuidae species occurrence prediction on sugar beet in conditions of Czech Republic. *Listy. Cukrov. Repar.* 138 (3), 106–110.

IDIDS (2023). International database on insect disinfestation and sterilization. Avaliable at: https://nucleus.iaea.org/sites/naipc/Pages/default.aspx (Accessed November 28, 2023).

Jiang, S., Fu, X. W., Jiang, S. S., Yang, X. M., Zhao, H. Y., and Wu, K. M. (2022a). Effect of X-ray irradiation on development, flight, and reproduction of *Spodoptera litura*. *Front. Physiol.* 13, 947848. doi:10.3389/fphys.2022.947848

Jiang, S., He, L. M., He, W., Zhao, H. Y., Yang, X. M., Yang, X. Q., et al. (2022b). Effects of X-ray irradiation on the fitness of the established invasive pest fall armyworm *Spodoptera frugiperda*. *Pest Manag. Sci.* 78 (7), 2806–2815. doi:10.1002/ps.6903

Judd, G., Arthur, S., Deglow, K., and Gardiner, M. (2011). Operational mark–release–recapture field tests comparing competitiveness of wild and differentially mass-reared codling moths from the Okanagan–Kootenay sterile insect program. *Can. Entomol.* 143 (3), 300–316. doi:10.4039/n11-005

Kapranas, A., Collatz, J., Michaelakis, A., and Milonas, P. (2022). Review of the role of sterile insect technique within biologically-based pest control – an appraisal of existing regulatory frameworks. *Entomol. Exp. Appl.* 170 (5), 385–393. doi:10.1111/eea.13155

Khattak, S. U. K., Howell, F. J., and White, L. D. (1989). Control of tropical spotted cutworm, *Amathes c-nigrum* (L), by gamma radiation. *Trop. Pest Manag.* 35 (1), 97–99. doi:10.1080/09670878909371328

Kim, J., Jung, S., Jang, S. A., Kim, J., and Park, C. G. (2015). X-ray radiation and development inhibition of *Helicoverpa armigera* Hübner (Lepidoptera: noctuidae). *Radiat. Phys. Chem.* 115, 148–152. doi:10.1016/j.radphyschem.2015.06.021

Klassen, W., and Vreysen, M. J. B. (2021). "Area-wide integrated pest management and the sterile insect technique," in *Sterile insect technique*. Editors V. A. Dyck, J. Hendrichs, and A. S. Robinson (Boca Raton , Florida: CRC Press), 75–112. doi:10.1201/9781003035572

Koyama, J., Kakinohana, H., and Miyatake, T. (2004). Eradication of the melon fly, *Bactrocera cucurbitae*, in Japan: importance of behavior, ecology, genetics, and evolution. *Annu. Rev. Entomol.* 49, 331–349. doi:10.1146/annurev.ento.49.061802.123224

Kumano, N., Haraguchi, D., and Tsurui-Sato, K. (2018). Effects of X-ray irradiation on male sperm transfer ability and fertility in the sweet potato weevils *Euscepes postfasciatus* (Coleoptera: Curculionidae) and *Cylas formicarius* (Coleoptera: brentidae). *Appl. Entomol. Zool.* 53 (4), 485–492. doi:10.1007/s13355-018-0578-4

Li, Y. J. (2006). Integration of sterile insect technique and egg parasitization (Trichogramma chilonis) for the eco-friendly management of Helicoverpa assulta (Lepidoptera: noctuidae). [dissertation/master's thesis]. Beijing, China: Chinese Academy of Agricultural Sciences.

Light, D. M., Ovchinnikova, I., Jackson, E. S., and Haff, R. P. (2015). Effects of X-ray irradiation on male navel orangeworm moths (Lepidoptera: Pyralidae) on mating, fecundity, fertility, and inherited sterility. *J. Econ. Entomol.* 108 (5), 2200–2212. doi:10.1093/jee/tov201

Mansour, M., and Mohamad, F. (2004). Effects of gamma radiation on codling moth, *Cydia pomonella* (L.), eggs. *Radiat. Phys. Chem.* 71 (6), 1125–1128. doi:10.1016/j.radphyschem.2003.12.051

Marec, F., and Vreysen, M. J. B. (2019). Advances and challenges of using the sterile insect technique for the management of pest Lepidoptera. *Insects* 10 (11), 371. doi:10.3390/insects10110371

Mastrangelo, T., Parker, A. G., Jessup, A., Pereira, R., Orozco-Dávila, D., Islam, A., et al. (2010). A new generation of X ray irradiators for insect sterilization. *J. Econ. Entomol.* 103 (1), 85–94. doi:10.1603/ec09139

M'Saad Guerfali, M., Hamden, H., Fadhl, S., Marzouki, W., Raies, A., and Chevrier, C. (2011). Improvement of egg hatch of *Ceratitis capitata* (Diptera: tephritidae) for enhanced output. *J. Econ. Entomol.* 104 (1), 188–193. doi:10.1603/ec10065

Neven, L. G., and Wakie, T. (2020). Effects of irradiation on codling moth (Lepidoptera: tortricidae) first through third instars in sweet cherries. *J. Entomol. Sci.* 55 (4), 570–577. doi:10.18474/0749-8004-55.4.570

Orozco, D., Hernandez, M. R., Meza, J. S., and Quintero, J. L. (2013). Do sterile females affect the sexual performance of sterile males of *Anastrepha ludens* (Diptera: tephritidae)? *J. Appl. Entomol.* 137 (5), 321–326. doi:10.1111/j.1439-0418.2012.01748.x

Osouli, S., Atapour, M., and Ahmadi, M. (2023). Effect of gamma irradiation on F1 generation and competitive ability of *Phyllocnistis citrella* and *Ostrinia nubilalis*, and evaluation of the sterile insect release ratio on plant infestation in field cages. *Entomol. Exp. Appl.* 171 (6), 475–486. doi:10.1111/eea.13299

Pérez-Staples, D., Shelly, T. E., and Yuval, B. (2012). Female mating failure and the failure of 'mating' in sterile insect programs. *Entomol. Exp. Appl.* 146 (1), 66–78. doi:10.1111/j.1570-7458.2012.01312.x

Plá, I., García de Oteyza, J., Tur, C., Martínez, M. Á., Laurín, M. C., Alonso, E., et al. (2021). Sterile insect technique programme against Mediterranean fruit fly in the Valencian community (Spain). *Insects* 12 (5), 415. doi:10.3390/insects12050415

Proverbs, M., Newton, J., and Campbell, C. (1982). Colding moth: a pilot program of control by sterile insect release in British Columbia. *Can. Entomol.* 114 (4), 363–376. doi:10.4039/Ent114363-4

Ramírez-Santos, E., Rendon, P., Gouvi, G., Zacharopoulou, A., Bourtzis, K., Cáceres, C., et al. (2021). A novel genetic sexing strain of *Anastrepha ludens* for cost-effective sterile insect technique applications: improved genetic stability and rearing efficiency. *Insects* 12 (6), 499. doi:10.3390/insects12060499

R Development Core Team (2023). *R: a language and environment for statistical computing, Version 4.3.1*. Austria: Vienna: R Foundation for Statistical Computing. Avaliable at: http://www.R-project.org.

Salem, H. M., Fouda, M. A., Abas, A. A., Ali, W. M., and Gabarty, A. (2014). Effects of gamma irradiation on the development and reproduction of the greasy cutworm, *Agrotis ipsilon* (Hufn.). *J. Radiat.* 7 (1), 110–115. doi:10.1016/j.jrras.2013.12.007

Saour, G., Hashem, A., and Jassem, I. (2022). Mating competitiveness of irradiated *Lobesia botrana* (Lepidoptera: tortricidae) in male-only and both sex release strategies under laboratory cage conditions. *Insects* 14 (1), 18. doi:10.3390/insects14010018

Shelly, T. E., and Manoukis, N. C. (2022). Mating competitiveness of *Bactrocera dorsalis* (Diptera: tephritidae) males from a genetic sexing strain: effects of overflooding ratio and released females. *J. Econ. Entomol.* 115 (3), 799–807. doi:10.1093/jee/toac027

Subchev, M., Toth, M., Szocs, G., Stan, G., and Botar, A. (1996). Evidence for geographical differences in pheromonal responses of male *Amathes c-nigrum* L. (Lep., Noctuidae). *J. Appl. Entomol.* 120 (1), 615–617. doi:10.1111/j.1439-0418.1996.tb01660.x

Therneau, T. (2023). A package for survival analysis in R. R package version 3.5-5. Avaliable at: https://CRAN.R-project.org/package.

Vaiserman, A. M., Koshel, N. M., and Voitenko, V. P. (2004). Effect of X-irradiation at larval stage on adult lifespan in *Drosophila melanogaster*. *Biogerontology* 5 (1), 49–54. doi:10.1023/b:bgen.0000017686.69678.0c

Venables, W. N., and Ripley, B. D. (2002). *Modern applied statistics with S*. fourth edition. New York: Springer. Avaliable at: https://www.stats.ox.ac.uk/pub/MASS4/.

Wang, L. M., Li, N., Ren, C. P., Peng, Z. Y., Lu, H. Z., Li, D., et al. (2023). Sterility of *Aedes albopictus* by X-ray irradiation as an alternative to γ-ray irradiation for the sterile insect technique. *Pathogens* 12 (1), 102. doi:10.3390/pathogens12010102

Weng, A. Z., Wang, A. J., Wang, L. Y., Mei, X. D., She, D. M., and Ning, J. (2019). Synthesis and bioactivities of novel fluorine–substituted sex pheromone analogues of spotted cutworm, *Xestia c-nigrum* Linnaeus. *Chin. J. Synth. Chem.* 27 (5), 329–334. doi:10.15952/j.cnki.cjsc.1005-1511.18075

Woods, B., Mcinnis, D. O., Steiner, E., Soopaya, A., Lindsey, J., Lacey, I., et al. (2016). Competitiveness of sterile light brown apple moths (Lepidoptera: tortricidae) in western Australia. *Fla. Entomol.* 99 (1), 135–148. doi:10.1653/024.099.sp117

Wright, L. C., James, D. J., Reyna, V., Conte, S. C. D., Gingras, S., Landolt, P., et al. (2010). Species composition of cutworm (Lepidoptera: noctuidae) larvae in south central Washington Vineyards. *Ann. Entomol. Soc. Am.* 103 (4), 592–596. doi:10.1603/AN09112

Wu, M. Y. (2020). Effect of diallyl trisulfide on sperm quality of Sitotroga cerealella (Olivier). [dissertation/master's thesis]. Wuhan, China: Huazhong Agricultural University.

Zhang, H. T., Liu, J. N., Tan, L., and Zhu, Y. (2020). Sexing of *Helicoverpa armigera* pupae based on machine vision. *Tob. Sci. Technol.* 53 (2), 21–26. doi:10.16135/j.issn1002-0861.2019.0127

Zhang, J. H., Li, N., Zhao, H. Y., Wang, Y. Q., Yang, X. Q., and Wu, K. M. (2023). Sterility of *Cydia pomonella* by X ray irradiation as an alternative to gamma radiation for the sterile insect technique. *Bull. Entomol. Res.* 113 (1), 72–78. doi:10.1017/S0007485322000323

Zhang, Y. J., Lu, Q., Gu, S. H., Lu, Y. H., and Wu, K. M. (2012). *Preparation and application of artificial diet for Agrotis ipsilon larvae China Patent No CN101584411B*. Beijing: Institute of Plant Protection, Chinese Academy of Agricultural Sciences.

Zhao, J., Li, S., Xu, L., Li, C., Li, Q., Dewer, Y., et al. (2022). Effects of X-ray irradiation on biological parameters and induced sterility of *Ephestia elutella*: establishing the optimum irradiation dose and stage. *Front. Physiol.* 13, 895882. doi:10.3389/fphys.2022.895882

frontiers | Frontiers in Physiology

TYPE Original Research
PUBLISHED 21 June 2024
DOI 10.3389/fphys.2024.1427385

OPEN ACCESS

EDITED BY
Bin Tang,
Hangzhou Normal University, China

REVIEWED BY
Agata Kaczmarek,
Polish Academy of Sciences, Poland
Saif Ul Malook,
University of Florida, United States

*CORRESPONDENCE
Xinzheng Huang,
huangxinzheng@cau.edu.cn
Cong'ai Zhen,
zhencongai@126.com

†These authors have contributed equally to this work

RECEIVED 03 May 2024
ACCEPTED 31 May 2024
PUBLISHED 21 June 2024

CITATION
Sun X, Li W, Yang S, Ni X, Han S, Wang M, Zhen C and Huang X (2024), Insecticidal activity and underlying molecular mechanisms of a phytochemical plumbagin against *Spodoptera frugiperda*. *Front. Physiol.* 15:1427385. doi: 10.3389/fphys.2024.1427385

Insecticidal activity and underlying molecular mechanisms of a phytochemical plumbagin against *Spodoptera frugiperda*

Xiaoyu Sun[1†], Wenxuan Li[2†], Shuang Yang[1], Xueqi Ni[1], Shengjie Han[3], Mengting Wang[1], Cong'ai Zhen[1*] and Xinzheng Huang[1*]

[1]Department of Entomology, MOA Key Lab of Pest Monitoring and Green Management, College of Plant Protection, China Agricultural University, Beijing, China, [2]College of Food Science and Nutritional Engineering, China Agricultural University, Beijing, China, [3]College of Horticulture and Plant Protection, Henan University of Science and Technology, Luoyang, China

Introduction: Plumbagin is an important phytochemical and has been reported to exhibit potent larvicidal activity against several insect pests, However, the insecticidal mechanism of plumbagin against pests is still poorly understood. This study aimed to investigate the insecticidal activities of plumbagin and the underlying molecular mechanisms against a devastating agricultural pest, the fall armyworm *Spodoptera frugiperda*.

Methods: The effects of plumbagin on *S. frugiperda* larval development and the activities of two detoxification enzymes were initially examined. Next, transcriptomic changes in *S. frugiperda* after plumbagin treatment were investigated. Furthermore, RNA-seq results were validated by qPCR.

Results: Plumbagin exhibited a high larvicidal activity against the second and third instar larvae of *S. frugiperda* with 72 h LC_{50} of 0.573 and 2.676 mg/g, respectively. The activities of the two detoxification enzymes carboxylesterase and P450 were significantly increased after 1.5 mg/g plumbagin treatment. Furthermore, RNA-seq analysis provided a comprehensive overview of complex transcriptomic changes in *S. frugiperda* larvae in response to 1.5 mg/g plumbagin exposure, and revealed that plumbagin treatment led to aberrant expression of a large number of genes related to nutrient and energy metabolism, humoral immune response, insect cuticle protein, chitin-binding proteins, chitin synthesis and degradation, insect hormone, and xenobiotic detoxification. The qPCR results further validated the reproducibility and reliability of the transcriptomic data.

Discussion: Our findings provide a valuable insight into understanding the insecticidal mechanism of the phytochemical plumbagin.

KEYWORDS

***Spodoptera frugiperda*, plumbagin, RNA-seq, detoxification enzyme, toxicological mechanism**

1 Introduction

The fall armyworm, *Spodoptera frugiperda* (J.E. Smith), a migratory, highly polyphagous, and widely distributed destructive lepidopteran pest species, is native to tropical and subtropical areas of the Americas (Kenis et al., 2023). Since 2016, this pest has invaded West Africa, and then rapidly spread to sub-Saharan Africa nations, Asia, and parts of Oceania such as southern Australia (Kenis et al., 2023; Tay et al., 2023). In China, *S. frugiperda* was first observed in January 2019 from maize field in Jiangcheng County, Yunnan Province (Guo et al., 2023; Sun et al., 2021), and then quickly spread to 27 provinces (autonomous regions and municipalities) across China, and thus being considered to be a major invasive crop pest posing a significant threat to crop production and agricultural food security (Wang et al., 2023). Generally, most farmers and agricultural practices in many invasive regions have relied primarily on the application of synthetic pesticides to manage *S. frugiperda*. Unfortunately, their improper application and excessive utilization have brought various negative effects such as nontarget toxicity, pesticide residue accumulation in agricultural products and the environment, and resistance of this pest to spinosad, diamides and *Bacillus thuringiensis* (Zhao et al., 2022; Tay et al., 2023). Over the past few years, significant progress has been made in the development of effective and sustainable management strategies to control this devastating pest in many recently invaded countries, including China. For example, effective and eco-friendly botanical pesticides have received increasing attention in sustainable agriculture, and are recognized as one of the most promising alternatives to synthetic insecticides for the development and practical implementation of integrated pest management programmes (Kenis et al., 2023).

Plumbagin, 5-hydroxy-2-methyl-1,4-naphthoquinone ($C_{11}H_8O_3$), is an important secondary metabolite and bioactive compound in plants originally isolated from the medicinal plant *Plumbago zeylanica* and has been reported to exhibit potent larvicidal activity against several insect pests, including *S. litura* (Tokunaga et al., 2004; Rajendra Prasad et al., 2012), *Achaea Janata* (Rajendra Prasad et al., 2012), *Trichoplusia ni* (Akhtar et al., 2012a), *Musca domestica* (Pavela, 2013), *Helicoverpa armigera* (Hu et al., 2018), *Pieris rapae* (Hu et al., 2018), *Mythimna separate* (Shang et al., 2019), *Nilaparvata lugens* (Shang et al., 2019), *S. littoralis* (Davila-Lara et al., 2021; Rahman-Soad et al., 2021), *Aedes aegypti* (de Oliveira et al., 2022), and three aphid species (Akhtar et al., 2012b), as well as acaricidal activity against the herbivorous mite *Tetranychus urticae* (Akhtar et al., 2012b). The results of these studies have indicated that plumbagin has great potential to be developed as a potent botanical insecticide and an alternative to synthetic insecticides. However, little is known about the acute toxicity of plumbagin on *S. frugiperda* and the underlying molecular mechanisms of larvae in response to plumbagin exposure.

Recently, rapid and remarkable developments in sequencing technology and increasing numbers of complete insect genomes have opened up new avenues for exploring global transcriptome changes reflecting the physiological state of insect pests to plant metabolites exposures, unveiling previously unknown mechanisms and mining functional genes (Lin et al., 2023; Li et al., 2023). Huang et al. (2018) used RNA-Seq and qPCR to characterize the expression levels of detoxification genes, especially P450 genes in *Sitophilus zeamais* responding to terpinen-4-ol, the main constituent of *Melaleuca alternifolia* essential oil. Li et al. (2023) analyzed transcriptome profiling of linalool-exposed *Pagiophloeus tsushimanus* larvae using RNA-seq and single-molecule real-time sequencing. Gene ontology enrichment of DEGs revealed that overall upregulation of DEGs encoding cytochrome P450s and cuticular proteins was the primary response characteristic in larvae upon exposure to linalool. The effects of several plant metabolites such as carvacrol (Liu et al., 2023), toosendanin (Lin et al., 2023), camptothecin (Shu et al., 2021a; Shu et al., 2021b), azadirachtin (Shu et al., 2021c), and chlorogenic acid (Lin et al., 2023) on gene expression profiles and enzyme activities in *S. frugiperda* larvae have recently been studied using RNA-seq and enzyme activity assays in order to elucidate the response mechanism. These findings indicated that these metabolites influenced the normal physiological activities of *S. frugiperda* at multiple levels.

In this study, the effects of plumbagin on *S. frugiperda* larval development and on the activities of two detoxification enzymes were examined to assess its bioactivity against this devastating agricultural pest. Next, transcriptomic changes of *S. frugiperda* after plumbagin treatment were investigated to elucidate the underlying molecular mechanism of its insecticidal activity. Furthermore, RNA-seq results were confirmed by qPCR. Our results will provide a better understanding of the toxicological mechanism of plumbagin used as a botanical pesticide against pests.

2 Material and methods

2.1 Insect

Eggs of *S. frugiperda* used in this study were supplied by the Institute of Plant Protection, Chinese Academy of Agricultural Sciences, which were collected from maize fields in Jiangcheng, Yunnan Province, China. The larvae were reared on artificial diet in a growth room at 26°C ± 1°C, 70% ± 5% relative humidity, with a photoperiod of 14:10 (L:D) as described previously (Su et al., 2023).

2.2 Bioassays and enzyme activity assays

Plumbagin (CAS number: 481-42-5) was purchased from Sigma-Aldrich. Dissolved in acetone, plumbagin was incorporated into the artificial diet at various concentrations of 3, 1.5, 0.75, 0.375, 0.1875, 0.09375 mg/g. Artificial diet incorporating acetone was used as control. A single second or third instar *S. frugiperda* larvae was placed in petri dish (35 mm in diameter × 2 cm in height) and reared on 1 g artificial diet. They were allowed to feed for 7 days, and mortality was recorded. Three biological replicates, each comprising a total of 20 larvae, were analyzed. The larval weight of surviving *S. frugiperda* was also recorded daily for 4 days.

Ten third instar larvae fed on diet containing 1.5 mg/g plumbagin were homogenized in 1 mL phosphate buffer solution. The homogenate was centrifuged for 20 min (13,000 rpm, 4°C), and the supernatants were collected for further enzyme activity assays. The enzyme activities of two detoxification enzymes carboxylesterase (CarE) and P450 were determined using the Carboxylesterase Test Kit (A133-1-1) and the Cytochrome P450 Assay Kit (H303-1-2) from Nanjing Jiancheng Bioengineering Institute (Jiangsu, China) following the manufacturer's protocol.

2.3 RNA isolation and illumina sequencing

Third-instar *S. frugiperda* larvae were provided with an artificial diet incorporating 1.5 mg/g plumbagin as described above for bioassays. The larvae fed with an artificial diet containing acetone were used as controls. After 3 days, the survival larvae were collected and then subjected to RNA extraction and RNA sequencing analysis. Total RNA extraction was performed using TRIzol reagent (Invitrogen) following the manufacturer's instructions. At least four biological replicates were analyzed for each treatment.

RNA purity was evaluated using the NanoPhotometer® spectrophotometer (IMPLEN, CA, United States). A total of 3 μg RNA per sample was utilized for cDNA library preparation with the NEBNext Ultra RNA Library Prep Kit according to the manufacturer's instructions. Samples were sequenced on an Illumina NovaSeq6000 platform (Biomics Biotech Co., Ltd., Beijing, China). Clean reads were aligned to the chromosome-level assembled genome of *S. frugiperda* available at http://v2.insect-genome.com/Organism/715 using TopHat v2.0.12 software. Gene Ontology (GO) and KEGG pathway enrichment analyses for differentially expressed genes (DEGs) were conducted using the GOseq R package and KOBAS software, respectively. Genes with a $\log_2|\text{fold change}| > 1$ and FDR < 0.05 were considered as DEGs.

2.4 qPCR validation

The qPCR validation was carried out based on SuperReal PreMix Plus (SYBR Green) reagent kit (TianGen, Beijing, China), according to the manufacturer's instructions (Huang et al., 2018) and using the same samples used for RNA-seq. The qPCR programme was 95°C for 10 min, followed by 40 cycles of 95°C for 15 s and 60°C for 30 s. The gene β-actin was used as a reference gene as described previously (Su et al., 2023). The primers for qPCR were listed in Supplementary Table S1.

2.5 Statistical analysis

POLO Plus software was used to calculate the median lethal concentration (LC_{50}), with corresponding 95% confidence interval (CI) and chi-square (χ^2) of the probit regression equation. For data on larval weight and enzyme activity assay, statistical analysis was performed using one-way analysis of variance (ANOVA) with LSD/Duncan pairwise comparison testing.

3 Results

3.1 Bioactivity of plumbagin against *Spodoptera frugiperda* larvae

The toxicity of plumbagin to *S. frugiperda* was determined using second or third instar larvae. The results showed that plumbagin exhibited significant insecticidal activity against *S. frugiperda* larvae, and the LC_{50} values for second instar and third instar were 0.573 and 2.676 mg/g, respectively (Table 1). The mortality rate of 1.5 mg/g plumbagin treatment after 7 days was 91.53% (Figure 1A). The survival larvae during 1.5 mg/g plumbagin treatment displayed lower weight compared to controls, with weight reduction from 43.57 to 15.90 mg after 4 days (Figure 1B).

3.2 Enzyme activities of two detoxification enzymes in *S. frugiperda* larvae after plumbagin exposure

Furthermore, enzyme activity assays revealed that 1.5 mg/g plumbagin treatment significantly improved the activities of the two detoxification enzymes CarE and P450 compared with the control, with a 4.13- and 1.72-fold increase, respectively (Figure 2).

3.3 Global transcriptome changes in *S. frugiperda* larvae after plumbagin exposure

Transcriptome sequencing of *S. frugiperda* larvae upon plumbagin exposure was conducted to explore the molecular mechanisms underlying the larvicidal activity of plumbagin. Nine independent cDNA libraries were generated, comprising four for the plumbagin treatment group and five for the control group. The raw reads number ranged from 41,489,334 to 45,978,878, while high quality clean reads varied between 40,213,076 and 45,148,130. The proportion of mapped clean reads in each sample ranged from 77.56% to 80.91% (Supplementary Table S2). Correlation within each group of experimental and control samples were generally high (Figure 3A). Principal component analysis (PCA) showed that the plumbagin-exposed samples and controls formed distinct clusters, indicating plumbagin exposure led to aberrant expression of genes in *S. frugiperda* larvae (Figure 3B).

3.4 Functional category of plumbagin-responsive DEGs in *S. frugiperda* larvae

After plumbagin exposure, a total of 1,614 genes with a $\log_2|\text{fold change}| > 1$ and FDR < 0.05 were identified as differentially expressed genes (DEGs) in *S. frugiperda* larvae. Among these DEGs, 445 were upregulated and 1,080 were downregulated (Figure 3C).

Functional enrichment analysis including GO annotation enrichment, KOG functional enrichment and KEGG pathway analysis were conducted to explore the functional categories of these DEGs (Figures 4, 5), which showed that the plumbagin treatment exhibited profound strong adverse effects on many essential genes involved in amino acid transport and metabolism (75 out of 104 DEGs), carbohydrate transport and metabolism (43 out of 54 DEGs), energy production and conversion (23 out of 28 DEGs), lipid transport and metabolism (51 out of 69 DEGs), nucleotide transport and metabolism (15 out of 23 DEGs), and replication, recombination and repair (31 out of 35 DEGs). Also, most DEGs related to humoral immune response (38 out of 50 DEGs), insect cuticle protein (21 out of 27 DEGs), insect hormone (27 out of 38 DEGs), detoxification enzymes (49 out of

TABLE 1 Toxicity of plumbagin against *S. frugiperda* larvae after 72 h of treatment.

Larval stage	Slope ± SE[a]	LC_{50} (95% CI)[b] mg/g	χ^2 (df)	*p*-value
2nd	2.690 ± 0.346	0.573 (0.471–0.696)	13.500 (13)	0.410
3rd	1.362 ± 0.243	2.676 (1.800–5.528)	13.781 (13)	0.389

[a]SE, standard error.
[b]95% CI, 95% confidence intervals.

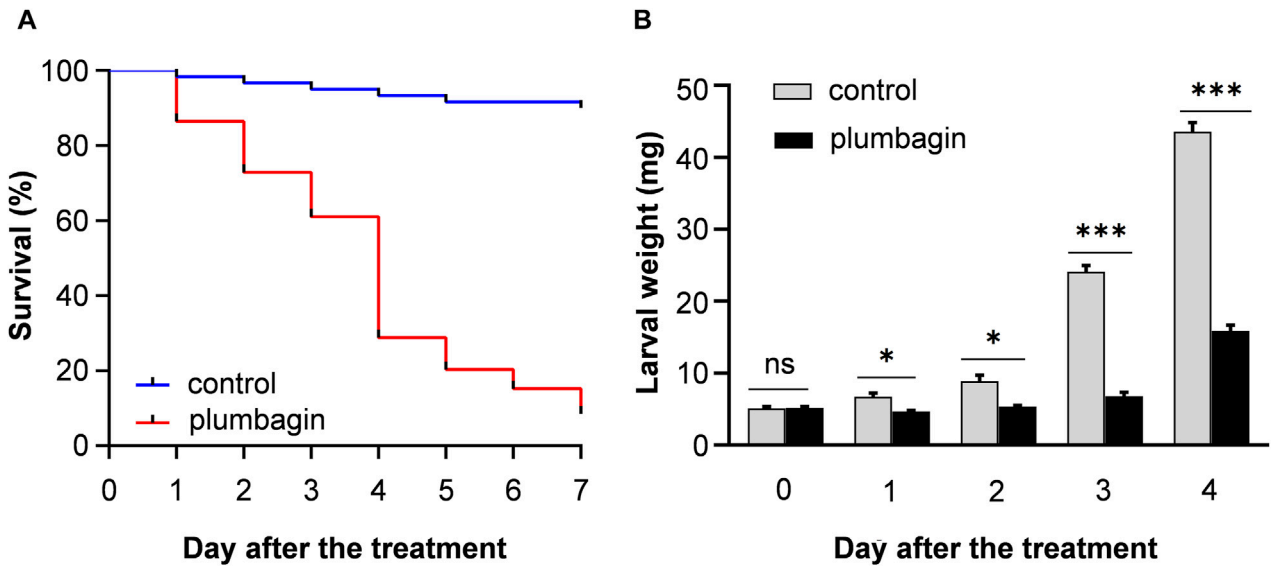

FIGURE 1
The survival rate **(A)** and larval weight **(B)** of *S. frugiperda* after 1.5 mg/g plumbagin treatment.

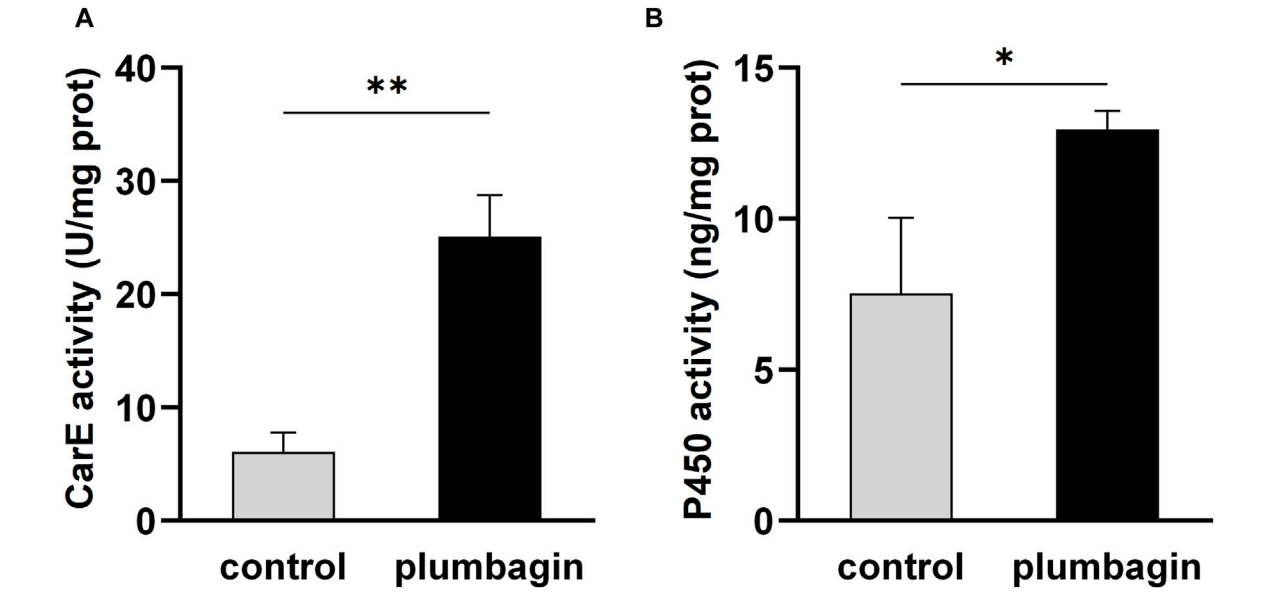

FIGURE 2
The activities of two detoxification enzymes in third-instar *S. frugiperda* larvae after 1.5 mg/g plumbagin treatment. **(A)** Carboxylesterase (CarE) activity. **(B)** P450 activity.

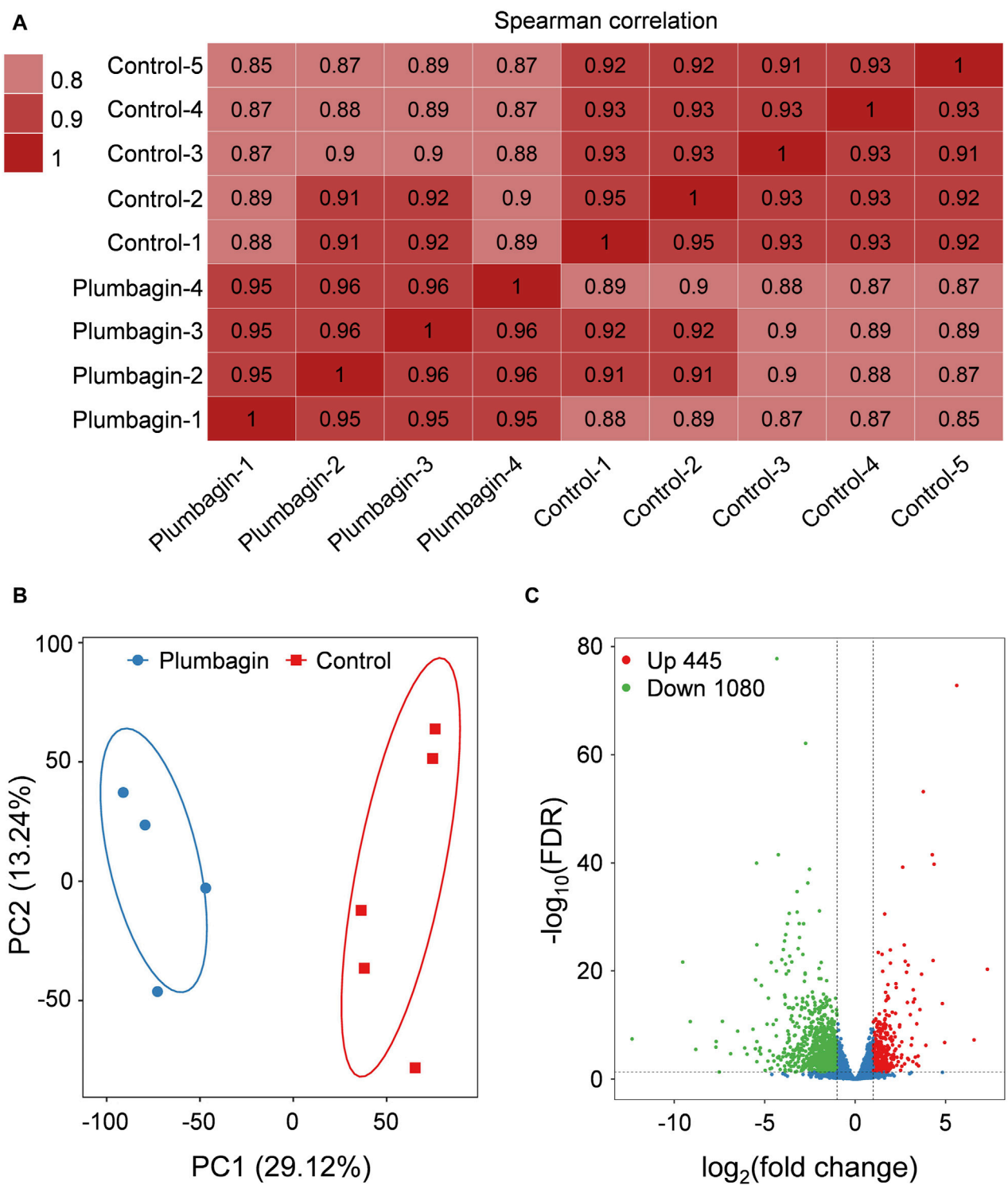

FIGURE 3
Transcriptome profile of RNA-Seq data. **(A)** Correlation matrix of the samples utilizing Spearman's correlation coefficients. **(B)** Principal component analysis of the samples. **(C)** Volcano plot of RNA-Seq data.

74 DEGs) and digestive enzymes (69 out of 81 DEGs) were downregulated. It is noteworthy that all DEGs associated with chitin synthesis and degradation (8 of 8) and chitin-binding proteins (15 of 15) were downregulated, while all of the 10 DEGs related to endocytosis were upregulated (Figures 4, 5).

3.5 Validation of transcriptomic data by qPCR

To validate the RNA-seq results, nine genes were analyzed by qPCR, which are involved in humoral immune response (XLOC_

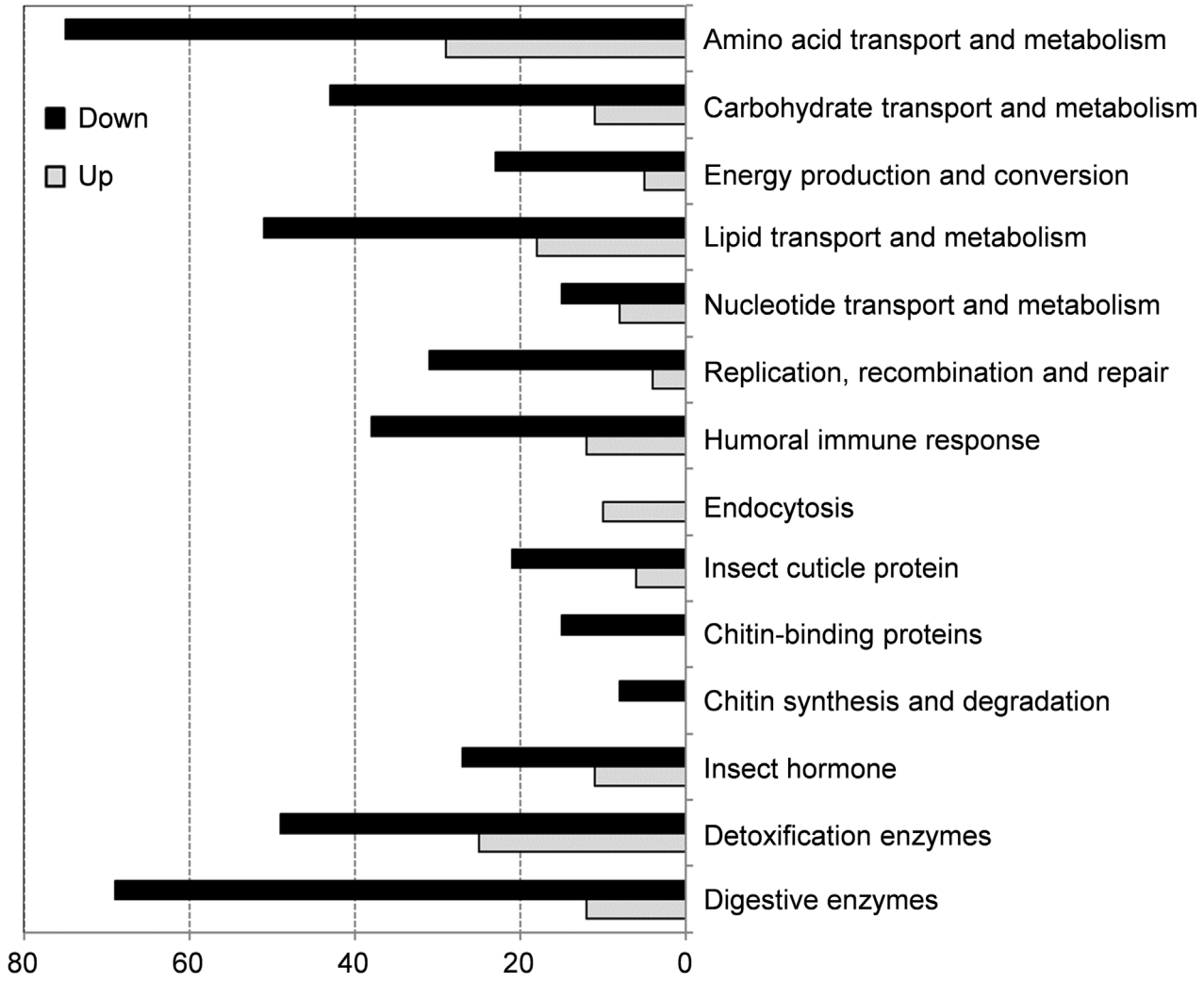

FIGURE 4
Enrichment analyses of differentially expressed genes (DEGs) in *S. frugiperda* larvae after 1.5 mg/g plumbagin treatment.

005114 and Sfru004462), insect hormone (Sfru007117) chitin synthesis and degradation (Sfru010180 and Sfru012164) detoxification enzymes (Sfru020044, XLOC_004422 and Sfru016345) digestive enzymes (Sfru017470) were selected and analyzed by qPCR. The qPCR results exhibited a high level of concordance with the transcriptomic data (Figure 6), confirming the reproducibility and reliability of the transcriptomic data.

4 Discussion

In this study, the bioassay experiments demonstrated that plumbagin, a natural small molecule naphthoquinone compound in plants, exhibited a high insecticidal activity against the larvae of the distributed destructive lepidopteran pest *S. frugiperda*, consistent with previously reported results that the secondary metabolite has high toxicity to several other lepidopteran pests (Tokunaga et al., 2004; Akhtar et al., 2012a; Rajendra Prasad et al., 2012; Hu et al., 2018; Shang et al., 2019; Dávila-Lara et al., 2021; Rahman-Soad et al., 2021). The findings demonstrated that plumbagin has great potential to serve as a botanical pesticide for controlling second or third instar larvae. However, according to the Globally Harmonized System (GHS) of Classification and Labelling of Chemicals, the toxicity and LC_{50} value of plumbagin against *S. frugiperda* classify it as a Class 4 acute toxicant for humans. This classification may restrict its use as a pesticide. To overcome this limitation, the encapsulation of plumbagin in nanocarriers could be a promising method, enhancing its bioactivity and allowing for reduced dosages and frequencies, thereby effectively minimizing harm to humans and mammals.

To better understand molecular mechanisms underlying the insecticidal effects of plumbagin against *S. frugiperda*, RNA-seq analysis and subsequent qPCR experiments were conducted, which demonstrated that plumbagin treatment could stimulate complex, global transcriptome changes in *S. frugiperda* larvae. Transcriptomic analysis indicated that plumbagin exposure had profound adverse effects on biological and metabolic processes of three nutrients (proteins, lipids and carbohydrates), which are the principal sources of nutrients and energy for insects, and are essential for their normal growth and development (Toprak et al., 2020). Most

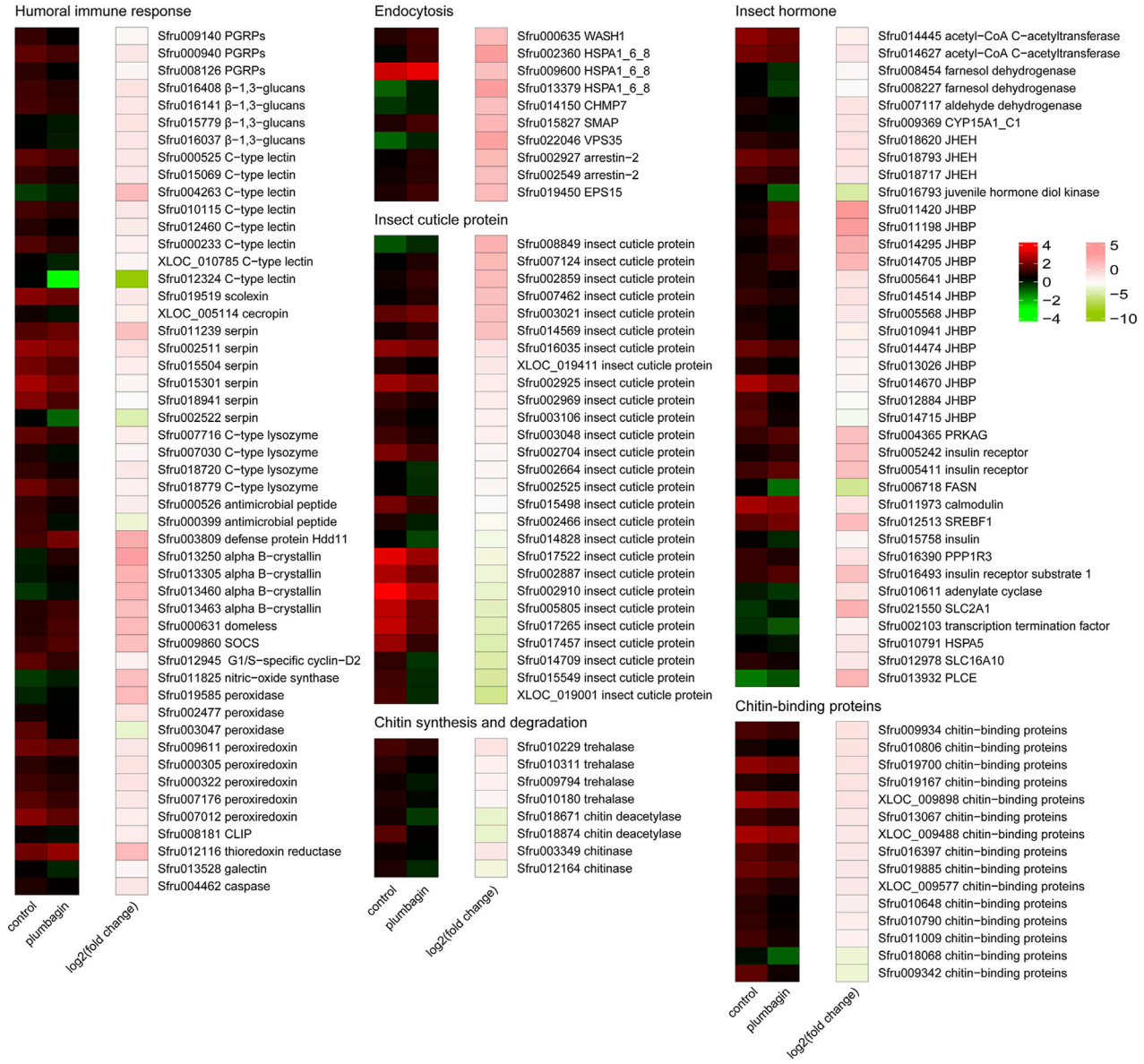

FIGURE 5
Heatmap analysis of differentially expressed genes (DEGs) in *S. frugiperda* larvae after plumbagin treatment. CLIP, clip domain serine protease; SOCS, suppressor of cytokine signaling 2; PGRPs, peptidoglycan recognition proteins; CHMP7, charged multivesicular body protein 7; HSPA1_6_8, heat shock 70 kDa protein 1/2/6/8; SMAP, stromal membrane-associated protein; VPS35, vacuolar protein sorting-associated protein 35; EPS15, epidermal growth factor receptor substrate 15; JHEH, juvenile hormone epoxide hydrolase; JHBP, haemolymph juvenile hormone binding protein; PRKAG, 5′-AMP-activated protein kinase, regulatory gamma subunit; FASN, fatty acid synthase, animal type; SREBF1, sterol regulatory element-binding transcription factor 1; PPP1R3, protein phosphatase 1 regulatory subunit 3A/B/C/D/E; SLC2A1, solute carrier family 2 (facilitated glucose transporter), member 1; HSPA5, heat shock 70 kDa protein 5; SLC16A10, solute carrier family 16 (monocarboxylic acid transporters), member 10; PLCE, phosphatidylinositol phospholipase C, epsilon; CYP15A1_C1, methyl farnesoate epoxidase/farnesoate epoxidase; WASH1, WAS protein family homolog 1.

DEGs related to amino acid transport and metabolism (75 out of 104 genes), lipid transport and metabolism (51 out of 69 genes), and carbohydrate transport and metabolism (43 out of 54 genes) were downregulated (Figures 4, 5). Moreover, most DEGs involved in protein digestion (7 of 8), lipid digestion (13 of 21), and carbohydrate digestion (49 of 52), were downregulated in *S. frugiperda* larvae after plumbagin treatment, which are important for absorption and utilization of these three nutrients. The general suppression of these growth-related genes indicated that plumbagin exposure displayed strong adverse effects on larval growth and development, strongly correlating with bioassay results. Similarly, carvacrol treatment significantly affect the expression levels of genes involved in the metabolism carbohydrates, lipids and proteins in *Lymantria dispar* (Chen et al., 2022).

Transcriptomic analysis showed that plumbagin treatment strongly altered the expression of genes encoding detoxification enzymes/proteins, including *CarEs* (5 up- and 17 downregulated genes), *P450s* (6 up- and 19 downregulated genes), *Glutathione S-transferases* (*GSTs*; 4 up- and 5 downregulated genes), *UDP-glycosyltransferases* (*UGTs*; 5 up- and 6 downregulated genes), *alkaline phosphatases*

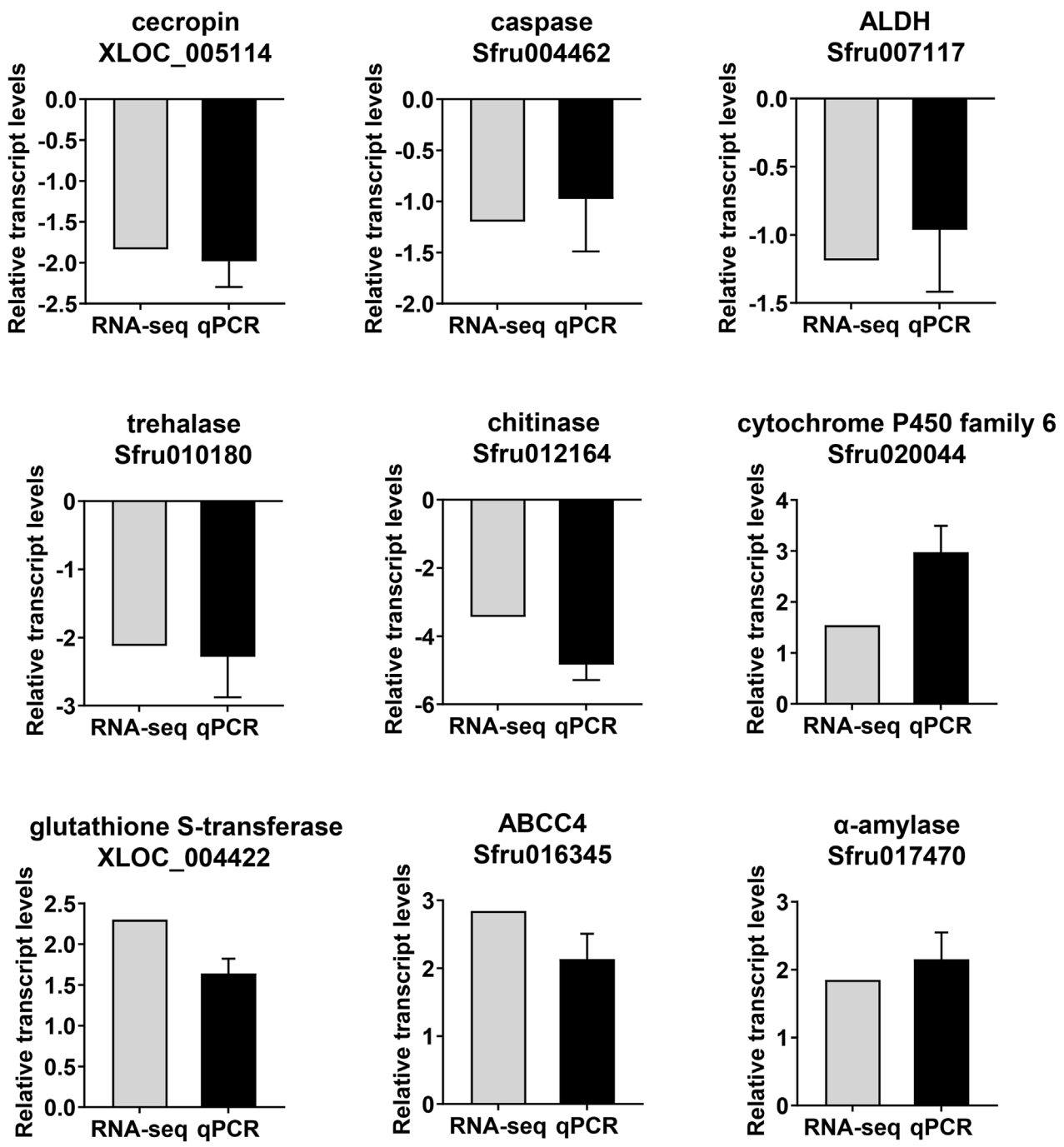

FIGURE 6
Comparison of expression levels of selected genes in RNA-seq and qPCR.

(2 downregulated genes), and *ABC transporters* (5 upregulated genes). These detoxification enzymes have been reported to play multiple roles in metabolic detoxification of a variety of xenobiotics (Amezian et al., 2021; Giraudo et al., 2015; Li et al., 2007; Vandenhole et al., 2021). For example, the UGT33 family member SfUGT33F28 in *S. frugiperda* is responsible for detoxification of the major maize defensive compound DIMBOA (2,4-dihydroxy-7-methoxy-1,4-benzoxazin-3-one) (Israni et al., 2020). CYP9A subfamily genes in two insect pests *Spodoptera exigua* and *S. frugiperda* collectively metabolize two furanocoumarin plant defense compounds (imperatorin and xanthotoxin) and three insecticides (pyrethroids, avermectins, and oxadiazines) (Shi et al., 2023). The carboxylesterase SexiCXE11 in *S. exigua* is able to degrade two plant allelochemicals pentyl acetate and (Z)-3-hexenyl caproate with >50% degradation (He et al., 2020). Although most DEGs responsible for CarEs and P450s were downregulated in *S. frugiperda* larvae (Figures 4, 5), enzyme activity assays revealed that plumbagin treatment led to a significant increase in enzyme activities of both CarEs and P450 (Figure 2). Possible explanations for this phenomenon could be the involvement of post-transcriptional regulatory mechanisms and the contributions of enzyme isoforms with different expression and

activity profiles. The inconsistency between RNA-seq data at the transcriptional level and enzyme assay results at the protein level are also reported in previous studies. For example, toosendanin exposure inhibited the expression of most DEGs encoding lipases, while it increased lipase enzyme activity in *S. frugiperda* larvae to overcome the adverse effects of the xenobiotic toosendanin (Lin et al., 2023). Notably, the six upregulated P450s (*Sfru004887*, *Sfru020044*, *Sfru009692*, *Sfru004769*, *Sfru011158* and *Sfru011561*) are mainly concentrated in the CYP6 family and CYP301 family, which are also induced by phytochemicals in other insects, such as *H. armigera* and *Aphis gossypii*, and are associated with plant allelochemical detoxification in insects (Vandenhole et al., 2021). The expression level of one *CYP301A1* gene (*Sfru020044*) were upregulated by 1.55- and 2.97 in RNA-seq and qPCR data, respectively, which was also induced by the phenolic monoterpenoid carvacrol in *S. frugiperda* larvae (Liu et al., 2023). Interestingly, all of five DEGs for the detoxification enzyme ABC transporters (*Sfru016345*, *Sfru007970*, *Sfru007513*, *Sfru007645* and *Sfru007518*) and all of two DEGs for sodium channel protein (*XLOC_025616* and *Sfru014814*), one type of the insecticide targets, were upregulated in plumbagin-treated larvae, highlighting their potential roles in *S. frugiperda* larvae in response to plumbagin exposure.

Plumbagin treatment led to the downregulation of many DEGs related to humoral immune responses. Almost all DEGs (14 of 15) associated with pattern recognition proteins/receptors including peptidoglycan recognition (*Sfru009140*, *Sfru000940* and *Sfru008126*), protein beta-glucan recognition protein (*Sfru016408*, *Sfru016141*, *Sfru015779* and *Sfru016037*) and c-type lectin including *Sfru000525*, *Sfru015069* and *Sfru004263*, which plays critical roles in initiating humoral immune responses (Tsakas et al., 2010), were downregulated. Besides, several other immune-related genes such as one *scolexin* (*Sfru019519*), one *cecropin* (*XLOC_005114*), four *C-type lysozymes* (*Sfru007716*, *Sfru007030*, *Sfru018720* and *Sfru018779*), two *antimicrobial peptides* (*Sfru000526* and *Sfru000399*), five *peroxiredoxin* (*Sfru009611*, and *Sfru000305*, *Sfru000322*, *Sfru007176* and *Sfru007012*) were also downregulated. Serpin (serine protease inhibitor) is a key negative regulator of melanization responses (Jiravanichpaisal et al., 2006). Almost all DEGs (5 of 6) for serpin, including *Sfru002511*, *Sfru015504*, *Sfru015301*, *Sfru018941* and *Sfru002522*, were downregulated, which suggested that serpin-mediated immunity might be activated by plumbagin treatment. Moreover, all of 10 endocytosis-related genes (*Sfru000635*, *Sfru002360*, *Sfru009600*, *Sfru013379*, *Sfru014150*, *Sfru015827*, *Sfru022046*, *Sfru002927*, *Sfru002549* and *Sfru019450*), all of 4 *alpha-crystallin* (*Sfru013250*, *Sfru013305*, *Sfru013460* and *Sfru013463*), and almost all DEGs (3 out of 4) involved in JAK-STAT signaling pathway (*Sfru000631*, *Sfru009860* and *Sfru009860*) were upregulated. These findings indicated that plumbagin treatment triggered complex immune responses in *S. frugiperda* larvae.

Cuticle proteins and chitin are the major components of insect cuticle and midgut peritrophic membrane (Shu et al., 2021b). After plumbagin treatment, most DEGs (21 of 27) for insect cuticle proteins, such as *Sfru008849*, *Sfru007124* and *Sfru002859*, and one DEG for skin secretory protein (*Sfru015138*) were downregulated. Similar to our results, Shu et al. (2022) reported that azadirachtin treatment led to the downregulation of many genes for cuticle proteins *S. frugiperda* larvae, whereas the DEGs related to cuticle proteins and skin secretory proteins were upregulated in *P. tsushimanus* larvae after linalool exposure to decrease the penetration of this volatile compound (Li et al., 2023). Besides, plumbagin inhibited the expression of all DEGs (8 genes) involved in chitin synthesis and degradation pathway, including four *trehalase* (Sfru010229, *Sfru010311*, *Sfru009794* and *Sfru010180*), two *chitin deacetylase* (*Sfru018671* and *Sfru018874*) and two *chitinase A* (*Sfru003349* and *Sfru012164*). Trehalase is the first enzyme in chitin biosynthesis, and suppression of trehalase resulted in lethality and morphological defects in several insects (Liu et al., 2019). In present study, all of 4 *trehalases* were downregulated, which might disrupt chitin synthesis and degradation, and consequently led to a decrease in chitin content. Also, all of 15 DEGs associated with chitin-binding proteins (Sfru009934, Sfru010806, Sfru019700, Sfru019167, XLOC_009898, Sfru013067, XLOC_009488, Sfru016397, Sfru019885, XLOC_009577, Sfru010648, Sfru010790, Sfru011009, Sfru018068 and Sfru009342) were downregulated, which play essential roles in forming and maintaining of chitin-containing structures (Tetreau et al., 2015).

5 Conclusion

In summary, our results illustrated that plumbagin treatment exhibited a high larvicidal activity against *S. frugiperda* larvae in the bioassay experiments. Consistently, a large number of the DEGs responsible for nutrient and energy metabolism, humoral immune response, insect cuticle protein, chitin-binding proteins, chitin synthesis and degradation, insect hormone, and xenobiotic detoxification were suppressed in RNA-seq data. Conversely, the expression of DEGs involved in endocytosis and the activities of the two detoxification enzymes CarE and P450 were enhanced after plumbagin treatment. These results will help to elucidate insecticidal mechanisms of botanical insecticides against pests.

Data availability statement

The transcriptome sequencing data presented in this study are deposited in the NCBI BioProject database (https://www.ncbi.nlm.nih.gov/bioproject), accession number PRJNA1119741. Further inquiries can be directed to the corresponding author.

Ethics statement

The manuscript presents research on animals that do not require ethical approval for their study.

Author contributions

XS: Investigation, Methodology, Writing–original draft. WL: Investigation, Methodology, Writing–original draft, Writing–review and editing. SY: Formal Analysis, Writing–original draft. XN: Formal Analysis, Writing–original draft. SH: Resources, Writing–original draft. MW: Resources, Writing–original draft. CZ: Conceptualization, Writing–original draft, Writing–review and editing. XH: Conceptualization, Writing–original draft, Writing–review and editing.

Funding

The author(s) declare that financial support was received for the research, authorship, and/or publication of this article. This work was supported by the National Key Research and Development Program of China (2021YFD1400701).

Conflict of interest

The authors declare that the research was conducted in the absence of any commercial or financial relationships that could be construed as a potential conflict of interest.

Publisher's note

Supplementary material

The Supplementary Material for this article can be found online at: https://www.frontiersin.org/articles/10.3389/fphys.2024.1427385/full#supplementary-material

References

Akhtar, Y., Isman, M. B., Lee, C. H., Lee, S. G., and Lee, H. S. (2012b). Toxicity of quinones against two-spotted spider mite and three species of aphids in laboratory and greenhouse conditions. *Ind. Crop Prod.* 37 (1), 536–541. doi:10.1016/j.indcrop.2011.07.033

Akhtar, Y., Isman, M. B., Niehaus, L. A., Lee, C. H., and Lee, H. S. (2012a). Antifeedant and toxic effects of naturally occurring and synthetic quinones to the cabbage looper, *Trichoplusia ni*. *Crop Prot.* 31 (1), 8–14. doi:10.1016/j.cropro.2011.09.009

Amezian, D., Nauen, R., and Le Goff, G. (2021). Comparative analysis of the detoxification gene inventory of four major *Spodoptera* pest species in response to xenobiotics. *Insect biochem. Mol. Biol.* 138, 103646. doi:10.1016/j.ibmb.2021.103646

Chen, Y. Z., Li, T., Yang, J., Li, Q. M., Zhang, G. C., and Zhang, J. (2022). Transcriptomic analysis of interactions between *Lymantria dispar* larvae and carvacrol. *Pestic. Biochem. Physiol.* 181, 105012. doi:10.1016/j.pestbp.2021.105012

Dávila-Lara, A., Rahman-Soad, A., Reichelt, M., and Mithöfer, A. (2021). Carnivorous *Nepenthes x ventrata* plants use a naphthoquinone as phytoanticipin against herbivory. *PLoS One* 16 (10), e0258235. doi:10.1371/journal.pone.0258235

de Oliveira, P. M. C., Sousa, J. P. B., Albernaz, L. C., Coelho-Ferreira, M., and Espindola, L. S. (2022). Bioprospection for new larvicides against *Aedes aegypti* based on ethnoknowledge from the Amazonian Sao Sebastiao de Marinau riverside community. *J. Ethnopharmacol.* 293, 115284. doi:10.1016/j.jep.2022.115284

Giraudo, M., Hilliou, F., Fricaux, T., Audant, P., Feyereisen, R., and Le Goff, G. (2015). Cytochrome P450s from the fall armyworm (*Spodoptera frugiperda*): responses to plant allelochemicals and pesticides. *Insect molec. Biol.* 24 (1), 115–128. doi:10.1111/imb.12140

Guo, J. F., Shi, J. Q., Han, H. L., Rwomushana, I., Ali, A., Myint, Y., et al. (2023). Competitive interactions between invasive fall armyworm and Asian corn borer at intraspecific and interspecific level on the same feeding guild. *Insect Sci.* doi:10.1111/1744-7917.13300

He, P., Mang, D. Z., Wang, H., Wang, M. M., Ma, Y. F., Wang, J., et al. (2020). Molecular characterization and functional analysis of a novel candidate of cuticle carboxylesterase in *Spodoptera exigua* degradating sex pheromones and plant volatile esters. *Pestic. Biochem. Physiol.* 163, 227–234. doi:10.1016/j.pestbp.2019.11.022

Hu, W. Y., Du, W. C., Bai, S. M., Lv, S. T., and Chen, G. (2018). Phenoloxidase, an effective bioactivity target for botanical insecticide screening from green walnut husks. *Nat. Prod. Res.* 32 (23), 2848–2851. doi:10.1080/14786419.2017.1380015

Huang, Y., Liao, M., Yang, Q. Q., Xiao, J. J., Hu, Z. Y., Zhou, L. J., et al. (2018). Transcriptome profiling reveals differential gene expression of detoxification enzymes in *Sitophilus zeamais* responding to terpinen-4-ol fumigation. *Pestic. Biochem. Physiol.* 149, 44–53. doi:10.1016/j.pestbp.2018.05.008

Israni, B., Wouters, F. C., Luck, K., Seibel, E., Ahn, S. J., Paetz, C., et al. (2020). The fall armyworm *Spodoptera frugiperda* utilizes specific UDP-glycosyltransferases to inactivate maize defensive benzoxazinoids. *Front. Physiol.* 11, 604754. doi:10.3389/fphys.2020.604754

Jiravanichpaisal, P., Lee, B. L., and Söderhäll, K. (2006). Cell-mediated immunity in arthropods: hematopoiesis, coagulation, melanization and opsonization. *Immunobiology* 211 (4), 213–236. doi:10.1016/j.imbio.2005.10.015

Kenis, M., Benelli, G., Biondi, A., Calatayud, P. A., Day, R., Desneux, N., et al. (2023). Invasiveness, biology, ecology, and management of the fall armyworm, *Spodoptera frugiperda*. *Entomol. Gen.* 43 (2), 187–241. doi:10.1127/entomologia/2022/1659

Li, S. Y., Li, H., Chen, C., and Hao, D. J. (2023). Tolerance to dietary linalool primarily involves co-expression of cytochrome P450s and cuticular proteins in *Pagiophloeus tsushimanus* (Coleoptera: Curculionidae) larvae using SMRT sequencing and RNA-seq. *BMC Genomics* 24 (1), 34. doi:10.1186/s12864-023-09117-7

Li, X. C., Schuler, M. A., and Berenbaum, M. R. (2007). Molecular mechanisms of metabolic resistance to synthetic and natural xenobiotics. *Annu. Rev. Entomol.* 52, 231–253. doi:10.1146/annurev.ento.51.110104.151104

Lin, D. J., Zhang, Y. X., Fang, Y., Gao, S. J., Wang, R., and Wang, J. D. (2023a). The effect of chlorogenic acid, a potential botanical insecticide, on gene transcription and protein expression of carboxylesterases in the armyworm (*Mythimna separata*). *Pestic. Biochem. Physiol.* 195, 105575. doi:10.1016/j.pestbp.2023.105575

Lin, Y. Z., Huang, Y. T., Liu, J. F., Liu, L. Y., Cai, X. M., Lin, J. T., et al. (2023b). Characterization of the physiological, histopathological, and gene expression alterations in *Spodoptera frugiperda* larval midguts affected by toosendanin exposure. *Pestic. Biochem. Physiol.* 195, 105537. doi:10.1016/j.pestbp.2023.105537

Liu, J. F., Lin, Y. Z., Huang, Y. T., Liu, L. Y., Cai, X. M., Lin, J. T., et al. (2023). The effects of carvacrol on development and gene expression profiles in *Spodoptera frugiperda*. *Pestic. Biochem. Physiol.* 195, 105539. doi:10.1016/j.pestbp.2023.105539

Liu, X. J., Cooper, A. M. W., Zhang, J. Z., and Zhu, K. Y. (2019). Biosynthesis, modifications and degradation of chitin in the formation and turnover of peritrophic matrix in insects. *J. Insect Physiol.* 114, 109–115. doi:10.1016/j.jinsphys.2019.03.006

Pavela, R. (2013). Efficacy of naphthoquinones as insecticides against the house fly, *Musca domestica* L. *Ind. Crop Prod.* 43, 745–750. doi:10.1016/j.indcrop.2012.08.025

Rahman-Soad, A., Dávila-Lara, A., Paetz, C., and Mithöfer, A. (2021). Plumbagin, a potent naphthoquinone from *Nepenthes* plants with growth inhibiting and larvicidal activities. *Molecules* 26, 825. doi:10.3390/molecules26040825

Rajendra Prasad, K., Suresh Babu, K., Ranga Rao, R., Suresh, G., Rekha, K., Madhusudana Murthy, J., et al. (2012). Synthesis and insect antifeedant activity of plumbagin derivatives. *Med. Chem. Res.* 21, 578–583. doi:10.1007/s00044-011-9559-7

Shang, X. F., Zhao, Z. M., Li, J. C., Yang, G. Z., Liu, Y. Q., Dai, L. X., et al. (2019). Insecticidal and antifungal activities of *Rheum palmatum* L. anthraquinones and structurally related compounds. *Ind. Crop Prod.* 137, 508–520. doi:10.1016/j.indcrop.2019.05.055

Shi, Y., Liu, Q., Lu, W., Yuan, J., Yang, Y., Oakeshott, J., et al. (2023). Divergent amplifications of CYP9A cytochrome P450 genes provide two noctuid pests with differential protection against xenobiotics. *Proc. Natl. Acad. Sci. U. S. A.* 120 (37), e2308685120. doi:10.1073/pnas.2308685120

Shu, B. S., Lin, Y. Z., Qian, G. Z., Cai, X. M., Liu, L. Y., and Lin, J. T. (2022). Integrated miRNA and transcriptome profiling to explore the molecular mechanism of *Spodoptera frugiperda* larval midgut in response to azadirachtin exposure. *Pestic. Biochem. Physiol.* 187, 105192. doi:10.1016/j.pestbp.2022.105192

Shu, B. S., Yang, X. M., Dai, J. H., Yu, H. K., Yu, J. K., Li, X. L., et al. (2021a). Effects of camptothecin on histological structures and gene expression profiles of fat bodies in *Spodoptera frugiperda*. *Ecotox. Environ. Safe.* 228, 112968. doi:10.1016/j.ecoenv.2021.112968

Shu, B. S., Yu, H. K., Li, Y. N., Zhong, H. X., Li, X. L., Cao, L., et al. (2022). Identification of azadirachtin responsive genes in *Spodoptera frugiperda* larvae based on RNA-seq. *Pestic. Biochem. Physiol.* 172, 104745. doi:10.1016/j.pestbp.2020.104745

Shu, B. S., Zou, Y., Yu, H. K., Zhang, W. Y., Li, X. L., Cao, L., et al. (2021b). Growth inhibition of *Spodoptera frugiperda* larvae by camptothecin correlates with alteration of the structures and gene expression profiles of the midgut. *BMC Genomics* 22 (1), 391. doi:10.1186/s12864-021-07726-8

Su, C. Y., Liu, S. S., Sun, M. X., Yu, Q. L., Li, C. Y., Graham, R. I., et al. (2023). Delivery of methoprene-tolerant dsRNA to improve RNAi efficiency by modified liposomes for pest control. *ACS Appl. Mater. Inter.* 15, 13576–13588. doi:10.1021/acsami.2c20151

Sun, X. X., Hu, C. X., Jia, H. R., Wu, Q. L., Shen, X. J., Zhao, S. Y., et al. (2021). Case study on the first immigration of fall armyworm, *Spodoptera frugiperda* invading into China. *J. Integr. Agr.* 20 (3), 664–672. doi:10.1016/S2095-3119(19)62839-X

Tay, W. T., Meagher, R. L., Czepak, C., and Groot, A. T. (2023). *Spodoptera frugiperda*: ecology, evolution, and management options of an invasive species. *Annu. Rev. Entomol.* 68, 299–317. doi:10.1146/annurev-ento-120220-102548

Tetreau, G., Dittmer, N. T., Cao, X. L., Agrawal, S., Chen, Y. R., Muthukrishnan, S., et al. (2015). Analysis of chitin-binding proteins from *Manduca sexta* provides new insights into evolution of peritrophin A-type chitin-binding domains in insects. *Insect biochem. Mol. Biol.* 62, 127–141. doi:10.1016/j.ibmb.2014.12.002

Tokunaga, T., Takada, N., and Ueda, M. (2004). Mechanism of antifeedant activity of plumbagin, a compound concerning the chemical defense in carnivorous plant. *Tetrahedron Lett.* 45 (38), 7115–7119. doi:10.1016/j.tetlet.2004.07.094

Toprak, U., Hegedus, D., Doğan, C., and Güney, G. (2020). A journey into the world of insect lipid metabolism. *Insect Biochem. Physiol.* 104 (2), e21682. doi:10.1002/arch.21682

Tsakas, S., and Marmaras, V. J. (2010). Insect immunity and its signalling: an overview. *Invert. Surviv. J.* 7 (2), 228–238.

Vandenhole, M., Dermauw, W., and Van Leeuwen, T. (2021). Short term transcriptional responses of P450s to phytochemicals in insects and mites. *Curr. Opin. Insect Sci.* 43, 117–127. doi:10.1016/j.cois.2020.12.002

Wang, H. H., Zhao, R., Gao, J., Zhang, L., Zhang, S., Liang, P., et al. (2023). Genetic architecture and insecticide resistance in Chinese populations of *Spodoptera frugiperda*. *J. Pest Sci.* 96 (4), 1595–1610. doi:10.1007/s10340-022-01569-2

Zhao, R., Wang, H. H., Gao, J., Zhang, Y. J., Li, X. C., Zhou, J. J., et al. (2022). Plant volatile compound methyl benzoate is highly effective against *Spodoptera frugiperda* and safe to non-target organisms as an eco-friendly botanical-insecticide. *Ecotox. Environ. Safe.* 245, 114101. doi:10.1016/j.ecoenv.2022.114101

frontiers | Frontiers in Physiology

TYPE Original Research
PUBLISHED 29 August 2024
DOI 10.3389/fphys.2024.1426169

OPEN ACCESS

EDITED BY
Natraj Krishnan,
Mississippi State University, United States

REVIEWED BY
Marcelo Hermes-Lima,
University of Brasilia, Brazil
Hamzeh Izadi,
Vali-E-Asr University of Rafsanjan, Iran

*CORRESPONDENCE
Bimalendu B. Nath,
bbnath@gmail.com

RECEIVED 30 April 2024
ACCEPTED 02 August 2024
PUBLISHED 29 August 2024

CITATION
Bomble P and Nath BB (2024) Impact of singular versus combinatorial environmental stress on RONS generation in *Drosophila melanogaster* larvae.
Front. Physiol. 15:1426169.
doi: 10.3389/fphys.2024.1426169

Impact of singular versus combinatorial environmental stress on RONS generation in *Drosophila melanogaster* larvae

Pratibha Bomble [1,2] and Bimalendu B. Nath[1,3]*

[1]Stress Biology Research Laboratory, Department of Zoology, Savitribai Phule Pune University, Pune, India, [2]Department of Zoology, Indira College of Arts Commerce and Science, Pune, India, [3]MIE-SPPU Institute of Higher Education, Doha, Qatar

We investigated environmentally correlated abiotic stressor desiccation (D), heat (H), and starvation (S) in the generation of reactive oxygen and nitrogen species (RONS) using *Drosophila melanogaster* larvae as an experimental model, subjected to either individual stressors or exposed to a combinatorial form of stressors (D + H, H + S, and D + S). The study was also extended to find synergistic endpoints where the impacts of all three stressors (D + H + S) were exerted simultaneously. We estimated the lethal time (LT_{20}) at specific doses using regression and probit analyses based on the larval survival. LT_{20} values were used as the base-level parameter for further oxidative stress experimental analysis work. First, all stressors led to the activation of a typical common oxidative stress-mediated response irrespective of the mode of exposure. As envisaged, *D. melanogaster* larvae exhibited a homeostatic stress tolerance mechanism, triggering an antioxidant defense mechanism, indicated by an elevated level of total antioxidant capacity and enhanced activities of superoxide dismutase, catalase, glutathione reductase, and glutathione peroxidase. In all types of stress-exposed regimes, we found a negative impact of stressors on the activity of mitochondrial enzyme aconitase. Elevated levels of other oxidative stress markers, viz., lipid peroxidation, protein carbonyl content, and advanced oxidative protein products, were obvious although the increment was treatment-specific. Desiccation stress proved to be the most dominant stressor compared to heat and starvation. Among the combination of stressors, rather than a single stressor, D + H impacted more than other binary stress exposures. Focusing on the impact of singular versus combinatorial stress exposure on RONS generation, we observed an increase in the RONS level in both singular and combinatorial forms of stress exposure although the magnitude of the increment varied with the nature of stressors and their combinations. The present study indicated an "additive" effect when all three stressors (D + H + S) operate simultaneously, rather than a "synergistic" effect.

KEYWORDS

oxidative stress, abiotic stressors, antioxidants, reactive oxygen and nitrogen species, *Drosophila*, aconitase

1 Introduction

For the last couple of decades, climatic scenarios have intensified various environmental stressors. Fluctuations in environmental conditions pose a risk to the survival of living organisms, impacting their physiology of adaptation. In natural environments, living organisms periodically experience various abiotic stressors, such as heat, starvation,

desiccation, hypoxia, and osmotic imbalance (Bijlsma and Loeschke, 2005; Bradley, 2009; Thorat et al., 2012; Thorat and Nath, 2018; Sokolova, 2021; Thorat et al., 2023). Insects, often considered barometers for environmental monitoring, have drawn the attention of stress biologists. Insects are routinely exposed to multiple environmental variations, thereby successfully occupying diverse ecological niches (Ramniwas et al., 2023; Thorat et al., 2023). Quite a few insect groups demonstrate remarkable tolerance, often selectively, toward abiotic stressors occurring either individually or simultaneously. One needs to choose either a stress-sensitive or stress-tolerant bioindicator insect model to investigate singular and multiple stress response mechanisms at the cellular, behavioral, and physiological levels (Hoffmann and Hercus, 2000; Holt and Miller, 2010).

A common stress-responsive biochemical signature observed in most abiotic stress conditions is the generation of reactive oxygen species (ROS), linking oxidative stress with desiccation, heat, and starvation (Malik and Storey, 2011; Thorat et al., 2016a; Zhang et al., 2019; Farahani et al., 2020; Miao et al., 2020; Pandey et al., 2020; Pati et al., 2024; Hermes-Lima et al 2015). Similar to ROS, reactive nitrogen species (RNS) are an additional set of free radicals and non-radical molecules generated under stress conditions, leading to nitrosative stress, and their significance is being revealed, mainly in plants (Del Río, 2015; Khan et al., 2023) and in pathophysiological circumstances in humans (Dalle-Donna et al., 2005; Wang et al., 2021). The generation of reactive oxygen and nitrogen species (RONS) occurs in many cell signaling pathways. Although many reports on RONS are available to date on plants exposed to multiple stressors, there are practically no studies carried out in non-human biota, especially in stress-bioindicator insects. Studies on RONS are warranted because the nitrosative stress responses can be exploited as a potential tool for biomonitoring environmental health.

The RONS generation follows species-specific strategies to combat singular and simultaneously acting multiple stressors. Recently, findings from our laboratory demonstrated a homeostatic response through RONS generation in a stress-resilient chironomid midge species, *Chironomus ramosus*, exposed to stressful fluctuations in temperature, humidity, and nutrient imbalances (Bomble and Nath, 2022). Having explored the effect of combinatorial stress on RONS generation in chironomid midge, an aquatic dipteran insect, we shifted our attention to drosophilid flies, which are an evolutionary distant and ecologically diverse dipteran terrestrial insect group. Among insects, the family Drosophilidae is one of the most well-investigated groups in stress biology, especially the popular model *Drosophila melanogaster*. The rationale for choosing *D. melanogaster* for the present study is its amenability to experimental manipulation. Previous work from our laboratory proved *D. melanogaster* not only as a stress-bioindicator species (Thorat et al., 2012) but also for laboratory-based simulation studies of environmental biotic and abiotic stress (Thorat and Nath, 2010; Thorat et al., 2016a; Thorat et al., 2016b). In the present paper, we investigated three abiotic stressors, desiccation (D), heat (H), and starvation (S), subjecting *D. melanogaster* larvae to each stressor individually or in combination, viz., either D + H, H + S, D + S, or D + H + S. We intended to know the status and level of attainment of antioxidant defense mechanisms in singular and combinatorial forms of stress exposure, and RONS served as the endpoints of our queries. Additionally, we explored the status of mitochondrial enzyme aconitase, which is a marker of stress at the cellular level (Gardner, 2002). This is the first report of RONS generation after combinatorial abiotic stress exposure in *D. melanogaster*, and the findings provided physiologically relevant insights.

2 Materials and methods

2.1 Rearing and maintenance of *Drosophila*

In this study, an inbred population of *D. melanogaster* (ORK strain) was maintained under controlled environmental conditions in a BOD incubator at 24°C ± 2°C. The *Drosophila* cultures were maintained in a nutrient-rich cornmeal–agar medium. To ensure the consistency of the experimental cohort, healthy early third-instar larvae were used for all experiments.

2.2 Stress treatment

2.2.1 Experimental design

A total of 10 larvae of *D. melanogaster* were used in each experiment, in which the larvae were exposed to either a desiccation, heat, and starvation stressor or combinations of these stressors. LT_{20} (lethal time required for 20% mortality in the population) values were taken as an endpoint for each experiment (Supplementary Table S1).

2.2.2 Desiccation

A measure of 500 g of silica gel was added to the desiccating chamber 12 h prior to its use in order to obtain <5% relative humidity (RH), which was monitored using a hygrometer. The larvae of *D. melanogaster* were desiccated in this chamber on dry tissue paper placed in a glass Petri dish. The LT_{20} values were taken as an endpoint for further experimental work. Untreated larvae were used as controls.

2.2.3 Heat

Heat stress was administered by transferring the larvae of *D. melanogaster* to incubators set at 37°C. The induction of HSP70 occurs as a response to heat stress in *Drosophila* at 37°C (Lindquist, 1980) and hence 37°C was used for the experiment.

2.2.4 Starvation

The larvae of *D. melanogaster* were removed from the rearing media, carefully cleaned, and then placed on wet tissue paper in a glass Petri plate without any nutrient medium. The starvation stress was applied at the LT_{20} time points (Supplementary Table S1).

2.2.5 Multiple stressors

For combined stress treatments, the larvae were concurrently exposed to combinations of two or three stressors, including desiccation with heat (D + H), heat with starvation (H + S), and starvation with desiccation (D + S) or three stressors (D + H + S) simultaneously. The endpoint for each experiment was determined as the lethal time required for 20% mortality in the population (LT_{20}). LT_{20} values were used as the base-level parameter across all treatments, enabling a comparison between singular and combinational stress effects. Each experiment was replicated

thrice per treatment and conducted under controlled laboratory conditions.

2.3 Assay of oxidative stress markers

2.3.1 Lipid peroxidation

The thiobarbituric acid reactive substance (TBARS) assay was conducted following the protocol outlined by Ohkawa et al. (1979), utilizing malondialdehyde (MDA) as the marker. A standard graph was plotted using 2 mM MDA, and calibration for subsequent dilutions was prepared accordingly to quantify MDA concentrations in the samples. For sample preparation, whole larvae of *D. melanogaster* (n = 80) from both treatment and control groups were homogenized in 1× phosphate-buffered saline (PBS) at specific time points. The resulting homogenates were centrifuged at 15,000 rpm for 30 min at 4°C to obtain the supernatant for further analysis. The supernatants were then mixed with a TBA reagent and subjected to a 60-min incubation in a boiling water bath alongside positive and negative controls, after which they were immediately transferred to ice for 10 min and then centrifuged at 8,000 rpm for 5 min. After centrifugation, the tubes were allowed to incubate at room temperature, and the absorbance was measured at 535 nm using a spectrophotometer. The concentration of MDA in the sample test was calculated in terms of μmol/mg of protein, providing a quantitative measure of lipid peroxidation levels.

2.3.2 Protein carbonyl content

The quantification of protein carbonyl content involved its reaction with 2.4 dinitrophenyl hydrazine (DNPH), producing a protein–hydrazone complex quantified spectrophotometrically at 360 nm, adhering to the protocol outlined in the Protein Carbonyl Colorimetric Assay Kit (Item No. 10005020, Cayman Chemical). The control and treated sets of larvae (n = 50) were washed with 1× PBS to remove adherent particles. Subsequently, the larvae were homogenized in an ice-cold buffer (50 mM phosphate and 1 mM EDTA, pH 6.7) and centrifuged at 10,000 g for 15 min at 4°C to yield supernatants for further analysis. Nucleic acids were removed using 10% streptomycin sulfate. The assay mixture, comprising the sample, DNPH, 2.5 M HCl, and 20% trichloroacetic acid (TCA), was centrifuged at 10,000 g for 10 min at 4°C. The pellet was re-suspended in 1 mL of a 1:1 ethanol/ethyl acetate mixture and centrifuged at 10,000 g for 10 min at 4°C, and the whole process was repeated twice. Subsequently, the pellet was re-suspended in 500 μL of guanidine hydrochloride and centrifuged at 10,000 g for 10 min at 4°C. The absorbance of the supernatant was then measured at 360 nm using a UV spectrophotometer, facilitating the quantification of protein carbonyl content.

2.3.3 Advanced oxidative protein products

The method described by Witko-Sarsat et al. (1996) was used to assess the levels of advanced oxidative protein products (AOPPs). Homogenates of larvae (n = 50) from both treated and control samples were incubated with potassium iodide in a rocking shaker at room temperature. Following this incubation period, ethyl acetate was added, and the spectrophotometric absorbance was measured at 340 nm. The absorbance values were normalized using a chloramine standard T-plot.

2.4 Assay for ROS generation

2.4.1 Measurement of superoxide radicals

Following stress treatment, *D. melanogaster* larvae (n = 50) were homogenized in 1× PBS and subsequently centrifuged at 5,000 rpm at 4°C for 10 min. The resulting supernatants were then incubated in a light-protected environment with a 2′,7′-dichlorodihydrofluorescein diacetate (DCF-DA; D399, Invitrogen) solution for 30 min to detect the presence of superoxide radicals ($O_2^{\cdot-}$). Post-incubation, the supernatants were analyzed using fluorimetry at wavelengths specific to the excitation and emission properties of the DCF-DA dye. A standard solution of DCF-DA dye was used, and the data were quantified in arbitrary fluorescence units.

2.4.2 Measurement of hydrogen peroxide

The Amplex Red Hydrogen Peroxide Assay Kit (A22188, Invitrogen) was utilized to ascertain the concentration of hydrogen peroxide in both the control and treated samples of *D. melanogaster*, following the manufacturer's guidelines. Post-stress treatment at respective time points, the larvae (n = 50) were homogenized in an assay buffer solution and subsequently centrifuged at 10,000 g for 15 min at 4°C. The resultant supernatant was carefully collected and combined with the reaction solution comprising the dye and horseradish peroxidase (HRP). The absorbance was measured at 560 nm using a microplate reader, and readings were normalized with a standard plot of H_2O_2.

2.5 Assay for RNS generation

2.5.1 Measurement of the total nitrate/nitrite concentration

The total nitrate/nitrite concentration was quantified using the Total Nitrate/Nitrite Colorimetric Assay Kit (780001, Cayman Chemical), following the manufacturer's protocol. Larvae from both the control and treated groups were homogenized in 1× PBS at pH 7.4 and subsequently centrifuged at 10,000 g for 20 min at 4°C to obtain the supernatant for further analysis. Nitrate/nitrite concentrations were determined by correlating the absorbance values with a standard plot of nitrate and nitrite concentration.

2.5.2 Measurement of nitric oxide radicals

The concentration of nitric oxide radicals was assessed using the fluorescent dye 4,5-diaminofluorescein diacetate (DAF-2DA; ab145283, Abcam), which is specific for reactive nitrogen species. Following stress treatment, the larvae were homogenized in 1× PBS and subsequently centrifuged at 5,000 rpm at 4°C for 10 min to obtain the supernatant. The supernatant was then incubated in the dark with a 4,5-DAF-2DA (Abcam) solution for 20 min to enable the detection of nitric oxide radicals. Post-incubation, the supernatants were analyzed by fluorimetry at dye-specific excitation and emission wavelengths (Ex/

Em = 491/513). The DAF-DA dye solution was run as the standard, and the data were represented in arbitrary fluorescence units.

2.6 Estimation of the total RONS concentration

Total RONS generation was quantified using the ROS-ID® Total ROS Detection Kit (ENZ-51011, Enzo Chemicals) in the larval hemolymph of *D. melanogaster* from both the control and treated groups, following the manufacturer's protocol. The Total ROS Detection Kit includes the oxidative stress detection reagent (Green, Ex/Em 490/525 nm) to directly monitor the reactive oxygen and/or nitrogen species (ROS/RNS). This non-fluorescent, cell-permeable detection probe reacts directly with a wide range of reactive species (hydrogen peroxide, peroxynitrite, and hydroxyl radicals), yielding a green fluorescent product. The samples were analyzed by fluorimetry using a microplate reader (FLUOstar Optima, BMG LABTECH, Germany) at dye-specific excitation and emission wavelengths (Ex/Em = 490/525 nm). Hemocytes from *D. melanogaster* were isolated using the cuticle puncture method. In brief, the larvae were carefully removed from the control and treated groups and thoroughly washed with Ringer's solution. The hemolymph was then collected from the larvae by bleeding into 1× PBS in a dissecting glass, and the collected hemolymph from both the control and treated groups was transferred into microcentrifuge tubes with Schneider's insect medium, and this sample was used for further analysis. The data obtained were represented in the form of arbitrary fluorescence units, providing a quantitative measure of the total RONS generation.

2.7 Microscopic study to investigate the status of reactive species

2.7.1 Salivary glands of *Drosophila melanogaster* larvae

Salivary glands from both control and treated early third-instar larvae of *D. melanogaster* were dissected and fixed in 4% paraformaldehyde after undergoing permeabilization treatment, preparing them for further study and analysis.

2.7.2 Assay for the visualization of ROS and RNS generation

Intracellular ROS were analyzed by fluorescence microscopy using 2′,7′-DCF-DA (Cayman Chemical). The differential interference contrast (DIC) image was used to visualize the structure of the tissue, and 4′,6-diamidino-2-phenylindole (DAPI), a fluorescent stain that binds strongly to A-T-rich regions in DNA, is used to label the nuclei of the cell; here, we used DAPI for counterstaining. The dissected salivary glands of *D. melanogaster* from both the control and treated groups were incubated with 2′,7′-DCF-DA (Abcam) dye to detect ROS and 4,5-DAF-2DA (Abcam) dye to detect RNS for 30 min, followed by counterstaining with DAPI for 5 min in the dark. The samples were then examined under a fluorescence microscope (Carl Zeiss), utilizing appropriate filters for DCF-DA (Ex/Em = 492–495/517–527), DAF-DA (Ex/Em = 491/513), and DAPI (Ex/Em = 358/461).

2.8 Estimation of aconitase enzyme activity

Mitochondria were extracted from early third-instar larvae of *D. melanogaster*, sourced from both the control and treated groups, utilizing the procedure outlined by Wen et al. (2016), with some adaptations. Aconitase activity was quantified spectrophotometrically using Thermo Fisher Scientific instruments, where NADPH formation was tracked at 340 nm using the coupled assay method developed by Gardner (2002). The isolated mitochondria served as the subcellular fractionated samples for the assessment of aconitase enzyme activity. Spectrophotometric measurement of aconitase activity was conducted using Thermo Fisher Scientific instruments, with NADPH formation monitored at 340 nm. The samples were then introduced into an assay buffer (comprising 50 mM Tris–HCl at pH 7.4, 0.6 mM $MnCl_2$, 5 mM sodium citrate, 0.2 mM $NADP^+$, 0.1% v/v Triton X-100, and 0.4 units/mL isocitrate dehydrogenase (Sigma) pre-equilibrated to 30°C). Each sample was assayed in quadruplicate, and readings were taken at 15-s intervals over 7 min. The resulting linear slopes were averaged to derive the measurement of aconitase activity for each sample.

2.9 Measurement of antioxidant enzymes

2.9.1 Preparation of the homogenate for antioxidant assay

To prepare the larval sample for antioxidant assay, larvae from the control and treated groups of *D. melanogaster* were homogenized in a protein extraction buffer, which contained 1 mM phenyl methyl sulfonyl fluoride (PMSF), 1 mM ethylenediaminetetraacetic acid (EDTA), 50 mM phosphate buffer (pH 7.2), and 0.1% Triton X-100. The buffer was maintained under chilled conditions until use. Larvae were added to the chilled buffer, homogenized, and then centrifuged at 14,000 rpm for 30 min at 4°C. This homogenate was used as a crude extract for determining the enzyme activity. The amount of protein obtained from the above homogenate was quantified using the Bradford method, with bovine serum albumin as the standard.

2.9.2 Superoxide dismutase assay

By using the principle described by Beauchamp and Fridovich (1971), the specific activity of superoxide dismutase (SOD) (EC 1.15.1.1) was determined by measuring its ability to inhibit the photochemical reduction of nitro blue tetrazolium (NBT) chloride. The reaction mixture consisted of 100 mM KPO_4 buffer, pH 7.8, 0.01 µM EDTA, 65 mML methionine, 750 µM NBT chloride, 2 mM riboflavin, and 50 µL of enzyme extract in a total volume of 3 mL. Riboflavin was added at the end, and the tubes were mixed by shaking. Two sets of the above reaction mixture were prepared: one set was kept under light conditions (20 W) while the other was kept under dark conditions for 30 min. Similarly, mixtures without the enzyme extract were kept under light and dark conditions and used

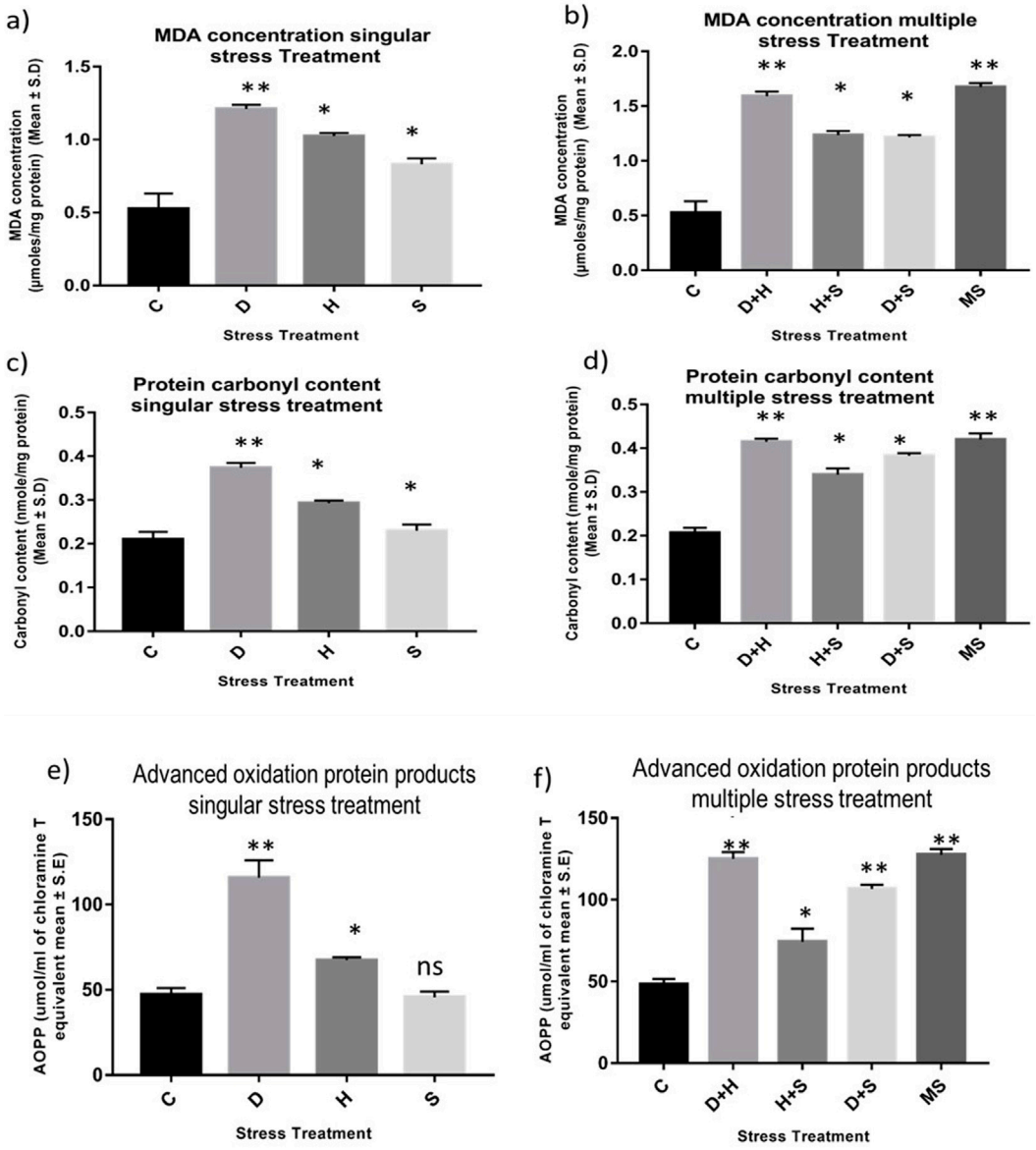

FIGURE 1
Impact of oxidative stress: Spectrophotometric measurement of **(A, B)** Lipid peroxidation (mean ± SD U/mg protein) **(C, D)** Protein Carbonyl content (mean ± SD U/mg protein) **(E,F)** AOPP (mean ± SD U/mL) in third instar larvae of *D. melanogaster*. Values represent mean and the vertical bars represent SD. Data shown are representative of three independent experiments. *** P <0.001; ** P < 0.01; * P < 0.05 indicates level of significance.

as controls. Absorbance was measured at 560 nm. One unit of SOD activity (U) was defined as the amount of enzyme required to cause 50% inhibition of the photoreduction rate of NBT. The results were expressed as unit activity (U)/mg of protein.

2.9.3 Catalase assay

The specific activity of the catalase (CAT) (EC 1.11.1.6) enzyme was measured by using the principle of its ability to convert H_2O_2 to a product, as described by Aebi (1983). The reaction mixture consisted of 100 mM phosphate buffer, pH 7.0, 20 mM H_2O_2, and 50 µL enzyme extract in a total volume of 1 mL in quartz cuvettes. The readings were taken at 240 nm at intervals of 30 s for 3 min to check changes in the amount of H_2O_2 using a spectrophotometer. One unit of enzyme was defined as the amount of enzyme required to convert 1 mol of H_2O_2 to a product in 1 s. The results were expressed in unit activity (U) per microgram (mg) of protein.

2.9.4 Glutathione reductase assay

The specific activity of glutathione reductase (GR) (EC 1.8.1.7) was determined by monitoring its ability to oxidize NADPH, as described by Goldberg and Spooner (1983). The assay mixture consisted of 100 mM phosphate buffer, pH 7.2, 0.17 mM NADPH, 0.5 mM EDTA, 2.2 mM oxidized glutathione, and 100 µL of enzyme extract in a total volume of 1 mL. All components were mixed properly, and the rate of oxidation of NADPH was monitored up to 5 min at intervals of 30 s by measuring the absorbance at 340 nm. The enzyme activity was calculated in terms of U/mg of protein.

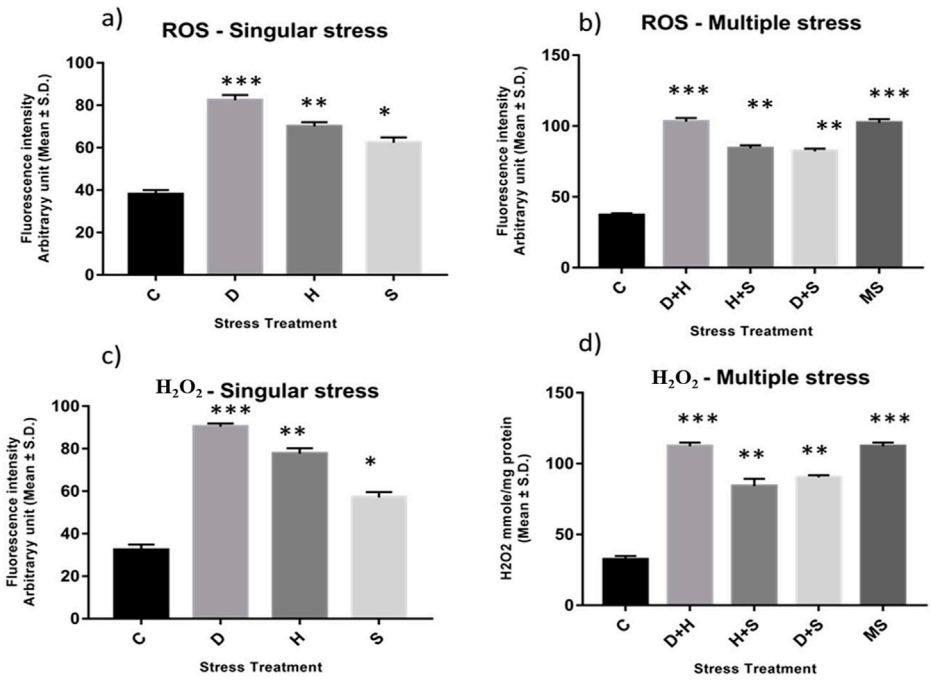

FIGURE 2
Spectrofluorometric measurement of ROS; **(A, B)** superoxide radical expressed as level of arbitrary unit (mean ± SD) **(C, D)** Quantification of Hydrogen peroxide nmole/mg of protein (mean ± SD) in third instar larvae of *D. melanogaster*. Values represent mean and the vertical bars represent SD. Data shown are representative of three independent experiments. *** $P < 0.001$; ** $P < 0.01$; * $P < 0.05$ indicates level of significance.

2.9.5 Glutathione peroxidase assay

To determine the specific activity of glutathione peroxidase (GPx) (EC 1.11.1.9), we used the method proposed by Lawrence and Burk (1976). For this assay, the reaction mixture consisted of 100 mM KPO_4 buffer, pH 7.0, 1 mM NaN_3, 0.2 mM NADPH, 1 U GR, 1 mM GSH, 0.25 mM H_2O_2, 1 mM EDTA, and 100 µL of enzyme extract in a total volume of 1 mL. Absorbance was measured at 340 nm for 5 min at an interval of 30 s. Enzyme activity was measured in terms of U/mg of protein.

2.9.6 Total antioxidant capacity

The antioxidants can inhibit the oxidation of 2,2′-azino-di-3-ethylbenzothiazoline sulfonic acid (ABTS) by metmyoglobin, and based on this, the absorbance was taken at 405 nm, according to the manufacturer's protocol (709001, Cayman Chemical). The capacity of the antioxidants in the sample to prevent ABTS oxidation was compared with that of Trolox, a water-soluble tocopherol analog, and was quantified as molar Trolox equivalents. The control and experimental larvae of *D. melanogaster* were homogenized in 100 µL of the extraction buffer (provided with a kit) and then centrifuged at 12,000 rpm for 15 min at 4°C, while the supernatants were used for further experiments. A standard curve was prepared using different concentrations of Trolox for calculating the total antioxidant capacity of samples.

2.10 Statistics

Different parameters were monitored in normal and stress-exposed third-instar larvae of *D. melanogaster*. An analysis of variance was carried out to find the significant differences in the means, considering each endpoint as a dependent variable and the duration of exposure (LT_{20} of each stressor and combination of stressors) as independent variables. The data were represented as the mean ± SD. The *post hoc* test was used for the statistical comparison between the groups, and Tukey's multiple comparisons test was carried out to determine statistical significance within the groups. A value of $p < 0.05$ was considered statistically significant (SPSS, version 12.0, SPSS Inc., Chicago, IL, United States).

3 Results

3.1 MDA, AOPP, and protein carbonyl content measurement

An increase in the concentration of MDA was evident in the treated larvae compared to the untreated larvae. The increase in the concentration of MDA was more significant in the case of heat stress with desiccation stress than in other combinatorial forms of stressors. When stressors are present in singular form, the increment in the level of MDA was more prominent in the case of desiccation than in the other two stressors, heat stress and starvation stress. The MDA concentration reached a maximum when all three stressors (MS) acted on the larvae simultaneously (Figures 1A, B). Protein carbonyl content is a known marker of protein oxidation, mainly caused by the highly reactive free radical species. The increase in the level of protein carbonyl content with stress treatment was conspicuous, but this increase was more

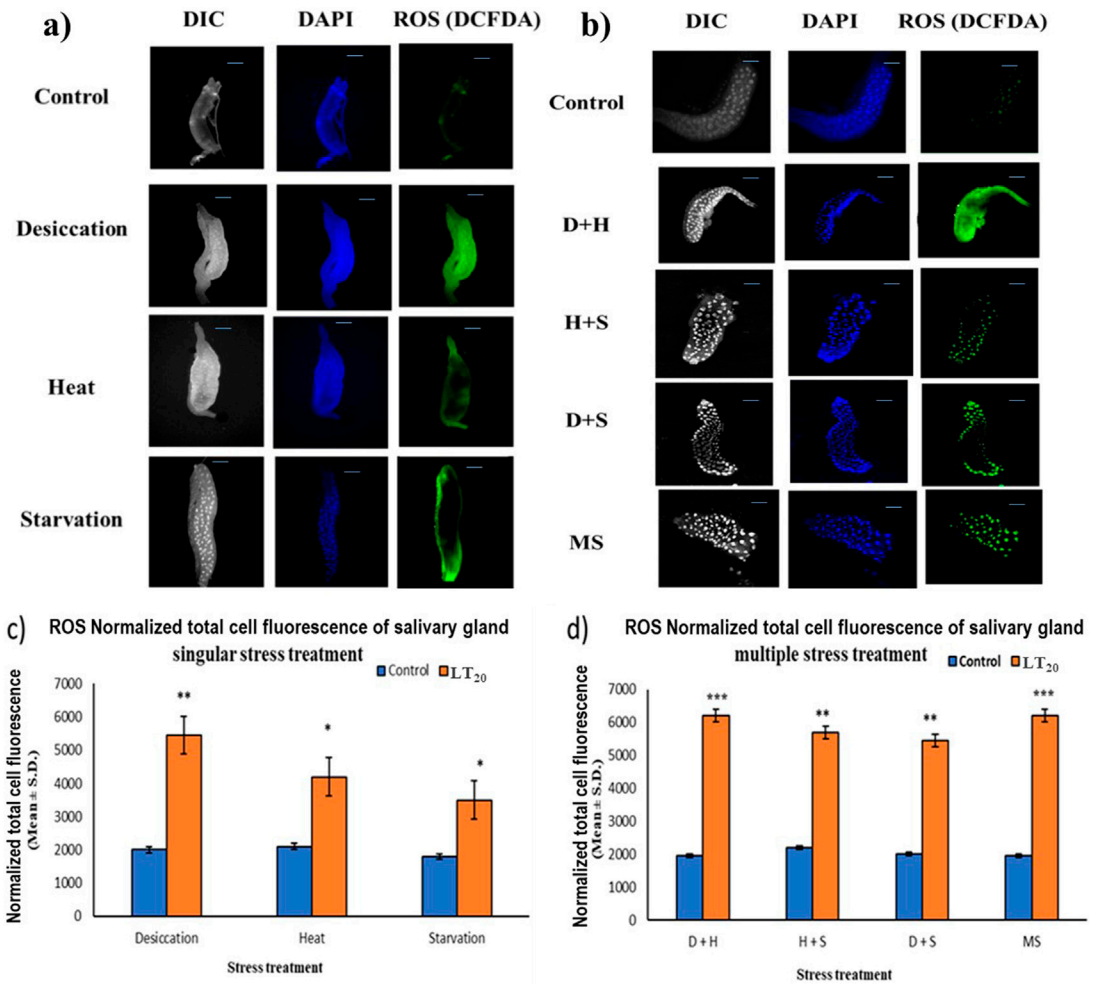

FIGURE 3
Microscopic visualization of ROS. Fluorescence microscopic images of *D. melanogaster* exposed to desiccation, heat, starvation, D + H, H + S, and D + S stress treatments compared against control salivary glands, following **(A)** singular stress and **(B)** combinatorial stress treatments to visualize reactive oxygen species. Normalized cell fluorescence intensity of **(C)** singular and **(D)** combinatorial stress treatments to quantify reactive nitrogen species. ***$p < 0.001$; **$p < 0.01$; and *$p < 0.05$; ns: non-significant. Scale bar: 200 μm. **(A,B)** Differential interference contrast panel for the ease of resolving the outline.

prominent in the case of desiccation than in other singular stressors like heat stress and starvation stress (Figure 1C). The results from combinatorial studies revealed that desiccation stress in combination with heat stress was more vulnerable than desiccation alone and also in other forms of combination. The impact of D + H apparently was equivalent to MS (Figure 1D). AOPPs are toxins formed through the reaction of chlorinated oxidants with proteins during oxidative stress. Here, an increase in the concentration of AOPP in desiccation-stressed larvae was observed compared to heat and starvation-stressed counterparts. Starvation stress did not exert its effect on the AOPP level, and the larvae maintained a similar level as observed in the control (Figure 1E). This increase was more evident in the combinatorial form (H + D) than in the form of singular stressors. The AOPP level was high, as observed in the case of D + H, when all three stressors (MS) acted on the larvae simultaneously (Figure 1F).

3.2 Quantification of ROS: superoxide radicals and hydrogen peroxide

An increase in the production of ROS resulting from stress induced an imbalance between oxidants and antioxidants, as evident from the enhanced level of superoxide radicals and hydrogen peroxide, along with the stress exposure, compared to the control. In singular form, the increase was more prominent in the case of desiccation stress than that in heat stress and desiccation stress. This increase was more evident under combinatorial and multiple stress conditions desiccation combined with heat stress (D + H) was more potent than desiccation combined with starvation stress (D + S) and heat combined with starvation stress (H + S). In the presence of more than one stressor, D + H impacted the same way when all three stressors (MS) acted simultaneously (Figures 2A–D).

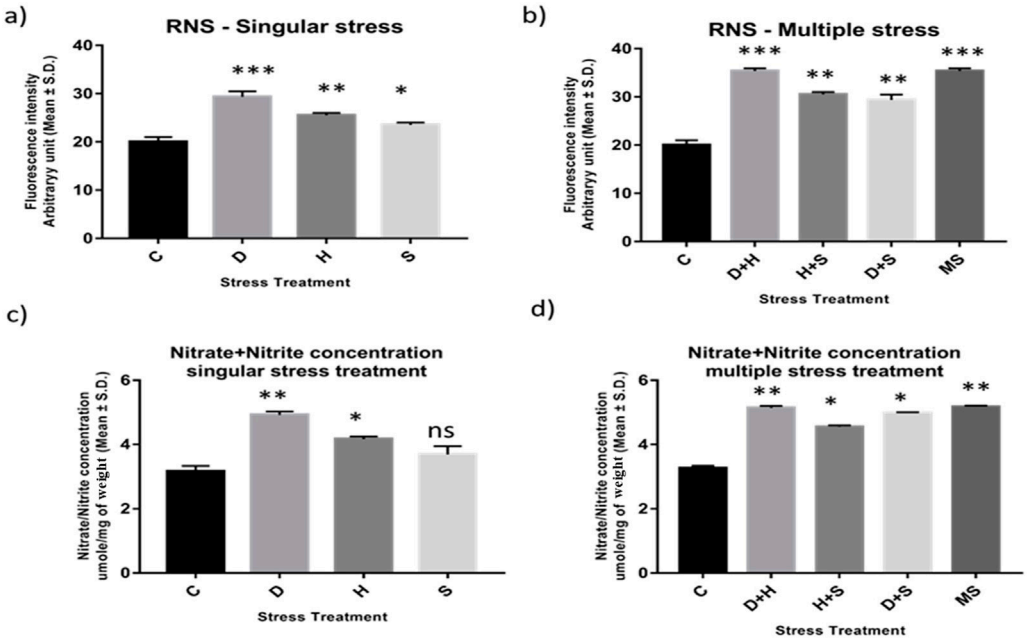

FIGURE 4
(A, B) Estimation of level of nitric oxide radical Arbitrary unit (mean ± SD) in third instar larvae of *D. melanogaster*. **(C, D)** Determination of Total Nitrate/Nitrite concentration umole/mg of weight (mean ± SD) in fourth instar larvae of *D. melanogaster*. Values represent mean and the vertical bars represent SD. Data shown are representative of three independent experiments. *** $P < 0.001$; ** $P < 0.01$; * $P < 0.05$ indicates significance level.

3.3 Reactive oxygen species imaging analysis

In fluorescence microscopic examination, the generation of ROS was validated in a metabolically active glandular tissue, the salivary glands of *D. melanogaster* larvae, and the ROS was quantified by green fluorescence intensity generated by the indicator DCF-DA dye. An increase in fluorescence intensity was observed with each stress treatment compared to the control salivary gland dissected from larvae without stress exposure. Salivary glands from desiccated larvae showed more green fluorescence intensity, indicative of higher levels of ROS in multiple stress treatments (Figures 3B, D) than in exposure to individual stressors (Figures 3A, C). When comparing the impact of singular stressors, desiccation stress generated more ROS than heat and starvation (Figures 3A, C). For a multiple stress regime, D + H and MS showed similar levels of elevation (Figures 3B, D).

3.4 Quantification of RNS: nitric oxide radical and nitrite/nitrate concentration

Abiotic stress administered in the present study induced oxidative stress, leading to the generation of nitrated species. RNS and the ratio of nitrate/nitrite concentration were all found to be elevated in the treated larvae of *D. melanogaster*. The treated larvae showed a higher ratio of nitrate/nitrite concentration and nitric oxide radicals than the corresponding control ones. While the increase was more prominent in the case of desiccation-stressed larvae than in the other singularly exposed larvae, the combinatorial exposure showed an increment notable in the case of heat with desiccation compared to other combinations. The consequences of D + H were similar to the impact of all three stressors (MS) on the larvae (Figures 4A–D).

3.5 Reactive nitrogen species imaging analysis

The increase in the intensity of green fluorescence resulting from the marker DAF-2DA dye was an indication of the presence of nitric oxide radicals. The metabolically active glandular tissue of the salivary glands of *D. melanogaster* was exposed to stress treatments as carried out in previous experiments, and the results showed an increase in green fluorescence intensity in the stressed larvae compared to the control larvae. The higher green fluorescence intensity was an indication of the elevated level of reactive species in the desiccated salivary glands than in the glands of the starved and heat stressed larvae. In combinatorial form, glandular tissues of the larvae subjected to desiccation combined with heat stress treatment showed higher fluorescence (Figures 5A–D).

3.6 Measurement of the total RONS and aconitase enzyme activity

The result of the collective measurement of RONS like hydrogen peroxide, peroxynitrite, and hydroxyl radicals showed the generation of total RONS, and it was more evident in the case of desiccation stress and also in combination with heat stress (Figures 6A, B). The quantification of mitochondrial aconitase enzyme activity showed that the concentration of the superoxide radical was inversely proportional to aconitase enzyme activity.

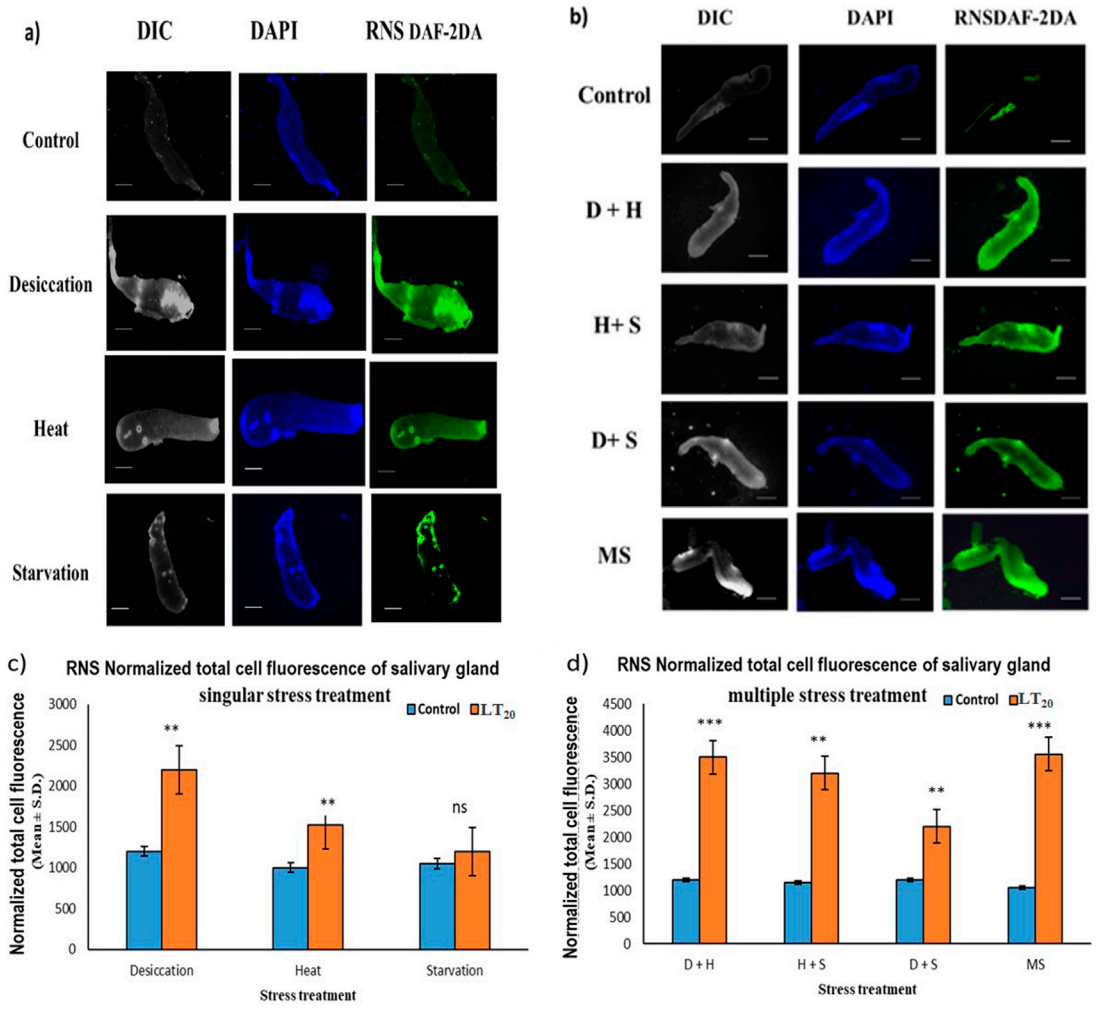

FIGURE 5
Fluorescence microscopic visualization of RNS: salivary gland images of *D. melanogaster* exposed to stress compared against the control with larvae subjected to **(A)** singular and **(B)** combinatorial stress treatments to visualize RNS. Normalized cell fluorescence intensity of **(C)** singular and **(D)** combinatorial treatment of salivary glands to quantify RNS. ***$p < 0.001$; **$p < 0.01$; and *$p < 0.05$ indicate significance levels. Scale bar: 200 µm. **(A,B)** DIC panel for the ease of resolving the outline.

Interestingly, the decrease in relative aconitase enzyme activity was more conspicuous in desiccated larvae than in the other singular stressors, while in combinations of stressors, it was more evident in D + H stress than in other combinations. As observed in other sets of experiments, the D + H impact resembled that of MS, where all stressors act together (Figures 7A, B).

3.7 Measurement of antioxidant enzyme activity

The data obtained from the quantification of antioxidant enzyme activity revealed that the specific activity of superoxide dismutase, catalase (Figures 8A–D), and glutathione peroxidase (Figures 9C, D) was directly proportional to stress treatment, while the specific activity of glutathione reductase was inversely proportional to stress treatment (Figures 9A, B). It was evident that the increase in the specific activity of SOD and catalase was more in the case of desiccation stress than that of heat stress and starvation stress (Figure 8A), while in combinatorial form, it was quite evident that the incremental change was prominent in the case of D + H compared to the other two combinations D + S and H + S (Figure 8B). Catalase showed a similar increase in activity with respect to stress treatments either in singular or multiple stress regimes (Figures 8C, D). Nevertheless, the total antioxidant capacity showed an increase in respective stressor-exposed larvae compared to the control. Furthermore, the increase in activity was higher in the case of desiccation stress and desiccation stress combined with heat stress than that in other singular and combinatorial stress exposure simultaneously (Figures 10A,B).

4 Discussion

The co-occurrence of heat, desiccation, and starvation as stressors has been well documented, and both plants and

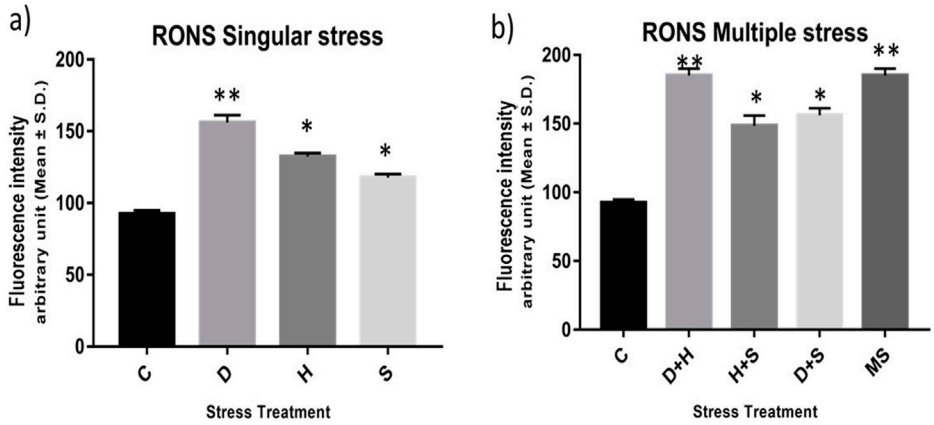

FIGURE 6
(A,B) Measurement of the total RONS fluorescence intensity arbitrary unit (mean ± SD) in third-instar larvae of *D. melanogaster*. Values represent the mean, and the vertical bars represent SD. Data shown are representative of three independent experiments. ***$p < 0.001$; **$p < 0.01$; and *$p < 0.05$ indicate significance levels.

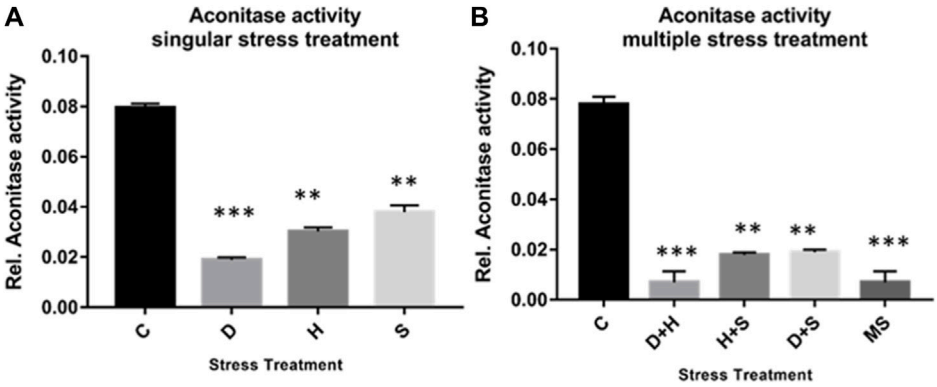

FIGURE 7
(A,B) Mitochondrial aconitase activity relative to the control with stress treatment (mean ± SD) in third-instar larvae of *D. melanogaster*. Values represent the mean, and the vertical bars represent SD. Data shown are representative of three independent experiments. ***$p < 0.001$; **$p < 0.01$; and *$p < 0.05$ indicate significance levels.

animals are equally vulnerable to such multi-stress environments. It is also well documented that in multi-stress environments, oxidative stress is one of the most common denominators of environmental stressors (Samet and Wages, 2018), and the occurrence of multiple stresses triggers an overproduction of ROS. Over a period, nitric oxide (NO) reacts rapidly with superoxide ($O_2^{\bullet -}$), producing peroxynitrite ($ONOO^-$) under excessive oxidation conditions, resulting in nitrosative stress. Under the nitrosative stress regime, additional RNS are generated (Figure 11). When the larvae of *D. melanogaster* were exposed to stressors either in singular or combinatorial form, the increase in RONS was evident, thereby confirming the convergence of desiccation stress, heat stress, and starvation stress in oxidative and nitrosative stress. The generation of ROS/RNS was always higher in the case of combinatorial stress than in singular exposure. The increased MDA concentration, protein carbonyl content, and AOPPs, damage markers of oxidative and nitrosative stress, further confirmed the biochemical and molecular signatures of the stress regime after desiccation stress, heat stress, and starvation stress, whether exposed individually or in combination. Previous reports of multi-stress environments have revealed that combinatorial responses are unique and cannot be extrapolated directly from the individual response to each type of stressor to which the organism is exposed. This might be due to the differential exposure of genes associated with the ROS gene network, as reported in *Arabidopsis* exposed to different stress treatments (Mittler et al., 2004; Mittler, 2006). In our study, stress-induced homeostasis could be ascertained through an increase in antioxidant activities. The antioxidant enzyme activity (SOD, CAT, and GPx) was higher, especially in combinatorial stress exposures, thereby suggesting how this defense system could manage oxidative and nitrosative stress, as well as cellular homeostasis. Other data on oxidative damage markers (MDA,

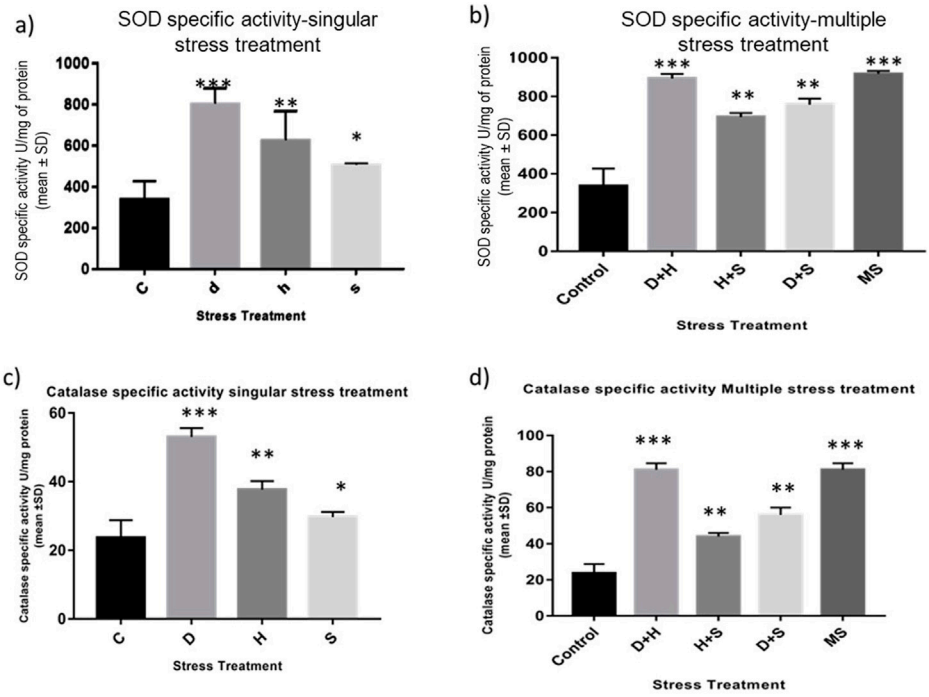

FIGURE 8
(A,B) Spectrophotometric measurement of **(A,B)** superoxide dismutase activity and **(C,D)** catalase activity of the whole larvae of *D. melanogaster* exposed to desiccation, heat, starvation, D + H, H + S, and D + S stress treatments compared with control groups and between treated groups. ***p < 0.001; **p < 0.01; and *p < 0.05 indicate significance levels.

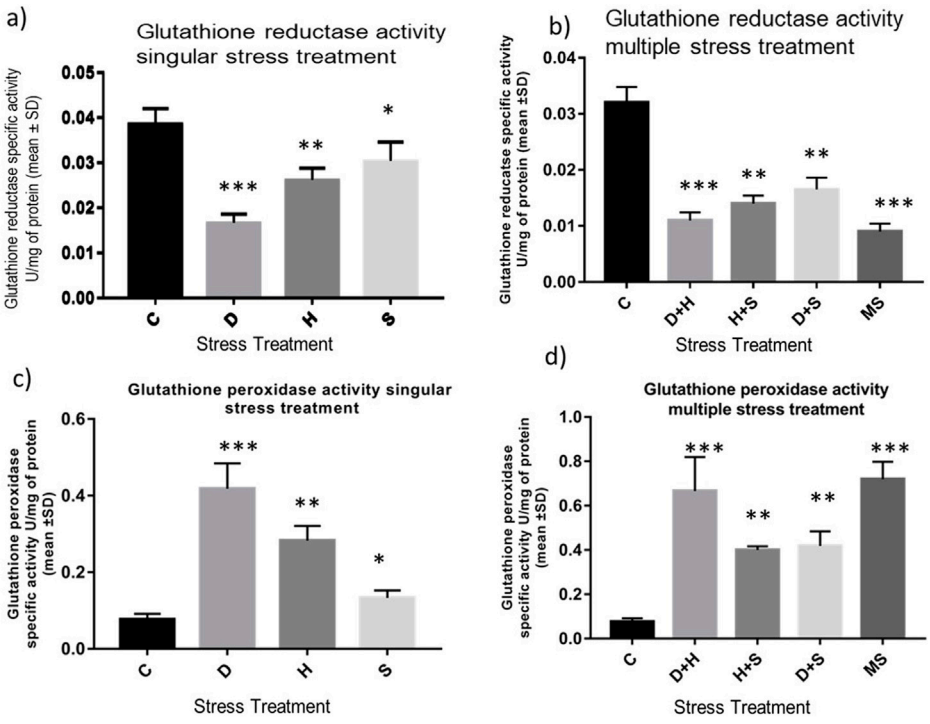

FIGURE 9
Determination of change in the activity of **(A,B)** glutathione reductase and **(C,D)** glutathione peroxidase of the whole larvae of *D. melanogaster* exposed to desiccation, heat, starvation, D + H, H + S, and D + S stress treatments compared with control groups and between treated groups. ***p < 0.001; **p < 0.01; and *p < 0.05 indicate significance levels.

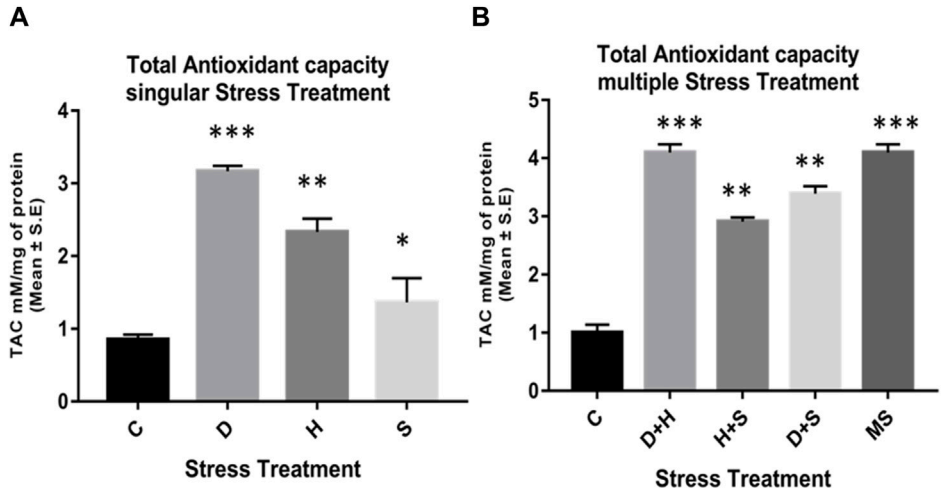

FIGURE 10
Quantification of the total antioxidant capacity of the whole larvae of *D. melanogaster* exposed to **(A)** singular and **(B)** multiple stress treatments compared with control groups and between treated groups. ***$p < 0.001$; **$p < 0.01$; and *$p < 0.05$ indicate significance levels.

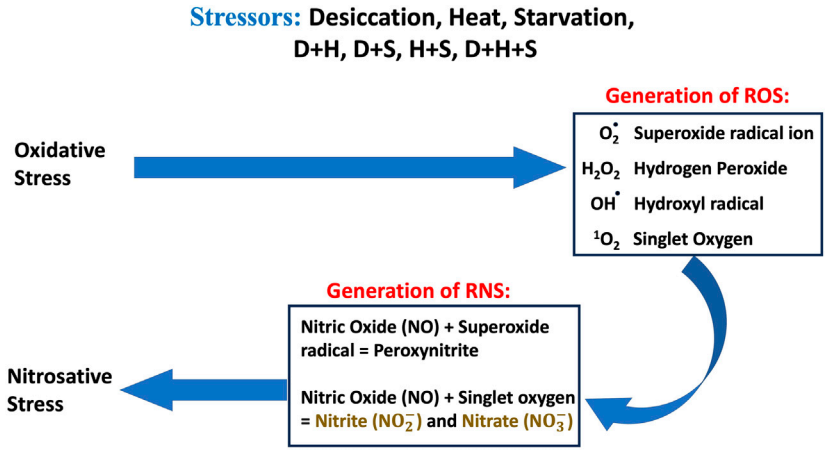

FIGURE 11
Schematic diagram of the overview of oxidative and nitrosative stress and generation of ROS and RNS.

protein carbonyl content, and AOPP) presented in this paper are analyzed, and desiccation was the most potent stressor, either acting individually or in combination with other stressors. Similar reports are available on other animals, where a combination of desiccation and heat stress can lead to greater lethal effects than those from different abiotic stress exposures (Jiang and Huang, 2001; Wang and Huang, 2004). Desiccation, as well as nutritional deprivation (starvation), can influence the thermal threshold of tolerance in insects by impacting homeostatic physiological mechanisms (Mitchell et al., 2017). In predatory mites, *Neoseiulus barkeri*, subjected to heat and desiccation stress, the mortality was mainly due to desiccation (Huang et al., 2019). Plants are also more vulnerable to desiccation-related stress while mitigating in a multi-stress environment. In *Brassica napus*, drought combined with heat stress led to more deleterious effects than drought alone. Moreover, in the presence of all three stressors, namely, drought + heat + nutrient deficiency, the damage is more than what might be due to a single stressor (Dikšaityte et al., 2020). In a seminal study on *D. melanogaster*, Bubliy et al. (2012) suggested that in a multi-stress environment, shared protective systems associated with plastic responses might be constrained. This study revealed that heat and desiccation hardening, along with acclimation to starvation, would incur metabolic costs, leading to reduced longevity (Bubliy et al., 2012). Our data on the total antioxidant enzyme activities (TAC) reflected a similar scenario. At the molecular level, several plants and animals respond through the expression of stress-responsive proteins like HSPs

(Nguyen et al., 2017; Yurina, 2023). Ongoing proteomic studies in our laboratory on *Drosophila* under a multi-stress environment indicated the upregulation of HSPs (Bomble and Nath, 2019). The superoxide anion radical $O_2^{\bullet-}$ is a major precursor of RONS production in cells, and an increase in this radical in a multi-stress environment ultimately leads to nitrosative stress (Ananda-Rivera et al., 2022). A higher level of $O_2^{\bullet-}$ generates additional RNS like nitrite (NO_2^-) and nitrate (NO_3^-) in a continuum (Figure 11). A higher level of $O_2^{\bullet-}$ and $ONOO^-$ generates additional RNS like nitrite (NO_2^-) and nitrite (NO_3^-) in a continuum (Figure 11). Since energy availability plays a crucial role in an organism's survival under a multi-stress environment, we focused on key mitochondrial enzymes involved in energy metabolism during the stress regime. We found the aconitase enzyme to be the best candidate for our present study because the aconitase enzyme is attacked by ROS and RNS. Aconitase activity in mitochondria has been reported to be a sensitive redox sensor of RONS (Tórtora et al., 2007; Lushchak et al., 2014). In the Krebs cycle, aconitase catalyzes citrate to isocitrate. However, during oxidative and nitrosative stress, aconitase is oxidized by nitric oxide (•NO), superoxide ($O_2^{\bullet-}$), and peroxynitrite ($ONOO^-$), generating inactive aconitase. In the present study, a significant inactivation of aconitase activity (Figure 9) was concomitant with the increase in the RONS level (Figure 8), both under singular and multiple stress regimes. Therefore, an increase in superoxide radical concentration, along with other RONS, might have led to the inactivation of the aconitase enzyme, as previously described (Liang et al., 1997; Miwa and Brand, 2005). Interestingly, the impact of desiccation stress was significantly higher than that of any other stressors impacting aconitase inactivation, whether exerting its effect singularly or in combination. This is the first report of multi-stressor-induced inactivation of aconitase through RONS in *Drosophila* or, for that matter, in any other terrestrial invertebrate animals. In *Drosophila*, the salivary gland provides an excellent experimental system for cellular, molecular, and physiological studies. The cells of salivary glands contain polytene nuclei and are metabolically active across all the developmental stages (Andrew et al., 2000). In the present study, we extended our biochemical experiments of ROS/RNS detection and quantification at the cellular level using salivary gland cells of *D. melanogaster* as the model tissue. Fluorescence microscopic detection of ROS (Figure 3) and RNS (Figure 6) in salivary gland cells corroborated biochemical findings, suggesting that a quantum of the multi-stress response was maximum during desiccation stress, as well as with other stressors in combination with desiccation. In recent literature, the impact of multiple stressors has been categorized into additive, synergistic, and antagonistic (Piggott et al., 2015; Simmons et al., 2021). If we compare the effects of two stressors, A and B, with the control C, the effect of A will be the change in the response above the baseline, represented as A−C. Similarly, the effect of B will be B−C. The stressor interaction will be "*additive*" if the sum of effects of A and B is above the baseline [response = (A + B) −C]. However, the interaction will be "*synergistic*" if the sum of the effects of A and B is greater than the sum of the effects of both treatments [response > (A + B)−C]. The impact of the simultaneous action of multiple stressors can be assessed using this paradigm (Fong et al., 2018) and conceptualized for inferring endpoints of multi-stress regimes (Piggott et al., 2015; Simmons et al., 2021). The findings of the present study revealed that the combinatory effect of stressors (D + H, H + S, D + S) was "*synergistic*" because the combined effect of two stressors was always greater than the sum of the effect when administered separately and was never equal (*additive*) to the mathematical summation of their impact when treated individually. This was evident in all the experimental results (Figures 1–6, 8, 10), except where the downregulation or inhibitory effect (*antagonistic*) served as a "proof of concept."

Considering all the endpoints, the present study strongly suggested that multiple stress responses depended on the type of individual stressor and the combination of stressors, leading to a synergistic effect. Although molecular signaling pathways of abiotic stresses like desiccation, heat, and starvation converge at some point to the oxidative stress pathway, signaling pathways are different in abiotic stressors (Knight and Knight, 2001; Lacal, 2017). Future studies will reveal the intricacies of signaling networks of desiccation stress, heat stress, and starvation stress and key signaling molecules involved in cross-talk.

5 Conclusion

The study found that all three stressors caused oxidative and nitrosative stress responses. Desiccation stress was the most significant stressor compared to heat stress and starvation stress. When stressors were combined, D + H had a greater impact than other pairs of stressors. The findings suggest that the level of oxidative and nitrosative stress depends on the specific stressors and their combinations. The study highlights the importance of considering RNS as a stress marker, not just focusing on ROS generation. Research on RONS will provide a more comprehensive understanding of oxidative stress biology. The findings of this paper could lead to new research directions on managing and restoring the environment, using *Drosophila* as an indicator.

Data availability statement

The original contributions presented in the study are included in the article/Supplementary Material; further inquiries can be directed to the corresponding author.

Ethics statement

The paper presents research on animals that does not require ethical approval for the study.

Author contributions

PB: conceptualization, formal analysis, investigation, methodology, software, validation, and writing–original draft. BBN: data curation, funding acquisition, project administration, resources, supervision, visualization, and writing–review and editing.

Funding

The author(s) declare that financial support was received for the research, authorship, and/or publication of this article. BBN acknowledges the partial funding received from RUSA-II Phase-II (RUSA-CBS-TH1) and remuneration as consultant to PB from the same fund. BBN also acknowledges the partial grant received from the Department of Zoology, Savitribai Phule Pune University, India.

Acknowledgments

PB and BBN acknowledge the technical and experimental assistance received from Kranti Meher, who worked as a trainee in the BBN laboratory. They also acknowledge infrastructural support from the Department of Zoology, and BBN acknowledges Savitribai Pule Pune University for providing necessary permission for research work as Emeritus Professor at the Department of Zoology and the administrative support from the EC at the MIE-SPPU Institute of Higher Education, Doha, Qatar.

Conflict of interest

The authors declare that the research was conducted in the absence of any commercial or financial relationships that could be construed as a potential conflict of interest.

Publisher's note

All claims expressed in this article are solely those of the authors and do not necessarily represent those of their affiliated organizations, or those of the publisher, the editors, and the reviewers. Any product that may be evaluated in this article, or claim that may be made by its manufacturer, is not guaranteed or endorsed by the publisher.

Supplementary material

The Supplementary Material for this article can be found online at: https://www.frontiersin.org/articles/10.3389/fphys.2024.1426169/full#supplementary-material

References

Aebi, H. E. (1983). "Catalase," in *Methods of enzymatic analysis*. Editor H. U. Bergmeyer (Weinheim: Verlag), 273–286.

Ananda-Rivera, A. K., Cruz-Gregorio, A., Arancibia-Hernandez, Y. L., Hernandez-Cruz, E., and Pedraza-Chaverri, J. (2022). RONS and oxidative stress: an overview of basic concepts. *Oxygen* 2, 437–478. doi:10.3390/oxygen2040030

Andrew, D. J., Henderson, K. D., and Seshaiah, P. (2000). Salivary gland development in *Drosophila melanogaster*. *Mech. Dev.* 92, 5–17. doi:10.1016/s0925-4773(99)00321-4

Beauchamp, C., and Fridovich, I. (1971). Superoxide dismutase: improved assays and an assay applicable to acrylamide gels. *Anal. Biochem.* 44 (1), 276–287. doi:10.1016/0003-2697(71)90370-8

Bijlsma, R., and Loeschke, V. (2005). Environmental stress, adaptation and evolution: an overview. *J. Evol. Biol.* 18, 744–749. doi:10.1111/j.1420-9101.2005.00962.x

Bomble, P., and Nath, B. B. (2022). Differential manifestation of RONS and antioxidant enzymes in response to singula versus combinatorial stress in *Chironomus ramosus*. *Stress Biol.* 2, 56. doi:10.1007/s44154-022-00077-8

Bomble, P. N., and Nath, B. (2019). Comparative susceptibility of *Chironomus* and *Drosophila* to exposure to each and combinations of the following stressors: desiccation, heat stress and starvation. *Eur. J. Environ. Sci.* 9 (1), 41–46. doi:10.14712/23361964.2019.5

Bradley, T. J. (2009). *Animal osmoregulation*. Oxford: Oxford University Press.

Bubliy, O. A., Kristensen, T. N., Kellermann, V., and Loeschcke, V. (2012). Plastic responses to four environmental stresses and cross-resistance in a laboratory population of *Drosophila melanogaster*. *Funct. Ecol.* 26, 245–253. doi:10.1111/j.1365-2435.2011.01928.x

Dalle-Donna, I., Scaloni, A., Giustarini, D., Cavarra, E., Tell, G., Lungarela, G., et al. (2005). Proteins as biomarkers of oxidative/nitrosative stress in diseases: the contribution of redox proteomics. Mass Spect. *Rev.* 24, 55–99. doi:10.1002/mass.20006

Del Río, L. A. (2015). ROS and RNS in plant physiology: an overview. *J. Exptl. Bot.* 66, 2827–2837. doi:10.1093/jxb/erv099

Dikšaityte, A., Virsile, A., Zaltauskaite, J., Januskaitiene, I., Praspaliauskas, M., and Pedisius, N. (2020). Do plants respond and recover from a combination of drought and heatwave in the same manner under adequate and deprived soil nutrient conditions? *Plant Sci.* 291, 110333. doi:10.1016/j.plantsci.2019.110333

Farahani, S., Bandani, A. R., Alizadeh, H., Goldansaz, S. H., and Whyard, S. (2020). Differential expression of heat shock proteins and antioxidant enzymes in response to temperature, starvation, and parasitism in the Carob moth larvae, Ectomyelois ceratoniae (Lepidoptera: Pyralidae). *PLoS ONE* 15 (1), e0228104. doi:10.1371/journal.pone.0228104

Fong, C. R., Bittick, S. J., and Fong, P. (2018). Simultaneous synergist, antagonistic and additive interactions between multiple local stressors all degrade algal turf communities on coral reefs. *J. Ecol.* 106, 1390–1400. doi:10.1111/1365-2745.12914

Gardner, P. R. (2002). Aconitase: sensitive target and measure of superoxide. *Methods Enzym.* 349, 9–23. doi:10.1016/S0076-6879(02)49317-2

Goldberg, D. M., and Spooner, R. J. (1983). "Assay of glutathione reductase," in *Methods of enzymatic analysis*. Editor H. V. Bergmeyen (Weinheim: Verlag Chemie), 258–265.

Hermes-Lima, M., Moreira, D. C., Rivera-Ingraham, G. A., Giraud-Billoud, M., Genaro-Mattos, T. C., and Campos, E. G. (2015). Preparation for oxidative stress under hypoxia and metabolic depression: revisiting the proposal two decades later. *Free Radic. Biol and Med* 89, 1122–1143. doi:10.1016/j.freeradbiomed.2015.07.156

Hoffmann, A. A., and Hercus, M. J. (2000). Environmental stress as an evolutionary force. *BioScience* 50, 217–226. doi:10.1641/00063568(2000)050[0217:ESAAEF]2.3.CO;2

Holt, E. A., and Miller, S. W. (2010). Bioindicators: using organisms to measure environmental impacts. *Nat. Edu. Knowdlege.* 3, 8.

Huang, J., Liu, M.-X., Zhang, Y., Kuang, Z.-Y., Li, W., Ge, C.-B., et al. (2019). Response to multiple stressors: enhanced tolerance of Neoseiulus barkeri hughes (Acari: phytoseiidae) to heat and desiccation stress through acclimation. *Insects* 10, 449. doi:10.3390/insects10120449

Jiang, Y., and Huang, B. (2001). Drought and heat stress injury to two cool-season turfgrasses in relation to antioxidant metabolism and lipid peroxidation. *Crop Sci.* 41, 436–442. doi:10.2135/cropsci2001.412436x

Khan, M., Ali, S., Al Azzawi, T. M. I., Saqib, S., Ullah, F., Ayaz, A., et al. (2023). The key roles of ROS and RNS as a signaling molecule in plant-microbe interactions. *Antioxidants* 12, 268. doi:10.3390/antiox12020268

Knight, H., and Knight, M. R. (2001). Abiotic stress signalling pathways: specificity and cross-talk. *talk* 6, 262–267. doi:10.1016/S1360-1385(01)01946-X

Lacal, C. T. (2017). *Signaling pathways in abiotic stress* (USA: Arcler Education Inc).

Lawrence, R. A., and Burk, R. F. (1976). Glutathione peroxidase activity in selenium-deficient rat liver. *Biochem. Biophys. Res. Commun.* 71 (4), 952–958. doi:10.1016/0006-291X(76)90747-6

Liang, J. Y., Levine, R. L., and Sohal, R. S. (1997). Oxidative damage during aging targets mitochondrial aconitase. *Proc. Natl. Acad. Sci. USA.* 94, 11168–11172. doi:10.1073/pnas.94.21.11168

Lindquist, S. (1980). Varying patterns of protein synthesis in Drosophila during heat shock: implications for regulation. *Dev Biol.* 77 (2), 463–479. doi:10.1016/0012-1606(80)90488-1

Lushchak, O. V., Piroddi, M., Gatti, F., and Lushchak, V. I. (2014). Aconitase post-translational modification as a key in linkage between Krebs cycle, iron homeostasis, redox signaling, and metabolism of reactive oxygen species. *Redox Rep.* 19, 8–15. doi:10.1179/1351000213Y.0000000073

Malik, A. I., and Storey, K. B. (2011). Transcriptional regulation of antioxidant enzymes by FoxO1 under dehydration stress. *Gene* 485, 114–119. doi:10.1016/j.gene.2011.06.014

Miao, Z. Q., Tu, Y. Q., Guo, P. Y., He, W., Jing, T. X., Wang, J. J., et al. (2020). Antioxidant enzymes and heat shock protein genes from liposcelis bostrychophila are involved in stress defense upon heat shock. *Insects* 11, 839. doi:10.3390/insects11120839

Mitchell, K. A., Bardman, L., Clusella-Trullas, S., and Terblanche, J. S. (2017). Effects of nutrient and water restriction on thermal tolerance: a test of mechanisms and hypotheses. *Comp. Biochem. Physiol. Pt.A.* 212, 15–23. doi:10.1016/j.cbpa.2017.06.019

Mittler, R. (2006). Abiotic stress, the field environment and stress combination. *Trends Plant Sci.* 11, 15–19. doi:10.1016/j.tplants.2005.11.002

Mittler, R., Vanderauwera, S., Gollery, M., and Van Breusegem, F. (2004). Reactive oxygen gene network of plants. *Trends Plant Sci* 9, 490–498. doi:10.1016/j.tplants.2004.08.009

Miwa, S., and Brand, M. D. (2005). The topology of superoxide production by complex III and glycerol-3-phosphase dehydrogenase in *Drosophila* mitochondria. *Biochim. Biophys. Acta* 1709, 214–219. doi:10.1016/j.bbabio.2005.08.003

Nguyen, A. D., DeNovellis, K., Resendez, S., Pustilnik, J. D., Gotelli, N. J., Parker, J. D., et al. (2017). Effects of desiccation and starvation on thermal tolerance and the heat-shock response in forest ants. *J. Comp. Physiol. B* 187, 1107–1116. doi:10.1007/s00360-017-1101-x

Ohkawa, H., Ohishi, N., and Yagi, K. (1979). Assay for lipid peroxides in animal tissues by thiobarbituric acid reaction. *Anal. Biochem.* 95 (2), 351–358. doi:10.1016/0003-2697(79)90738-3

Pandey, J. P., Jena, K., Tiwari, R. K., and Sahay, A. (2020). Starvation modulates the immuno-oxidative stress and cocoon characteristics of tasar silkworm Antheraea mylitta. *Am. J. Biochem. Mol. Biol.* 10, 23–34. doi:10.3923/ajbmb.2020.23.34

Pati, S. G., Panda, F., Bal, A., Paital, B., and Sahoo, D. K. (2024). Water deprivation-induced hypoxia and oxidative stress physiology responses in respiratory organs of the Indian stinging fish in near coastal zones. *PeerJ* 12, e16793. doi:10.7717/peerj.16793

Piggott, J. J., Townsend, C. R., and Matthaei, C. D. (2015). Reconceptualizing synergism and antagonism among multiple stressors. *Ecol. Evol.* 5, 1538–1547. doi:10.1002/ece3.1465

Ramniwas, S., Tyagi, P. K., Sharma, A., and Kumar, G. (2023). Editorial: abiotic stress and physiological adaptive strategies of insects, *Front. Physiol.*, 14:1210052. doi:10.3389/fphys.2023.1210052

Samet, J. M., and Wages, P. A. (2018). Oxidative stress from environmental exposures. *Curr. Opin. Toxicol.* 7, 60–66. doi:10.1016/j.cotox.2017.10.008

Simmons, B. I., Blyth, P. S. A., Blanchard, J. L., Clegg, T., Delmas, E., Garnier, A., et al. (2021). Refocusing multiple stressor research around the targets and scales of ecological impacts. *Nat. Ecol. Evol.* 5, 1478–1489. doi:10.1038/s41559-021-01547-4

Sokolova, I. (2021). Bioenergetics in environmental adaptation and stress tolerance of aquatic ectotherms: linking physiology and ecology in a multi-stressor landscape. *J. Exp. Biol.* 224, jeb236802. doi:10.1242/jeb236802

Thorat, L., Mani, K-P., Thangaraj, P., Chatterjee, S., and Nath, B. B. (2016a). Downregulation of dTPS1 in *Drosophila melanogaster* larvae confirms involvement of trehalose in redox regulation following desiccation. *Cell Stress and Chaperones* 21, 285–294. doi:10.1007/s12192-015-0658-0

Thorat, L., and Nath, B. B. (2010). Effect of water hyacinth *Eichhornia crassipes* root extracts on midge *Chironomus ramosus* larva: a preliminary note. *Physiol. Entomol.* 35, 391–393. doi:10.1111/j.1365-3032.2010.00745.x

Thorat, L., and Nath, B. B. (2018). Insects with survival kits for desiccation tolerance underextreme water deficits. *Front. Physiol.* 9, 1843. doi:10.3389/fphys.2018.01843

Thorat, L., Oulkar, D., Banerjee, K., and Nath, B. B. (2016b). Desiccation stress induces developmental heterochrony in *Drosophila melanogaster*. *J. Biosci.* 41, 331–339. doi:10.1007/s12038-016-9628-7

Thorat, L., Paluzzi, J-P., Pflüger, H-J., and Nath, B. B. (2023). Editorial: insects and changing environments: emerging perspectives on abiotic stress tolerance mechanisms. *Front. Physiol.* 14, 1191318. doi:10.3389/fphys.2023.1191318

Thorat, L. J., Gaikwad, S. M., and Nath, B. B. (2012). Trehalose as an indicator of desiccation stress in *Drosophila melanogaster* larvae: a potential marker of anhydrobiosis. *Biochem. Biophys. Res. Commun.* 419, 638–642. doi:10.1016/j.bbrc.2012.02.065

Tórtora, V., Quijano, C., Freeman, B., Radi, R., and Castro, L. (2007). Mitochondrial aconitase reaction with nitric oxide, S-nitrosoglutathione, and peroxynitrite: mechanisms and relative contributions to aconitase inactivation. *Free Radic Biol Med.* 42 (7), 1075–1088. doi:10.1016/j.freeradbiomed.2007.01.007

Wang, F., Yuan, Q., Chen, F., Pang, I., Pan, C., Xu, F., et al. (2021). Fundamental mechanisms of the cell death caused by nitrosative stress. *Front. Cell Dev. Biol.* 20, 742483. doi:10.3389/fcell.2021.742483

Wang, Z. L., and Huang, B. R. (2004). Physiological recovery of Kentucky bluegrass from simultaneous drought and heat stress. *Crop Sci.* 44, 1729–1736. doi:10.2135/cropsci2004.1729

Wen, C. A., Bajracharya, R., Towarnicki, S. G., and Ballard, W. O. (2016). Assessing bioenergetic functions from isolated mitochondria in Drosophila melanogaster. *J. Biol. Methods.* 3 (2), e42. doi:10.14440/jbm.2016.112

Witko-Sarsat, V., Friedlander, M., Capeillère-Blandin, C., Nguyen-Khoa, T., Nguyen, A. T., Zingraf, J., et al. (1996). Advanced oxidation protein products as a novel marker of oxidative stress in uremia. *Kidney Int.* 49 (5), 1304–1313. doi:10.1038/ki.1996.186

Yurina, N. P. (2023). Heat shock proteins in plant protection from oxidative stress. *Mol. Biol.* 57, 951–964. doi:10.1134/S0026893323060201

Zhang, D.-W., Xiao, Z.-J., Zeng, B.-P., Li, K., and Tang, Y.-L. (2019). Insect behavior and physiological adaptation mechanisms under starvation stress. *Front. Physiol.* 10, 163. doi:10.3389/fphys.2019.00163

Frontiers in Physiology

Understanding how an organism's components work together to maintain a healthy state

The second most-cited physiology journal, promoting a multidisciplinary approach to the physiology of living systems - from the subcellular and molecular domains to the intact organism and its interaction with the environment.

Discover the latest Research Topics

See more →

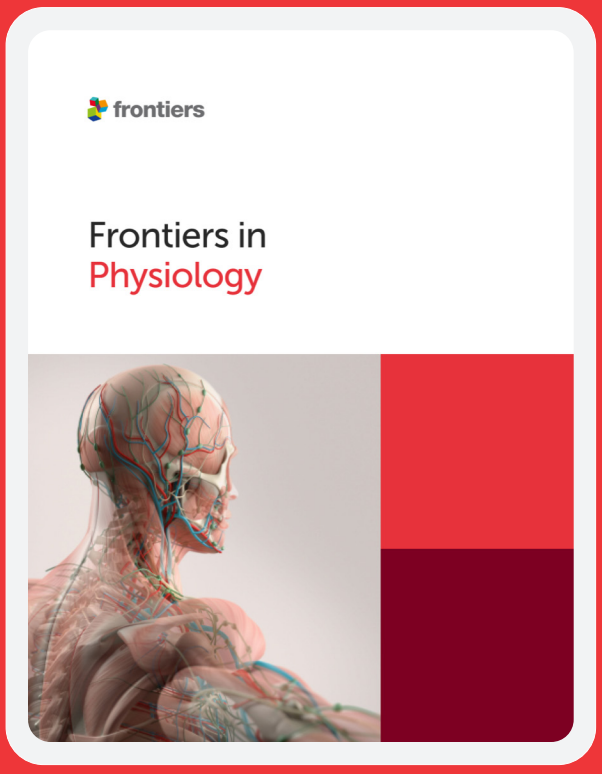

Frontiers

Avenue du Tribunal-Fédéral 34
1005 Lausanne, Switzerland
frontiersin.org

Contact us

+41 (0)21 510 17 00
frontiersin.org/about/contact